

249

Topics in Current Chemistry

Editorial Board:

**A. de Meijere · K. N. Houk · H. Kessler · J.-M. Lehn · S.V. Ley
S. L. Schreiber · J. Thiem · B. M. Trost · F. Vögtle · H. Yamamoto**

Topics in Current Chemistry

Recently Published and Forthcoming Volumes

Anion Sensing

Volume Editor: Stibor, I.
Vol. 255, 2005

Organic Solid State Reactions

Volume Editor: Toda, E.
Vol. 254, 2005

DNA Binders and Related Subjects

Volume Editors: Waring, M.J., Chaires, J.B.
Vol. 253, 2005

Contrast Agents III

Volume Editor: Krause, W.
Vol. 252, 2005

Chalcogenocarboxylic Acid Derivatives

Volume Editor: Kato, S.
Vol. 251, 2005

New Aspects in Phosphorus Chemistry V

Volume Editor: Majoral, J.-P.
Vol. 250, 2005

Templates in Chemistry II

Volume Editors: Schalley, C.A.,
Vögtle, F., Dötz, K.H.
Vol. 249, 2005

Templates in Chemistry I

Volume Editors: Schalley, C.A.,
Vögtle, F., Dötz, K.H.
Vol. 248, 2004

Collagen

Volume Editors: Brinckmann, J.,
Notbohm, H., Müller, P.K.
Vol. 247, 2005

New Techniques in Solid-State NMR

Volume Editor: Klinowski, J.
Vol. 246, 2005

Functional Molecular Nanostructures

Volume Editor: Schlüter, A.D.
Vol. 245, 2005

Natural Product Synthesis II

Volume Editor: Mulzer, J.
Vol. 244, 2005

Natural Product Synthesis I

Volume Editor: Mulzer, J.
Vol. 243, 2005

Immobilized Catalysts

Volume Editor: Kirschning, A.
Vol. 242, 2004

Transition Metal and Rare Earth Compounds III

Volume Editor: Yersin, H.
Vol. 241, 2004

The Chemistry of Pheromones and Other Semiochemicals II

Volume Editor: Schulz, S.
Vol. 240, 2005

The Chemistry of Pheromones and Other Semiochemicals I

Volume Editor: Schulz, S.
Vol. 239, 2004

Orotidine Monophosphate Decarboxylase

Volume Editors: Lee, J.K., Tantillo, D.J.
Vol. 238, 2004

Long-Range Charge Transfer in DNA II

Volume Editor: Schuster, G.B.
Vol. 237, 2004

Long-Range Charge Transfer in DNA I

Volume Editor: Schuster, G.B.
Vol. 236, 2004

Spin Crossover in Transition Metal Compounds III

Volume Editors: Gülich, P., Goodwin, H.A.
Vol. 235, 2004

Spin Crossover in Transition Metal Compounds II

Volume Editors: Gülich, P., Goodwin, H.A.
Vol. 234, 2004

Spin Crossover in Transition Metal Compounds I

Volume Editors: Gülich, P., Goodwin, H.A.
Vol. 233, 2004

Templates in Chemistry II

Volume Editors:

Christoph A. Schalley, Fritz Vögtle, Karl Heinz Dötz

With contributions by

F. Aricó · J. D. Badjic · P. Bäuerle · D. H. Busch · S. J. Cantrill

M. G. J. ten Cate · B. X. Colasson · M. Crego-Calama

C. Dietrich-Buchecker · M. Emgenbroich · A. H. Flood · B. C. Gibb

A. J. Hall · A. Kaiser · Z. R. Laughrey · K. C.-F. Leung · Y. Liu

D. N. Reinhoudt · J.-P. Sauvage · B. Sellergren · J. F. Stoddart



Springer

The series *Topics in Current Chemistry* presents critical reviews of the present and future trends in modern chemical research. The scope of coverage includes all areas of chemical science including the interfaces with related disciplines such as biology, medicine and materials science. The goal of each thematic volume is to give the nonspecialist reader, whether at the university or in industry, a comprehensive overview of an area where new insights are emerging that are of interest to a larger scientific audience.

As a rule, contributions are specially commissioned. The editors and publishers will, however, always be pleased to receive suggestions and supplementary information. Papers are accepted for *Topics in Current Chemistry* in English.

In references *Topics in Current Chemistry* is abbreviated Top Curr Chem and is cited as a journal.

Visit the TCC content at springerlink.com

Library of Congress Control Number: 2004108949

ISSN 0340-1022

ISBN-10 3-540-23087-4 Springer Berlin Heidelberg New York

ISBN-13 978-3-540-23087-8 Springer Berlin Heidelberg New York

DOI 10.1007/b98632

This work is subject to copyright. All rights are reserved, whether the whole or part of the material is concerned, specifically the rights of translation, reprinting, reuse of illustrations, recitation, broadcasting, reproduction on microfilms or in any other ways, and storage in data banks. Duplication of this publication or parts thereof is only permitted under the provisions of the German Copyright Law of September 9, 1965, in its current version, and permission for use must always be obtained from Springer-Verlag. Violations are liable to prosecution under the German Copyright Law.

Springer is a part of Springer Science+Business Media

springeronline.com

© Springer-Verlag Berlin Heidelberg 2005

Printed in Germany

The use of general descriptive names, registered names, trademarks, etc. in this publication does not imply, even in the absence of a specific statement, that such names are exempt from the relevant protective laws and regulations and therefore free for general use.

Cover design: KünkelLopka, Heidelberg/design & production GmbH, Heidelberg

Typesetting: Fotosatz-Service Köhler GmbH, Würzburg

Printed on acid-free paper 02/3141/xv – 5 4 3 2 1 0

Volume Editors

Priv-Doz. Dr. Christoph A. Schalley
c.schalley@uni-bonn.de

Prof. Dr. Fritz Vögtle
voegtle@uni-bonn.de

Prof. Dr. Karl H. Dötz
doetz@uni-bonn.de

Kekulé-Institut für Organische
Chemie und Biochemie
Gerhard-Domagk-Str. 1
53121 Bonn, Germany

Editorial Board

Prof. Dr. Armin de Meijere
Institut für Organische Chemie
der Georg-August-Universität
Tammannstraße 2
37077 Göttingen, Germany
ameijer1@uni-goettingen.de

Prof. Dr. Horst Kessler
Institut für Organische Chemie
TU München
Lichtenbergstraße 4
85747 Garching, Germany
kessler@ch.tum.de

Prof. Steven V. Ley
University Chemical Laboratory
Lensfield Road
Cambridge CB2 1EW, Great Britain
svl1000@cus.cam.ac.uk

Prof. Dr. Joachim Thiem
Institut für Organische Chemie
Universität Hamburg
Martin-Luther-King-Platz 6
20146 Hamburg, Germany
thiem@chemie.uni-hamburg.de

Prof. Dr. Fritz Vögtle
Kekulé-Institut für Organische Chemie
und Biochemie der Universität Bonn
Gerhard-Domagk-Straße 1
53121 Bonn, Germany
voegtle@uni-bonn.de

Prof. Kendall N. Houk
Department of Chemistry and Biochemistry
University of California
405 Hilgard Avenue
Los Angeles, CA 90024-1589, USA
houk@chem.ucla.edu

Prof. Jean-Marie Lehn
Institut de Chimie
Université de Strasbourg
1 rue Blaise Pascal, B.P.Z 296/R8
67008 Strasbourg Cedex, France
lehn@chimie.u-strasbg.fr

Prof. Stuart L. Schreiber
Chemical Laboratories
Harvard University
12 Oxford Street
Cambridge, MA 02138-2902, USA
sls@slsiris.harvard.edu

Prof. Barry M. Trost
Department of Chemistry
Stanford University
Stanford, CA 94305-5080, USA
bmtrost@leland.stanford.edu

Prof. Hisashi Yamamoto
Arthur Holly Compton Distinguished
Professor
Department of Chemistry
The University of Chicago
5735 South Ellis Avenue
Chicago, IL 60637
773-702-5059, USA
yamamoto@uchicago.edu

Topics in Current Chemistry also Available Electronically

For all customers who have a standing order to Topics in Current Chemistry, we offer the electronic version via SpringerLink free of charge. Please contact your librarian who can receive a password for free access to the full articles by registration at:

springerlink.com

If you do not have a subscription, you can still view the tables of contents of the volumes and the abstract of each article by going to the SpringerLink Homepage, clicking on "Browse by Online Libraries", then "Chemical Sciences", and finally choose Topics in Current Chemistry.

You will find information about the

- Editorial Board
- Aims and Scope
- Instructions for Authors
- Sample Contribution

at springeronline.com using the search function.

Preface

When we invited authors to contribute to the first Topics in Current Chemistry volume on “Templates in Chemistry”, the resonance was overwhelming and encouraged us to edit a second volume which together with the first one provides an even broader overview of and a deeper insight into the template topic adding new aspects and new views.

The present volume begins with a chapter by Daryle H. Busch, the pioneer in the field, who puts molecular templates into the context of their 40 years’ history. In view of the many different new aspects appearing in the current chemistry literature, we sometimes tend to lose sight of the long and successful history of templates. Therefore, this chapter may well serve as a reminder of the wealth of chemistry that developed from the template strategy even several decades ago.

The other contributions to the present volume are organized roughly in order of the decreasing bond strengths involved and the increasing complexity of the systems under study. Zachary Laughrey and Bruce Gibb review templated macrocycle formation starting with covalent templates and proceeding to other, weaker interactions involving coordinative and hydrogen bonds. The third chapter by Achim Kaiser and Peter B  uerle is devoted to macrocycle formation through coordination to Pt(II). Then, Fraser Stoddart and his colleagues describe the templated synthesis of interlocked molecules, followed by an overview on molecular knots by Jean-Pierre Sauvage and his coworkers. The two latter chapters thus continue a theme which was already touched on in the first volume on templates in this series of monographs. David Reinhoudt et al. show how templation can assist the hierarchical self-assembly of complex hydrogen-bonded rosette-type aggregates. Finally, imprinted polymers which form around a template and – after its removal – can recognize guest molecules or even accelerate reactions, form the topic of the last chapter by B  rje Sellergren and his colleagues. These two final chapters thus deal with increasingly complex and structurally rich systems which were not possible without the use of templates. This nicely illustrates how templates help to tame complexity by a suitable design of smaller and simpler building blocks.

We believe that this volume not only provides excellent and comprehensive overviews for expert readers, but also certainly shows that there are many new aspects of templates still to be discovered for readers not so familiar with the chemistry presented here.

Contents

First Considerations: Principles, Classification, and History	
D. H. Busch	1
Macrocycle Synthesis Through Templatation	
Z. R. Laughrey · B. C. Gibb	67
Macrocycles and Complex Three-Dimensional Structures Comprising Pt(II) Building Blocks	
A. Kaiser · P. Bäuerle	127
Templated Synthesis of Interlocked Molecules	
F. Aricó · J. D. Badjic · S. J. Cantrill · A. H. Flood · K. C.-F. Leung · Y. Liu · J. F. Stoddart	203
Molecular Knots	
C. Dietrich-Buchecker · B. X. Colasson · J.-P. Sauvage	261
Templatation in Noncovalent Synthesis of Hydrogen-Bonded Rosettes	
M. Crego-Calama · D. N. Reinhoudt · M. G. J. ten Cate	285
Imprinted Polymers	
A. J. Hall · M. Emgenbroich · B. Sellergren	317
Author Index Volumes 201–249	351
Subject Index	369

Contents of Volume 248

Templates in Chemistry I

Volume Editors: Christoph A. Schalley · Fritz Vögtle · Karl Heinz Dötz
ISBN 3-540-22547-1

Spacer-Controlled Multiple Functionalization of Fullerenes

C. Thilgen · S. Sergeyev · F. Diederich

Chromium-Templated Benzannulation and Haptotropic Metal Migration

K. H. Dötz · B. Wenzel · H. C. Jahr

Supramolecular Templating in the Formation of Helicates

M. Albrecht

Hydrogen-Bond-Mediated Template Synthesis of Rotaxanes, Catenanes, and Knotanes

C. A. Schalley · T. Weilandt · J. Brüggemann · F. Vögtle

Template-Controlled Synthesis in the Solid State

L. R. MacGillivray · G. S. Papaefstathiou · T. Friščić · D. B. Varshney ·
T. D. Hamilton

Gels as Templates for Nanotubes

J. H. Jung · S. Shinkai

First Considerations: Principles, Classification, and History

Daryle H. Busch (✉)

University of Kansas, Department of Chemistry and Center for Environmentally Beneficial Catalysis, 1501 Wakarusa Drive, Bldg A, Lawrence Kansas 66047, USA
busch@ku.edu

1	Introduction	2
1.1	The Borromean Link	4
2	Elements that Compose Templates	6
3	Kinds of Templates	11
3.1	Metal Ion Anchored Templates	11
3.2	π - π Templates	12
3.3	Hydrogen Bond Anchored Templates	13
3.4	Hydrophobically Enhanced Templates	15
4	History	17
4.1	The Template Route to Macrocyclic Ligands	17
4.1.1	The Quest and Discovery	17
4.1.2	Concept Development and Missed Opportunities to Recognize Templates	21
4.2	The Template Route to Molecular Cage Ligands	22
4.2.1	The Quest and Discovery	22
4.2.2	Concept Development and Missed Opportunities	26
4.3	The Template Route to Catenanes	26
4.3.1	The Quest and Discovery	26
4.3.2	Concept Development and Missed Opportunities	35
4.4	The Template Route to Rotaxanes	35
4.4.1	The Quest and Discovery	35
4.4.2	Concept Development and Missed Opportunities	50
4.5	The Template Route to Knots	50
4.5.1	The Quest and Discovery	50
4.5.2	Concept Development and Missed Opportunities	57
5	Molecular Templates – a Limited Field with an Unlimited Future	58
	References	59

1**Introduction**

Despite a 40 year history, molecular templates continue to open new frontiers in chemistry. They greatly facilitated the availability, study, and exploitation of macrocyclic molecules and the many chemical developments associated with macrocyclic ligands and receptor chemistry. The use of molecular templates to optimize catanane and rotaxane formation (in their many small molecule, dendritic, and polymeric manifestations) and the yielding by templates of both simple and composite molecular knots has opened the universe constituted by the orderly entanglement of molecules of various topologies. Chemists stand at the border of that new land of great promise and toy with the simplest of examples while coveting the ultimate, for example, template-generated molecular scale computer elements or new kinds of materials such as 3-dimensional substances woven at the molecular level. As is typical of true frontiers of knowledge, each unique advance opens the way for myriads of other advances. One example of a new interlocked form of matter constitutes the creation of a new molecular species of unknown and, perhaps, unexpected properties. We now recognize the parallel nature of synthetic chemical templates (which we have called molecular templates) and DNA, the marvelous template of nature that implements genetic information and directs the construction of whole organisms, molecule by molecule. Remarkably, it has been shown that DNA can produce a most extensive and astounding list of topological motifs in its multitude of molecular entanglements [1]. Here we deal with the orderly molecular entanglements and interlocked structures that chemists have managed to make from small molecules.

Chemists and physicists have long been the pico- and nanoscientists, but popular literature and public fascination with extremes of all kind have made words like nanoscience and nanotechnology common language. The molecular scientists and the public equally expect new marvels from these realms, at least in molecular electronics and molecular machines. Chemical templates will provide guiding principles for many advances as these ambitions are realized. A clear point of application for molecular templates is the building of nanostructures in the direction proceeding from the smallest of atomic and molecular components to the nanoscale final product. The new fields of dynamic organic chemistry [2] and dynamic combinatorial chemistry [3] exemplify exciting chemical frontiers that have a less than universally recognized, but undeniable, relationship to molecular templates. In fact, the equilibrium molecular template described at a later point in this discussion is a very early recognized example making use of dynamic organic chemistry.

Along with the concept of complementarity, the principles of molecular templates provide the foundations for understanding the vast array of scenarios in which interactions occur between individual atomic or molecular entities, regardless of the complexity of the examples involved. In a templated process, molecular entities, or their components, actively organize complementary

entities, resulting in selected results that would be highly improbable in the absence of the templating interaction. A second feature of template processes is the common, but not essential, use of molecular/atomic entities as anchors that facilitate the selected result but which, post reaction, can be removed, leaving the highly improbable structure as a stable entity.

A simple example, the formation of a rotaxane, dramatizes the essential relationships (Fig. 1). A rotaxane is a molecularly interlocked molecule in which a relatively linear molecule occupies a threaded position through a cyclic molecule; bulky groups at both ends of the linear molecule prevent it from slipping out of the ring. Over 40 years ago, Frisch and Wasserman wrote about molecular topology and the formation of such simple interlocked structures as interlocked rings (catenanes) and knots in molecules [4]. As part of their investigations, they considered the probability that linear molecules might thread through appropriately sized cyclic molecules, as required for rotaxane or catenane formation (by certain mechanisms), and concluded that it would be a tiny fraction. Harrison and Harrison [5] performed elaborate experiments in which threadings were repeated some 70 times with a result indicating that the likelihood of threading linear molecules through molecular rings is something like 10^{-3} . Experimenters confront numbers of this magnitude with varied reactions ranging from “this is so improbable it doesn’t deserve attention” to “it happens; maybe we can make it happen more often – maybe much more often”. In fact, if the random result is unfavorable then it is appropriate to find ways

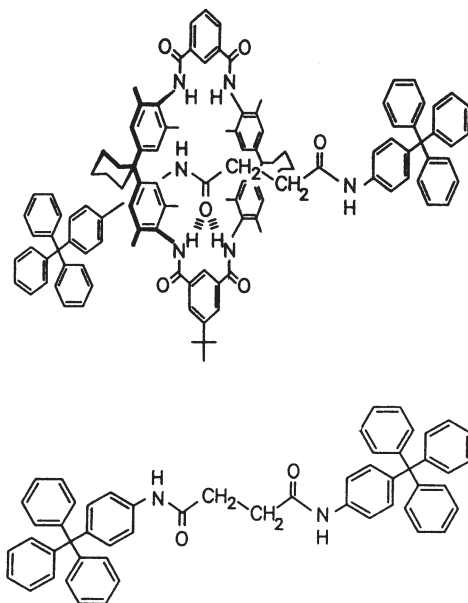


Fig. 1 Example of a rotaxane [140]. Reprinted with permission from Wiley-VCH. Copyright 1997

to exert control in order to create a favorable result, and that is what molecular templates do.

Many researchers have demonstrated the impact of templates on the yields of such threading reactions with strongly contrasting results. At the limit, one can anticipate quantitative formation of the pseudo-rotaxane, made possible by a template interaction between complementary linear and cyclic molecules. A pseudo-rotaxane involves the threading of the axle into the ring but without the blocking groups at the ends of the linear molecule. Removable anchors, employed to hold the parts together while rotaxanes are formed, have most commonly been protons, cationic metal ions (such as Cu^+ , Ru^{2+} , Zn^{2+} , or Fe^{2+}), or π - π stacking. It must be emphasized that many of the ultimate applications of designed orderly molecular entanglements, be they interlocked or the product of an open topology, require enormous numbers of identical repetitive events, e.g., the weaving of linear molecules, or the construction of a computer chip based on millions of molecular sites. Achieving these goals will require an essentially complete reaction at each step. Otherwise the cumulative error, or incompleteness, may produce a useless product.

Before becoming immersed in the total content of this subject let us enjoy the beauty, excitement, and immensity of what is probably the most elegant success, to date, of the synthetic molecular template.

1.1

The Borromean Link

Adopting, for the moment, one of many histories of this famous image – an ancient Italian family logo has attracted the attention of chemists interested in stereochemistry since the beginning of discussions on subjects that may be called chemical topology. The motif is usefully perceived as three oval rings, each in its own plane, which is orthogonal to the planes of the other two rings, and all three rings have a common center of gravity (Fig. 2). The rings are collectively inseparable, but once one ring is broken, the other two are liberated – an intriguing topological parody of a demanding social scenario. A nicely planned strategy by Siegel et al. provided the template synthesis of a motif that correctly positioned two of the three rings, linked by two templating ions [6]. Molecular turns of the octahedral Sauvage type (based on a Cu^+ anchor, vide infra) were used for one of the rings, while the other ring used a modification that focused the reactive centers away from its copper(I) anchor. The success of that work boded well for synthesis by these seekers of the first Borromean motif. However, history interceded. To quote Dr. Siegel from his review on chemical topology in *Science* [7] “Chichak et al. report on page 1308 that they combined the equilibrium-based methods of imine formation with the templation power of zinc ions to effect an elegant one-step total synthesis of a Borromean link from 18 precursors. Their strategy uses a set of endo- and exo-oriented ligands designed to form an oriented trigonal bipyramidal unit around zinc ions, six of which assemble into the Borromean link.” The X-ray

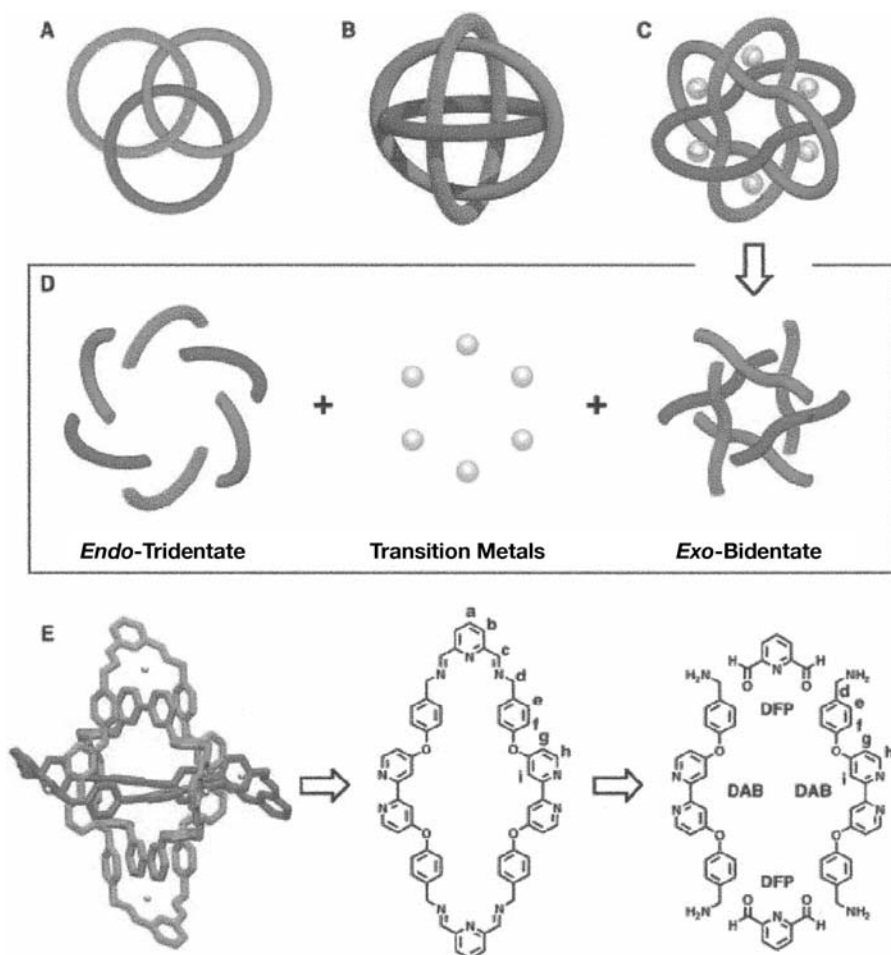


Fig. 2 Three representations of the Borromean link (Venn rings, orthogonal rings and template). Excerpted with permission from [8]. Copyright 2004 AAAS

structure determination confirmed the achievement of Stoddart and his colleagues [8].

The achievement was remarkable in a number of ways. It involved what is probably the most complicated template in the chemical literature, based on six zinc(II) ions and both convergent (or endo-directed) and divergent (or exo-directed) molecular turns (Fig. 2). In contrast to the overall complexity of the templating system, the reactants were relatively simple. The divergent component was a dipyriddy while the convergent component was an α,α' -diiminopyridyl unit formed by a thermodynamic, or equilibrium, templating process. Top of the outstanding characteristics of the template is the fact that it involves both kinetic and thermodynamic template components, a combination that should

become common. Both of these distinctive template types were used in their fully modern contexts. The combination is extremely powerful; the components of the kinetic template hold the subjugated components in place while the thermodynamic components find their final disposition at equilibrium. In the classic equilibrium template [9] the reactants form their normal distribution of products and the anchoring/selecting factor (often a metal ion) selects the product that binds best, combines with it and shifts the equilibrium accordingly. Only the authors know the extent to which alternative components were selected and rejected in failure, but their final choices contain still another special feature.

The choice of zinc as the template anchor provided a second opportunity for flexibility in the reacting system because zinc, being a spherical ion, is adaptable when it comes to coordination numbers and coordination geometries. So, this template system allowed the chemistry to determine critical features both in the Schiff base reaction steps and in the basic stereochemistry of the metal ion anchor. Further, the yield in this scientific triumph was 90%. The success over the enormous challenge of synthesizing the molecular embodiment of the Borromean link suggests that the science of using the molecular template has reached a level of maturity from which scientists may be expected to produce new molecular entanglements and interlocked structures of profound significance, despite the equally profound challenges they represent.

2 Elements that Compose Templates

The history of templates is most readily appreciated with an understanding of the most basic underlying relationships. These elements make molecular templates very special and, from the standpoint of controlling matter, extremely powerful. After having worked with templates, off and on, for close to 40 years, the author offered a definition for a molecular template [10] “a chemical template organizes an assembly of atoms, with respect to one or more geometric loci, in order to achieve a particular linking of atoms.” That simple statement does capture the essence of a molecular template, but it fails to consider the complexity of a templating process. Missing are several levels of complexity, including:

1. The general kind of template, whether it is a kinetic or equilibrium template
2. The essential elements that must be present in a template and how they depend on the specific purpose of the template
3. The centricity of the template, i.e., whether it involves a single center or two or more such centers, and whether those centers are independent or cooperative
4. Complementarity

From the time when they were first reported and given their universally accepted name, it has been clear that there are two kinds of molecular templates:

Kinetic templates. The template affects the sequence of events that determine the structural changes during the course of the reacting process [9b, 11].

Equilibrium (or thermodynamic) templates. The reaction between organic components produces a variety of products but one, or more, of those products is/are sequestered in the course of the template process, shifting the equilibrium in favor of that product(s) [9a, 12].

The kinetic and equilibrium template processes are illustrated in Figs. 3 and 4. The most common molecular templates control processes that create topological or other related effects: ring closure, cage formation, catenane (interlocking rings) formation, tying of molecular knots, creating the Borromean link. Consequences dependent on size relationships are also significant in the case of real molecules, as in rotaxane formation and entrapping of ions or molecules in

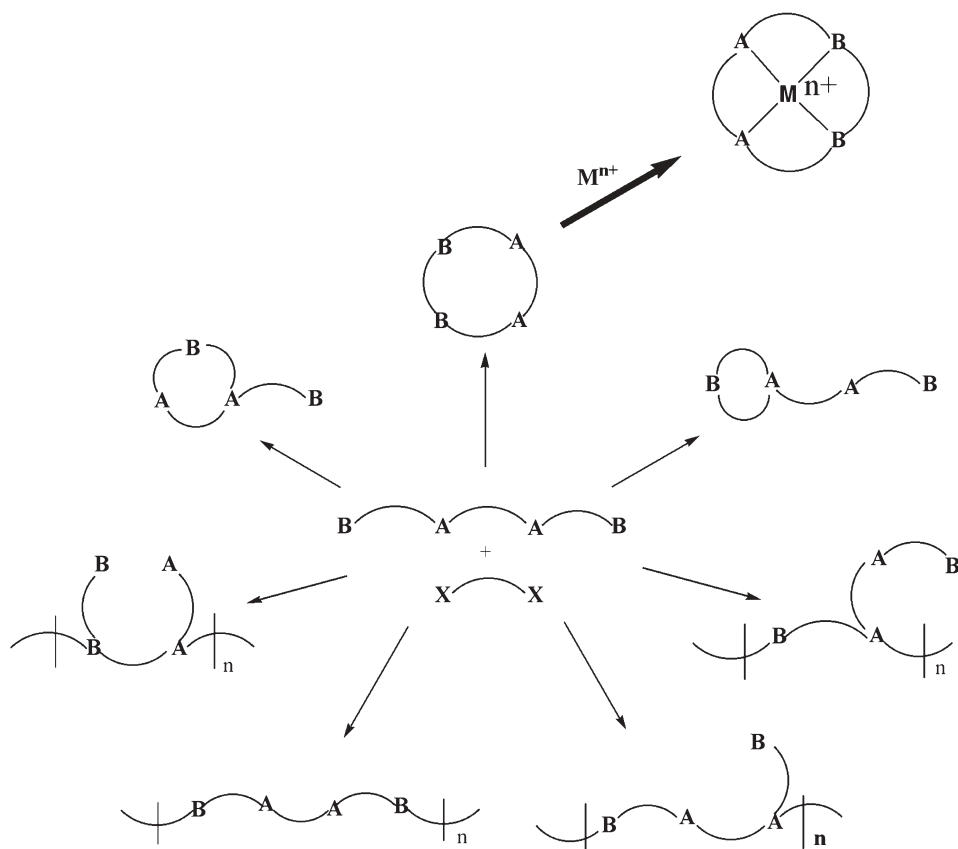


Fig. 3 Equilibrium molecular template. At equilibrium the organic reactants form multiple products. A metal ion binds to a single product and sequesters that product. The equilibrium shifts to generate more of that product

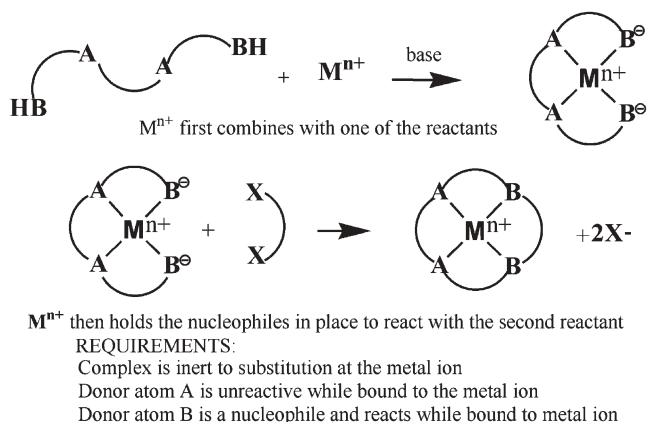


Fig. 4 Kinetic molecular template. A 2-site template adds one edge to tetradentate macrocycle

cage structures, but these constraints are not topological in nature. To facilitate separation of the product selected by the templating process, the Sanders group has made good use of immobilized axle molecules that select complementary rings from a variety of reversibly formed products [13]. Fig. 5 illustrates the simple elements of templates and a few of the associated motifs. The black dots represent anchors, about which the template organizes the assembly of atoms. The anchors can be any atom, ion, or group of atoms that reversibly links to the entities that are to be joined together in the templating process, but most often they are metal ions, protons (often multiple), the stacking of aromatic rings having complementary acid-base properties, anions, or some combination of these interactive entities. In certain cases the anchor may be virtual, as in the case of attractive forces between chemical groups that are to be united in the templating process, e.g., the Stoddart template, *vide infra*. The curved lines near the black dots are “molecular turns” and examples of molecular structures that have served as molecular turns are given in Fig. 6. In the left side of Fig. 5a, two turns are organized orthogonally about a single anchor. Proceeding from this point, the addition of one link that joins the ends of a single turn would create a ring with an axle molecule penetrating through it. This is a pseudo-rotaxane. It is pseudo because the axle could, probably would, slip away if the anchor were removed, and an essential element of most template processes is that the anchor is removed after the links are added. If blocking groups are added to the ends of the axle molecule in the pseudo-rotaxane before the anchor is removed, then the product is a true [2]rotaxane and its permanence is assured if the blocking groups are too big to slip through the ring that has been formed about the axle and the anchor. The [2] means that two separate molecules are trapped in this molecularly interlocked structure. Fig. 5b represents the reaction of a fused pair of molecular turns with a complementary fused linker, producing a cage.

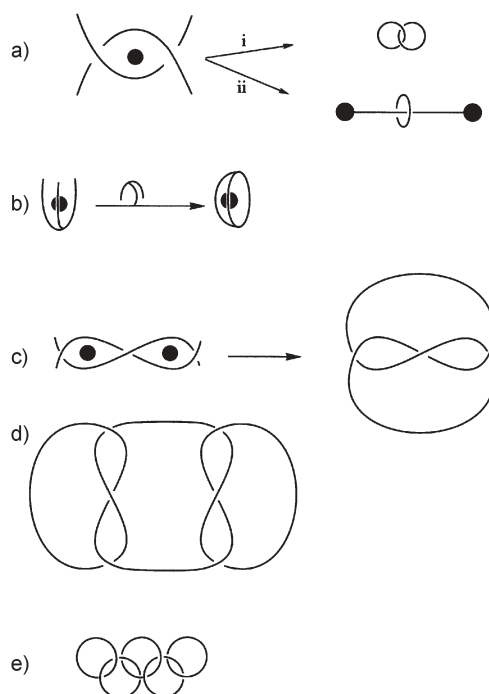


Fig. 5 Elements of a molecular template. **a** Cross-over composed of two convergent molecular turns (*curved lines*) and a metal ion (*black circle*). Adding one link produces a rotaxane; adding two links completes a catenane. **b** Two fused turns bound to a metal ion anchor that combines with a fused link to form a cage. **c** Two pairs of correlated turns wrapped about two anchors that add two links create a trefoil knot. **d** Composite knot formed by two linked pairs of 2-center templates, making a total of four anchors, eight turns, and 4 cross-overs in the composite template [164]. Reproduced with permission from Elsevier

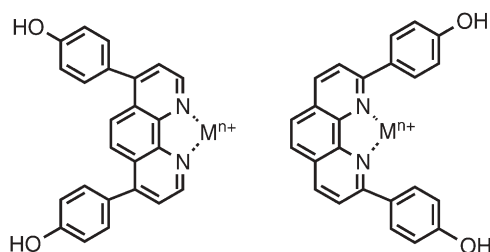


Fig. 6 Convergent and divergent molecular turns for use in metal ion anchored templates. **a** Convergent turn of the Sauvage type. **b** Similar divergent [165]

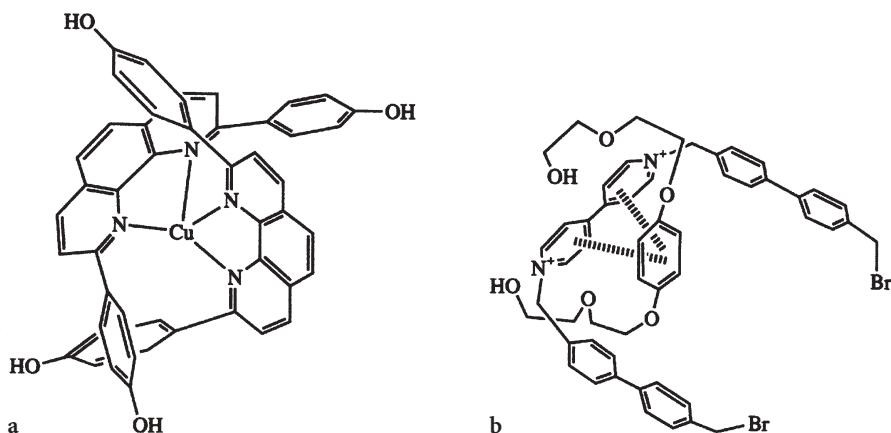


Fig. 7 Cross-overs used in **a** the Sauvage template and **b** the Stoddart template. Dietrich and Sauvage used a Cu^+ as the anchor in their template. π - π stacking replaces the atom or molecule in the Stoddart template [166]

Figure 5c shows two anchors combined with two pairs of linked turns and the linked turns are not independent of each other. They are constrained to be the inverses of each other (one up and one down). If linkages are made as indicated in the figure, a molecular knot has been tied. If instead, links had been made between the ends closest to each other on the right and left sides of the picture, respectively, then the product would have been a single large ring. Figure 5d shows a 4-anchor template in which two pairs of constrained curves are independently linked into a single large loop. The completed product of the template is shown and it represents a square knot – a composite knot [14]. Figure 5e simply shows the chain of five interlocked rings dubbed olympiadane.

Figure 6 illustrates two very different kinds of turns, the convergent molecular turn on the right and the divergent molecular turn on the left. The convergent turn was used in all of the examples described above except the rotaxane, in which either turn could be used for the curve that is not linked, i.e., the axle molecule. The divergent, or exo-directed, turn was an essential element in the closing of the Borromean link and in the related publication cited above. Two very important cross-overs are illustrated in Fig. 7, that of the ground-breaking Cu^+ anchored template of Dietrich-Buchecker and Sauvage [15] and the extremely productive π - π template of Stoddart [16]. As shown, the π - π template has, in effect, a virtual anchor. The attraction between the electron-poor paraquat dication and the electron-rich dioxypyphenylene group dominates the interactions between the molecules being subjected to a template-directed reaction.

3

Kinds of Templates

When viewing all kinds of molecular architectures, templates are most often classified in terms of the anchors that dominate the key attractions facilitating their functions. The expertise of the researchers is sometimes reflected in the nature of the template anchor. On that basis the list of kinds of templates includes metal ion anchor, molecule anchor, hydrogen bond anchor, π - π anchor, and hydrophobic anchor. Each of these is briefly illustrated below. In the historical sections that follow, the efficacies of the templates are more clearly displayed.

3.1

Metal Ion Anchored Templates

Fig. 7a shows the essential elements of a very simple metal ion anchored template. The pair of turns cross the tetrahedral copper(I) ion, anchor orthogonally, and provide direct routes to pseudo-rotaxanes and catenanes, depending on whether one or two links are added to close macrocycles about the Cu^+ ion. The relationship between the molecular turns and the metal ion anchor is very important. The tetrahedral ion creates an orthogonal cross-over when the ligating turns are didentate, i.e., each uses two of the four coordination sites on the tetrahedral ion. As described below, this template dominated the pioneering contributions to catenane, rotaxane, and knotane synthesis using metal ion anchored templates. However, closely parallel templating relationships can be achieved using octahedral metal ions, such as iron(II) [17] or ruthenium(II) [18], as anchors and properly derivatized tridentate ligands as molecular turns. This is illustrated for ruthenium in Fig. 8. As indicated in the discussion of the Borromean link above, zinc(II) ion has also been used and may have been

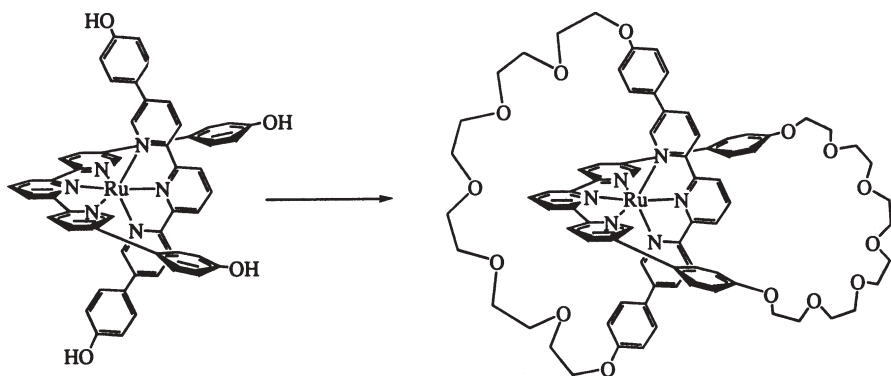


Fig. 8 Octahedral anchor for template synthesis of catenanes and rotaxanes [166]. Reproduced with permission from Elsevier

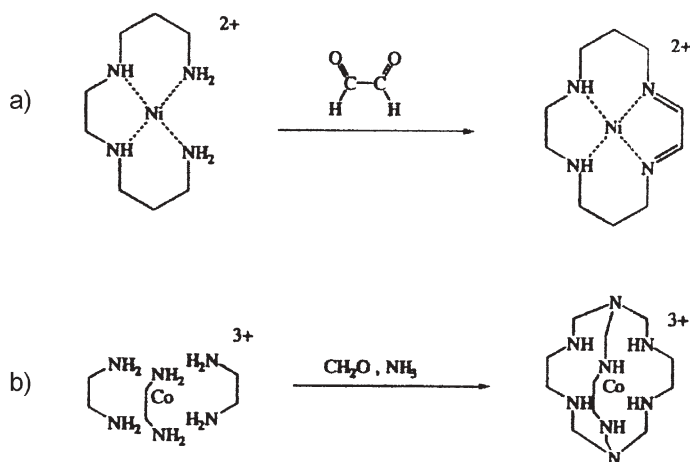


Fig. 9 Templates for macrocycle and cage ligand synthesis [166]. Reproduced with permission from Elsevier

effective because of its ability to accommodate to the needed coordination number and coordination geometry (*vide supra*). Building on reports by Schröder et al. [19] and Busch et al. [20], Leigh and associates have produced catenanes using a template based on a tridentate Schiff base ligand [21]. These studies make octahedral anchors and tridentate turns easy synthetic targets.

The earliest template targets were not interlocked molecules but macrocyclic and completely encapsulating ligands. These goals were achieved by use of different versions of the metal ion anchored template. For macrocycles, planar ions are very widely employed, as shown in Fig. 9a for the formation of the critical intermediate in Barefield's synthesis of the key macrocycle called cyclam (1,4,8,11-tetraazacyclotetradecane) [22]. In principle, the cage formation shown in Fig. 9b uses a fused linker binding to a fused set of three turns, but in this case, the linker is assembled *in situ* [23].

3.2

π - π Templates

The so-called π - π template has been enormously successful in the synthesis of interlocked structures and devices based on their architectures. This contrasting kind of template might well be viewed as building on a virtual anchor or anchors. The obvious and persistent interaction is between aromatic rings that become permanent members of the structure. The π - π template is perhaps best illustrated with an example that is typical of the general concept of anchor-based templates, but is atypical of the most elegant work using these templates. In this novel example, a phenanthrene molecule serves as the anchor. Through π - π stacking the anchor attracts two electron-poor paraquat moieties to it,

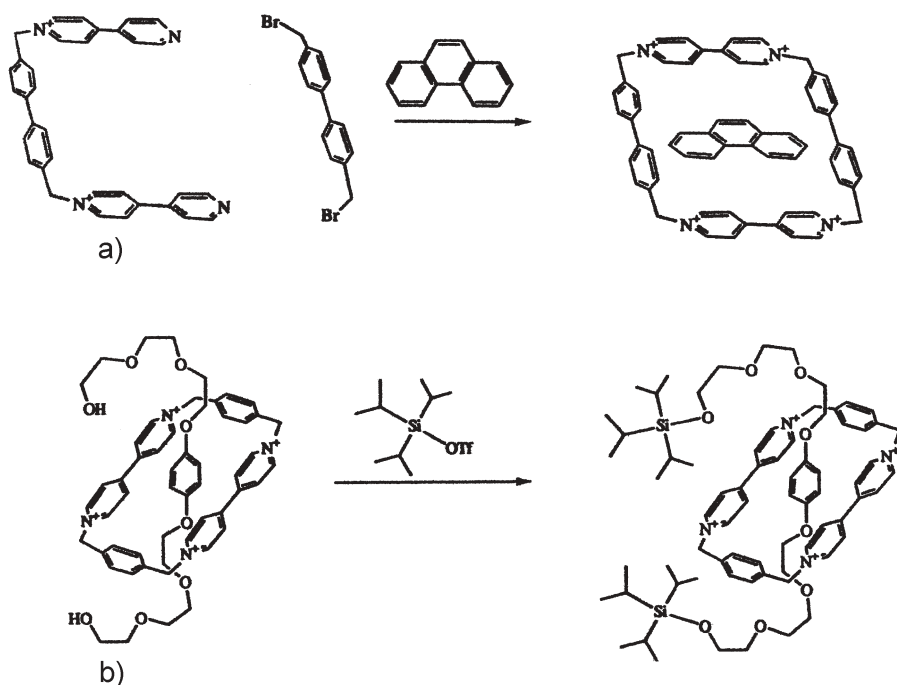


Fig. 10 π - π template. **a** Atypical example that shows the relationships well. **b** Typical example of the template at work [166]. Reproduced with permission from Elsevier

creating a molecular turn which is closed into a ring by reaction with a suitable linking agent (Fig. 10a) [24]. A more representative example of the template is shown in Fig. 10b, where the electron-rich part of the axle molecule is attracted to the electron-poor part of the macrocycle, leading to pseudo-rotaxane formation. Blocking of the free end of the axle molecule locks it in place completing the template synthesis of the rotaxane, assuring that the anchor cannot be removed [25]. It has been shown that the π - π stacking in these templates is reinforced by hydrogen bonding between α -hydrogens on the bipyridinium groups and the oxygen atoms of the partnered structural unit.

3.3

Hydrogen Bond Anchored Templates

Two specific families of templates of this kind are most prominent in the literature on this most versatile and subtle of templates. The simpler of these makes use of secondary ammonium cations as sources of the positively charged hydrogen atom donors and, most commonly, the oxygen atoms of crown ethers as the electron pair donors in the hydrogen bond formation. Because of the nature of the H-bonding atoms, the template is limited in complexity. Even in this case,

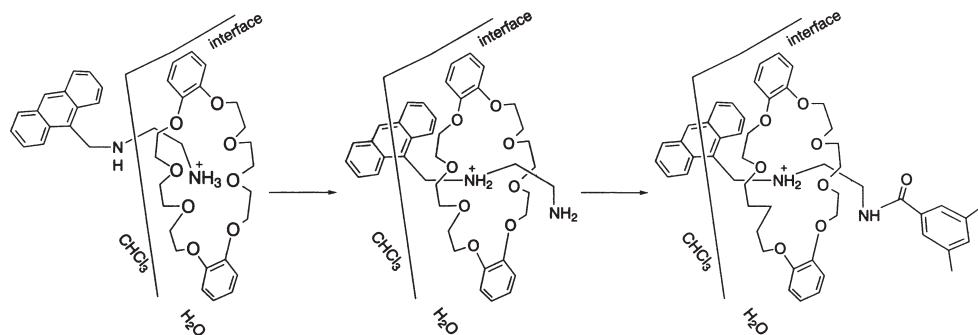


Fig. 11 Scheme that produced the first secondary ammonium ion/crown ether rotaxane [26]. Reproduced by permission of The Royal Society of Chemistry

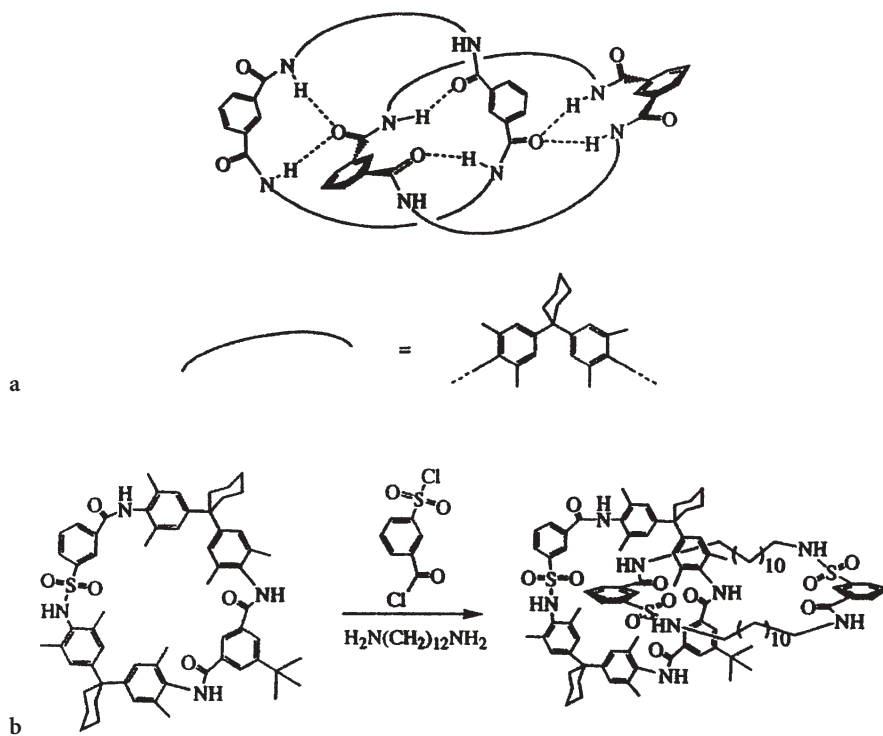


Fig. 12 HVL hydrogen-bonding template. **a** Hydrogen bonding pattern in first product of the template. **b** Illustration of the versatility of the template [166]. Reproduced with permission from Elsevier

the anchoring process may involve complicated multi-atom interactions, hence the increased subtlety of these systems. The scheme that produced the first crown ether/secondary ammonium ion rotaxane is shown in Fig. 11 [26].

An amide based template is equally important and applicable in rather different ways. Here we identify this template family as the HVL template in recognition of three important contributors to its development and application, Drs. Hunter, Vögtle, and Leigh. The HVL template capitalizes on the class of interactions that controls much of the conformational chemistry of proteins and DNA, hydrogen bonding arising from the amide function. Principle groups are secondary amides appropriately placed, often as 1,3-diacyl derivatives of benzene. In fact, the chemistry usually begins with a diamine and a diacyl chloride. An early example of the hydrogen bonding is shown in Fig. 12a [27], and the versatility of the template is partially displayed in Fig. 12b [28]. Recognizing the generality of the templating effectiveness of pairs of transoid amide hydrogen bonding sites, and the similarity of adjacent amino acid groups in peptide chains, Leigh and associates used stoppered glycylglycine as a templating axle molecule to prepare a [2]rotaxane via a clipping process (*vide infra*) [29].

3.4

Hydrophobically Enhanced Templates

The hydrophobic interiors of the cyclodextrins (cyclic oligomers of (α -1–4) linked D-glucose, containing 6, 7, or 8 units) have been used in pioneering and in very recent research to produce impressive results [30]. To act as templates, the cyclodextrins (CDs) usually bind linear components of organic molecules inside their hydrophobic cavities, and the attraction can be large. This selectivity for hydrophobic moieties supports the attribution to hydrophobic effects. In aqueous solution, putting the hydrophobic group into the cavity replaces the interaction of the apolar organic moiety with the polar solvent by interactions between the relatively low polarity organic guest and host. This is accompanied by release of water from the cavity, with a parallel consequence. Because of the presence of hydroxyl groups and ether oxygens at the peripheries of the cone-shaped host, hydrogen bonding is also possible. The complexity of the interactions is great [30a]. In the sense that one does not focus on specific atom–atom interactions, the templating process is very general; many types of guest/host complexes can be formed. Almost any molecule having a multi-methylene chain or an aromatic ring is a potential guest, and a candidate for the anchor site in a turn that may be used in a template. Early studies on interlocked molecules produced rotaxanes with cobalt(III) complexes as blocking groups (Fig. 13) [31].

Cucurbituril [32] has emerged in recent years as a comparable host molecule of similar yet different properties than those of cyclodextrins. Cucurbituril is a macrocycle that self-assembles through condensation of glycouril with formaldehyde. Its cavity resembles that of α -cyclodextrin in size, but the cucurbituril is symmetrical and often represented as a cylinder, whereas cy-

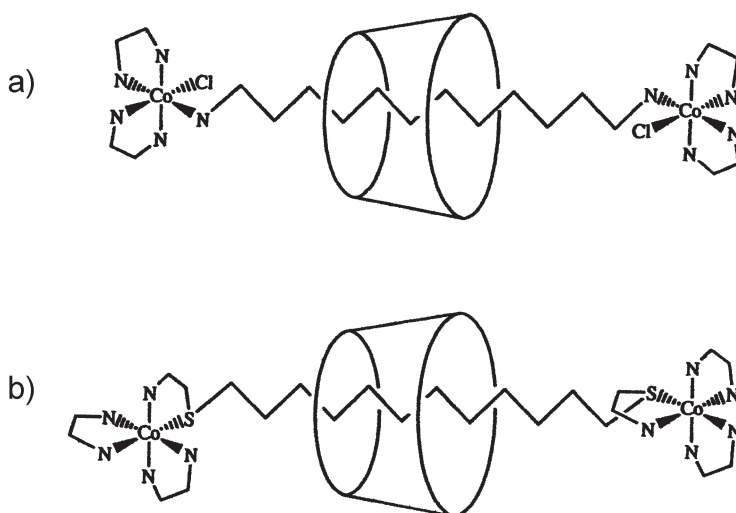


Fig. 13 Early [2]rotaxanes based on cyclodextrins and using metal complexes as blockers [166]. Reproduced with permission from Elsevier

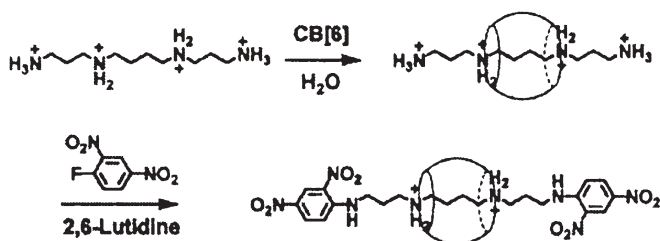


Fig. 14 Examples of simple rotaxanes using cucurbituril as the ring and tetramine axles [32]. Reproduced by permission of The Royal Society of Chemistry

clodextrins are represented as segments of cones. Like CDs, cucurbituril has a large (diameter ~ 5.7 Å) hydrophobic cavity, and its entries are both lined with polar groups capable of potent hydrogen bonding interactions. Early studies of pseudo-rotaxane formation (i.e., threading axles into the ring) showed a high selectivity in the case of α , ω -diammonium cations having varying polymethylene chain lengths, $^+\text{NH}_3(\text{CH}_2)_n\text{NH}_3^+$. Formation constants increased from 2.5 M^{-1} at $n=3$ to $8,600 \text{ M}^{-1}$ at $n=6$; the number then decreased to 1.5 M^{-1} at $n=9$ [33]. With the assumption that the ammonium ions hydrogen-bond to the peripheral carbonyls of the cucurbituril, the hexamethylene chain leads to good complementarity between host and guest. The formation of interlocked molecules has made effective use of the anchoring properties of this fascinating molecule. A simple rotaxane is shown in Fig. 14.

4

History

Each topological motif that has characterized the progress of template chemistry has its own distinctive history: macrocycles, cage compounds, catenanes, rotaxanes, knots, and the Borromean link. In all cases it is likely that the possibilities were discussed sometime before the concept was replaced by experimental reality. Further, in retrospect, others may have produced a template product or products of a given motif without realizing its structure. In contrast to the architectural motifs of chemistry, it is not clear that the concept of a molecular template was so broadly discussed, possibly because interest in the methodology (directed versus statistical reaction pathway) has always been secondary to the object itself (macrocycles, catenanes, knots, etc.).

4.1

The Template Route to Macrocyclic Ligands

4.1.1

The Quest and Discovery

There is perhaps a small place in history for recording the process that first established this or that concept of vast generality. Over time, templates have given rise to an enormous array of elegant molecular architectures that would be very difficult to produce in the absence of templating interactions. However, the concept of a molecular template was first demonstrated and put to extensive use in the quest for broad families of the simplest of such motifs, macrocyclic ligands for metal ions. In the early 1950s, the author became fascinated with the notion that the collection of linear and branched di-, tri-, tetra-, and even higher polyamines (such as ethylenediamine, diethylenetriamine, triethylenetetramine), which seemed to reflect the inventory of polyamine ligands, did not contain a cyclic structure. Nature provides cyclic ligands (e.g., porphyrins) and industry had produced cyclic ligands as pigments (phthalocyanines) but the common amines, thioethers, phosphines, and ethers did not include large polyfunctional rings.

In the simplest image, such a macrocyclic ligand structure would encircle a metal ion within the same plane as the metal ion. Molecular models suggested that such rings might contain 12–16 members and coordination chemistry preferred four or five, more or less evenly spaced, ligating atoms. At that point in time, the early 1950s, these macrocycles were viewed as difficult to synthesize because of their specific ring sizes and because polyfunctionality was involved.

Kekule's hoop-snake vision of the structure of benzene plays a role here. Every chemistry student has heard the story and it resides in our memories. The snake would be better positioned to grab its tail if it were held in the shape of a hoop by evenly spaced spokes that link it to a central point, more like a wheel than a hoop. Therefore, if a ligand molecule having four ligating atoms were able to react with itself, ring closure might be greatly favored by letting

the molecule wrap itself around a metal ion (Fig. 15a). Just considering square planar coordination structures, it immediately follows that there is a large array of possible ways to develop this general idea. The reaction could be bimolecular with the tetradentate ligand serving as a difunctional molecule, say a nucleophile, and adding the fourth edge to the “square” by reacting with a difunctional electrophile (Fig. 15b). Indeed this was the model used in the seminal example of a planned kinetic template synthesis (Fig. 16a) [9, 11, 34]. If such a ring closure could be accomplished by adding the fourth edge to a macrocycle, then it should be equally possible to add two such edges to a bis(didentate) complex involving a planar metal ion (Fig. 15c). Serendipity provided

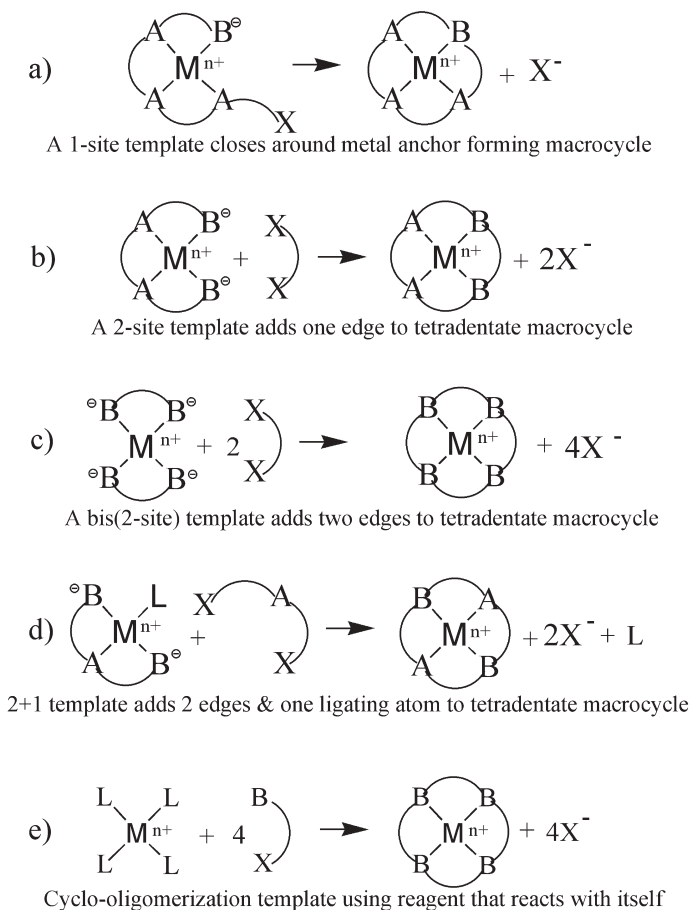
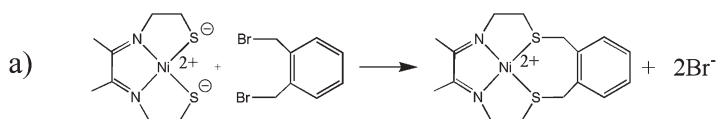


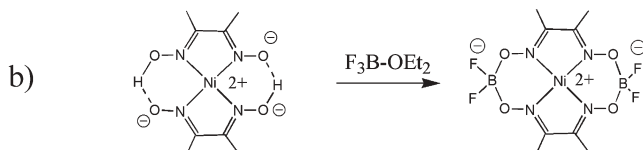
Fig. 15 First campaign in the realm of template synthesis: template pathways to planar tetradentate macrocycles. **a** One-bond pathway closes a single side of the square. **b** Two-bond pathway adds an edge to one side of the square. **c** Four-bond pathway adds two edges to the square. **d** Three-bond pathway adds two edges and a donor atom to the square. **e** Cyclo-oligomerization adds all donors and edges to the square

two examples of the same reaction early on in the history of template chemistry (Fig. 16b) [35]. Given those cases, obviously it should be possible to start with a tridentate ligand and simultaneously add the fourth ligating atom and close the ring along two edges (Fig. 15d). Examples of this reaction also emerged early in the history of molecular templates and macrocyclic ligand chemistry (Fig. 16c) [36]. Finally, with well chosen self-reacting bifunctional molecules it should be possible to produce cyclo-oligomers (Fig. 15e), and these also appeared very early in template and macrocycle chemistry (Fig. 16d) [37]. During the years 1962–1964, these templating pathways were used to make new families of macrocyclic ligands, mostly by the Busch group.

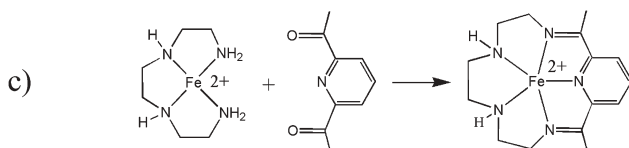
Of course this is only the beginning of the abundance of templating relationships, and one can follow similar expansions of capabilities beginning with other templates. A marvelous example is the analysis and exploitation of



A 2-site template was among 4 early pathways to the (then) new macrocycles
Thompson MC, Busch DH, (1962) Chem Eng News(Sept. 17 1962):57



Bis(2-site) template introduced from two labs with similar products
Schrauzer GN, (1962) Ber 95:1438; Umland F, Thierig D (1962) Angew Chem 74:388



A 2+1 template produces pentadentate (and sexadentate) macrocycle(s)
Curry JD, Busch DH, (1964) J Am Chem Soc 86:592

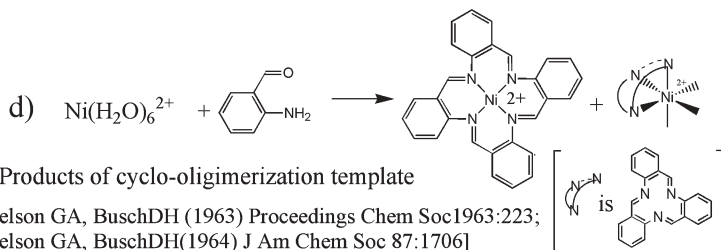


Fig. 16 Early examples of template formation of macrocyclic complexes: **a** Two-bond pathway, **b** Four-bond pathway, **c** Three-bond pathway, and **d** cyclo-oligomerization

increasing numbers of linearly connected orthogonal-orienting templating centers, a small part of which is shown in Fig. 17.

The story only starts here. Research leading to the first products developed by way of molecular templates and the synthesis of broad areas of macrocyclic ligands gained the support of the U.S. National Institutes of Health in 1959. Early studies were dedicated to the design of kinetic templates. Since metal ions served as the anchors for the templates, attention focused on the organic chemical reactions that ligands can undergo while bound to metal ions. This added to the impetus for growth of the field that has been labeled “ligand reactions”. Early research dedicated to making the template concept work focused on reactions in which the ligating atoms could serve as nucleophiles, such as coordinated mercaptide ions, amides of the type NH_2^- , RNH^- , $\text{RR}'\text{N}^-$, and alkoxide ions [38]. By-products of these investigations ranged from new ligands containing nitrogen and/or sulfur donors and their mono-, di-, and trimeric transition metal complexes [39], to improved understanding of the reactions in which electro-

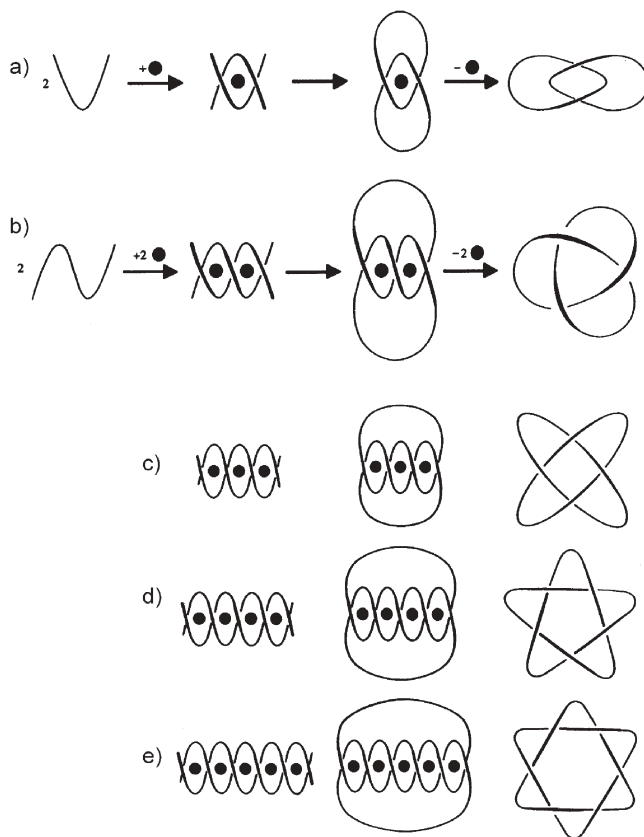


Fig. 17 Template patterns and molecular architecture resulting from one- to five-anchor molecular templates [75]. Reproduced with permission from Elsevier

philic centers add to coordinated mercaptide and oxime functions [40]. These studies led directly to the first recognized examples of both kinetic and equilibrium template reactions (Fig. 16). Attention also focused on reactions that might proceed by attack on the atom α to the ligating atom, including nucleophiles like the oxygen atom of a kappa-1, nitrogen-bound oxime function (Fig. 16b) or the NH_2 group of a coordinated hydrazone or hydrazide function. Investigations also included aldehydes and ketones, whose carbonyl carbon atoms would be expected to increase in electrophilic character upon coordination of the oxygen atom to a metal ion. The latter may be involved in numerous templated Schiff base, and related, reactions, e.g., Figs. 16c and 16d.

As often is true in science, after the first few macrocyclic ligands were synthesized using the metal ion anchored template effect, the successful synthesis of macrocyclic ligands became commonplace. What once appeared to be difficult became more or less easy. Early on, template methods were so well recognized as the major source of macrocycles that it was appropriate to emphasize examples where no template was involved [41]. Notable special applications of templates continue in macrocycle chemistry. The use as a template of the glyoxal-derived bis(aminal) moiety, as devised by Weisman [42], has been described as a powerful route to C-functionalized tetraazamacrocycles [43]. It is interesting that certain hydrogen bonding templates are so effective at catenane formation that special measures are required to produce the simple macrocycles [44], including formation of the rotaxane as a step along the way [45]. Reviews and monographs provide ready insight into that pioneering work [46].

4.1.2

Concept Development and Missed Opportunities to Recognize Templates

Prior to the developments summarized here, it is apparent that chemists had not sought to add the general molecular motif of macrocyclic ligands to the array of structures of the common polydentate ligands containing the usual nitrogen, oxygen, sulfur, and phosphorus donor atoms. On the other hand, in retrospect, there can be no doubt that metal ions help in the synthesis of unnatural porphyrins and phthalocyanines, perhaps by exerting template effects. Also, the first explorations of the oligomeric complexes of *o*-aminobenzaldehyde almost certainly produced mixtures of the complexes of trimeric and tetrameric macrocycles derived from that monomer, but the ligands in those complexes were not characterized as macrocycles in those early studies. Most deserving of comment, Posner [47] had produced a macrocyclic complex of zinc in 1898, but the structure was not known until proven by Melson and Busch in 1964 [37]. Similarly, it has been pointed out that Reppe's cyclotetramerization of ethyne may have proceeded through a templating process, providing another example of a template-directed macrocyclization reaction and this one may have been observed in 1948 [48]; however, that is speculation. The discovery [49] that acetone solutions of tris(ethylenediamine)nickel(II) form macrocycles derived from two molecules of ethylenediamine and four molecules of acetone may

involve templated condensation, but it has been shown that the macrocyclic ligand forms in the absence of the metal ion. [41c]. Consequently, if there is a template effect it probably is of the equilibrium type. Further, this outstanding contribution to macrocyclic chemistry, like many important discoveries, was serendipitous and reflected a gift for recognizing the fully unexpected, rather than achieving the goal of a professional mission. The development by Pedersen of the crown ethers, the crown jewel of macrocyclic chemistry, was an outstanding achievement of organic synthesis. Later, in demonstrating an improved synthesis Greene deduced the involvement of a metal ion template in the preferred procedure [50]. Additional examples of what might have been recognized as templated macrocycles have been cited in other reviews [51].

4.2

The Template Route to Molecular Cage Ligands

4.2.1

The Quest and Discovery

Ligands shaped as cages were first suggested in 1963 [52] and elaborated on in 1965 [53]. Boston and Rose [54] published the first example 4 years later. This outstanding research used a 3-dimensional template in which tris(dimethylglyoximate)iron(II), and the corresponding cobalt(III) complex, reacted with $\text{Et}_2\text{O} \cdot \text{BF}_3$ to produce a cage in which two BF_2^{+} units linked all three dimethylglyoximate units that occupy each of two opposite faces of the coordination octahedron of the iron(II) or cobalt(III) complex (Fig. 18). The second example

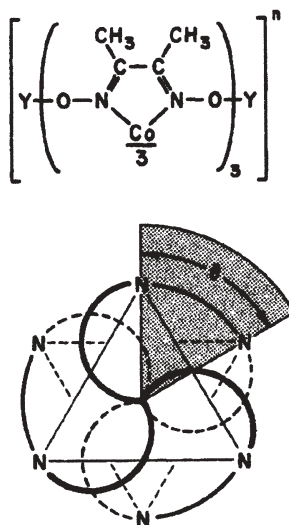


Fig. 18 First cage complex – dubbed a clathro-chelate. Reprinted with permission from [167]. Copyright 1973, American Chemical Society

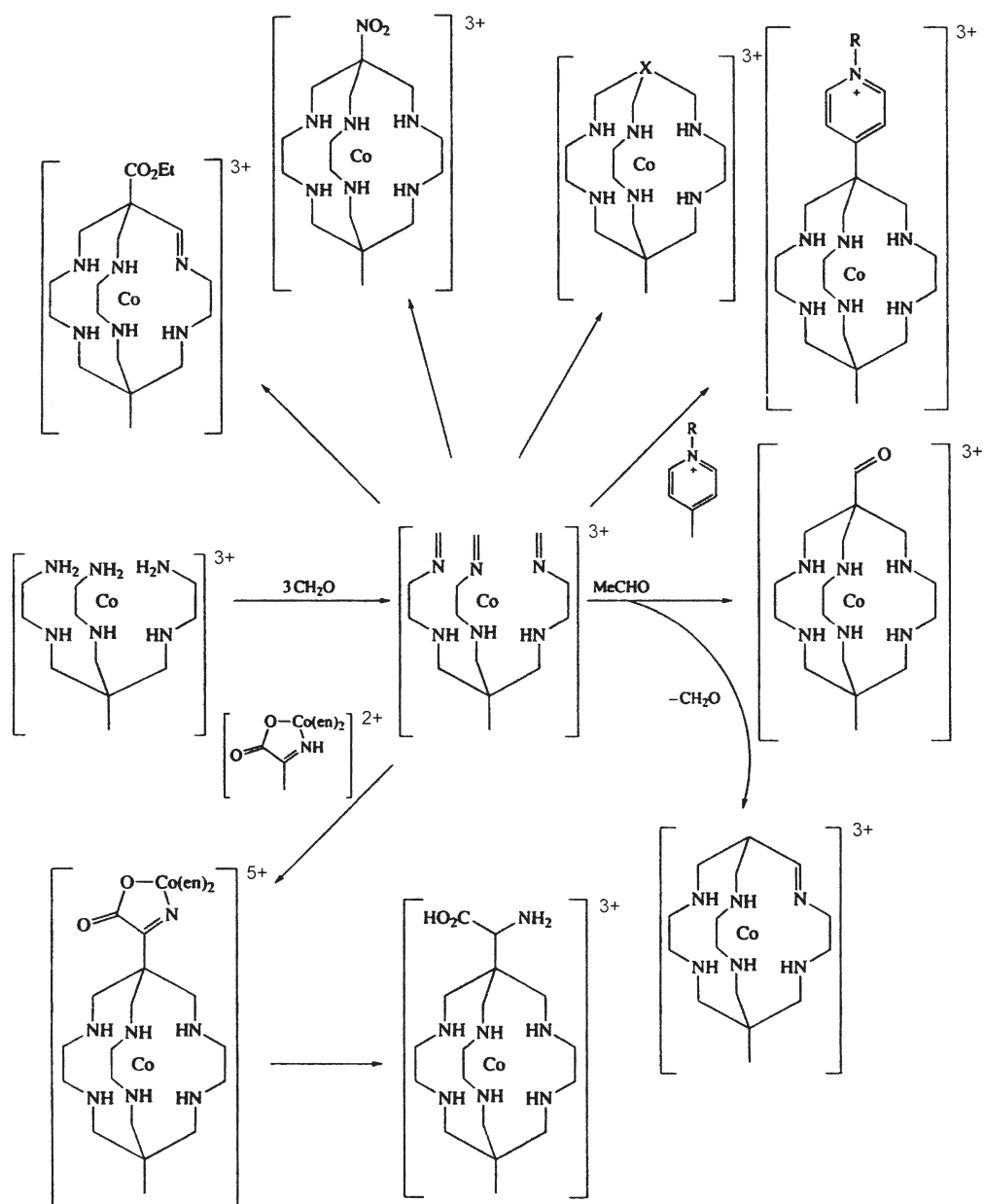


Fig. 19 Polyamine octahedral cages of Sargeson et al. [51] p 5. Reproduced with permission from Elsevier

appeared a few years later when a hexadentate tripodal ligand, tris(aldoximo-6-pyridyl)phosphine was closed around the metal ion with the same structural moiety (BF^{2+}) [55]. In these cases, the templating reaction occurs at the oxygen atoms α to the donor atoms of the ligands that are held in place by the metal ion. More recently many variations of these structures have been achieved using different aromatic and aliphatic dioximes and, for closing groups, boric acid, other boron halides, organoboron compounds, tin(IV) halides, and silicon derivatives [56]. The chemistry of this templating motif was extended to saturated polyamine ligands by Sargeson and his collaborators, who prepared aliphatic polyamine cages that have been labeled sepulchrates. The reaction of tris(ethylenediamine)cobalt(III) with formaldehyde and ammonia produces the cage complex shown in Fig. 19 in 74% yield in a single step [57]. Since these template reactions work best for substitution-inert metal ions, cobalt(III), chromium(III), rhodium(III), and platinum(IV) have been used [58]. The rearrangement to form cages of certain of the bridged, planar tetradentate ligands known as cyclidenes is testimony to the stabilities of cage complexes (Fig. 20) [59]. Recent development of extended tris-bipyridyl molecular cages provides a new and versatile family of metal ion cages [60]. In their development of models for the siderophores of nature, Raymond and associates prepared outstanding cage ligands, using an unusual kind of template (Fig. 21) [61]. The new cage ligands were designed specifically for binding iron(III), and the presence of the iron(III) ion as a templating anchor increases the yield of cage from 3.5% to 40%. As Fig. 21 shows, this is an unusual template. The reactive sites are quite remote from the anchoring metal ion. However, the metal ion locks the precursor complex into a structure that orients the remote reactive sites suitably for formation of the desired product. The square planar cyclidene complexes also template their reactive sites in remote locations suitable for ring closure because of the conformation locked in by complexing to a

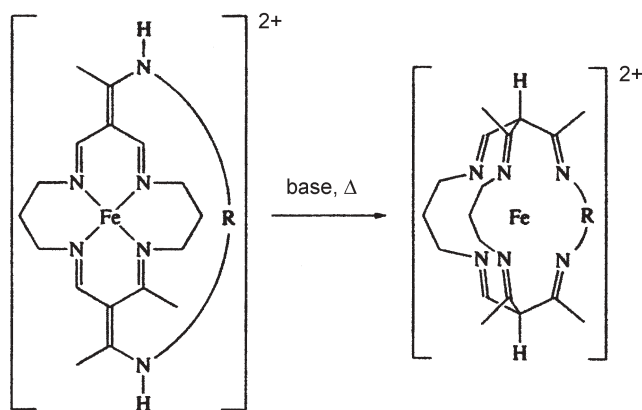


Fig. 20 Cage by rearrangement of a bridged macrocycle. [51] p 1. Reproduced with permission from Elsevier

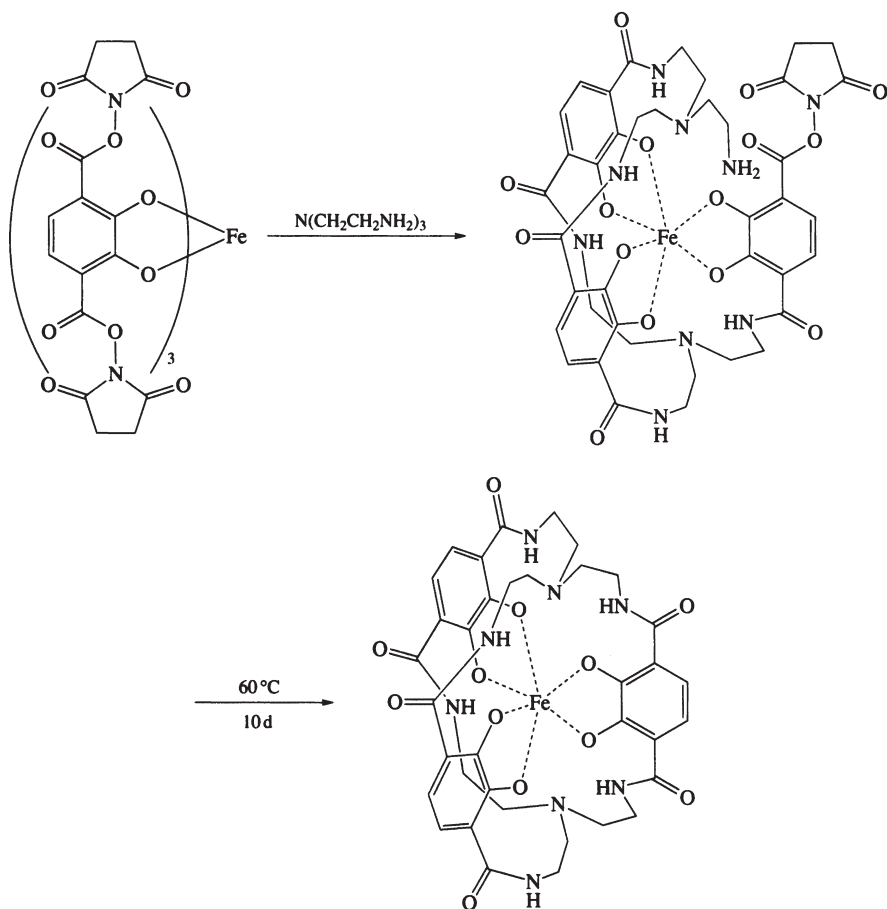


Fig. 21 Ligand cage designed after nature's siderophores. [51] p 8, Scheme 1. Reprinted with permission. Copyright 1991, American Chemical Society

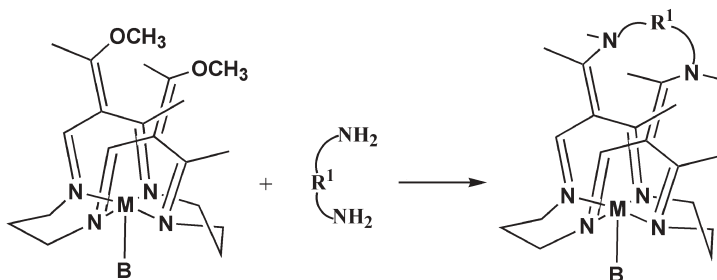


Fig. 22 Cyclidene ligands template formed molecules with a cavity for binding of a substrate, i.e., O_2 or an organic molecule, depending on the size of the cavity

metal ion, in this case nickel(II) [62]. The added group acts as a roof over a cavity within which special groups may be brought into close contact with the metal ion. Examples are the binding of the O_2 molecule (in the case of small cavities) or serving as a hydrophobic receptor for erstwhile substrates (in the case of large cavities) (Fig. 22).

4.2.2

Concept Development and Missed Opportunities

It is very likely that Feigl produced the first cage ligands and their metal complexes in developing an indirect colorimetric method for the detection of tin [63]. The addition of stannous chloride to a solution containing iron(III) and dimethylglyoxime produces a dark red color. It is highly likely that the tin(IV) produced by the redox reaction bridges triplets of oxime oxygens forming a cage complex similar to that in Fig. 18.

4.3

The Template Route to Catenanes

4.3.1

The Quest and Discovery

In 1960, Wasserman [64] achieved the first proof of the existence of a catenane molecule, but was not able to obtain the pure interlocked compound. Diethyl tetratriacontanedioate, $EtO_2C(CH_2)_{32}CO_2Et$, was converted to the cyclic acyloin in a solvent composed of 1:1 xylene: $C_{34}H_{63}D_5$, where the latter is the corresponding deuterium-labeled, 34-membered cyclic hydrocarbon. The reaction yielded a mixture of the free acyloin and its catenane with the labeled hydrocarbon ring, $C_{34}H_{63}D_5$. Subsequent separations and oxidation of the acyloin back to the corresponding acid demonstrated the presence of the catenane, originally reported to be present as about 1% of the acyloin (Fig. 23). Subsequently the yield was revised to .01% [65]. In 1963, Frisch and Wasserman [4] published the first theoretical treatment of chemical topology, mainly considering catenanes and simple knots. These early studies demonstrated the limitations of statistical approaches to catenane synthesis. In conclusion, the threading process essential to both catenane and rotaxane synthesis occurs in only a small fraction of the molecules of a mixture of a cyclic molecule and an axle molecule.

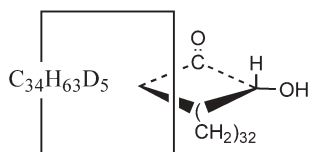


Fig. 23 First catenane to be reported in the chemical literature

The first synthesis of pure catenanes was reported several years later by Lüttringhaus and Schill who clearly demonstrated the need for intervention by some structure-determining method in order to produce catenanes in significant yields [66]. Lüttringhaus and Schill introduced a profoundly complex *directed* route to catenanes, using organic chemical reactions to build a precursor molecule in which the rings to be interlocked are held in place by covalent bonds during the building of the precursor. Subsequently, the links between the rings were removed, producing the catenane (Fig. 24). The critical stereochemical feature in the synthetic scheme is the orthogonality between the plane of the benzene ring (and much of the first large ring) and the plane of the two functional groups anchoring the second large ring. This design exploits the tetrahedral stereochemistry in much the same way that Sauvage et al. did in template syntheses of catenanes and knots (vide infra). In the 16-step synthesis, the overall yield of catenane is low, but the yield in the second ring closure step is substantial (~30%). Indeed it is this step that is the point of failure in less constrained, directed approaches to catenane formation [67]. The challenges of the elegant work of Lüttringhaus and Schill dramatize the value of template syntheses. The ultimate template route is capable of producing quantitative yields in a small number of steps, usually one or two.

Later, the success with statistical threading in the synthesis of rotaxanes led to their application in the synthesis of catenanes by Agam et al. [68]. The Agam et al. synthesis (Fig. 25) represents a landmark in the progress toward ready catenane synthesis. Beginning with a statistical yield of rotaxane of 18.5%, the catenane was produced from that point in 14% yield.

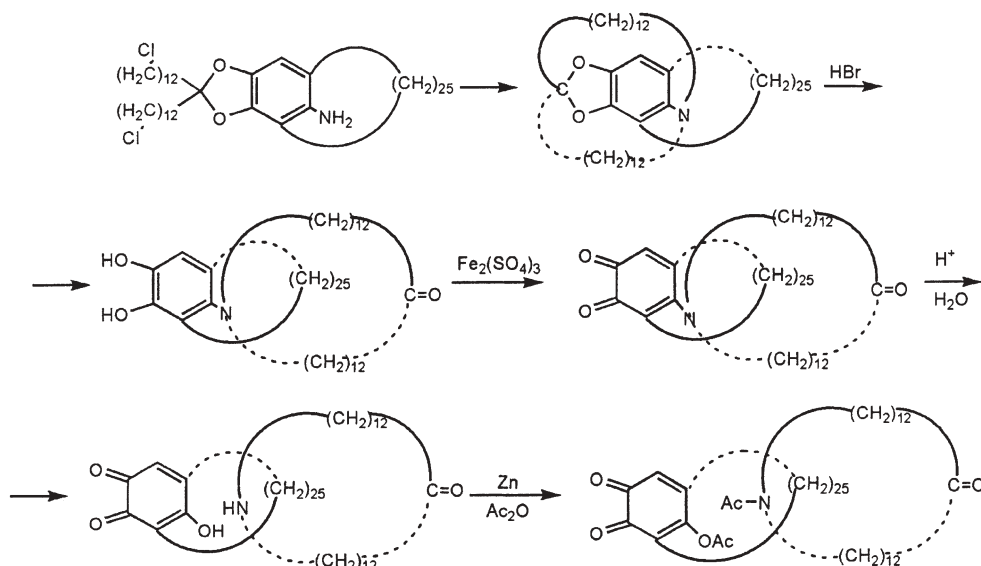


Fig. 24 “Directed” organic synthesis of the first pure catenane

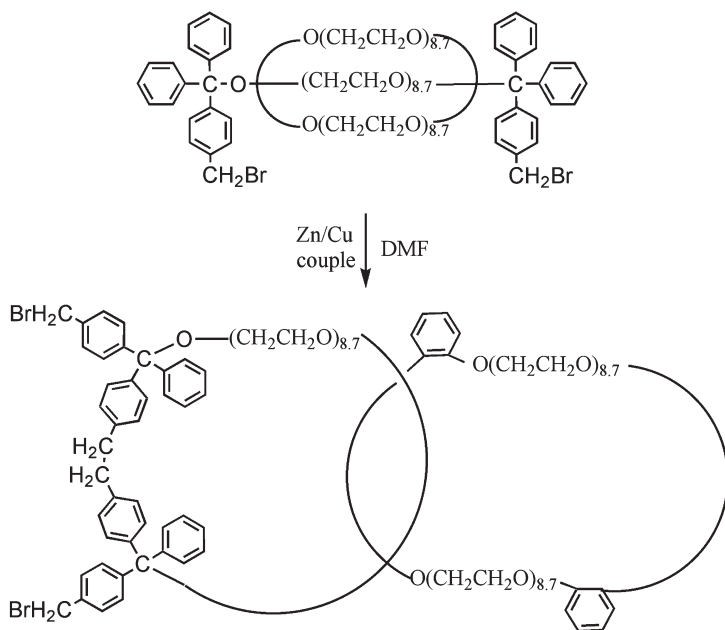


Fig. 25 Successful catenane synthesis based on good yields in synthesis of rotaxane precursor [68b]. Reprinted with permission. Copyright 1976, American Chemical Society

The development of broad areas of chemistry based on interlocked structures and other template-based molecular motifs has occurred whenever particularly successful new templates have been created. The history of catenanes illustrates this fact very clearly. Having the knowledge of molecular templates and their successful use by others in the synthesis of macrocycles and cages, Sauvage and Dietrich-Buchecker invented a new template for the closure of pairs of interlocking rings, catenanes. The achievement of a successful template synthesis of a catenane constitutes a major accomplishment in the progress of the fields of interlocked molecular structures and template chemistry. That classic work opened the way to many new architectures, and led to ever more complicated structures and potential applications. In that first template system, which was adequate to generate complicated molecular motifs in good yield, the tetrahedral copper(I) ion serves as the anchor. When combined with their prototypical molecular turn, 2,9-bis(p-hydroxyphenyl)-1,10-phenanthroline, the template orients the two turns orthogonally, providing a 90° cross-over between them (Fig. 26). Knot theory calls these elements “crossings” [14], but since this is not a discussion of knot theory the similar term “cross-over” is used. When combined with a proper linker (the diiodo derivative of pentaethylene glycol), the desired catenate is formed [69]. In a second approach [70], one macrocycle is prepared in advance and bound to the copper(I) ion. A molecular turn then threads through the coordinated macrocycle, binds to copper and, in a subse-

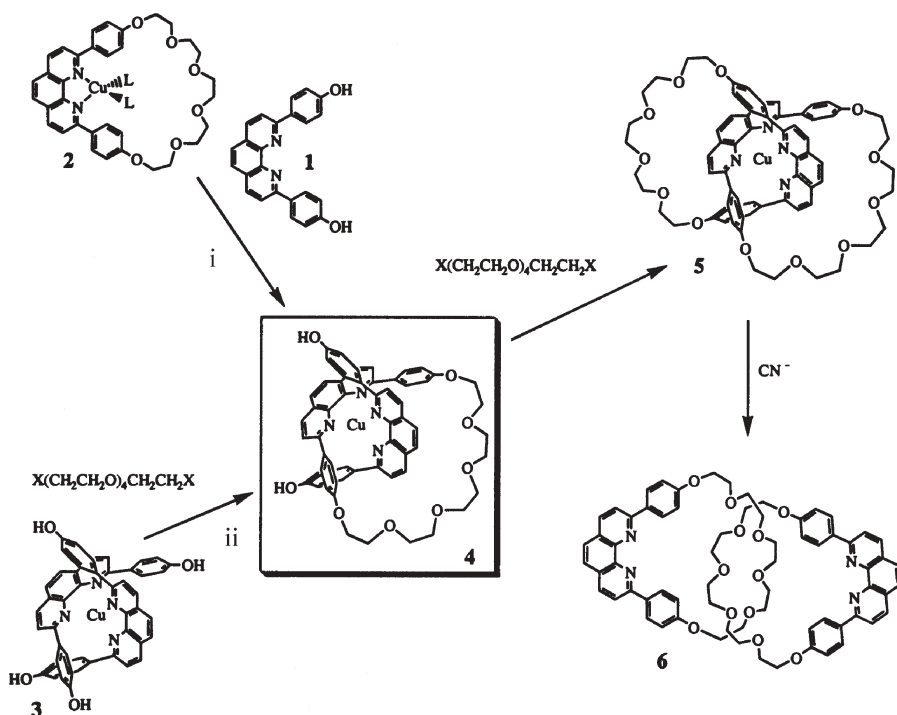


Fig. 26 Tetrahedral metal ion template of Dietrich-Buchecker and Sauvage based on the Cu^+ ion as anchor and the didentate diphenol substituted phenanthroline convergent turn [166]. Reproduced with permission from Elsevier

quent step, combines with a linker, completing the catenane formation. In both approaches, removal of the copper(I) with cyanide leads to isolation of the pure organic catenane. The yields were 27% and 42% for the 2-turn and ring-turn methods, respectively. Over the course of many uses and elaborations, this template has ultimately produced catenanes in almost quantitative yields (93%). The high yields were achieved by converting the bimolecular steps to unimolecular, using ring-closing metathesis (Fig. 27) [71]. With these developments, template syntheses are becoming sufficiently efficient to be used in continuous 1-, 2-, and 3-dimensional materials syntheses where the same process must be repeated many, many times in order to yield the high molecular weight products. Complementary tetrahedral copper(I) and didentate molecular turns have been replaced by equally complementary octahedral ions and tridentate turns, using ruthenium(II) and iron(II) ions [17–18]. Momenteau's porphyrins have been used in the ring-turn synthesis of a trimetallic [2]-catenane having interlocked basket-handle porphyrins [72]. The use of pairs of metal ions produced [3]catenates and [3]catenanes [73]. Other motifs include necklace-type oligocatenates [74]. The many architectures and linkages created by these templates are summarized in reviews [75].

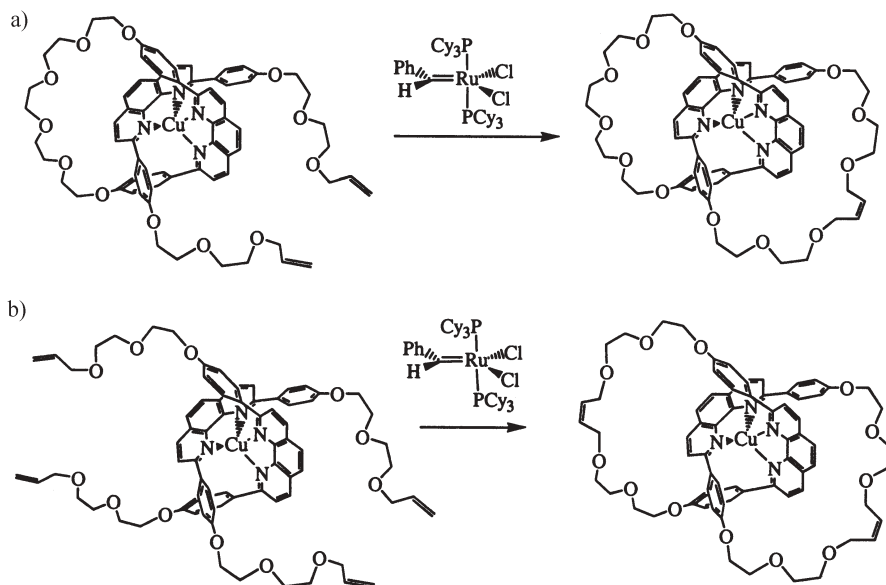


Fig. 27 High yield catenane synthesis by converting a bimolecular process to unimolecular, use of the Grubbs cyclization methodology [166]. Reproduced with permission from Elsevier

The development of an extremely general template utilizing π - π donor/acceptor interactions provided parallel developments of great importance. The opening and exploitation of this chemistry is found in the enormous works of Stoddart and his collaborators. In solvents of moderate polarity and, in some cases, with the help of high pressures, the π -electron-deficient aromatic dication paraquat forms strong complexes with electron-rich aromatic groups exemplified by those functions in bis-*p*-phenylene34crown10 (Fig. 28) [76]. To produce the multitude of derivatives of this template, a molecular turn had to

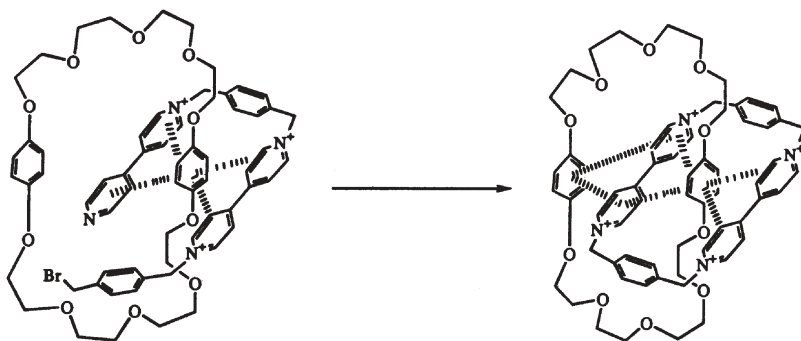


Fig. 28 First example of catenane formation using Stoddart's template [166]. Reproduced with permission from Elsevier

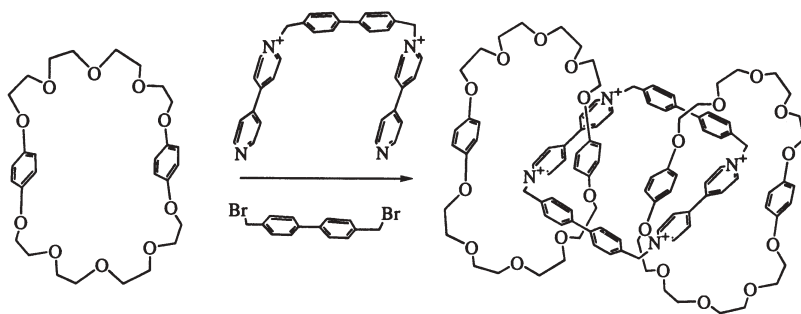


Fig. 29 Application of the π - π template to synthesize a [3]rotaxane. First example of catenane formation using Stoddart's template [166]. Reproduced with permission from Elsevier

be created and this was in the form of a bis(paraquat) bifurcated by a phenylene moiety. Crystal structures have shown that the attraction involves hydrogen bonding of the hydrogens of the methyl groups of the paraquat to the oxygens of the hydroquinone moieties, in addition to the π - π stacking [77]. The template synthesis of Stoddart's first [2]catenane gave a remarkable 70% yield [78]. A kinetic study of the formation of the simple Stoddart catenanes provided a model for the dynamics of the templating process [79]. Although much variety characterized the work of this group with interlocked structures, an early goal was stated to be polycatenanes [76]. The linking ring was enlarged for this purpose and the first [3]catenane of this class was soon synthesized

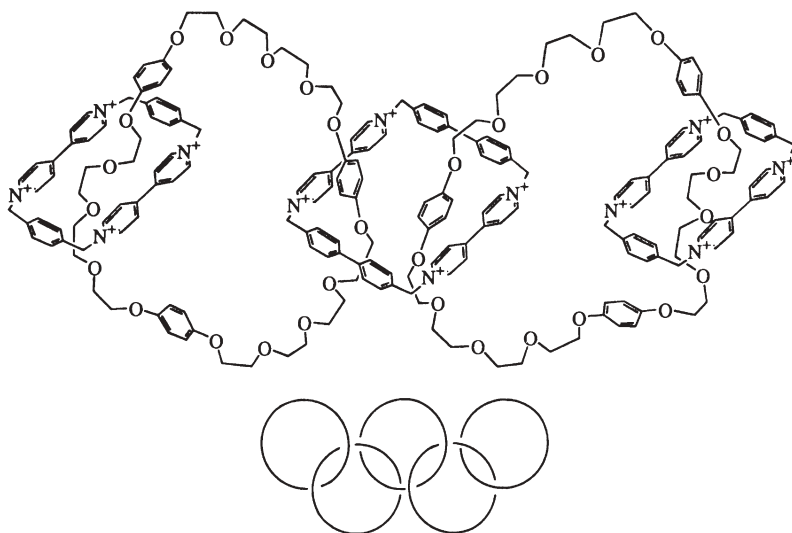


Fig. 30 Olympiadane, formed using the π - π template, is a chain of five macrocycles in an interlocked sequence as in a classic macroscopic chain [166]. Reproduced with permission from Elsevier

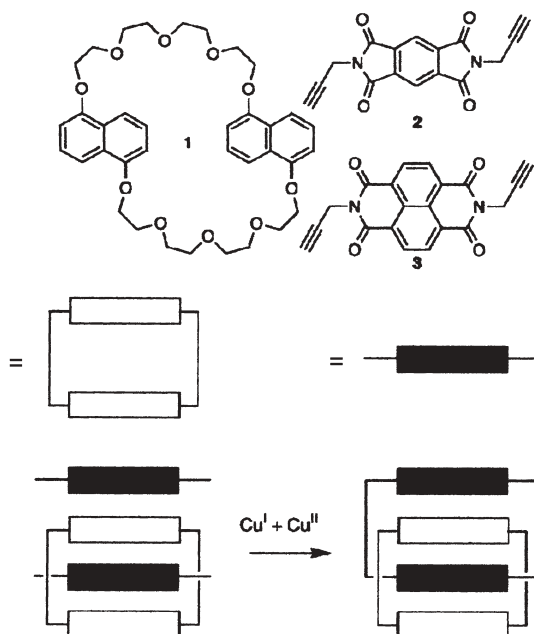


Fig. 31 Potent π - π template based on neutral electron-poor components [82]. Reproduced by permission of The Royal Society of Chemistry on behalf of the Centre National de la Recherche Scientifique

(Fig. 29). Extending the chain length to five rings produced the landmark labeled “olympiadane” (during a year of the Olympics), (Fig. 30), and a branched [7]catenane was also produced [80]. For more complete descriptions of these historical developments, see reviews [81].

A second template based on π - π stacking has been developed by the Sanders group. Using a crown ether ring containing two naphthyl groups, two neutral electron-deficient, aromatic diimide molecules provide the foundation of these templates (Fig. 31) [82]. Catenanes have been formed by three distinctly different reactions: kinetically controlled Glaser-Hay coupling of terminal acetylene groups, thermodynamically controlled Grubbs coupling of terminal vinyl groups, and Mitsunobu alkylation of the nitrogens of the aromatic diimide functions of the electron-poor aromatic molecules (Fig. 32) [83].

A third class of template ranks among the most versatile of the templates known to date. The [2]catenane marking its beginning was discovered by Hunter while studying the synthesis of a 2+2 macrocycle formed from isophthaloyl chloride and a well-designed dianiline derivative of cyclohexane [84]. In addition to the desired product he also isolated the bisamine shown in Fig. 33. Remarkably, the high dilution reaction of that bisamine with isophthaloyl chloride resulted in the [2]catenane (in 34% yield), in addition to the macrocycle he had sought to synthesize. It was suggested that the hydrogen bonding pat-

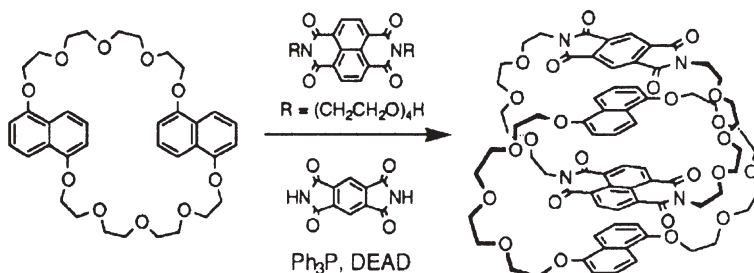


Fig.32 Examples of catenanes formed with the Sanders π - π template [83a]. Reprinted with permission. Copyright 2000, American Chemical Society

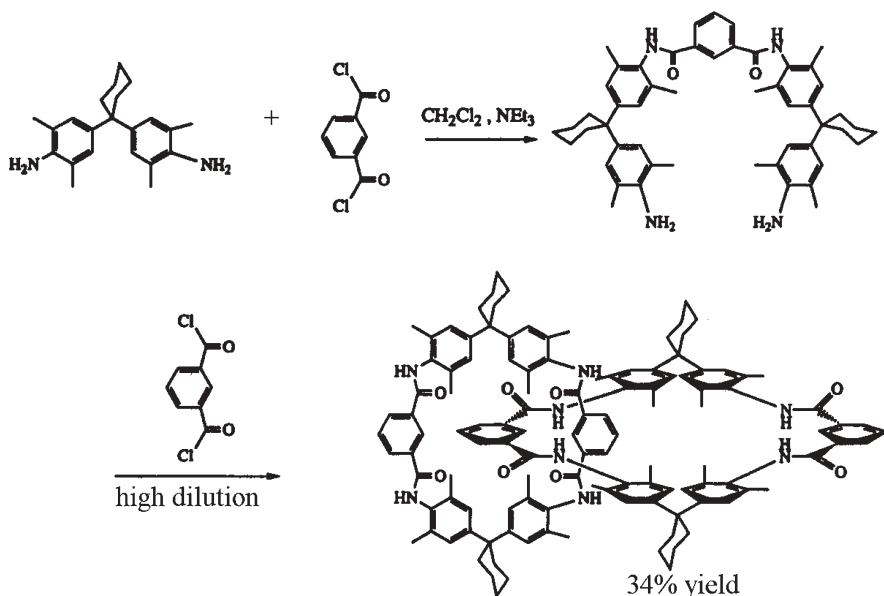


Fig.33 Reaction leading to discovery of the HVL template by Hunter [166]. Reproduced with permission from Elsevier

tern between the two macrocycles in that [2]catenane typify the anchor and turn of this new template. Although the templating must be quite different, it seems appropriate to reflect on another case of serendipitous catenane synthesis [85]. In the course of synthesizing 42crown14, Gibson and Lee found the corresponding [2]catenane in 8% yield.

We continue with the discussion of the template given the short title HVL in recognition of the major early contributors to the field (Hunter, Vögtle, and Leigh). By studying the effect of substituents on the 5-position of the isophthaloyl groups, Vögtle deduced the mechanistic scheme shown in Fig. 34 [86]. Replacing one of the phenyl groups with a furan ring, Vögtle observed what he calls translational isomers in 8% and 20% yield [87].

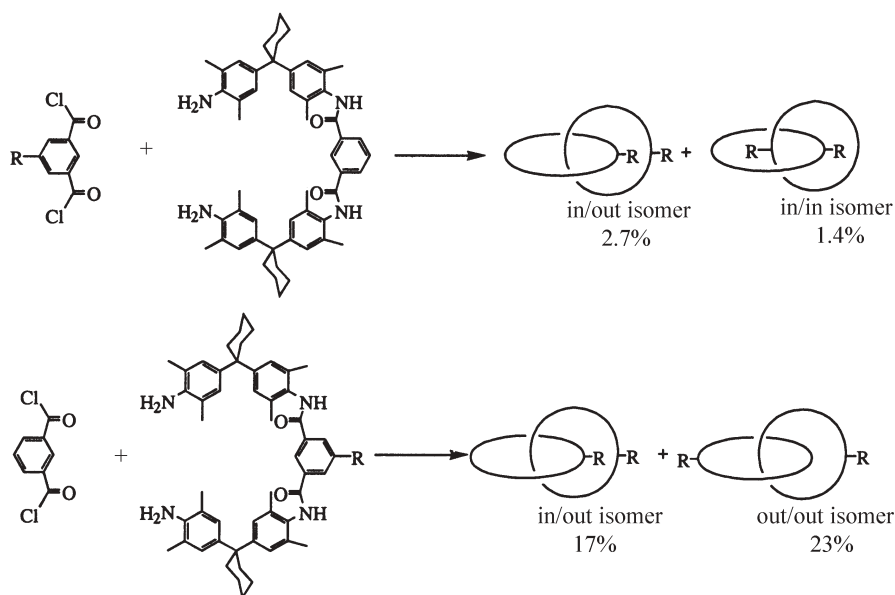


Fig. 34 Effect of substituents on the isomer distribution in catenane synthesis using the HVL template [166]. Reproduced with permission from Elsevier

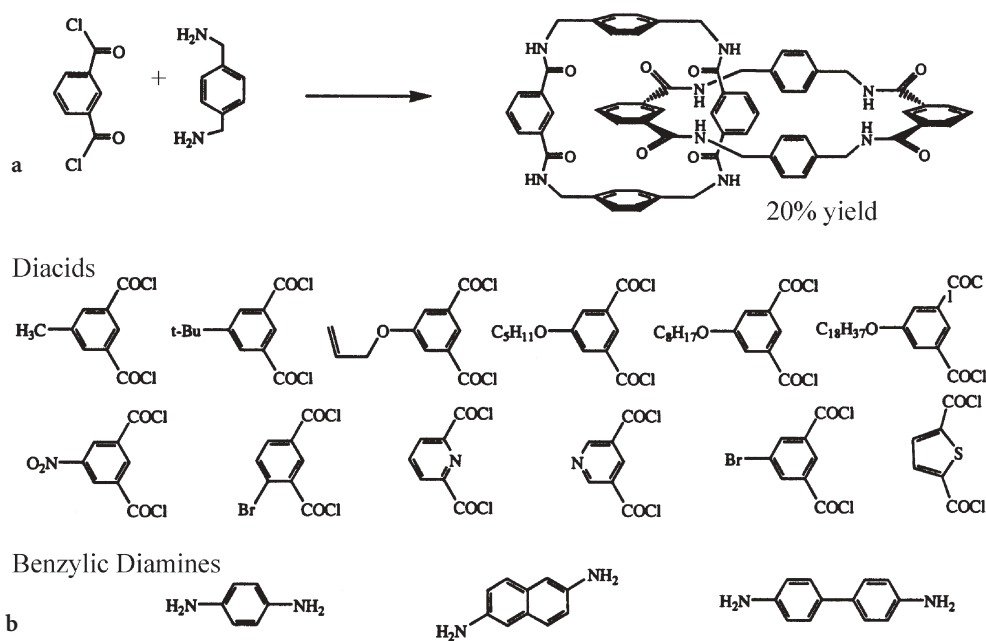


Fig. 35 Leigh's discovery that simple benzamides react with many iso-phthaloylchlorides to form catenanes [166]. Reproduced with permission from Elsevier

Leigh found that simpler amines readily form [2]catenanes in much the same way and that some of these adjust their conformations in response to environmental conditions, exposing either polar or apolar components, depending on the nature of the solvent (Fig. 35) [88]. In these studies a broader range of structural components was used than in earlier studies. A major contribution was the realization that the components need not be so rigid as had originally been thought. Incorporation of long-chain aliphatic moieties in his catenanes led Vögtle to the same conclusion [89].

4.3.2

Concept Development and Missed Opportunities

The formation of interlocked molecular rings was a topic for discussion early in the 20th century, with the most often cited example being a seminar given by Willstätter in Zurich in 1912 [4, 90]. Lüttringhaus et al. discussed alternative approaches to catenanes in 1958 [91], but the first catenane was successfully synthesized several years later. The possible existence of interlocking rings was suggested for polysiloxanes [92] and polymeric phosphonitrile chloride [93] in 1953 and 1959, respectively, but without confirmation. D. Lemal has been attributed with anticipating the work of Lüttringhaus and Schill in the form of directed synthesis of catenanes, and Closson is said to have suggested the use of metal ions as in the work of Dietrich-Buchecker and Sauvage using a copper(I) anchored template. These suggestions reflect naked concepts that emerged fully clothed at later points in time. However, they soundly illustrate how conceptual advances proceed almost subliminally until the opportune combination of researchers and subject lead to their substantive demonstration.

4.4

The Template Route to Rotaxanes

4.4.1

The Quest and Discovery

In the paper that initiated molecular topology, Frisch and Wasserman point out the parallel isomerism between a rotaxane and its molecularly interlocked parts and a catenane and its corresponding parts [4]. Topologically, the blocked axle and the ring of a true rotaxane are separable; in the real world, that may not be true for a given example. The practical difference distinguishes between a pseudo-rotaxane and a true rotaxane. Harrison observed the unique behavior of a single ring-size in his study of rotaxanes (he called them hooplaanes) with fixed blocked axles and rings of varying sizes [94]. Ring sizes between 25 and 28 formed true rotaxanes while those of larger ring-size quickly separated. The rotaxane involving the unique ring size of 29 had the property of appearing stable, yet it could be synthesized with the blocking groups already in place on

the axle. This first example of rotaxane synthesis by “slippage” (Fig. 36) heralded a concern that persisted for years: “Rotaxane or pseudo-rotaxane: That is the question!” [95].

Harrison and Harrison demonstrated the statistical probability of pseudo-rotaxane formation by the threading method [96]. The C30 acyloin macrocycle was bound to a Merrifield resin and repeatedly treated with an axial ligand, decane-1,10-diol, followed by a blocking agent, triphenylmethylchloride. Analysis was conducted on the hydrolysis products and after a total of 70 cycles, some 6% of the rotaxane was calculated to have been formed, giving a probability of pseudo-rotaxane formation of about 10^{-3} . Much later (2002), Bravo, Orain and Bradley used the Stoddart template to produce polymer-bound rotaxanes in useful amounts and high purity [97].

Researchers seeking catenanes became involved in rotaxane synthesis because of the intermediacy of such structures in catenane synthesis by the so-called “threading” route. Schill and Zollenkopf [98] extended the directed organic synthesis methodology to rotaxanes. Relative to the catenane preparation, the procedure was remarkably simple. Of the four common methods for template synthesis (Fig. 36), all but slippage can be, and have been, achieved by template routes, and all of those specific templates described in the development of catenane chemistry have played roles in the history of rotaxanes. An early example of use of a metal ion to template the formation of a rotaxane was reported by Gibson, employing the Sauvage template [99]. Stoddart et al. applied their π - π

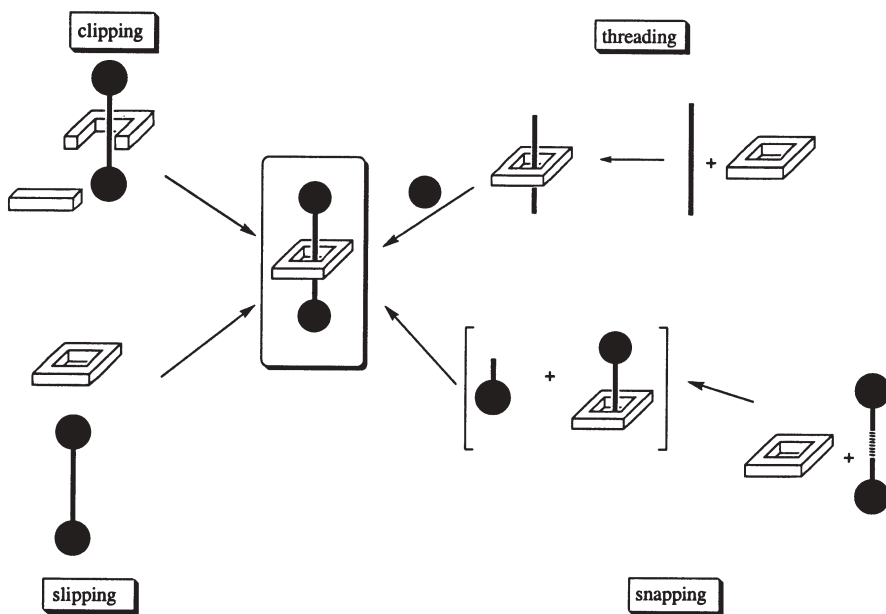


Fig. 36 Pathways for the formation of rotaxanes [166]. Reproduced with permission from Elsevier

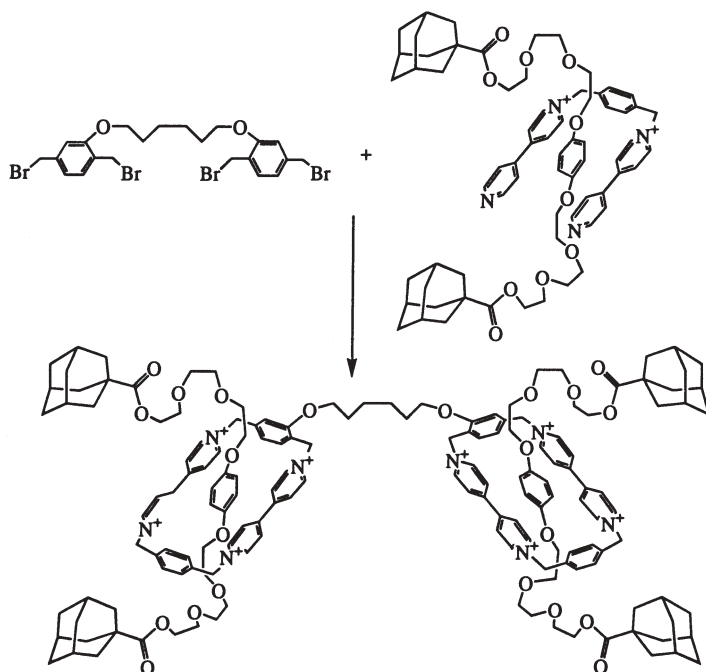


Fig. 37 Clipping reactions with two templated axle molecules produces a bis[2]rotaxane [166]. Reproduced with permission from Elsevier

template to an early example of rotaxane synthesis by clipping. Figure 37 shows an example of a bis[2]rotaxane formed by a double clipping reaction [100]. The ability of ammonium ions to bind to crown ethers was known from the time of Pedersen's classic work with crown ethers [101], but early work with small crown ethers suggested that secondary alkylammonium ions were not likely to form pseudo-rotaxanes, a view contradicted by the threading of cyclic molecules on polyglycols or polyamines [102]. A logical extension produced the first simple hydrogen-bond templated [2]rotaxanes (Fig. 38) [26], an advance followed quickly by additional examples. The application of a second hydrogen-bond template, that based on amides, to [2]rotaxane synthesis was reported in 1995 [103, 104]. Threading groups are diacid dichlorides, and pseudo-rotaxane formation was reported to be favored by complementarity of both hydrogen bonding and π - π interactions. This template system soon yielded a [3]rotaxane [105] and a bis[2]rotaxane based on a pair of linked rings [106]. A novel twist, the [2]rotaxane between an amide-based macrocycle and an amide/sulfonamide axle was used as a template to link the axle and ring together, producing a [1]rotaxane [107]. Using the same chemistry, the rings of two [2]rotaxane molecules were linked together to form a [3]-rotaxane [108]. The inverse process, linking of the axles of a pre-formed [2]-rotaxane, was also used to produce a [3]rotaxane [108]. By performing the linking process in two steps it has been possible

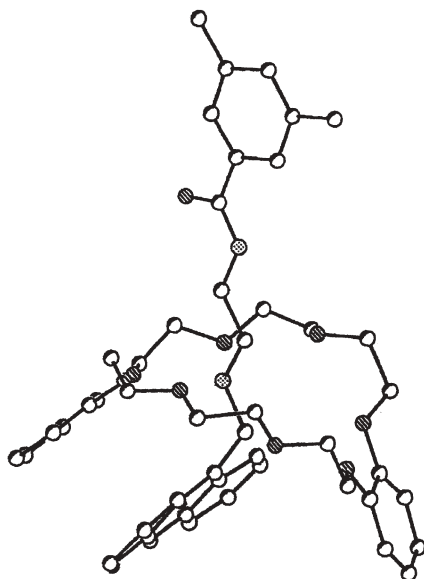


Fig. 38 Structure of the first rotaxane between a crown ether and a secondary ammonium cation [166]. Reproduced with permission from Elsevier

to make unsymmetrical ring-linked bis[2]rotaxanes in high purity. A tris[2]rotaxane was synthesized by utilizing a branched triplet of rings (Fig. 39). In all of the preceding work, it has been assumed that the axle molecule must have an aromatic ring to perform as an effective template. Subsequent studies with, for example, succinic acid derivatives have proven that amide functions provide excellent threading, *vide infra*.

The tetraamide macrocycles are most notable for the strong hydrogen-bond donor function of the ring in rotaxanes, and the Vögtle group has used this to produce an extremely important new template reaction of much generality [109, 110]. They have shown that this highly positive environment is sufficiently complementary to small anions (F^- , Cl^- , Br^- , I^- , AcO^- , NO_3^- , $H_2PO_4^-$) to give large binding constants in the non-coordinating polar solvent CD_2Cl_2 . The interaction has been used to create a new kind of template reaction that constitutes the ideal pattern for rotaxane synthesis by the “snapping” pathway (Fig. 36). In this template, a nucleophile, that will add the blocking reagent to the axle, complexes with the macrocycle and its reactive atom locates near the ring’s interior. When the electrophile approaches by entering the ring, the nucleophilic process occurs within vicinity of the ring in such a manner that it completes the synthesis of both the blocked axle and the rotaxane in a single step. The precursor nucleophile/ring complex is modeled by the anion complexes studied by Vögtle et al. Alternatively, the process can be designed so that the nucleophilic and electrophilic roles of the blocking reagent and axle stem may be reversed [110b]. The results of the Vögtle group are highly successful, having produced

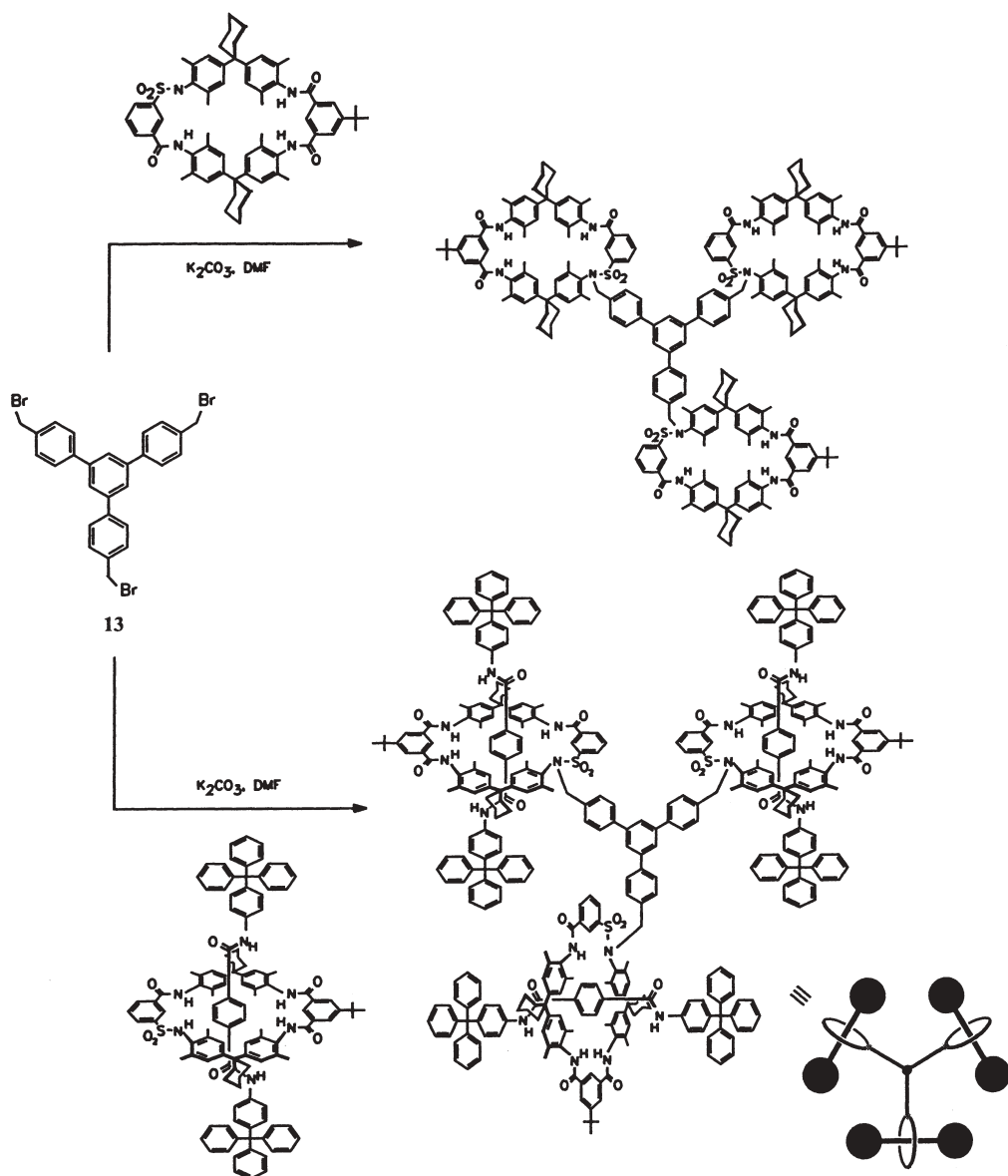


Fig. 39 Synthesis of a tris[2]rotaxane [108]. Reprinted with permission from Wiley-VCH. Copyright 1997

a rotaxane yield of 95% in the first systems reported. Whereas the authors focus on the critical complexing of the nucleophile as hydrogen bonding between the anion and the ring, it may be that the phenols they have used bind as neutral molecules, as the authors point out. It is probably not necessary that the nucleophile be an anion; it merely needs to have a high proclivity toward serving as a hydrogen-bond acceptor, i.e., primary amines might serve as nucleophiles in such systems. This combining of the nucleophilic property and the binding ability of blocker precursors is an exciting contribution to template chemistry. The development of superior new template methods with such high yields has made rotaxanes' structural features available for use in molecular design in general. Schalley et al. exploited the binding ability of phenols by locating such a functional group mid-axle, providing strong hydrogen-bond templating for rotaxane formation [111].

As a second example of high yield syntheses in broad families of rotaxanes, consider the equally important rotaxanes devised and exploited by the Stoddart researchers, those based on a so-called π - π template. With well-designed axle molecules, they successfully improved the yields of rotaxanes in their paraquat macrocycle systems to as high as 81% [112].

Building on a history of anion receptor studies, Beer and associates have made excellent use of anions as anchors in template chemistry [113]. Strongly hydrogen-bonding U-shaped receptors (*turns* in template jargon) are combined with a chloride or bromide ion in solvents that are not highly competitive in the formation of hydrogen bonds. In acetone, the 3,5-diamido pyridinium ion shown in Fig. 40 binds chloride ion and simultaneously binds to the macrocyclic diamide shown in the same figure, carrying the pyridinium ion with it as an axle molecule in the resulting pseudo-rotaxane. Further, in acetone the binding of the pyridinium ion receptor, or similar receptors, to chloride was shown to exhibit high binding constant values (6,600 at 25 °C). In a later report, this group extended the designs to template formation of a true [2]rotaxane. The *n*-hexyl groups of the axle molecule were replaced by bis(*t*-butyl) substituted 4-trityl phenyl groups and this pre-blocked axle molecule was bound to the chloride axle molecule. The glycol ether portion of the previously used macrocycle was replaced by two uncoupled $-\text{OCH}_2\text{CH}_2\text{OCH}_2\text{CH}_2\text{OCH}_2\text{CH}=\text{CH}_2$ groups. With both linear amides wrapped about the chloride ion, the allylic

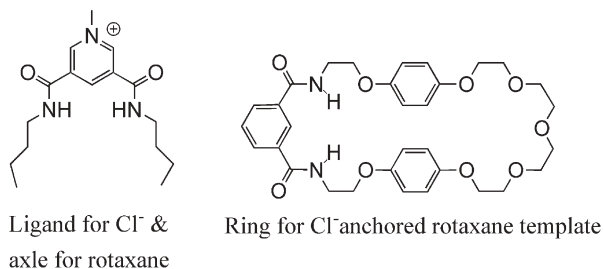


Fig. 40 Axle and macrocycle for chloride ion anchored formation of pseudo-[2]rotaxane

groups were subjected to Grubbs ring-closing metathesis reaction, completing the [2]rotaxane synthesis [114]. The Beer group has recently altered the macrocycle design to incorporate a luminescent moiety and extended their pseudo-rotaxane synthesis to the new molecule [115].

If [2]rotaxanes were, at first, difficult to make, higher rotaxanes were a great challenge and this too has been overcome. Hydrogen-bonded templates provide good examples of the relative difficulty of synthesizing both [2]- and [3]rotaxanes. Stoddart and his collaborators used 1,2,3-triazole stoppered secondary ammonium axles and a symmetrical 1,4-phenylene linked 28crown8 [116] to produce [2]- and [3]rotaxanes in yields of 30% and 10%, respectively, a difference that reflects the relative difficulty of [3]rotaxane synthesis. The fusing together of the axle molecules of two “semi-rotaxanes”, by oxidation of terminal mercaptans to form a disulfide group, was employed by Kolchinski et al. to produce a [3]rotaxane in a remarkable yield of at least 84% (Fig. 41) [117]. Because the [3]rotaxane is believed to be formed by a bimolecular reaction involving two semi-rotaxane precursor molecules, the threading of the precursor is presumed to be at least 90%. Takata and collaborators have applied the concept of dynamic organic chemistry to make essentially the same [3]rotaxane from the previously formed, separate axle and ring molecules. Benzene thiol was used as the thiophilic nucleophile that labilized the disulfide linkage in the axle molecule so the [3]rotaxane could be formed by the snapping mechanism (58% yield), along with some [2]rotaxane (8% yield) [118]. Comparison of the yields of the kinetic template of Kolchinski with the thermodynamic template of Takata suggests that the kinetic template route is more efficient in this particular case. Leigh et al. have also used the thermodynamic template to form rotaxanes, using the labilizing ability of the Grubbs olefin metathesis reaction [119].

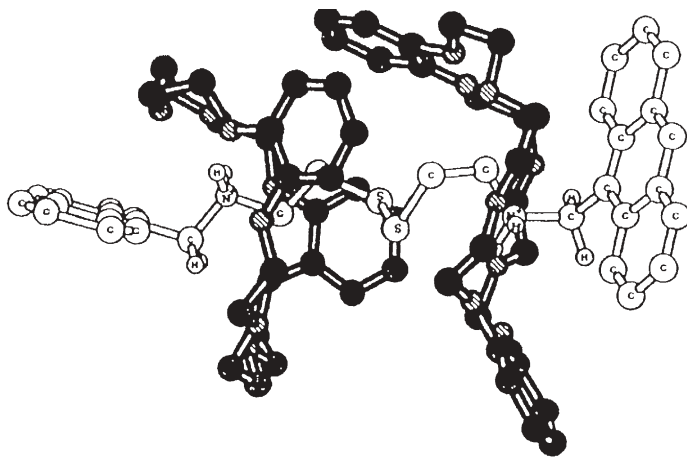


Fig. 41 [3]Rotaxane produced in 84% yield by oxidative coupling of two mercaptoammonium axles [166]. Reproduced with permission from Elsevier

Loeb and Wisner [120] responded to Stoddart's conclusion that the combination of the components from the crown ether/hydrogen bond template and the π - π template (paraquat dication) show little tendency to form rotaxanes by introducing a new pyridinium cation derivative, 1,2-bispyridinium ethane dication, as a new axle for crown ethers that has a greater charge concentration. The crystal structure of the resulting rotaxane showed that this new axle molecule is nicely complementary to DB24Cr8 (Fig. 42). Substituents at the 4-positions of the pyridine rings affect binding, with electron withdrawing groupings increasing the affinity of axle for ring. The work was extended to [3]rotaxanes [121] and molecular shuttles [122].

Using the amine/crown ether (BPP34C10) template, the Stoddart group expanded the range of interlocked molecules with additional examples of doubly threaded [2]rotaxanes, the corresponding [3]rotaxanes, and remarkable double threaded [3]rotaxanes [123]. Using a 3-armed axle molecule, these researchers prepared and characterized compounds including a singlet, a doublet, and a triplet of [2]rotaxane moieties in a single molecule. They consider the triplet to be an early generation rotaxane dendrimer [124]. Fitting the template parts in which both the axle and ring are trifunctionally distributed leads to what Stoddart and group call a mechanically interlocked bundle [125].

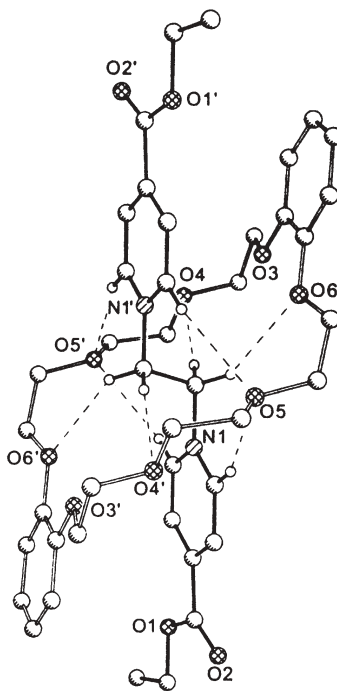


Fig. 42 [2]Rotaxane templated by an ethylenedipyridinium dication [120a]. Reprinted with permission from Wiley-VCH and authors. Copyright 1998

Axles with two binding sites are of interest for two reasons. In addition to their value as parts of templates for [3]rotaxane formation, they are the motif most often used in research directed at molecular switches and their many applications (machines, electronics, smart materials, sensors, etc). In what appears to be revelation of a concept before its time for application, it has been shown that one can use blocking agents to assure the site occupied during synthesis of a shuttle-precursor rotaxane by threading [126]. By use of both the H-bonding template and the π - π template, novel [3]rotaxanes have been prepared [127]. Because this chapter focuses on historical and introductory material, discussion of molecular design and demonstration directed at molecular devices has not been included.

When the two essential components of a rotaxane are combined in a single molecule, novel architectures arise, two of which are obvious, cyclic oligomers and acyclic polymers (Fig. 43). So-called hermaphroditic rotaxanes are formed when the rings and axles of two molecules are combined mutually with each other, forming cyclic dimers [128]. Elaboration of the chemistry of the dimers

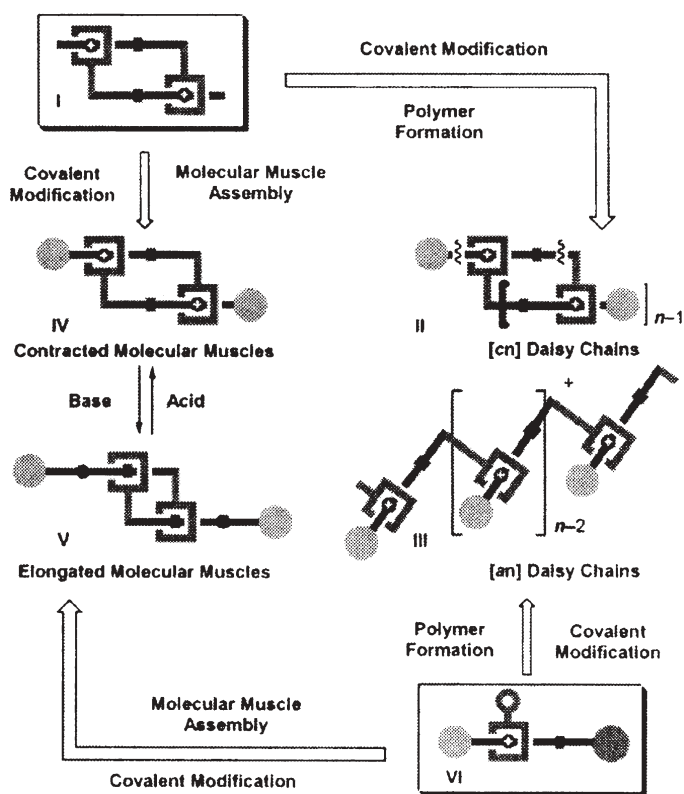


Fig. 43 Hermaphroditic and daisy chain rotaxanes [128]. Reproduced by permission of The Royal Society of Chemistry

is being pursued with a vision of contractile materials resembling muscle tissue in function. Examples of cyclic dimers and trimers, based on a number of the familiar templates, have been studied [128, 129]. The second architecture is labeled the daisy-chain polymer. This architecture exists when each molecule serves as a ring toward a different molecule of the same kind while serving as an axle to a third molecule. Stoppering would convert a pseudo-[*n*]rotaxane to a true polymeric [*n*]rotaxane (alternatively called poly[2]rotaxane).

Equally important to the development of new motifs and better synthetic methods are studies that reveal the structural and environmental factors that affect the kinetics and thermodynamics of pseudo-rotaxane formation because they should guide in the design of templates for threading in general, not just for rotaxane synthesis. Using the prototypic axle and ring, dibenzylammonium ion (DBA) and dibenzo-24-crown-8 (DB24C8) (Fig. 44), Stoddart et al. showed the great impact of solvents on the threading process [130]. At 25 °C, the equilibrium constant decreased as follows (*K*, M⁻¹): chloroform 27,000, acetonitrile 460, acetone 360, and no threading in dimethyl sulfoxide. The behavior in mixed solvents is indicated by the value for chloroform/acetonitrile (1,700 M⁻¹) [131]. A more dramatic example of dominating solvent effects was provided by the reaction of the axle bis(cyclohexylmethyl)ammonium hexafluorophosphate with a sixfold excess of the same ring, DB24C8. About 98% of the axle molecule is converted to the pseudo-rotaxane by reflux in methylene chloride for 32 days. The solid was dissolved in 3:1 deuterio chloroform and deuterio acetonitrile and no evidence for dissociation was found after standing for weeks at room temperature. The behavior is very different in DMSO; the rotaxane dissociates completely within 18 h at 25 °C [132].

Cucurbit[7]uril (CR7) and its complementary axles respond very differently to solvent types. CR7 binds dimethylviologen cation strongly in aqueous media (Fig. 45) [133]. This testifies to the highly polar environment associated with CR7. That environment contrasts sharply with the hydrophobic interior of cyclodextrins, yet the equilibrium constants for binding of tetramethyl- β -cyclodextrin to the tetraphenyl porphyrins having sulfonate functions on hydro-

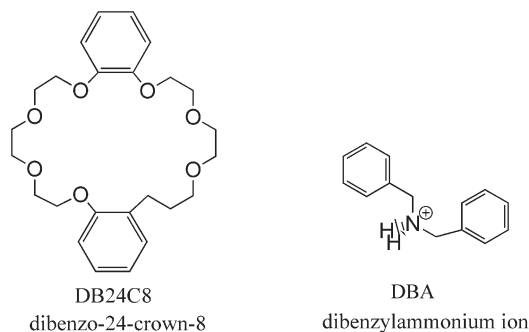


Fig. 44 Prototypical axle and ring for measurement of equilibrium constants for pseudo-rotaxane formation

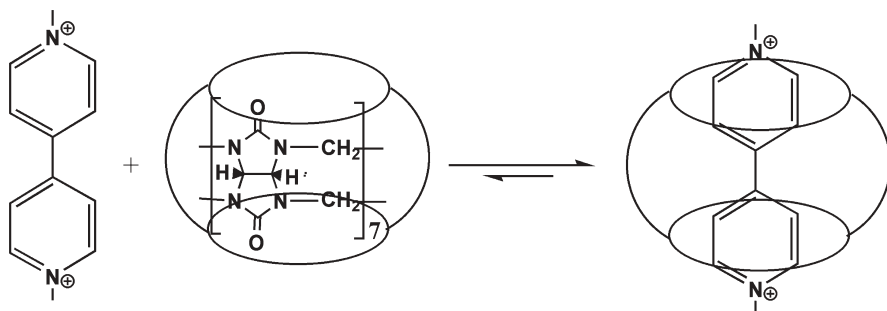


Fig. 45 Binding equilibrium for methylviologen and Cucurbit[7]uril [133]. Copyright 2002, National Academy of Sciences, U.S.A

carbon chains are too large to measure in aqueous solution, but give values of $8,700 \text{ M}^{-1}$ in ethylene glycol and 290 M^{-1} in methanol at 25°C ; no binding was observed in DMSO [134].

Clearly, threading is favored in some solvents and not in others. Further, the threading process can reach equilibrium very slowly. Considering the dynamics of molecules above absolute zero, the statistics of threading seems to resemble the throwing of fine wires at the holes in needles, with the needles moving about freely. Surely the collections of trajectories, conformations, and orientations favorable to threading are small compared to the total array of those same motional properties for a solution containing threads and rings of appropriate complementarity to facilitate threading. Attractions between charges and dipoles doubtless help, but the intervention of solvent molecules is certainly a powerful factor that may or may not help.

Substituent effects were evaluated with the macrocycle DB24C8 and *p*-disubstitution of the axle molecule DBA. The equilibrium constant for pseudo-rotaxane formation increases smoothly with the increasing electron withdrawing power of the substituent. This decreases the basicity of the ammonium ion and increases the polarity of its protons. In turn, this increases the hydrogen bonding ability of the axle molecule. As expected, electron donating methyl groups decrease the equilibrium constant. The equilibrium constant for binding is almost doubled when one ether oxygen in the ring is replaced by a pyridine nitrogen. The larger basicity of the nitrogens produces stronger hydrogen bonds to the ammonium group of the threading molecule [135]. The position of the benzo groups of DB24CR8 has very little effect on binding [136].

For a fixed ring size, e.g., DB24C8, steric effects associated with the axle molecule are expected because of the necessary complementarity between the ring and the threading moiety. This is supramolecular jargon saying that the axle has to be small enough to slip through the ring, but large enough to get maximum benefit from hydrogen bonding. An interesting example involves changing the axle molecule to a DBA analog (but with cyclopentyl, cyclohexyl, or cycloheptyl rings instead of the phenyl ring) in a study of the rates of formation and

dissociation of the pseudo-rotaxane [95]. Bis-*p*-*i*-propylphenyl ammonium ion provided the standard for comparison with an association rate constant of $3.2 \times 10^{-3} \text{ M}^{-1} \text{ s}^{-1}$, a dissociation rate of $1.3 \times 10^{-6} \text{ s}^{-1}$, and an equilibrium constant (formation) of $2,470 \text{ M}^{-1}$. The cyclopentyl derivative reacts more rapidly than the reference standard while the cyclohexyl derivative reacts more slowly, but, remarkably, those two axle molecules have identical equilibrium constants of 110 M^{-1} . Above, it was reported that the cyclohexyl derivative reacts at a very slow rate (reaction complete in 32 days in methylene chloride). The smaller cyclopentyl derivative reacts on the second/minute time scale, while the larger cycloheptyl derivative does not form a pseudo-rotaxane.

Clifford and Busch [137] have determined the equilibrium constants for pseudo-[2]rotaxane formation for a single crown ether, benzo-24crown8 (B24C8), and almost 30 axle molecules selected to show the influences of the group that must penetrate the ring as the anchoring ammonium ion approaches the ring oxygens. For simplicity the axles all have a single threading group, with the other substituent on the secondary ammonium function always the same and serving as a blocking group (Fig. 46). Results with nine normal alkyl derivatives showed that the binding of a hydrogen-bonded axle to a crown ether is not sensitive to the length of a linear alkane group extending from the secondary ammonium template. Specifically, axles with hexyl and octadecyl groups had the same equilibrium constant (178 M^{-1}) for pseudo-rotaxane formation while that with a propyl group (149 M^{-1}) differed by less than 20%. More completely, for the *n*-alkyl groups through nonyl, plus octadecyl, the equilibrium constants ranged from 120 to 180 M^{-1} , with a mean of $160 \pm 20 \text{ M}^{-1}$. The seven measurable values show no systematic variations, including no indication of an odd-even variation. It was concluded that the *K* values for *n*-alkanes are the same within the uncertainties of the measurements. In contrast, qualitative observations show very clearly that the relative rates of binding differed markedly, depending on chain length. Axles having alkyl (or related) groups shorter than pentyl bind rapidly on the NMR timescale while longer chains are, on that scale, slow to bind.

Branching by adding a methyl group to the alkyl moiety greatly impedes binding when the methyl group is located α to the amine nitrogen, but it shows

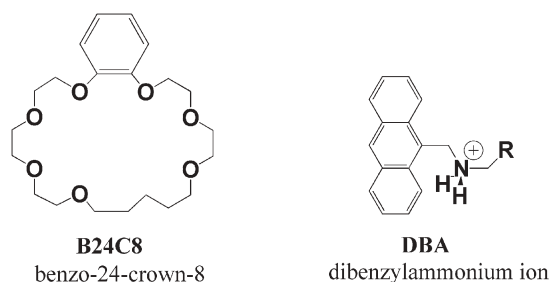


Fig. 46 Axle and wheel for determination of equilibrium constants for pseudo-rotaxane formation

relatively little effect if attached at a greater distance from the template site. For example, equilibrium constants (K, M^{-1}) vary as follows for butyl groups: *n*-Bu 127, *sec*-Bu 43.5, *iso*-Bu 12.9, and *tert*-Bu no threading observed. Also, for the series, *i*-propyl, *i*-butyl, *i*-pentyl, the branch is increasingly remote from the ammonium group in that sequence and K increases in the same sequence, 17, 43, 164 M^{-1} . Interestingly, the cyclohexyl derivative displays an affinity (K) identical with that of the *i*-propyl derivative. However, the binding rate for the cyclohexyl derivative is slow, but probably not for precisely the same reason that *n*-alkyls of chain length greater than five are slow. This branching effect is probably attributable to the size of the ring, rendering the axle and ring non-complementary when it is placed in the region near the hydrogen bonding site.

In contrast, the effect of relative remoteness of a group was found to be reversed in the case of phenyl groups, e.g., (K, M^{-1}) benzyl 94, 2-phenethyl 194, 3-phenylpropyl 282. The effects of substituents on the remote ends of alkyl groups are varied: OH groups give a small but real decrease in K values compared to the simple alkyl group whereas carboxylic acid functions enhance the binding, e.g., $K=177$ for an *n*-hexyl substituent and $K=223$ for the 6-amino-hexanoic acid derivative and $K=280$ for the 5-aminopentanoic acid derivative.

With DB24C8 and a similar axle molecule having one end blocked and a carboxylic acid function on the other, Zhender and Smithrud observed an increase in affinity with chain length [138]. The increased affinity with increasing chain length for the phenyl and carboxylic acid groups may arise from some additional associative interactions that are facilitated by increasing flexibility of the linkage for longer chains. On the other hand, the decrease in affinity that accompanies a terminal OH group may be attributable to competitive binding with the solvent, both within and outside the macrocycle. The presence of strong binding groups on the macrocycle that can only bind on its outside has been found to impair threading [139].

For the amide-based templates of the HVL type (Fig. 47) the following equilibrium constants ($K M^{-1}$) were determined for pseudo-rotaxane formation [140]: *m*-chlorosulfdioxybenzoyl chloride 66, phenyl benzoic amide 282, the partially blocked succinate having a 4-trityl phenyl amide group and a benzyl ester group 696. Clearly the much used axle (*m*-chlorosulfdioxybenzoyl chloride) binds least strongly. The affinity for the amide-containing axles implicates the carbonyl oxygens of the macrocycle in complexation. As the authors state, the affinity for the succinate axle proves that there is no requirement for an aromatic ring in the structure of the axle molecule. Reflecting on the manner in which the known axles bind in amide-based templates, Leigh et al. [141] reasoned that pseudo-rotaxane formation should be favored by locking the amide functions of the axle molecule into a conformation optimizing the threading relationships. They applied the principle and achieved a record 97% yield of rotaxane formation by what may be viewed as a clipping process.

Whereas it has been shown that paraquat has little affinity for crown ethers of what would seem to be appropriate size, Loeb and Wisner [120] have shown that ethylene dipyridinium cations, which have more concentrated charges, form

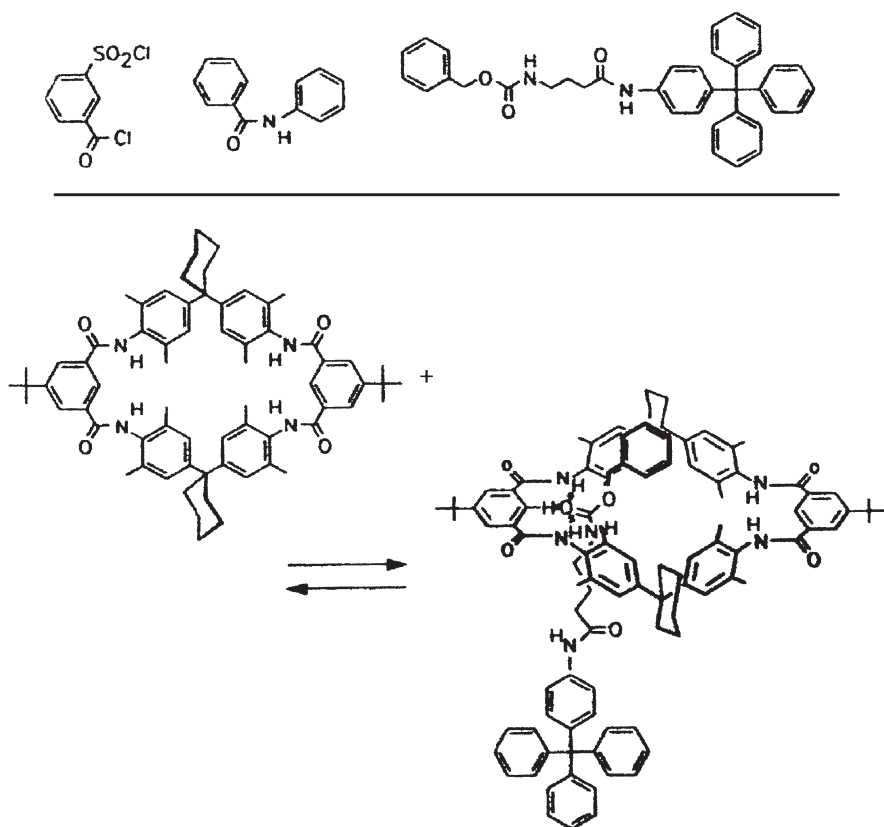


Fig. 47 Binding of acid chloride and amide axles to Vögtle's tetraamide macrocycle [140]. Reprinted with permission from Wiley-VCH. Copyright 1997

pseudo-rotaxanes in acetonitrile. Substituents at the 4-positions on the pyridine rings lead to the following equilibrium constants for disubstituted dipyridinium cation as axle and for the ring shown in Fig. 42 above, in acetonitrile solution at 25 °C (K , M^{-1}): *DB24C8* – H 180, CH_3 230, Ph 320, CO_2Et 1200. *B24C8* – H 195, CH_3 205, Ph 300, CO_2Et 740. *24C8* – H 165, CH_3 105, Ph 160, CO_2Et 320. The effect of π stacking on these results is apparent in the higher values for constants, especially when electron withdrawing substituents are in place. The crystal structure of the rotaxane shows a dramatic example of hydrogen bonding by electron-poor hydrogens attached to methylene groups. Kim, Jeon, Ko, and Kim [142] find that the dicationic methyl viologen binds more strongly than do the partially reduced radical cation or the neutral fully reduced species.

Kawaguchi and Harada [143] found a major charge effect on both the kinetics and thermodynamics of pseudo-rotaxane formation between dodecamethylene- α,ω -diammonium ions and α -cyclodextrin. NH_3^+ ions at the extremities gave the axle a +2 total charge; replacing $-NH_3^+$ with $-^+NC_5H_4-C_5H_4N^+$ provided a second

example with a +2 charge; quaternizing the second nitrogen of the bipyridine group gave a +4 charge; alkylating that second pyridine group with a 2-ammonium ethyl group ($-^+NC_5H_4-C_5H_4N^+-CH_2CH_2NH_3^+$) gave an axle molecule with a +6 charge. The kinetics of binding and release of the +2 and +4 charged axles were rapid on the NMR time scale while the +6 charged axle both complexed very slowly with the cyclodextrin and formed a stable pseudo-rotaxane. Is charge a second way, in addition to size, to block a rotaxane and convert it from pseudo- to true rotaxane? Investigations continue in other laboratories as well [144].

Discrimination between chiral threads by a chiral ring has been found in the binding constants for pseudo-rotaxane formation by Stoddart and associates (Fig. 48) [145]. For host (RR)PF₆, axle molecules gave the following chiral selectivities (K_{RR}/K_{SS}): axle #3 3.3, axle #4 3.0, axle #5 1.1. These values show that the selectivity decreases with distance of the chiral centers from the binding center of the axle molecule, varying from a significant K_{RR}/K_{SS} of 3.3 to an

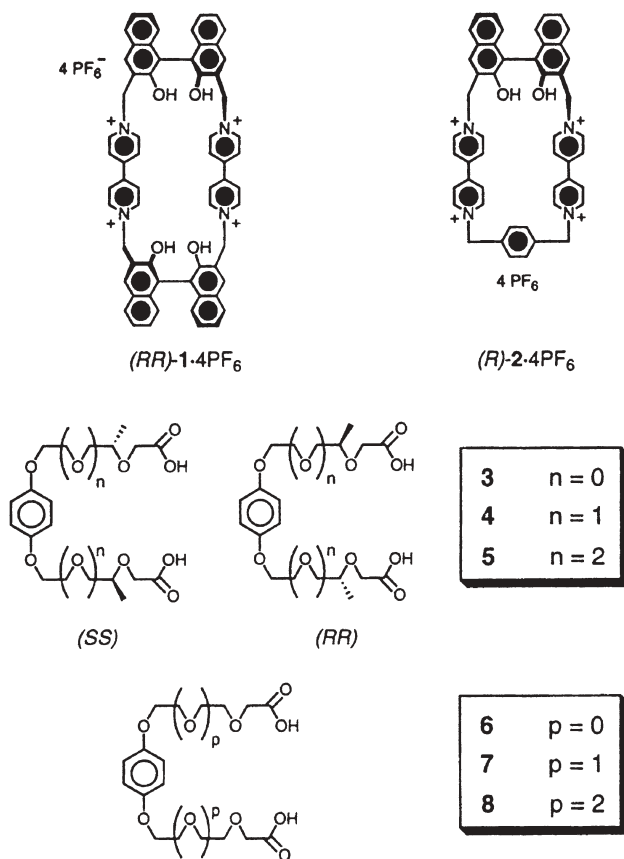


Fig. 48 Enantioselective discrimination in π - π template assembly of pseudo-[2]rotaxane [145]. Reprinted with permission from Wiley-VCH and authors. Copyright 1998

insignificant 1.1. This behavior is consistent with the more general observation that axles composed of 1,5-dioxynaphthalene units flanked by multiple ethyloxy units form rotaxanes in increasing yields as the number of units decreases. Zilkha et al. studied the statistical threading of polyethylene glycol through crown ethers, including some oligo-crown ethers. They fit their data with a mathematical model for the threading system [146].

4.4.2

Concept Development and Missed Opportunities

Paradoxically, from among the basic motifs of interlocked structures and molecular topology, rotaxanes emerge today as arguably the most versatile of molecular building components, or even tools, while historically the catenane almost always occupied center stage. The tradition of focusing on challenges using catenanes reflects a proper response to the true topological isomerism of a catenane in comparison to its two composing rings. In contrast, a true rotaxane and its composing parts, the axle and ring, are not topological isomers because, in principle, they are not composite for topological reasons but for reasons retaining a metric factor. Frisch and Wasserman [4] mention the rotaxane to reflect on its topological insignificance. Sokolov comments on the behavioral similarities of rotaxanes and catenanes, despite their topological difference – and then finds utility in rotaxanes. Schill finds that making rotaxanes is only a minor challenge compared to making catenanes. Pioneers like Sauvage and Stoddart focused their group's early efforts on catenanes. Even in work on molecular devices, catenanes were used before rotaxanes.

In our world of practical matters, like designing the first molecular machine or the first nano-chip for a computer, metrics are often matters of importance. The cliché “reinventing the wheel” ignores a critical relationship. Except in cartoons, outer space, magnetically levitated and constrained conditions, and maybe a few other situations, the wheel is useless without an axle. The rotaxane is the molecular invention of the wheel and axle combination. Rotaxanes empower the wheel on the molecular scale. The rotaxane was not so much discussed in the early history of the field of this book because the focus was on the most fundamental relationships, not on the applications. Today's compulsion to exploit the utility of molecules and ions has created a new focus.

4.5

The Template Route to Knots

4.5.1

The Quest and Discovery

The synthesis of molecular knots was first achieved with DNA [147] and in the copper(I)-templated chemistry of Sauvage [148]. The first synthetic molecular trefoil knot was synthesized by a template using two copper(I) ions as anchors

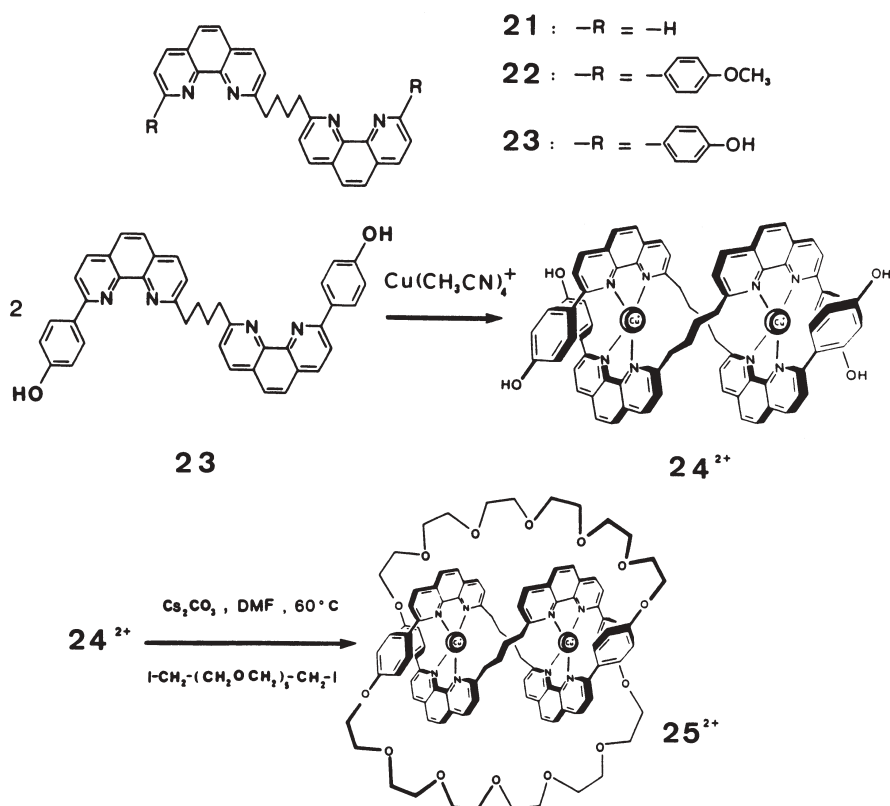


Fig. 49 Two-center tetrahedral copper(I) template-based synthesis of the first molecular trefoil knot [149a]. Reproduced by permission of The Royal Society of Chemistry on behalf of the Centre National de la Recherche Scientifique

joined together by pairs of ditopic didentate chelating ligands, each of which constituted a linked pair of molecular turns (Fig. 49) [149]. The ring-closing reagent (linker) was the diiodo derivative of hexaethyleneglycol. Depending on which pair of phenolic oxygen atoms react with the linker, three products were predicted: a single large ring, a [2]catenane, and a trefoil knot (Fig. 50). The links between the two didentate groups that the ring-closing reagent forms are critical. This is emphasized by the three systematic possible products given in Fig. 50. However, such a system, if not properly designed, might generate polymeric complexes or the ligand might simply engulf a single metal ion. In the first report of successful trefoil knot synthesis, the most abundant product was the least interesting, the single large ring; however, a small amount (3%) of the trefoil knot was also formed. The necessary intermediate is properly described as a dinuclear double helical complex.

Several years later, using ring-closing metathesis and reducing the ring-closing process to a unimolecular reaction (Fig. 51), the same investigators have

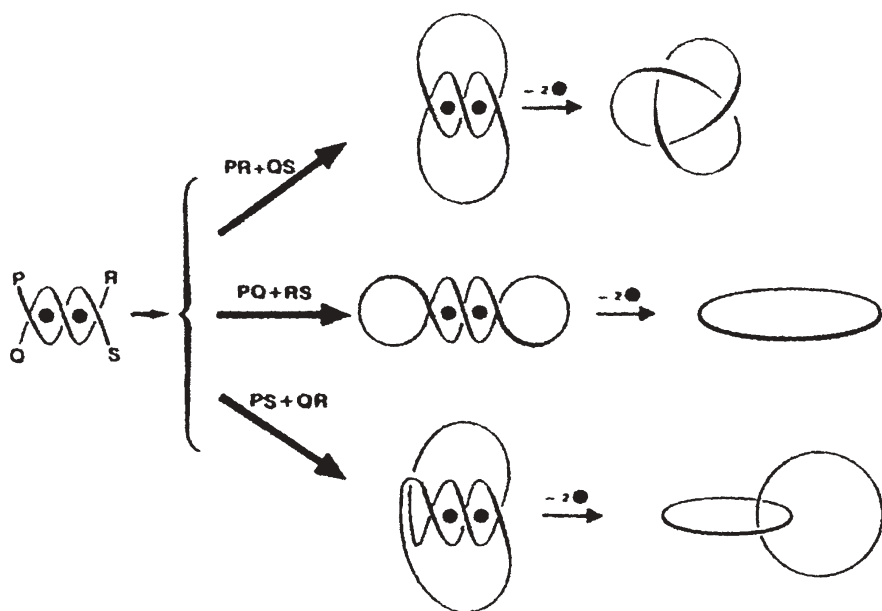


Fig. 50 Three possible products from a 2-center tetrahedral copper(I) template: trefoil knot, large ring, catenane [149a]

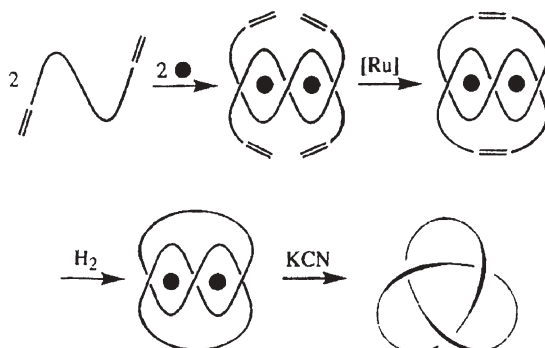


Fig. 51 High yield synthesis of a molecular trefoil knot using the Grubbs ring-closing methodology. Reprinted with permission from [150]. Copyright 1999 American Chemical Society

succeeded in producing molecules with the topology of a trefoil knot in high yield (74%) [150]. The intermediate used was again a helical dinuclear dicopper(I) complex. It was also shown that a parallel path to a trefoil knot was obtainable (in 20% yield) using octahedral iron(II) and a tridentate 2,2',2''-terpyridine ligand moiety. This work clearly makes these unusual molecular motifs available in non-trivial amounts.

The copper(I)-based templates have been extended to include the tying of composite knots as well, specifically, those composed of two trefoil knots [151]. Figure 52 shows the three competing 4-anchor template intermediates. The two diastereomeric isomers of this composite of two trefoil knots are items F and G. In F, the two dinuclear helical template components have the same chirality. In street language, this knot is the granny. The more symmetrical knot represented by G is a square knot. In a complicated and challenging process a yield of ~3% of the composite knot was obtained.

A second template yielded a trefoil knot in 1997 (Fig. 53) [152]. Stoddart et al. reported the formation of a knot using their π - π donor/acceptor template. The corresponding knot and unknot were isolated in 0.6% and 0.3% yields, respectively.

In contrast to the two systems just described, the hydrogen bonding template system (HVL) developed by Hunter, Vögtle, and Leigh, provided a trefoil knot serendipitously – in 20% yield in the discovery example (Fig. 54) [153].

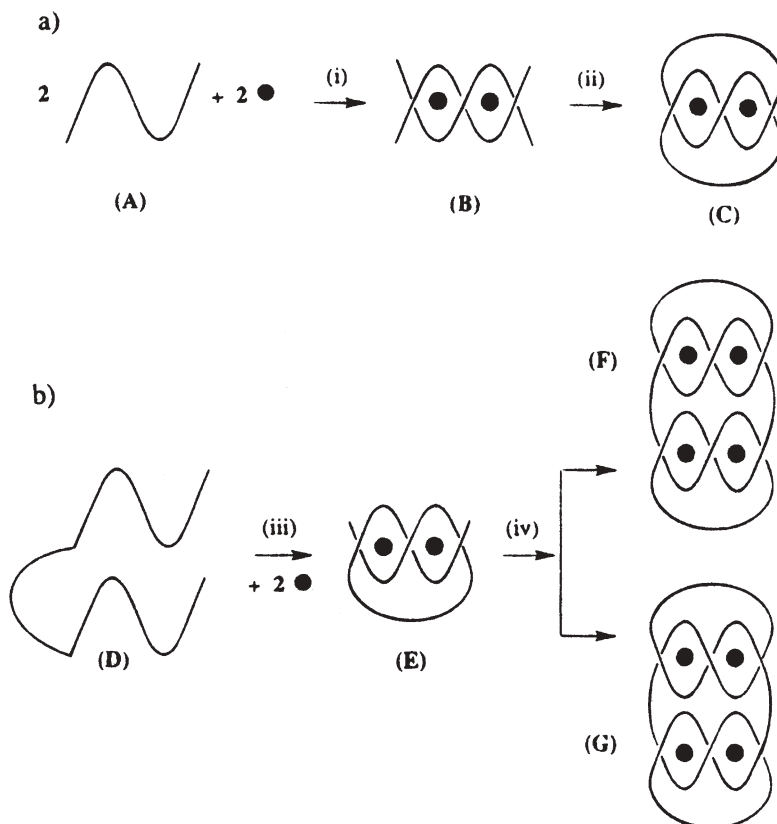


Fig. 52 Molecular template for formation of composite knots known colloquially as the square knot (g) and the granny (f). Reprinted with permission from [151]. Copyright 1996 American Chemical Society

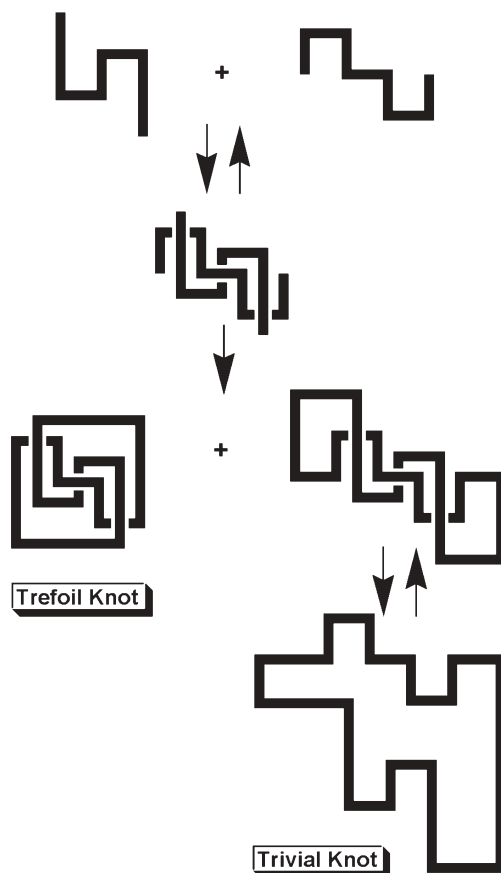


Fig. 53 Molecular π - π template for formation of trefoil knot [152]. Reprinted with permission from Wiley-VCH and authors. Copyright 1997

The research team led by Vögtle quickly exploited their discovery, producing a total of six distinct molecular knots templated by hydrogen bonding interactions due to amide functions within large macrocycles (Fig. 54) [154]. In these reactions three molecules of a pyridine-2,6-dicarbonyl dichloride (labeled B in Fig. 54) combine with three molecules of a previously prepared tetrafunctional molecule having terminal amino groups and internal amide functions (A in Fig. 54). B may have substituents such as Cl, OCH₃, or OCH₂Ph. In that second paper, these investigators also report the resolution of the knots into enantiomers and assignment of absolute configurations. From molecular simulations, it is clear that the knotanes (the new name for such molecules) have relatively fixed conformations. Researching a range of structural modifications that facilitate knot formation provided foundations for a postulated mechanism for knot tying in this 3+3 system. A supramolecular template is postulated in which a strand, representing partial completion of the condensation, forms

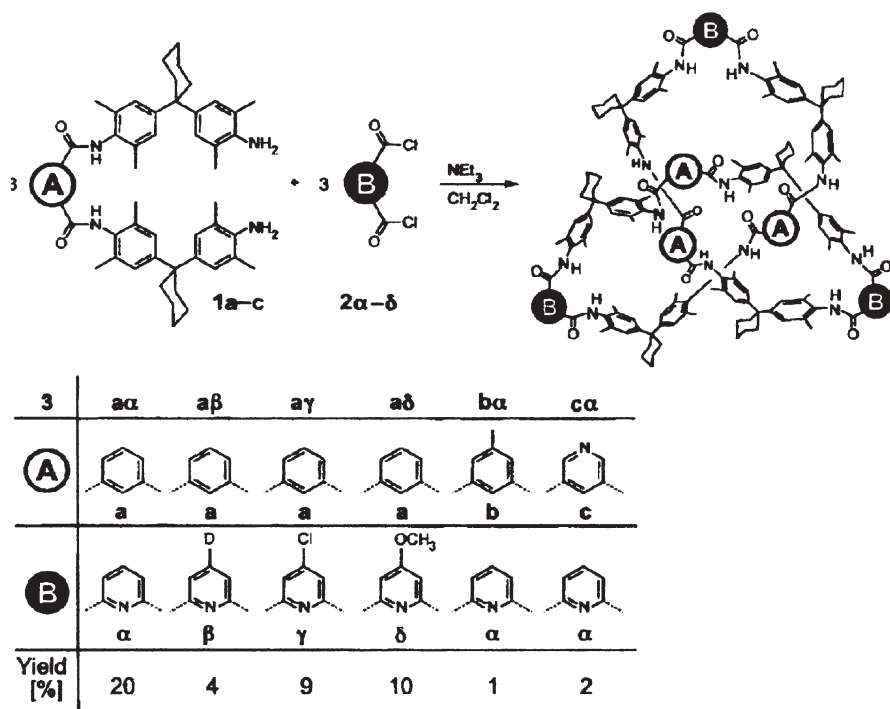


Fig. 54 Molecular knot formed by the HVL hydrogen-bond template [154]. Reprinted with permission from Wiley-VCH and authors. Copyright 2001

a host loop through hydrogen bonding, and an acid chloride molecule threads the loop and condenses with terminal amide groups (Fig. 55). Hunter and Mayers [155] reported the formation of a knot from a pre-synthesized oligomer of sufficient length to wrap around a metal ion when that element was supplied. This is the only example of a knot formed by templating the conformation-determining process. The example also differs in the fact that the knot is not a knot according to knot theory, since the ends of the strand are not joined together. In practical terms that latter requirement is not important; in topology it is a determining factor.

It should be emphasized that the hypothesis that a molecular strand forms a loop that successively hosts a threading event is of very broad significance. The threading of loops is a basic process for macroscopic orderly entanglements and controlling such processes at the molecular level will eventually facilitate major advances in the complexities of nanoscopic interlocked structures. The range of fabric-like orderly molecular entanglements that might be produced is small so long as the threading is limited to passing linear molecules through closed molecular rings, e.g., the obvious molecular fabric is patterned after the chain-mail used in ancient body armor. Extending the molecular threading process to loops formed in the usual way, but with a linear molecule,

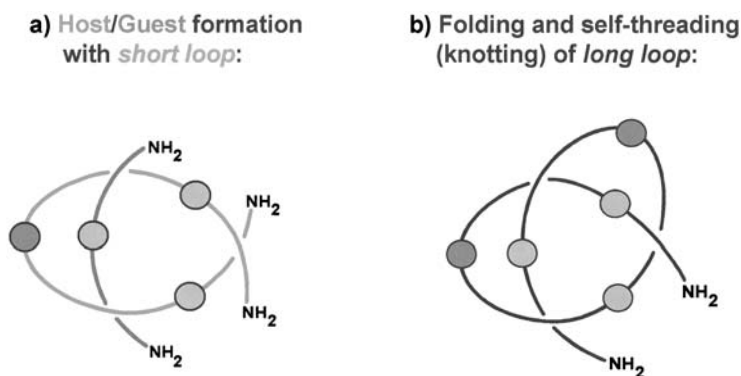


Fig. 55 Key host loop and thread proposed in models for mechanism of formation of the HVL knot. Reprinted with permission from FJ Vögtle

opens a larger topological array including assemblies of knots, as in macramé, but better typified by knitting and crocheting.

Vögtle et al. have shown that knotanes may be used as substituents, or as centers for the attachment of substituents, in very general terms [156]. Beginning with a tris(benzyloxy) knotane, deprotection with hydrogen over Pd on carbon produces a mixture of mono-, di-, and trihydroxy knotanes. Reaction of the latter with first and second generation dendryl bromides (Fig. 56) produced mixtures of dendryl-substituted knotanes that were separable by HPLC (Fig. 57). The tribenzyloxy knotane and the tridendryl knotane (1st generation) were resolved into enantiomers and, again, absolute configurations were assigned. In the case of the second generation dendrimers, only the mono- and disubstituted knotanes were isolated in pure form. In combining these large knotanes with multiples of dendrimers the basic knot unit has been defined as a chiral tecton: “A nano-sized chiral core that allows for the orientation of three substituents in space” [157].

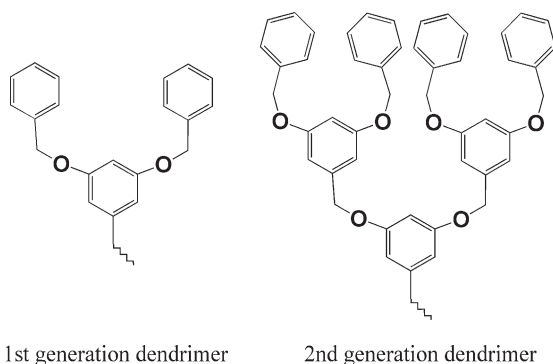


Fig. 56 First and second generation dendrimers used with knotanes

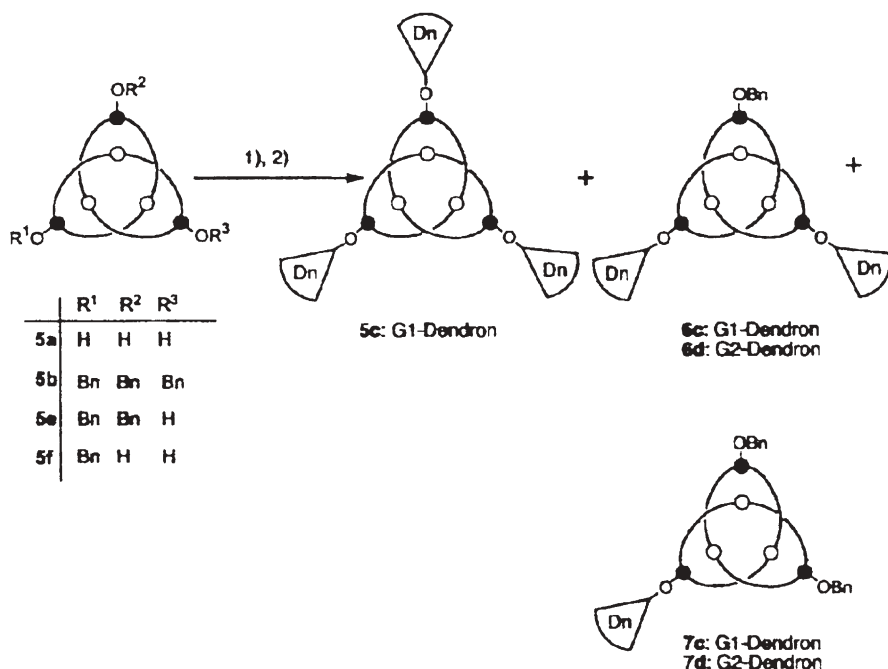


Fig. 57 Dendronized molecular knots. Reprinted with permission from [156]. Copyright 2002 Wiley-VCH

Synthesis of the pure tris(allyloxy) knotane in 5% yield opened the way to useable amounts of mono- and trihydroxy knotanes for further study [158]. Reaction of the monohydroxy knotane with biphenyl-4,4'-disulfonyl chloride in the presence of Et₃N in acetonitrile gave a dumbbell-shaped molecule in which two large knotanes were attached to a single linear unit. This unusual molecule existed in racemic and meso forms and all isomers were separated. This kind of dumbbell molecule could conceivably force the stoppers or ring in a rotaxane to rotate in a predetermined direction, a requirement of molecular machines [159]. Choosing an axle of sufficient length to accommodate the large knotane as a blocking group and a macrocycle with which it was known to have a template relationship, these investigators succeeded in synthesizing a knot-blocked rotaxane in 19% yield. The availability of the mono- and trihydroxy-knotanes also facilitated the synthesis of an example of diastereoisomeric species in which topologically chiral and centrochiral units have been linked covalently [160].

4.5.2

Concept Development and Missed Opportunities

The formation of knots in molecular strands has been studied for several decades. The possibility of such a strand first forming a loop and then thread-

ing through it was considered by Frisch and Wasserman [4] in 1962 and they estimated the probability a chain 80 carbons long would exist as a knot to be 10^{-3} to 10^{-2} . Sauvage [75a] lends credence to that perspective saying: "Despite the simplicity of the concept, this approach has, to our knowledge, never been attempted due to the low probability a chain has to tie a knot before its ends A and B find each other and connect." Frisch and Wasserman also first considered the Mobius strip approach, and Walba conceived an ingenious solution to the problem of creating a molecular Mobius strip having three half-twists. Schill and coworkers attempted synthesis of the trefoil knot by both the Mobius strip principle [161] and by extension of his directed synthesis methods [162], but without success. In 1973, Sokolov offered a third possibility based on a tris(didentate)transition metal complex serving as a template [163]. However, the design of the corresponding linking agent appears to be very challenging.

As we study the template that created the Borromean link or as we puzzle over the fate and/or uses of Vögtle's dendrimerized knotanes- (perhaps serving as chiral tectons) we are like mountain climbers following a well-marked trail up to misty heights, but without the struggles of the first pioneering effort to reach those heights. History has value to researchers for many reasons: detailed knowledge accumulates and what was learned, if it was true, it still is true; it can inspire us and provide a basis for celebrating the advances of our fields; it can humanize our necessarily uncompromising encounter with experimental reality; it can guide us to not make the kinds of mistakes made by others; it shows us that the seemingly impossible challenges of today become the records of accomplishment in time. I exaggerate – but to many of us, all things are possible but nothing is easy.

5

Molecular Templates – a Limited Field with an Unlimited Future

At the cutting edge of research today, rotaxanes and catenanes figure most heavily in studies inspired by the concepts of functional molecular devices, and templates are important in their design and synthesis. The most often repeated motif is a [2]rotaxane or [2]catenane with a pair of binding sites on a ring whose affinity for the axle/other ring inverts when the switch is thrown. Of course when the affinity reverses, the axle/second ring migrates to the newly favored site. Oxidation-reduction, acid-base reactions and photo-excitation are among the switching mechanisms used. Conversely, the axle of a [2]rotaxane may have two binding sites of invertible affinities for the cyclic molecule, resulting in the corresponding response, i.e., the axle promptly moves from the first site of binding to the one favored after the switch is thrown. Motivations vary from switches and sensors to actual molecular scale machines and computer parts – and beyond. Similarly, molecular cages have been followed by molecules with much larger 3-dimensional cavities, viewed as possible molecular scale reactors or delivery vessels for medicines. While templating will con-

tinue to be critical to the design and preparation of such futuristic molecules and to their applications in materials, catalysts, drugs, and electronics, those subjects are beyond the purpose of this historical introduction. Further, the word template has many meanings to a variety of science communities. The term arises in many aspects of biology and medicine (including enzymology, drug design, membranes, genetics, and imaging among others) and in many areas of the materials realm, ranging over biological aspects, separations, durable materials, and electronics. It follows that the segment of the literature summarized here is very limited. Of the 81,000+ references responding to the word “template” in *Chemical Abstracts*, only a tiny fragment have been mentioned here. The choice not to consider templates where the influential elements exceed the molecular scale is easiest to justify. Similarly, the biological, astronomical, and electronic uses of the term can be cleanly delineated from those covered here. It has been a more arbitrary matter to not consider most of the work associated with polymers, including molecularly imprinted polymers. It is hoped that the reader will be tolerant of that and other similar decisions that were necessary in order to focus on the basic considerations relating to so-called small molecules.

References

1. Seeman NC (1997) *Acc Chem Res* 30:357
2. a) Furlan RLE, Otto S, Sanders JKM (2002) *PNAS* 99:4801; b) Rowan SJ, Cantrill SJ, Graham RLC, Sanders JKM, Stoddart JF (2002) *Angew Chem Int Ed Engl* 41:898
3. Lehn J-M (1999) *Chem Eur J* 5:2455
4. Frisch E, Wasserman E (1961) *J Am Chem Soc* 83:3789
5. Harrison IT, Harrison S (1967) *J Am Chem Soc* 89:5723
6. Loren JC, Yoshizawa M, Haldimann RF, Linden A, Siegel JS (2003) *Angew Chem Int Ed Engl* 42:5702
7. Siegel JS (2004) *Science* 304:1256
8. Chichak KS, Cantrill SJ, Pease RR, Chiu S-H, Cave GWV, Atwood JL, Stoddart JF (2004) *Science* 304:1308
9. a) Thompson MC, Busch DH (1964) *J Am Chem Soc* 86:213; b) Thompson MC, Busch DH (1964) *J Am Chem Soc* 86:3651
10. Busch DH (1993) *J Inclusion Phenomena Molec Recog* 12:389
11. Thompson MC, Busch DH (1962) *Chem Eng News* September 17 1962:57
12. Thompson MC, Busch DH (1962) *J Am Chem Soc* 84:1762
13. Roberts SL, Furlan RLE, Cousins GRL, Sanders JKM (2002) *Chem Comm* 2002:938
14. Adams CC (1994) *The knot book*. Freeman, New York
15. Dietrich-Buchecker CO, Marnot PA, Sauvage J-P, Kintzinger JP, Maltese P (1984) *New J Chem* 8:573
16. Amabilino DB, Stoddart JF (1995) *Chem Rev* 95:2725
17. Piguet C, Bernardinelli G, Williams AF, Bocquet B (1995) *Angew Chem Int Ed Engl* 34:582
18. Ward M, Sauvage J-P (1991) 30:3869
19. Blake AJ, Lavery AJ, Hyde TI, Schroder MJ (1989) *J Chem Soc Dalton Trans* 1989:965
20. Vance AL, Alcock NW, Heppert JA, Busch DH (1998) *Inorg Chem* 37:6912

21. Leigh DA, Lusby PJ, Teat SJ, Wilson AJ, Wong JKY (2001) *Angew Chem Int Ed Engl* 40:1538
22. Barefield KE, Wagner F, Herlinger AW, Dahl AR (1976) *Inorg Synth* 16:220
23. Creaser II, Harrowfield JM, Herlt AJ, Sargeson AM, Springborg J, Gene RJ, Snow MR (1977) *J Am Chem Soc* 99:3181
24. Bühner M, Geuder W, Gries W-K, Hünig S, Koch M, Poll T (1988) *Angew Chem Int Ed Enl* 27:1553
25. Anelli PL, Ashton PR, Ballardini R, Balzani R, Delgado M, Gandolfi MT, Goodnow TT, Kaifer AE, Philp D, Pietraszkiewicz M, Prodi L, Reddington MV, Slawin AMZ, Spencer N, Stoddart JF, Vincent C, Williams DJ (1992) *J Am Chem Soc* 114:193
26. Kolchinski AG, Busch DH, Alcock NW (1995) *Chem Comm* 1995:1289
27. Adams H, Carver FJ, Hunter CA (1995) *Chem Comm* 1995:809
28. Baumann S, Jäger R, Ahuis F, Kray B, Vögtle F (1997) *Liebigs Ann/Recueil* 1997:761
29. Leigh EA, Murphy A, Smart JP, Slawin AMZ (1997) *Angew Chem Int Ed Engl* 36:728
30. a) Fenyvesi E, Szenté L, Russell NR, McNamara M (1996) *Comp Supramolec Chem* 3:305; b) Harada A (2001) *Acc Chem Res* 34:456
31. a) Ogina H (1981) *J Am Chem Soc* 103:1303; b) Yamanari K, Shimura Y (1983) *Bull Chem Soc Jpn* 56:2283
32. Kim K (2002) *Chem Soc Rev* 31:96
33. Mock WL, Shih N-Y (1986) *J Org Chem* 51:4440
34. Busch DH, Burke JA, Jicha DC, Thompson MC, Morris ML (1963) *Adv Chem Series* 37:125
35. Schrauzer GN (1962) *Ber* 95:1438; Umland F, Thierig D (1962) *Angew Chem* 74:388
36. Curry JD, Busch DH (1964) *J Am Chem Soc* 86:592
37. a) Melson GA, Busch DH (1963) *Proc Chem Soc* 1963:223; b) Melson GA, Busch DH (1964) *J Am Chem Soc* 86:4830; c) Melson GA, Busch DH (1964) *J Am Chem Soc* 86:4834; d) Melson GA, Busch DH (1964) *J Am Chem Soc* 87:1706
38. Busch DH (1963) *Adv Chem Series* 37:1
39. a) Jicha DJ, Busch DH (1962) *Inorg Chem* 1:872; b) Robinson MA, Busch DH (1963) *Inorg Chem* 2:1171; c) Wrathall JW, Busch DH (1963) *Inorg Chem* 2:1182; d) Brubaker GR, Busch DH (1966) *Inorg Chem* 5:2110; e) Jicha DC, Busch DH (1962) *Inorg Chem* 1:878; f) Busch DH, Jicha DC (1962) *Inorg Chem* 1:884.
40. a) Krause RA, Jicha DC, Busch DH (1961) *J Am Chem Soc* 83:528; b) Busch DH, Burke JA, Jicha DC, Thompson MC, Morris ML (1963) *Adv Chem Series* 37:125; c) Busch DH, Jicha DC, Thompson MC, Wrathall JW, Blinn E (1964) *J Am Chem Soc* 86:3642
41. a) Truex TJ, Holm RH (1971) *Chem Comm* 1971:285; b) Honeybourne CL, Lucas C, Burchill P (1978) *Inorg Synth* 18:44; c) Hay RW, Lawrence GA, Curtis NF (1975) *J Chem Soc Dalton Trans* 1975:591; d) Owston PG, Peters R, Ramsammy E, Tasker PA, Trotter J (1980) *Chem Comm* 1980:1218
42. Weisman GR, Rogers ME, Wong EH, Jasinski JP, Paight ES (1990) *J Am Chem Soc* 112:8604
43. Boschetti F, Denat F, Espinosa E, Lagrange J-M, Guillard R (2004) *Chem Comm* 2004:588
44. Carver FJ, Hunder CA, Shannon RJ (1994) *Chem Comm* 1994:1277
45. Johnston AG, Leigh DA, Murphy A, Smart JP, Deegan MD (1996) *J Am Chem Soc* 118:10662
46. a) Busch DH (1967) *Helv Chim Acta* 1967:174; b) Melson G (1979) *Coordination chemistry of macrocyclic compounds*. Plenum, New York; c) Lindoy LF (1989) *The chemistry of macrocyclic ligand complexes*. Cambridge University Press, Cambridge, UK; d) Busch DH (1994) *Ligand design for enhanced molecular organization selectivity and specific sequencing in multiple receptor ligands and orderly molecular entanglements*. In: Fabbrizzi L, Poggi A (eds) *Transition metals in supramolecular chemistry*. Kluwer, Netherlands, p 55

47. Posner T (1898) *Berichte* 1898:656
48. Reppe W, Schlichting O, Klager K, Toepel T (1948) *Liebigs Ann Chem* 560:1
49. a) Curtis NS, House DA (1961) *Chem Ind* 1961:1708; b) Curtis NF (1968) *Coord Chem Rev* 3:3
50. Greene RN (1972) *Tetrahedron Lett* 1972:1793
51. Busch DH, Vance AL, Kolchinski AG (1996) Molecular template effect: Historical view, principles, and perspectives. In: Atwood JL, Davies JED, MacNicol DD, Vögtle F (eds) *Comprehensive supramolecular chemistry*, vol 9. Elsevier, New York, p 5
52. Busch DH (1963) *Adv Chem Series* 37:1
53. Busch DH (1964) *Rec Chem Prog* 25:107
54. Boston DR, Rose NJ (1968) *J Am Chem Soc* 90:6859
55. a) Parks JE, Wagner BE, Holm RH (1970) *J Am Chem Soc* 92:3500; b) Parks JE, Wagner BE, Holm RH (1971) *Inorg Chem* 10:2472
56. a) Muller JG, Takeuchi KJ (1989) *Polyhedron* 8:1391; b) Voloshin YZ, Trachevskii VV (1994) *J Coord Chem* 31:147
57. a) Creaser II, Harrowfield JM, Herlt AJ, Sargeson AM, Springborg J, Geue RJ, Snow MR (1977) *J Am Chem Soc* 99:3181; b) Creaser II, Geue RJ, Harrowfield JM, Herlt AJ, Sargeson A, Snow MR, Springborg J (1982) *J Am Chem Soc* 104:6016
58. a) Geue RJ, Hohn A, Ramph SE, Sargeson AM, Willis AC (1994) *Chem Comm* 1994:1513; b) Boucher HA, Lawrance GA, Lay PA, Sargeson AM, Bond AM, Sangster DF, Sullivan JC (1983) *JACS* 105:4652; c) Harrowfield JM, Herlt AJ, Lay PA, Sargeson AM (1983) *JACS* 105:5503; d) Marasami T, Endicott JF, Burbaker GR (1983) *J Phys Chem* 87:5057; e) Suh MP, Shiu W, Kim D, Kim S (1984) *Inorg Chem* 23:618; f) Brown KN, Geue RJ, Hambley TW, Hockless DCR, Rae AD (2003) *Org Biomol Chem* 1:1598
59. Bowman K, Riley DP, Busch DH, Corfield PWR (1975) *J Am Chem Soc* 97:5036
60. Perkins DF, Lindoy LE, Meehan GV, Turner P (2004) *Chem Comm* 2004:152
61. a) McMurray TJS, Raymond RN, Smith PH (1990) *Science* 244:938; b) Garrett TM, McMurry TJ, Hosseini MW, Reyes ZE, Hahn FE, Raymond KN (1991) *JACS* 113:2965
62. a) Schammel WP, Mertes KSB, Christoph GG, Busch DH (1979) *J Am Chem Soc* 101:1622; b) Stevens JC, Jackson PJ, Schammel WP, Christoph GG, Busch DH (1980) *J Am Chem Soc* 102:3283; c) Busch DH (1980) *Pure Appl Chem* 52:2477; d) Herron N, Cameron JH, Neer GL, Busch DH (1983) *J Am Chem Soc* 105:298; e) Busch DH, Stephenson NA, (1991) Inclusion compounds. In: Atwood JL, Davies JED, MacNicol DD (eds) *Inorganic and physical aspects of inclusion*, vol 276. Oxford University Press, Oxford, p 310
63. Feigl F (1919) *Chem Ztg* 163:30
64. Wasserman E (1960) *JACS* 82:4433
65. Wasserman E (1962) *Sci Amer* 207–5:94
66. a) Schill G, Lüttringhaus A (1964) *Angew Chem* 76:567; b) Schill G (1965) *Chem Ber* 98:2906; b) Schill G (1967) *Chem Ber* 100:2021
67. a) Lüttringhaus A, Isele G (1967) *Angew Chem Intl Ed Engl* 6:956; b) Schill G, Beckmann W, Vetter W (1973) *Angew Chem Intl Ed Engl* 12:665
68. a) Agam G, Graiver D, Zilkha A (1976) *J Am Chem Soc* 98:5206; b) Agam G, Zilkha A (1976) *J Am Chem Soc* 98:5214
69. Dietrich-Buchecker CO, Sauvage J-P (1983) *Tetrahedron Lett* 24:5095
70. Dietrich-Buchecker CO, Sauvage J-P (1984) *J Am Chem Soc* 106:3043
71. Mohr B, Weck M, Sauvage J-P, Grubbs RH (1997) *Angew Chem Int Ed Engl* 36:1308
72. Momenteau M, Le Bras F, Loock B (1994) *Tetrahedron Lett* 35:3289
73. a) Sauvage J-P, Weiss J (1985) *JACS* 107:6108; b) Guilhem J, Pascard C, Sauvage J-P, Weiss J (1988) *JACS* 110:8711; c) Dietrich-Buchecker CO, Khemiss A, Sauvage J-P (1986) *Chem*

- Comm 1986:1376; d) Dietrich-Buchecker CO, Khemiss A, Sauvage J-P (1985) JACS 107:8711
74. Bitsch F, Dietrich-Buchecker CO, Sauvage J-P, Van Dorsselaer A (1991) JACS 113:4023
75. a) Chambron J-C, Dietrich-Buchecker C, Sauvage J-P (1996) Transition metals as assembling and templating species: synthesis of catenanes and molecular knots. In: Atwood JL, Davies JED, MacNicol DD, Vögtle F (eds) Comprehensive supramolecular chemistry, vol 9. Elsevier, Oxford, UK, p 43; b) Collin J-P, Dietrich-Buchecker C, Gavina P, Jimenez-Molero MC, Sauvage J-P (2001) Acc Chem Res 34:477; c) Sauvage J-P (1990) Acc Chem Res 23:319; d) Dietrich-Buchecker C, Rapenne G, Sauvage J-P (1999) Coord Chem Rev 185–186:167
76. Ambinino DB, Stoddart JF (1995) Chem Rev 95:2725
77. a) Allwood BL, Spencer N, Shahriari-Zavareh H, Stoddart JF, Williams DJ (1987) Chem Comm 1987:1064; b) 78. Ashton PR, Slawin AMZ, Spencer N, Stoddart JF, Williams DJ (1987) Chem Comm 1987:1066
78. Ashton PR, Goodnow TT, Kaifer AE, Reddington MV, Slawin AMZ, Spencer N, Stoddart JF, Vincent JC, Williams DJ (1989) Angew Chem Int Ed Engl 28:1396
79. D'Acerno C, Doddi G, Ercolani G, Mencarelli P (2000) Chem Eur J 6:3540
80. a) Amabilino DB, Ashton PR, Reder AS, Spencer N, Stoddart JF (1994) Angew Chem Int Ed Engl 33:1286; b) Ashton PR, Baldoni V, Balzani V, Claessens CG, Credi A, Hoffmann A, Raymo FM, Stoddart JF, Venturi M, White AJP, Williams DJ (2000) Eur J Org Chem 2000:1121
81. a) Colquhoun HM, Stoddart JF, Williams DJ (1986) Angew Chem Int Ed Engl 25:487; b) Langford SJ, Pérez-García L, Stoddart JF (1995) Supramol Chem 6:11; c) Philip D, Stoddart JF (1996) Angew Chem Int Ed Engl 35:1154; d) Ambilino DB, Raymo FM, Stoddart JF (1996) Donor-acceptor template-directed synthesis of catenanes and rotaxanes. In: Atwood JL, Davies JED, MacNicol DD, Vögtle F (eds) Comprehensive supramolecular chemistry. Elsevier, Oxford, UK, p 43; Fyfe MCT, Stoddart JF (1999) Coord Chem Rev 183:139; f) Balzani V, Credi A, Raymo EM, Stoddart JF (2000) Angew Chem Int Ed Engl 39:3348; g) Pease AR, Jeppesen JO, Stoddart JF, Luo Y, Collier CB, Heath JR (2001) Acc Chem Res 34:433
82. Zhang Q, Hamilton DG, Feeder N, Teat SJ, Goodman JM, Sanders JKM (1999) New J Chem 23:897
83. a) Hansen JG, Feeder N, Hamilton DG, Gunter MJ, Becher J, Sanders JKM (2000) Org Letters 2:449; b) Hamilton DG, Daview JE, Prodi L, Sanders JKM (1998) Chem Eur J 4:608; c) Hamilton DG, Feeder N, Teat SJ, Sanders JKM (1998) New J Chem 22:1019
84. a) Hunter CA (1992) JACS 114:5303; b) Hunter CA (1991) Chem Comm 1991:749
85. Gibson HW, Lee S-H (2000) Can J Chem 78:347
86. a) Hildebrandt O-S, Meier S, Schmidt W, Vögtle F (1994) Angew Chem Int Ed Engl 33:1767; b) Vögtle F, Meier S, Hoss R (1992) Angew Chem Int Ed Engl 31:1619
87. Ottens-Hildebrandt S, Nieger M, Rissanen K, Rouvinen J, Meier S, Harder G, Vögtle F (1995) Chem Comm 1995:777
88. a) Johnston AG, Leigh DA, Pritchard RJ, Deegan MD (1995) Angew Chem Int Ed Engl 34:1209; b) Johnston AG, Leigh DA, Nezhad L, Smart JP, Deegan MD (1995) Angew Chem Int Ed Engl 34:1212; c) Leigh DA, Moody K, Smart JP, Watson KJ, Slawin AMZ (1996) Angew Chem Int Ed Engl 35:306
89. Baumann S, Jäger R, Ahui F, Kray B, Vögtle F (1997) Liebigs Ann/Recueil 1997:761
90. Schill G (1971) Catenanes, rotaxanes and knots. Academic, New York
91. Lüttringhaus A, Cramer F, Prinzbach H, Henglein FM (1958) Annalen 613:185
92. Frisch H, Martin I, Mark H (1953) Monatsh 84:250
93. Patat F, Derst P (1959) Angew Chem 71:105

94. Harrison IT (1972) *Chem Comm* 1972:231
95. Ashton PR, Baxter I, Fyfe MCT, Raymo FM, Spencer N, Stoddart JF, White AJP, Williams DJ (1998) *J Am Chem Soc* 120:2297
96. Harrison IT, Harrison S (1967) *JACS* 89:5723
97. Bravo JA, Orain D, Bradley M (2002) *Chem Comm* 2002:194
98. Schill G, Zjollenkopf H (1969) *Annalen* 721:53
99. Gibson HW, Breda MC, Engen PT (1994) *Prog Polym Sci* 19:843
100. Ashton PR, Huff J, Menzer S, Parsons IW, Preece JA, Stoddart JF, Tolley MS, White AJP, Williams DJ (1996) *Chem Eur J* 2:31
101. Pedersen CJ (1967) *JACS* 89:7017
102. a) Harada A, Kamachi M (1990) *Chem Comm* 1990:1322; b) Harada A, Li J, Kamachi M (1992) *Nature* 356:325; c) Wenz G, Keller B (1992) *Angew Chem Int Ed Engl* 31:197
103. Vögtle F, Mandel M, Meier S, Ottens-Hildebrandt S, Ott F, Schmidt T (1995) *Liebigs Ann* 1995:739
104. Lindoy LF (1995) *Nature* 376:293
105. Vögtle F, Dünnwald T, Händel M, Jäger R, Meier S, Harder G (1996) *Chem Eur J* 2:640
106. Jäger R, Händel M, Harren J, Rissanen K, Vögtle F (1996) *Liebigs Ann* 1996:1201
107. Reuter C, Mohry A, Sobanski A, Vögtle F (2000) *Chem Eur J* 6:1674
108. Dünnwald T, Jäger R, Vögtle F (1997) *Chem Eur J* 3:2043
109. Hübner GM, Glaser J, Seel C, Vögtle F (1999) *Angew Chem Int Ed Engl* 38:383
110. a) Reuter C, Wienand W, Hübner GM, Seel C, Vögtle F (1999) *Chem Eur J* 5:2692; b) Reuter C, Vögtle F (2000) *Org Lett* 2:593; c) Hübner GM, Reuter C, Seel C, Vögtle F (2000) *Synthesis* 1:103
111. Ghosh P, Mermagen O, Schalley CA (2002) *Chem Comm* 2002:2628
112. Bravo JA, Raymo FM, Stoddart JF, White AJP, Williams DJ (1998) *Eur J Org Chem* 1998:2565
113. a) Wisner JA, Beer PD, Drew MGB (2001) *Angew Chem Int Ed Engl* 40:3606; b) Wisner JA, Beer PD, Berry NG, Tomapatanaget B (2002) *PNAS* 99:4983
114. Wisner JA, Beer PD, Drew MGB, Sambrook MR (2002) *J Am Chem Soc* 124:12469
115. Curiel D, Beer PD, Paul RL, Cowley A, Sambrook MR, Szemes F (2004) *Chem Comm* 2004:1162
116. a) Ashton PR, Glink PT, Stoddart JF, Tasker PA, White AJP, Williams DJ (1996) *Chem Eur J* 2:729; b) Ashton PR, Glink PT, Stoddart JF, Menzer S, Tasker PA, White AJP, Williams DJ (1996) *Tetrahedron Lett* 37:6217
117. Kolchinski AG, Alcock NW, Roesner RA, Busch DH (1998) *Chem Comm* 1998:1437
118. Furusho Y, Hasegawa T, Tsuboi A, Kihara N, Takata T (2000) *Chem Lett* 2000:18
119. Hannam JS, Kidd TJ, Leigh DA, Wilson AJ (2003) *Org Lett* 5:1907
120. a) Loeb SJ, Wisner A (1998) *Angew Chem Int Ed Engl* 37:2838; b) Loeb SJ, Wisner A (1998) *Chem Comm* 1998:2757
121. Loeb SJ, Wisner JA (2000) *Chem Comm* 2000:845
122. Loeb SJ, Wisner JA (2000) *Chem Comm* 2000:1939
123. Glink PT, Schiavo C, Stoddart JF, Williams DJ (1996) *Chem Comm* 1996:1483
124. Amabilino DB, Ashton PR, Belohradsky M, Ramo FM, Stoddart JF (1995) *Chem Comm* 1995:751
125. Baddjic JD, Balzani V, Credi A, Lowe JN, Silvi S, Stoddart JF (2004) *Chem Eur J* 10:1926
126. Cao J, Fyfe CT, Stoddart JF (2000) *J Org Chem* 65:1937
127. Ashton PR, Ballardini R, Balzani V, Fyfe MCT, Gandolfi MT, Martinez-Diaz M-V, Morosina M, Schiavo C, Shibata K, Stoddart JF, White AJP, Williams DJ (1998) *Chem Eur J* 4:2332

128. Chiu S-H, Roway SJ, Cantrill SJ, Stoddart JF, White AJP, Williams DJ (2002) *Chem Comm* 2002:2948
129. a) Jimenez-Molera MC, Dietrich-Buchecker C, Sauvage J-P (2002) *Chem Eur J* 8:1456; b) Hoshino T, Miyauchi M, Kawaguchi Y, Yamaguchi H, Harada A (2000) *J Am Chem Soc* 122:9876
130. Ashton PR, Campbell PJN, Chrystal EJT, Glink PT, Menzer S, Philip D, Spencer N, Stoddart JF, Tasker PA, Williams DJ (1995) *Angew Chem Int Ed Engl* 34:1865
131. Ashton PR, Fyfe MCT, Hickingbottom SK, Stoddart JF, White AJP, Williams DJ (1998) *J Chem Soc Perkin Trans* 2:2117
132. Elizarov AR, Chang T, Chiu S-H, Stoddart JF, (2002) *Org Letters* 4:3565
133. Kim H-J, Jeon WS, Young HK, Kim K (2002) *PNAS* 99:5007
134. Kano K, Nishiyabu R, Asada T, Kuroda Y (2002) *J Am Chem Soc* 124:9937
135. Chang T, Heiss AM, Cantrill SJ, Fift MCT, Pease AR, Rowan SJ, Stoddart JF, White AJP, Williams DJ (2000) *Org Letters* 2:2947
136. Ashton PR, Christal EJT, Glink PT, Menzer S, Schiaro C, Spencer N, Stoddart JF, White AJP, Williams DJ (1996) *Chem Eur J* 2:709
137. Clifford T, Busch DH (2002) *PNAS* 99:4830
138. Zhender DW, Smithrud DB (2001) *Org Lett* 3:2485
139. Thomas C, Kolchinski AG, Busch DH (1999) unpublished results
140. Jäger R, Baumann S, Fischer M, Safarowsky O, Nieger M, Vögtle F (1997) *Liebigs Ann* 1997:2269
141. Gatti FG, Leigh DA, Nepogodiev SA, Slawin AM, Teat SJ, Wong JKY (2001) *J Am Chem Soc* 123:5893
142. Kim H-J, Jeon WS, Ko YH, Kim K (2002) *PNAS* 99:5007
143. Kawaguchi Y, Harada A (2000) *J Am Chem Soc* 122:3797
144. a) Avram L, Cohen Y (2002) *J Org Chem* 67:2639; b) Giastas P, Mourtzis N, Yannakopoulou K, Mavridis IM (2002) *J Inclusion Phen Macrocyclic Chem* 44:247; c) Kim B-S, Hong J-I (2002) *Chem Lett* 2002:336; d) Hwang HJ, Lee S, Part JW (2000) *Bull Korean Chem Soc* 21:245
145. Asakawa M, Jansses HM, Meijer EW, Pasini D, Stoddart JF (1998) *Eur J Org Chem* 1998:983
146. Agam G, Graiver D, Zilkha A (1976) *J Am Chem Soc* 98:5206
147. Seeman NC (1997) *Acc Chem Res* 30:357
148. Dietrich-Buchecker C, Sauvage P-P (1989) *Angew Chem Int Ed Engl* 28:189
149. a) Dietrich-Buchecker CO, Sauvage J-P (1992) *New J Chem* 16:277; b) Dietrich-Buchecker C, Sauvage J-P, De Cian A, Fischer J (1994) *Chem Comm* 1994:2231
150. Rapenne G, Dietrich-Buchecker C, Sauvage J-P (1999) *JACS* 121:994
151. Carina RF, Dietrich-Buschecker C, Sauvage J-P (1996) *JACS* 118:9110
152. Ashton PR, Matthews OA, Menzer S, Raymo M, Spencer N, Stoddart JF, Williams DJ (1997) *Liebigs Ann* 1997:2485
153. Safarowsky O, Nieger M, Fröhlich R, Vögtle F (2000) *Angew Chem Int Ed Engl* 39:1616
154. Vögtle F, Hunten A, Vogel F, Buschbeck S, Safarowsky O, Recker J, Parham A-H, Knott M, Müller WM, Müller U, Okamoto Y, Kubota T, Lindne W, Francotte E, Grimme S (2001) *Angew Chem Int Ed* 40:2468
155. Hunter CA, Mayers PC (2001) *Nature* 411:763
156. Janosch R, Müller WM, Müller U, Kubota K, Okamoto Y, Nieger M, Vögtle FJ (2002) *Chem Eur J* 8:4434
157. Hirsch A, Vostrowsky O (2001) *Top Curr Chem* 217:51
158. a) Lukin O, Recker J, Böhmer A, Müller WM, Kubota T, Okamoto Y, Nieger M, Fröhlich R, Vögtle F (2003) *Angew Chem Int Ed Engl* 42:442; b) Lukin O, Müller WM, Müller U, Kaufmann A, Schmidt C, Leszczynski J, Vögtle F (2003) *Chem Eur J* 9:3507

159. a) Pease AR, Jeppesen J, Stoddart JF, Luo Y, Collier CP, Heath JR (2001) *Acc Chem Res* 34:433; b) Ballardini R, Balzani V, Credi A, Gandolfi M, Venturi M (2001) *Acc Chem Res* 34:445; c) Harada A (2001) *Acc Chem Res* 24:456; d) Schalley CA, Beizai, K, Vögtle F, (2001) *Acc Chem Res* 34:465; e) Collin J-P, Dietrich-Buchecker C, Gavina MC, Jiménez-Molero MC, Sauvage J-P (2001) *Acc Chem Res* 34:4776; f) Amendola V, Fabbrizzi L, Magano C, Pallavicini P (2001) *Acc Chem Res* 34:488
160. Lukin O, Yoneva A, Vögtle F (2004) *Eur J Org Chem* 2004:1236
161. a) Schill G, Tafelmair F (1971) *Synthesis* 10:546; b) Schill G, Keller U, Fritz H (1983) *Chem Ber* 116:3675
162. a) Schill G, Doerjter G, Logemann E, Fritz H (1974) *Chem Ber* 112:3603; b) Schill G, Boeckmann J (1974) *Tetrahedron* 30:1945
163. Sokolov VI (1973) *Russian Chem Rev* 42:452
164. Hubin TJ, Busch DH (2000) *Coord Chem Rev* 200–202:5
165. Hubin TJ, Busch DH (1999) *Adv Supramol Chem* 5:334
166. Hubin TJ, Kolchinski AG, Vance AL, Busch DH (1999) *Adv Supramol Chem* 5:237
167. Boston DR, Rose NJ, (1968) *J Am Chem Soc* 95:4163

Macrocycle Synthesis Through Templatation

Zachary R. Laughrey · Bruce C. Gibb (✉)

Department of Chemistry, University of New Orleans, New Orleans LA 70148, USA
bgibb@uno.edu

1	Introduction	67
2	Scope of the Review	68
3	Macrocycle Synthesis Through Templatation	69
3.1	Covalent Bonds Between Template and Macrocycle	69
3.2	Ion-Ion Interactions Between Template and Macrocycle	71
3.3	Ion-Dipole Interactions (Including Coordinative Bonds) Between Template and Macrocycle	76
3.4	Hydrogen Bonds Between Template and Macrocycle	94
3.5	Cation- π Interactions Between Template and Macrocycle	111
3.6	π - π Stacking Between Template and Macrocycle	114
3.7	Van der Waals Forces Between Template and Macrocycle	117
3.8	Miscellaneous Non-covalent Interactions	119
4	Conclusions	121
	References	122

Abstract This review highlights the major advances over the last 5 years in the templated synthesis of carbon-based macrocycles. With selected examples, it focuses on the literature describing several developing areas of research including dynamic combinatorial libraries/dynamic covalent chemistry, and the extrapolation of templated macrocyclic synthesis to topologically complex structures.

Keywords Macrocycle · Templatation

Abbreviations

DCL Dynamic combinatorial library

RCM Ring closing metathesis

1 Introduction

Templates have been used through the ages to ensure that a desired object has the required shape. Thus, to build an arch or bridge from stone blocks, it is first necessary to construct a scaffold or template that takes the form of the archway.

The masonry is then built on this, before the scaffolding is removed to reveal the final structure. Likewise, a sheet-metal panel that forms part of the body of a car is pressed from a similarly shaped template, while a sculpture may be cast from a template that is a “negative” of the desired form.

At the molecular scale, templates ensure that out of a myriad of possible chemical reactions, only the one that leads to the target is promoted. Thus, DNA is a template for the synthesis of RNA, which in turn is a template for protein synthesis. Nature used templation to make humans, long before humans used templation to manipulate Nature. Although chemical templates have been around since time immemorial, it was not until the structure of duplex DNA was identified in 1953 [1] that the term “templation” entered the chemical lexicon. Shortly thereafter Todd suggested that templates might one day be used to control chemical processes [2], but it wasn’t until 1963/64 that Busch and his coworkers obliged by reporting the first synthetic, chemical templation process [3]. Since that time, templation in synthetic chemical systems has grown and diversified immensely; most famously perhaps with Pedersen’s templated synthesis of crown ethers [4, 5].

2

Scope of the Review

Two recent books thoroughly review the templation literature prior to 1999 [6, 7]. This review highlights the major conceptual advances over the last 5 years in the templated synthesis of carbon-based macrocycles. It is therefore not intended to be comprehensive. Within the last 5 years, over 500 papers have been published on the topic of “macrocycle/templation”. A perusal of these papers reveals that about two-thirds of these report on the continuing efforts to form new catalysts and contrast reagents for medical imaging with tried and trusted cyclam derivatives; particularly mono- and multinuclear transition metal and lanthanide complexes of Schiff-bases [8–10]. Readers interested in this topic are directed towards a recent review [11]. This review focuses on the remaining third of the literature that describes several developing areas of research such as dynamic combinatorial libraries (DCL)/dynamic covalent chemistry [12], or the extrapolation of templated macrocyclic synthesis to topologically more complex catenanes or knots [13–15]. Several caveats should be added to this statement. This review will not cover (poly-macrocyclization) carceplex reactions [16–19] nor the synthesis of porphyrins and polypyrrolic macrocycles [20, 21]. Both these important topics have been recently surveyed. Likewise, this review will not comprehensively cover macrocyclization reactions such as the McMurray reaction or ring closing metathesis (RCM). These popular synthetic methods have on occasion been shown to involve templation [22]. However, the majority of literature examples are framed in the context of synthesis rather than templation. As a result, most of the specific systems were not examined for template effects. That said, RCM does figure prominently in this review, as a tool

to close macrocycles that are being templated by other means. In addition, the different ligation methods used to form large cyclic peptides will not be specifically covered by this review [23].

3

Macrocycle Synthesis Through Templatation

This review is organized according to the interactions between template and incipient macrocycle. As most cases of templatation occur through more than one type of interaction, this categorization is by no means unequivocal. In ambiguous cases, we have categorized the example according to the interaction that is observed to or believed to predominate. Although this categorization is not always ideal at the level of individual templatation processes, it does give an interesting picture of the “popularity” of the different methods of templatation.

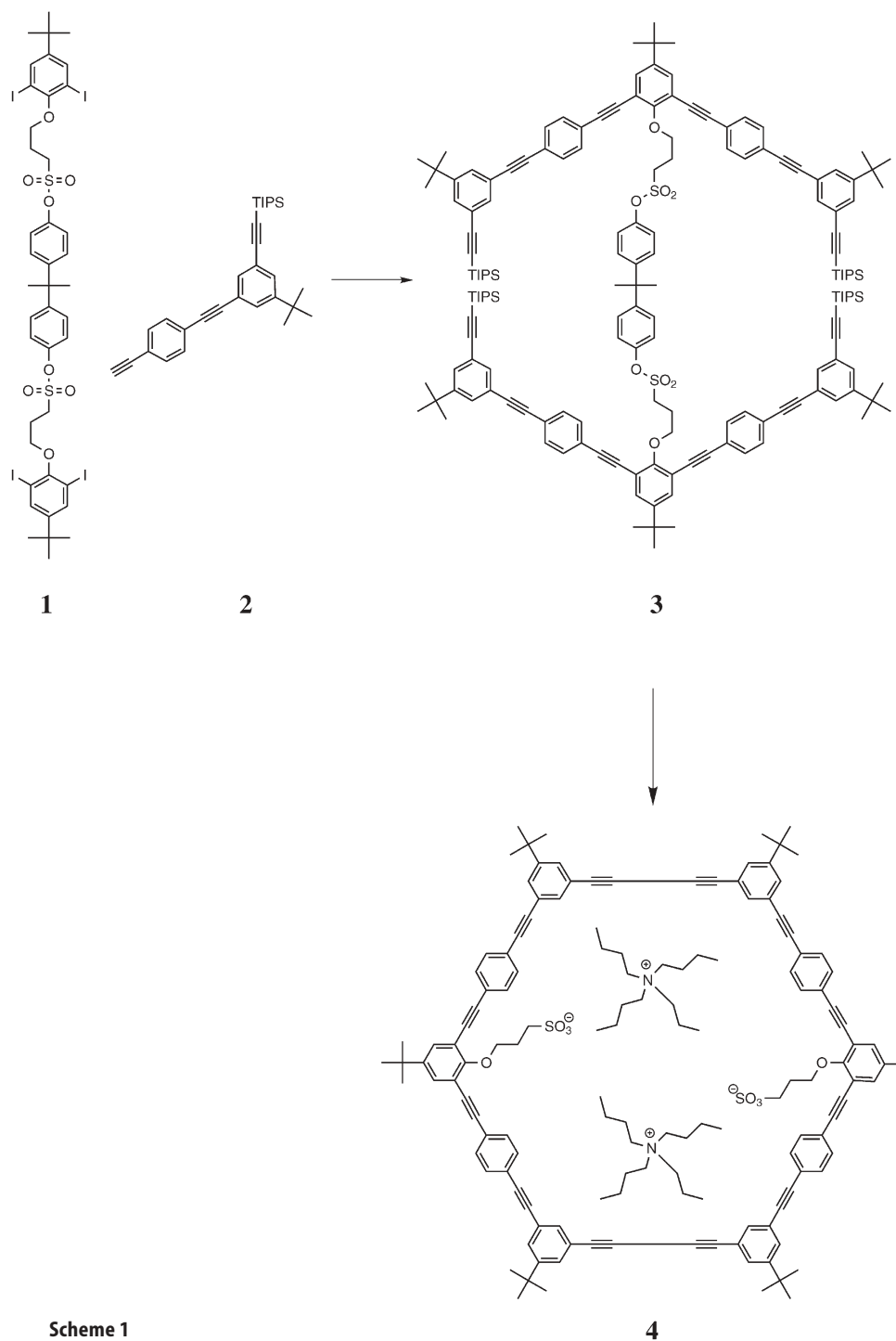
3.1

Covalent Bonds Between Template and Macrocycle

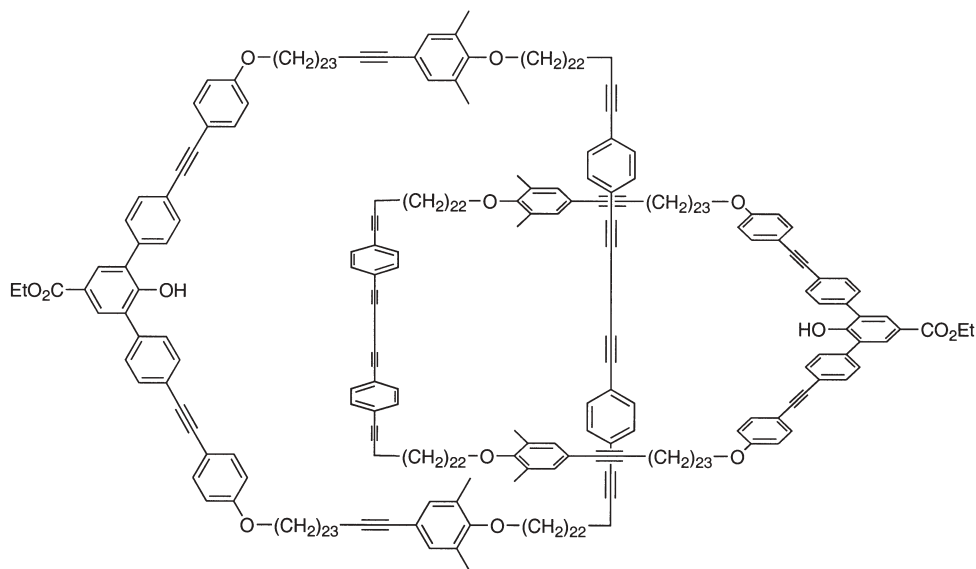
The majority of templatation approaches involve non-covalent forces between incipient macrocycle and template; the use of covalent bonding is less well studied. As a strategy, covalent linking between template and precursor has the disadvantage that the template must be removed in a subsequent step. However, the strong bonding in the precursor helps ensure that the templatation process goes according to plan and in high yield. Two strategies are apparent. The template may be “linear”. In other words, it is joined to the incipient macrocycle at two sites. Alternatively, the template may have more than two bonding sites that radiate out from its center.

The Höger group has utilized a number of different functionalities including carboxylic and sulfonic ester linkages to connect premacrocycle and template [24–27]. As with other covalent approaches, the template also acts as a protecting group for the functionality present in the final macrocycle. By way of example, the oxidative coupling of tetra-iodide **1** and silane **2** led to **3** (Scheme 1). Removal of the protecting groups, oxidative coupling and removal of the bis-phenol A template gave the desired macrocycle **4** in 85% yield.

In working towards the synthesis of polymeric catenanes, the Godt group has used covalent bonding to template the synthesis of very large macrocycles. The [2]catenane **5** comprised of two interlocked 147-membered rings, was synthesized by using a carbonate linker to joint the necessary subunits. Thus, coupling the phenol groups of **6** and **7** with phosgene, gave **8** (Scheme 2), which upon oxidative cyclization gave the corresponding precatenane. Hydrolysis of the carbonate group gave the desired [2]catenane **5** [28, 29]. However, even with such a “sure” template, the inherent flexibility of each chain led to some inter-strand macrocyclization and the formation of **9**. A slightly different approach



Scheme 1



5

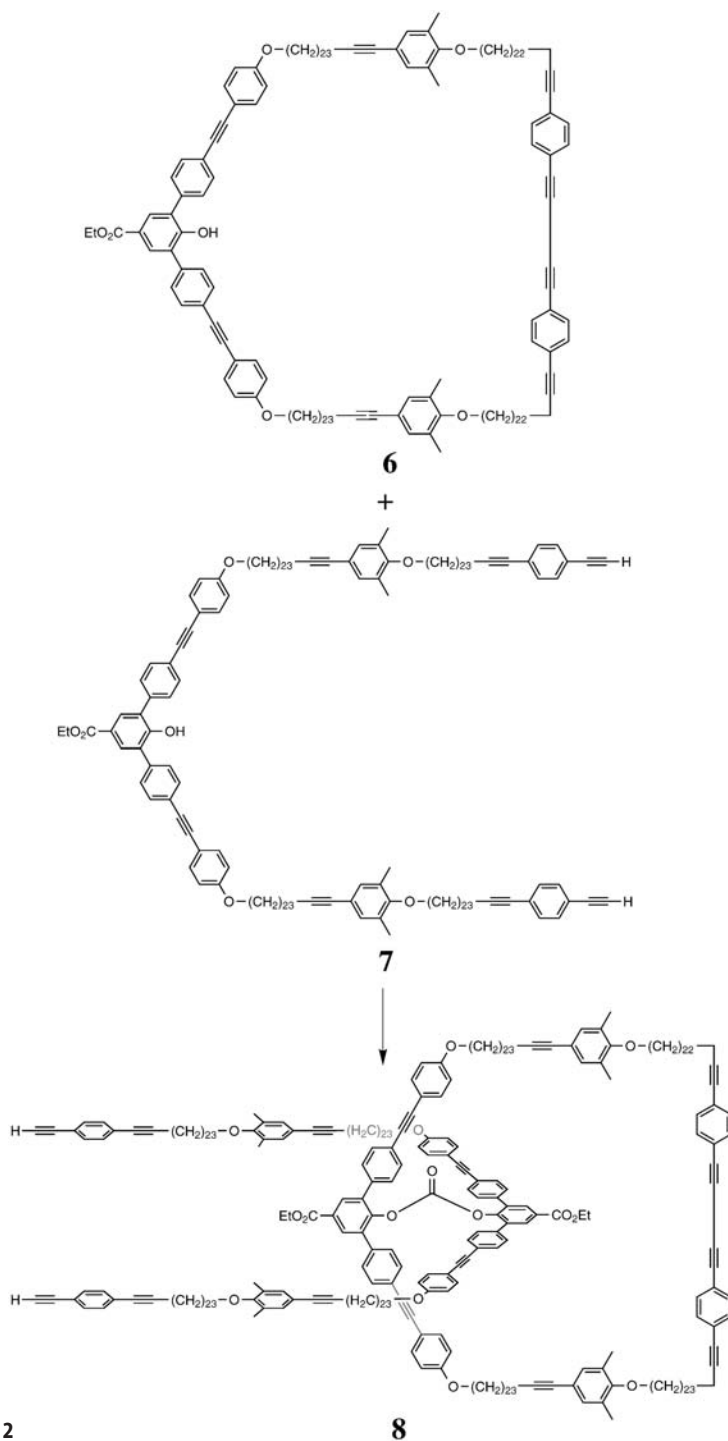
has also been reported in which, for example, two molecules of **10** are joined by reacting the phenol groups with phosgene, before (bis)cyclization and subsequent removal of the template [30]. However, in such cases the major product produced in 65% yield was “dimer” macrocycle **11**.

Resorcinarenes such as **12** have recently been identified by the Gibb group as examples of covalent templates possessing four, radiating, bonding sites [31, 32]. In the first step (Scheme 3), one set of moieties is added to the resorcinarene in a stereoselective manner to make a series of deep-cavity cavitands (**13**). Next, these tethered groups are linked together to form a series of molecular baskets, e.g., **14**. These molecules possess interesting hosting properties in their own right [33]. However, treatment with BBr_3 results in the cleavage of the four acetal groups of these types of compounds and the isolation of macrocycles such as **15** in very good yields.

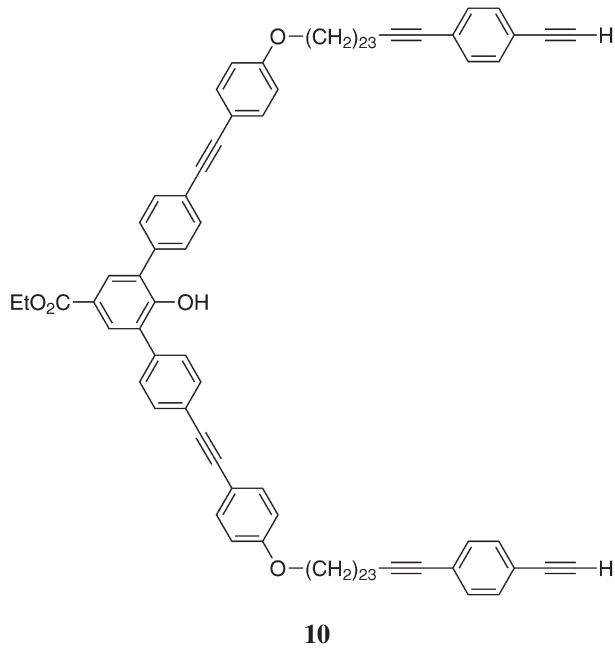
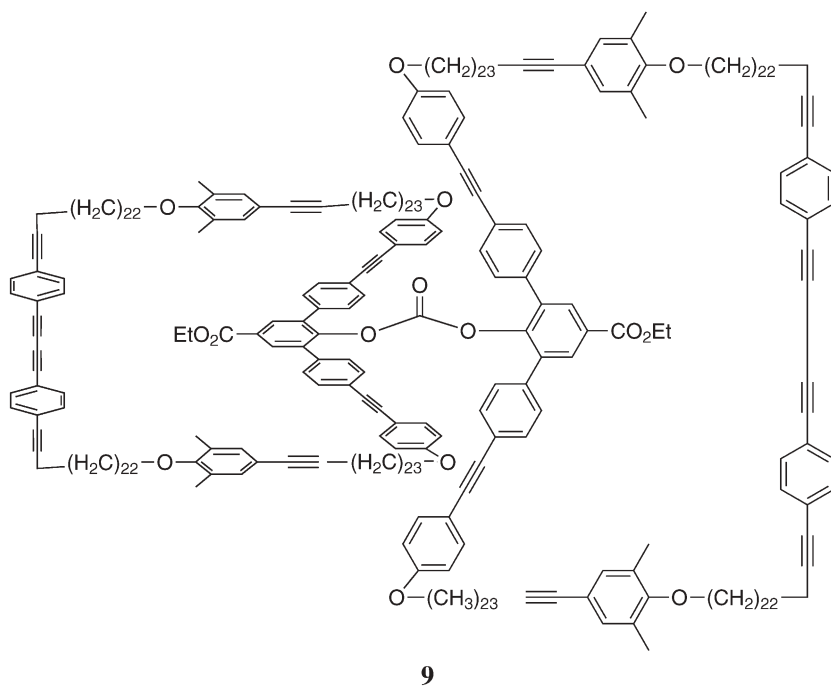
3.2

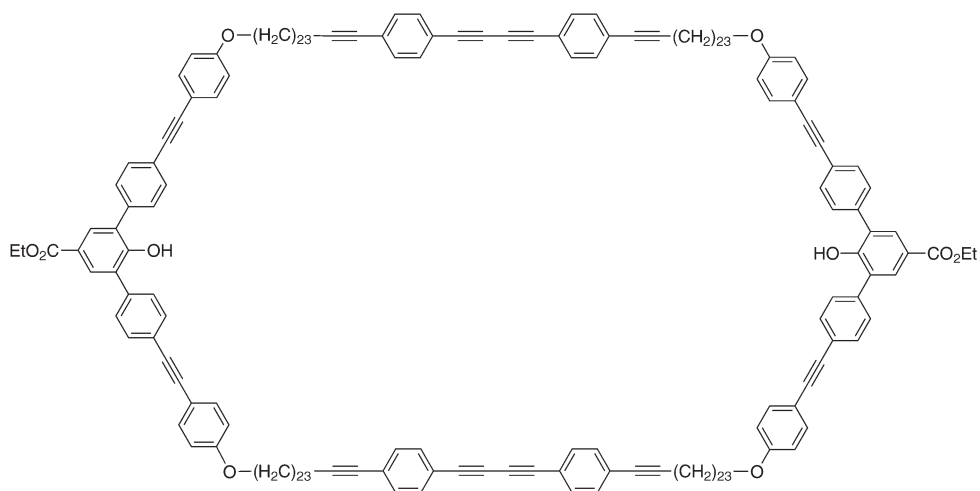
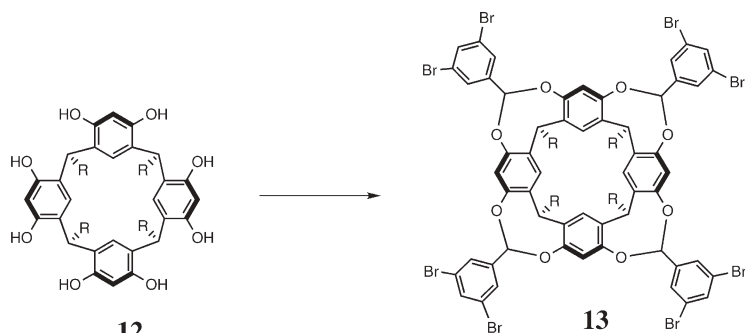
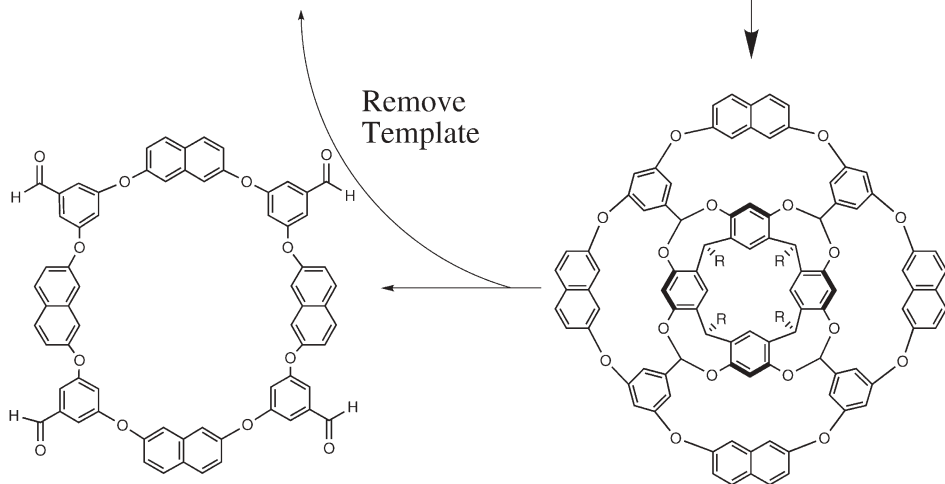
Ion-Ion Interactions Between Template and Macrocycle

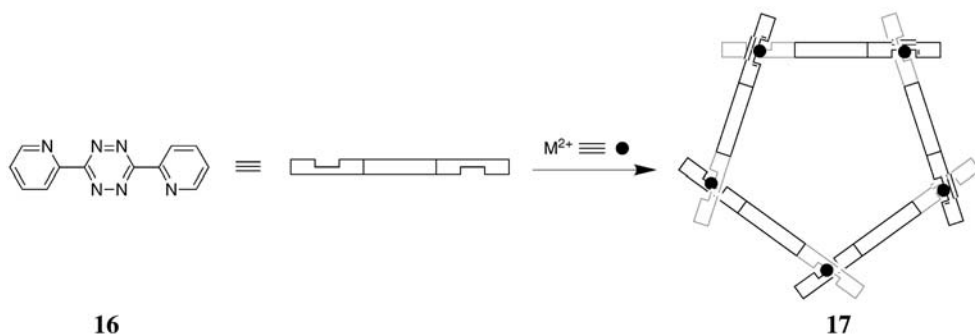
The bulk of templates are smaller than the intended product; the interactions between template and incipient macrocycle radiate out from the former. Such an example involving ion-ion interactions has been reported by the Dunbar group (Scheme 4). Thus, mixing of ligand **16** and either Ni^{2+} or Zn^{2+} results in the formation of either molecular squares [34], or molecular pentagons [35], depending on the counter-ion of the metal. The solid-state structure of the pentagon **17** shows the SbF_6^- counter ion filling the cavity of the host. However, this



Scheme 2

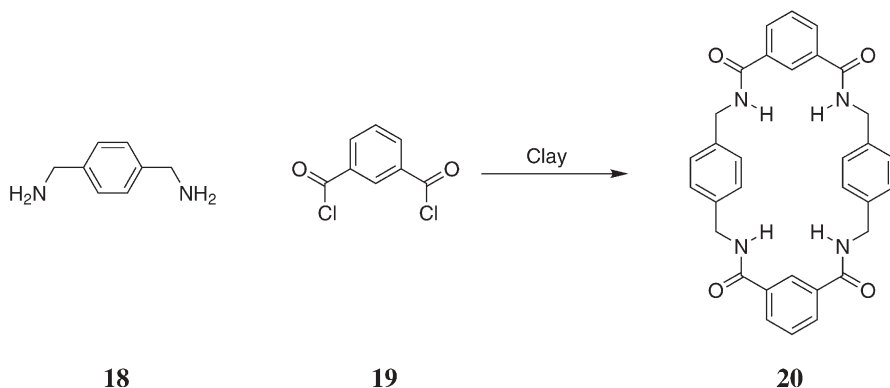


**11****12****13****Scheme 3****15****14**

**Scheme 4**

cavity is too big for smaller anions such as BF_4^- . Thus, in the presence of tetrafluoroborate salts, the same reaction leads to the formation of the corresponding square.

A recent trend in the literature is the development of the “opposite” strategy to the one just outlined, whereby the template is larger than the target. To switch supramolecular dialects, the template becomes the host rather than the guest. One example of this strategy is the use of smectite clays [36]. Thus, when the dihydrochloride salt of diamine **18** is inserted between the layers of clay, a pillared clay structure is formed that is capable of taking up the neutral diamine. The resulting intercalated hemisalt is then treated with acid chloride **19** to give a 60% yield of macrocycle **20** (Scheme 5). In the absence of the template, the precursors form polymers or undergo self-templation to form the corresponding [2]catenane. By this strategy, a number of tetra-amide macrocycles were synthesized in yields between 30 and 65% [37].

**Scheme 5**

3.3

Ion-Dipole Interactions (Including Coordinative Bonds) Between Template and Macrocycle

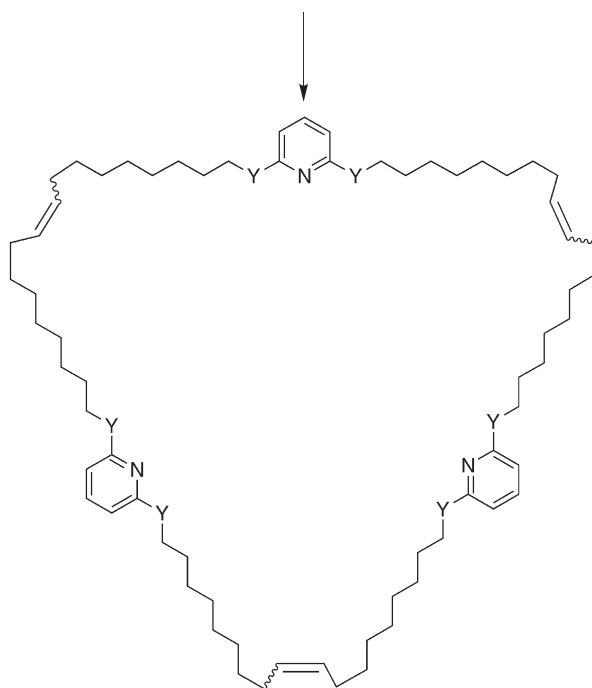
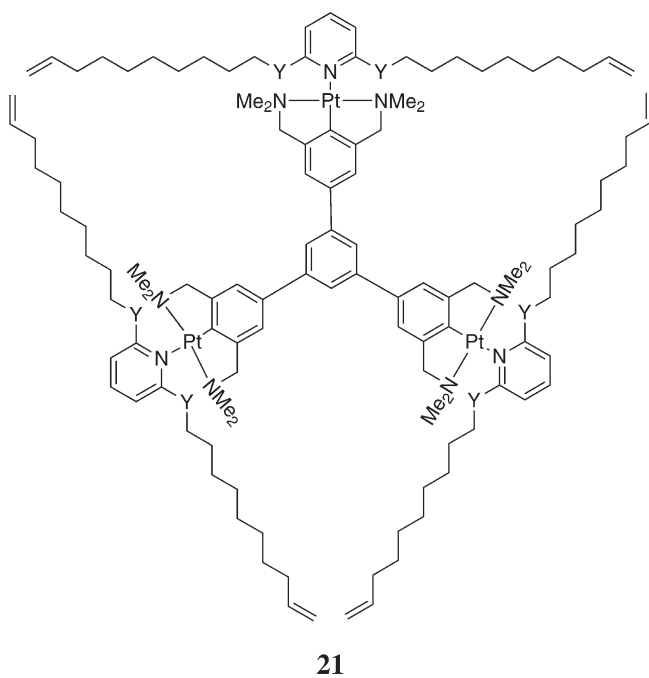
Along with hydrogen bonding, metal coordination continues to be one of the most popular means by which to affect templation. The recent literature has reported upon the synthesis of both macrocycles and higher topology entities such as helical structures, catenanes and knots. The different examples given below illustrate several points including the importance of phenanthroline and bipyridine ligands for coordinating to the (metal ion) template, and the utility of the RCM strategy to efficiently perform macrocyclizations.

With regard to the formation of macrocycles, major new thrusts have included the development of dynamic combinatorial libraries, new strategies for phosphocrown synthesis, and the use of more “traditional” templation strategies in the total syntheses of natural products. As just alluded to, RCM plays a role in many of these cases. An example of the efficacy of the RCM strategy has been reported by van Koten in the synthesis of 69- and 72-membered macrocycles [38, 39]. Thus, treatment of complex **21** ($Y=O$) with a Grubbs catalyst and removal of the template gave macrocycle **22** ($Y=O$) in 67% yield (Scheme 6). As the macrocycle existed as a mixture of *cis* and *trans* isomers, the double bonds were reduced quantitatively to yield the corresponding alkane. By a similar templation process, the slightly larger macrocycle **22** ($Y=CH_2O$) was formed in 44% yield.

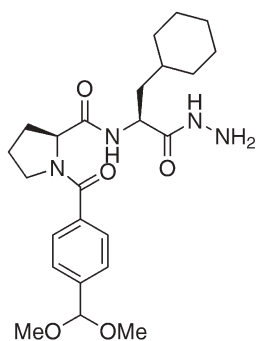
A major focus of the Sanders group is the development of dynamic combinatorial libraries. In a study of the generation of macrocyclic hydrazones via the acid catalyzed reaction between bifunctional building blocks containing a hydrazine group and a protected aldehyde, they noted that the addition of lithium and sodium iodides adjusted product distribution [40, 41]. For example, in the absence of a template **23** formed the corresponding “dimer”, “trimer” **24**, “tetramer”, “pentamer” and “hexamer”, with the cyclic “tetramer” predominating. In contrast, upon addition of LiI the ‘trimer’ complex accounted for more than 95% of the products of the library. Neutralization froze the library and allowed the isolation of **24**. An analysis of its complexation properties showed that lithium ion coordination to the carbonyl groups of the macrocycle was important to assembly. Nevertheless, assembly was entropically driven.

Ammonium ions have also been used by the Sanders group as templates in macrocyclizations with **25** [42]. The relative affinities of the various templates for the isolated receptors correlated with their ability to focus the library. The same group have also noted that immobilization of the template on a solid support need not effect its ability to focus a library [43]. Thus, the selection and amplification of trimer **26** with benzyltrimethyl ammonium ion occurred both in solution and when the template was immobilized on a solid support.

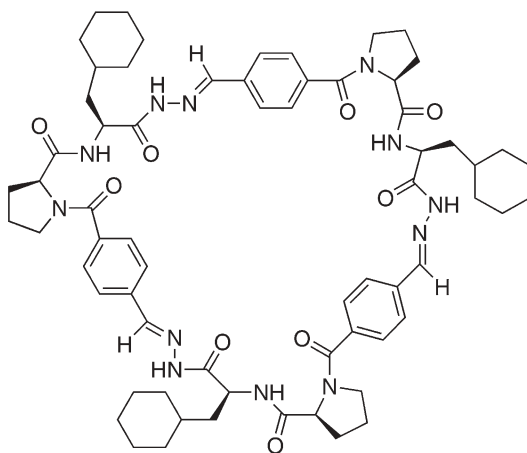
The Sanders group have also reported on the use of palladium-catalyzed allyl transesterifications to reversibly form macrocycles (Scheme 7) [44]. In the absence of a suitable template, porphyrin dimer **27** ($R=\text{hexyl}$) and succinic acid reacted to produce macrocycle **28** ($X=-CH_2CH_2-$) in less than 2% yield. In con-



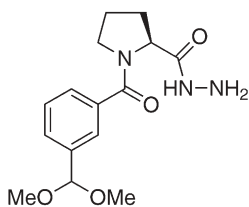
Scheme 6



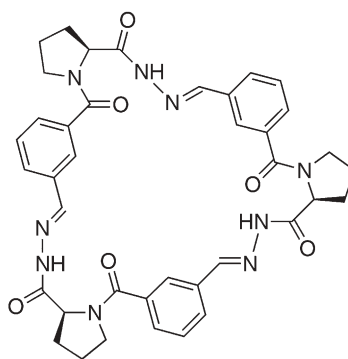
23



24



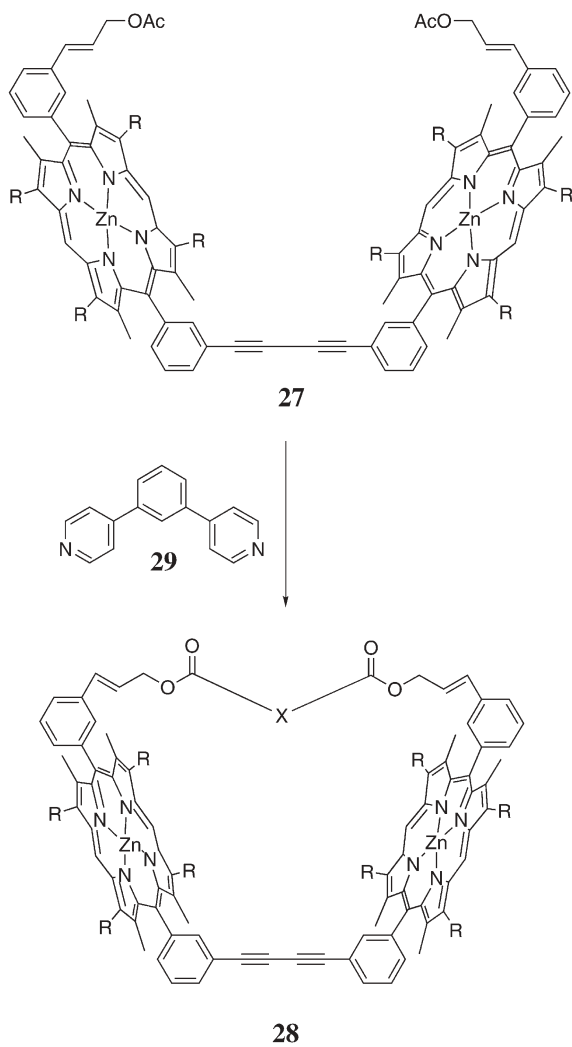
25



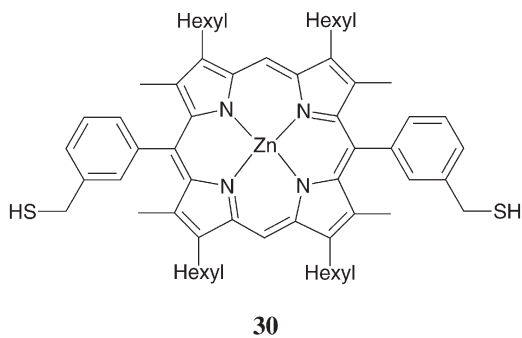
26

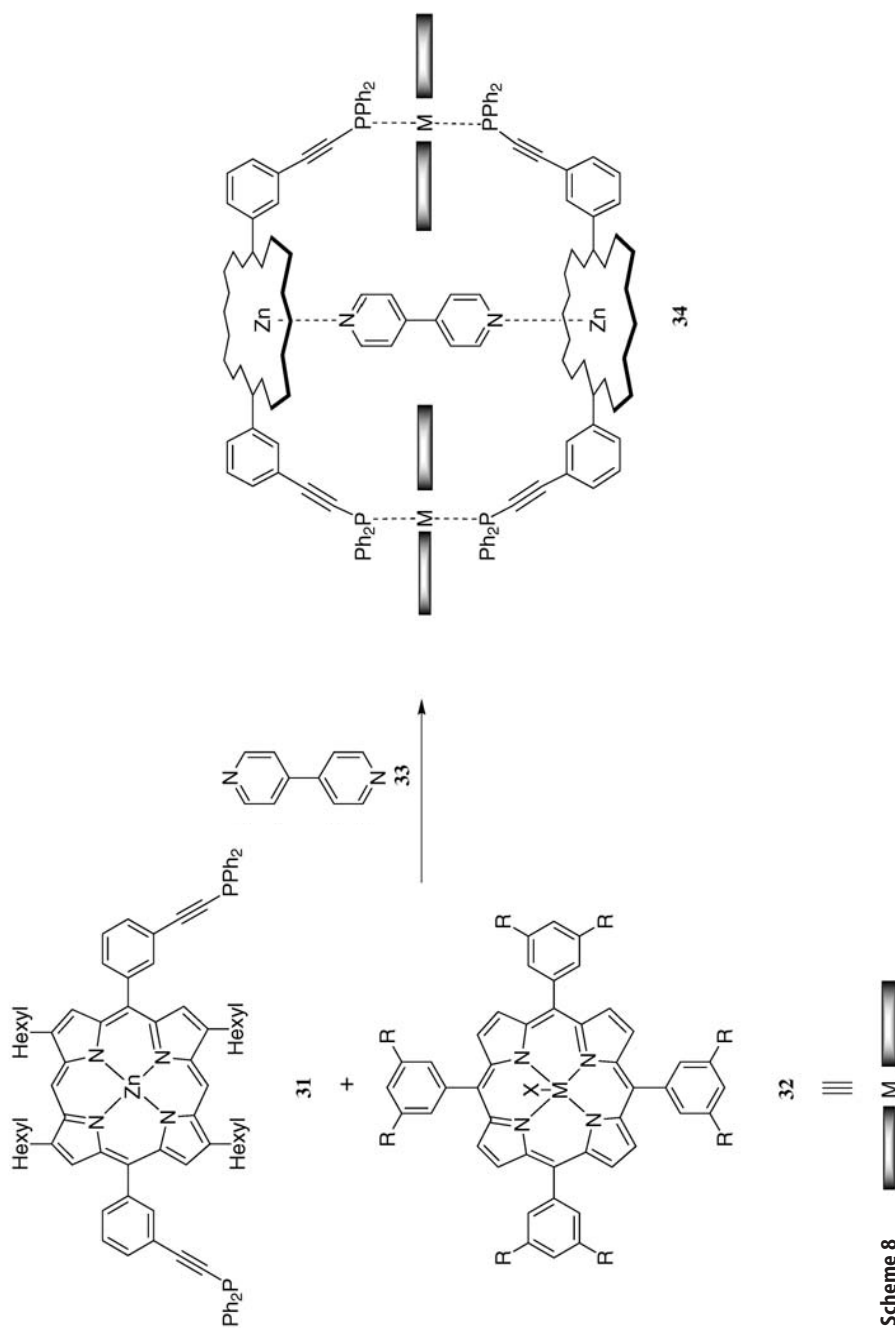
trast, addition of template **29** to the reaction resulted in a 10% yield of the desired product. An analogous system in which the porphyrin subunits are driven together by the formation of disulfide bonds has also been reported [45]. These studies centered on the oligomerization and cyclization of bis-thiol **30**. Templates could be used to control the library of products such that the dimer, trimer or tetramer predominated.

A final example from the Sanders group is the use of DCLs to form mixed-metal porphyrin cages (Scheme 8) [46]. Combining two equivalents of zinc porphyrin **31**, two equivalents of porphyrins such as **32** containing either ruthenium or rhodium centers, and one equivalent of a template such as 4,4-bipyridine **33**, leads to cage structures of general structure **34**. Variations in the structure of the template, and the structures of the Ru/Rh porphyrins, identified which combinations of subunits lead to successful assembly.

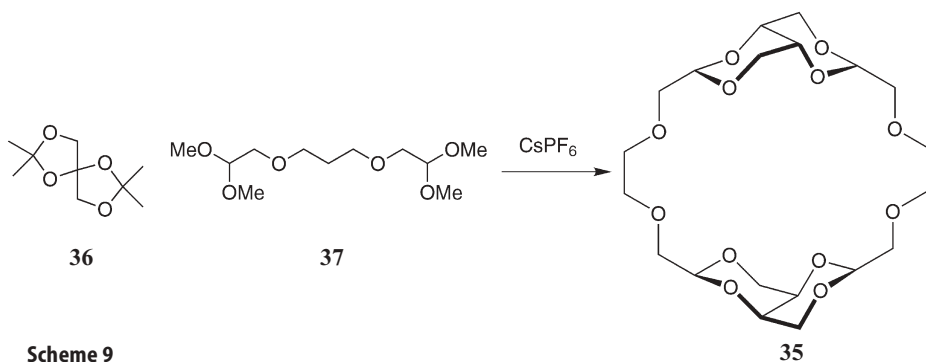


Scheme 7



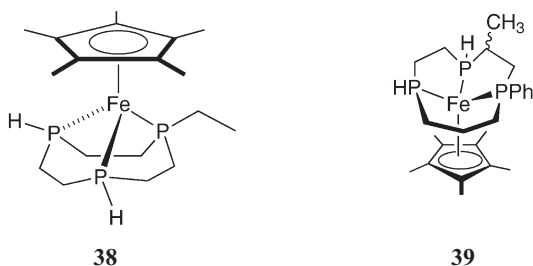


Dynamic covalent chemistry has also been used to efficiently form macrocyclic polyether **35** (Scheme 9) [47]. In the absence of a template, transacetalations between subunits **36** and **37** generated a library of products in which both the number of subunits that come together and the constitution of the bis-acetal moieties were variables. The addition of CsPF₆ focused the library such that **35** constituted >95% of the library. Scale-up led to an un-optimized 58% yield of the macrocycle, whereas the stepwise (kinetic) approach to the same compound gave a maximal overall yield of 1.4%.

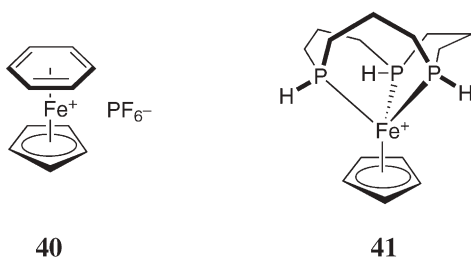


Scheme 9

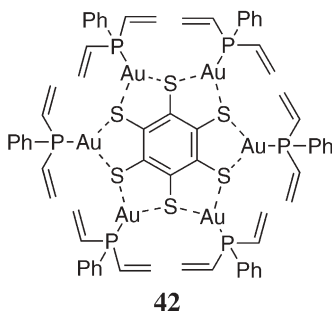
The synthesis of phosphorus-containing macrocycles has lagged somewhat behind the synthesis of crown ethers and aza-crowns. Towards closing this gap, the Edwards group has recently pioneered new approaches to small triphosphorus macrocycles. Using $[\eta^5\text{-CpFeL}_3]^+$ complexes they have synthesized in a step-wise manner the first examples of 9-membered [48, 49] (**38**) and 10-membered [50] (**39**) triphosphorus macrocycles. In these particular cases, the stereochemically controlled liberation of the ligand have yet to be reported.



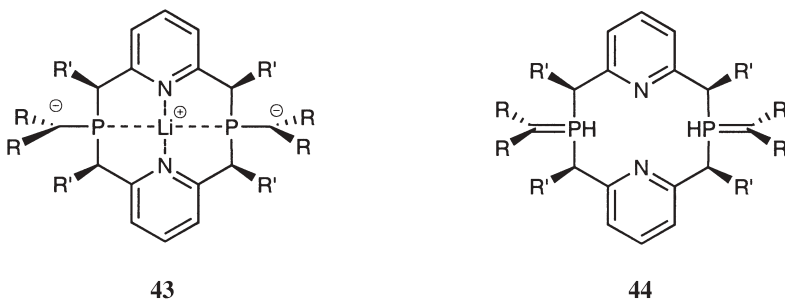
Using a similar template, the same group has also reported the synthesis of substituted 1,5,9-triphosphacyclododecanes [51]. For instance, when the benzene ring in complex **40** was displaced with three allylphosphines and the resulting triallylphosphine irradiated, macrocycle **41** was formed. Alkylation of the phosphorus atoms could then be carried out, before the macrocycle was liberated from the template.



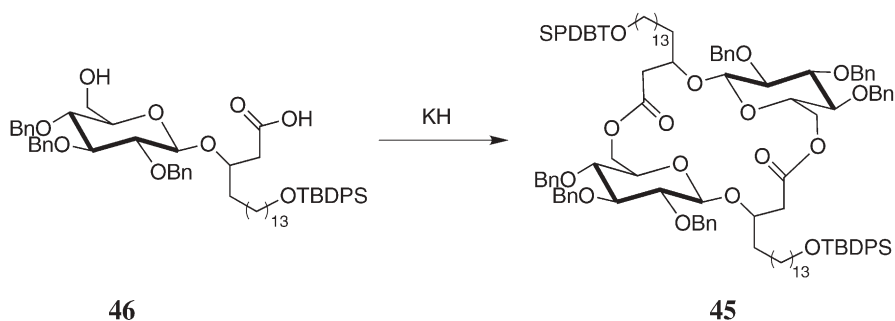
The templated synthesis of much larger polyphosphine macrocycles has been reported by Harnisch and Angelici [52]. Their ingenious approach is to use benzenhexathiolate as a template. Treatment with $((\text{CH}_2\text{CH})_2\text{PhP})\text{AuCl}$ leads to “golden wheel” **42**, which upon irradiation gave the templated macrocycle.



Metal ion templation has also been used in the synthesis of anionic macrocycles **43** ($\text{R}=\text{Ph}$ or SiMe_2). Protonation of the tetra-phenyl species led to the corresponding phosphorus/nitrogen macrocycle that formed complexes of unusual geometry [53]. In contrast, the chemistry of the octa-silyl derivative **43** ($\text{R}=\text{SiMe}_2$) was quite different [54]. Protonation instead led to the P-H ylide **44** ($\text{R}=\text{SiMe}_2$). Calculations suggested that steric crowding led to the high kinetic stability of the ylide.

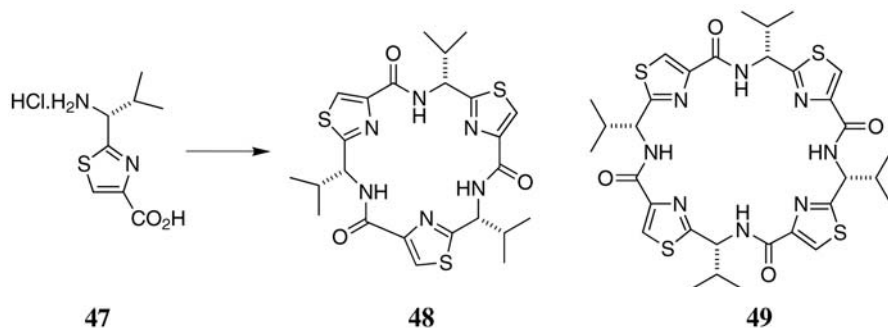


Some of the more traditional templation approaches are sufficiently well understood that they are beginning to be applied to the total synthesis of structurally complex natural products. By way of example, the Fürstner group has used templation processes in their elegant syntheses of complex glycolipids [55]. For example, the lactide core of Cycloviracin B₁ **45**, is built by the templated combination of two equivalents of **46** (Scheme 10). In the absence of potassium ion, coupling the fragments leads to the formation of a cyclic monomer (28%), the desired dimer **45** (37%), and several other oligomeric products (35%). Using potassium hydride as the base resulted in a 75% of the desired core, and allowed the efficient synthesis of the target [56, 57]. Sodium and cesium ions proved less efficient templates. The isolation of appreciable amounts allowed the full structural assignment of Cycloviracin B₁ and an investigation of its antiviral properties [56]. A similar strategy was implemented by Cleophax et al. in the synthesis of the macrocyclic core of cycloviracin and glucolipsin [58].



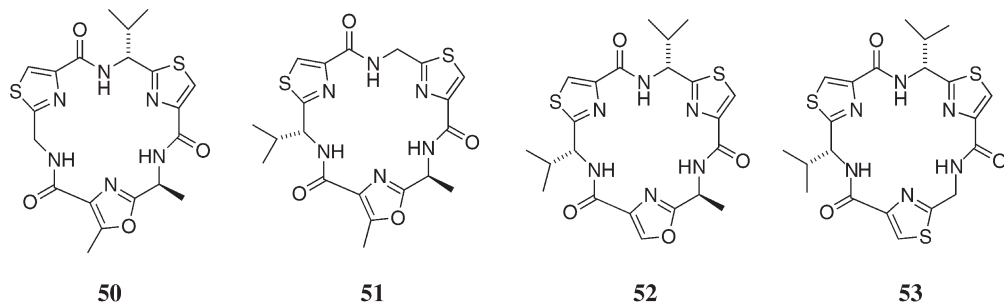
Scheme 10

Pattenden et al. have examined the metal templated cyclooligomerization of modified amino acids to form unusual marine metabolites and related derivatives. The treatment of **47** with a coupling reagent and *i*-Pr₂NEt gave a 95% yield of trimer **48** and tetramer **49** in a 3:1 ratio (Scheme 11); the subunit is predisposed to cyclize [59].



Scheme 11

Adding metal ions to the reaction changed its outcome such that the ratio of products varied from 4:1 to 7:3. Furthermore, when a 1:1:1 mixture of three different amino acid derivatives were subjected to the same macrocyclization conditions, of a possible eleven products, only nostricyclamide **50** and three other products **51**, **52**, and **53** could be isolated in a combined yield of 65% [60]. In this system, the addition of copper ions gave a 2:1 mixture of nostracyclamide **50** and **51** (ca. 20% yield), whereas silver ions resulted only in a 15% yield of **52**.



Remaining on the topic of using templation to form otherwise difficult to synthesize natural products, Hesse recently published a shortened synthesis of the spermidine (+)-(*S*)-dihydroperiphylline [61]. The key step in this synthesis is the Cs⁺ templated *bis*-alkylation of **54** with bis(methylsulfonyl)propane to give intermediate **55** in 78% yield (Scheme 12).

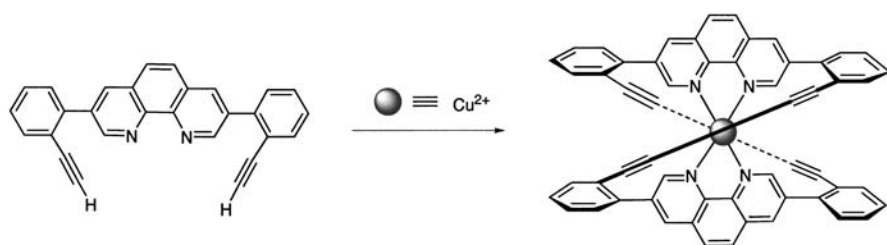


Scheme 12

54**55**

The recent synthesis of topologically more complex structures via ion-dipole interactions has relied heavily on bipyridine and phenanthroline ligands. RCM has also proven to be a useful tool in such syntheses.

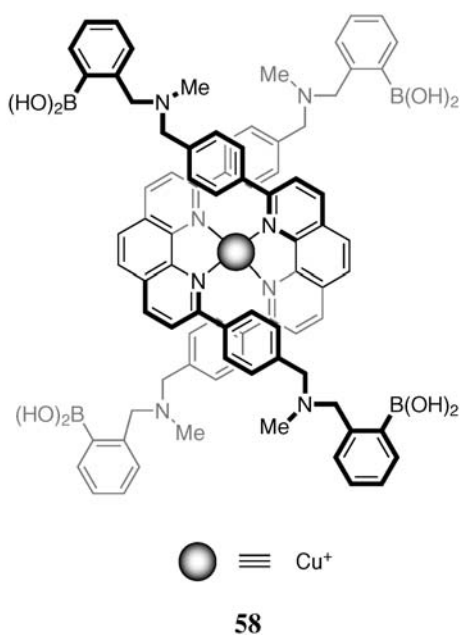
With respect to the formation of helical structures, Heuft and Fallis recently revealed the synthesis of helical cyclophane **56**, available from phenanthroline **57** in 84% yield (Scheme 13) [62]. Copper(II) acted as both template and reagent for this conversion. One equivalent of copper acetate gave the corresponding complex, a subsequent 5.5 equivalents was used to covalently join the two phenanthrolines. If only six equivalents of copper ion were added to the solution of the ligand, a yield of only 15% was obtained.



Scheme 13 57

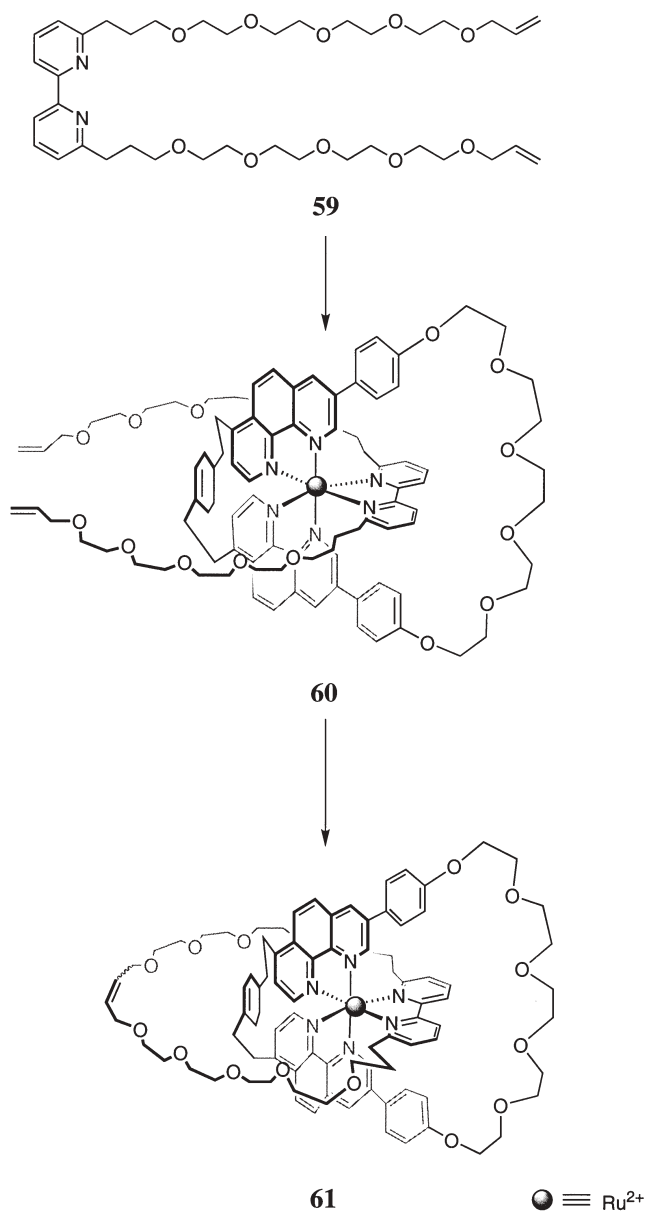
56

Phenanthroline derivatives and copper ion templation have also been used to form helicates and catenates comprised in part by sugars [63]. The requisite precursor complex **58** was formed by treating the corresponding phenanthroline ligand with copper ion. Addition of sugars to solutions of this complex led to one of two types of products. Two equivalents of glucose for example partake in *inter*-strand linking to form a helicate, whereas two molecules of maltopentose form *intra*-strand links to give the corresponding catenate.



Both strategies of [2]catenane synthesis, threading and double ring closure, have figured prominently in the recent literature. Research from the Sauvage group has examined the formation of [2]catenanes using ruthenium ions [64, 65] and rhodium ions as templates [66]. In the first instance, threading 6,6'-di-

substituted bipyridine **59** through the respective macrocyclic ruthenium complex gave catenane precursor **60** in 56% yield (Scheme 14). Ring-closing metathesis then gave catenate **61** in 68% yield [64, 65]. The related, rhodium-templated catenane with slightly shorter, 4,4'-alkene chains on the bipyridine moiety, was obtained via a less efficient threading (14%) and RCM (34%) processes [66].



Scheme 14

Scheme 15

62

63

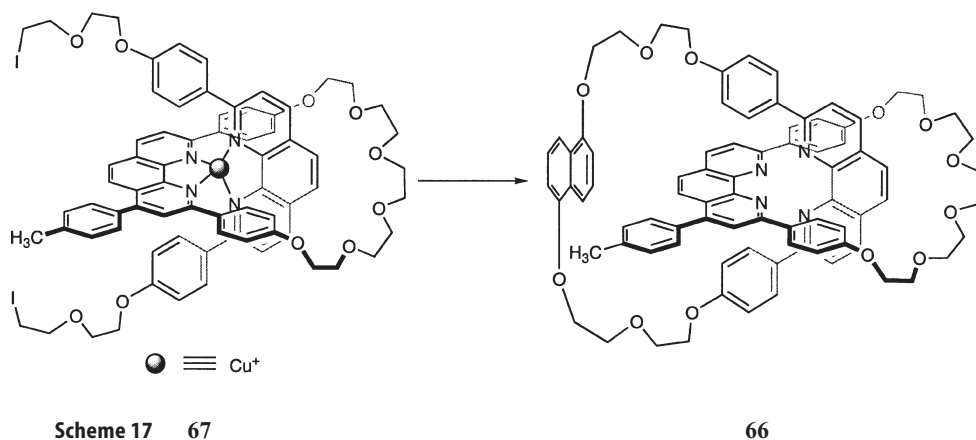
● ≡ Ru²⁺

Scheme 16

64 $\xrightarrow{\hspace{2cm}}$ 65

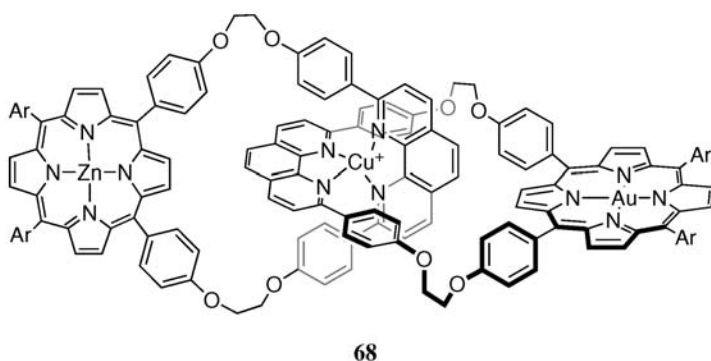
Legend: $\bullet \equiv \text{Zn}^{2+}$

Copper templation led to the stereochemical curiosity **66**. Thus, reaction between complex **67** and 1,5-dihydroxynaphthalene, followed by removal of the copper ion, led to **66** in 35% yield (Scheme 17) [69]. [2]Catenane **66** is an example of an achiral molecule that possesses two enantiomeric conformations that are interchangeable only via chiral conformations.

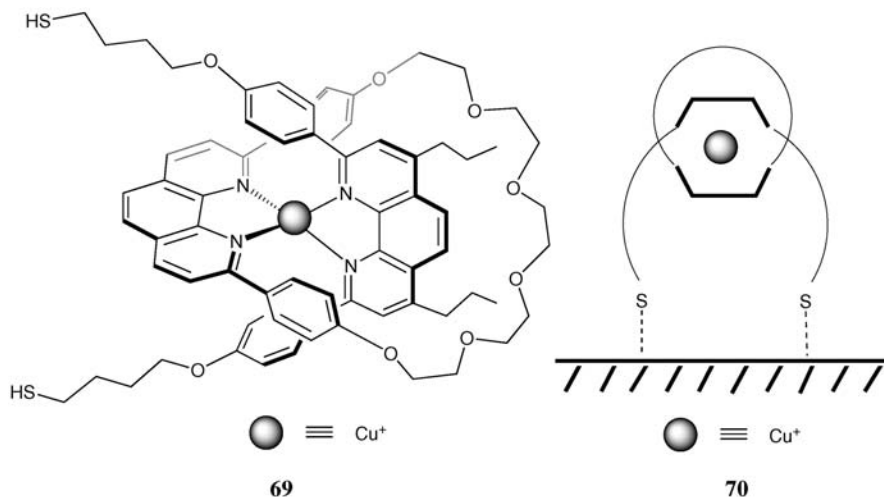


A similar alkylation strategy has been used to synthesize [2]catenanes possessing gold and zinc metalated porphyrins for studying intramolecular photo-induced electron transfer [70]. The most efficient strategy for synthesizing catenane **68** (Ar=3,5-di-*tert*-butylphenyl), was to start with the zinc porphyrin macrocycle and form the respective copper complex. Subsequently, a phenanthroline moiety was threaded through the macrocycle, and bis-alkylated with a gold metalated porphyrin to form **68**.

An intriguing catenane reported by Kern et al. is in part constituted from a gold surface [71]. The first step in the synthesis was the copper-templated syn-



thesis of rotaxane **69**. The second macrocycle was completed when a solution of this molecule was exposed to a gold surface. Cyclic voltammetry was used to confirm that the thiol groups coordinated to the gold surface to make the unusual catenane structure **70**.

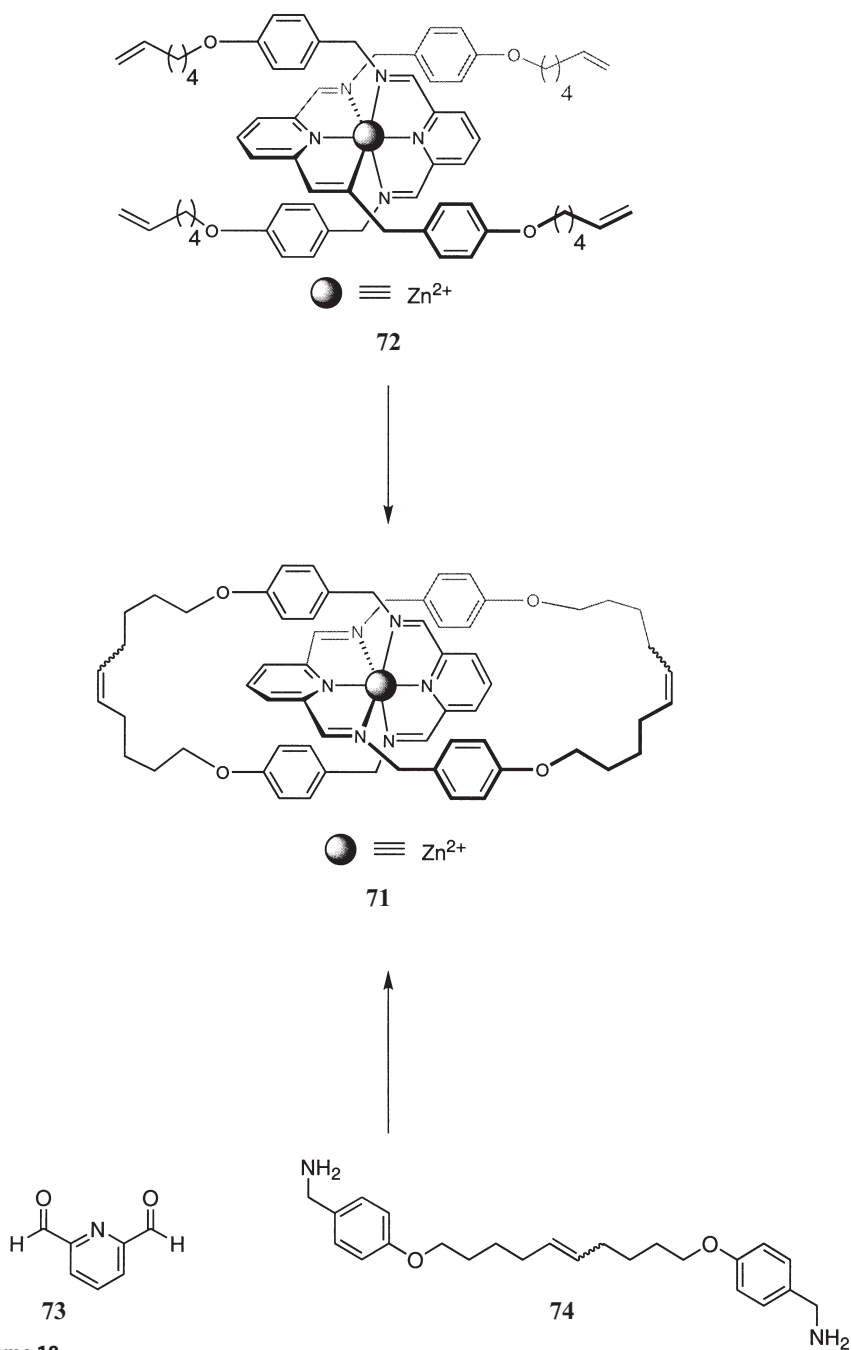


Schiff base chemistry lies at the heart of catenanes reported by Leigh and his group [72]. Catenane **71** (Scheme 18) can be formed by either pre-forming the zinc-Schiff base complex **72** and exposing it to RCM conditions, or by condensing aldehyde **73** and amine **74** in the presence of zinc.

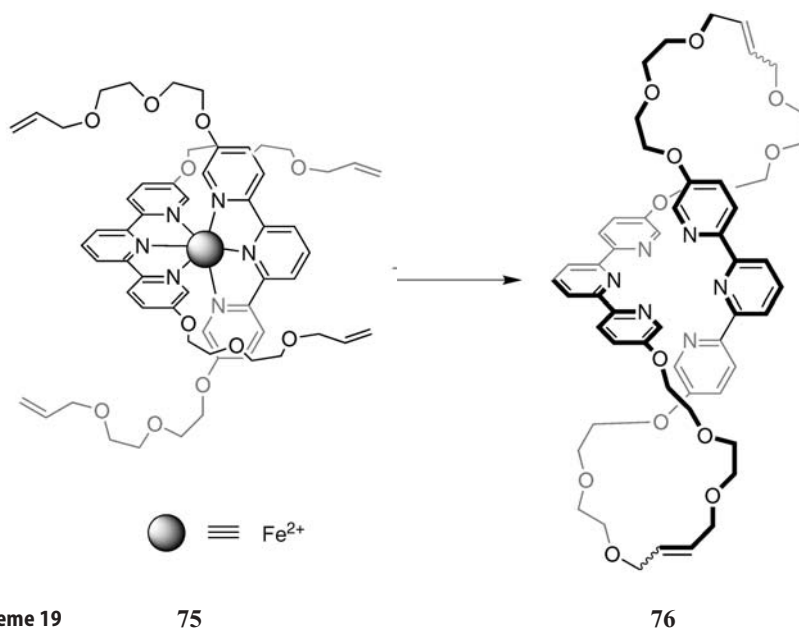
Although an extremely efficient process, metal ion templation nevertheless can lead to unexpected products. Normally, less than quantitative yields of the target can be attributed to the formation of polymer; a problem that becomes worse as the distance between the termini that are being tethered and the metal template increases. However, In the case of RCM upon **75** (Scheme 19), the lack of catenane product could not be attributed to polymer formation. Instead, after reaction and demetallation, macrocycle **76** was isolated in 70% yield. The metal ion can bring the two ligands together, but it cannot force their “arms” to intertwine sufficiently for catenane formation [73].

Moving to more complex topologies, a Cu(I) template has been used to form the doubly interlocked [2]catenane **77** (Scheme 20) [74]. The order by which the reaction components were combined was not important. Either ligand **78** could be first treated with copper ion to form **79**, and then the palladium complex **80** added, or because of the reversibility of Pd-N bonds, the palladium macrocycle **81** could be first formed before the copper template was added. Lengthening the ligand resulted in the formation of a singly interlocked [2]catenane [75, 76].

The Sauvage group has also used the combination of RCM and metal ion coordination to phenanthroline moieties to form doubly interlocked [2]cate-



Scheme 18



Scheme 19

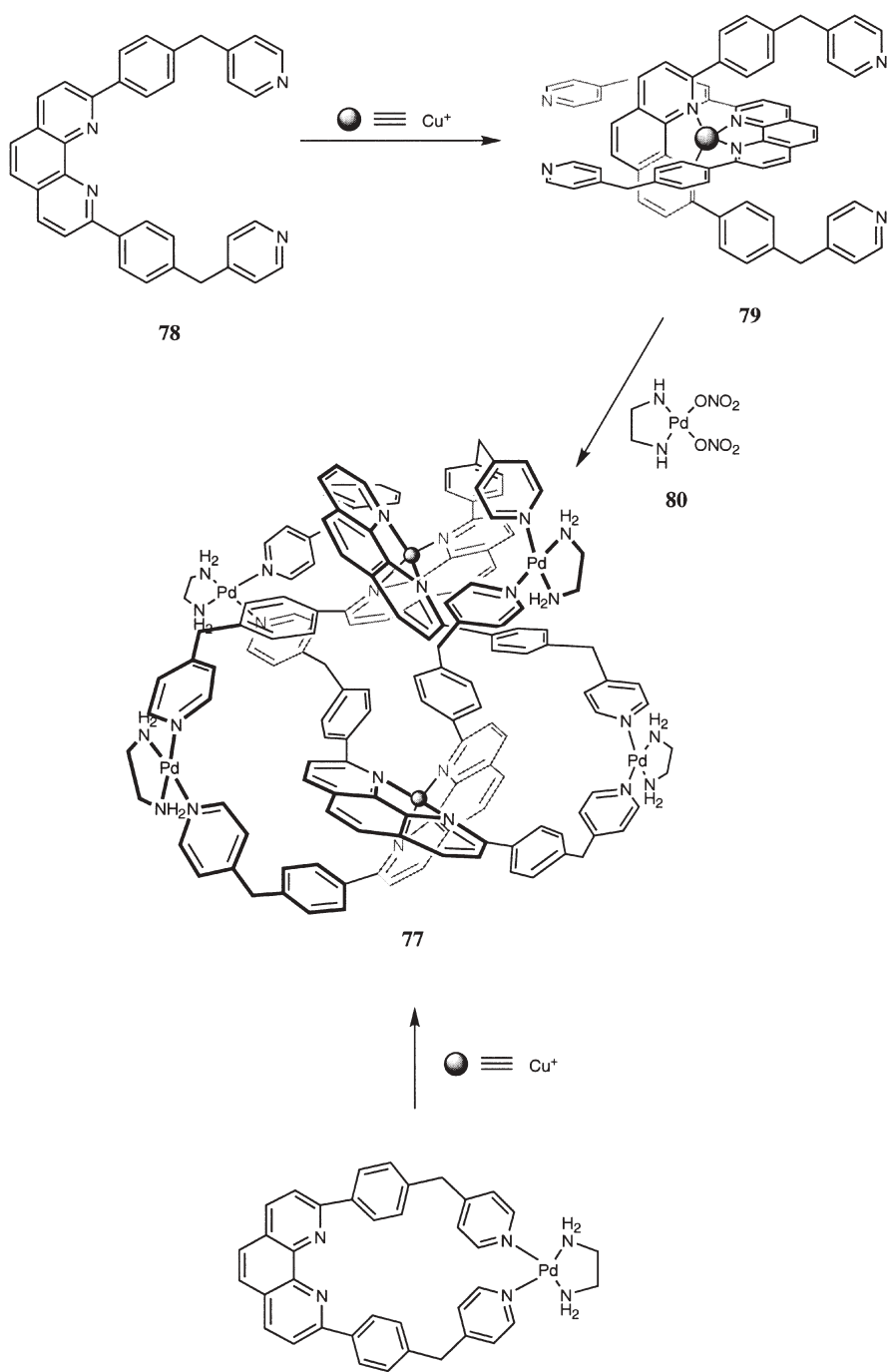
75

76

nane **82** (Scheme 21) [77]. The complexation of ligand **83** and three lithium ions occurred quantitatively, but the reaction mixture obtained after RCM proved inseparable. Metal ion exchange provided a means to purification. Thus, exchange with copper ion, separation, and subsequent demetallation gave the target **82** in about 30% yield.

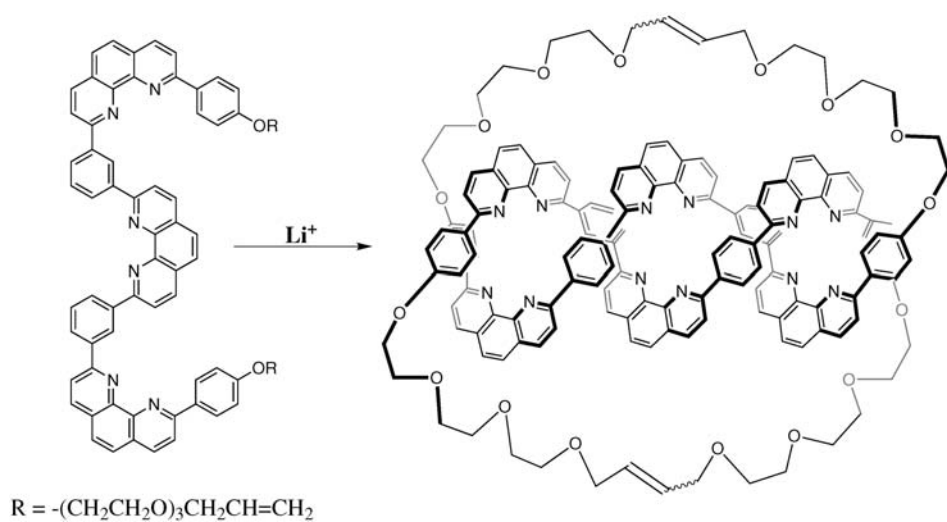
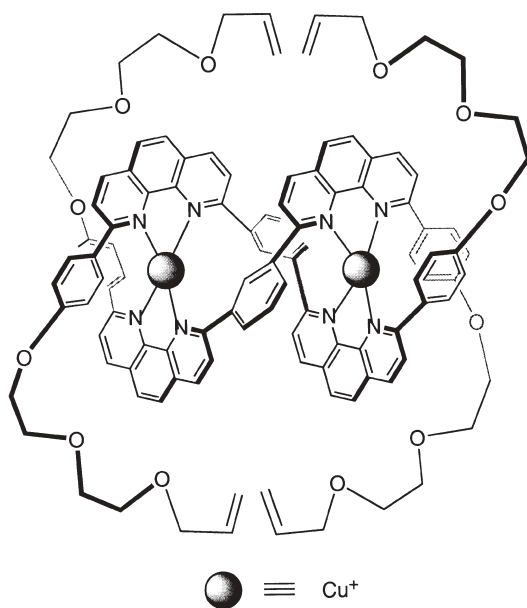
Similarly, the Sauvage group have also used templation to synthesize molecular knots [78]. For example, *bis*-copper(I) complex **84**, prepared in quantitative yield from the corresponding ligand and salt, gave the anticipated knot after RCM and demetallation. The yield for the RCM step was 75%. A related iron(II) templated knot using terpyridine ligands was also synthesized, although its larger macrocyclic structure led to a lower yield in the metathesis step. Likewise, the formation of related knot **85** by alkylation of the bisphenanthroline core with 1,17-diiodohexaethyleneglycol, was less efficient than the RCM protocol. The macrocycle was prepared in 29% yield. In this particular case, however, the two enantiomers of the knots were isolated by complexing with enantiopure binaphthyl phosphate [79].

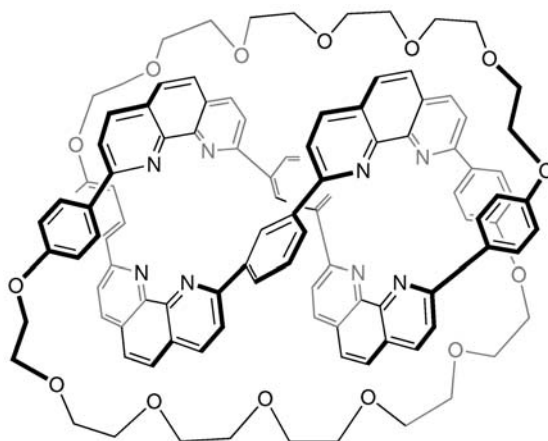
Towards the topologically complex Borromean link, Siegel et al. recently reported the synthesis of **86** (Scheme 22); templation was used to efficiently synthesize both rings [80]. Thus, copper ion templation during a modified Eglinton reaction upon **87** led to the $\text{87}_2\text{Cu}$ complex that underwent oxidative coupling. Removal of the template led to **88** in over 90% yield. Subsequently, after reduction of the alkyne groups and formation of *bis*-complex **89**, alkylation with 6,6'-bisbromomethyl-2,2'-bipyridine gave **86** in 49% yield.



Scheme 20

81

**83****82****Scheme 21****84**



85

3.4

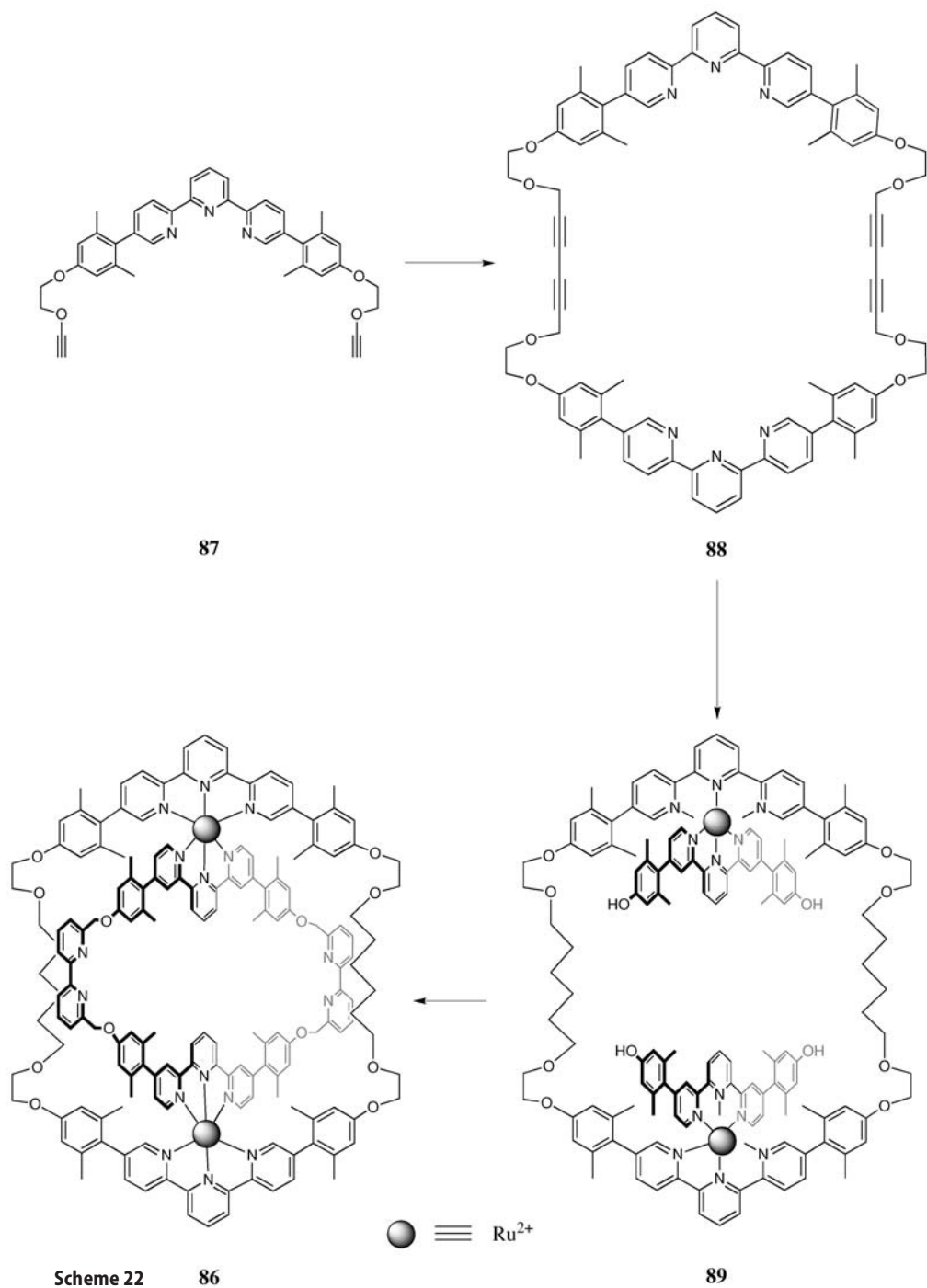
Hydrogen Bonds Between Template and Macrocyclic

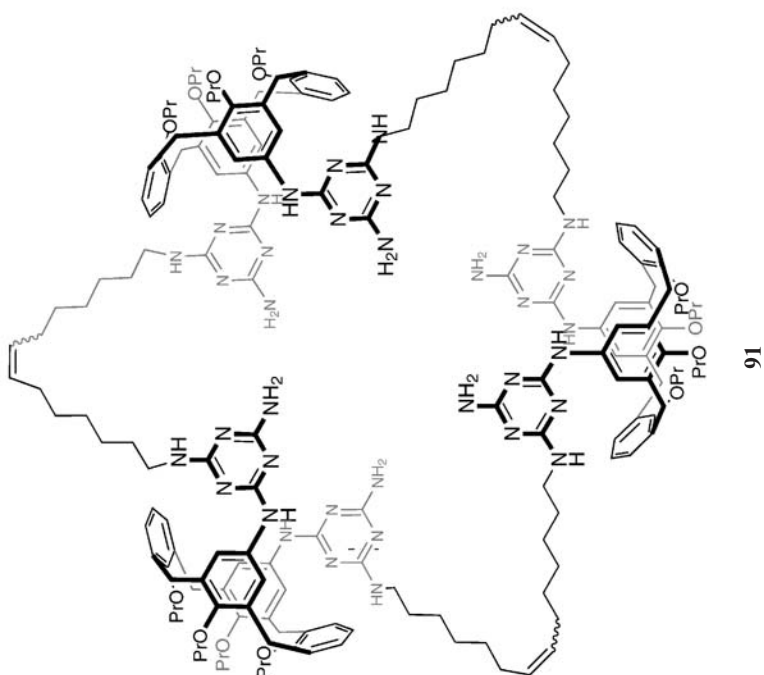
The strength and directionality of hydrogen bonds make them, along with ligand/metal coordination, the most popular means to bring about templation. Over the last 5 years, hydrogen bond templation has allowed access to macrocycles, catenanes, rotaxanes and knots of ever increasing size and constitutional/stereochemical complexity.

A large macrocycle has been formed by the barbituric acid templated co-joining of three calixarenes [81]. The stitching together of calix[4]arene subunits in the supramolecular complex **90** using RCM protocols led to a 96% yield of the 123-membered ring product **91** (Scheme 23). Changes to the solvent, substituents on the calixarene, the lengths of the unsaturated chains, and the nature of the calixarene itself all had a dramatic influence on the outcome of the ring closure.

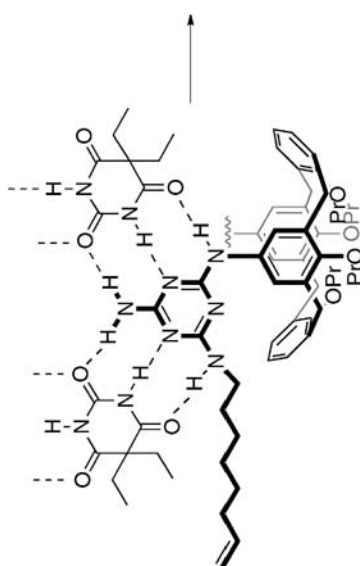
An X-ray analysis suggests that relatively rare C–H...Cl[−] hydrogen bonding is a component of the chloride-templated synthesis of a number of macrocycles [82–84]. Thus, the treatment of **92** with **93** leads to macrocycle **94** in up to 70% yield when chloride ion was used as a template (Scheme 24). A similar “1+3” synthesis leading to **95** gives this bis-xylyl derivative in 88% yield. In the absence of an anionic template, or one that was too large, yields of these macrocycles were between 13 and 42%. Kinetic analysis confirms the proposed templation process [83].

A large proportion of the recent rotaxane and catenane syntheses involves a templation process developed in the Stoddart group; namely the reaction between **96** and **97** that, in the presence of π -electron rich aromatic templates, forms cyclobis(paraquat-*p*-phenylene) (CBPQT⁴⁺) **98** (Scheme 25). A number



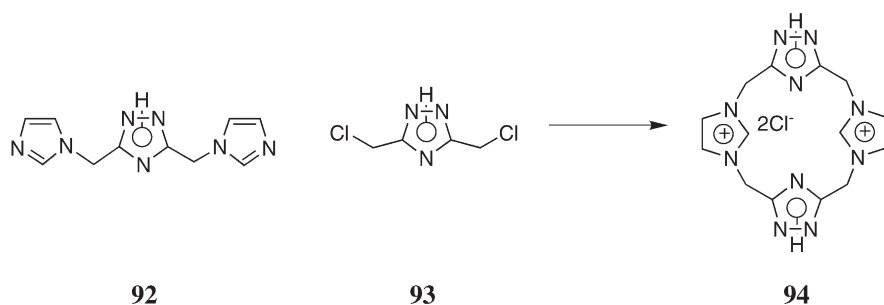


91

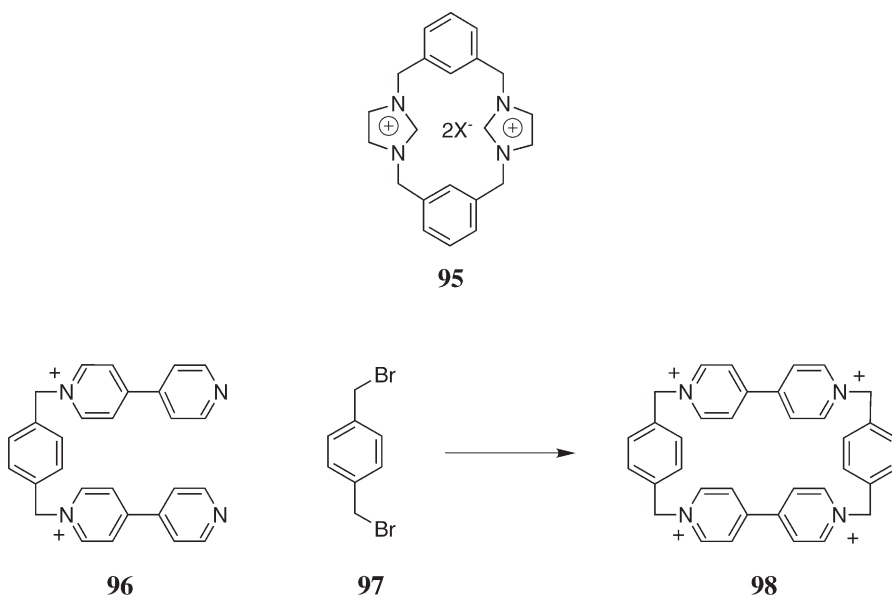


90

Scheme 23



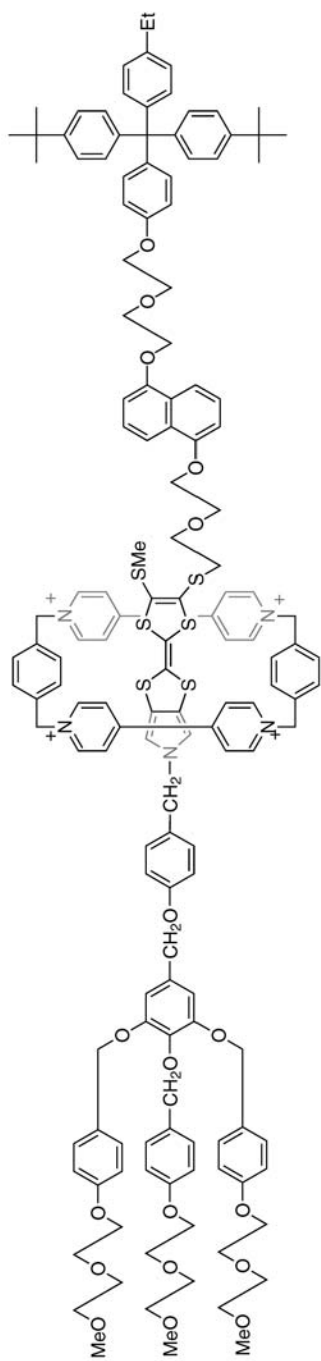
Scheme 24



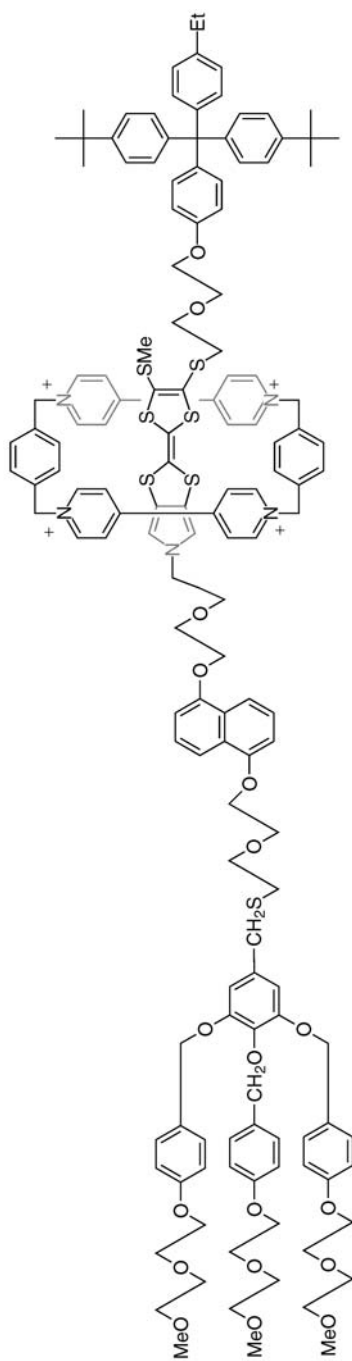
Scheme 25

of non-covalent forces lie at the heart of these “clipping” processes, including: C–H \cdots O hydrogen bonds, π – π stacking, and C–H \cdots π interactions, which makes their classification by intermolecular force tricky. Relative weighing of these non-covalent forces suggest, however, that C–H \cdots O hydrogen bonding is the major contributor to complexation [85]. The efficiency of this templation process [86, 87] provides a ready means to synthesize a broad range of species for molecular machine and molecular switch development [88, 89].

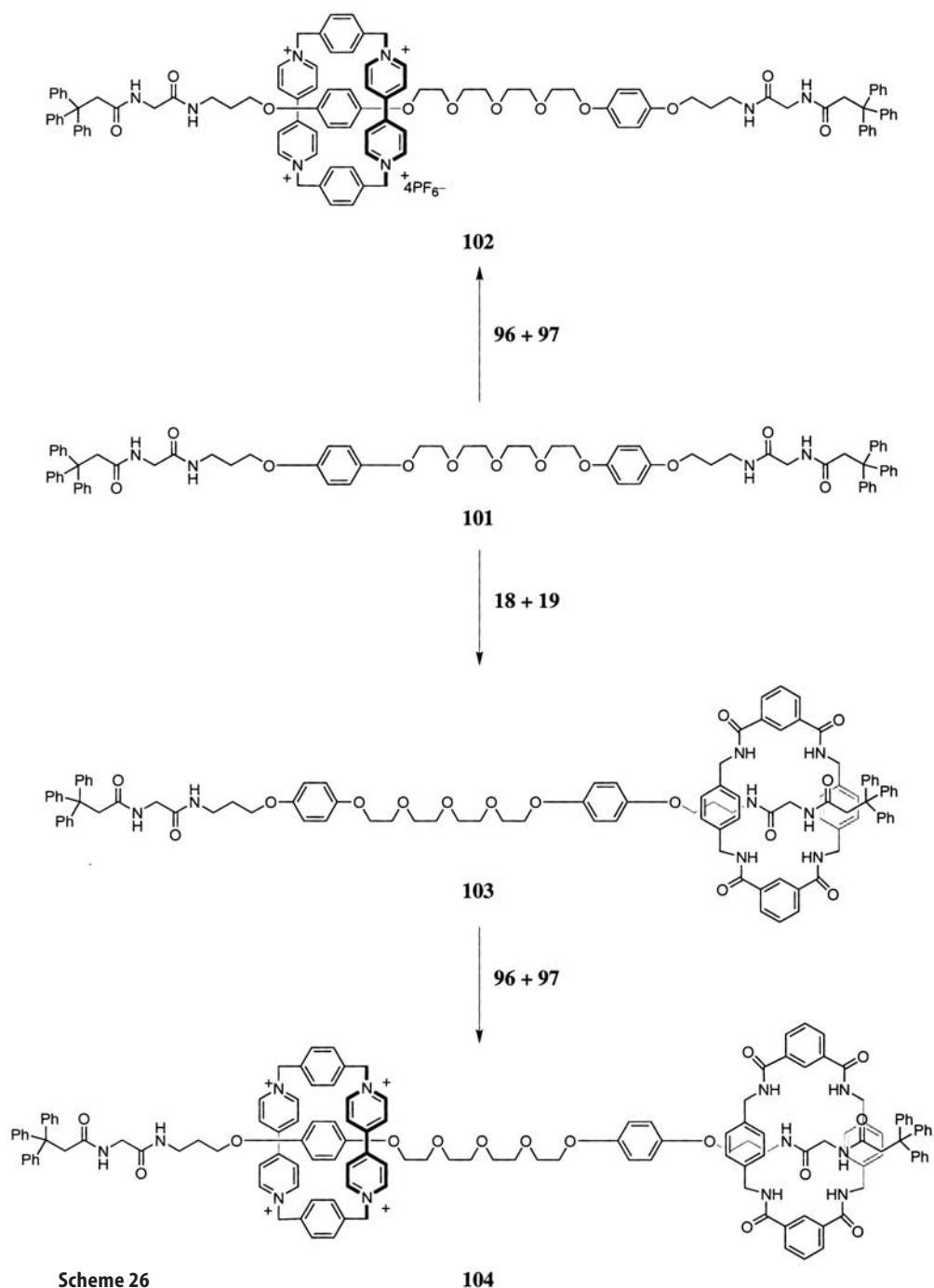
Recent rotaxane developments involving templated macrocycle synthesis have focused on the development of amphiphilic, two-station [2]rotaxanes for the fabrication of molecular electronic devices [90, 91]. Compounds **99** and **100** are two examples that each possess hydrophobic and dendritic hydrophilic stoppers, and two stations – a tetrathiafulvalene (TTF) group and a 1,5-dihydroxynaphthalene group (DNP) – which the CBPQT $^{4+}$ moiety shuttles between depending on the



99



100



Scheme 26

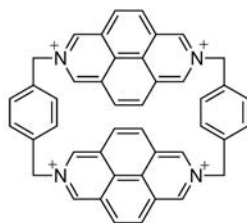
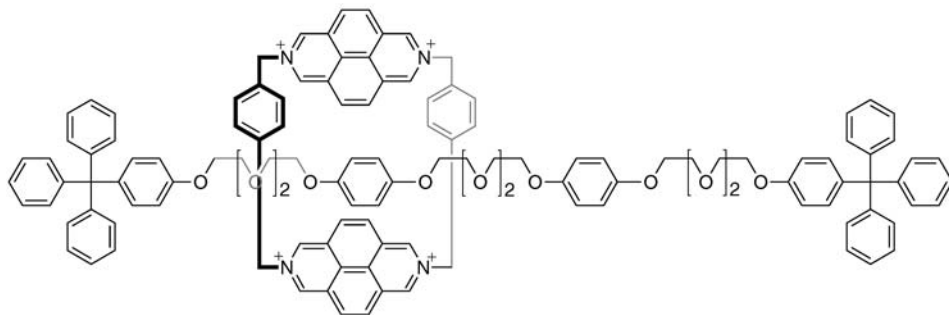
104

oxidation state of the TTF group. The constitution of rotaxane **99** is such that the translocation of the CBPQT⁴⁺ moiety from one station to the next means that it must surmount the –SMe group on the TTF station. Thus, translocation is slower in this rotaxane. The clipping process in which the (CBPQT⁴⁺) moiety is built around each dumbbell occurred in 23% and 47% yield respectively.

In other work on [2]rotaxanes, the Stoddart group have used similar clipping processes to form 9,10 and 2,6-dioxyanthracene containing rotaxanes [92] and rotaxanes possessing either chiral centers or planar chirality. Studies upon these latter derivatives gave insight into the three degenerate dynamic processes that these [2]rotaxanes can undergo [93].

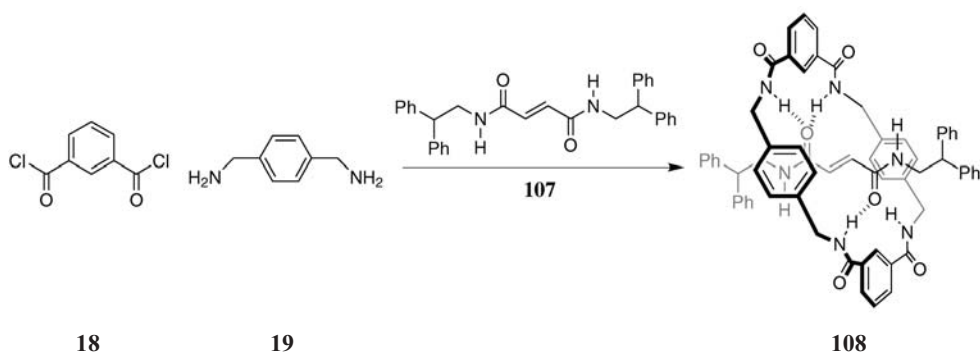
Building on this [2]rotaxane work, Li and associates have synthesized [3]rotaxanes that possess two different macrocycles around the dumbbell [94, 95]. To take one example (Scheme 26), dumbbell **101** when treated with **96** and **97** led to [2]rotaxane **102** in 36% yield. Alternatively, by treating the dumbbell with *p*-xylenediamine **18** and 1,3-phthaloyl dichloride **19** the glycine moiety could be used to template the synthesis of **103** in 18% yield. Invoking the hydroquinone template once again, subsequent treatment with **96** and **97** gave the hetero-[3]rotaxane **104** in 54% yield. NMR analysis of this and other derivatives provided a wealth of information pertaining to the movement of components in these complexes.

Diazapyrenium macrocycle **105** has also been used as the π -electron deficient component of rotaxanes (and catenanes) [96]. This macrocycle forms

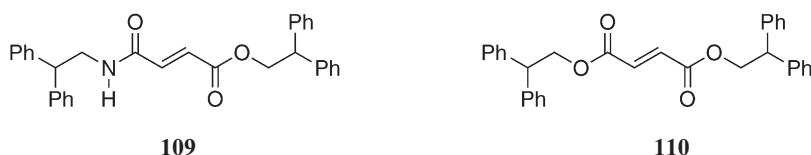
**105****106**

stronger non-covalent interactions with electron-rich moieties than the corresponding bipyridinium **98**. As a result, the clipping of the macrocycle to form rotaxane **106** occurs in 45% yield, whereas the corresponding bipyridinium derivative is formed in 23% yield.

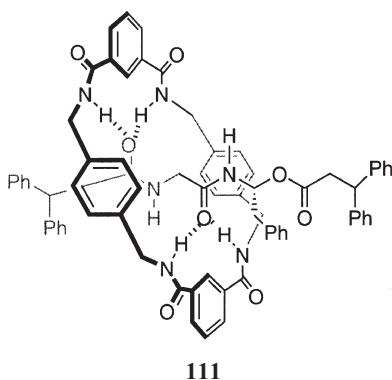
The Leigh group recently reported a “world record” for the facile synthesis of a [2]rotaxane [97]. A five-component assembly involving two equivalents each of xylylene diamine **18** and isophthaloyl dichloride **19**, and one equivalent of dumbbell **107** gave the corresponding rotaxane **108** in a remarkable 97% yield (Scheme 27). Conformational preferences of the immediate precursor to the macrocycle are an important contributor to this yield, but hydrogen bonding between amide groups, as evidenced in both the solution and solid states, is essential. This excellent example of templation allowed weaker hydrogen bond acceptors to be examined as templates. Thus, the corresponding dumbbells **109** and **110**, in which one or two ester groups replace the amide groups of **107**, gave their respective rotaxanes in 35 and 3% yield. Both were characterized by X-ray crystallography. NMR was also used to examine the strength of hydrogen bonding between each dumbbell and its encircling macrocycle.



Scheme 27



In a study of information transmission in chemical systems, the same macrocycle has been wrapped around dumbbells comprised of dipeptides to form rotaxanes such as **111** [98]. An examination of six X-ray structures revealed how much the macrocycle component was distorted in the rotaxane. Low yields were obtained in cases where the macrocycle underwent little distortion, high distortion was observed in high yielding cases. Hence, the ability of a flexible macrocycle precursor to wrap around an unsymmetrical

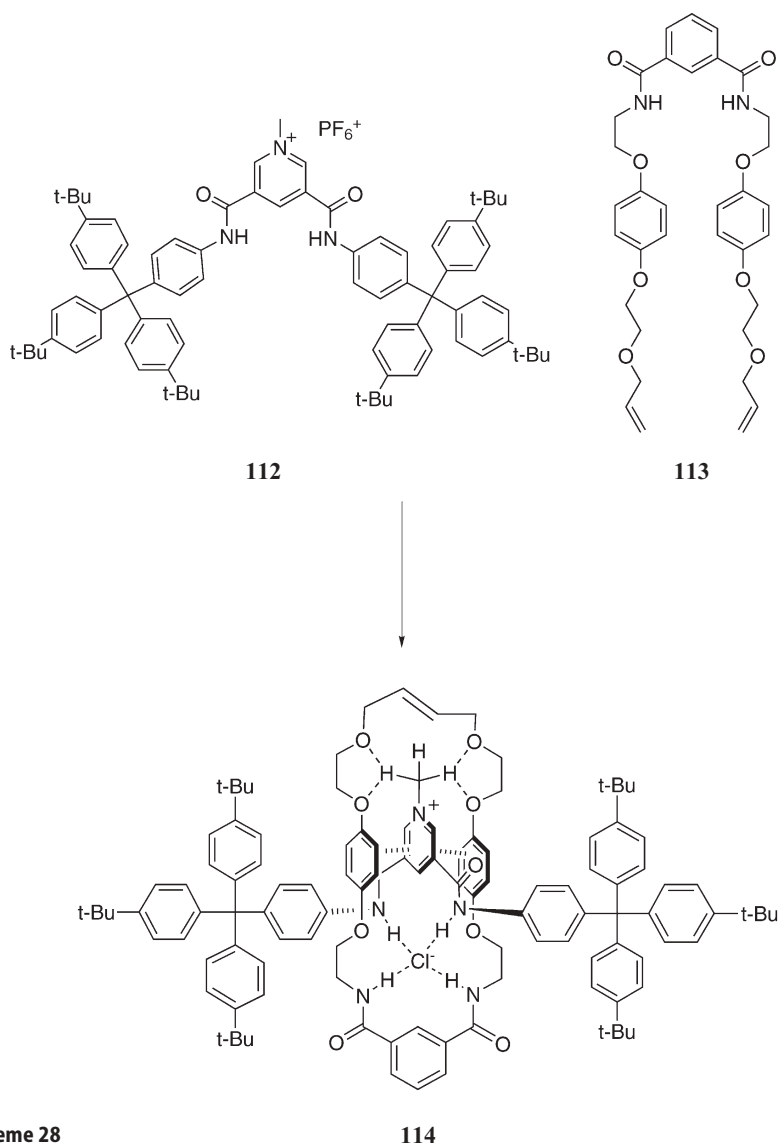


hydrogen-bonding template determines, and thus relates, reaction yield and symmetry distortion in the product.

In related work, the *E-Z* rotamer distribution of the dipeptide dumbbells of rotaxanes such as **111** was examined as a function of solvent. In apolar solvents, where hydrogen bonds between ring and dumbbell exist, the latter adopts primarily an *E* conformation. In contrast, in polar solvents, no rotamer dominates [99]. More recently, the circular dichroism (CD) response of dipeptide rotaxanes have been examined as a function as solvent. In solvents where hydrogen bonding between dumbbell and macrocycle is not possible, the CD signature of these chiral entities is weak. However, in apolar solvents, hydrogen bonding between chiral dumbbell and achiral macrocycle allows the chirality to be transmitted from the dumbbell, via the macrocycle, to the diphenylmethane rotaxane stopper. The result is a dramatic increase in the CD signature of the rotaxane [100].

N-H \cdots Cl $^-$ and C-H \cdots O hydrogen bonds, are the principle driving forces behind the anion templated rotaxane synthesis reported by Beer et al. (Scheme 28) [101]. Dumbbell **112** is designed to bind chloride ion via its amide N-H groups, while premacrocycle **113** is designed to bind both chloride ion (via its amide N-H groups) and the electron-deficient pyridinium ring of the dumbbell (via π -stacking and C-H \cdots O hydrogen bonds). The resulting ternary complex was treated under RCM conditions to yield the rotaxane **114** in 47% yield. That the chloride ion was central to the synthesis was demonstrated by carrying out an analogous reaction with a hexafluorophosphate salt; no product was observed.

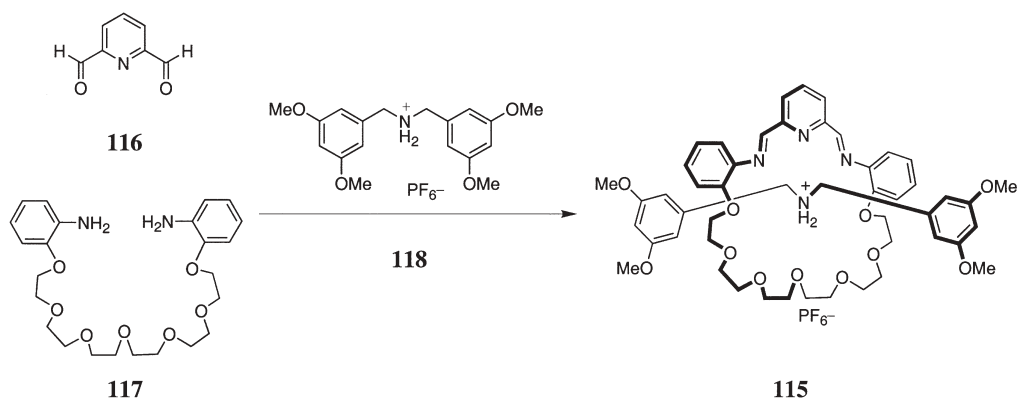
Hydrogen bonding is also important in the templated synthesis of [2]rotaxane **115** (Scheme 29) [102]. This molecule, the first dialkylammonium ion-based [2]rotaxane to be formed by a clipping process, was formed by the condensation of **116** and **117** in the presence of template **118**. In the absence of the template, indeterminate compounds were made. However, the reaction came into focus in the presence of the template, and the reduction of the imine bonds led to the corresponding amine being isolated in 70% yield. Extending this work, an analysis of [2]rotaxane formation as a function of different dialdehydes and different



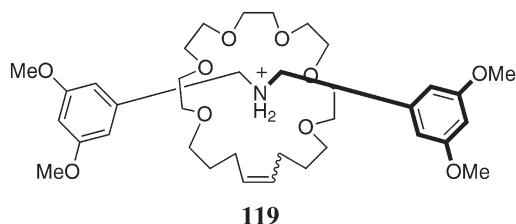
Scheme 28

templates revealed that furan containing macrocycles and π -electron-deficient templates gave the most thermodynamically stable rotaxanes. In contrast, pyridine-containing macrocycles gave the more kinetically stable rotaxanes [103]. RCM conditions were used in the synthesis of related rotaxane **119**. Clipping of the terminal olefin around the bis(3,5-dimethoxybenzyl)ammonium ion lead to a 73% yield of the rotaxane [104].

In recent catenane research, the Stoddart group have investigated the templated synthesis of [2]-, [3]-, [5]-, and [7]catenanes [105] as well as lower sym-



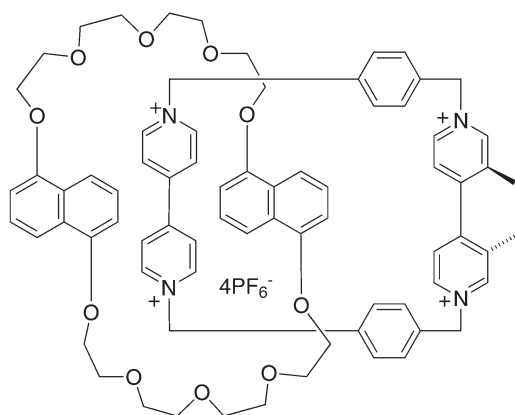
Scheme 29



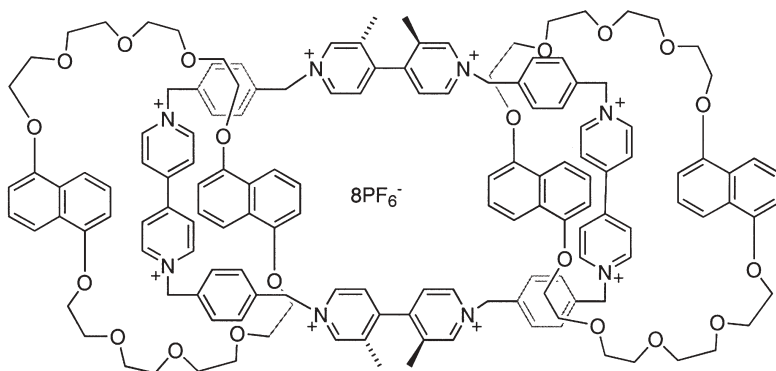
metry [2]- and [3]catenanes [106]. In regards to lower symmetry cavitands, the templated formation of **120** and **121** in 9 and 24% yields, respectively, allowed a detailed structural analysis of these stereochemically complex molecules. For example, [2]catenane **120** exists as 16 stereoisomers, but only one diastereomer predominates. Continuing on the stereochemical theme, templation under high pressure leads to **122** in 34% yield. This catenane possesses both elements of planar and helical chirality. However, even though it can potentially exist as four inter-converting stereoisomers, it spontaneously resolves into one enantiomer in the solid state [107].

The templated synthesis and X-ray crystallography analysis of chiral [2]catenane **123** has been reported by the Vögtle group [108]. Hydrogen bonding between the macrocyclic template and the incipient, second macrocycle led to its synthesis in 17%. The catenane is chiral because the mono-sulfonamide groups and the amide groups, give each macrocycle directionality. Therefore, each ring is itself chiral when fixed in a plane. Catenation fixes each macrocycle plane relative to the other, and therefore chirality is bestowed on the molecule as a whole.

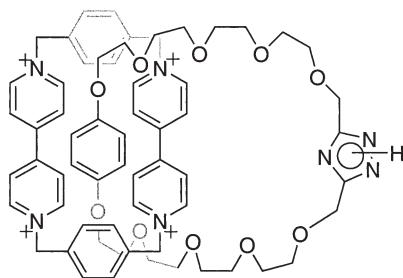
A clipping protocol has also been used to form self-complexing [2]catenanes. A yield of 18% was observed for **124**, which was shown to dimerize in both the solution and solid state [109, 110]. Such self-complexing [2]catenanes possess central voids that are important for recognition, a feature that often allows the generation of [3]catenanes as “side products” in high yields [110].



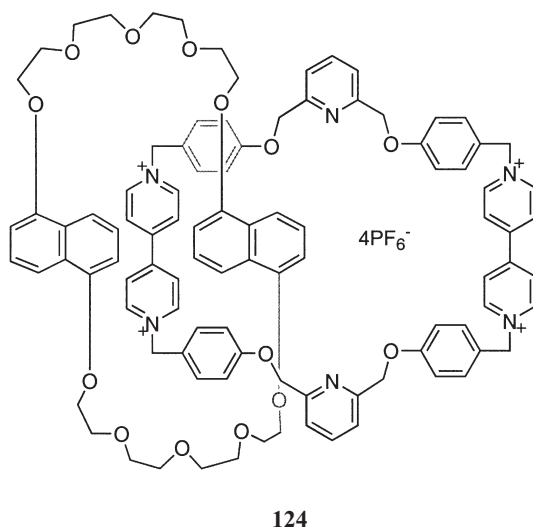
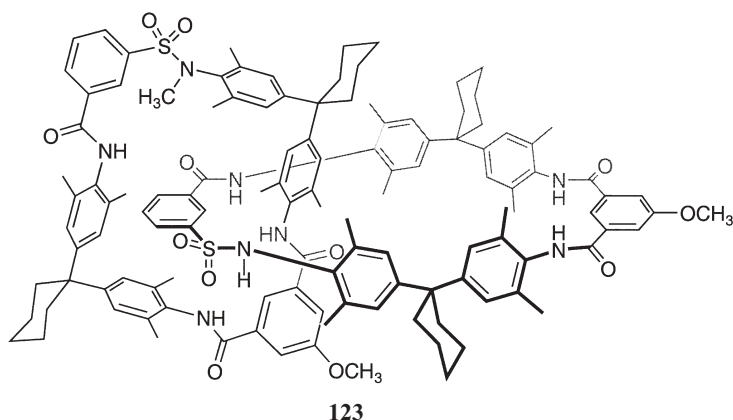
120



121

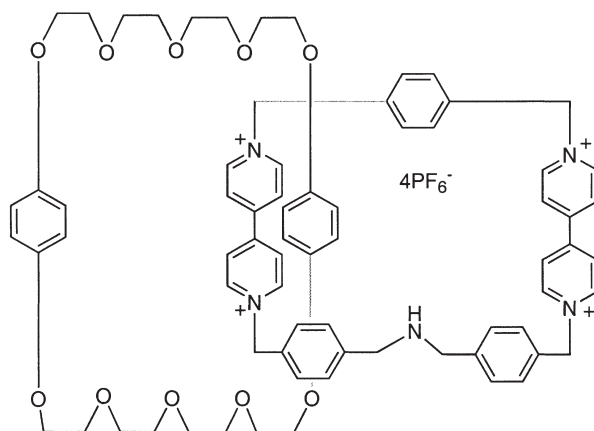


122

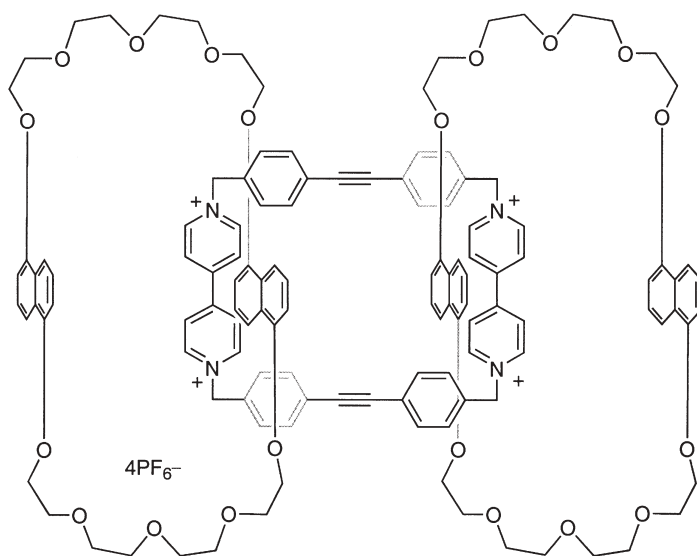


Recently, the Stoddart group has been investigating the formation of “duel mode” switching in catenanes incorporating bipyridinium and dialkylammonium recognition sites. For example, [2]catenane **125**, synthesized in 12% yield by clipping the CBPQT⁴⁺ derivative around the crown ether, demonstrated AND logic gate behavior. Thus, in its 4+ form, and two-electron reduced 2+ form, the crown ether macrocycle was observed to reside around a bipyridinium moiety, while the addition of one proton led to the shift of the crown ether to the now alkyl ammonium site. A two-electron oxidation shifted the crown back to one of the pyridinium groups [111].

The synthesis of [3]catenanes possessing binding pockets has shed light on the importance of CH...O hydrogen bonds in these polyether/bipyridinium templation processes. Catenane **126** for example, formed in an excellent 42% yield,



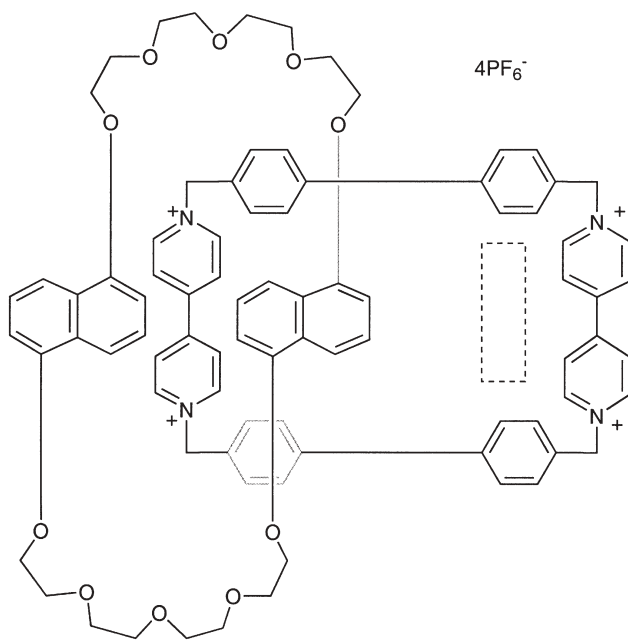
125



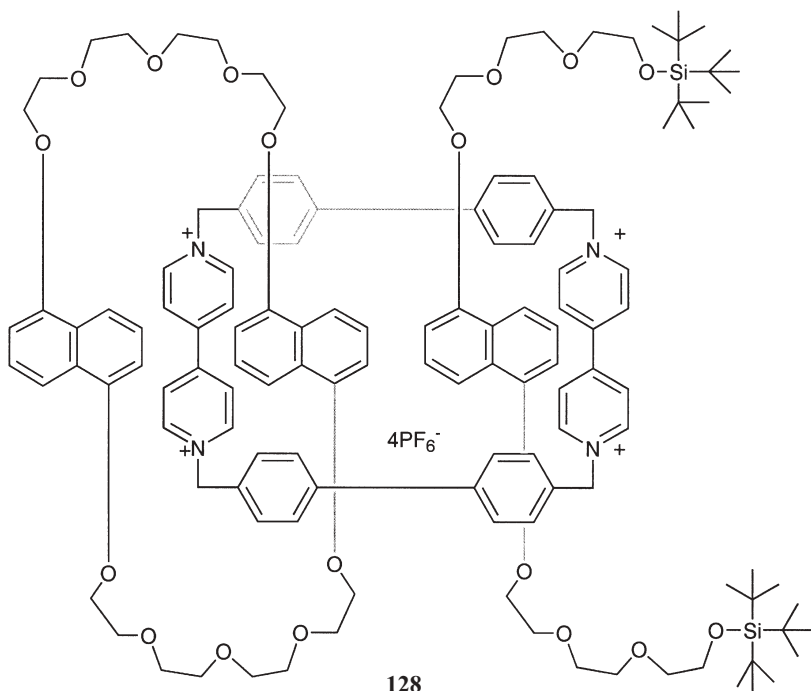
126

does not bind bipyridinium guests even though it possesses an ideal pocket for doing so [85]. Calculations suggest that one of the main reasons why this is so, and hence why no [4]catenanes can be formed in the templation reaction, is the lack of CH \cdots O interactions between host and bipyridinium guest [85, 112].

In contrast, [2]catenane 127 does bind guests in its cavity. Included in the list of guests for this catenane are dumbbell compounds that result in the formation of rotacatenanes such as 128. The predisposition of this [2]catenane to bind guests is reflected in the poor templated yields of its synthesis [113].



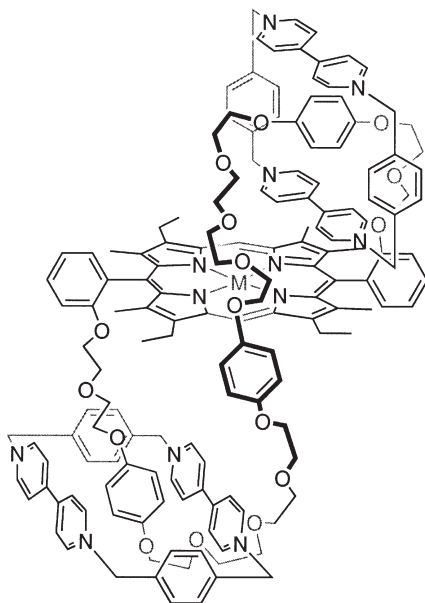
127



128

[2]Catenane **127** is formed in only 8% yield whereas the corresponding side-product [3]catenane, which does not possess an empty cavity, is formed in 35% yield.

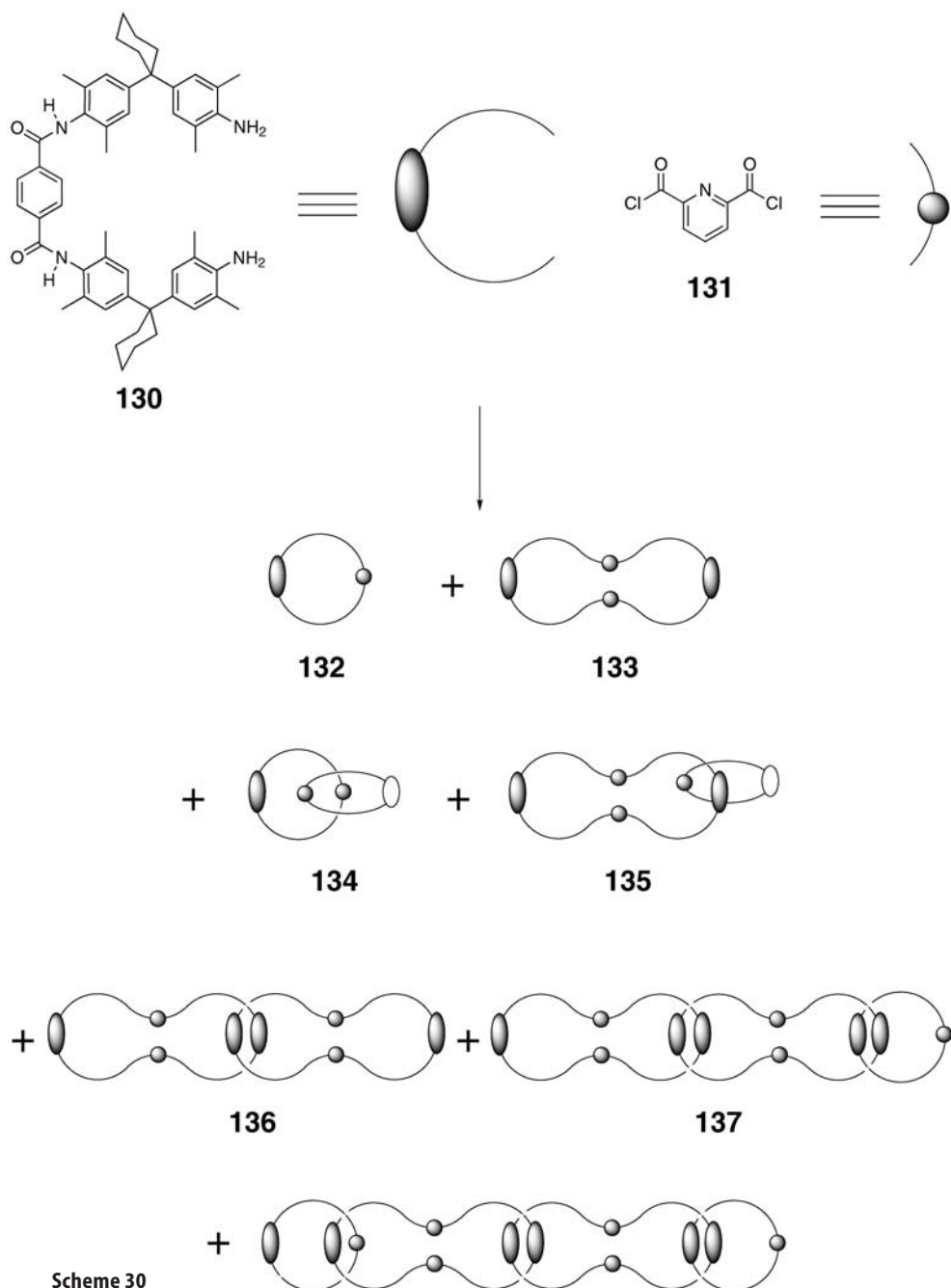
This same clipping process has been used by the Gunter laboratory to assemble porphyrin-containing catenanes [114]. They synthesized a number of different atropisomeric, strapped porphyrins and studied their ability to template CBPQT⁴⁺ formation around the 1,4-dioxybenzene(or 1,5-dioxynaphthalene)/crown ether straps. By way of example, twisted [3]catenane **129** was formed in 21% yield from the corresponding twisted, strapped porphyrin.

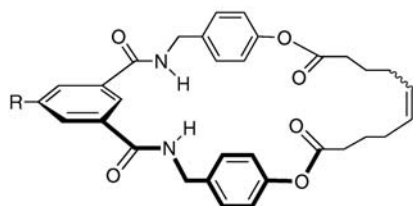


129

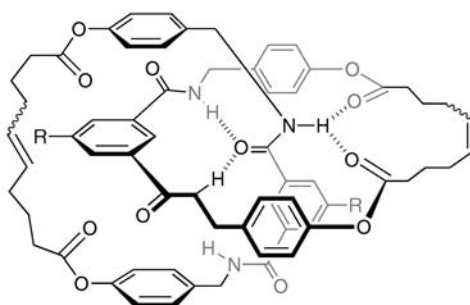
The Vögtle group has used hydrogen bond templatation to form oligo-catenanes. In an examination of the factors leading to successful oligo-catenanes formation, they identified terephthalic acid **130** and pyridine **131** (Scheme 30) as the most successful subunits from a range of compounds [115]. These led to the formation of two macrocycles **132** and **133** in 9% and 17% yield, and five different catenanes. The [2]catenanes **134**, **135** and **136** in 3%, 14%, and 10%, respectively, and the [3]catenane **137** and [4]catenane **138** each in 2% yield.

An example of reversible catenane formation from the Leigh group involves ring opening and ring closing metathesis with a Grubbs catalyst [116]. Thus, in the presence of the catalyst, a 0.2 M solution of macrocycle **139** gives a >95% yield of catenane **140**, whereas at a concentration of 2×10^{-4} M, the catenane gives macrocycle **140** in >95% yield.





139



140

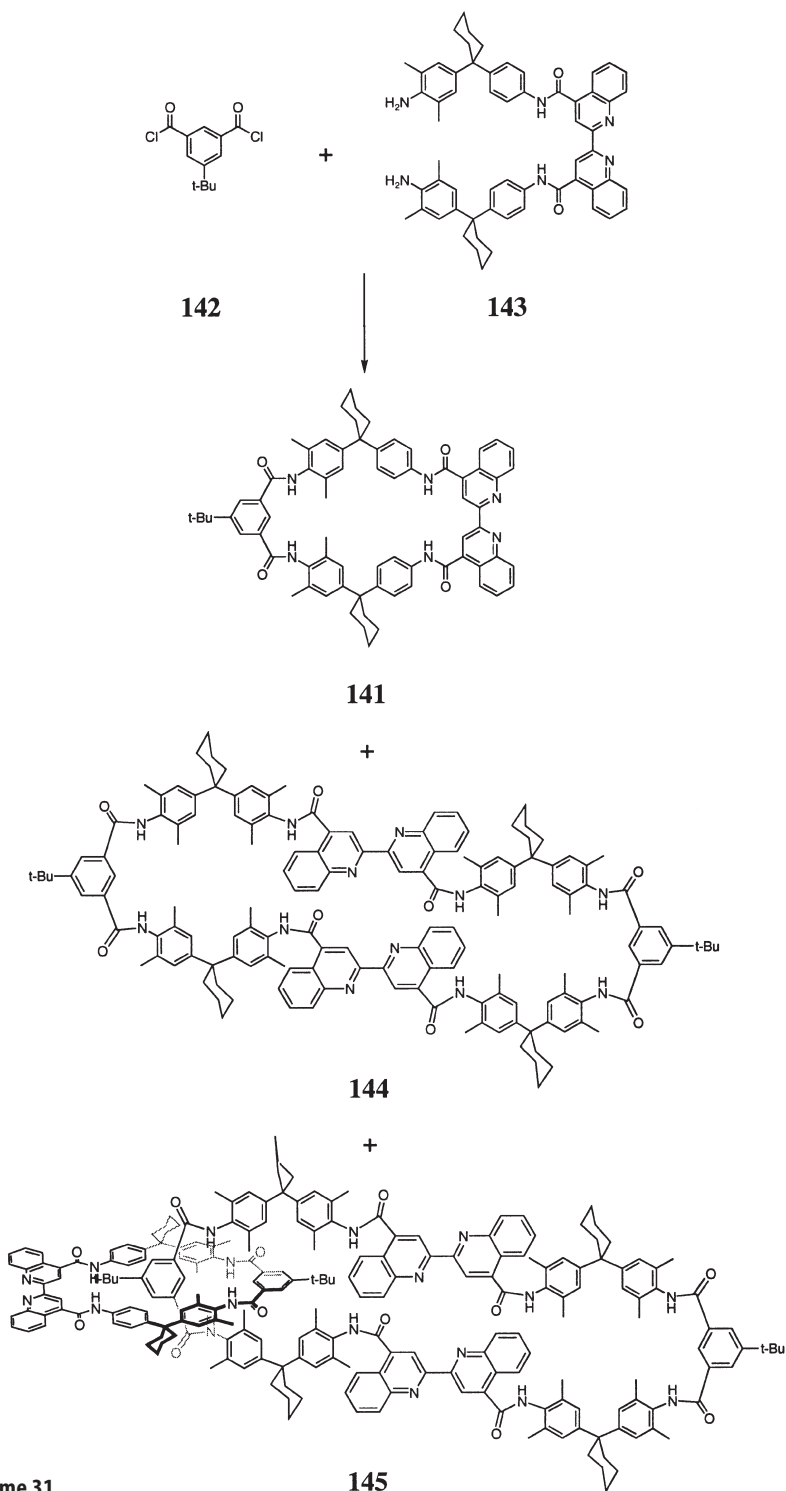
The templated synthesis of catenanes and rotaxanes is also a facet of the Schalley group's research [117]. Macrocycle **141** (Scheme 31), required for the synthesis of rotaxanes, was synthesized in 10% yield by the base-promoted combination of **142** and **143**. Also produced in this reaction were the corresponding [2]catenane (1%), the larger macrocycle **144** (32%), and the [2]catenane **145** (7%).

The Vögtle group has also used hydrogen bonding to template the formation of molecular knots [118, 119]. For example, a remarkable yield of 20% was recorded for chiral, trefoil knot **146** by mixing diamine **147** and pyridine **131** in the presence of base (Scheme 32). The subtle change from terephthaloyl to phthaloyl moiety of the diamine, switches the assembly system from poly-catenane synthesis (Scheme 30) to knot formation. The Vögtle group have also derivatize different knots with dendritic wedges to improve their solubility [120].

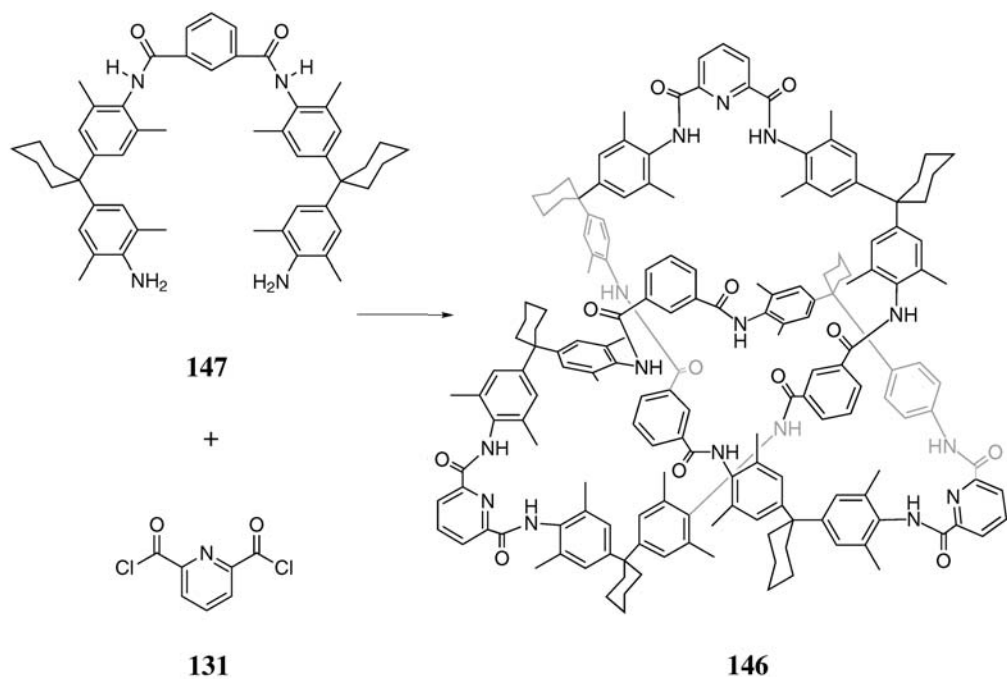
3.5

Cation- π Interactions Between Template and Macrocycle

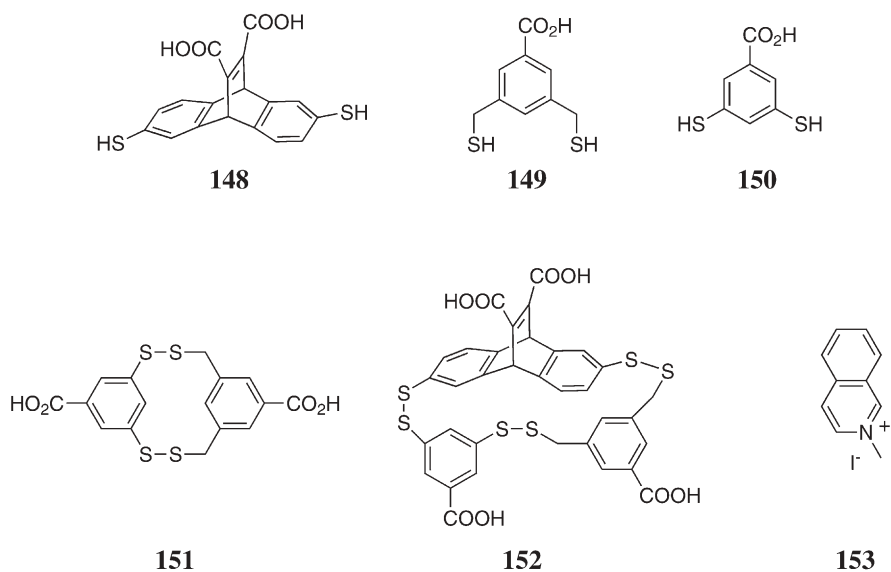
In their investigations into different dynamic combinatorial libraries, the Sanders group have identified a system that can amplify the formation of selected macrocycles, even though the differences between the respective binding constants for target macrocycle and corresponding template are small [121]. Thus, in the absence of a template, the three thiols **148**, **149** and **150** leads to a library of literally dozens of macrocycles with mixed dimer **151** and mixed trimer **152** as the major components. On the other hand, the addition of 2-methylisoquinoline **153** to the library led to a large proportion of **154**, whereas trimer **155** was formed in good yield if the template was the *N*-methylated morphine derivative **156**. Microcalorimetric studies on the isolated hosts revealed that template binding was enthalpy driven, suggesting that it is dominated by electrostatic forces such as cation- π interactions. These results also demonstrated that these library member amplifications arose even though the binding constants for matched host-guest pairs **155**·**153** and **154**·**156** were only 6–24 times

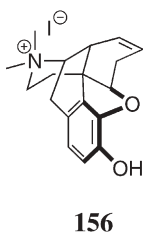
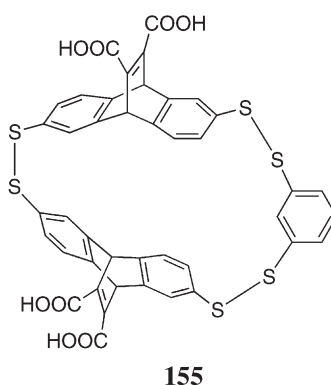
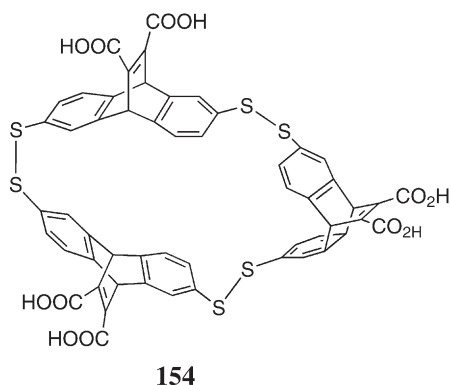


Scheme 31



Scheme 32





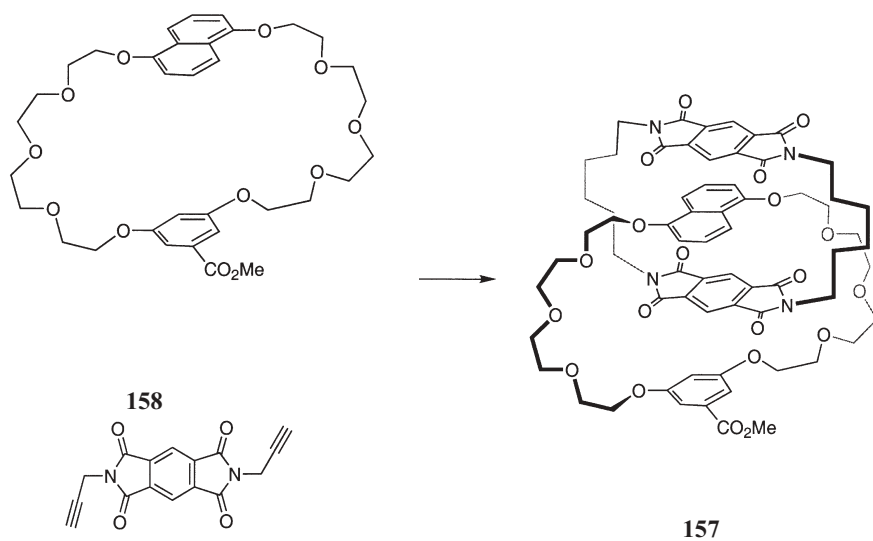
greater than for the mismatched pairs **154**·**153** and **155**·**156**. Small association constants can have sizable effects in dynamic libraries.

3.6

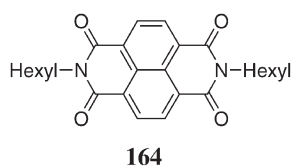
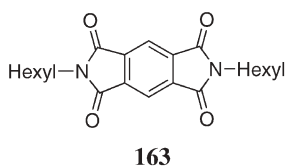
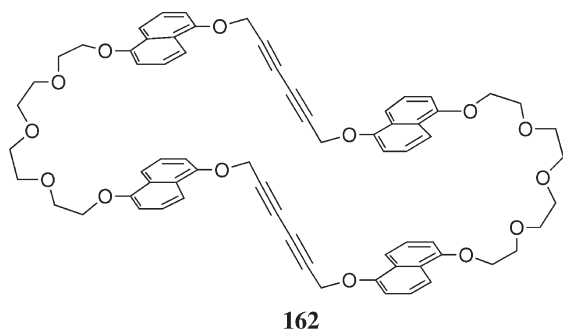
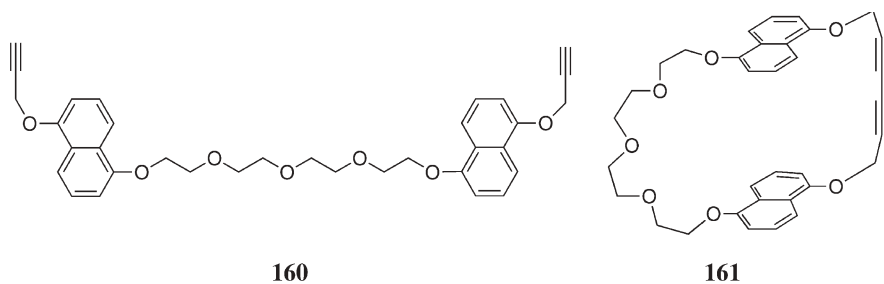
π - π Stacking Between Template and Macrocyclic

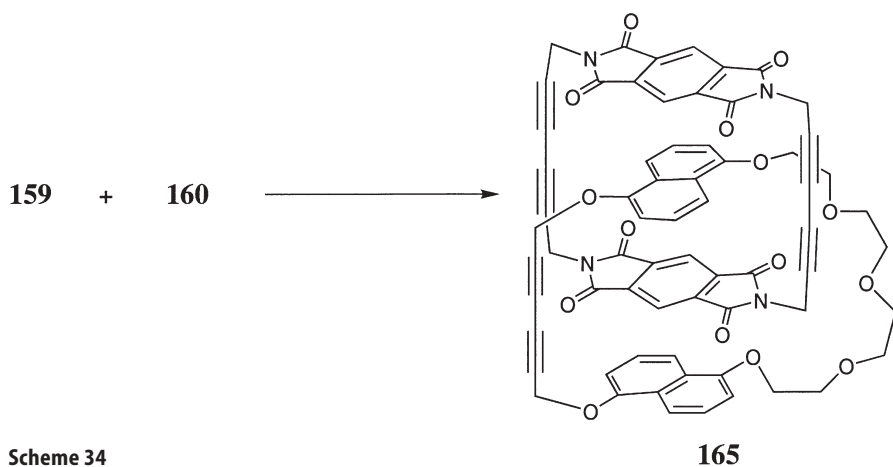
A number of catenanes have recently been synthesized using π - π stacking between template and macrocycle. The Sanders group have formed [2]catenanes such as **157** (Scheme 33) by the combination of crown ether **158** and bisacetylene **159** under Glaser coupling conditions and then reduction of the di-alkyne groups. Driven primarily by π - π stacking (although C-H...O hydrogen bonding may also be important), the catenane is formed in 30% yield [122].

Expanding on this protocol, the group has also investigated the cyclization of diacetylene **160**. Monomer **161** and dimer **162** were prepared in ca. 40% and 2% yields, respectively. In contrast, the addition of template **163** to the oxidative coupling process led to ca. 70% of **161** and 4% of **162**, whereas the larger template **164** gave ca. 54% and 15% of the monomer and dimer, respectively [123]. These two successes led to an investigation of the possibility of carrying out a tandem cyclization process. Thus, when a 2:1 ratio of **159** and **160** were combined under the standard coupling conditions, the yield of [2]catenane **165** was ca. 14% (Scheme 34).



Scheme 33



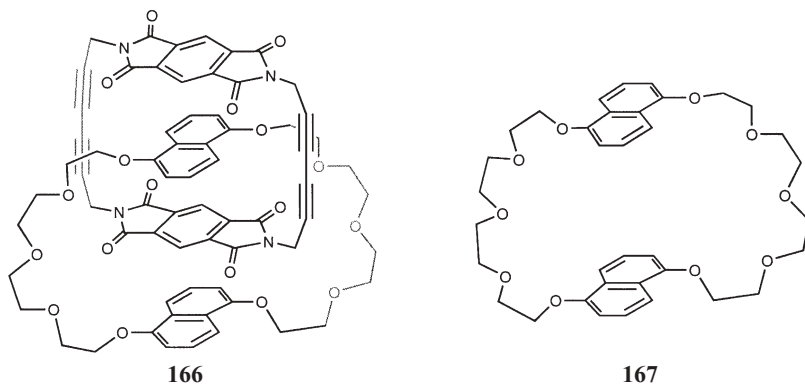


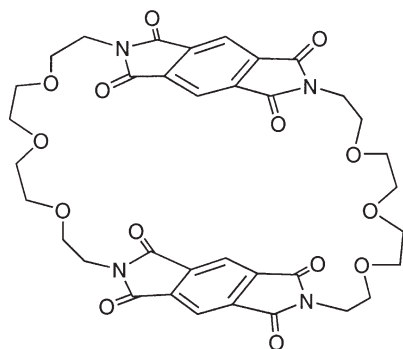
Scheme 34

From the following observations, it has been suggested that C–H···O hydrogen bonding may also be important in these macrocyclizations:

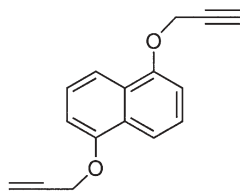
1. Catenane **166** is formed in 38% yield by building diimide **159** around macrocycle **167**.
2. Diimide **159** possesses weakly acidic hydrogen atoms adjacent to the amide nitrogen that interact in the solid state with the ether oxygens of the other macrocycle.
3. The “opposite” assembly, the combination of **168** and **169** to make the isomeric catenane fails; neither of the subunits possesses acidic hydrogens. Such non-covalent interactions may explain why macrocycle **168** and diimides **170** and **171** undergo [2]catenane formation via Mitsunobu alkylation [124]

The Gunter group have also used diimide/hydroquinol(naphthoquinol) stacking in the synthesis of porphyrin-containing catenanes [125]. Several systems were studied. The most successful were those adorned with solubilizing groups. Thus using Glaser coupling, **172** (R=Hexyl) was synthesized in 60%

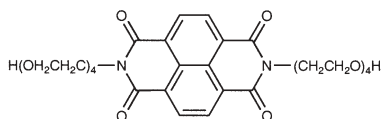




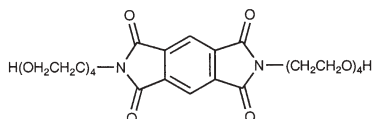
168



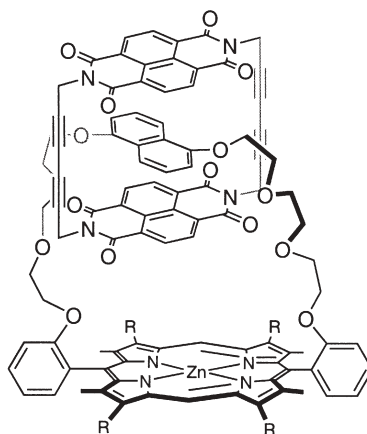
169



170



171



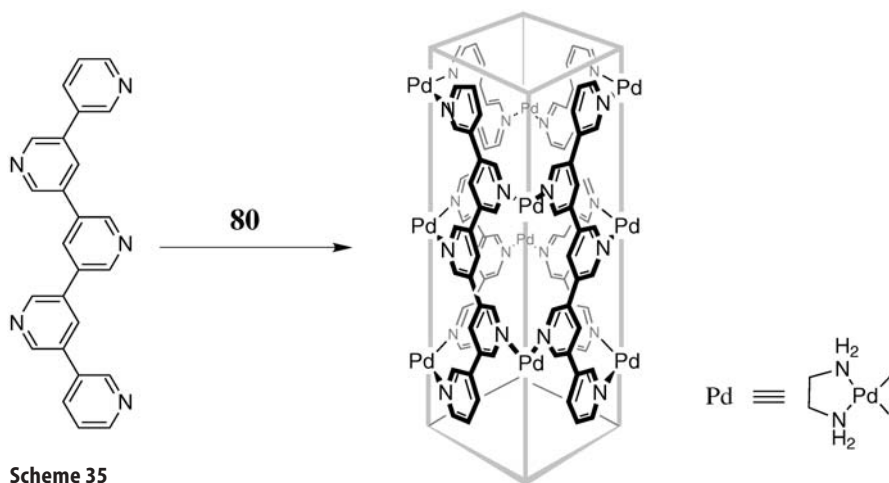
172

yield from the strapped, zinc porphyrin and two equivalents of propynyl substituted diimide [125].

3.7

Van der Waals Forces Between Template and Macrocycle

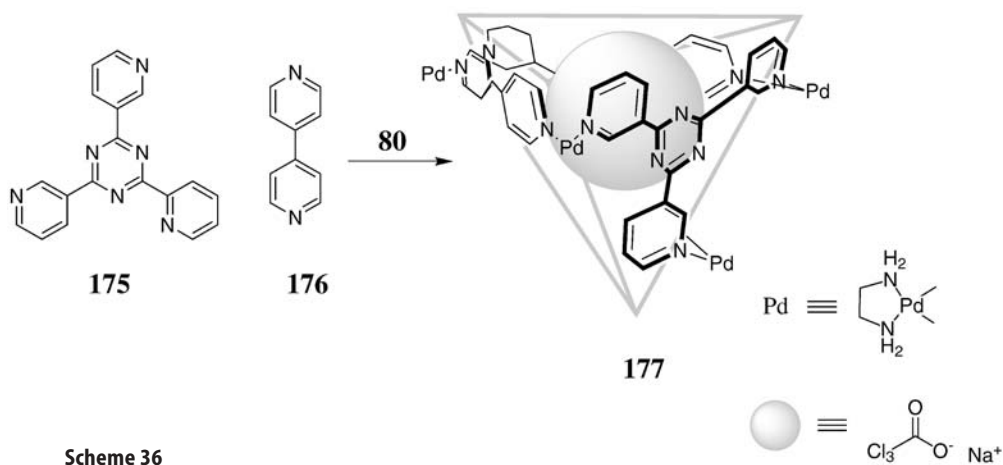
Fujita has reported that the synthesis of tube 173 requires a template [126] (Scheme 35). In the absence of a template, the combination of five equivalent



Scheme 35

of palladium species **80** and two equivalent of oligo-pyridine **174** leads to a multitude of products. Upon addition of *p*-terphenyl or 4,4'-biphenylenedicarboxylic acid the desired tube **173** was formed quantitatively in a matter of hours. However, rotund guests such as adamantane derivatives did not engender tube formation.

When the same palladium species **80** and five different ligands were mixed together, a complex mixture of macrocycles that constituted a DCL was formed [127]. Difference-NMR of the mixture, with and without a template molecule, identified the species formed upon addition of template. Thus within the mixture, the sodium salt of trichloroacetic acid templated the coming together of two equivalents of **175** and one equivalent of **176** to form host **177** (Scheme 36).

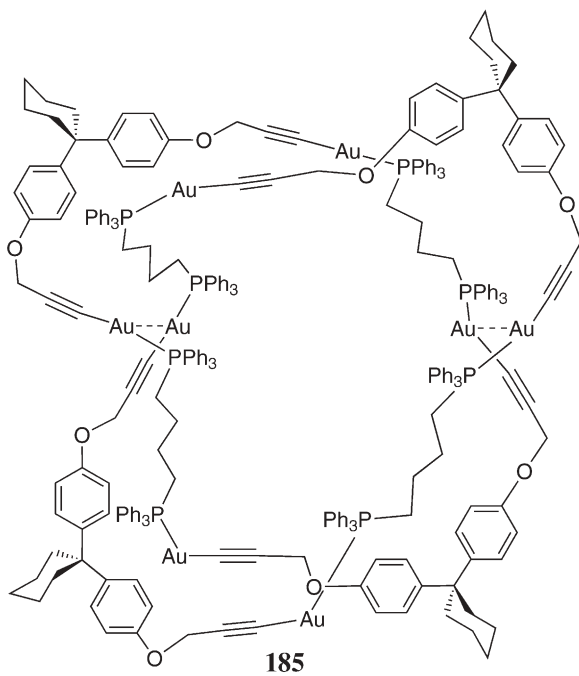
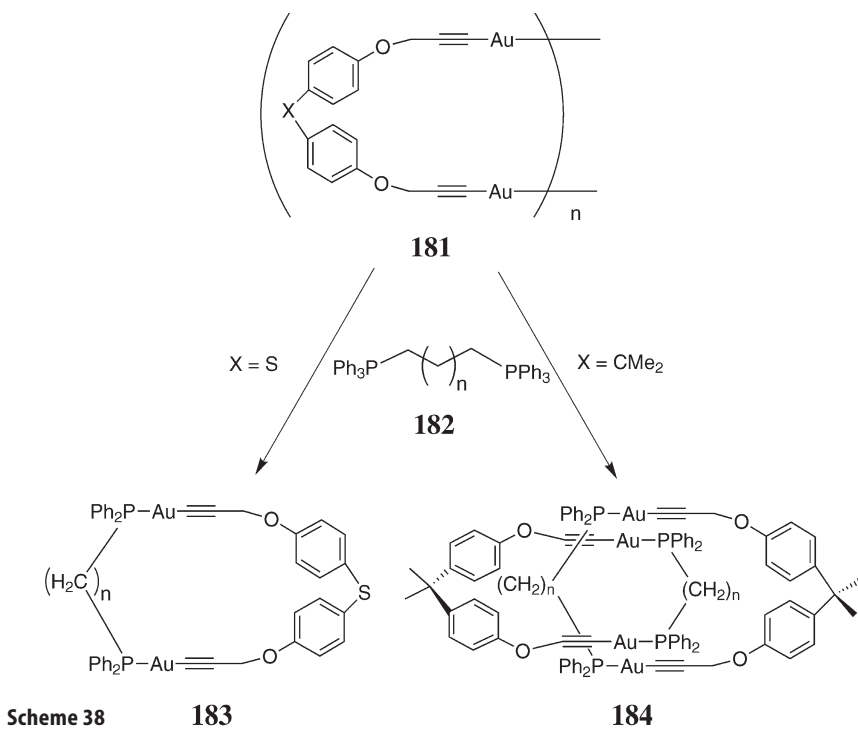


Scheme 36

178



Puddephatt has reported that gold diacetylene **181** (X=various) reacts with diphosphane ligand **182** (n=various) to form a number of products depending on the nature of the group X and the length of the carbon chain in the diphosphane. If X=S, monocycle **183** is formed (Scheme 38), if X=CMe₂, [2]catenane **184** is formed, whereas if X=cyclohexylidene the doubly braided [2]catenane



185 is formed [129–132]. Changing the length of the diphosphane ligand has revealed cases where the corresponding macrocycle is formed, cases where the [2]catenane is observed, and an example where both macrocycle and [2]catenane exist in dynamic equilibrium [133]. X-ray crystallography indicates that the principle driving force in the formation of these species is attractive Au...Au interactions.

The Dawson group have demonstrated the synthesis of a peptide catenane that assembles via the hydrophobic effect and the gamut of non-covalent forces [134]. Based on the tetramerization domain of the tumor suppressor protein (residues 325–356), the synthesized polypeptide forms a U-shaped helix-turn-sheet motif that dimerizes in an intertwining manner **186** (structure adapted from the Protein Data Bank; file 1OLG) The free N and C-termini of each peptide were connected together using a native chemical ligation process. The resulting catenane was more stable than the dimer complex and resisted both thermal and chemical denaturation [135].



186

4

Conclusions

As the aforementioned examples attest to, research into templated macrocyclizations and the synthesis of topologically complex molecules continues apace. Over the last 5 years, most non-covalent forces have been used to bring premacrocycle and template together. The two most common approaches have utilized metal ion coordination – particularly transition metal ion coordination – and hydrogen bonding. Other non-covalent forces, such as π – π stacking and cation– π interactions have proved useful, as has the strategy of using covalent bonds to link template and precursor. Regardless of the strategy, the future will likely bring larger macrocycles, topologically more complex entities, and improved yields as the field's understanding of the strengths and limitations of these exquisite reactions improves.

References

1. Watson JD, Crick FHC (1953) *Nature* 171:737
2. Todd AR (1956) In: Todd AR (ed) *Perspectives in organic chemistry*. Interscience, New York
3. Melson GA, Busch DH (1963) *Proc Chem Soc London*:223
4. Pedersen CJ (1967) *J Am Chem Soc* 89:7017
5. Pedersen CJ (1988) *Angew Chem Int Ed Engl* 27:1021
6. Diederich F, Stang PJ (2000) *Templated organic synthesis*. Wiley-VCH, Weinheim
7. Gerbeleu NV, Arion VB, Burgess J (1999) *Template synthesis of macrocyclic compounds*. Wiley-VCH, Weinheim
8. McAuley A, Subramanian S (2000) *Coord Chem Rev* 200-202:75
9. Arion VB, Revenco M, Gradinaru J, Simonov Y, Kravtsov V, Gerbeleu N, Saint-Aman E, Adams F (2001) *Rev Inorg Chem* 21:1
10. Hubin TJ (2003) *Coord Chem Rev* 241:27
11. Hernández-Molina R, Mederos A (2004) *Comprehensive coordination chemistry II: From biology to nanotechnology*:411
12. Rowan SJ, Cantrill SJ, Cousins GRL, Sanders JKM, Stoddart JF (2002) *Angew Chem Int Ed Engl* 41:898
13. Raymo FM, Stoddart JF (1999) *Chem Rev* 99:1643
14. Hubin TJ, Busch DH (2000) *Coord Chem Rev* 200-202:5
15. Breault GA, Hunter CA, Mayers PC (1999) *Tetrahedron* 55:5265
16. Jasat A, Sherman JC (1999) *Chem Rev* 99:932
17. Warmuth R, Yoon J (2001) *Acc Chem Res* 34:95
18. Warmuth R (2001) *Eur J Org Chem* 423
19. Sherman JC (2003) *Chem Commun* 1617
20. Sessler JL, Camiolo S, Gale PA (2003) *Coord Chem Rev* 240:17
21. Chandrashekar TK, Venkatraman S (2003) *Acc Chem Res* 36:676
22. Fürstner A (2000) In: Diederich F, Stang PJ (eds) *Templated organic synthesis*. Wiley-VCH, Weinheim, Chap. 9
23. Li P, Roller PP, Xu J (2002) *Curr Org Chem* 6:411
24. Fischer M, Höger S (2003) *Eur J Org Chem* 441
25. Höger S (1999) *Macromolecular Symposia* 142:185
26. Höger S (1999) *J Polym Sci Part A: Polym Chem* 37:2685
27. Höger S, Meckenstock A-D (1999) *Chem Eur J* 5:1686
28. Ünsal Ö, Godt A (1999) *Chem Eur J* 5:1728
29. Duda S, Godt A (2003) *Eur J Org Chem* 3412
30. Shah MR, Duda S, Müller B, Godt A, Malik A (2003) *J Am Chem Soc* 125:5408
31. Li X, Upton TG, Gibb CLD, Gibb BC (2003) *J Am Chem Soc* 125:650
32. Gibb BC (2003) *Chem Eur J* 9:4862
33. Laughrey ZR, Gibb CLD, Senechal T, Gibb BC (2003) *Chem Eur J* 9:130
34. Campos-Fernández CS, Clérac R, Dunbar KR (1999) *Angew Chem Int Ed* 38:3477
35. Campos-Fernández CS, Clérac R, Koomen JM, Russell DH, Dunbar KR (2001) *J Am Chem Soc* 123:773
36. Georgakilas V, Gournis D, Petridis D (2001) *Angew Chem Int Ed* 40:4286
37. Georgakilas V, Gournis D, Bourlinos AB, Karakassides MA, Petridis D (2003) *Chem Eur J* 9:3904
38. Chuchuryukin AV, Dijkstra HP, Suijkerbuijk BMJM, Gebbink RJMK, van Klink GPM, Mills AM, Spek AL, van Koten G (2003) *Angew Chem Int Ed* 42:228
39. Chuchuryukin AV, Dijkstra HP, Suijkerbuijk BMJM, Gebbink RJMK, van Klink GPM, Mills AM, Spek AL, van Koten G (2003) *Russian J Org Chem* 39:422

40. Furlan RLE, Ng Y-F, Otto S, Sanders JKM (2001) *J Am Chem Soc* 123:8876
41. Roberts SL, Furlan RLE, Otto S, Sanders JKM (2003) *Org Biomol Chem* 1:1625
42. Furlan RLE, Ng Y-F, Cousins GRL, Redman JE, Sanders JKM (2002) *Tetrahedron* 58:771
43. Roberts SL, Furlan RLE, Cousins GRL, Sanders JKM (2002) *Chem Commun* 938
44. Kaiser G, Sanders JKM (2000) *Chem Commun* 1763
45. Kieran AL, Bond AD, Belenguer AM, Sanders JKM (2003) *Chem Commun* 2674
46. Stulz E, Scott SM, Bond AD, Teat SJ, Sanders JKM (2003) *Chem Eur J* 9:6039
47. Fuchs B, Nelson A, Star A, Stoddart JF, Vidal S (2003) *Angew Chem Int Ed Engl* 42:4220
48. Edwards PG, Newman PD, Malik KMA (2000) *Angew Chem Int Ed* 39:2922
49. Edwards PG, Whotton ML, Haigh R (2000) *Organometallics* 19:2652
50. Edwards PG, Newman PD, Hibbs DE (2000) *Angew Chem Int Ed* 39:2722
51. Price AJ, Edwards PG (2000) *Chem Commun* 899
52. Harnisch JA, Angelici RJ (2000) *Inorg Chim Acta* 273
53. Ekici S, Nieger M, Glaum R, Niecke E (2003) *Angew Chem Int Ed* 42:435
54. Ekici S, Gudat D, Nieger M, Nyulaszi L, Niecke E (2002) *Angew Chem Int Ed* 41:3368
55. Fürstner A (2004) *Eur J Org Chem* 943
56. Fürstner A, Albert M, Mlynarski J, Matheu M, DeClercq E (2003) *J Am Chem Soc* 125:13132
57. Fürstner A, Albert M, Mlynarski J, Matheu M (2002) *J Am Chem Soc* 124:1168
58. Bailliez V, de Figueiredo RM, Olesker A, Cleophax J (2003) *Tetrahedron Lett* 44:9151
59. Blake AJ, Hannam JS, Jolliffe KA, Pattenden G (2000) *Synlett* 1515
60. Bertram A, Pattenden G (2001) *Synlett* 12:1873
61. Sergeyev SA, Hesse M (2002) *Helv Chim Acta* 85:161
62. Heuft MA, Fallis AG (2002) *Angew Chem Int Ed* 41:4520
63. Yamamoto M, Takeuchi M, Shinkai S (2002) *Tetrahedron* 58:7251
64. Mobian P, Kern J-M, Sauvage J-P (2003) *J Am Chem Soc* 125:2016
65. Mobian P, Kern J-M, Sauvage J-P (2003) *Helv Chim Acta* 86:4195
66. Mobian P, Kern J-M, Sauvage J-P (2003) *Inorg Chem* 42:8633
67. Arico F, Mobian P, Kern J-M, Sauvage J-P (2003) *Org Lett* 5:1887
68. Hamann C, Kern J-M, Sauvage J-P (2003) *Inorg Chem* 42:1877
69. Chambron J-C, Sauvage J-P, Mislow K, De Cian A, Fischer J (2001) *Chem Eur J* 7:4086
70. Linke M, Fujita N, Chambron J-C, Heitz V, Sauvage J-P (2001) *New J Chem* 25:790
71. Kern J-M, Raehm L, Sauvage J-P (1999) *Comptes Rendus de l'Académie des sciences. Série II. Fascicule C, Chimie* 2:41
72. Leigh DA, Lusby PJ, Teat SJ, Wilson AJ, Wong JKY (2001) *Angew Chem Int Ed* 40:1538
73. Belfrekh N, Dietrich-Buchecker C, Sauvage J-P (2000) *Inorg Chem* 39:5169
74. Ibukuro F, Fujita M, Yamaguchi K, Sauvage J-P (1999) *J Am Chem Soc* 121:11014
75. Dietrich-Buchecker C, Geum N, Hori A, Fujita M, Sakamoto S, Yamaguchi K, Sauvage J-P (2001) *Chem Commun* 1182
76. Dietrich-Buchecker C, Colasson B, Fujita M, Hori A, Geum N, Sakamoto S, Yamaguchi K, Sauvage J-P (2003) *J Am Chem Soc* 125:5717
77. Dietrich-Buchecker C, Sauvage J-P (1999) *Chem Commun* 615
78. Rapenne G, Dietrich-Buchecker C, Sauvage J-P (1999) *J Am Chem Soc* 121:994
79. Dietrich-Buchecker C, Rapenne G, Sauvage J-P, Cian AD, Fischer J (1999) *Chem Eur J* 5:1432
80. Loren JC, Yoshizawa M, Haldimann RF, Linden A, Siegel JS (2003) *Angew Chem Int Ed Engl* 42:5702
81. Cardullo F, Calama MC, Snellink-Ruel BHM, Weidmann J-L, Bielejewska A, Fokkens R, Nibbering NMM, Timmerman P, Reinhoudt DN (2000) *Chem Commun* 367
82. Alcalde E, Ramos S, Pérez-García L (1999) *Org Lett* 1:1035
83. Ramos S, Alcalde E, Doddi G, Mencarelli P, Pérez-García L (2002) *J Org Chem* 67:8463

84. Alcalde E, Alvarez-Rúa C, García-Granda S, García-Rodríguez E, Mesquida N, Pérez-García L (1999) *Chem Commun* 295
85. Houk KN, Menzer S, Newton SP, Raymo FM, Stoddart JF, Williams DJ (1999) *J Am Chem Soc* 121:1479
86. Doddi G, Ercolani G, Franconeri S, Mencarelli P (2001) *J Org Chem* 123:4950
87. Bravo JA, Orain D, Bradley M (2002) *Chem Commun* 194
88. Balzani V, Gómez-López M, Stoddart JF (1998) *Acc Chem Res* 31:405
89. Balzani V, Credi A, Raymo FM, Stoddart JF (2000) *Angew Chem Int Ed Engl* 39:3348
90. Jeppesen JO, Nielsen KA, Perkins J, Vignon SA, Di Fabio A, Ballardini R, Gandolfi MT, Venturi M, Balzani V, Becher J, Stoddart JF (2003) *Chem Eur J* 9:2982
91. Jeppesen JO, Perkins J, Becher J, Stoddart JF (2000) *Org Lett* 2:3547
92. Ballardini R, Balzani V, Dehaen W, Dell'Erba AE, Raymo FM, Stoddart JF, Venturi M (2000) *Eur J Org Chem* 591
93. Ashton PR, Bravo JA, Raymo FM, Stoddart JF, White AJP, Williams DJ (1999) *Eur J Org Chem* 899
94. Zhao X, Jiang X-K, Shi M, Yu Y-H, Xia W, Li Z-T (2001) *J Org Chem* 66:7035
95. Chen L, Zhao X, Chen Y, Zhao C-X, Jiang X-K, Li Z-T (2003) *J Org Chem* 68:2704
96. Ashton PR, Boyd SE, Brindle A, Langford SJ, Menzer S, Pérez-García L, Preece JA, Raymo FM, Spencer N, Stoddart JF, White AJP, Williams DJ (1999) *New J Chem* 23:587
97. Gatti FG, Leigh DA, Nepogodiev SA, Slawin AMZ, Teat SJ, Wong JKY (2001) *J Am Chem Soc* 123:5983
98. Brancato G, Coutrot F, Leigh DA, Murphy A, Wong JKY, Zerbetto F (2002) *Proc Natl Acad Sci USA* 99:4967
99. Clegg W, Gimenez-Saiz C, Leigh DA, Murphy A, Slawin AMZ, Teat SJ (1999) *J Am Chem Soc* 121:4124
100. Asakawa M, Brancato G, Fanti M, Leigh DA, Shimizu T, Slawin AMZ, Wong JKY, Zerbetto F, Zhang S (2002) *J Am Chem Soc* 124:2939
101. Wisner JA, Beer PD, Drew MGB, Sambrook MR (2002) *J Am Chem Soc* 124:12469
102. Glink PT, Oliva AI, Stoddart JF, White AJP, Williams DJ (2001) *Angew Chem Int Ed* 40:1870
103. Horn M, Ihringer J, Glink PT, Stoddart JF (2003) *Chem Eur J* 9:4046
104. Kilbinger AFM, Cantrill SJ, Waltman AW, Day MW, Grubbs RH (2003) *Angew Chem Int Ed* 42:3281
105. Ashton PR, Baldoni V, Balzani V, Claessens CG, Credi A, Hoffmann HDA, Raymo FM, Stoddart JF, Venturi M, White AJP, Williams DJ (2000) *Eur J Org Chem* 7:1121
106. Tseng H-R, Vignon SA, Celestre PC, Stoddart JF, White AJP, Williams DJ (2003) *Chem Eur J* 9:543
107. Alcalde E, Perez-Garcia L, Ramos S, Stoddart JF, Vignon SA, White AJP, Williams DJ (2003) *Mendeleev Comm* 100
108. Mohry A, Vögtle F, Nieger M, Hupfer H (2000) *Chirality* 12:76
109. Cabezon B, Cao J, Raymo FM, Stoddart JF, White AJP, Williams DJ (2000) *Angew Chem Int Ed* 39:148
110. Cabezon B, Cao J, Raymo FM, Stoddart JF, White AJP, Williams DJ (2000) *Chem Eur J* 6:2262
111. Ashton PR, Baldoni V, Balzani V, Credi A, Hoffmann HDA, Martínez-Díaz M-V, Raymo FM, Stoddart JF, Venturi M (2001) *Chem Eur J* 7:3482
112. Raymo FM, Bartberger MD, Houk KN, Stoddart JF (2001) *J Am Chem Soc* 123:9264
113. Amabilino DB, Ashton PR, Bravo JA, Raymo FM, Stoddart JF, White AJP, Williams DJ (1999) *Eur J Org Chem* 1295
114. Gunter MJ, Farquhar SM, Jeynes TP (2003) *Org Biomol Chem* 1:4097
115. Schwanke F, Safarowsky O, Heim C, Silva G, Vögtle F (2000) *Helv Chim Acta* 83:3279

116. Kidd TJ, Leigh DA, Wilson AJ (1999) *J Am Chem Soc* 121:1599
117. Li X-Y, Illigen J, Nieger M, Michel S, Schalley CA (2003) *Chem Eur J* 9:1332
118. Vögtle F, Hoss R, Händel M (2002) *Template or host/guest relations*. Wiley-VCH, Weinheim
119. Vögtle F, Hüntel A, Vogel E, Buschbeck S, Safarowsky O, Recker J, Parham A-H, Knott M, Müller WM, Müller U, Okamoto Y, Kubota T, Lindner W, Francotte E, Grimme S (2001) *Angew Chem Int Ed* 40:2468
120. Recker J, Müller WM, Müller U, Kubota T, Okamoto Y, Nieger M, Vögtle F (2002) *Chem Eur J* 8:4434
121. Otto S, Furlan RLE, Sanders JKM (2002) *Science* 297:590
122. Zhang Q, Hamilton DG, Feeder N, Teat SJ, Goodman JM, Sanders JKM (1999) *New J Chem* 23:897
123. Hamilton DG, Prodi L, Feeder N, Sanders JKM (1999) *J Chem Soc Perkin Trans* 1:1057
124. Hansen JG, Feeder N, Hamilton DG, Gunter MJ, Becher J, Sanders JKM (2000) *Org Lett* 2:449
125. Gunter MJ, Farquhar SM (2003) *Org Biomol Chem* 1:3450
126. Aoyagi M, Biradha K, Fujita M (1999) *J Am Chem Soc* 121:7457
127. Kubota Y, Sakamoto S, Yamaguchi K, Fujita M (2002) *Proc Natl Acad Sci USA* 99:4854
128. Yamanoi Y, Sakamoto Y, Kusukawa T, Fujita M, Sakamoto S, Yamaguchi K (2001) *J Am Chem Soc* 123:980
129. McArdle CP, Irwin MJ, Jennings MC, Puddephatt RJ (1999) *Angew Chem Int Ed* 38:3376
130. McArdle CP, Vittal JJ, Puddephatt RJ (2000) *Angew Chem Int Ed* 39:3819
131. McArdle CP, Jennings MC, Vittal JJ, Puddephatt RJ (2001) *Chem Eur J* 7:3572
132. McArdle CP, Irwin MJ, Jennings MC, Vittal JJ, Puddephatt RJ (2002) *Chem Eur J* 8:723
133. Mohr F, Jennings MC, Puddephatt RJ (2003) *Eur J Inorg Chem*:217
134. Yan LZ, Dawson PE (2001) *Angew Chem Int Ed* 40:3625
135. Blankenship JW, Dawson PE (2003) *J Mol Biol* 327:537

Macrocycles and Complex Three-Dimensional Structures Comprising Pt(II) Building Blocks

Achim Kaiser · Peter B  uerle (✉)

Department of Organic Chemistry II, University of Ulm, Albert-Einstein-Allee 11,
89081 Ulm, Germany
peter.baeuerle@chemie.uni-ulm.de

1	Introduction	129
1.1	Usage of Pt(II) Units as Supramolecular Building Blocks	129
1.2	Strategies for the Synthesis of Pt(II) Macrocycles	131
1.2.1	Choice of Building Blocks	131
1.2.2	Choice of Reaction Conditions	134
1.2.3	Characterization of Pt(II) Macrocycles	134
2	Survey of Pt(II) Macrocycles	135
2.1	Division of Different Structures	135
2.2	Macrocycles by Pt-N Coordination	136
2.2.1	Macrocycles Containing Nucleobases	136
2.2.2	Macrocycles with Exocyclic Diamine Ligands	141
2.2.3	Square Macrocycles with Exocyclic Ligands Other than Diamines	144
2.2.4	Molecular Polygons Other than Squares (Triangles, Hexagons, Cyclodimers) and Equilibria Thereof	149
2.3	Macrocycles by Pt-C Coordination	158
2.3.1	Macrocycles with Bridging Cyanide and Isocyanide Ligands	158
2.3.2	Macrocycles with Bridging Acetylide Ligands	161
2.4	Macrocycles by Pt-P Coordination	175
2.5	Macrocycles by Unusual Pt Coordination	179
3	Related Structures and Topologies	182
3.1	2D Compounds with Cyclic Substructures	182
3.2	3D (Cage) Structures	183
3.3	Catenanes	191
4	Concluding Remarks	196
	References	197

Abstract Metalla-macrocycles and complex three-dimensional structures containing Pt(II) building blocks are becoming increasingly attractive and the focus of research due to their highly effective synthesis by supramolecular self-organization and templating processes, their enhanced stability in comparison to the analogous Pd(II) complexes and their attractive properties arising from their (multi)cyclic structures. In this comprehensive review, many aspects of Pt(II) macrocyclic structures are considered and the development of this exciting field is described from the beginning of the 1990s, covering literature until the middle of 2004.

We have surveyed and organized the diverse data by first describing relevant Pt(II) building blocks, which are frequently used as a scaffold due to their defined angles and binding vectors. In an extensive second section, the various Pt(II) macrocycles are organized and described according to the mode of binding of the Pt(II) metal centres to the bridging ligands, most frequently Pt-N, Pt-C and Pt-P. Structures are summarized according to their molecular geometries – squares and rectangles, triangles, hexagons and cyclodimers. Very recent developments such as reactions and applications of these sophisticated molecular architectures are also taken into account. The third section describes even more complicated 2D compounds, 3D cage structures and topological architectures such as catenanes comprising Pt(II) centres, which are effectively formed by self-assembly processes. Interesting features such as controlled host-guest chemistry, selective molecular recognition and interesting material properties now come into range.

Keywords Platinum(II) complexes · Macrocycles · Cages · Catenanes · Supramolecular coordination · Self-assembly processes

Abbreviations

BINAP	2,2'-Bis(diphenylphosphino)-1,1'-binaphthyl
BINOL	2,2'-Dihydroxy-1,1'-binaphthyl
bipy	Bipyridine
bpz	2,2'-Bipyrazine
CD	Circular dichroism
Chiraphos	2,3-Bis(diphenylphosphino)butane
COD	Cycloocta-1,5-diene
C _p	Cyclopentadiene
CSI(-MS)	Coldspray ionization (mass spectrometry)
d(GpG)	2'-Deoxyguanylyl(3'→5')2'-deoxyguanosine
dppe	1,2-Bis(diphenylphosphino)ethane
dppee	1,2-Bis(diphenylphosphino)ethylene
dppf	1,1'-Bis(diphenylphosphino)ferrocene
dppm	Bis(diphenylphosphino)methane
dppp	1,3-Bis(diphenylphosphino)propane
<i>ee</i>	Enantiomeric excess
<i>en</i>	Ethane-1,2-diamine
ESI(-MS)	Electron spray ionization (mass spectrometry)
FAB(-MS)	Fast atom bombardment (mass spectrometry)
FT-ICR(-MS)	Fourier transform ion cyclotron resonance (mass spectrometry)
isonic	Isonicotinic acid
MALDI-(TOF)	Matrix-assisted laser desorption/ionization (time-of-flight)
	mass spectrometry
MLCT	Metal-to-ligand charge transfer
MO(s)	Molecular orbital(s)
OTf ⁻	Triflate (anion)
TBDMS-	<i>tert</i> -Butyldimethylsilyl
TIPS-	Triisopropylsilyl

1

Introduction

1.1

Usage of Pt(II) Units as Supramolecular Building Blocks

Supramolecular chemistry is of growing interest, as especially self-organization is seen as an important way to highly functional and complex systems. In particular, chemists are increasingly fascinated by large rings, molecular polygons or more complex 3D structures formed by supramolecular self-assembly processes. Complicated structures, which some years ago one only could dream of, can now be built from suitable precursors in one step. Recent reviews are available dealing with various aspects of this topic, such as supramolecular 2D and 3D coordination chemistry [1–7], structural and conformational control of functions [8] or the role of guest molecules interacting with supramolecular host systems [9, 10], as well as for special metal-free macrocyclic systems [11].

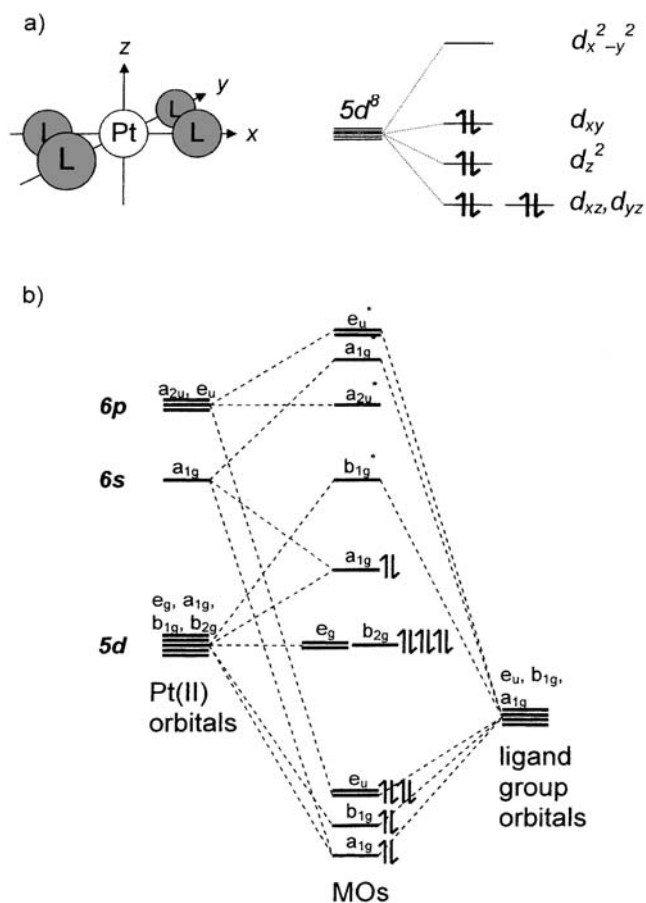
Many examples of metalla-macrocycles rely on Pd(II) coordination chemistry as the key element. During the last decade, however, the number of interesting (macrocyclic) structures built with corresponding Pt(II) units has steadily increased. Since no specialized review on this most modern topic of increasing importance is available so far, we would therefore like to present an overview and describe the up-to-date status on (self-assembled) metalla-macrocycles and complex multicyclic structures comprising Pt(II) units as the coordinating building blocks.

At first glance, the trend to use Pt(II) as crucial building block seems not quite reasonable since platinum chemicals are rather expensive and the low solubility or product mixtures often cause experimental problems. The reason for this contradiction is given by the unique properties of Pt(II) complexes.

As a late d^{10} transition metal, the element platinum comprising $5d$, $6s$ and $6p$ orbitals prefers a 16-electron valence shell rather than an 18-electron configuration. The most important oxidation state of Pt consequently is Pt(II), having a d^8 valence electron configuration that fully contributes to Pt(II) complexes. The remaining eight electrons come from four ligands around the central metal to form Pt(II)L₄ complexes.

A square planar coordination is energetically more favourable than a tetrahedral coordination due to the splitting of the originally degenerated metal d orbitals, as shown in Scheme 1a. Scheme 1b depicts a more detailed MO scheme for such a square planar d^8 complex, reflecting the symmetrically allowed valence orbital interactions. In this case, the 16 electrons occupy the energetically lowest lying bonding and non-bonding orbitals, while the anti-bonding orbitals remain unoccupied.

The main attractivity and value for the use of Pt(II) units in (supramolecular) chemistry comes from their inherent stability and rather low reactivity in



Scheme 1 Qualitative picture of the orbital levels in square planar Pt(II) complexes. **a** Splitting of the d orbital levels due to the influence of the ligand electrons. **b** MO scheme of the metal and ligand valence orbitals, considering symmetry-allowed interactions

the final complex. The geometry aspect adds to these advantages and opens up structural variations: Square planar Pt(II) complexes can either act as important 90° building blocks, i.e. as corner elements for the construction of molecular squares when the bridging ligands are *cis*-connected to the Pt(II), or as 180° linear spacers having a *trans*-Pt(II) arrangement. When macrocycles comprise a *cis*-arranged Pt unit, the so-called bite angle can be fine-tuned to a certain extent by the use of different chelating ligands. Ligand variation at the metal is a valuable factor in general, since additional modification of the resulting macrocyclic structure becomes possible.

Recently, host-guest chemistry has become an important topic in the field of macrocycles. In particular, multiply charged platina-macrocycles are the result of incorporation of Pt-N coordinated moieties. This leads to an enhanced sol-

ubility in polar or protic organic solvents, and furthermore provides ionic interactions for the inclusion of anionic guest molecules.

Another major interest in the implementation of Pt(II) into large cyclic structures is the expectation of special physical and materials properties, such as non-linear optical effects. The *d* orbitals of the metal often give important contributions to the MOs of the whole macrocyclic system. This may lead to a polarization of the excited state, which in particular provides hyperpolarizability as a basic requirement for non-linear optics.

1.2

Strategies for the Synthesis of Pt(II) Macrocycles

For the preparation of Pt(II) macrocycles several considerations have to be made concerning the building blocks and the reaction conditions. This section will give a brief introduction to the choice of appropriate building blocks and reaction conditions in order to successfully prepare these compounds and to characterize the products.

1.2.1

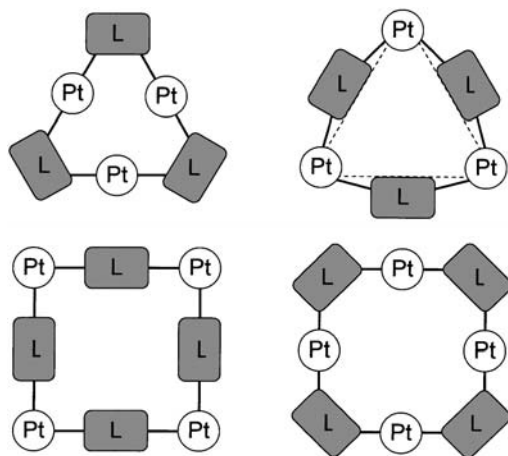
Choice of Building Blocks

Of course, the synthesis of Pt(II) macrocycles always involves a suitable Pt(II) precursor complex. Already at this point, questions concerning the type of ligands and the configuration of the resulting complex have to be addressed. Typically, the configuration (*cis/trans*) at the metal centre is retained during reactions, and from these the *trans*-configuration is the more stable one. In this respect, *cis*-to-*trans* isomerizations have been reported (e.g. structure **Bosch1**) [12], while the reverse way is more difficult to achieve [13]. To ensure the retention of a desired *cis*-configuration in the resulting macrocycle, chelating ligands such as 1,2-bis(diphenylphosphino)ethane (dppe), 1,1'-bis(diphenylphosphino)ferrocene (dppf), 1,3-bis(diphenylphosphino)propane (dppp), or ethane-1,2-diamine (en) may be used. With such bidentate ligands, the bite angle at the Pt centre may be fine tuned: a larger bridge in the chelating ligand ensures an increased bite angle, but at the same time the disadvantage of steric hindrance might arise.

As leaving groups in the Pt(II) precursor complexes, weakly bound ligands such as cycloocta-1,5-diene (COD), halogenides (Hal^-), triflate (OTf^-), or nitrate (NO_3^-) are quite useful. When these leaving groups act as counter-anions for the resulting charged Pt(II) macrocycles, and this is in particular true in the case of NO_3^- , they might have an important impact on the stability of the macrocyclic complex. Furthermore, they may influence the dynamic equilibria that sometimes come into play.

In most cases, the macrocycles are intentionally prepared by a directional bonding method: the “binding vectors” (representing the directions of the coordination bonds to which the difunctional ligand and metal precursors are

capable) form angles that can be assigned to geometric structures and polygons. As already pointed out in the previous section, Pt(II) can thereby act as a 90° (*cis*) or 180° (*trans*) building block, which directly results in basic frameworks of cyclic tri- and tetranuclear Pt(II) complexes (Scheme 2). The combination of Pt(II) with ligands of different bite angles may result in a variety of geometric structures and molecular polygons, some of which are depicted in Scheme 3 [6b,c].

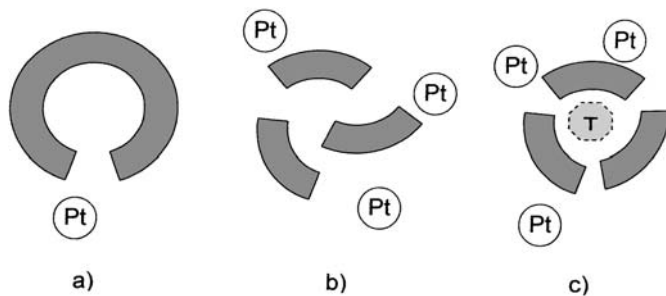


Scheme 2 Possible approaches to molecular coordination triangles and squares (L =bridging ligand)

Building Blocks	60°	90°	109.5°	120°	180°
60°					
90°					
109.5°					
120°					
180°					

Scheme 3 Selective formation of different geometric structures by appropriate choice of corner and bridging units [6b,c]

Typically, these frameworks are formed by self-assembly processes. If this strategy is not applicable, which is mostly the case for the preparation of mixed metal macrocycles, the following general strategies (depicted in Scheme 4) might be used for the construction of corresponding coordination macrocycles:



Scheme 4 Strategies for the synthesis of coordination macrocycles (T =template): **a** using a “preformed” macrocycle, **b** by self assembly, and **c** by a template synthesis

Preformed cycles. Here, the macrocycle is already preformed to a certain extent and (intramolecular) ring closure is the crucial step. In order to allow efficient ring closure reactions, a configuration or conformation of the precursor is needed in which the end groups (that are to be connected) come into close proximity to each other. This method probably gives the best control over product formation.

Self-assembly. Rather rigid bifunctional building blocks and Pt precursors with predefined geometry (size and angles) are reacted in a specific stoichiometry to form the macrocycle. Typically, a mixture of various ring sizes and number of metal centres should be expected as well as linear oligomers or polymers. Therefore, well-defined and optimized geometries of the building blocks are necessary so that finally the multi-component system can self-organize into distinct structures. Thermodynamically, the cyclic structures are normally the most stable compounds. If the Pt–ligand bond formation is reversible, which is mainly the case for Pt–N bonds, long reaction times and heating are favourable for macrocycle formation. Entropy usually prefers smaller ring sizes, hence, strained macrocycles become available with this method.

Template synthesis. The addition of a template leads to a pre-organization of one component around the template due to hydrophobic or ionic interactions. Efficient formation of the macrocyclic product is then obtained by connecting these prearranged moieties with the second component. Finally, the template is removed to yield the desired macrocycles. The template approach is especially important and useful for the formation of complex 3D structures (see Sect. 3).

1.2.2

Choice of Reaction Conditions

Although the reaction works at room temperature for most Pt-N and Pt-P complexes, heating might be necessary to drive the equilibrium from kinetically formed linear oligomers to thermodynamically favoured macrocyclic products. This reaction control can be applied in particular for Pt-N coordinated compounds where the Pt-N bond is stable at room temperature but becomes labile when heated up to about 100 °C. Typically, the metalla-macrocycle is formed as a multiply charged salt that precipitates from aqueous or non-polar organic solvents, shifting the equilibrium towards the macrocyclic products.

In contrast to Pt-N and Pt-P coordination chemistry, Pt-C bond formation is not reversible. Here, the macrocyclization is kinetically controlled and does not need a long reaction time. In the case of acetylide ligands, the precursors are rather instable and are therefore generated in situ from trialkylsilyl-protected reactands. Pt(II) acetylide complex formation can then be achieved by copper(I) iodide as a catalyst [14].

1.2.3

Characterization of Pt(II) Macrocycles

Characterization and structure elucidation of Pt(II) systems can be best done by NMR, IR and mass spectrometry methods. In most Pt(II)-based systems phosphorous-containing ligands are involved. Therefore, ^{31}P -NMR is (besides other NMR methods) an excellent tool. The position of the phosphorous signal represents a good indication for the environment, i.e. the geometry at the Pt centre.

Further characterization of Pt(II)-macrocyclic systems is often provided by IR spectroscopy. Especially in the case of Pt(II)-acetylide complexes, characteristic bands for the $\text{C}\equiv\text{C}$ triple bond are found.

The complicated structures are typically well supported by mass spectrometry using fast atom bombardment (FAB) as ionization method [15]. For more labile compounds, which may decompose even under mild ionization conditions such as FAB, matrix-assisted laser desorption/ionization (MALDI) or electron spray ionization (ESI) can be used. Yamaguchi, Fujita et al. developed cold spray ionization mass spectrometry (CSI) as a modification of ESI at low temperatures [16], whereas Schalley, Lützen et al. successfully utilized advanced Fourier transform ion cyclotron mass spectrometry (FT-ICR-MS) for high-resolution measurements [17].

2

Survey of Pt(II) Macrocycles

2.1

Division of Different Structures

The following sorting criteria for the numerous Pt(II) macrocycles can be used:

Geometry of the macrocycle. The large group of molecular squares and triangles is frequently the topic of reviews on coordination-driven self-assembly. However, some macrocycles that are not shape-persistent cannot be accounted to a specific geometry. Furthermore, in several cases equilibria between two different geometries are observed.

Configuration of the Pt moiety. Either *cis*- or *trans*-configurations of the bridging ligands are possible at the Pt centres. Since some macrocycles include both *cis*- and *trans*-arranged Pt units within the same molecule, this criterion is not well suited.

Synthetic strategy. As presented in Sect. 1.2, there are different approaches for construction of Pt(II) macrocycles. Because they all may lead to very similar structures, a good comparison is not possible.

Properties of the macrocycles. Some of the macrocycles presented in this review have been investigated in terms of their chemical and physical behaviour, such as host-guest chemistry, subsequent modification, chirality or non-linear optical properties. A satisfying comparison might be difficult because large differences in these properties might arise from only small structural modifications.

Coordination type of the bridging ligand. Typically, the bridging ligands such as *N*-hetarenes, phosphines or acetylides are bound to the metal centre by Pt-N, Pt-P or Pt-C coordination, respectively. This aspect is often congruent with the synthetic strategy for preparation of Pt(II) macrocycles. Since only few exceptions exist in which several binding modes are operative in one molecule, we therefore chose the coordination type of the bridging ligands to the Pt(II) centre as the main criterion to divide the examples cited in this review into the corresponding Sects. 2.2 to 2.5. Within these sections we grouped the members according to their geometry. For clarity, instead of using the typical lengthy and complicated nomenclature of the presented macrocycles, we named them after the corresponding author(s) of the cited publication (e.g. "Author1").

2.2

Macrocycles by Pt-N Coordination

2.2.1

Macrocycles Containing Nucleobases

Coordination of heteroaromatic nitrogen ligands to Pt(II) is the key to many synthetic Pt(II) macrocycles, including the first examples inspired by biochemical research in the 1980s. The biological importance of the anticancer drug “Cis-platin” led to detailed studies on the binding modes of Pt compounds to nucleobases, resulting in various macrocyclic structures.

As an example, in the 1970s Lock et al. reported a cyclic dimer formed from *cis*-Pt(NH₃)₂Cl₂ and 1-methylthymine, in which the nucleobase binds to the Pt(II) moieties by nitrogen and oxygen atoms [18]. Further reports on similar structures followed, e.g. by Lippert et al. [19] or Fanchiang [20]. As these complexes might rather be considered “macrochelates” than “macrocycles”, their structures are not shown here. Meanwhile, the investigation of Pt insertion into DNA fragments has developed into an important field of research on its own and we will describe some representative examples; a complete survey would go far beyond the scope of this review.

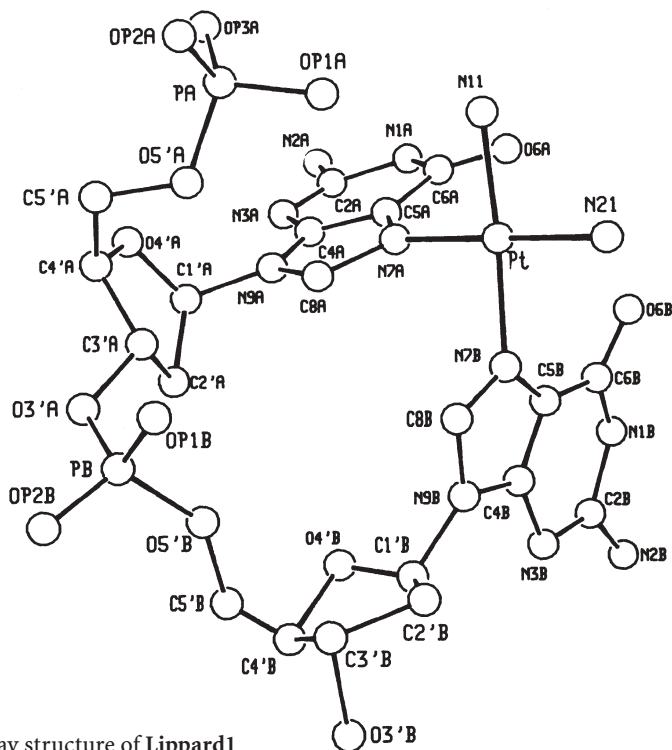


Fig. 1 X-ray structure of Lippard1

In 1985, Lippard et al. presented the first X-ray structure analysis of platina-macrocyclic **Lippard1**, which is assembled from $\{\text{Pt}(\text{NH}_3)_2\}^{2+}$ and the DNA intrastrand d(GpG). The Pt(II) centre here is surrounded by four nitrogen ligands: two ammonia and two guanosine moieties, the latter being linked by a phosphate unit (Fig. 1) [21].

Longato et al. reported in 1995 the impressive hexaplatina-macrocyclic **Longato1**, which readily self-assembles in D_2O from six 9-methylguanine and six $\text{Pt}(\text{PMe}_3)_2(\text{NO}_3)_2$ precursor molecules (Fig. 2) [22a]. The structure was confirmed by X-ray structure analysis and shows an S_3 -symmetric compound, in which the bridging guanine units are alternately located below and above the ring plane of the six Pt(II) centres.

Besides these examples, the cyclic trimer **Longato2** is formed from $\text{Pt}(\text{PMe}_3)_2(\text{OH})_2$ and 1-methylcytosine as the nitrate or the perchlorate salt (the latter being described as “unpredictably explosive”) after heating in water for 6 days at 80 °C. (Fig. 3) [22b]. In this trisplatina-macrocyclic, the cytosine units are arranged on one side of the plane which is formed by the three Pt(II) corners, whereas the six phosphine ligands face the opposite side.

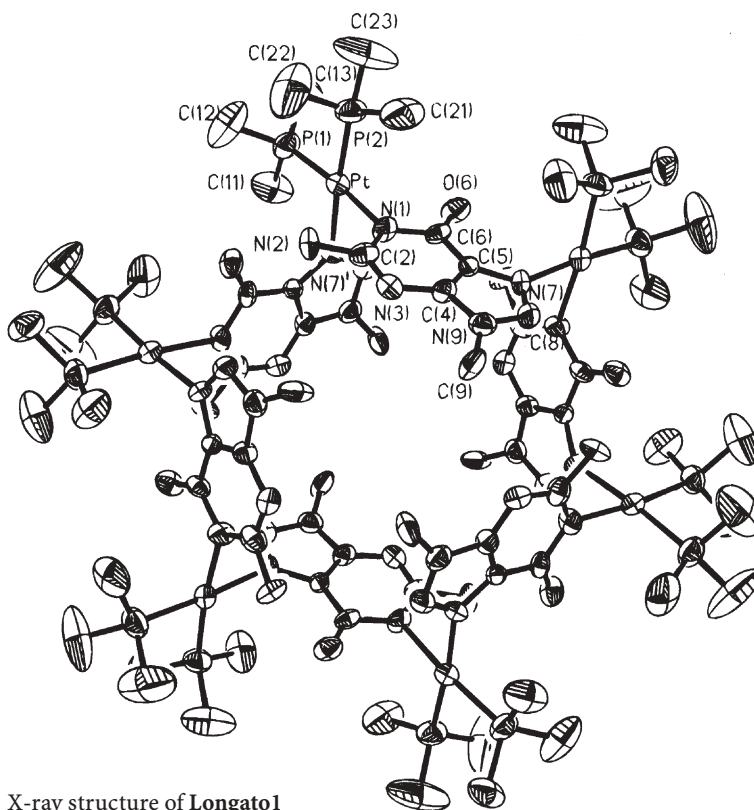


Fig. 2 X-ray structure of Longato1

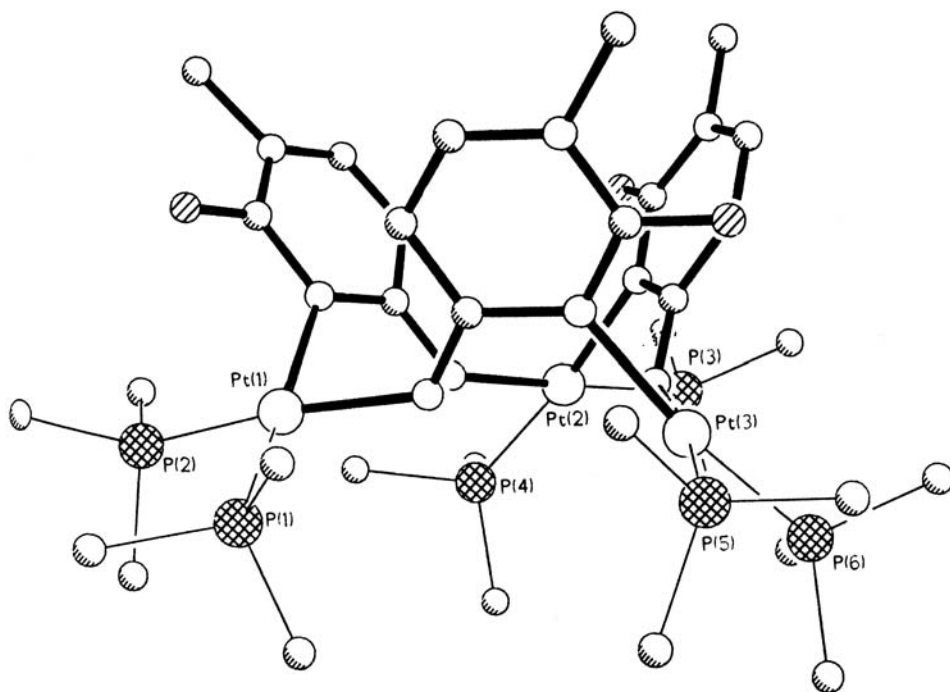


Fig. 3 X-ray structure of Longato2

Lippert et al. broadly investigated macrocycles consisting of Pt(II) and nucleobases, and later on extended their research to related Pt(II)-macrocycles in which other *N*-heterocyclic systems act as bridges between the Pt centres [23, 24]. By 1981 Lippert had already postulated the cyclic tetranuclear Pt(uracilate) complex $\{\text{Pt}(\text{en})(\text{u-}N^1, N^3)\}_4$ **Lippert1** (Fig. 4) [24r]. However, a thorough characterization of this “molecular box” by crystal structure analysis only appeared in 1992 [24q]. The platina-macrocyclic **Lippert1** results from an initially formed mixture of linear complexes after stirring for several days at room temperature. In contrast to most of the existing Pt-N coordinated complexes (vide ultra), one nitrogen atom in a uracil ligand is bound as an anion. The OH groups of the resulting positively charged complex can be deprotonated around pH 8 to a neutral, highly soluble product. From its structure, **Lippert1** can be considered as a metal analogue of calix[4]arenes. An equilibrium between various conformations was observed due to the rotational freedom around the Pt-N bonds, whereby the “1,3-alternate” form is the predominant one (see Fig. 4). By deprotonation, or addition of metal ions such as Ag^+ , the equilibrium can be shifted to a “pinched cone” conformation. Each of the possible conformations can be stabilized by additional metal cations [24d,e,m,n,o]. In recognition experiments it was found that only the “cone” conformation is able to complex sulfonate anions [24e]. Navarro, Lippert et al. and Mutikainen, Randaccio, Lippert et al. also reported an analogous tetrameric macrocycle with 2-hydroxypyrimidine

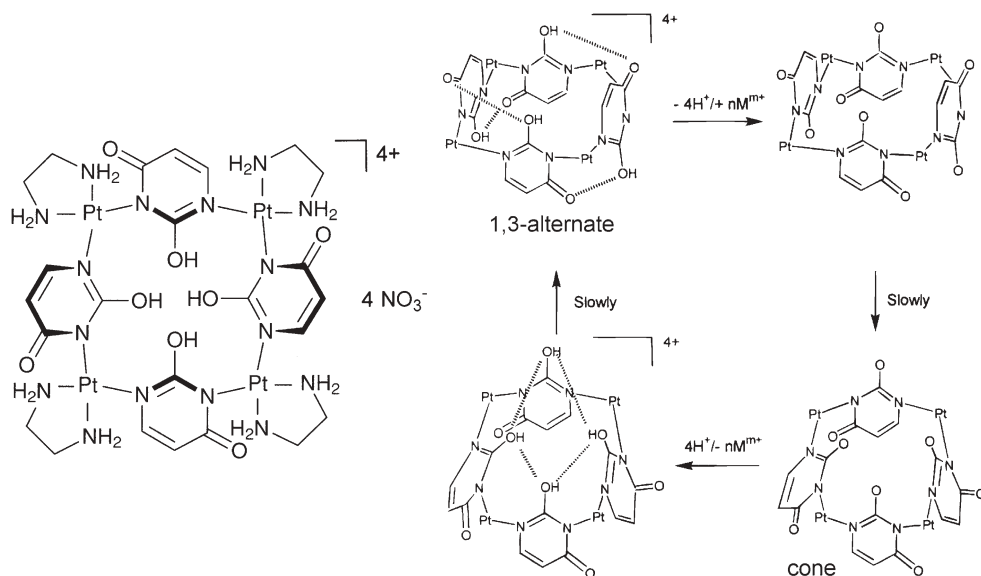


Fig. 4 Macrocycle Lippert1 and the conformational equilibria. Pt=Pt(en); M is omitted in the structures for sake of clarity

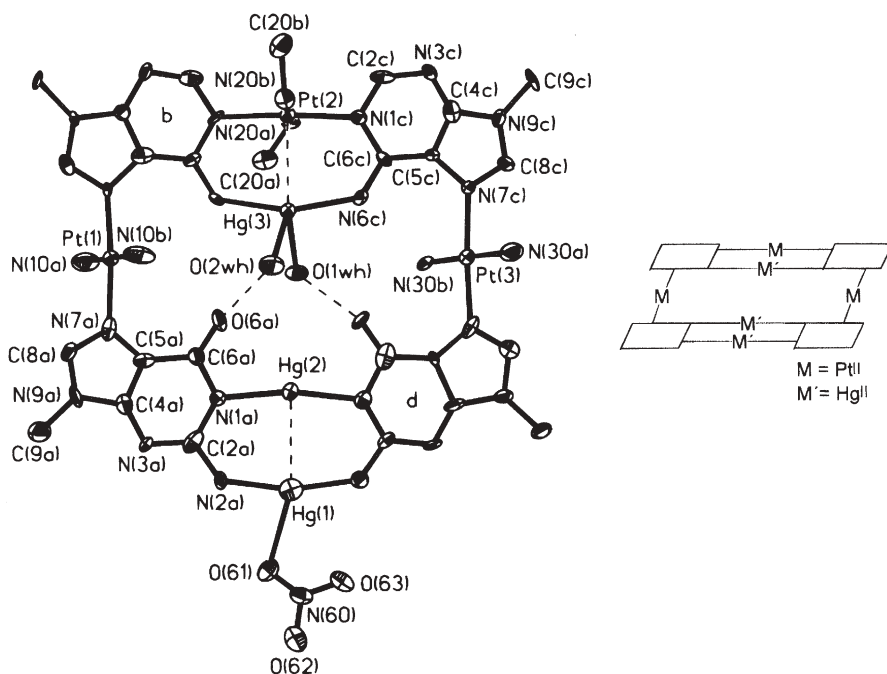


Fig. 5 X-ray structure and sketch of Lippert2

ligands, as well as several mixed hexa- or octanuclear cycles comprising uracilate and *trans*-Pt(II), which represent further interesting examples [24c,m,n].

The molecular rectangle **Lippert2**, consisting of *trans*-Pt(II), linear Hg(II) and guanine units, is quantitatively formed due to the ideal binding vectors of guanine which virtually adopt a 90° angle (Fig. 5) [24i,l,p].

The similar “molecular rectangle” **Lippert3** with two Ag(I) and two Pt(II) moieties could be obtained by reaction of AgNO₃ and a *trans*-Pt(II) precursor comprising 9-methyladenine and 9-methylhypoxanthinate as ligands (Fig. 6) [24a].

As successfully applied for **Lippert1**, the concept of switching the ligand conformation by post-modification of the metalla-macrocycle was extended to cyclic trimers containing 2,2'-bipyrazine (bpz) units [24b,f,g,h,j,k]. The bpz ligand connects to the Pt(II) corners by a *trans*-4,4' coordination to form the molecular triangle **Lippert4a** in 35% yield (Fig. 7). In this macrocycle the pyrazine rings are distorted by 21–27° and remain more or less perpendicular to the molecular plane [24j,k]. This coordination mode allows the formation of a triangle because the favourable 90° angles at the Pt corners remain intact. The addition of an second metal precursor complex such as Pd(II)(en) results in the formation of hexametalla-macrocycle **Lippert4b** [24b,f,g] in which the bipyra-

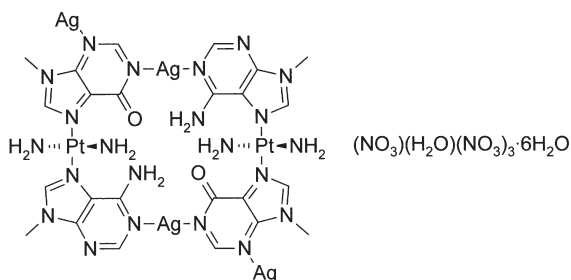


Fig. 6 Macrocycle **Lippert3**

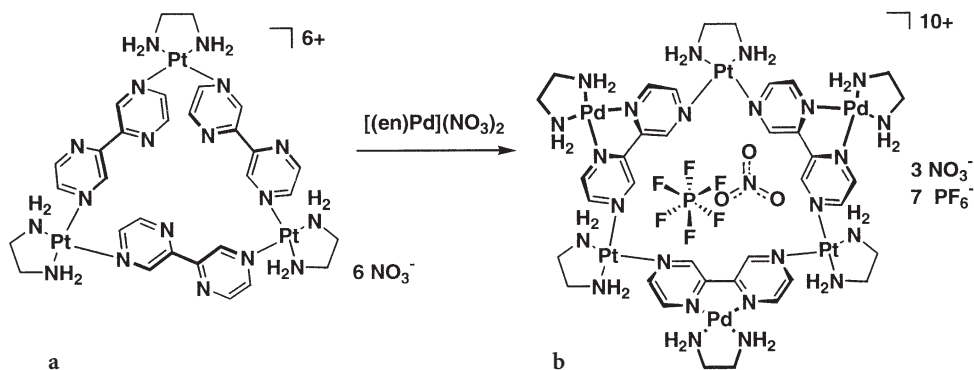


Fig. 7 Macrocycle **Lippert4a** and conversion to macrocycle **Lippert4b**

zines are twisted and chelate three Pd(II) units by 2,2'-coordination at the remaining nitrogen atoms. The three Pt and Pd centres are arranged in an alternating up/down fashion which, similar to macrocycle **Lippert1**, resembles a calix[3]arene and is capable of complexing anions such as PF_6^- and NO_3^- . In the solid state, the macrocycles are stacked, forming anion channels with a diameter of 6.24–6.42 Å [24h].

2.2.2

Macrocycles with Exocyclic Diamine Ligands

While the examples described so far have concentrated on bridging ligands with biologic relevance, it was the ground-breaking work of Fujita et al. and Stang et al. that established a huge variety of novel metalla-macrocylic structures formed by self-assembly processes. Molecular polygons or more sophisticated molecular topologies, such as catenanes or Platonic and Archimedean structures, boosted a field on its own which receives much attention (see also Sect. 3 and reviews of Fujita et al. [5] and Stang et al. [6]). In 1991, Fujita, Ogura et al. were in fact the first to report a molecular square comprising *cis*-Pt(II)(en)-corners and 4,4'-bipyridine bridging ligands [25c,e]. The reaction of Pt(II)(en)(NO_3)₂ and the bipyridine in D_2O first resulted in a mixture of linear oligomers. Nevertheless, when heating the reaction mixture to 100 °C for 4 weeks (!), the macrocycle **Fujita1** (Fig. 8) could then be identified and its formation could be monitored by ^1H -NMR [25e]. NMR studies in aqueous solutions showed that the macrocycle is capable of complexing small aromatic ether molecules, however, with relatively small association constants in the range $K_a = 10^2 \text{ L mol}^{-1}$ [25d]. The intermolecular interactions are most probably of hydrophobic nature and are due to the quasi-perpendicular conformation of the 4,4'-bipyridine units.

When [4,7]phenanthroline is used as a bridging ligand instead of 4,4'-bipyridine, a completely different macrocylic structure results, which is quan-

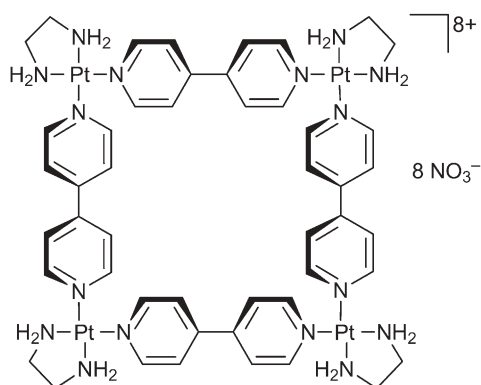


Fig. 8 Macrocycle **Fujita1**

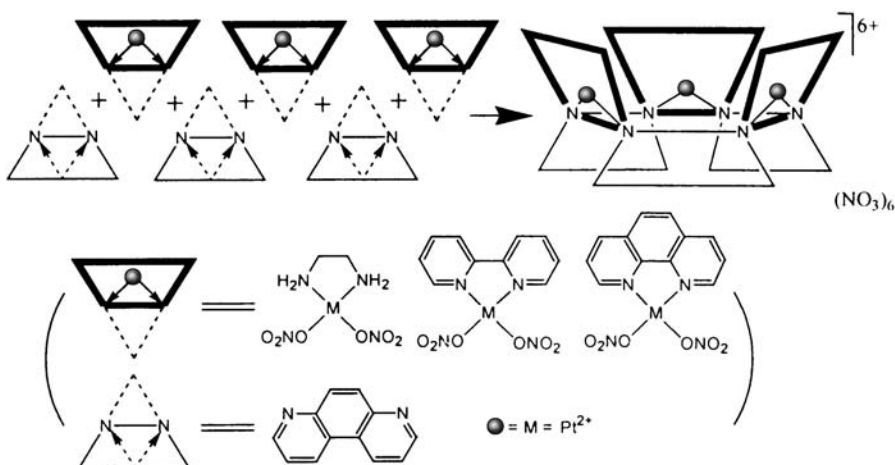


Fig. 9 Macrocycle **Yu1**

titatively formed in D_2O within minutes, as reported by Yu et al. [25a,b]. Due to the 60° angle of the binding vectors of the nitrogen lone pairs in $[4,7]$ phenanthroline, three *cis*-arranged $\text{Pt}(\text{II})(\text{en})$ corners form a triangle with a crown-like structure. Replacement of the bidentate en-ligands at the $\text{Pt}(\text{II})$ centres by $2,2'$ -bipyridine or $[1,10]$ phenanthroline, which occurs at 100°C in the presence of excess NaNO_3 , gives the crown-like structure **Yu1** comprising strong aromatic receptor moieties (Fig. 9).

An interesting mixed-metal motif was presented by Dunbar et al., who obtained the square **Dunbar1** (Fig. 10) comprising isonicotinate (isonic) bridging ligands and mixed Pt and Re corners in 42% yield [26]. Here, each Re corner consists of two linked Re atoms, each of them coordinating to one of the oxygen atoms of the carboxylate moieties. A further cyclic assembly with isonic ligands, in which Pt is not only bound by nitrogen, but also via oxygen, is presented in Sect. 2.5.

A kind of strain-free truncated triangle, in which the Pt corners comprise a bite angle of 90° , was reported by Kim et al., who used flexible linkers to build the macrocyclic oligorotaxane (or “necklace”) **Kim1** (Fig. 11) [27]. The interlocked ring system was obtained in 90% yield in a one-pot reaction by stirring a mixture of the $\text{Pt}(\text{II})$ precursor, the exocyclic en-ligand and cucurbituril in refluxing water. The reaction could be monitored by NMR and the structure was confirmed by X-ray structure analysis. With longer reaction times, an equilibrium between the molecular triangle and a corresponding square evolved, yielding an almost 1:1 mixture of the trimeric and tetrameric necklace. On the other hand, the cyclotetramers could be selectively obtained by tuning the threading ligands in terms of length and connectivity to the coordinating groups (3-pyridyl- vs. 4-pyridyl-) [27a].

A similar flexible molecular triangle with the non-symmetric bridging ligand *N*-(4-pyridinyl)isonicotinamide was reported by Puddephatt et al. [28]. From

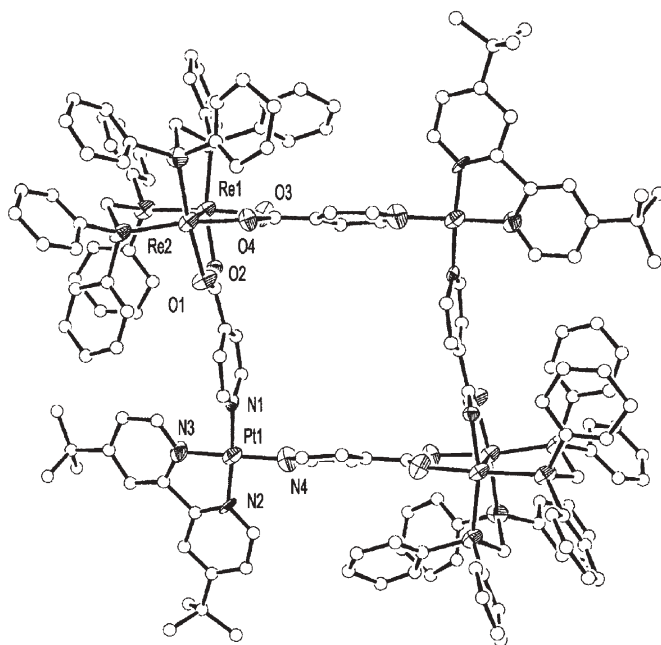


Fig. 10 X-ray structure of macrocycle Dunbar1

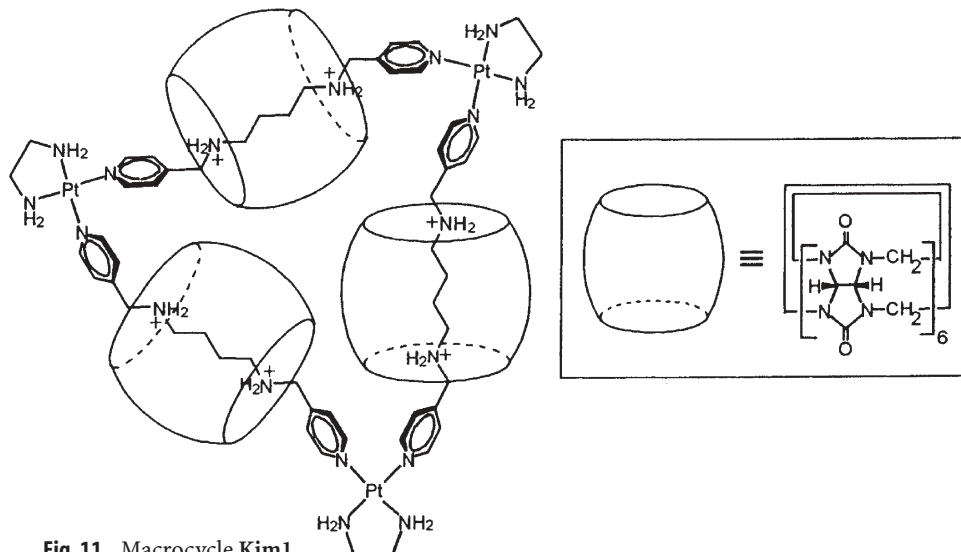


Fig. 11 Macrocycle Kim1

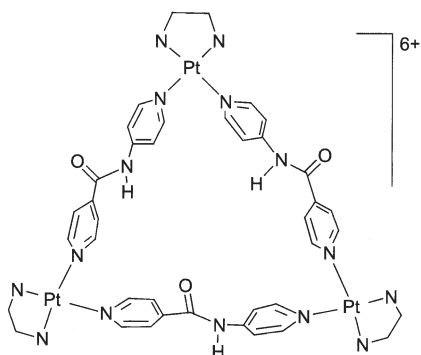


Fig. 12 Macrocycle **Puddephatt1**

the two different possible combinations, the less symmetric trimer **Puddephatt1** (Fig. 12) is formed in favour of a potential triangle with C_3 symmetry, as was confirmed by X-ray structure analysis. The packing pattern in the crystal reveals association of the molecules by stacking, which is caused by hydrogen bonding between the amide groups. However, the authors do not exclude the possibility that in solution other structures such as molecular squares may exist.

2.2.3

Square Macrocycles with Exocyclic Ligands Other than Diamines

The same type of self-assembled molecular square such as **Fujita1** was reported in 1994 by Stang et al. [15,29f,g]. In contrast to **Fujita1**, the molecular square **Stang1** forms at room temperature with 4,4'-bipyridine when, instead of the en-ligand, the bidentate phosphine ligand dppp is used in the Pt(II) precursor complex (Fig. 13). Interestingly, the successful implementation of PEt_3 instead

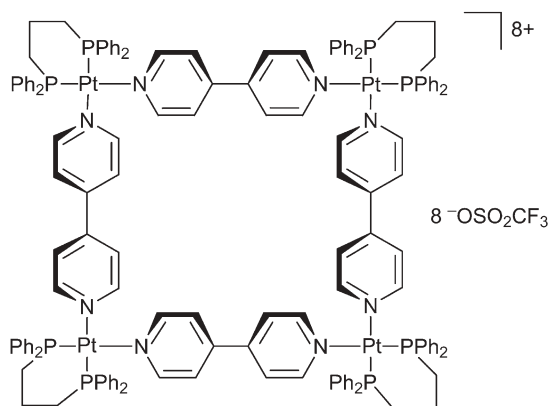


Fig. 13 Macrocycle **Stang1**

of dppp proved that a chelating ligand is not absolutely necessary to retain the *cis*-geometry at the metal centre.

In the following years, Stang et al. reported a variety of metalla-macrocycles based on the previous type including Pt(II) diphosphine corner units. Various bridging ligands, e.g. diazapyrene and diazabenzoperylene, have been used yielding macrocycles with extended cavities. Furthermore, variation of the structures were achieved at the exocyclic bidentate ligands of the Pt(II) centres or by replacement of two opposite Pt(II) corners with other 90° elements such as Pd(II), T-shaped iodonium moieties or oxygen-bonded TiCp₂ units. Since much of this work has already been covered by reviews published in 1997 and 1998 [6c,d], here, we only focus on some prominent examples.

Very aesthetic and complex multimetallic structures result when *meso*-(4'-pyridyl)-substituted metalloporphyrins are reacted with Pt(II) precursors to form the comparable molecular squares **Stang2** (by Stang et al., Fig. 14) [29e] and **Lehn1** (by Lehn et al., Fig. 15) [30]. Such a cyclic arrangement of porphyrin moieties is particularly striking because one can regard them as a mimic for the natural light harvesting systems in the photosynthetic reaction centre. Detailed structural analyses of the porphyrin squares by NMR indicate that, in contrast to macrocycles such as **Fujita1** (vide infra), only the pyridine rings are twisted perpendicular to the molecular plane, while the porphyrins, representing the larger part of the bridging ligand, remain in the plane of the square. As had been seen before with self-coordinated Zn-porphyrin arrays, the coordinated metal has a

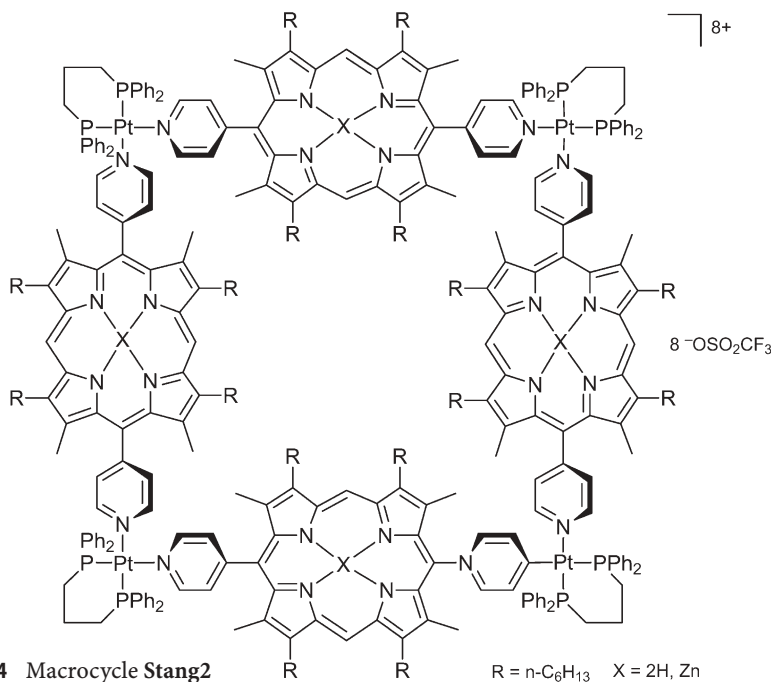


Fig. 14 Macrocycle **Stang2**

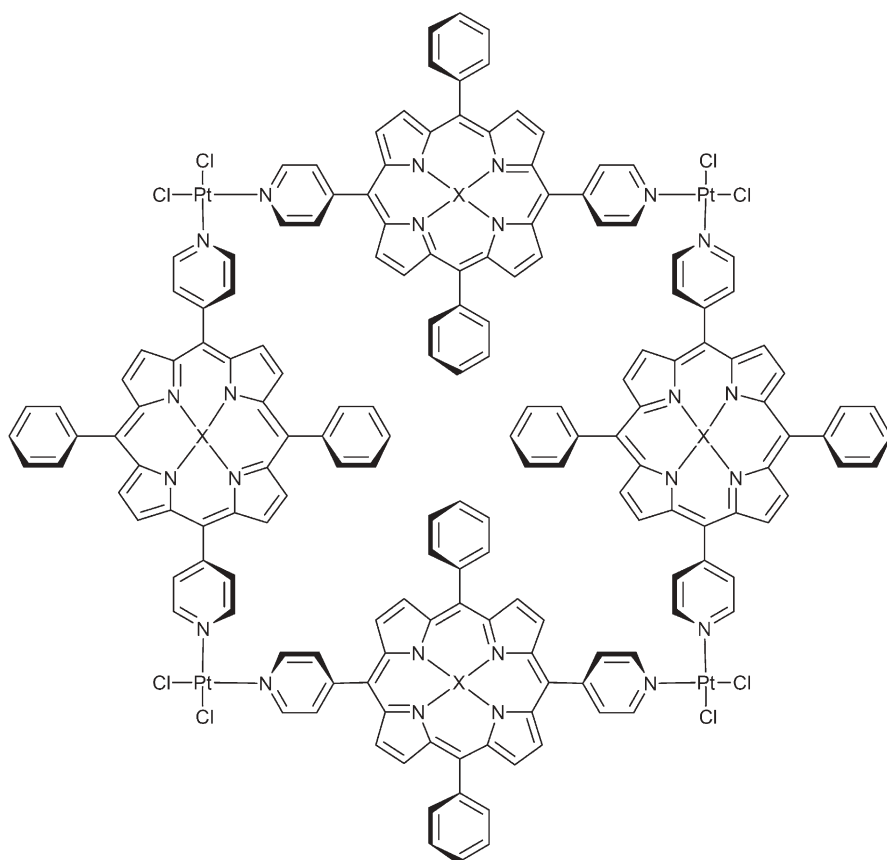


Fig. 15 Macrocycle Lehn1

X = 2H, Zn

strong influence on their spectroscopic behaviour; for example, the Soret- and Q-band absorptions are strongly enhanced [29e]. Stang et al. further demonstrated the possibility of using substituted porphyrins not only as a linear building block, but also as 90° corner elements for molecular Pt(II) squares [29a].

The replacement of the porphyrin unit by other dye molecules leads, e.g., to the molecular square **Würthner1**, which is formed by self-assembly in excellent yields and comprises *N,N*-dipyridyl-substituted perylene tetracarboxylic acid diamide as the bridging ligand (Fig. 16) [31]. This type of novel supramolecularly arranged dye aggregate shows intriguing photophysical data. Among them, the high fluorescence quantum yield of the ligand remains almost unchanged in the Pt(II) molecular square. The authors ascribe this effect to a decoupling of the perylene chromophore and the metal binding sites, caused by the perpendicular arrangement of the ligands with respect to the molecule plane. A similar macrocycle, which exhibits a triangle–square equilibrium, is presented in Sect. 2.2.4.

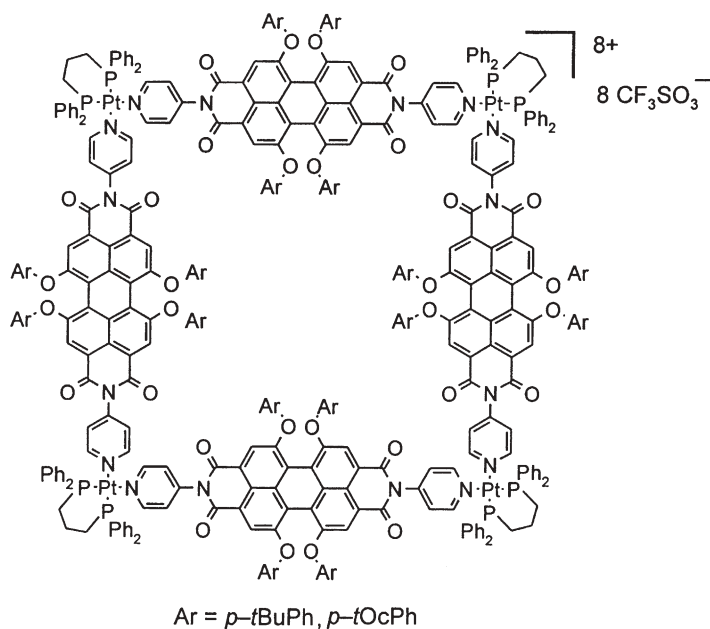


Fig. 16 Macrocycle Würthner1

The resulting cavity of the molecular squares may be suited for the inclusion of guest molecules, which was shown by Stang et al. for mixed metallic macrocycles such as **Stang3** (Fig. 17) [29b–d]. Although only little interaction was found with electron-rich compounds such as 1,4-dihydroxybenzene, it was possible to bind Ag^+ cations from silver triflate in a “tweezer” fashion, in which Ag^+ is bridging and connected to two ethynyl units adjacent to the Pt(II) corners. This coordination mode could be proven by NMR, IR and mass spectrometry. Remarkably, the resulting $\text{Ag}(\text{I})$ complexes of **Stang3** can themselves capture guest molecules, such as pyrazines or phenazines, to form a “diagonal” in the molecular square (Fig. 17) [29b].

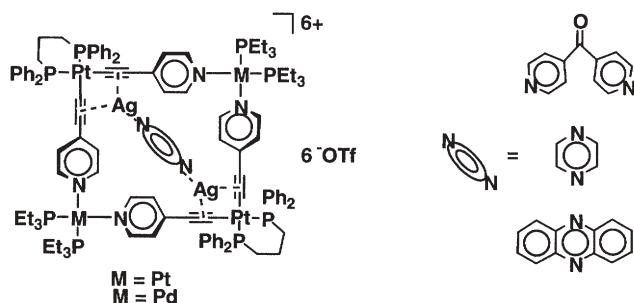


Fig. 17 Silver complex of macrocycle **Stang3** with different guest molecules

Post-modification of a molecular square by photo-isomerization of reactive bridging ligands was attempted by Lees et al. [32a]. Among other mixed metal molecular squares that have been reported by this group [32b], **Lees1** (Fig. 18) is particularly interesting due to its *trans*-diazo or *trans*-stilbene units, which constitute the bridging ligands between the two Pt(II) and Re(III) corners.

The ligand configuration at the double bond can be isomerized by light and thermally reverted. In contrast to the corresponding Pd(II) macrocycles, which

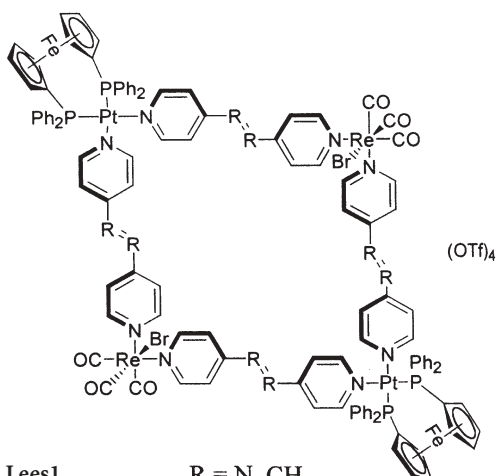


Fig. 18 Macrocycle **Lees1**

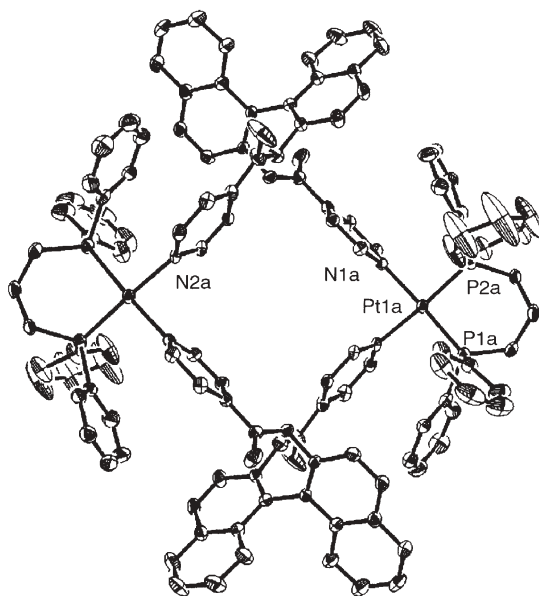


Fig. 19 X-ray structure of macrocycle **Hong1**

due to the *cis*-configuration of the bridging ligand convert to a cyclic dimer by irradiation, the Pt(II) analogues dissociate and do not form dimers upon irradiation. This was accounted for by the more stable nature of the Pt-N bond compared to the Pd-N bond, which prevents reorganization. However, after heating the solution of the follow-up products for 2 days, the original mixed metalla-macrocycle **Lees1** could be fully recovered.

The group of Hong used a BINOL (2,2'-dihydroxy-1,1'-binaphthyl) ester of isonicotinic acid as a bridging ligand. In the reaction of the racemic mixture of the BINOL ester with Pt(II)(dppf), the rectangular bis-platina-macrocycle **Hong1** (Fig. 19) was selectively formed [33]. NMR and X-ray structure analysis revealed that one *S* and one *R* ligand are incorporated in the macrocycle, showing a self-discrimination process.

2.2.4

Molecular Polygons Other than Squares (Triangles, Hexagons, Cyclodimers) and Equilibria Thereof

Due to the ideal 90° angle of the frequently used Pt(II) diphosphine precursors, most examples of Pt(II) macrocycles take the shape of a square or a rectangle. However, other molecular geometries, which may be strained, recently came up when the resulting binding angles either at the bridging ligands or at the Pt centre differ from 90° or 180°. Since metal-ligand interactions are typically reversible, equilibria between various molecular geometries may arise.

In this respect, the reversible transformation of a molecular square to a corresponding triangle was found by Stang et al. for the macrocycle **Stang4**, in which more or less flexible *trans*-bis(4-pyridyl)ethylene linkers are used as bridging ligands (Fig. 20) [34d]. The equilibration is accelerated by addition of water and was monitored by NMR spectroscopy. Although the squared configuration tends to crystallization, in solution the formation of a triangular structure is strongly favoured. Exchange of the triflate counter ions by the larger cobalticarbaborane anion ($\text{CoB}_{18}\text{C}_4\text{H}_{22}$) led to a further stabilization,

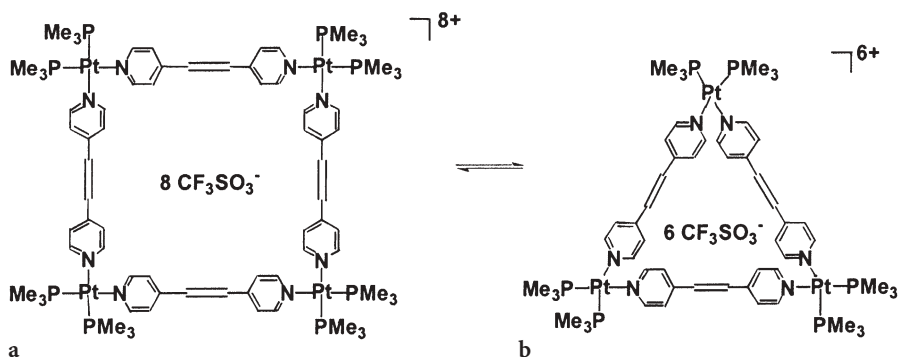


Fig. 20 Equilibrium between square **Stang4a** and triangle **Stang4b**

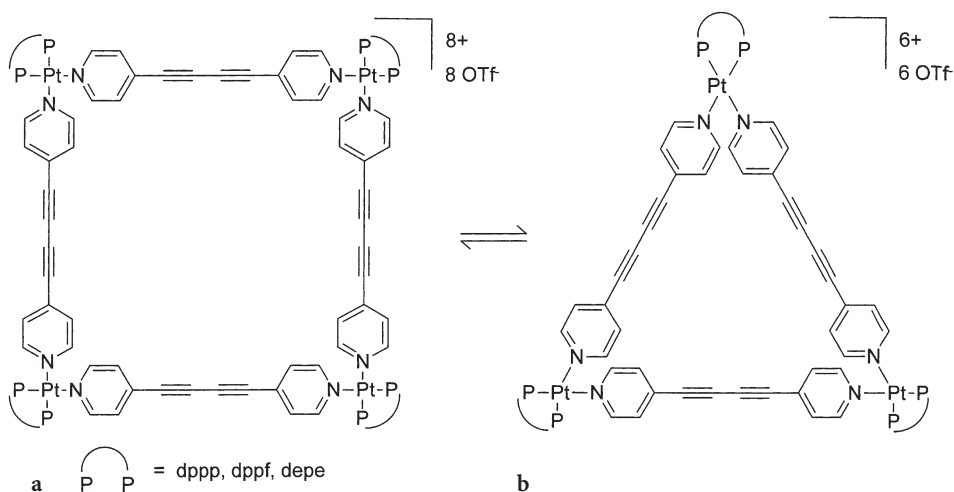


Fig. 21 Equilibrium between square **Ferrer1a** and triangle **Ferrer1b**

so that for the triangular form crystals suitable for X-ray analysis could be grown.

In the case of the similar macrocycle **Ferrer1** (Fig. 21) comprising 1,4-bis(4-pyridyl)butadiyne linkers, by increasing the concentration a shift of the square-trimer equilibrium towards the squared form resulted while the triangle is still the predominant species [35]. For the assembly process and equilibrium formation, length, basicity and flexibility of the spacer seem to play a major role, whereas the bite angle of the diphosphine ligand has rather less influence. Host-guest experiments of macrocycle **Ferrer1** with PF_6^- or OTf^- anions gave different results. In the former case enhancement of the luminescence of the macrocycle was found by the addition of the anion; in the latter case fluorescence was quenched.

Equilibria between molecular squares and triangles seem to be a quite general phenomenon. Würthner et al. synthesized the enlarged Pt(II) macrocycle **Würthner2** (Fig. 22), comprising a diazadibenzoperylene as bridging ligand. NMR studies in deuterated nitromethane clearly showed an almost 1:1 ratio of the square and the corresponding triangle [36]. The structures were assigned based on NMR and ESI-FT-ICR-MS results as well as on molecular modelling, which gave insight into the steric situations of the two related geometries. Repulsion between the phenyl groups of the exocyclic dppp ligand and the phenoxy substituents at the bay region of the diazadibenzoperylene is more pronounced for the molecular square. Therefore, most likely this steric interaction seems to be the driving force for the formation of the less hindered triangle. In contrast to the Pt(II) macrocycle **Würthner1** (vide infra), spectroscopic investigations on this macrocycle showed effective quenching of the pyrene fluorescence.

A very thorough investigation of square-triangle equilibria for the related Pt(II) macrocycles **SchalleyLützen1–3** containing 4,4'-bipyridine, *trans*-di(4-

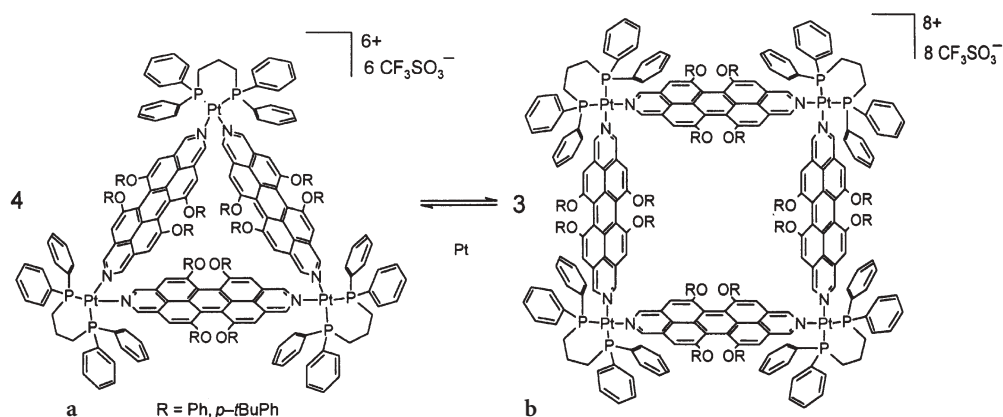


Fig. 22 Equilibrium between triangle Würthner2a and square Würthner2b

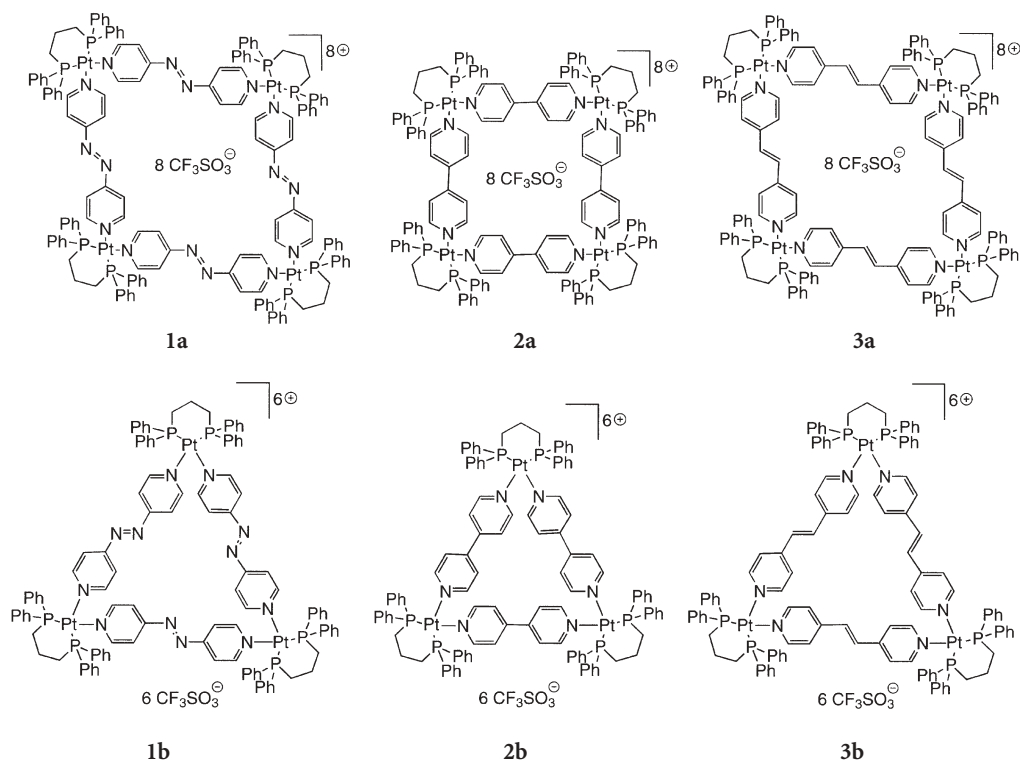


Fig. 23 Square molecules SchalleyLützen1a–3a and corresponding triangles Schalley Lützen1b–3b

pyridyl)ethylene and *trans*-4,4'-azopyridine as bridging ligands (Fig. 23) was recently described by Schalley, Lützen et al. [17]. The equilibrium and the ligand-exchange behaviour of these dynamic systems were examined by different techniques such as FT-ICR and tandem mass spectrometry as well as gas phase experiments. Thus, very important insight in the defragmentation pathways of the investigated Pt(II)-macrocycles was obtained.

In the preceding examples, the molecular triangles were difficult to isolate from the square-triangle equilibria because, due to the 90° *cis*-Pt(II) corners, they only exist in a truncated or strained form. However, Stang et al. showed that a true 60° tecton results from a phenanthrene that is disubstituted in 2,9-position with reactive Pt(II) units [34c]. Reaction of this corner element with the linear bridging ligand *trans*-[bis(4-pyridylethynyl)-bis(triethylphosphine)]platinum(II) in acetone gives the unique and stable molecular triangle **Stang5** (Fig. 24) in excellent yield within a few hours. Interestingly, in the solid state the nonaplatina triangles stack and form large channels.

Surprisingly, reaction of *cis*-Pt(PMe₃)₂(OTf)₂ with the rather small pyrazine in nitromethane resulted in the formation of the molecular triangle **Stang6** (Fig. 25) instead of the expected molecular square [34f,g]. Entropic reasons are

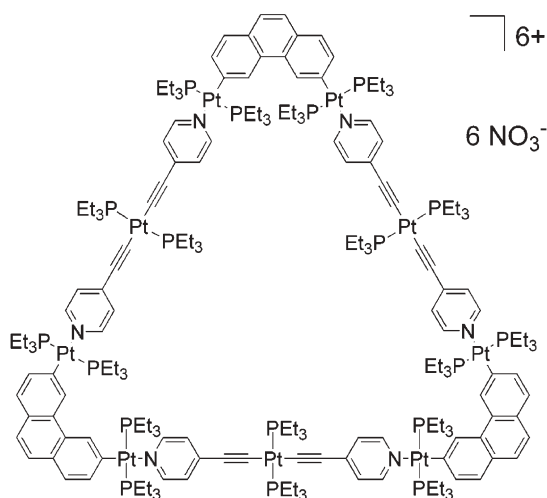


Fig. 24 Macrocycle **Stang5**

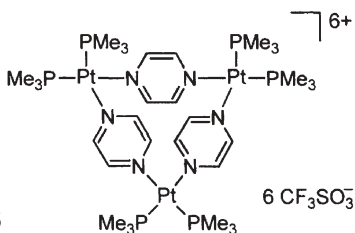


Fig. 25 Macrocycle **Stang6**

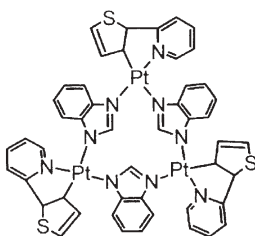


Fig. 26 Macrocycle **ChanChe1**

considered to be the driving force for the formation of this strained structure. The strain is not only accommodated by the reduced N–Pt–N angle of 82–83°, but also by the reduced centroid(pyrazine)–N–Pt angles of 167–171°. These values are remarkable, as Pt(II) typically tries to keep the rectangular coordination even in strained macrocycles (compare, e.g., **Bosch1**, Sect. 2.3.2).

Precursor complexes that can function as 60° tectons and exclusively form triangles are quite rare. In this respect, Chan, Che et al. took benzimidazole as a bridging ligand in which the nitrogen atoms span binding vectors of approximately 150° [37]. Reaction of benzimidazole with *cis*-Pt(II) as the corner element resulted in truncated triangle **ChanChe1** (Fig. 26). The crystal structure analysis of **ChanChe1** revealed a slight distortion of the Pt coordination sphere from the plane, which probably causes the *syn*, *anti*, *anti* orientation of the benzimidazole units with respect to the plane of the triangle.

That geometric structures other than squares, rectangles or triangles can be selectively formed was shown by Chi, Addicott, Stang et al. when various Pt(II) precursors complexes were used that allowed 90°, 120° or 180° angles in combination with di(3-pyridyl)ethyne or 1,4-di(3-pyridyl)-1,3-butadiyne, respectively [34b]. Strain-free hexagons **ChiAddicottStang1–2** or truncated hexagon **ChiAddicottStang3** (Fig. 27) were formed, although entropy should favour smaller macrocycles.

Utilizing the same type of building blocks, the formation of molecular hexagons **Rendina1–2** (Fig. 28) from isonic and *trans*-configured Pt(II) precursors by self-assembly was reported by Rendina et al. [38]. The rather rare non-covalent Pt(II) hexagons are kept together by hydrogen bonding due to the typical dimerization of carbonic acid groups. Appreciable association constants of up to 10⁴ L² mol^{–2} were determined.

The hexagonal Pt(II) macrocycle **Stang7a** (Fig. 29) was obtained by reaction of bis(4-pyridyl)ketone, which opens a perfect 120° angle, and *cis*-Pt(PEt₃)₂-(OTf)₂ [34h]. If the trisplatinum-macrocycle is crystallized from acetone/water, the original structure is not obtained, but the corresponding cyclodimer **Stang7b**. Hydration of the keto groups leads to a reduction of the binding vectors from 120° to 109° and to a more favourable cyclodimer, which then precipitates and shifts the equilibrium. A similar cyclodimer was directly obtained by reaction of *cis*-Pt(II) diphosphine and bis(4-pyridyl)silanes [34h]. X-ray structure analysis showed that the pyridyl rings are twisted out of the rhom-

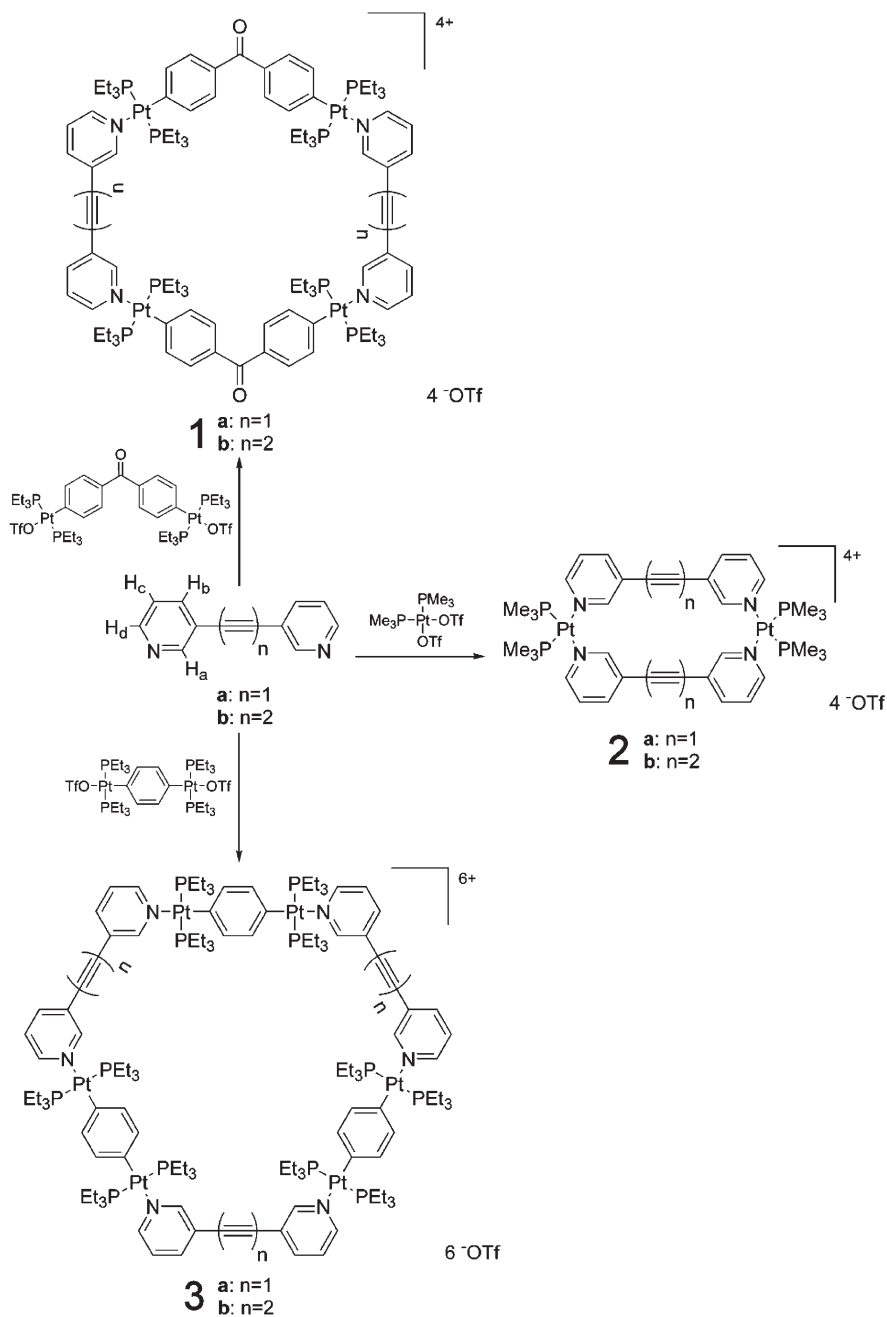


Fig. 27 Preparation of macrocycle **ChiAddicottStang1–3** from the same bridging ligand with different Pt(II) precursors

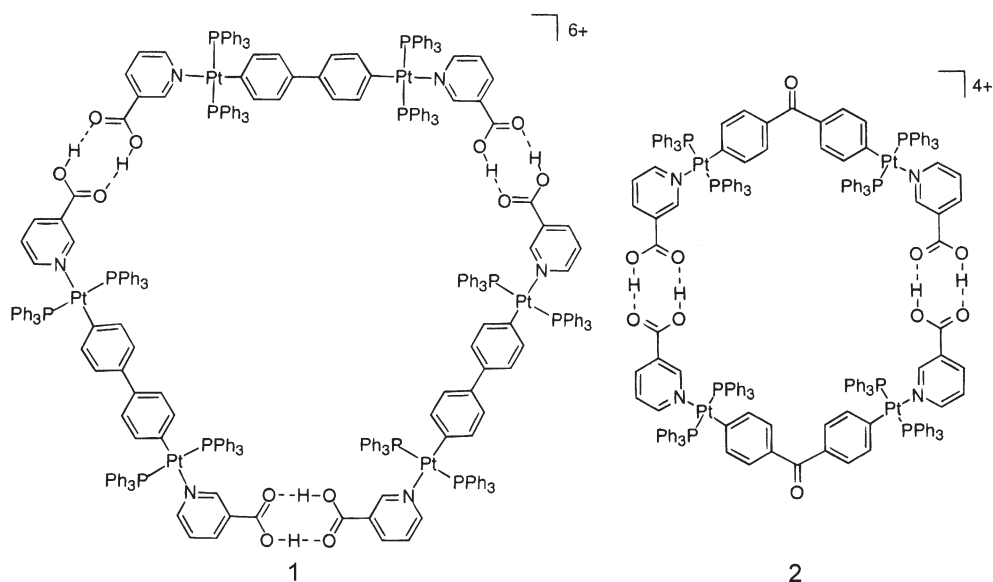


Fig. 28 Macrocycle **Rendina1** and **Rendina2**

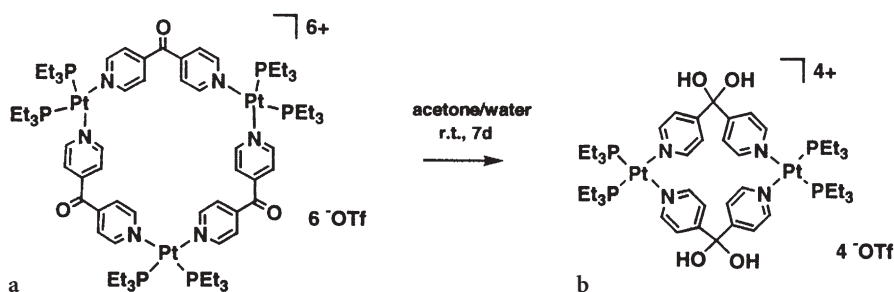


Fig. 29 Macrocycle **Stang7a** and conversion to **Stang7b**

boidal plane and that the N-Pt-N angle is decreased to 81–82°, similar to the molecular triangle **Stang6**.

On the other hand, a dynamic equilibrium between a rhomboidal bis-platina structure **Stang8a** and the corresponding hexagonal trisplatina-macrocycle **Stang8b** (Fig. 30) was observed for the self-assembly of *cis*-Pt(II) diphosphine and (4-pyridylethynyl)pyridine [34a]. The crystal structure analysis of the cyclodimer shows that ring strain is accommodated at the Pt corners at which, similar to the structures **Stang7b** and **Stang6**, the N-Pt-N angle is reduced from 90° to 81.3°. Most of the remaining strain is presumably accommodated in the acetylene connected bridging ligand and in the distortion of the rhomboidal structure from planarity.

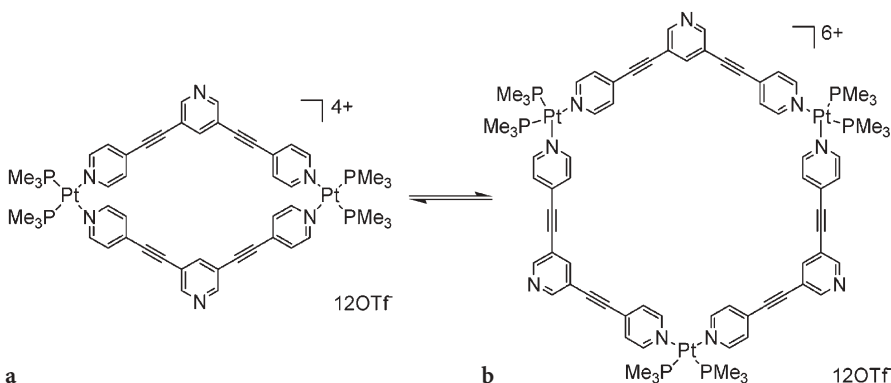


Fig. 30 Equilibrium between rhomboid **Stang8a** and hexagon **Stang8b**

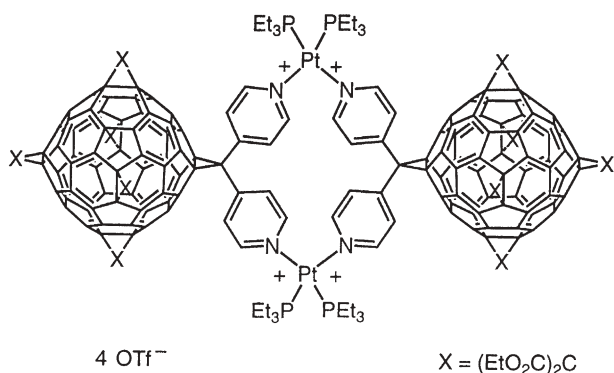


Fig. 31 Macrocycle **Diederich1**

Very similar to cyclodimeric Pt(II) macrocycle **Stang7b**, Diederich et al. reported the synthesis of the C₆₀-functionalized bis-platina cyclodimer **Diederich1** (Fig. 31) [39]. The macrocycle was rapidly obtained in quantitative yield only after the fullerene moieties had been exhaustively substituted with malonic ester groups in order to enhance the solubility of the precursor. As was the case for the previously described structures, the coordination of the ligands at the Pt(II) centre proves to be quite flexible, showing a reduced N-Pt-N angle of 82–83°.

The truncated tetrakis-platina hexagon **KuehlStang1** was obtained when a bent bridging ligand such as 2,5-bis[(4-pyridyl)ethynyl]furane is combined with Pt “clips” comprising an 1,8-anthracenyl ligand and *trans*-Pt(II) diphosphines (Fig. 32) [34e]. Here, the counterions obviously play an important role: mechanistic investigations showed that anion exchange of the initially released nitrate anions with hexafluorophosphate stabilized the product. On the other hand, an immediate addition of a PF₆⁻ salt to the reaction mixture prevents

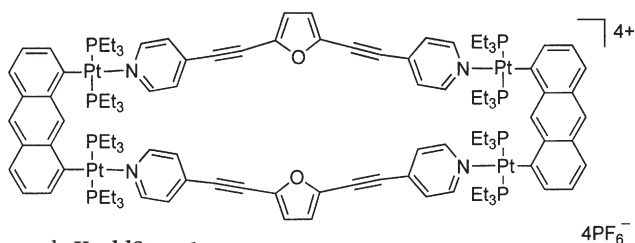


Fig. 32 Macrocycle KuehlStang1

kinetic formation of the macrocycle and results in an excess of linear oligomers. This result clearly underlines the importance of nitrate as a counterion in substitution reactions at Pt(II) centres.

Flexibility in terms of structural isomerism was found by Hanan et al. for the cyclodimeric macrocycle **Hanan1** (Fig. 33) built from *cis*-Pt(II) diphosphines and *N,N'*-bis(3-pyridyl)-2,6-pyridinedicarboxamide [40]. A rotation of the 3-pyridyl units in the bridging ligand leads to either a *syn*- or an *anti*-conformation with respect to the plane of the Pt(II) diphosphine corners. Temperature-dependant NMR spectroscopy revealed a rotational energy barrier of 30 kJ mol⁻¹, which allows “flipping” of the macrocycle without the need for breaking bonds. This flexibility permits an induced fit to bind BF₄⁻ anions in a 1:1 stoichiometry, which consequently raised the rotational energy barrier to about 45–50 kJ mol⁻¹.

A rather exceptional monoplantina-macrocycle involving one Pt(II)(dppp) corner and a bis-pyridyl bridging ligand was synthesized by a ring-closure reaction and has been used as the encircling ring in rotaxane **Jeong1** (Fig. 34) [41]. In contrast to the previously described rotaxane **Kim1** (vide infra), here, the threading of a linear chain through the macrocycle is subsequently obtained due to directed hydrogen bondings. As the rotaxane formation was slow on the NMR time scale, the rate constant was determined to be 6.2 (±0.1) s⁻¹.

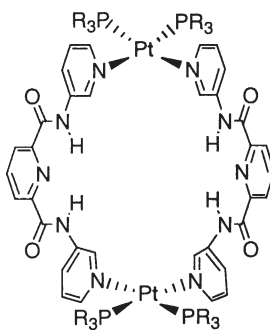


Fig. 33 Macrocycle Hanan1

anti R = Et
 R = *n*-Bu

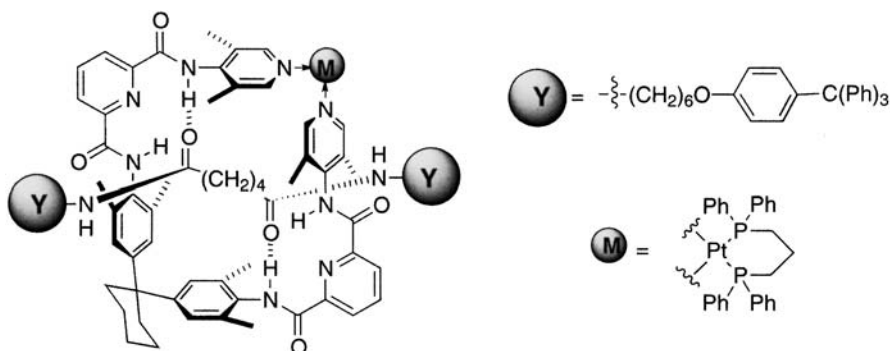


Fig. 34 Macrocycle Jeong1

2.3

Macrocycles by Pt-C Coordination

2.3.1

Macrocycles with Bridging Cyanide and Isocyanide Ligands

Another larger group of Pt(II) macrocycles comprises Pt-C coordination modes when typically cyanides, isocyanates or acetylides are used as bridging ligand.

For example, a mixed Pt-C and Pt-N bonded macrocycle was obtained by Che et al. [42]. Reaction of K₂[PtCl₄] with hydrazine hydrate and *tert*-butyl isocyanide (*t*-BuNC) in refluxing water surprisingly yielded hexagon **Che1** (Fig. 35) in which the six Pt corners are bridged with cyanide spacers and are further coordinated to exocyclic carbene ligands, which form from hydrazine and the isocyanide. Due to the almost 90° angles at the Pt(II) and the linear coordination mode of the cyanide ligands, the structure of the macrocycle is not planar and instead resembles a cube with two missing opposite corners. Unlike the majority of the Pt(II) macrocycles, **Che1** shows luminescence because of metal-to-ligand charge transfer (MLCT) to the exocyclic carbene ligands.

By mixing a tetracyanoplatinum(II) precursor with Cu(II) and 2,2'-bipy, Falvello and Tomás prepared the cyanide-bridged molecular square **FalvelloTomás1** (Fig. 36) in which the Pt(II) corners are coordinated to four carbons, the Cu(II) corners to four nitrogens and one aqua ligand, providing a square planar configuration for each platinum centre and a distorted square pyramidal coordination environment for each copper unit [43]. Additionally, by analogous reactions the corresponding Rh- and Ir-containing Pt(II) macrocycles could be synthesized. The mixed macrocycles showed very low solubility. Single crystals could only be obtained by dissolution of the macrocycles in ammonium hydroxide, which probably caused a break-up of the solid state structure due to coordination, while slow evaporation of NH₃ from this solution resulted in the precipitation of single crystals.

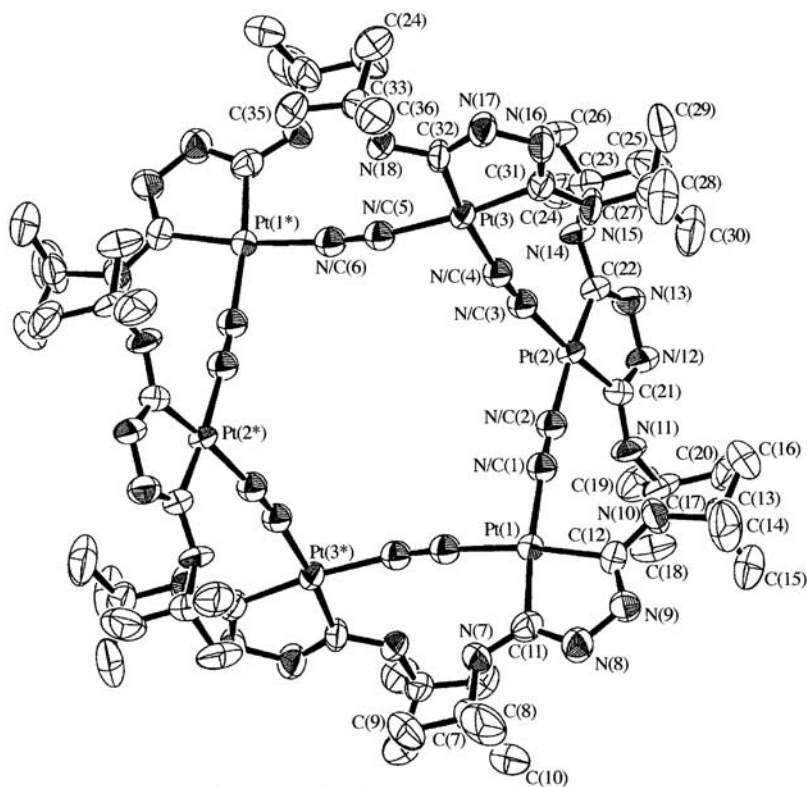


Fig. 35 X-ray structure of macrocycle Che1

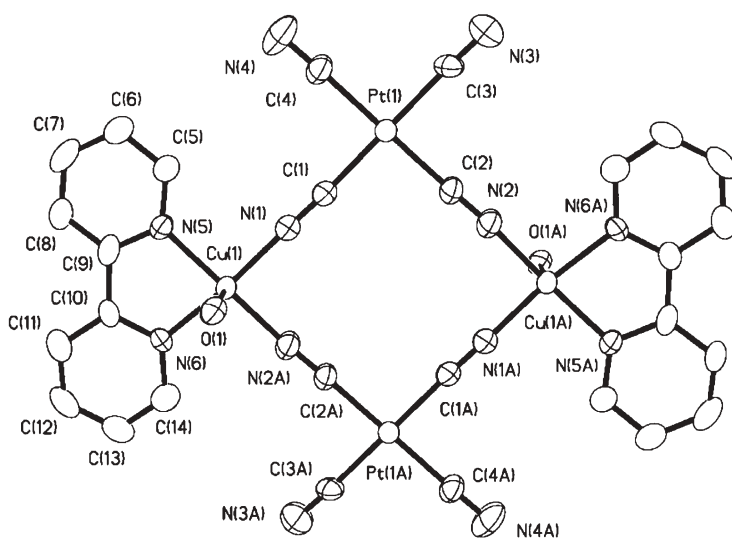


Fig. 36 X-ray structure of macrocycle FalvelloTomás1

Using a similar *cis*-dicyanoplatinum(II) precursor, Forniés, Lalinde et al. synthesized the molecular trisplatina triangles **ForniésLalinde1** and the mixed metal molecular squares **ForniésLalinde2** (both in Fig. 37), comprising two Rh or Ir corners in moderate yields [44]. Both macrocycles comprise platinum centres that are coordinated to four carbons as typical structural elements. Macrocycle **ForniésLalinde2** can be further modified by two additional Pt(II) ligands that bind to two exocyclic acetylide ligands by σ - and π -coordination and thus form a hexanuclear metallamacrocycle.

The same authors further extended the size of molecular Pt(II) squares incorporating cyanide ligands by reacting *cis*-Pt(II) diacetylide with an equivalent of triphenyltin cation in acetone [44]. Macrocycle **ForniésLalinde3**, which is hardly soluble, precipitated from the solution and was characterized by IR as

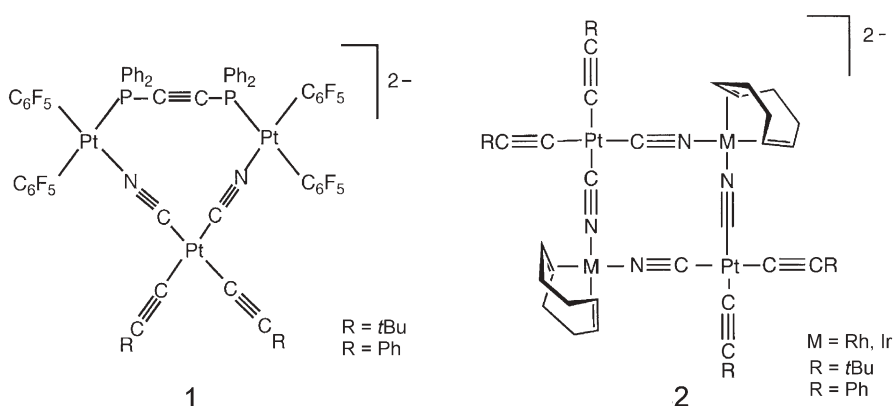


Fig. 37 Macrocyces **ForniésLalinde1** and **ForniésLalinde2**

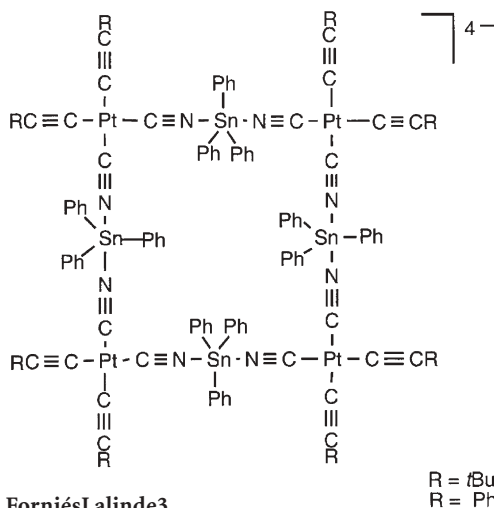


Fig. 38 Macrocycle **ForniésLalinde3**

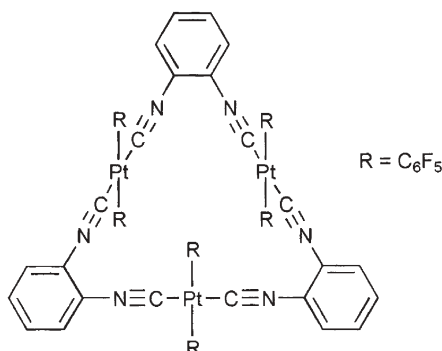


Fig. 39 Macrocycle **Espinet1**

well as ^1H -NMR spectroscopy. The structure comprises linear $(\text{CN})\text{SnPh}_3(\text{NC})$ edges connecting four Pt(II) corners (Fig. 38).

A rare example of an equilateral molecular triangle was reported by Espinet et al. [45]. The trisplatina-macrocycle **Espinet1** (Fig. 39) was obtained in good yield by stirring 1,2-phenylene diisocyanide and *trans*- $\text{Pt}(\text{C}_6\text{F}_5)_2(\text{AsPh}_3)_2$ for 2 h in dichloromethane. The small distance (ca. 5.65 Å) of the three Pt(II) moieties causes an unusual arrangement of the pentafluorophenyl ligands: while the phenyl plane normally is perpendicular to the Pt(II) coordination plane, X-ray structure analysis of **Espinet1** revealed an average torsion of 54° instead of 90°. The six phenyl units are twisted in the same sense leading to a $\text{C}_{3\text{h}}$ symmetry.

2.3.2

Macrocycles with Bridging Acetylide Ligands

Although the diversity of macrocycles with Pt(II)-acetylide bonds is as vast as for those with Pt-N bonds, there are structural motifs that exist for both types of macrocycles. An important “trick” for the construction of Pt-C macrocycles is the preassembly of Pt(II) corners already bearing the bridging ligands. For example, Lees et al. reported the Pt(II) acetylide squares **Lees2–3** (Fig. 40) comprising two Pt(II) and two Re(I) corners, in analogy to their Pt-N coordinated hybrid macrocycles **Lees1** (vide infra) [32b]. In contrast to **Lees1**, in **Lees2–3** the Pt(II) moiety bearing the *cis*-connected bridging ligands was assembled first and then reacted with $\text{Re}(\text{CO})_5\text{Br}$. The photophysical properties of **Lees2–3** are different in comparison to the Pt-N bonded counterparts **Lees1**, i.e. the luminescence is quenched. In NMR experiments no evidence for host-guest assemblies of macrocycle **Lees2–3** and 1,3,5-trimethoxybenzene or aromatic sulfonates, respectively, could be detected, indicating that no π - π or hydrophobic interactions are operative.

For Bruce et al. butadiyne-bridged molecular square **Bruce1** (Fig. 41), two *cis*-Pt(II)/bridging ligand assemblies were coupled with the two remaining Pt(II) corners under high dilution conditions in the presence of sodium acetate

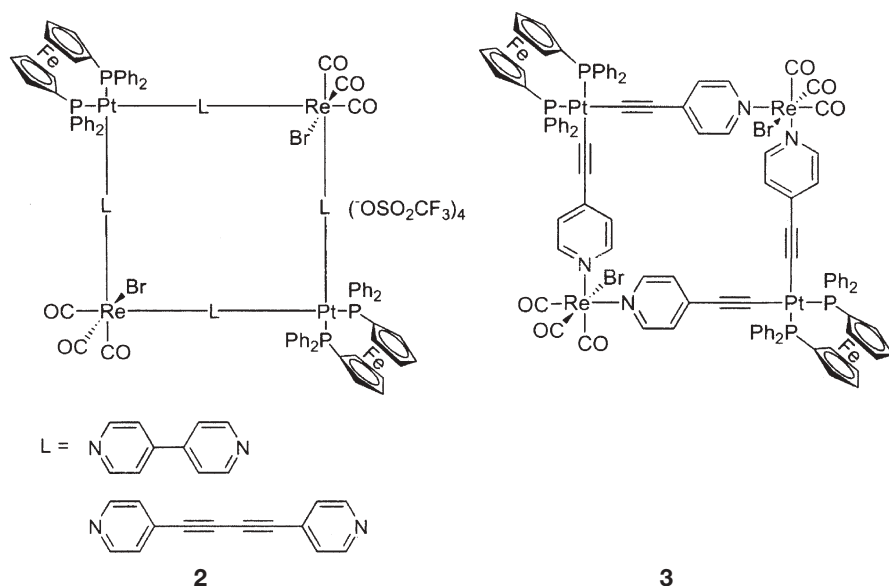


Fig. 40 Macrocycles Lees2 and Lees3

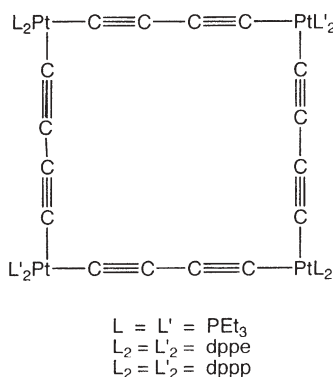


Fig. 41 Macrocycle Bruce1

[46]. Alternative usage of diethylamine resulted in the formation of dialkylammonium-macrocycle adducts, which in mass spectrometric characterizations gave additional peaks. Apparently, a triangular structure with a missing Pt(II) diphosphine group was formed by reductive elimination. Bruce et al. furthermore investigated whether Cu^+ or Ag^+ cations would interact with the acetylide triple bonds in a “tweezer”-like coordination, but a clear proof for such a structure could not be presented.

By copper-catalyzed oxidative dimerization of a *trans*-Pt(II) component with a U-shaped structure bearing terminal acetylene units, Diederich et al. were able to synthesize molecular square **Diederich2** (Fig. 42) in 92% yield [47].

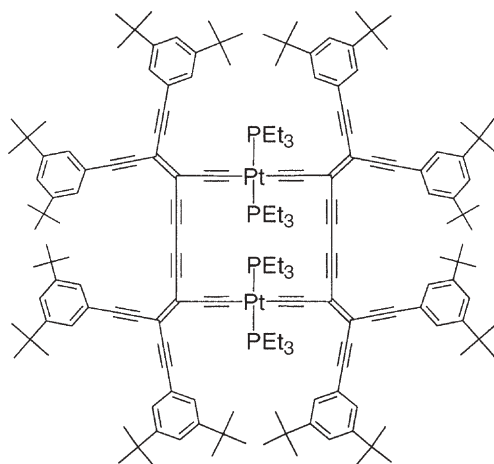


Fig. 42 Macrocycle Diederich2

Here, perfect 90° angles are provided by the cross-conjugated 1,1-diethynylene ethene units. The macrocycle could be characterized by NMR and MALDI-TOF mass spectrometry, while FAB-MS led to a complete fragmentation of the molecule.

Tessier, Youngs et al. used the preassembly approach to build the molecular square **TessierYoungs1** (Fig. 43) [48a]. Therefore, a *cis*-Pt(II) diphosphine diacetylide precursor was reacted with *cis*-Pt(PR₃)₂Cl₂ in almost quantitative yield. The product was found to be air stable, but decomposed slowly in halogenated solvents. In contrast, the larger octaplatina molecular square **TessierY-**

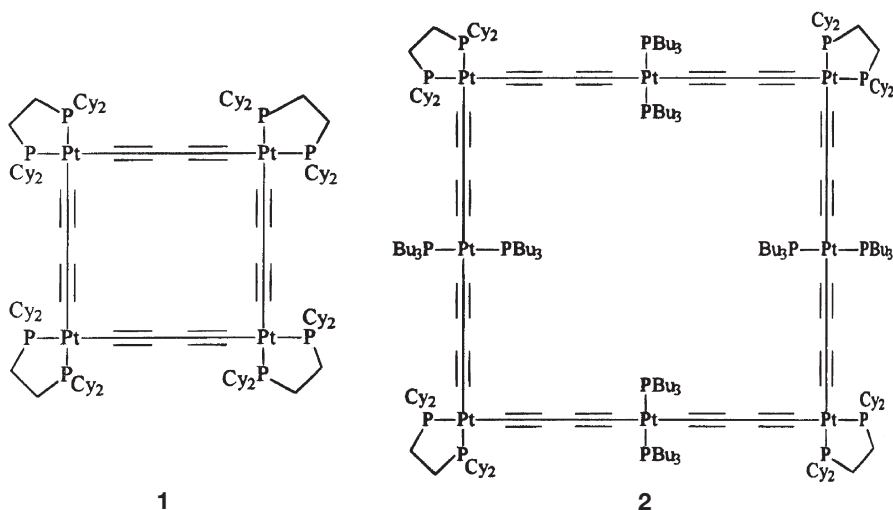


Fig. 43 Macrocycles TessierYoungs1 and TessierYoungs2

Youngs2 (Fig. 43) was prepared by self-assembly of the Pt(II) corners and *trans*-Pt(II) diphosphine diacetylide spacers [48a]. **TessierYoungs2** represents a most interesting structure comprising four *cis*-arranged and four *trans*-arranged Pt(II) bis-acetylide moieties. Reaction of the macrocycle with an excess of Ag^+ salts gave tweezer complexes in which Ag^+ is contained in ratios of 1:1 to 1:4.

Further macrocycles prepared by the group of Tessier and Youngs take advantage of preformed, almost cyclic fragments with terminal acetylide functions. In the final step, under high dilution conditions and Cu^+ catalysis, these fragments are reacted in good yields with Pt(II) corners to the triangular shaped structures **TessierYoungs3–4** (Fig. 44) [48c]. Due to the high strain of the molecular triangle, the C-Pt-C angles are reduced to $81\text{--}83^\circ$ and the Pt-C-C angles to $170\text{--}175^\circ$. To further accommodate the strain, the planes spanned by the P-Pt-P (exocyclic ligands) and the C-Pt-C atoms (macrocyclic plane) are distorted against each other by 18° .

Similarly, the butterfly-like, bicyclic structure **TessierYoungs5a** (Fig. 45) was synthesized, in which the Pt(II) tetraacetylide centre connects two triangular moieties [48b]. Addition of HgCl_2 results in the “double-tweezer” complex **TessierYoungs5b** by coordination of two Hg(II) atoms to acetylene units at the outer “pockets”, which was deduced from X-ray structure analysis.

Haley et al. described the synthesis of the triangular monoplatina-macrocycle **Haley1** (Fig. 46), which in contrast to **Tessier3**, contains a *trans*-configured Pt(II) diacetylide fragment in one edge of the triangle [49a]. The synthesis started from a “preoriented” acyclic precursor having triisopropyl silanyl- (TIPS)-protected terminal acetylene groups. After deprotection with

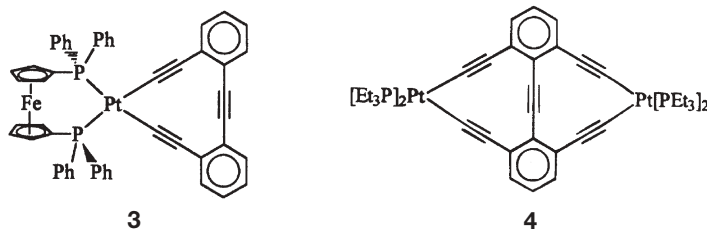


Fig. 44 Macrocycles **TessierYoungs3** and **TessierYoungs4**

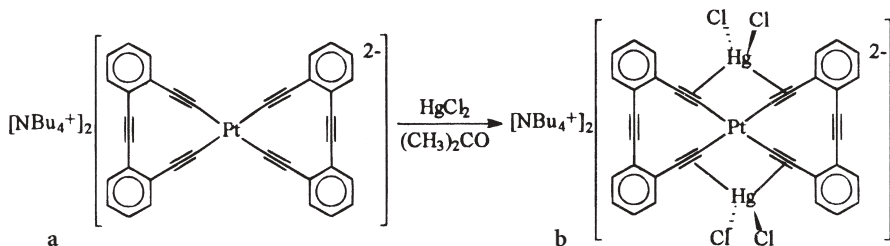


Fig. 45 Macrocycle **TessierYoungs5a** and conversion to **TessierYoungs5b**

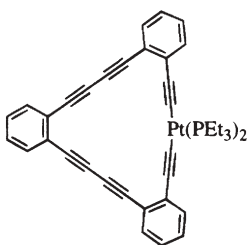


Fig. 46 Macrocycle **Haley1**

base, stannylation and Cu^+ -catalyzed transmetalation with a *trans*-Pt(II) diphosphine, the macrocycle was isolated in 65% yield. Since the insertion of the Pt(II) moiety exerts some strain in the macrocycle, a slight deviation of the square planar Pt(II) geometry from the ideal 180° coordination and the plane of the macrocycle was detected by X-ray structure analysis. Compared to the corresponding Pt-free dehydrobenzo[18]annulene, in UV spectra the absorption maximum of **Haley1** exhibits a bathochromic shift. This finding is in contrast to linear systems, where insertion of a *trans*-Pt(II) unit leads to a small hypsochromic shift [47].

In an analogous way Haley et al. synthesized the corresponding dehydrobenzo[15]annulene and dehydrobenzo[14]annulene platina-macrocycles **Haley2** (Fig. 47) and **Haley3** (Fig. 48) [49b]. In **Haley2**, a *trans*-Pt(II) diphosphine unit was used to close the ring, whereas for **Haley3** ring formation could only be achieved by the use of a *cis*-Pt(II)(dppe) precursor.

Using the same synthetic route, the more complicated “bowtie”-shaped bi-macrocycle **Haley4** (Fig. 49), which contains two *trans*-arranged Pt(II) units, was synthesized in 21% yield [49b].

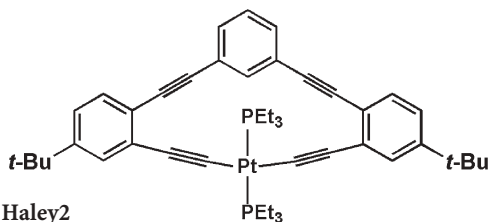


Fig. 47 Macrocycle **Haley2**

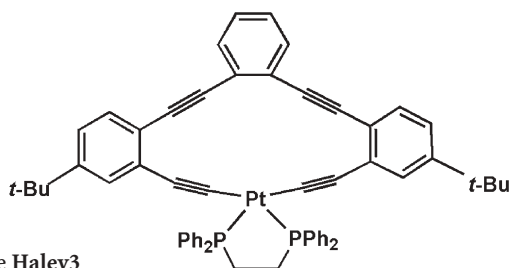


Fig. 48 Macrocycle **Haley3**

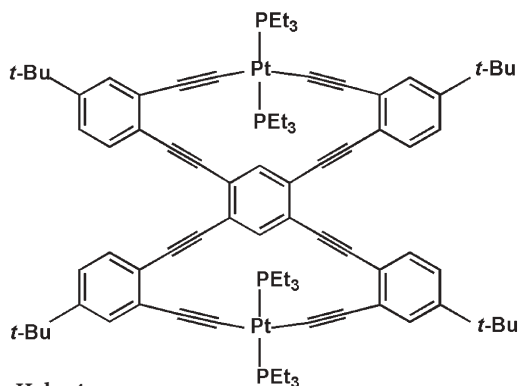


Fig. 49 Macrocycle Haley4

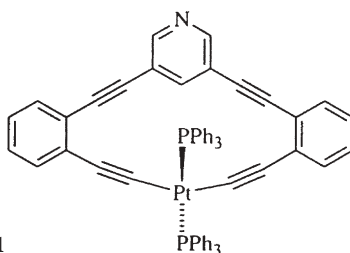


Fig. 50 Macrocycle Bosch1

Similar to the strained macrocycle **Haley2**, Bosch et al. reported the synthesis of the monoplantina-macrocycle **Bosch1** (Fig. 50), which contains a *meta*-branched pyridyl unit instead of a *meta*-phenylene unit as in **Haley2** [12]. Although a *cis*-Pt(II) diphosphine precursor was used as starting material, a *trans* configuration at the Pt(II) centre is found in the macrocycle and unequivocally proven by X-ray structure analysis. *Cis*-to-*trans* isomerizations at Pt(II) centres are known and might be induced by the usage of CuI and diethylamine for the cyclization reaction. In the case of macrocycle **Bosch1**, the isomerization is dictated by the steric environment of the small dialkyne ligand.

Tykwinski et al. used similar structural elements to build up platina-macrocycles **Tykwinski1a–2a** (Fig. 51 and Fig. 52) [13, 50]. A 3,5-diethynylated pyridine and exocyclic (1,1-diethynyl)ethene units as tectons provide curvature, so that ring closure reaction with *trans*-Pt(II) diphosphine effectively gave the monoplantina cyclyne **Tykwinski1a** in 70% yield and the bis-platina hexagon **Tykwinski2a** in 45% yield. In comparison to the previously described system **Bosch 1** (vide infra), metalla-cyclyne **Tykwinski1a** is substantially larger and less strained showing a non-distorted C–Pt–C angle of 178–180°. Furthermore, the pyridine unit provides an exocyclic binding site that can react with another Pt(II) complex. While the preparation of macrocycle **Bosch1** included a *cis*-to-*trans* isomerization at the Pt(II) centre, Tykwinski et al. showed the very interesting switching of *trans*-configured Pt(II) macrocycles **Tykwinski1a–2a** to

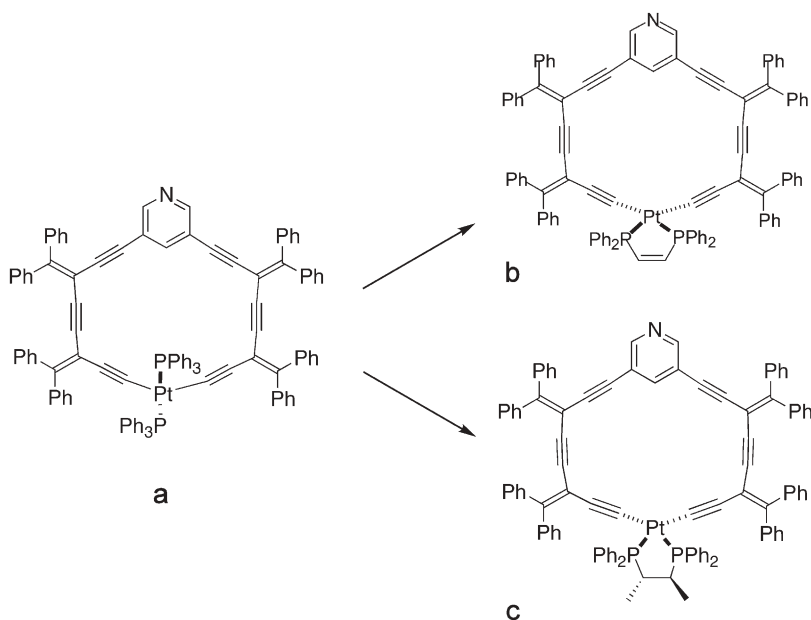


Fig. 51 Macrocycle **Tykwinski1a** and conversion to **Tykwinski1b** and **Tykwinski1c**, respectively

the corresponding *cis* systems **Tykwinski1b–2b**, which were obtained in 87% and 71% yield, respectively [13b]. This highly effective ligand exchange reaction is triggered when the *trans*-complexes are treated with the chelating ligand 1,2-bis(diphenylphosphino)ethylene (dppe) in dichloromethane. The *cis*-complex **Tykwinski1b** shows increased strain, since the Pt(II) moiety bends out of the plane of the macrocycle to retain a 89° C-Pt-C angle, while the Pt-C-C and C-C-C angles are reduced to about 170° . Very recently, this exchange reaction was extended to chiral chelating phosphine ligands, when *trans*-macrocyclic **Tykwinski1a** was treated with *S,S*-Chiraphos to form enantiopure **Tykwinski1c** in 73% [13a]. In the same way, **Tykwinsky2a** was reacted with either *R,R*- or *S,S*-Chiraphos to give the corresponding chiral macrocycles **Tykwinsky2c** in 92% and 96% yield, respectively.

Ligand exchange as the penultimate step bears a major advantage over the use of chiral precursors for macrocycle formation, as both enantiomers are easily accessible from the same macrocyclic precursor compound. CD spectra of the chiral molecules **Tykwinski2c–4c** (Figs. 52, 53, and 54) showed that the chirality of the ligand is transduced to the whole macrocycle, caused by an energetically favoured ligand conformation and the resulting steric interaction of the phosphine phenyl groups with the acetylide ligands [13a]. This chiral influence is somewhat reduced for the rather strained macrocycle **Tykwinski2c**, while the fully conjugated chromophore system of **Tykwinski4c** shows the strongest response.

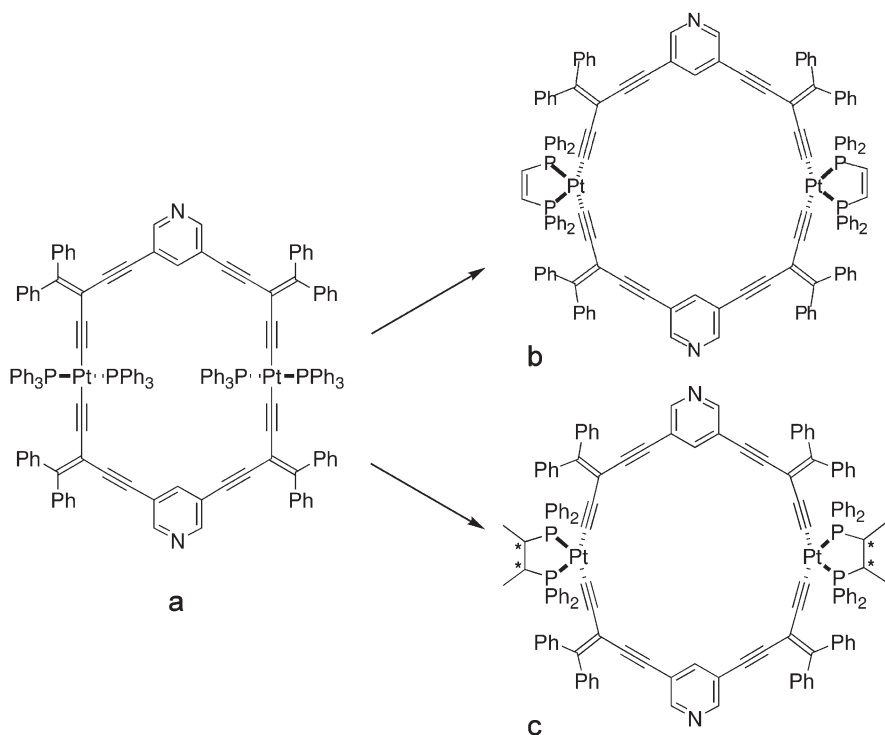


Fig. 52 Macrocycle **Tykwinski2a** and conversion to **Tykwinski2b** and **Tykwinski2c**, respectively

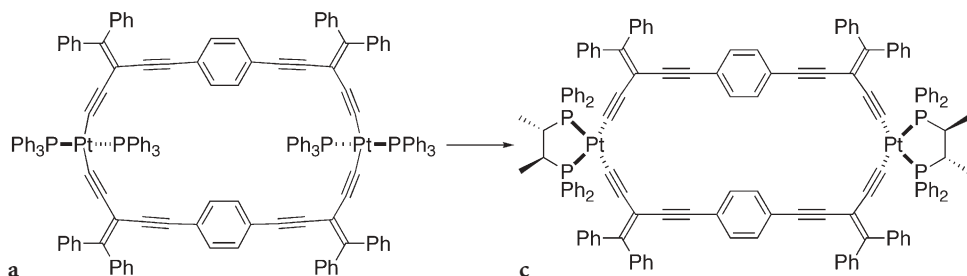


Fig. 53 Macrocycle **Tykwinski3a** and conversion to **Tykwinski3c**

While for the Pt-N coordinated macrocycles of Stang et al. chirality can be introduced by exocyclic chiral ligands at the Pt corners, as represented in square **Stang9** (Fig. 55) [29b], Lin et al. took advantage of chiral BINOL units implemented as building blocks *within* the cyclic array. By Cu⁺-catalyzed self-assembly of the linear 4,4'-bis(alkynyl)-BINOL and a *cis*-Pt(II) diphosphine precursor, the molecular triangles **Lin1a-d** were obtained in medium yields of 38–45% (Fig. 56) [51d]. The Pt(II) macrocycles were designed as catalysts

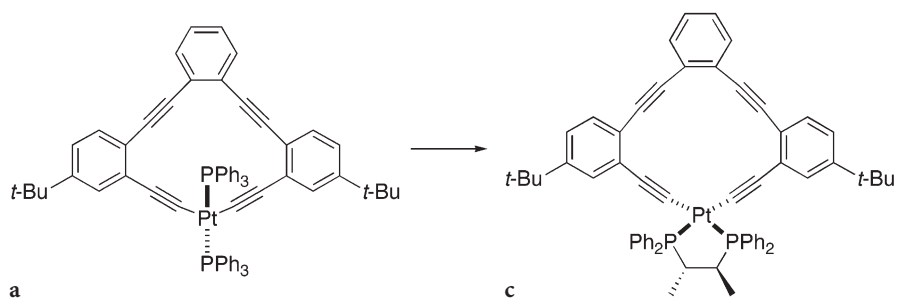


Fig. 54 Macrocycle Tykwinski4a and conversion to Tykwinski4c

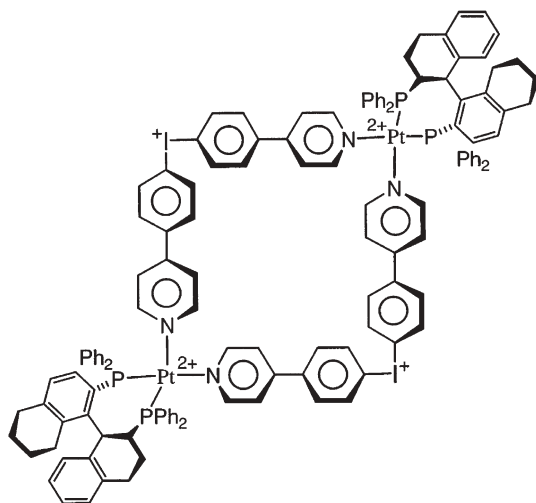


Fig. 55 Macrocycle Stang9

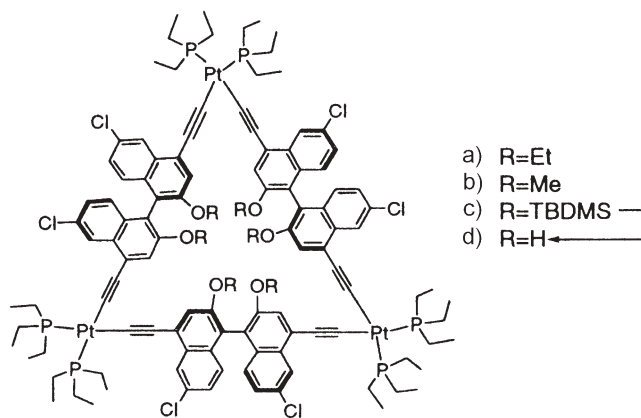


Fig. 56 Macrocycle Lin1

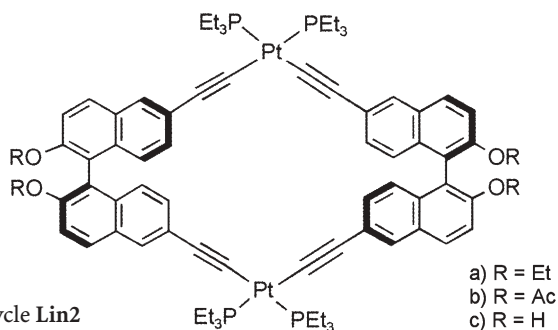


Fig. 57 Macrocycle **Lin2**

comprising a chiral cavity or pocket. A deprotonated form was successfully employed in the asymmetric reduction of aromatic aldehydes with $\text{Ti}(\text{O}^i\text{Pr})_4$ and ZnEt_2 . The resulting chiral alcohols were obtained with an *ee* value higher than 90%, while catalysis with the free ligand only led to excesses less than 80%.

Alkynyl substitution at the 6,6'-positions of BINOL turned the bridging ligand to a corner building block, which by reaction with a *cis*-Pt(II) diphosphine gave rhomboid **Lin2** (Fig. 57) in 49–59% yield [51c]. X-ray structure analysis showed a slightly distorted geometry at the Pt(II) centre comprising C–Pt–C angles from 82.4–101.3°. Similar to **Lin1**, this type of structure was used in a deprotonated form for asymmetric reduction of aldehydes, yielding chiral alcohols with very good *ee* values.

3,3'-Bis(alkynyl)-substituted BINOL and *cis*-Pt(II) diphosphine provided the analogous rhomboid **Lin3** (Fig. 58) in 79–81% yield [51a]. In this case, deprotonated **Lin3** was not catalytically active in stereoselective aldehyde reductions due to the steric hindrance around the inwards-pointing hydroxy groups. Therefore, the active Ti-BINOLate complex could not be formed. The reaction of the 3,3'-disubstituted BINOL derivative with *trans*-Pt(II) units resulted in polymers instead of cyclic oligomers [52].

While the aforementioned substitution patterns at the BINOL moieties in combination with *cis*-Pt(II) precursors resulted in discrete macrocycles, reac-

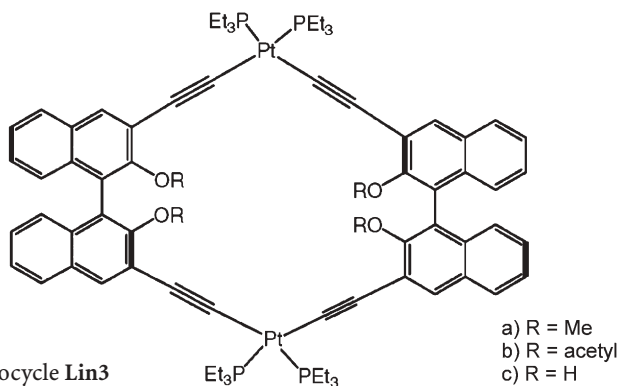


Fig. 58 Macrocycle **Lin3**

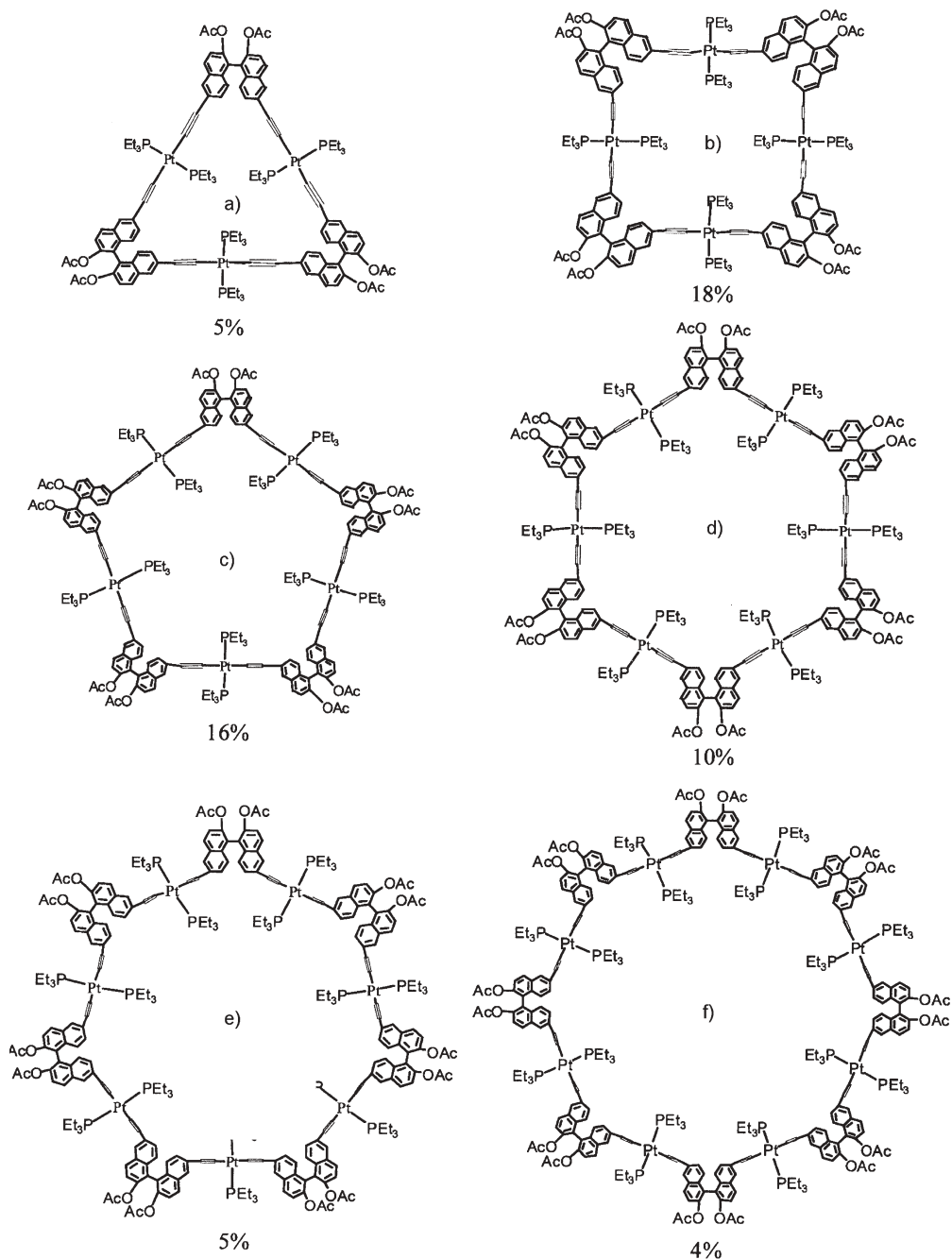


Fig. 59 Isolated compounds of the macrocyclization to macrocycle **Lin4**

tion of a 6,6'-disubstituted BINOL with *trans*-Pt(II) yielded a mixture of macrocycles **Lin4** (Fig. 59), ranging from the cyclotrimer to the cyclooctamer. The individual macrocycles could be obtained after chromatography in 5–18% yield [51b]. A reason for the statistical formation of various ring sizes might be the flexibility of the dihedral angle at the BINOL building block, which is able to adopt different bite angles and binding vectors without generating much strain.

A diethynylated biferrocene was used by Yamazaki, Haga et al. as a similar non-rigid building block in a Cu⁺-catalyzed macrocyclization with *cis*-Pt(II) diphosphine [53]. **YamazakiHaga1** (Fig. 60) forms as a mixture of cyclic oligomers ranging from the cyclodimer to the cyclotetramer, which were isolated in rather low yields. Employment of PMe₃ instead of PBu₃ as exocyclic Pt(II) ligand yielded rather selectively the cyclic tetramer in 22% yield. The X-ray structure analysis of this molecule reveals a rhomboidal geometry comprising two *trans*-Pt(II) moieties and two biferrocenyl units as opposite edges. Electrochemical investigations by cyclic and differential pulse voltammetry revealed only weak interaction and conjugation of the biferrocene units due to the rather insulating character of the Pt(II) spacers.

A series of oligothiophene-containing platina-macrocycles were synthesized by Bäuerle et al. in excellent yields. Reaction of an α,α' -diethynylated terthiophenes with Pt(II)(dppp) units did not give the expected square, but a strained cyclodimer **Bäuerle1a** (Fig. 61) by a four component self-assembly process in 91% yield. This cyclodimer subsequently served as a template for an oxidatively induced reductive elimination of the Pt(II) corners with iodine and led to the highly strained and fully conjugated metal-free macrocycle **Bäuerle1b** in 54% yield [54]. Therefore, this novel Pt(II) metal template approach was a major improvement compared to the former “statistical” route [55] and one of the first applications of effectively formed Pt(II) macrocycles as intermediates for the synthesis of conjugated macrocycles.

Meanwhile, in the course of our efforts to work out a generally applicable synthetic protocol for the transition metal-directed synthesis of diacetylene

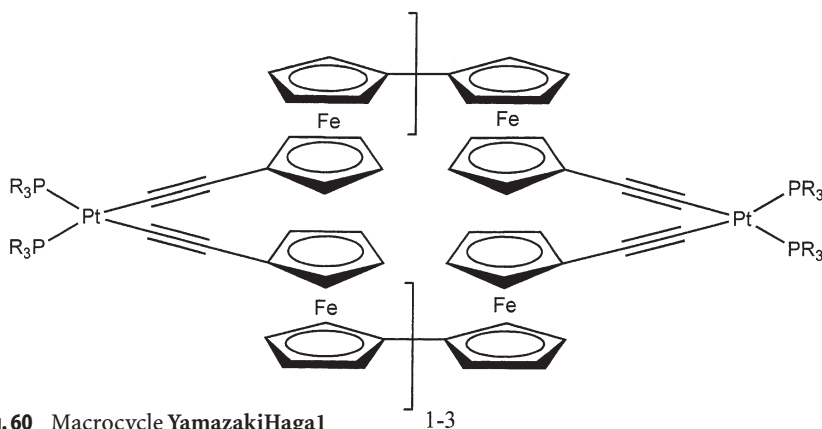


Fig. 60 Macrocycle YamazakiHaga1

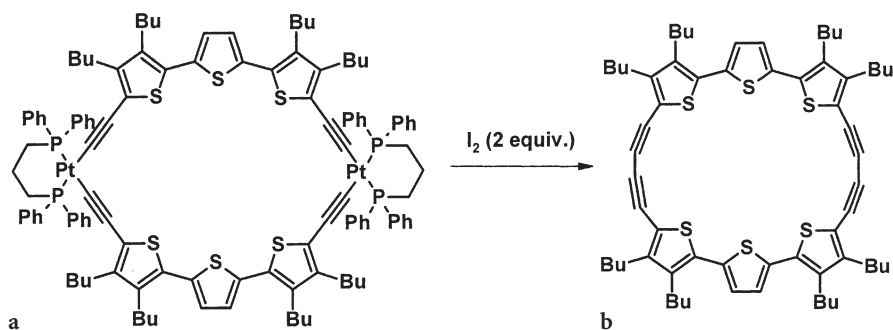


Fig. 61 Macrocycle Bäuerle1

bridged macrocycles, differently substituted α, α' -diethynylated terthiophenes were reacted with the Pt(II)(dppp) precursor to give corresponding Pt(II) cyclodimers **Bäuerle2–3** in 86% and 80% yield, respectively (Fig. 62) [56].

Furthermore, the length of the bridging oligothiophene unit could be extended to a quater-, quinque- and septithiophene, yielding platina-macrocycles **Bäuerle4–6** in 80–86% yield (Fig. 62, 63) [56, 57].

The broad applicability of the metal template approach was further shown by the synthesis of monoplatina-macrocycles **Bäuerle7–9** in which a

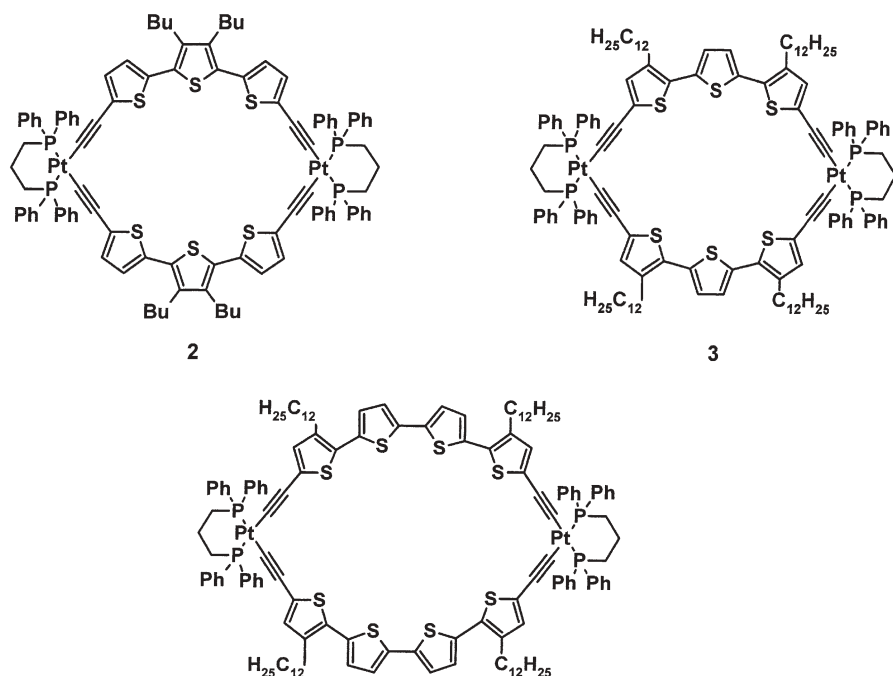


Fig. 62 Macrocycles Bäuerle2–4

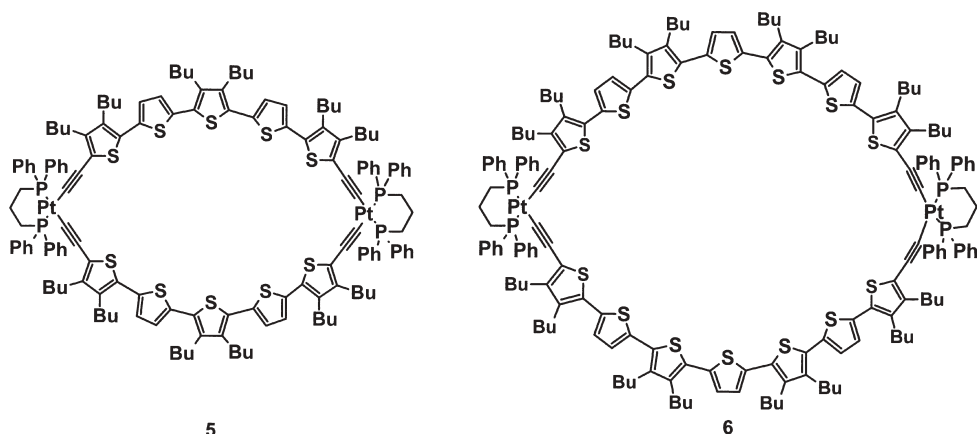


Fig. 63 Macrocycles Bäuerle5–6

Pt(II)(dppp) diacetylide corner is connected to a bent bis(oligothienyl)phenanthroline unit (Fig. 64) [57, 58]. Good yields (70%) are obtained only in the case of the terthienyl derivative, whereas the corresponding longer quater- and quinquethiophene only lead to low yields (23%, 9%), which is probably due to unfavourable conformations of the precursor molecules for the macrocyclization process.

With respect to the subsequent elimination reaction that is applied to this type of platina-macrocycles to form the conjugated macrocycles, we also varied the bite angle at the Pt(II) corner by using bidentate phosphine ligands other than dppp, which opens an angle of 91° . dppm and dppf span extreme angles of 72° and 108° , respectively, are well tolerated and gave platina-macrocycles Bäuerle10–11 in 80–85% yield (Fig. 65) [59].

Haley et al. synthesized the monoplatina-macrocycle **Haley5a**, however in this case, reductive elimination to conjugated macrocycle **Haley5b** was not

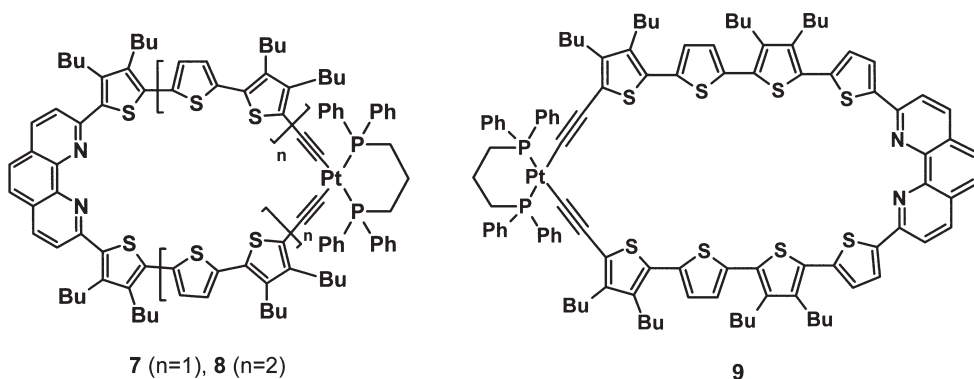


Fig. 64 Macrocycles Bäuerle7–9

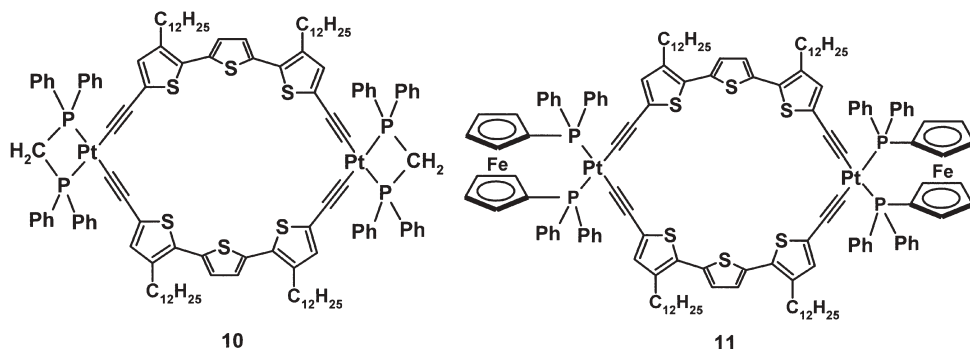


Fig. 65 Macrocycles Bäuerle10–11

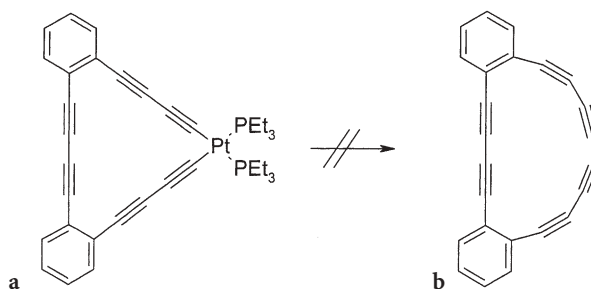


Fig. 66 Attempted route to obtain macrocycle Haley5b from Haley5a

successful as the still-unknown macrocycle **Haley5b** would probably bear too much strain (Fig. 66) [11a].

2.4

Macrocycles by Pt-P Coordination

Although they are commonly used as exocyclic ligands for Pt(II), phosphines are not that often used as bridging ligands for platina-macrocycles. One reason for this might be the lack of rigidity of the phosphine macrocycles, as rotation around the Pt(II)-P bond is easily possible. More flexible spacers, though, make a directional bond approach to macrocycles tedious or even impossible, and result in structures that are not shape-persistent. Nevertheless, the geometric behaviour of Pt(II) compounds is often controlled by diphosphine ligands, and a lot of work has been devoted to the field of Pt(II) diphosphine complexes. We therefore refer to reviews, e.g. Bessel, Takeuchi et al. [60] review *trans*-spanning diphosphine ligands giving a very detailed picture of research in this area. We will only concentrate on few examples here.

Gladysz et al. achieved the cyclization to a *trans*-Pt(II) diphosphane macrocycle by first preparing an acyclic Pt(II) precursor with two phosphine moieties

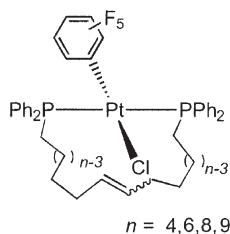


Fig. 67 Macrocycle Gladysz1

in *trans*-position. The alkene end groups of the phosphine ligands were then linked by an intramolecular metathesis cyclization to form macrocycle **Gladysz1** (Fig. 67) as a mixture of *E/Z* isomers in 78% yield [61b,e]. This macrocycle was subsequently hydrogenated over Pd/C to remove the double bond in 54% yield.

Using the same method with a precursor carrying four alkene groups, the bimacrocyclic system **Gladysz2** (Fig. 68) could be obtained after hydrogenation in moderate yield as a mixture of *syn* (31%) and *anti* (7%) isomers (regarding the two phosphine phenyl groups) [61a,e]. Shorter alkyl chains at such a precursor complex, however, mainly resulted in products with two separate rings on each side of the Pt.

More recently, this strategy was extended to prepare *trans*-Pt(II) diphosphane macrocycle **Gladysz3** (Fig. 69) by alkyne metathesis [61c]. Hydrogena-

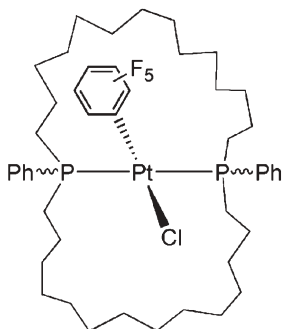


Fig. 68 Macrocycle Gladysz2

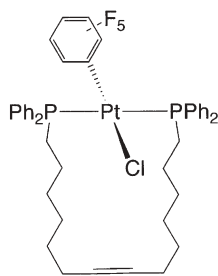


Fig. 69 Macrocycle Gladysz3

tion of the alkyne moiety with Pd/C and hydrogen led to the same saturated product (in 87% yield) as hydrogenation of **Gladysz1**.

When *cis*-configured Pt(II) precursor complexes are used instead of *trans*-Pt(II) complexes, monoplatina- and bis-platina-macrocycles **Gladysz4a–b** (Fig. 70) are formed in equilibrium and seem to interconvert having the equilibrium on the side of the cyclic monomer **Gladysz4a** [61a].

A directional bond formation strategy was elaborated by Faraone et al. Upon mixing diphosphinito ligands in a 1:1 ratio with Pt(COD)I₂, the cyclic dimers **Faraone1a–b** (Fig. 71) precipitate from the solution [62]. From X-ray structure analysis the authors concluded that the cavity of the macrocycles, with critical interatomic distances of ca. 4 Å, is too small to allow binding of even small guest molecules. While cyclic trimers or tetramers would certainly increase the chances of establishing host-guest chemistry, formation of such species was not observed. The preference of the cyclodimer over larger cyclooligomers is assumed to be due to both the geometry of the ligands and the strong Pt–P bonds.

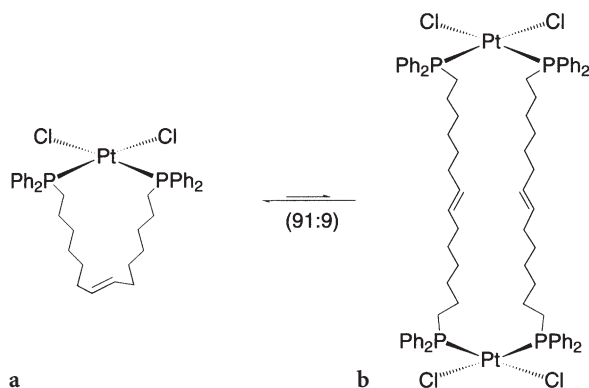


Fig. 70 Equilibrium between cyclic monomer **Gladysz4a** and cyclic dimer **Gladysz4b**

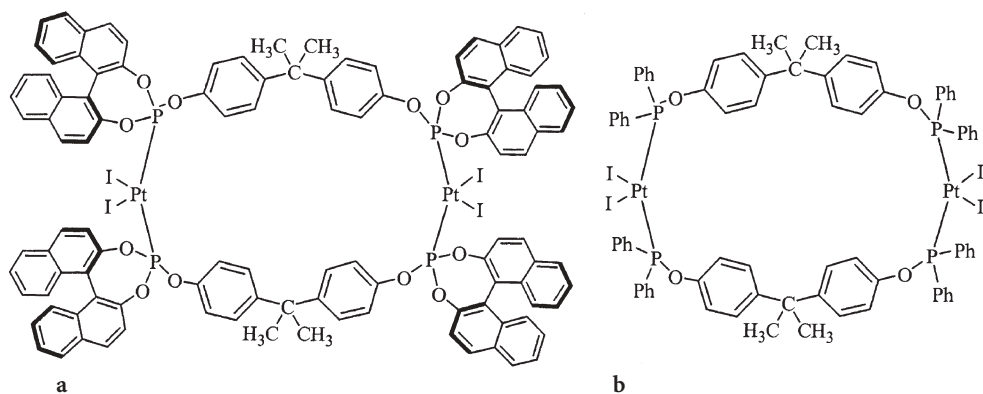


Fig. 71 Macrocycles **Faraone1a** and **Faraone1b**

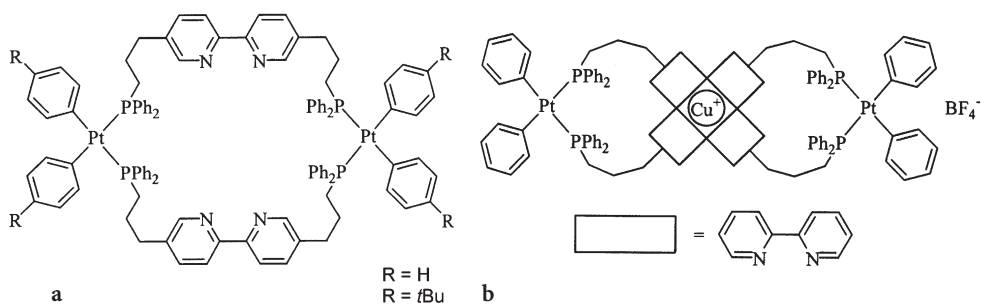


Fig. 72 Macrocycle **Lindner1a** and the resulting mixed metalla-macrocycle **Lindner1b**

By starting with a 2,2'-bipyridyl-containing diphosphine ligand, Lindner et al. introduced functionality in terms of endotopic binding sites to their macrocycles [63]. Although the diplatina-macrocycles **Lindner1a** (Fig. 72) are formed in only 20–23% yield, their solubility was much higher than that of a corresponding cyclodimer, comprising longer alkyl spacers and chlorine substituents at the Pt(II) corners, which forms in high yields under high-dilution conditions (not shown here). After addition of [Cu(CH₃CN)₄][BF₄] to macrocycle **Lindner1a**, the trisubstituted Pt(II)-Cu(I)-Pt(II) complex **Lindner1b** (Fig. 72) could be obtained in good yields. The macrocyclic system should exhibit a “figure-eight” conformation due to the tetrahedral coordination of Cu⁺ and the bipyridine bridging ligands.

A more rigid system has been prepared by Manners et al. by using a linear phosphinoacetylene ligand. Thus, the reaction of 1,4-diethynyl diphosphine and K₂PtCl₄ selectively gave the trisplatin triangle **Manners1a** (Fig. 73) in quantitative yield [64]. The macrocycle is strained, which is indicated by the X-ray structure analysis; with dihedral angles of 59–69° between the P-C-C atoms. Addition of KI to the system **Manners1a** in a 1:1:1 mixture of CHCl₃/CH₂Cl₂/

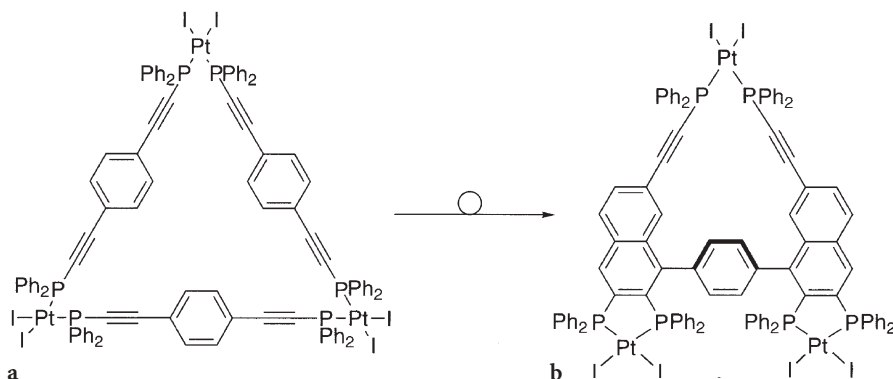


Fig. 73 Macrocycle **Manners1a** and conversion to **Manners1b**

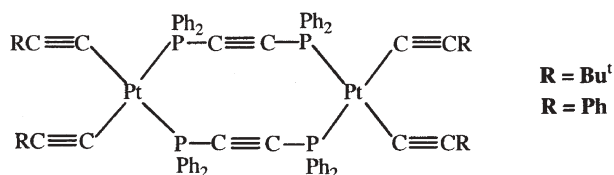


Fig. 74 Macrocycle ForniésLalinde4

CH_3CN resulted in a cyclization reaction and rearrangement providing the triangle **Manners1b**, which includes helical chirality.

Interestingly, by the use of shorter diphosphinoalkynyl ligands, cyclodimers are formed in high yields, as presented in the hexagon **ForniésLalinde4** (Fig. 74), reported by Forniés, Lalinde et al. [65a].

This type of structure has been known for a longer time and a variety of corresponding dinuclear Pt(II) cycles having other diphosphine ligands is known [65]. Early work on bis(diphenylphosphino)methane (dppm) bridged compounds is, e.g., summarized in a review by Puddephatt [66]. Although these complexes sometimes are named “macrocyclic”, the expression “macrochelate” would be more appropriate (see also introduction to Sect. 2.2.1).

2.5

Macrocycles by Unusual Pt Coordination

Bonds between the soft metal Pt(II) and hard oxygen atoms are considered to be rather unstable [67, 68]. Only very recently, Mukherjee, Stang et al. reported for the first time Pt(II) macrocycles with Pt-O coordinated bridging ligands. For example, reaction of a bis-Pt(II) phenanthrenyl precursor with various dicarboxylates in aqueous acetone resulted almost quantitatively in macrocycles **MukherjeeStang1** (Fig. 75) [67a].

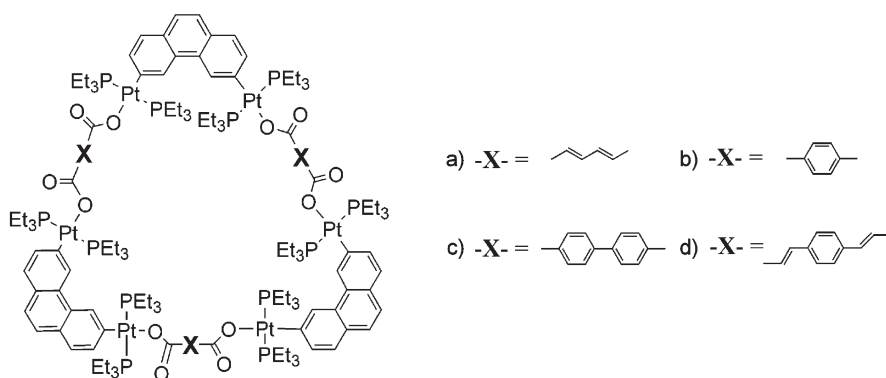


Fig. 75 Macrocycles MukherjeeStang1

More generally speaking, the concept of directional bonding was shown to work very effectively for Pt-O bound macrocycles: Reaction of the 60° bis-Pt(II) phenanthrenyl precursor with linear or quasi-linear bridging ligands resulted in the triangularly shaped systems **MukherjeeStang1**; the same bis-Pt(II) tecton reacted with a dicarboxylate that spans a 120° angle to yield the rhomboids **MukherjeeStang2** (Fig. 76) [67a]. In contrast, the U-shaped bis-Pt(II) anthracenyl “clamps” formed rectangles **MukherjeeStang3** (Fig. 77) [67a] and **MukherjeeStang4** (Fig. 78) [67b] by reaction with linear or quasi-linear ligands. The structures of these macrocycles have been confirmed by X-ray

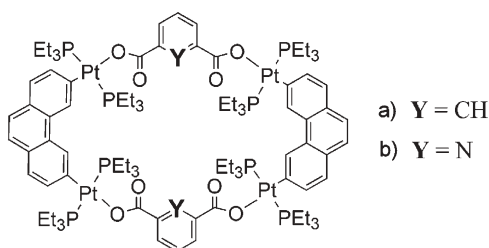


Fig. 76 Macrocycles **MukherjeeStang2**

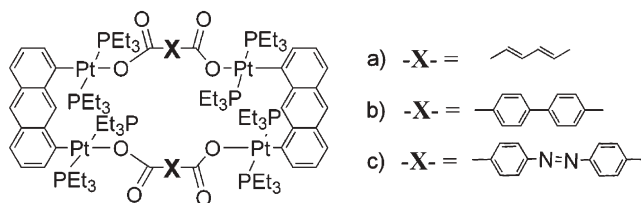


Fig. 77 Macrocycles **MukherjeeStang3**

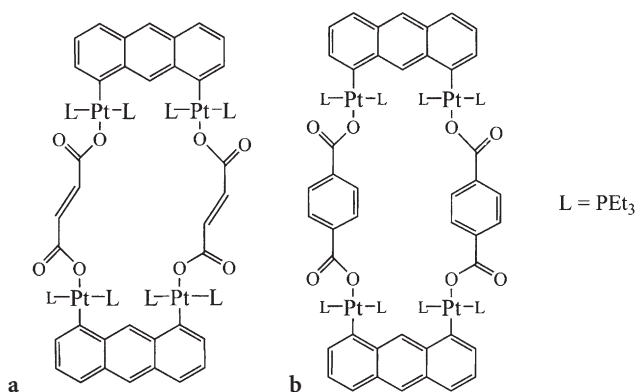


Fig. 78 Macrocycles **MukherjeeStang4**

structure analysis. Interestingly, only few of these molecules form stacks with cavities or channels in the solid state, while this is quite common for nitrogen bound macrocycles.

Hor et al. presented the Pt(II) square **Hor1** (Fig. 79) in which the Pt(II) corners are bound to the N and O atoms of isonicotinic acid [69]. For the reaction, a bis-Pt bithienyl precursor was used which reacted upon mixture with isonicotinic acid to the C_4 symmetric macrocycle **Hor1**. In contrast to macrocycle **Dunbar1** (see Sect. 2.2.2), the C=O oxygen atom is not involved in a coordinative bond.

Using the same metathesis strategy as for the P-coordinated macrocycles, Gladysz et al. synthesized the sulfur-coordinated macrocycles **Gladysz5a** and **Gladysz5b** (Fig. 80), which could be obtained in 55% and 24% yield, respectively [61d]. Unlike the macrocycles **Gladysz4a/b**, these two forms did not interconvert, and *tert*-butyl substitution at the sulfur suppressed the formation of dinuclear cycles.

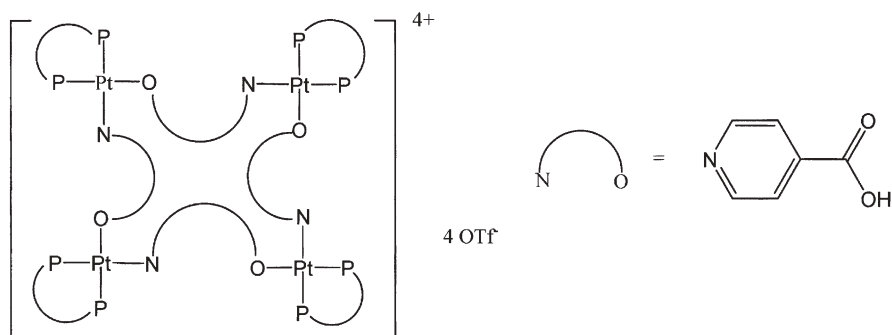


Fig. 79 Macrocycle **Hor1**

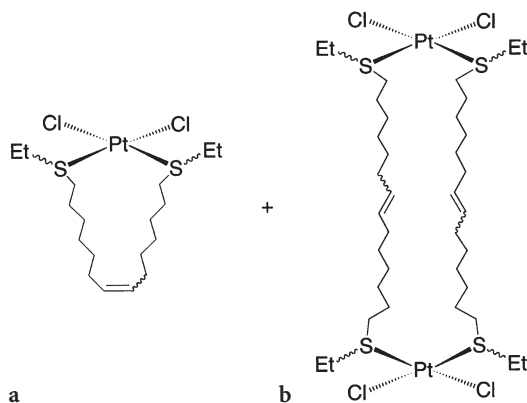


Fig. 80 Cyclic monomer **Gladysz5a** and dimeric byproduct **Gladysz5b**

3

Related Structures and Topologies

3.1

2D Compounds with Cyclic Substructures

In this small section, network structures are presented in which Pt(II) macrocycles are substructures of a 2D structure.

In this respect, Drain et al. prepared the “porphyrin band” **Drain1** (Fig. 81) comprising four tetrapyrrolylporphyrins that are held together by *cis*-arranged Pt(II) centres [70]. Such a “grid” may be considered as the 2D extension of the porphyrin Pt(II) macrocycles **Stang2** and **Lehn1** (Sect. 2.2.3).

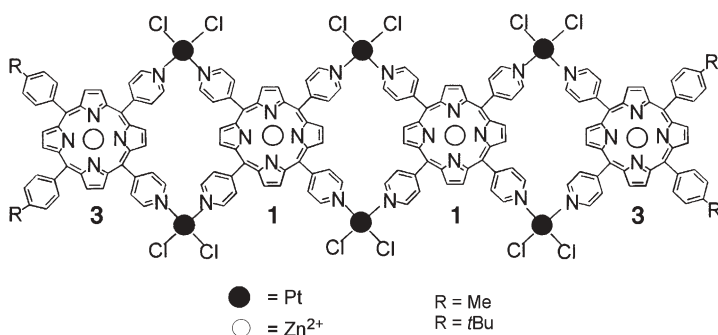


Fig. 81 Macrocycle array **Drain1**

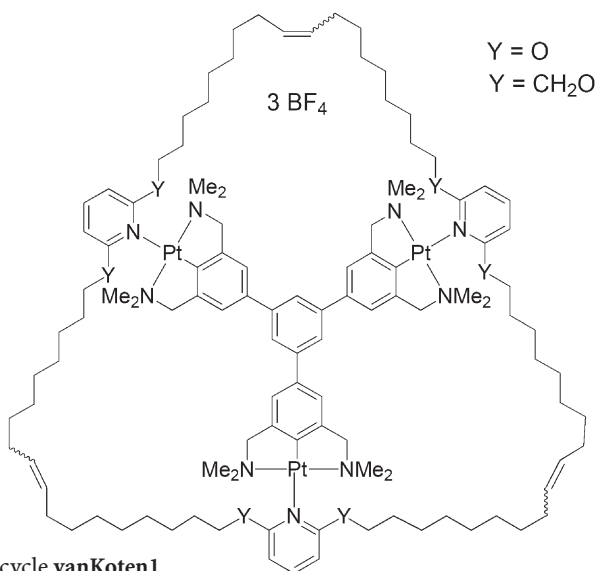


Fig. 82 Macrocycle **vanKoten1**

In Sect. 2.4, a structure of the Gladysz group comprising two “annulated” macrocyclic rings involving Pt(II) has been presented (**Gladysz2**). Closely related to this macrocycle is the work of van Koten et al. who used a trigonal tris-Pt(II) template to preorganize *meta*-alkyl substituted pyridine ligands bearing olefinic groups at the termini of the side chains [71]. By ring-closing metathesis, the outer cyclic array was closed to form the grid **vanKoten1** (Fig. 82), which formally consists of three annulated Pt(II) macrocycles. The Pt(II) template was removed later on by addition of aqueous NaCl to yield a Pt-free macrocycle. After hydrogenation of the olefinic moieties, the Pt(II) template was again recognized by the Pt-free macrocycle ring as a guest molecule.

3.2

3D (Cage) Structures

Meanwhile, a number of 3D structures and topologies exist that have been built from Pt(II) building blocks or Pt(II) macrocycles by using the same methods as described before for the macrocycle formation.

The first 3D structures containing Pt(II) were probably not seen as supramolecular assemblies, but rather as (simple) organometallic complexes. This is because they mainly were not synthesized in a “directional” way, but for example by pyrolysis of a metal and a ligand mixture. In 1985, Strähle published the trinuclear cage complex **Strähle1** (Fig. 83), which contains six pyrazole

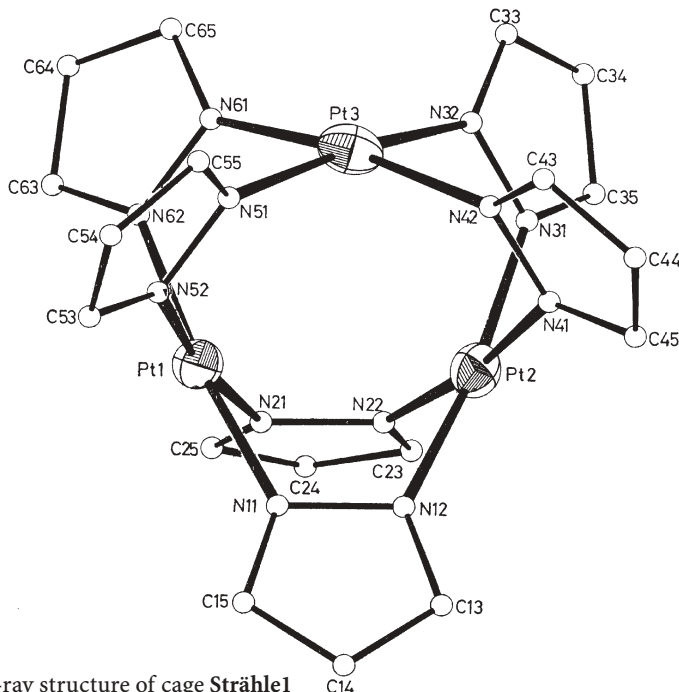


Fig. 83 X-ray structure of cage **Strähle1**

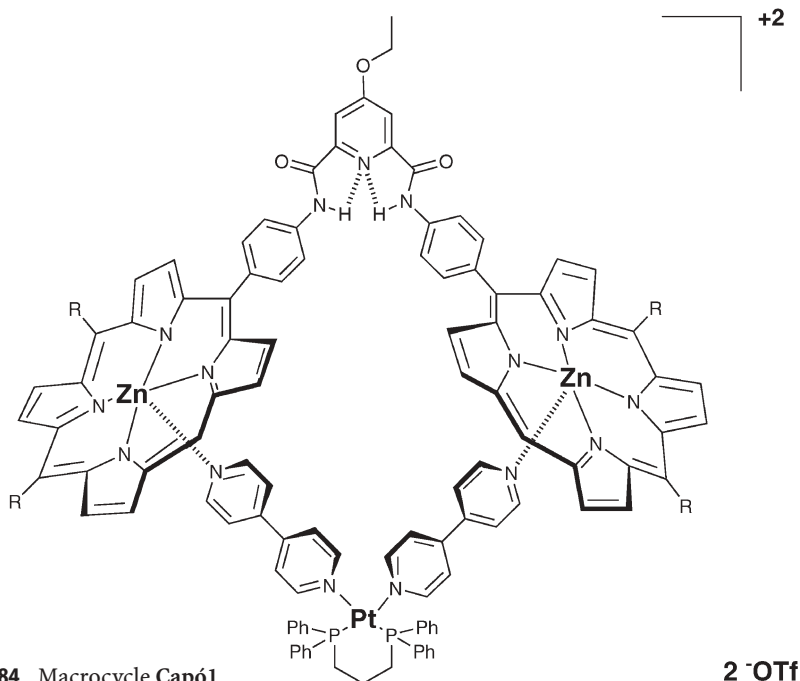


Fig. 84 Macrocycle **Cap61**

bridging ligands and is formed in 20% yield among a polymeric mixture [72]. The structure was verified by X-ray structure analysis and should rather be considered as a macrochelate.

Capó et al. reported the self-assembly of a bis-zinc porphyrin pincer molecule with a *cis*-Pt(II)(dppp) bis-4,4'-bipyridyl precursor to form the 3D cyclic structure **Cap61** (Fig. 84) [73]. Hereby, the vectors of the 4,4'-bipyridyl ligands, which form a 90° angle, directly point to the central Zn atoms of the porphyrin moieties. The quantitative formation of the macrocycle was proven by ¹H-NMR spectroscopy, which showed a high upfield shift of those 4,4'-bipyridyl protons that point to the porphyrin units. A high Zn-N binding constant of $\sim 10^8 \text{ L}^2 \text{ mol}^{-2}$ was determined. Additionally, significant shifts of the absorption maxima could be seen in the UV-Vis spectra by titration of the porphyrin precursor with the Pt(II) precursor and 4,4'-bipyridine.

A cage built from tetracyano-substituted cavitands, linked by Pt(II) corners, was presented by Dalcanale et al. [74]. The molecular cage **Dalcanale1** (Fig. 85), in which the two “bowl” units are linked by four Pt(II)dppp atoms through the cyano units, seems to trap one of the triflate counter ions. The cage molecule can be reversibly disassembled by addition of a competing ligand such as NEt₃.

“Half” cages built from a *cis*-Pt(II) precursor and thymine or uracil ligands have been very recently presented by Krebs et al. [75]. The resulting pentanuclear structures **Krebs1** (Fig. 86), obtained in rather low yields of ca. 15–20%, contain one monoplatinum and two diplatinum centres as the three “corners”

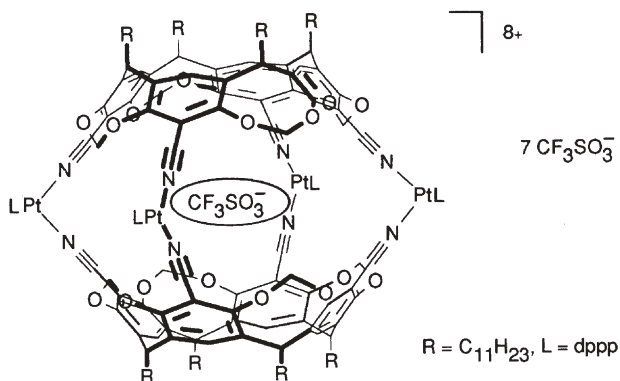


Fig.85 Cage Dalcane1

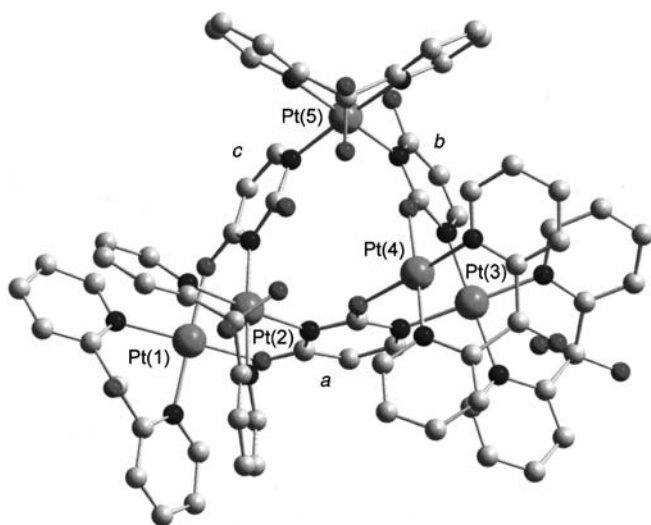


Fig.86 X-ray structure of cage Krebs1

which are bridged by the nucleobases. The ability of the system **Krebs1** to coordinate small anions such as nitrate to different edges of the Pt_5 complex by hydrogen bonds points to a close relation to metalla-calixarenes.

The synthesis of more flexible cage structures has been shown by Lindner et al. [76]. The trinuclear 3D structure **Lindner2** (Fig. 87) was prepared by the self-assembly of a 1,3,5-alkylated benzene scaffold that is functionalized by diphenylphosphine ligands at the termini of the alkyl chains and a *cis*-configured Pt(II) precursor under high dilution conditions [76a,c]. The cage molecule **Lindner2** was formed as the major product and no linear oligomers were observed. X-ray structure analysis showed the incorporation of dichloromethane as a guest molecule into the cavity of the cage by a reversible complexation/decomplexation process. The more complicated hexanuclear cage

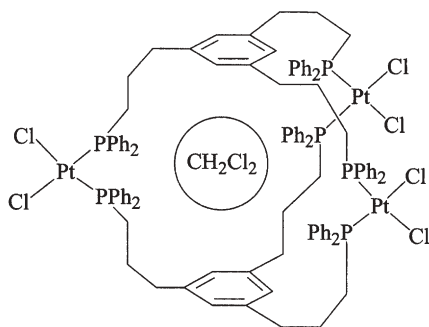


Fig. 87 Cage **Lindner2** with included CH₂Cl₂ guest molecule

Lindner3 (Fig. 88) was only formed in traces during the reaction, as proven by mass spectrometry [76c].

When similar 1,3,5-trisubstituted benzene scaffolds were reacted with *trans*-configured Pt(II) building blocks, comparable prism-like structures **Lindner4** (Fig. 89) were prepared comprising various alkyl chain lengths [76b]. The yield depended on the length of the alkyl side chains and dropped from 68% for ethylene to 37% for butylene bridges, while the formation of polymeric material increased. Although certain flexibility is introduced in these cages due to the alkyl chains and they should therefore be ideally suited for guest inclusion by induced fit, those experiments failed because of either too weak complexation behaviour by an eventually blocked access to the cage or by competing self-association due to π - π stacking. A side reaction detected in both systems **Lindner2** and **Lindner4** when longer alkyl chains were implemented seemed to be the formation of “intramolecular” 2D chelate complexes [76a].

With the same stoichiometry of Pt(II) corners and trigonal phosphine ligands, Balch et al. obtained the prism **Balch1** (Fig. 90) in moderate yields [77].

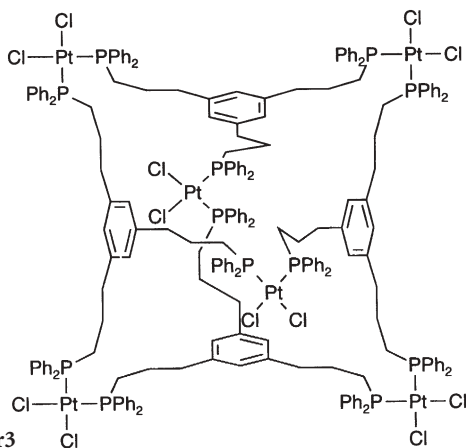


Fig. 88 Cage **Lindner3**

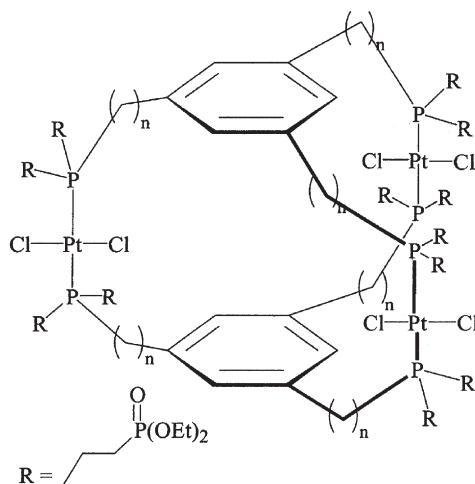


Fig. 89 Cage Lindner4

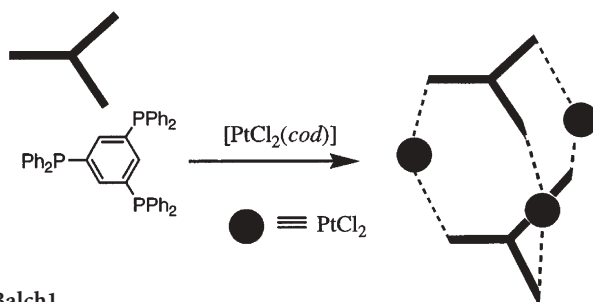


Fig. 90 Cage Balch1

Similar to **Lindner2–4**, the cage molecule **Balch1** comprises 1,3,5-tris(triphenylphosphane)-substituted benzene moieties resulting in a very low solubility that allowed characterization only by X-ray structure analysis in the solid state.

The best known examples (and also the largest number) of 3D structures have been published by the groups of Fujita [78] and Stang [79].

By self-assembly of the planar trigonal tris(4-pyridyl)-1,3,5-triazine ligand and Pt(II)(en) corner units, the “molecular lock” **Fujita2** (Fig. 91) has been prepared using sodium adamantanecarboxylate as a templating agent, which can be removed by heating afterwards [16a, 78c,e]. The cage molecule is capable of incorporating small neutral guest molecules that can diffuse through the “pores” of the capsule [16a, 78c]. Therefore, the capsule may act as a catalyst for the reaction of molecules within the cavity. Since the product that is formed cannot escape from the capsule, even otherwise reactive and labile species such as a siloxane cyclotrimer can be prepared, as shown by Kusakawa, Fujita et al. [78c].

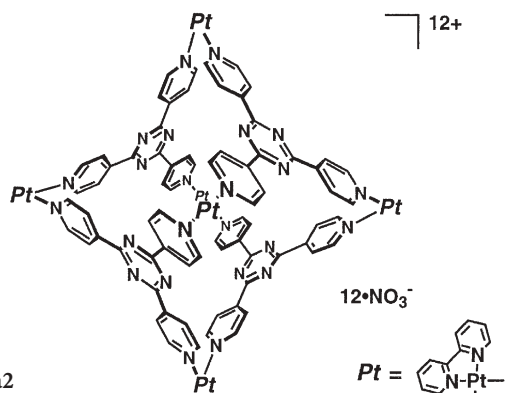


Fig. 91 Cage Fujita2

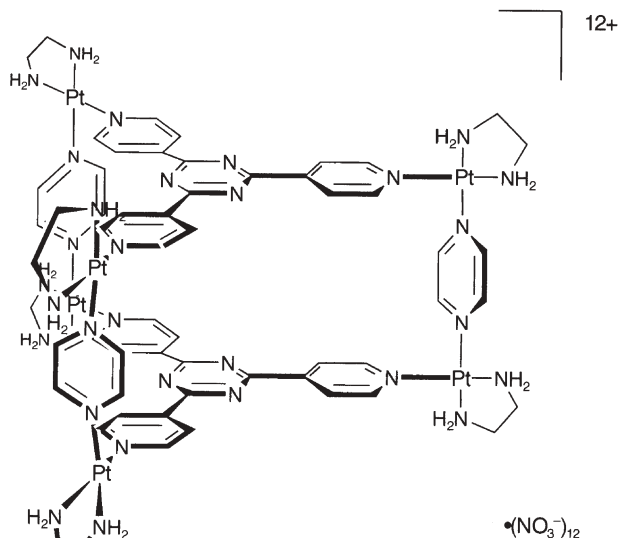











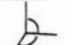


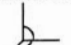







Fig. 92 Catenane Fujita3

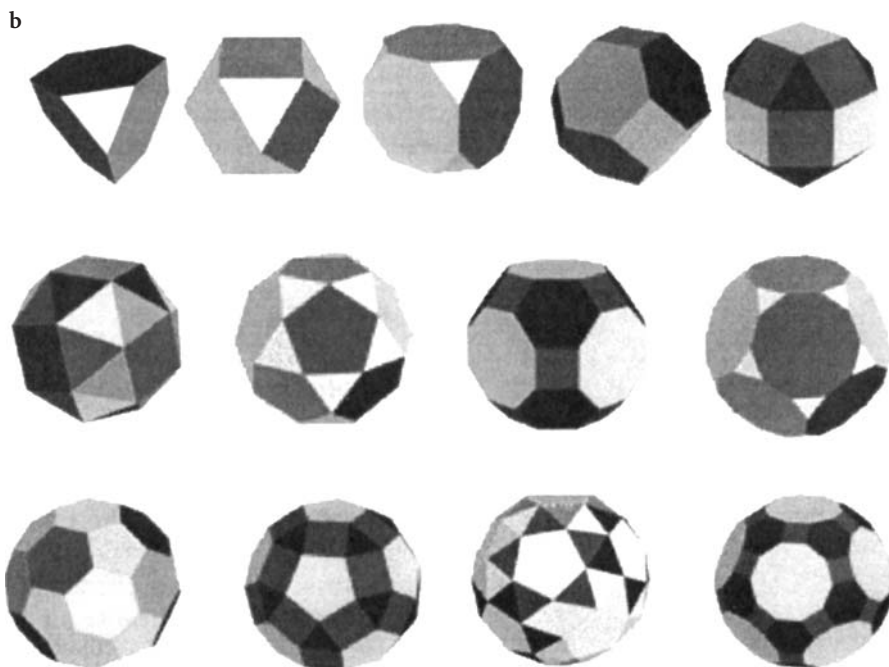
By addition of pyrazine together with a triphenylene template to the same reactand mixture that is used for **Fujita2**, the prism-like cage **Fujita3** (Fig. 92) forms instead [78a]. After extraction of the template with chloroform, cage molecule **Fujita3** is capable of intercalating different aromatic guest molecules, e.g. pyrene.

Using a slightly different mixture of the same components, the interlocked prism **Fujita4** (Fig. 93) could be obtained [78e].

Finally, Stang and his group managed to build a number of Platonic and Archimedean geometric structures (Scheme 5) from mixtures of specially de-

a

Building Blocks	 84-90°	 109.5°	 180°	 90° angular	 109.8° angular
 120° planar					
 109.8° angular					
 90° angular					
 180°					
 84-90°					



Scheme 5 a Selective formation of 3D solids using directional building blocks. b Typical Platonic and Archimedean geometric structures [6]

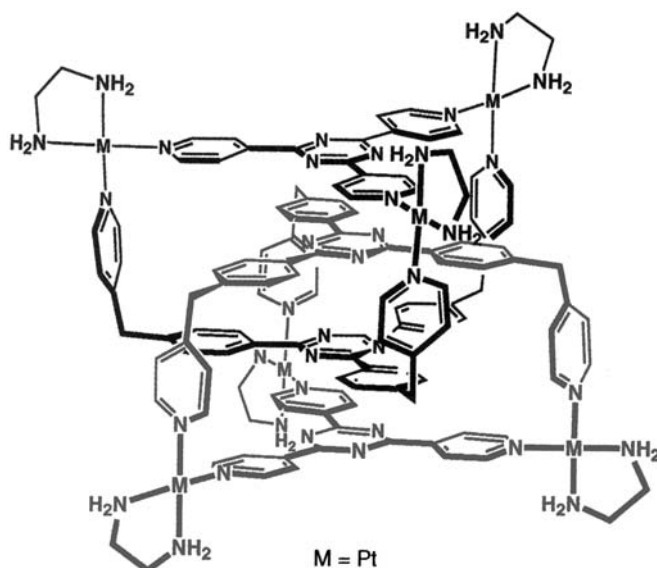


Fig. 93 Cage Fujita4

signed ligands and Pd(II) or Pt(II) moieties. As a complete survey of this work would go far beyond the scope of this review, some reviews of Stang et al. on this topic, which at least cover this work until 2002, are recommended [6]. We will discuss here some of the most interesting examples containing Pt(II) units.

The truncated tetrahedron **StangOlenyuk1** (Fig. 94) was prepared from a tripod-shaped 1,3,5-tris(4-ethynylpyridyl)-substituted benzene and a *cis*-Pt(II) precursor [79f]. The noticeable features of the cage complex are the exocyclic BINAP ligands which add chirality to the highly symmetric 3D structure and minimize a loss of entropy due to their rigid conformation.

An even more complicated cage structure is represented by the cuboctahedra **Stang10** (Fig. 95), which in this case combines tritopic trisplatina and angular bipyridyl precursor units [79e]. Remarkably, despite the high charge, the big cuboctahedra are very soluble in common organic solvents. Identification of the highly symmetric 3D structures was possible by NMR spectroscopy and elemental analysis, as well as ESI-MS, the results of the latter being in excellent agreement with calculated values [79d,e].

Very recently, the cage structures **ChiAddicottStang4–5** (Fig. 96), comprising *trans*-Pt(II) units in the “clip” moieties, have been reported to form in excellent yields [79a]. The chiral structure of the cage **ChiAddicottStang5** is most noticeable and could be assembled from the *R* or the *S* tritopic precursor. The structure was confirmed by NMR, elemental analysis and ESI-MS as well as by comparison with crystal structures of analogous compounds [79b].

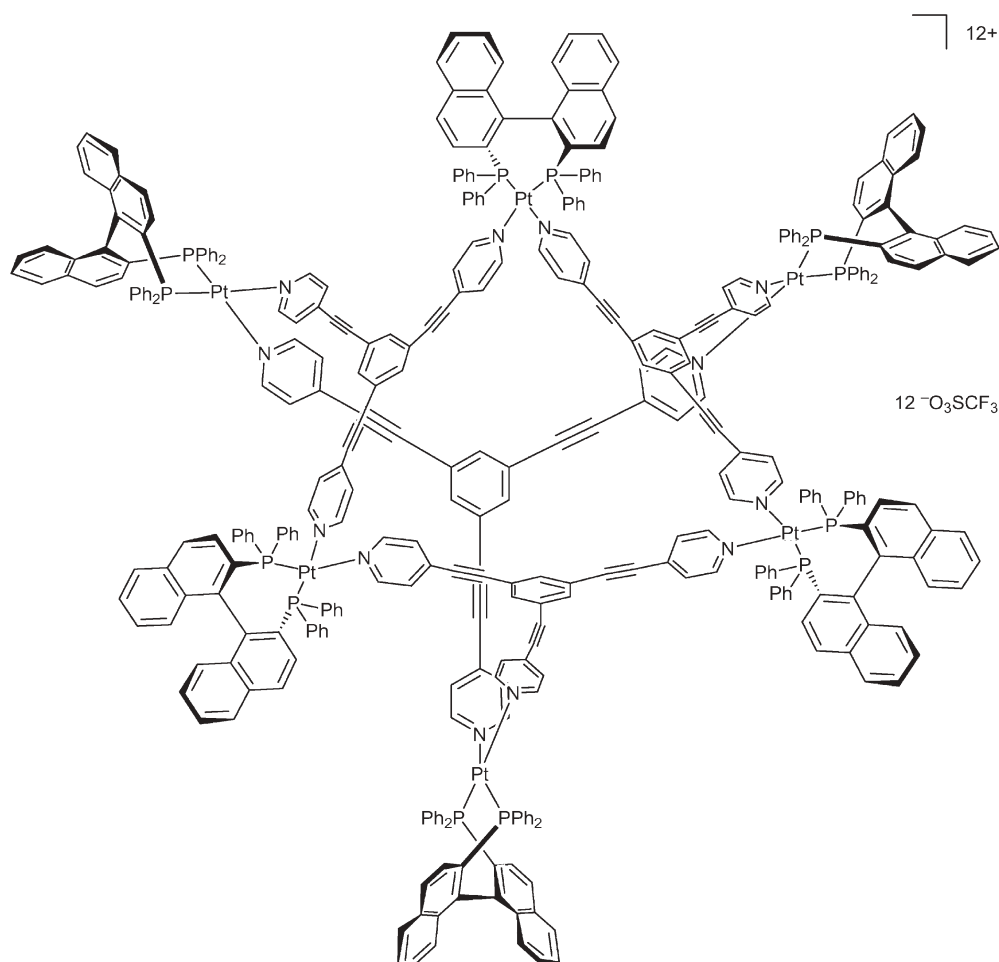


Fig. 94 Truncated tetrahedron StangOlenyuk1

Furthermore, the analogous prisms **KuehlStang2–3** (Fig. 97) including the same clip motif but with planar tops and bottoms, have been reported by Kuehl, Stang et al. [79c].

3.3 Catenanes

In general, catenanes represent interlocked macrocycles that are held together by a so-called mechanical bond and have become an intensively investigated field. Several synthetic approaches towards this molecular topology have been developed in the last two decades, utilizing highly efficient templating strategies [80] and self-assembly processes [81].

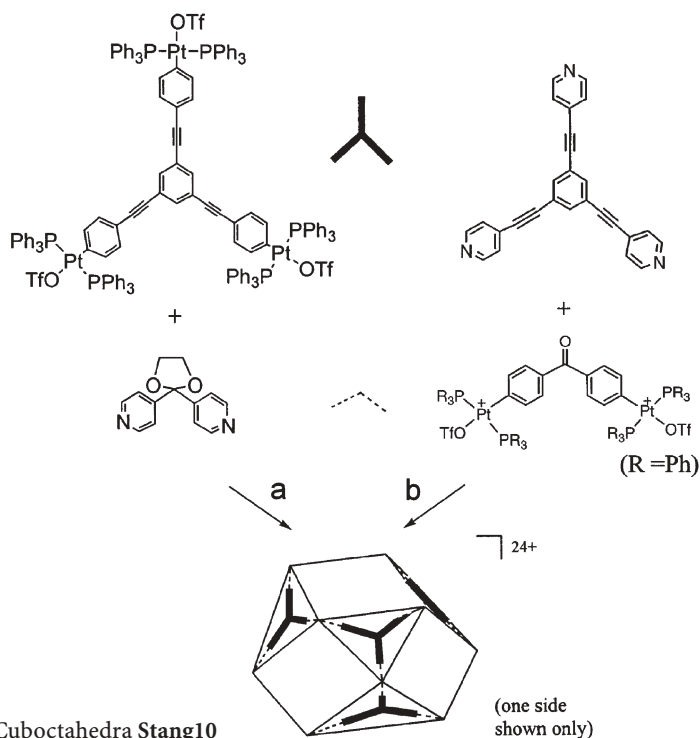


Fig. 95 Cuboctahedra Stang10

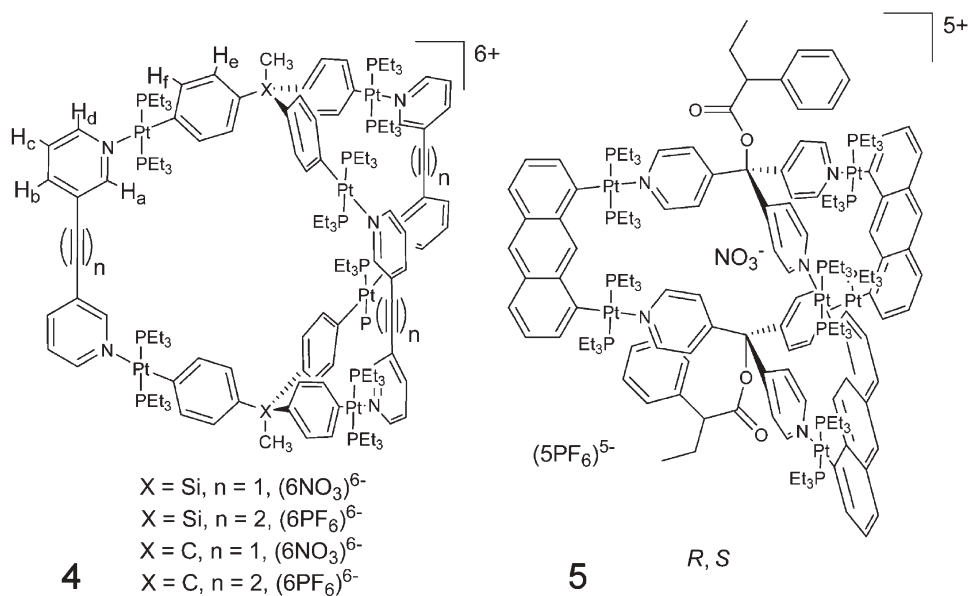


Fig. 96 Prisms ChiAddicottStang4 and ChiAddicottStang5

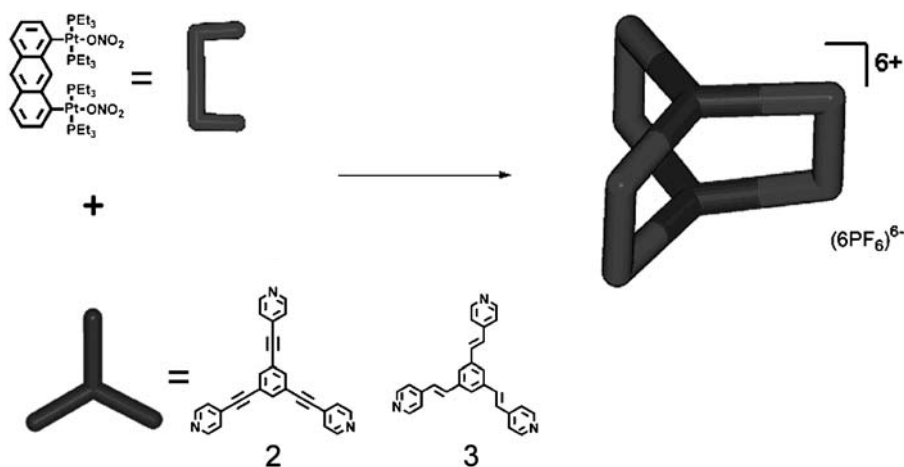


Fig. 97 Prisms KuehlStang2 and KuehlStang3

Catenanes can be prepared as thermodynamically controlled products without the use of a template, as shown by Fujita, Ogura et al. While the precursor macrocycles are formed under kinetic control, heating at 100 °C for 24 h resulted in an interlocking of two macrocycles to form the corresponding tetranuclear Pt(II) catenane **FujitaOgura1** (Fig. 98) [82b–c].

Selective cross-catenation of two analogous Pd(II) and Pt(II) macrocycles comprising tetrafluorobenzene units in the cyclic array was achieved by Fujita et al. [82a]. Without formation of homo-catenanes, the mixed metal catenane

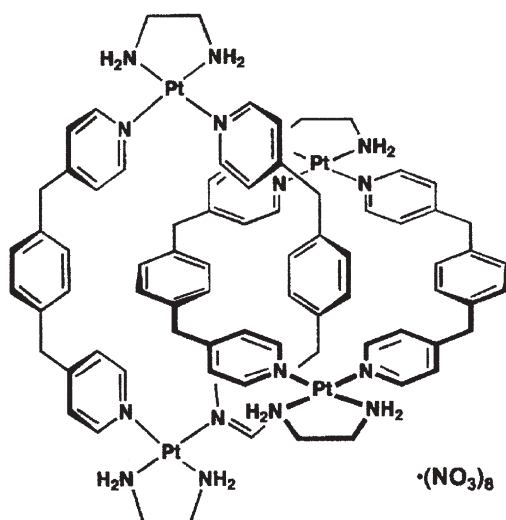


Fig. 98 Catenane FujitaOgura1

Fujita5 (Fig. 99) is formed in high yield within 3 h at room temperature. This elegant approach makes use of the kinetically labile Pd(II)-pyridine coordination, so that the Pd(II) macrocycle can thread through the inert Pt(II) macrocycle directed by π -donor/ π -acceptor interactions of benzene units in one macrocycle with tetrafluorobenzene units in the other one.

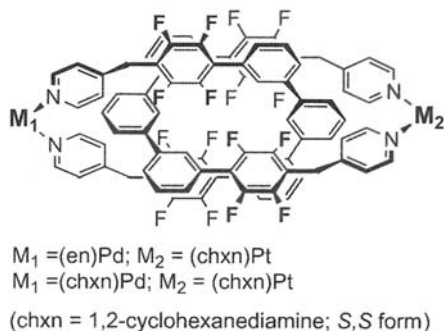


Fig. 99 Catenanes Fujita5

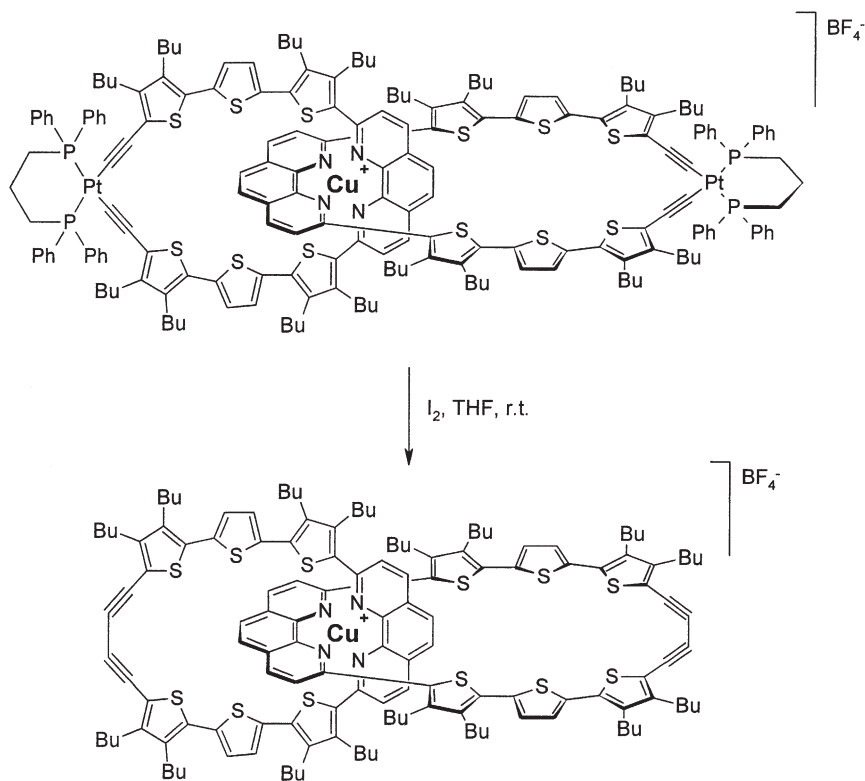


Fig. 100 Catenanes Bäuerle12

A strategy towards the synthesis of the first interlocked π -conjugated macrocycles was developed by Bäuerle et al. by extending their metal-template approach, which has already been described for oligothiophene-containing Pt(II) macrocycles (see Sect.2.3.2). A tris-metallated catenate was synthesized by heteroleptic Cu^+ complexation of phenanthroline Pt(II) macrocycle **Bäuerle7** and the open-chained ligand to form a “pseudorotaxane” under thermodynamic control. Ring closure with Pt(II)(dppp) gave bis-platina-Cu(I) catenate **Bäuerle12** (Fig. 100) in 43% yield. Subsequent 1,1-reductive elimination of the Pt(II) corners with iodine led to the corresponding conjugated Cu(I) catenate in 41% yield. Characterization and structural proof were made by ^1H -NMR spectroscopy and ESI-FT-ICR mass spectrometry [58]. Due to the very small ring size of the interlocked macrocycles it was not possible to remove the Cu^+ central atom.

This problem was solved by synthesizing the larger bis-platina-Cu(I) catenate **Bäuerle13** (Fig. 101), which contains quaterthiophene instead of terthiophenes units. It is obtained by homoleptic complexation of the open-chain compound with Cu^+ and subsequent macrocyclization with Pt(II)(dppp). Reductive elimination and decomplexation of the central copper yielded the first conjugated catenane [83].

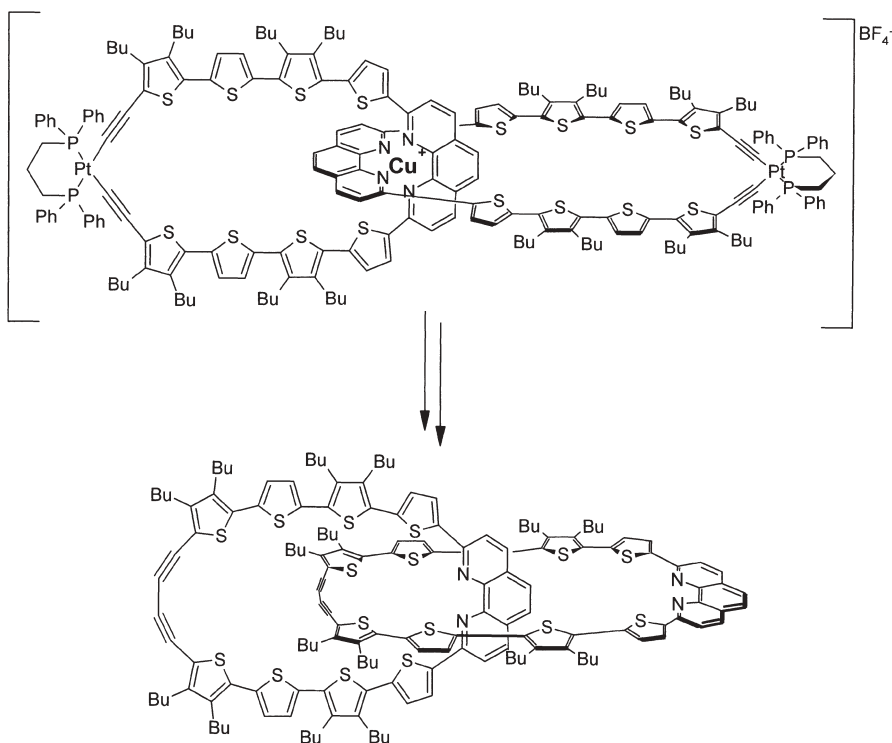


Fig. 101 Catenanes **Bäuerle13**

These examples demonstrate that Pt(II) complexation reactions can not only be used for the efficient synthesis of complicated molecular topologies and geometries, but also as templates and intermediates for the formation of the corresponding “metal-free” and covalently linked structures.

4

Concluding Remarks

The intention of this review was to give an overview of the state-of-the-art in the use of Pt(II) moieties in macrocyclic and topological chemistry. The many examples show that a lot of very creative work has already been done in this strongly growing field.

However, we do not want to conclude without stressing some closely related aspects. Many reports on the formation of Pt(II) macrocycles are in conjunction with corresponding Pd(II) compounds, therefore by comparison one general conclusion can be drawn: the Pd(II) analogues possess weaker bonds and are therefore prone to undergo equilibration. Because of this feature, it is easier to build up 3D structures or to achieve the thermodynamically most stable product with Pd(II) instead of Pt(II) building blocks, where bond formation is less reversible and hence unwanted side products are much more probable. Fujita et al. reported the equilibrium between the (entropically favoured) triangular and (strain-free) square assembly **Fujita6** (Fig. 102), the Pd analogue

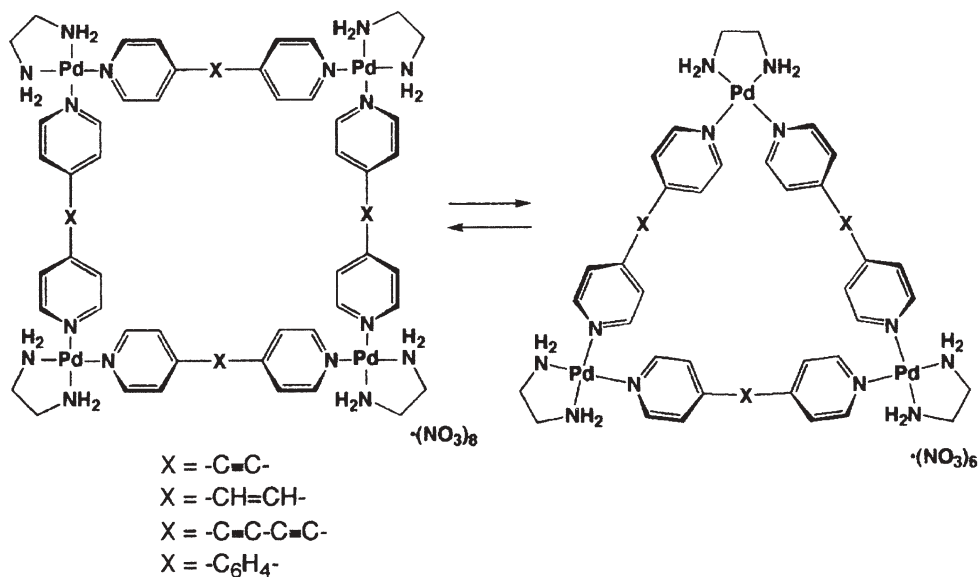


Fig. 102 Equilibrium between squared Pd(II) macrocycle **Fujita6a** and the triangular form **Fujita6b**

of Fujita [84]. The ratio between these two forms can be adjusted even at room temperature by just varying the concentration, whereas the Pt(II) square is completely stable.

If acetylides are reacted with Pd(II), very often only the C-C coupling product is observed because elimination from the Pd-bis-acetylide complex is very fast, in contrast to the corresponding isolable Pt complexes [85].

The coordination patterns for Pt(II), especially coordination to acetylides, are also seen in a number of linear structures. Pt(II) has been incorporated into a number of molecular wires, polymers and networks. The interest thereby is mainly in the electronic nature and conductivity of these compounds and the change upon the addition of Pt. Although they are not part of this review, their structures are often closely related to macrocycles.

In summary, the increasing number of Pt(II) macrocycles and complex 3D structures shows that Pt(II) is a very valuable building block for macrocyclic and topological chemistry. Its major advantages are good stability towards air and moisture (especially compared to the Pd(II) analogues), the usually good to excellent yields in formation, and the applicability both as a 90° and 180° construction element with which a directional synthesis of a specific structure (e.g. molecular squares) can be achieved. Furthermore, Pt(II) can act as a building block for more sophisticated 3D structures as well as a template for the synthesis of strained conjugated macrocycles and catenanes.

References

1. a) Diederich F, Stang PJ (2000) (eds) *Templated organic synthesis*. Wiley-VCH, Weinheim; b) Sauvage J-P, Hosseini MW (1996) (eds) *Templating, self-assembly and self-organization*. In: Lehn J-M (ed) *Comprehensive supramolecular chemistry*, vol 9. Pergamon, Oxford; c) Lehn J-M (1995) *Supramolecular chemistry – concepts and perspectives*. Wiley-VCH, Weinheim; d) Vögtle F (1991) *Supramolecular chemistry*. Wiley, Chichester
2. a) Holliday BJ, Mirkin CA (2001) *Angew Chem* 113:2076; b) Holliday BJ, Mirkin CA (2001) *Angew Chem Int Ed* 40:2022
3. a) Swiegers GF, Malefetse TJ (2002) *Coord Chem Rev* 225:91; b) Swiegers GF, Malefetse TJ (2000) *Chem Rev* 100:3483
4. Jones CJ (1998) *Chem Soc Rev* 27:289
5. a) Fujita M (1998) *Chem Soc Rev* 27:417; b) Fujita M, Ogura K (1996) *Bull Chem Soc Jpn* 69:1471
6. a) Seidel SR, Stang PJ (2002) *Acc Chem Res* 35:972; b) Leininger S, Olenyuk B, Stang PJ (2000) *Chem Rev* 100:853; c) Olenyuk B, Fechtenkötter A, Stang PJ (1998) *J Chem Soc, Dalton Trans* 1707; d) Stang PJ, Olenyuk B (1997) *Acc Chem Res* 30:502
7. Dinolfo PH, Hupp JT (2001) *Chem Mater* 13:3113
8. Schalley CA, Lützen A, Albrecht M (2004) *Chem Eur J* 10:1072
9. Johnson DW, Raymond KN (2001) *Supramol Chem* 13:639
10. a) Vilar R (2003) *Angew Chem* 115:1498; b) Vilar R (2003) *Angew Chem Int Ed* 42:1460
11. a) Marsden JA, Palmer GJ, Haley MM (2003) *Eur J Org Chem* 2355; b) Yamaguchi Y, Yoshida Z-i (2003) *Chem Eur J* 9:5430; c) Grave C, Schlüter AD (2002) *Eur J Org Chem* 3075; d) Bodwell GJ, Satou T (2002) *Angew Chem* 114:4175; e) Bodwell GJ, Satou T (2002) *Angew Chem Int Ed* 41:4003; f) Haley MM, Pak JJ, Brand SC (1999) *Top Curr Chem*

- 201:81; g) de Meijere A, Kozhushkov SI (1999) *Top Curr Chem* 201:1; h) Youngs WJ, Tessier CA, Bradshaw JD (1999) *Chem Rev* 99:3153
12. Bosch E, Barnes L (2000) *Organometallics* 19:5522
13. a) Campbell K, Johnson CA II, McDonald R, Ferguson MJ, Haley MM, Tykwinski RR (2005) (submitted); b) Campbell K, McDonald R, Ferguson MJ, Tykwinski RR (2003) *J Organomet Chem* 683:379
14. Sonogashira K, Yatake T, Tohda Y, Takahashi S, Hagihara N (1977) *Chem Commun* 291
15. a) Whiteford JA, Rachlin EM, Stang PJ (1996) *Angew Chem* 108:2643; b) Whiteford JA, Rachlin EM, Stang PJ (1996) *Angew Chem Int Ed* 35:2524
16. a) Sakamoto S, Yoshizawa M, Kusukawa T, Fujita M, Yamaguchi K (2001) *Org Lett* 3:1601; b) Sakamoto S, Fujita M, Kim K, Yamaguchi K (2000) *Tetrahedron* 56:955
17. Schalley CA, Müller T, Linnartz P, Witt M, Schäfer M, Lützen A (2002) *Chem Eur J* 8:3538
18. Lock CJL, Peresie HJ, Rosenberg B, Turner G (1978) *J Am Chem Soc* 100:3371
19. Neugebauer D, Lippert B (1982) *Inorg Chim Acta* 67:151
20. Fanchiang Y-T (1986) *J Chem Soc, Dalton Trans* 135
21. a) Sherman SE, Gibson D, Wang AH-J, Lippard SJ (1988) *J Am Chem Soc* 110:7368; b) Sherman SE, Gibson D, Wang AH-J, Lippard SJ (1985) *Science* 230:412
22. a) Longato B, Bandoli G, Trovó G, Marasciulo E, Valle G (1995) *Inorg Chem* 34:1745; b) Schenetti L, Bandoli G, Dolmella A, Trovó G, Longato B (1994) *Inorg Chem* 33:3169
23. a) Navarro JAR, Lippert B (2001) *Coord Chem Rev* 221:219; b) Zangrando E, Pichierri F, Randaccio L, Lippert B (1996) *Coord Chem Rev* 156:275; c) Lippert B (1989) *Prog Inorg Chem* 37:1
24. a) Rother IB, Willermann M, Lippert B (2002) *Supramol Chem* 14:189; b) Schnebeck R-D, Freisinger E, Glahé F, Lippert B (2000) *J Am Chem Soc* 122:1381; c) Navarro JAR, Freisinger E, Lippert B (2000) *Inorg Chem* 39:2301–2305; d) Navarro JAR, Freisinger E, Lippert B (2000) *Eur J Inorg Chem* 147; e) Navarro JAR, Janik MBL, Freisinger E, Lippert B (1999) *Inorg Chem* 38:426; f) Schnebeck R-D, Freisinger E, Lippert B (1999) *Angew Chem* 111:235; g) Schnebeck R-D, Freisinger E, Lippert B (1999) *Angew Chem Int Ed* 38:168; h) Schnebeck R-D, Freisinger E, Lippert B (1999) *Chem Commun* 675; i) Lüth MS, Freisinger E, Glahé F, Müller J, Lippert B (1998) *Inorg Chem* 37:3195; j) Schnebeck R-D, Randaccio L, Zangrando E, Lippert B (1998) *Angew Chem* 110:128; k) Schnebeck R-D, Randaccio L, Zangrando E, Lippert B (1998) *Angew Chem Int Ed* 37:119; l) Lüth MS, Freisinger E, Glahé F, Lippert B (1998) *Inorg Chem* 37:5044; m) Rauter H, Mutikainen I, Blomberg M, Lock CJL, Amo-Ochoa P, Freisinger E, Randaccio L, Zangrando E, Chiarparin E, Lippert B (1997) *Angew Chem* 109:1353; n) Rauter H, Mutikainen I, Blomberg M, Lock CJL, Amo-Ochoa P, Freisinger E, Randaccio L, Zangrando E, Chiarparin E, Lippert B (1997) *Angew Chem Int Ed* 36:1296; o) Rauter H, Hillgeris EC, Erxleben A, Lippert B (1994) *J Am Chem Soc* 116:616; p) Schreiber A, Hillgeris EC, Lippert B (1993) *Z Naturforsch B* 48:1603; q) Rauter H, Hillgeris EC, Lippert B (1992) *Chem Commun* 1385; r) Lippert B (1981) *Inorg Chem* 20:4326
25. a) Yu S-Y, Huang H, Liu H-B, Chen Z-N, Zhang R, Fujita M (2003) *Angew Chem* 115:710; b) Yu S-Y, Huang H, Liu H-B, Chen Z-N, Zhang R, Fujita M (2003) *Angew Chem Int Ed* 42:686; c) Aoyagi M, Biradha K, Fujita M (1999) *Bull Chem Soc Jpn* 72:2603; d) Fujita M, Yazaki J, Ogura K (1991) *Tetrahedron Lett* 32:5589; e) Fujita M, Yazaki J, Ogura K (1991) *Chem Lett* 1031
26. a) Bera JK, Basca J, Smucker BW, Dunbar KR (2004) *Eur J Inorg Chem* 368; b) Bera JK, Smucker BW, Walton RA, Dunbar KR (2001) *Chem Commun* 2562
27. a) Park K-M, Kim S-Y, Heo J, Whang D, Sakamoto S, Yamaguchi K, Kim K (2002) *J Am Chem Soc* 124:2140; b) Whang D, Park K-M, Heo J, Ashton P, Kim K (1998) *J Am Chem Soc* 120:4899

28. a) Qin Z, Jennings MC, Puddephatt RJ (2003) *Inorg Chem* 42:1956; b) Qin Z, Jennings MC, Puddephatt RJ (2001) *Chem Commun* 2676
29. a) Fan J, Whiteford JA, Olenyuk B, Levin MD, Stang PJ, Fleischer EB (1999) *J Am Chem Soc* 121:2741; b) Müller C, JA Whiteford, Stang PJ (1998) *J Am Chem Soc* 120:9827; c) Whiteford JA, Lu CV, Stang PJ (1997) *J Am Chem Soc* 119:2524; d) Manna J, Kuehl CJ, Whiteford JA, Stang PJ, Muddiman DC, Hofstadler SA, Smith RD (1997) *J Am Chem Soc* 119:11611; e) Stang PJ, Fan J, Olenyuk B (1997) *Chem Commun* 1453; f) Stang PJ, Cao DH, Saito S, Arif AM (1995) *J Am Chem Soc* 117:6273; g) Stang PJ, Cao DH (1994) *J Am Chem Soc* 116:4981
30. Drain CM, Lehn J-M (1994) *Chem Commun* 2313
31. a) Würthner F, Sautter A, Schmid D, Weber PJA (2001) *Chem Eur J* 7:894; b) Würthner F, Sautter A (2000) *Chem Commun* 445
32. a) Sun S-S, Anspach JA, Lees AJ (2002) *Inorg Chem* 41:1862; b) Sun S-S, Anspach JA, Lees AJ, Zavalij PY (2002) *Organometallics* 21:685
33. Kim TW, Lah MS, Hong J-I (2001) *Chem Commun* 743
34. a) Yamamoto T, Arif AM, Stang PJ (2003) *J Am Chem Soc* 125:12309; b) Chi K-W, Addicot C, Arif AM, Das N, Stang PJ (2003) *J Org Chem* 68:9798; c) Kryschenko YK, Seidel SR, Arif AM, Stang PJ (2003) *J Am Chem Soc* 125:5193; d) Schweiger M, Seidel SR, Arif AM, Stang PJ (2002) *Inorg Chem* 41:2556; e) Kuehl CJ, Huang SD, Stang PJ (2001) *J Am Chem Soc* 123:9634; f) Schweiger M, Seidel SR, Arif AM, Stang PJ (2001) *Angew Chem* 113:3575; g) Schweiger M, Seidel SR, Arif AM, Stang PJ (2001) *Angew Chem Int Ed* 40:3467; h) Schmitz M, Leininger S, Fan J, Arif AM, Stang PJ (1999) *Organometallics* 18:4817
35. Ferrer M, Rodríguez L, Rossell O (2003) *J Organomet Chem* 158
36. Sautter A, Schmid DG, Jung G, Würthner F (2001) *J Am Chem Soc* 123:5424
37. a) Lai S-W, Chan MC-W, Peng S-M, Che C-M (1999) *Angew Chem* 111:708; b) Lai S-W, Chan MC-W, Peng S-M, Che C-M (1999) *Angew Chem Int Ed* 38:669
38. Gianneschi NC, Tiekink ERT, Rendina LM (2000) *J Am Chem Soc* 122:8474
39. a) Habicher T, Nierengarten J-F, Gramlich V, Diederich F (1998) *Angew Chem* 110:2019; b) Habicher T, Nierengarten J-F, Gramlich V, Diederich F (1998) *Angew Chem Int Ed* 37:1916
40. Baer AJ, Koivisto BD, Côté AP, Taylor NJ, Hanan GS, Nierengarten H, Dorselaer AV (2002) *Inorg Chem* 41:4987
41. Chang S-Y, Jang H-Y, Jeong K-S (2003) *Chem Eur J* 9:1535
42. a) Lai S-W, Cheung K-K, Chan MC-W, Che C-M (1998) *Angew Chem* 110:193; b) Lai S-W, Cheung K-K, Chan MC-W, Che C-M (1998) *Angew Chem Int Ed* 37:182
43. Falvello LR, Tomás M (1999) *Chem Commun* 273
44. Forníés J, Gómez J, Lalinde E, Moreno MT (2004) *Chem Eur J* 10:888
45. Espinet P, Soulantica K, Charmant JPH, Orpen AG (2000) *Chem Commun* 915
46. Bruce MI, Costuas K, Halet J-F, Hall BC, Low PJ, Nicholson BK, Skelton BW, White AH (2002) *J Chem Soc, Dalton Trans* 383
47. Faust R, Diederich F, Gramlich V, Seiler P (1995) *Chem Eur J* 1:111
48. a) ALQaisi SM, Galat KJ, Chai M, Ray DG III, Rinaldi PL, Tessier CA, Youngs WJ (1998) *J Am Chem Soc* 120:12149; b) Zhang D, McConville DB, Tessier CA, Youngs WJ (1997) *Organometallics* 16:824; c) Bradshaw JD, Guo L, Tessier CA, Youngs, WJ (1996) *Organometallics* 15:2582–2584
49. a) Pak JJ, Weakley TJR, Haley MM (1997) *Organometallics* 16:4504; b) Johnson CA II, Haley MM (personal communication)
50. Campbell K, McDonald R, Ferguson MJ, Tykwinski RR (2003) *Organometallics* 22:1353
51. a) Hua J, Lin W (2004) *Org Lett* 6:861; b) Jiang H, Lin W (2003) *J Am Chem Soc* 125:8084; c) Jiang H, Hu A, Lin W (2003) *Chem Commun* 96; d) Lee SJ, Hu A, Lin W (2002) *J Am Chem Soc* 124:12948

52. Takahashi S, Onitsuka K, Takei F (2000) *Macromol Symp* 156:69
53. Mori Y, Kasai T, Takesada T, Komatsu H, Yamazaki H, Haga M-A (2001) *Chem Lett* 996
54. Fuhrmann G, Debaerdemaeker T, Bäuerle P (2003) *Chem Commun* 948
55. Krömer J, Rios-Carreras I, Fuhrmann G., Musch C, Wunderlin M, Debaerdemaeker T, Mena-Osteritz E, Bäuerle P (2000) *Angew Chem Int Ed Engl* 39:3481
56. Ammann M, Enßle M, Fuhrmann G, Kaiser A, Kilickiran P, Mena-Osteritz E, Bäuerle P (2003) *Polym Preprints* 44:379
57. Fuhrmann G, Kilickiran P, Bäuerle P (submitted) *Eur J Org Chem*
58. Ammann M, Schalley CA, Rang A, Bäuerle P (submitted) *Chem. Eur J*
59. Fave C, Bäuerle P (unpublished results)
60. Bessel CA, Aggarwal P, Marschilok AC, Takeuchi KJ (2001) *Chem Rev* 101:1031
61. a) Shima T, Bauer EB, Hampel F, Gladysz JA (2004) *J Chem Soc, Dalton Trans* 1012; b) Bauer EB, Hampel F, Gladysz JA (2003) *Organometallics* 22:5567; c) Bauer EB, Szafert S, Hampel F, Gladysz JA (2003) *Organometallics* 22:2184; d) Ruwwe J, Martín-Alvarez JM, Horn CR, Bauer EB, Szafert S, Lis T, Hampel F, Cagle PC, Gladysz JA (2001) *Chem Eur J* 7:3931; e) Bauer EB, Ruwwe J, Martín-Alvarez JM, Peters TB, Bohling JC, Hampel FA, Szafert S, Lis T, Gladysz JA (2000) *Chem Commun* 2261
62. Arena CG, Drommi D, Faraone F, Graiff C, Tiripicchio A (2001) *Eur J Inorg Chem* 247
63. Lindner E, Veigel R, Ortner K, Nachtigal C, Steimann M (2000) *Eur J Inorg Chem* 959
64. Baumgartner T, Huynh K, Schleidt S, Lough AJ, Manners I (2002) *Chem Eur J* 8:4622
65. a) Falvello LR, Forniés J, Gómez J, Lalinde E, Martín A, Martínez F, Moreno MT (2001) *J Chem Soc, Dalton Trans* 2132; b) Xu D, Murfee HJ, van der Veer WE, Hong B (2000) *J Organomet Chem* 596:53; c) Oberhauser W, Bachmann C, Stampfl T, Brüggeller P (1997) *Inorg Chim Acta* 256:223
66. Puddephatt RJ (1983) *Chem Soc Rev* 12:99
67. a) Mukherjee PS, Das N, Kryschenko YK, Arif AM, Stang PJ (2004) *J Am Chem Soc* 126:2464; b) Das N, Mukherjee PS, Arif AM, Stang PJ (2003) *J Am Chem Soc* 125:13950
68. Greenwood NN, Earnshaw A (1984) *Chemistry of the elements*. Pergamon, Oxford
69. Teo P, Koh LL, Hor TSA (2003) *Inorg Chem* 42:7290
70. a) Drain CM, Nifiatis F, Vasenko A, Batteas JD (1998) *Angew Chem* 110:2478–2481; b) Drain CM, Nifiatis F, Vasenko A, Batteas JD (1998) *Angew Chem Int Ed* 37:2344
71. a) Chuchuryukin AV, Dijkstra HP, Suijkerbuijk BMJM, Klein Gebbink RJM, van Klink GPM, Mills AM, Spek AL, van Koten G (2003) *Angew Chem* 115:238; b) Chuchuryukin AV, Dijkstra HP, Suijkerbuijk BMJM, Klein Gebbink RJM, van Klink GPM, Mills AM, Spek AL, van Koten G (2003) *Angew Chem Int Ed* 42:228
72. Burger W, Strähle J (1985) *Z Anorg Allg Chem* 529:111
73. Capó M, Ballester P (2004) *Tetrahedron Lett* 45:1055
74. a) Jacopozi P, Dalcanele E (1997) *Angew Chem* 109:665; b) Jacopozi P, Dalcanele E (1997) *Angew Chem Int Ed* 37:613
75. a) Rauterkus MJ, Krebs B (2004) *Angew Chem* 116:1321; b) Rauterkus MJ, Krebs B (2004) *Angew Chem Int Ed* 43:1300
76. a) Lindner E, Khanfar M, Steinmann M (2001) *Eur J Inorg Chem* 2411–2419; b) Lindner E, Khanfar M (2001) *J Organomet Chem* 630:244–252; c) Lindner E, Hermann C, Baum G, Fenske D (1999) *Eur J Inorg Chem* 679–685
77. Van Calcar PM, Olmstead MM, Balch AL (1996) *Chem Commun* 2597
78. a) Kumazawa K, Biradha K, Kusukawa T, Okano T, Fujita M (2003) *Angew Chem* 115:4039; b) Kumazawa K, Biradha K, Kusukawa T, Okano T, Fujita M (2003) *Angew Chem Int Ed* 42:3909; c) Yoshizawa M, Kusukawa T, Fujita M, Yamaguchi K (2000) *J Am Chem Soc* 122:6311; d) Fujita M, Fujita N, Ogura K, Yamaguchi K (1999) *Nature* 400:52; e) Ibukuro F, Kusukawa T, Fujita M (1998) *J Am Chem Soc* 120:8561

79. a) Chi K-W, Addicott C, Kryschenko YK, Stang PJ (2004) *J Org Chem* 69:964; b) Kuehl CJ, Kryschenko YK, Radhakrishnan U, Seidel SR, Huang SD, Stang PJ (2002) *Proc Natl Acad Sci* 99:4932; c) Kuehl CJ, Yamamoto T, Seidel SR, Stang PJ (2002) *Org Lett* 4:913; d) Leininger S, Fan J, Schmitz M, Stang PJ (2000) *Proc Natl Acad Sci* 97:1380; e) Olenyuk B, Whiteford JA, Fechtenkötter A, Stang PJ (1999) *Nature* 398:796; f) Stang PJ, Olenyuk B, Muddiman DC, Smith RD (1997) *Organometallics* 119:3094
80. a) Gerbelevu NV, Arion VB, Burgess J (1999) *Template synthesis of macrocyclic compounds*. Wiley-VCH, Weinheim; b) Diederich F, Stang PJ (eds) (2000) *Templated organic synthesis*. Wiley-VCH, Weinheim; c) Sauvage JP, Dietrich-Buchecker C (eds) (1999) *Molecular catenanes, rotaxanes, and knots*. Wiley-VCH, Weinheim
81. Fujita M (1999) *Acc Chem Res* 32:53
82. a) Hori A, Kataoka H, Okano T, Sakamoto S, Yamaguchi K, Fujita M (2003) *Chem Commun* 182; b) Fujita M, Ogura K (1996) *Supramol Sci* 3:37; c) Fujita M, Ibukuro F, Yamaguchi K, Ogura K (1995) *J Am Chem Soc* 115:4175
83. Ammann M (2003) Thesis, University of Ulm
84. Fujita M, Sasaki O, Mitsuhashi T, Fujita T, Yazaki J, Yamaguchi K, Ogura K (1996) *Chem Commun* 1535
85. Edelbach BL, Lachicotte RJ, Jones WD (1998) *J Am Chem Soc* 120:2843

Templated Synthesis of Interlocked Molecules

Fabio Aricó · Jovica D. Badjic · Stuart J. Cantrill · Amar H. Flood ·
Ken C.-F. Leung · Yi Liu · J. Fraser Stoddart (✉)

California NanoSystems Institute and Department of Chemistry and Biochemistry,
University of California, Los Angeles, 405 Hilgard Avenue, Los Angeles, CA 90095, USA
fabio@chem.ucla.edu, jovica@chem.ucla.edu, cantrill@chem.ucla.edu, amarf@chem.ucla.edu,
cflung@chem.ucla.edu, yliu@chem.ucla.edu, stoddart@chem.ucla.edu

1	Introduction	205
2	Kinetic Approaches to the Synthesis of Interlocked Molecules	209
2.1	Transition Metal Templates	209
2.2	π -Donor/ π -Acceptor Templatation	211
2.2.1	Charged Templates	211
2.2.2	Neutral Templates	213
2.3	Hydrogen Bond Templatation	214
2.3.1	Amide Templates	214
2.3.2	Ammonium Ion Templates	216
2.3.3	Anion Templates	218
2.3.4	Dipyridiniummethane Templates	218
2.4	Summary	218
3	Thermodynamic Approaches to the Synthesis of Interlocked Molecules	221
3.1	Introduction	221
3.2	Synthesis of Interlocked Molecules by Slippage	221
3.3	Ring-Closing Metathesis Mediated Syntheses	223
3.4	Ammonium Ion Templated Syntheses	225
3.5	Disulfide-Based Systems	233
3.6	Summary	235
4	Multivalency and Interlocked Molecules	236
5	Templating the Future of Technology	243
5.1	Molecular Switching	243
5.2	Surface Switching	246
5.3	Molecular Electronics	248
5.4	Summary	250
6	Conclusions and Perspectives	251
	References	251

Abstract Mechanically interlocked molecular compounds can be synthesized in high yields by using template-directed assistance to covalent synthesis. Catenanes and rotaxanes are two classes of mechanically interlocked molecules that have been prepared using a variety of methods such as “clipping”, “slipping”, and “threading-followed-by-stoppering”, under both kinetic and thermodynamic regimes. These different methods have utilized a range of templates such as transition metals, π -donor/ π -acceptors, and hydrogen-bonding motifs. Multivalency has emerged as another tool to aid and abet the supramolecularly assisted synthesis of mechanically interlocked molecules. Recent advances in our understanding of the nature of the mechanical bond has led to the construction of molecular machines with controllable motions that have, in one instance, been introduced into molecular electronic devices.

Keywords Catenanes · Dynamic chemistry · Molecular machines · Multivalency · Rotaxanes

Abbreviations and Symbols

B24C8	Benzo[24]crown-8
BIPY ²⁺	4,4'-Bipyridinium
BN24C8	Benzo-2,3-naphtho[24]crown-8
Bu	Butyl
24C8	[24]Crown-8
CBPQT ⁴⁺	Cyclobis(paraquat- <i>p</i> -phenylene)
CT	Charge-transfer
CV	Cyclic voltammetry
Cy	Cyclohexyl
DB24C8	Dibenzo[24]crown-8
DEAD	Diethyl azodicarboxylate
DMF	Dimethylformamide
DMSO	Dimethyl sulfoxide
DN24C8	2,3-Dinaphtho[24]crown-8
DN38C10	1,5-Dinaphtho[38]crown-10
DNP	1,5-Dioxynaphthalene
Et	Ethyl
Grubbs I	First generation Grubbs catalyst
Grubbs II	Second generation Grubbs catalyst
HMPT	Hexamethylphosphoric triamide
LB	Langmuir-Blodgett
Me	Methyl
MPTTF	Monopyrrolotetrathiafulvalene
N24C8	2,3-Naphtho[24]crown-8
NMR	Nuclear magnetic resonance
RCM	Ring-closing metathesis
RORCM	Ring-opening ring-closing metathesis
SAM	Self-assembled monolayer
<i>tert</i>	Tertiary
TFAA	Trifluoroacetic anhydride
THF	Tetrahydrofuran
Tr	Triphenylmethyl (Trityl)
TTF	Tetrathiafulvalene

1

Introduction

Interlocked molecules [1–5] consist of two or more components that are held together as a consequence of mechanical linking rather than by covalent bonds. The interest of the scientific community was initially piqued by the challenges inherent in their efficient syntheses, as well as by their relatively unconventional architectures – a fascinating aspect of their structure that marries topology [6] with chemistry. Catenanes [7–14] and rotaxanes [15–26] are the archetypal examples of such mechanically interlocked compounds. They merely represent the forerunners, however, of an ever-expanding family of more intricate assemblies [27]. Catenanes (from the Latin *catena*, meaning “chain”) are comprised of two or more mechanically interlocked macrocycles, whereas simple rotaxanes (from the Latin *rota* and *axis*, meaning “wheel” and “axle”, respectively) contain a linear dumbbell-shaped component – bearing bulky end-groups or “stoppers” – around which one or more macrocycles are trapped. No longer esoteric curiosities, catenanes and rotaxanes are now being explored [28–29] as prototypical molecular machines – an intriguing application that arises from the ability to control the relative translations of interlocked components within any given molecular assembly. Molecular devices such as logic gates, switches, and shuttles are now a reality [28–29].

A common retrosynthetic disconnection shared by generic [2]rotaxane and [2]catenane structures invokes (Fig. 1) a [2]pseudorotaxane precursor, in which a linear molecule is threaded through a macrocyclic one. Post-assembly modification of the threaded [2]pseudorotaxane superstructure can proceed in two ways: (i) macrocyclization of the linear component affords a [2]catenane (Fig. 1a), whereas (ii) end-capping of the linear component with sufficiently large groups – a process often referred to as “stoppering” (Fig. 1b) – results in the formation of a [2]rotaxane. A complementary “clipping” strategy (Fig. 1c), in which an acyclic precursor is cyclized around a linear dumbbell-shaped template, has also been developed for the synthesis of rotaxanes. An alternative approach to prepare rotaxanes, called “slippage” (Fig. 1d), proceeds by heating the preformed macrocycle and dumbbell together in order to slip the macrocycle past the bulky stoppers to produce the thermodynamically favored rotaxane.

Each of these strategies requires the precise geometrical positioning of two or more molecules prior to the formation of the final covalent bond, i.e., the one that defines the ultimate molecular entity. When left to chance, the fragments are highly unlikely to be oriented in the arrangement necessary for the creation of an interlocked molecule – the statistics are not kind! Consequently, early “statistical” approaches [7, 15] were poor yielding, relying upon tedious repetition and arduous purification protocols to generate even the smallest quantities of catenanes and rotaxanes. Covalent-directed approaches followed [1] but they fared little better since they required complex multi-step syntheses. Paradigms, however, have a habit of shifting; the chemical landscape was about

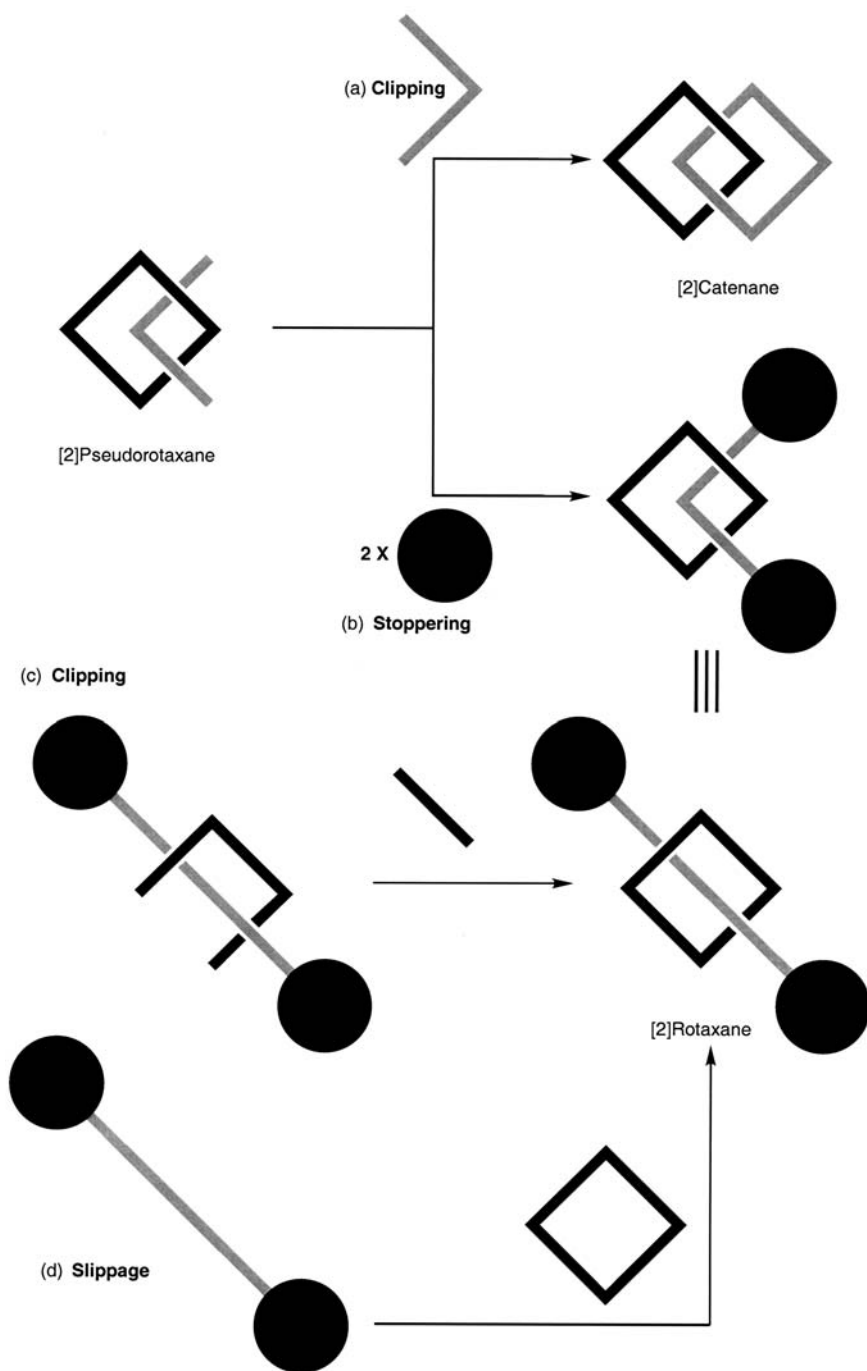


Fig. 1 Schematic representation of the synthesis of a [2]catenane by *a* clipping, and of a [2]rotaxane by *b* stoppering, *c* clipping, and *d* slippage

to change. The field of host-guest chemistry [30] gained momentum (and, in some circles, changed its name [31]) as the latter half of the twentieth century wore on, and it was only a matter of time before the principles and practices of supramolecular chemistry were applied to the formation of interlocked molecules. The template-directed strategies that we continue to develop and hone up to this day were born [8, 32–41]. Whether hydrogen-bonding [42–48] or metal-ligand interactions, [49–53] π - π stacking [54–60] or hydrophobic binding, [61–65] molecular recognition and the intermolecular forces – that we are now beginning to comprehend and exploit – are the foundations upon which the field of mechanically interlocked molecules are built.

To date, the final bond-forming reaction employed in the majority of mechanically interlocked molecule syntheses have been performed under kinetic control. Such protocols can result in the irreversible formation of undesired (non-interlocked) side-products, potentially reducing the efficiency of the interlocking processes. By contrast, however, a reversible thermodynamically controlled approach allows for a “proof-reading” step in which “incorrect” structures are consumed and their component parts recycled back into an equilibrating mixture [66–71]. For example, in a stoppering reaction performed (Fig. 2a) under reversible conditions, the formation of a dumbbell-shaped component does not represent a dead end, as it would if this reaction was performed under kinetic control (*vide supra*). In this case, such an undesired structure can simply re-equilibrate and its components can go on to form the desired dynamic [2]rotaxane product. Furthermore, thermodynamic approaches for the syntheses of mechanically interlocked compounds are not limited to stoppering reactions. The thermodynamically controlled clipping (Fig. 2b) of a macrocyclic component around a preformed dumbbell-shaped molecule can also be envisaged. In fact, there are many ways by which dynamic [2]catenanes and [2]rotaxanes can be assembled, depending upon whether just one or both of the components possess, within their framework, bonds that can be made and broken reversibly. Additionally, the possibility exists for mechanically interlocked molecules to be assembled (Fig. 2c) directly from their constituent components. For example, by mixing two preformed macrocycles with one another – at least one of which contains a reversibly formed bond – it is possible, under the appropriate conditions, to reproduce the conjurer’s “magic rings” trick, wherein two apparently “closed” rings can be linked together, one through the other, to form a [2]catenane.

This article surveys, in an appropriate historical context, the state-of-the-art when it comes to the formation of mechanically interlocked molecules – under both kinetic and thermodynamic regimes – and concludes with a vision of what the future may hold, especially if we choose the right templates!

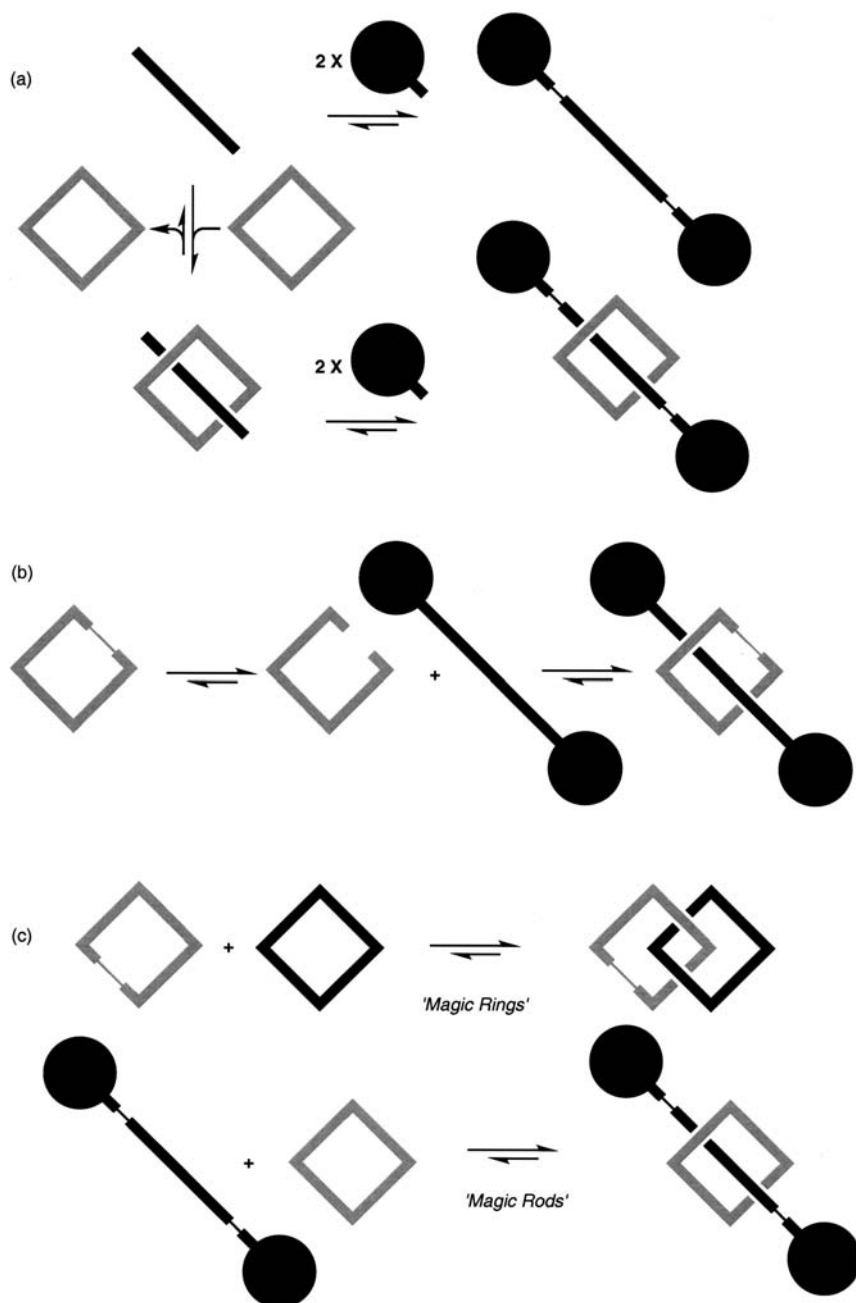


Fig. 2 Schematic representations depicting the thermodynamically controlled synthesis of a [2]rotaxane using *a* the stoppering methodology and *b* the clipping methodology. *c* Represents the magic interlocked molecules. The *thinner lines* represent the reversibly formed covalent bonds

2

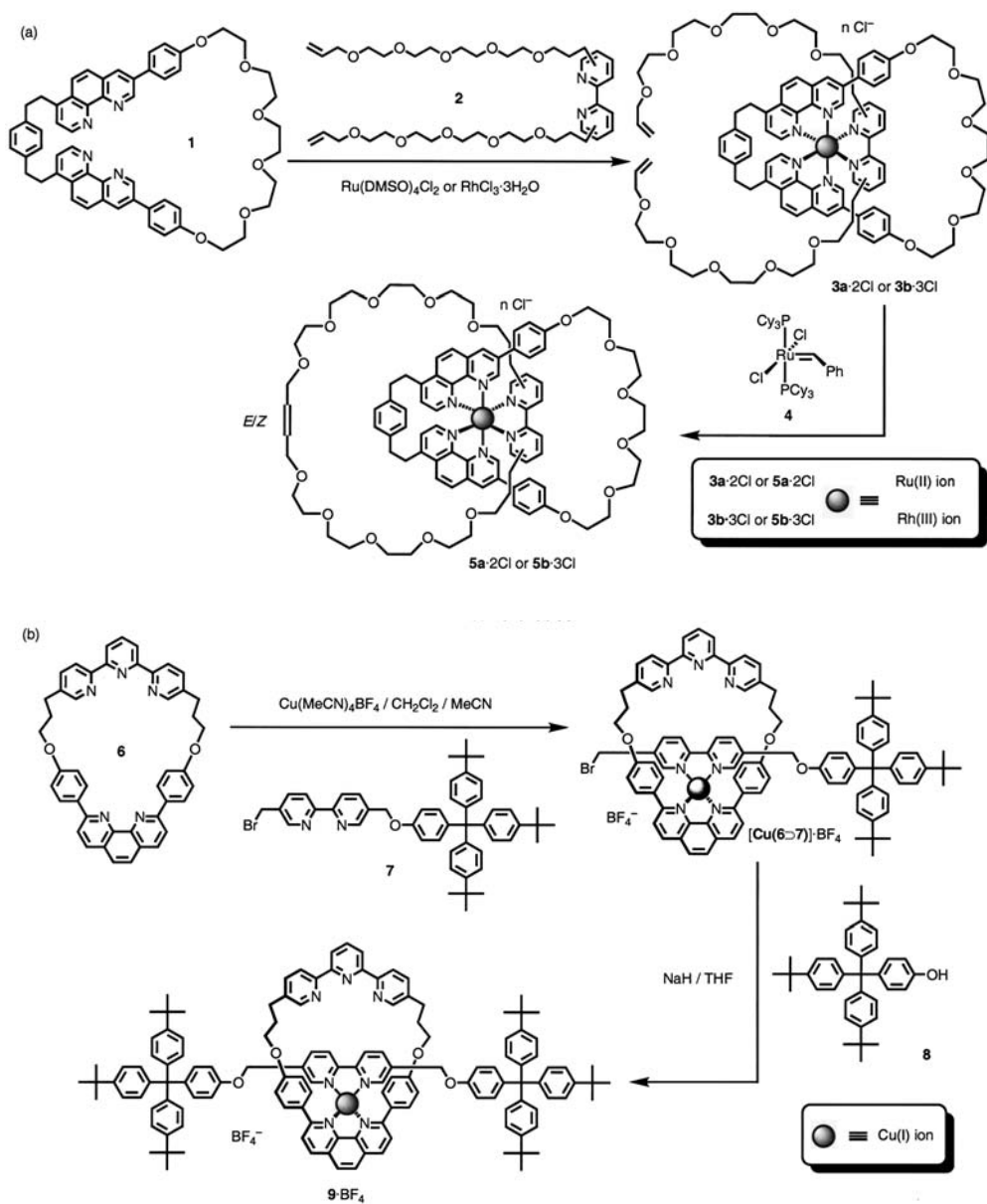
Kinetic Approaches to the Synthesis of Interlocked Molecules

2.1

Transition Metal Templates

Kinetic templates, such as transition metals, have been used for over two decades in the synthesis of catenanes and rotaxanes on account of their ability to gather and coordinate organic ligands in a geometrically precise fashion. In 1983, Sauvage [8] reported the first metal-templated protocols for the synthesis of catenanes and outlined a general procedure for using various transition metals as synthetic templates. Since then, the synthesis of a string of exotic catenanes and rotaxanes [72–73] has been demonstrated. Recently, Sauvage has reported [74–75] the synthesis of metal-templated [2]catenanes, for which an alkene terminated 2,2'-bipyridine derivative **2** (Scheme 1a) is chelated with a pre-formed bisphenanthroline macrocycle **1** in the presence of a Ru(II) or a Rh(III) metal center to afford stable, octahedral coordination complexes, which correspond to the pseudorotaxanes **3a**·2Cl or **3b**·3Cl, respectively. These pseudorotaxanes can be transformed into the corresponding olefin-linked [2]catenates **5a**·2Cl or **5b**·3Cl, respectively, by using a ring-closing metathesis (RCM) methodology on the two terminal alkenes with the catalyst **4** (Grubbs I) in 68% or 34% yield, respectively. Conversely, a Cu(I)-templated [2]rotaxane **9**·BF₄ [76] can be prepared (Scheme 1b) by means of a threading-followed-by-stoppering approach. In this case, a 2,2'-bipyridine derivative **7** is treated with a phenanthroline-terpyridine-containing macrocycle **6** in the presence of Cu(I) ions, resulting in the formation of a tetrahedral coordination complex – namely a semirotaxane [Cu(6⇌7)]·BF₄. Subsequently, alkylation of the complex [Cu(6⇌7)]·BF₄ with the stoppering reagent **8** gives the desired Cu(I)-templated rotaxane **9**·BF₄ in a yield of 20% for the final two steps. The X-ray crystal structure of the rotaxane **9**·BF₄ confirmed that the Cu(I) complex adopts a tetrahedral structure with the coordination of the two different bidentate ligands, 2,2'-bipyridine and phenanthroline with the Cu(I) metal center. It was demonstrated [76] that the Cu(I)-templated [2]rotaxane **9**·BF₄ undergoes controllable rotary motion (pirouetting) of the macrocycle around the dumbbell's axis following the oxidation and reduction of the Cu metal center. Specifically, the Cu(I) ion favors a four-coordinate ligand set in a tetrahedral geometry, a requirement satisfied by the 2,2'-bipyridine and phenanthroline ligands, whereas Cu(II) ion favors a five-coordinate geometry with 2,2'-bipyridine and terpyridine ligands.

These recent examples demonstrate the ability of metal-ion templates to facilitate the construction of interlocked molecules – and represent only the tip of the iceberg. Over the past two decades, Sauvage and others have employed a wide range of metal-ligand interactions to facilitate the efficient synthesis of both catenanes and rotaxanes, in addition to other complex intertwined molecular architectures, e.g., molecular knots.



Scheme 1 Syntheses of the metal-templated [2]catenanes 5a-2Cl/5b-3Cl and the [2]rotaxane 9·BF₄ by a ring-closing metathesis and an alkylation, respectively

2.2

π -Donor/ π -Acceptor Templatation

2.2.1

Charged Templates

The first synthesis of a [2]catenane utilizing the templating effects of charged π -donor/ π -acceptor noncovalent bonding interactions was reported [77] in 1989. Since then, charged π -donor/ π -acceptor templates have continued to play an important role in the syntheses of catenanes and rotaxanes on account of their high self-assembling efficiency [78]. Thus far, the preparation of catenanes and rotaxanes [61, 79–80] has taken advantage of strong binding affinities ($K_a > 3,000 \text{ M}^{-1}$ in MeCN at 298 K) between (Fig. 3) the charged π -electron-deficient tetracationic cyclophane, cyclobis(paraquat-*p*-phenylene) (CBPQT⁴⁺) $10 \cdot 4\text{PF}_6$ and π -electron-rich compounds, such as aromatic ethers **11** and **12**. This complexation is driven by π – π stacking and charge-transfer (CT) interactions [81–82], as well as by [C–H \cdots O] hydrogen bonding [83–84]. By far the most effective π -donors for the preparation of charged catenanes and rotaxanes are those [85] based on tetrathiafulvalene (TTF) **13** and their mutual recognition by the π -electron-deficient cyclophane $10 \cdot 4\text{PF}_6$. The binding constant between TTF (**13**) and $10 \cdot 4\text{PF}_6$ to form a 1:1 inclusion complex (i.e., a [2]pseudorotaxane) was determined to be ca. $10,000 \text{ M}^{-1}$ in MeCN at 298 K. Even higher binding constants have been obtained [86] for some pyrrole-fused TTF derivatives. The pioneering work in the development of charged π -donor/ π -acceptor recognition motifs led to the preparation of a myriad of novel catenanes [87–92], including the [5]catenane “Olympiadane” [87] and other functional rotaxanes [26, 93–96].

In 1998, the Stoddart group [90] reported that the bistable [2]catenanes **17a**· 4PF_6 and **17b**· 4PF_6 can be prepared (Scheme 2a) by template-directed synthesis that utilizes the appropriate preformed macrocyclic polyether **14a/b**. The reaction of the horseshoe-like dicationic salt **15**· 2PF_6 , under high dilution with the dibromide **16** in the presence of the macrocyclic template **14a/b**, affords either the 1,4-dioxybenzene-containing [2]catenane **17a**· 4PF_6 or the

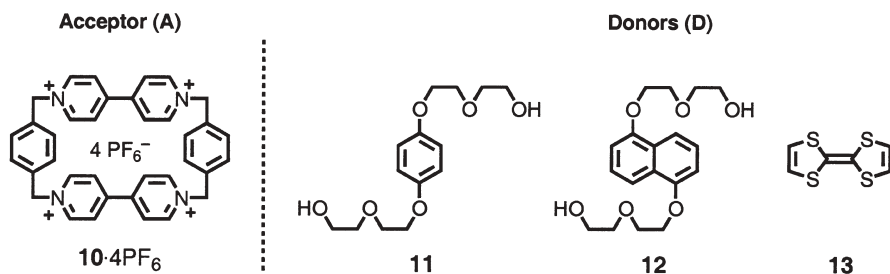
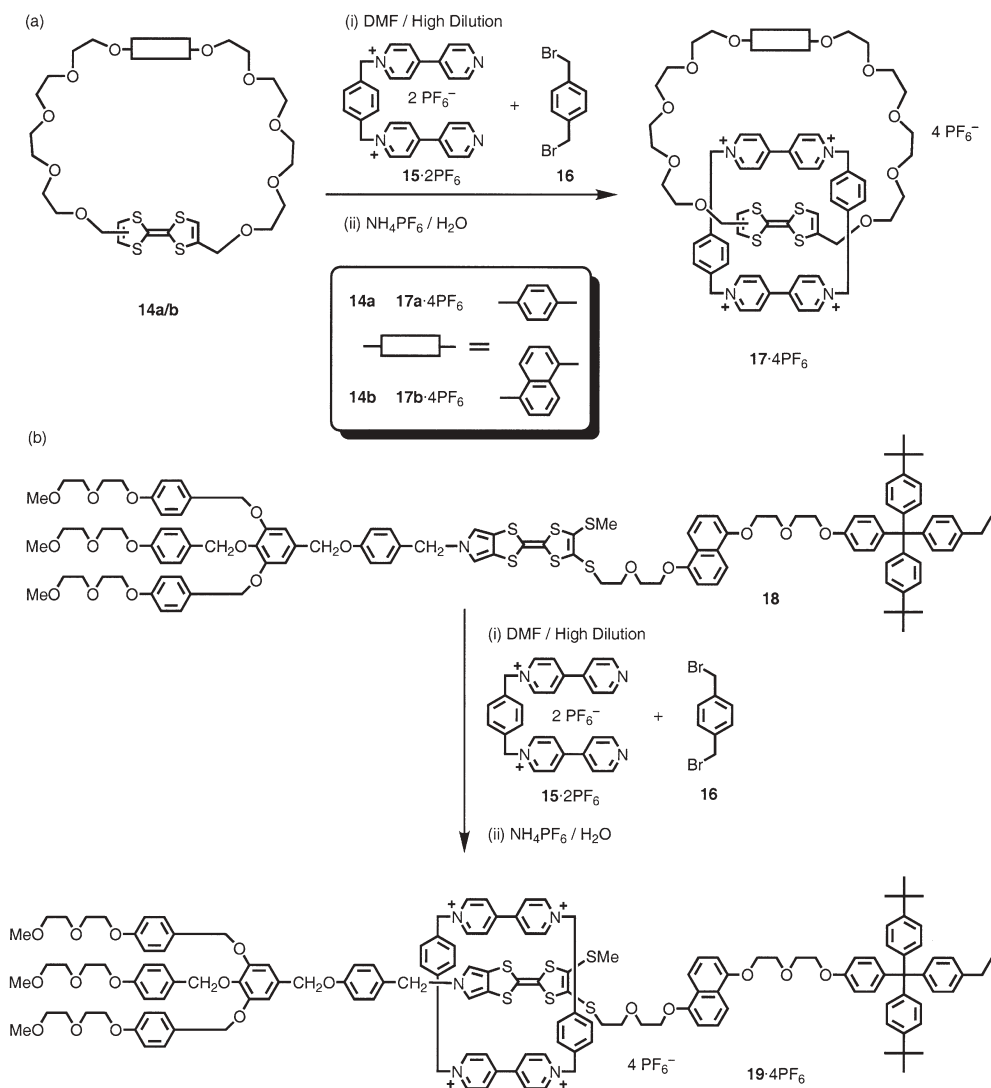


Fig. 3 Some examples of a π -electron acceptor (A) and some donors (D)

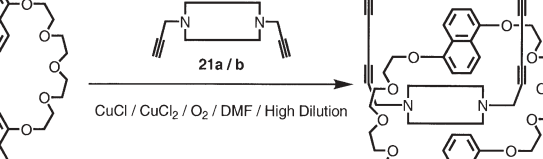


Scheme 2 Template-directed syntheses of the charged π -donor/ π -acceptor [2]catenanes $17\text{a}\cdot 4\text{PF}_6$ / $17\text{b}\cdot 4\text{PF}_6$ and the [2]rotaxane $19\cdot 4\text{PF}_6$ by clipping reactions around TTF units

1,5-dioxynaphthalene (DNP)-containing [2]catenane $17\text{b}\cdot 4\text{PF}_6$. The [2]catenanes were obtained in yields of 23 and 43%, respectively, following counterion exchange with ammonium hexafluorophosphate. The X-ray crystal structure of the [2]catenane $17\text{b}\cdot 4\text{PF}_6$ revealed that the tetracationic CBPQT⁴⁺ cyclophane encircles the TTF unit, leaving the DNP ring system to interact with the outer face of one of the bipyridinium rings of the cyclophane. Interestingly, the [2]catenanes $17\text{a}\cdot 4\text{PF}_6$ and $17\text{b}\cdot 4\text{PF}_6$ exhibit controllable, reversible circumro-

2.2.2 Neutral Templates

(a)



20

21a / b

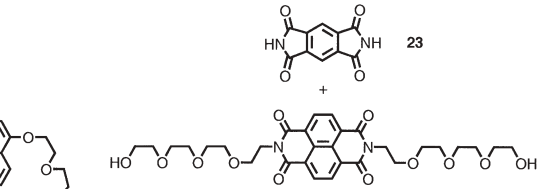
$\text{CuCl} / \text{CuCl}_2 / \text{O}_2 / \text{DMF} / \text{High Dilution}$

22a / b

21a or 22a

21b or 22b

(b)



20

23

24

$\text{PPh}_3 / \text{DEAD} / \text{THF} / \text{High Dilution}$

25

DEAD \equiv $\text{EtO}_2\text{C}-\text{N}=\text{N}-\text{CO}_2\text{Et}$

Scheme 3 Template-directed syntheses of neutral π -donor/ π -acceptor [2]catenanes **22a/22b** and **25**

DNP-based macrocycle **20** (DN38C10) is treated separately with the bisacetylene **21a** or **21b** utilizing the Glaser–Hay oxidative homo-coupling reaction, the [2]catenane **22a** is produced as an orange-red solid in 38% yield and the [2]catenane **22b** as a purple solid in 52% yield, respectively [99–100]. From the X-ray crystal structural analysis of the [2]catenane **22a**, both the 3.5 Å π – π interaction and the weak, intramolecular [N–C–H \cdots O] hydrogen bonds are observed and are believed to be essential for maintaining the self-assembled structures. Moreover, an acetylene-free [2]catenane **25** (Scheme 3b) can be constructed from the same starting macrocycle **20** with pyromellitimide **23** and diol **24** under Mitsunobu dehydrating reaction conditions to give the product **25** as a deep-red solid in 17% yield [101]. In the synthetic studies of other similar neutral [2]catenanes, the authors [97] conclude that the acidic methylene protons adjacent to the diimide unit facilitate the formation of the [2]catenanes from the macrocycle **20** by additional [N–C–H \cdots O] hydrogen bonding.

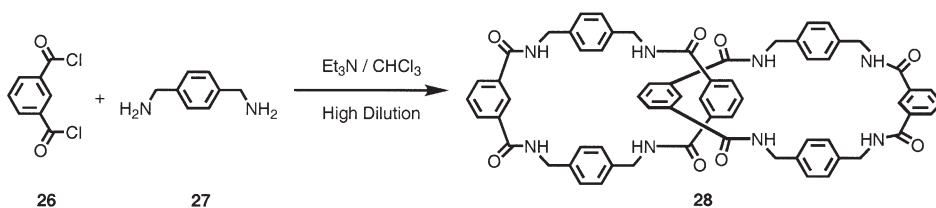
2.3

Hydrogen Bond Templatation

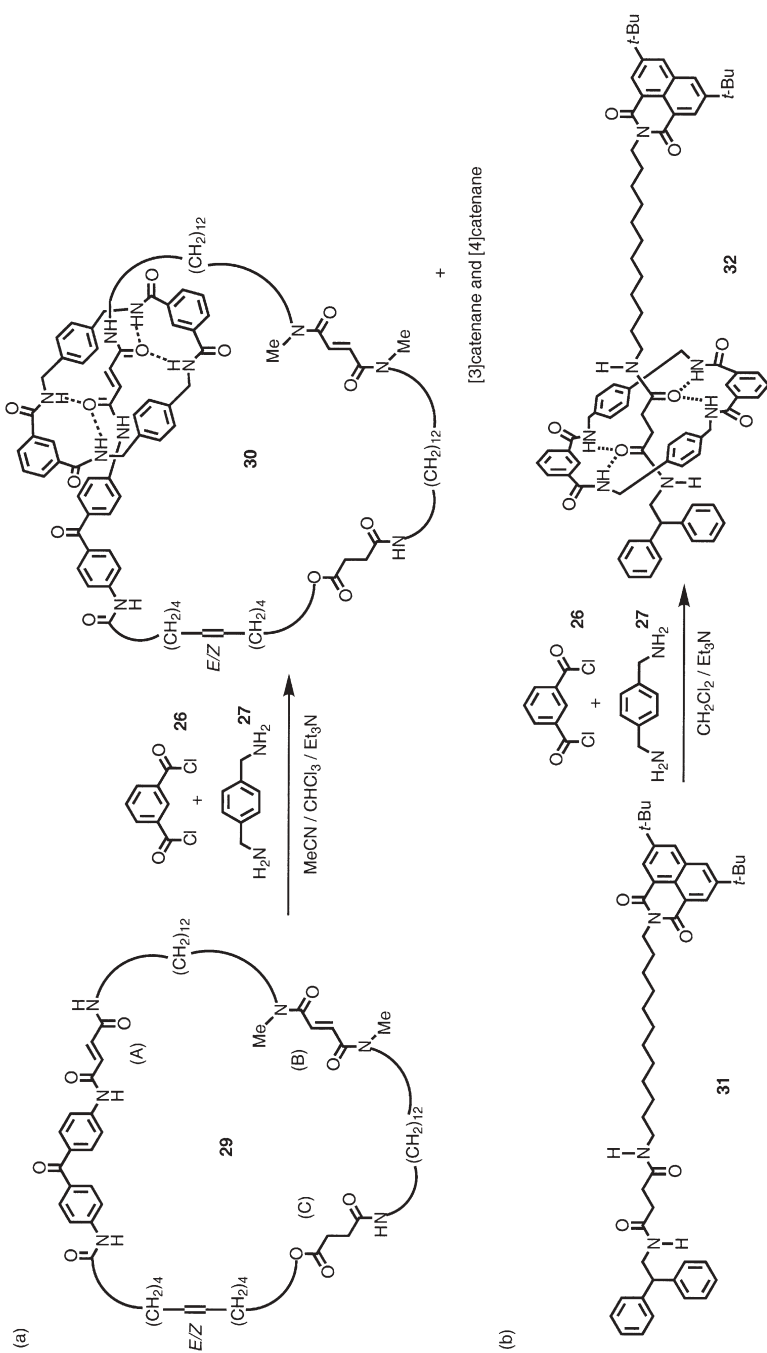
2.3.1

Amide Templates

In 1992, Hunter [102] and Vögtle [103] reported separately that amide-based [2]catenanes can be prepared in reasonable yields by amide-forming reactions such that the intermediates are held in place by strong [C=O \cdots H–N] hydrogen-bonds [104]. Subsequently, in 1995, Leigh [9] published a convenient one-step preparation (Scheme 4) of an amide-based [2]catenane **28**. The synthesis involves simply mixing isophthaloyl chloride **26** and *p*-xylylenediamine **27** in the presence of triethylamine to furnish the [2]catenane **28** in a 20% yield by a double [2+2] macrocyclization. The catenane formation is facilitated by two types of interactions – the [C=O \cdots H–N] hydrogen-bonds as well as π – π interactions between phenylene rings – in a minimally spaced system. Based on this landmark research, Leigh [105] has recently reported the synthesis (Scheme 5a) of a “three-station” amide-based [2]catenane **30**, which serves as the basis for a unidirectional photochemically driven molecular motor. To



Scheme 4 One-pot hydrogen bonding-assisted synthesis of the amide-based [2]catenane **28** from the acyclic starting materials **26** and **27**



Scheme 5 Template-directed syntheses of the amide-based [2]catenane **30** and the [2]rotaxane **32** from the acyclic starting materials **26** and **27**

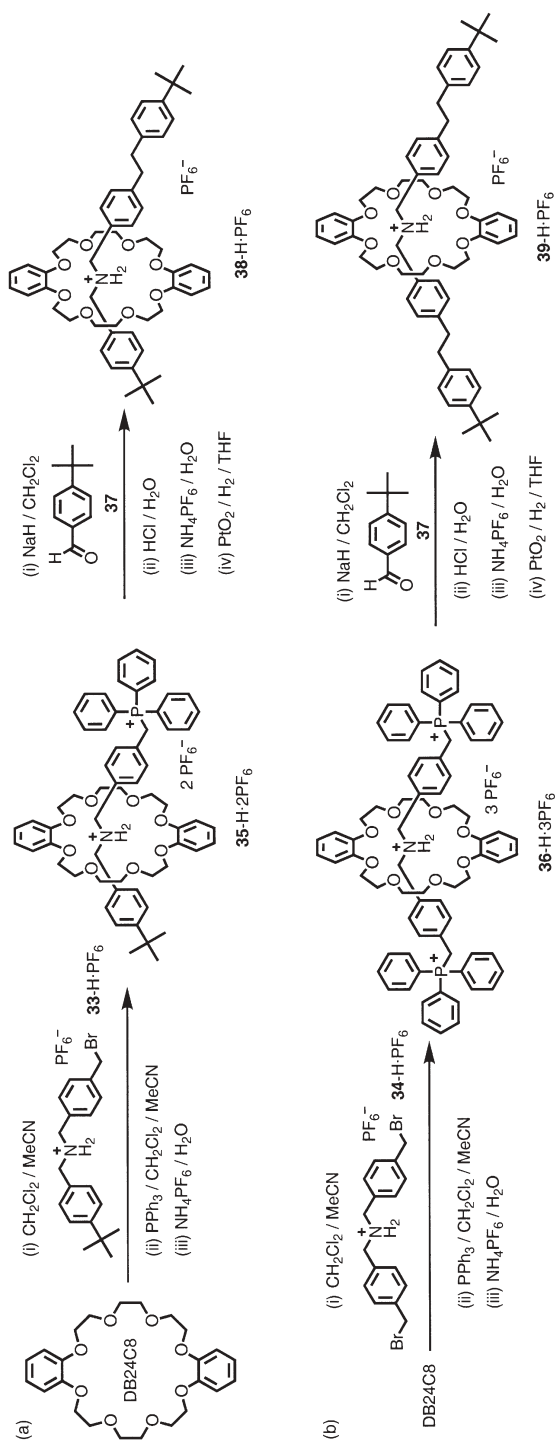
begin with, a large amide-based macrocycle **29**, which consists of (a) a secondary amide fumaramide group, (b) a tertiary amide fumaramide group, and (c) a succinic amide ester group, is treated with isophthaloyl chloride **26** and *p*-xylylenediamine **27** to yield, following a [2+2] macrocyclization, the [2]catenane **30** as the major product in 50% yield. ¹H-NMR spectroscopy confirmed that the newly formed macrocyclic lactam was situated at the secondary amide fumarmide moiety by forming a close-to-ideal hydrogen-bonding geometry. And, as expected, [3]- and [4]catenanes were obtained as bonuses from the one-pot reaction as minor products.

Employing a similar hydrogen bonding-induced macrocyclization strategy, various amide-based [2]rotaxanes can be constructed [106–112]. One example [110] is that of a [2]rotaxane **32** (Scheme 5b) that can be synthesized in a 59% yield from a succinamide and naphthalimide-containing compound **31** with a standard one-pot formation of the macrocyclic lactam from compounds **26** and **27**. Upon electrochemical stimulation, the [2]rotaxane **32** displays bistable switching behavior in which the macrocyclic lactam ring moves from the succinamide station to the naphthalimide station. Furthermore, by using similar synthetic strategies described above, other amide-based [2]catenanes [113–116] and amide-based [2]rotaxanes [117] have also been reported.

2.3.2

Ammonium Ion Templates

It is well known [16, 118–119] that crown ethers, such as [18]crown-6 and [24]crown-8 are ideal hosts for binding both with primary alkyl- and secondary dialkyl-ammonium ions as a result of strong [N⁺–H...O] hydrogen-bonding interactions. The Stoddart group [17, 120–121] has recently reported that ammonium-containing [2]rotaxanes **35**·H·2PF₆, **36**·H·3PF₆, **38**·H·PF₆ and **39**·H·PF₆ (Scheme 6) can be synthesized by templation between dibenzo[24]crown-8 (DB24C8) and dialkylammonium salts **33**·H·PF₆ or **34**·H·PF₆. The synthesis [122–123] involves a threading-followed-by-stoppering approach. In all these cases, one-end-capped dialkylammonium salt **33**·H·PF₆ (Scheme 6a) or the non-end-capped ammonium salt **34**·H·PF₆ (Scheme 6b) is threaded into DB24C8, followed by stoppering with triphenylphosphine to afford [2]rotaxanes **35**·H·2PF₆ in 80% or **36**·H·3PF₆ in 55% yield, respectively. Subsequently, the triphenylphosphonium stoppers can be modified to become aryl stoppers by Wittig reactions with, for example, the aldehyde **37**. Such reactions, followed by catalytic hydrogenation, yield new [2]rotaxanes **38**·H·PF₆ or **39**·H·PF₆, respectively, both in about 50% yield. During the post-modification reactions, there is no evidence for the escaping of the crown ether from the dumbbell component. The X-ray crystal structures of the [2]rotaxane **38**·H·PF₆ and **39**·H·PF₆ reveal that both the ammonium protons and the α-methylene protons adjacent to the nitrogen atom contribute to the hydrogen bonding with the DB24C8 component.



Scheme 6 Template-directed synthesis of the dialkylammonium ion-based [2]rotaxanes 35-H-2PF₆, 36-H-3PF₆, 38-H-PF₆ and 39-H-PF₆ under kinetic control

2.3.3

Anion Templates

In the presence of appropriate macrocycles, the use of phenoxy anion templates directs the synthesis of [2]rotaxanes [124–129] in high yielding reactions. In 1999, Vögtle [124] reported that a macrocyclic lactam **40** (Scheme 7a) is a good acceptor for a *p*-tritylphenoxy anion as a result of forming [N–H \cdots O $^-$] hydrogen bonds. In this case, an intermediate complex [40 \supset 41] $^-$ is subsequently reacted with a trityl end-stoppered alkylbromide **42**, affording an amide-containing [2]rotaxane **43** in 95% yield. By using a similar synthetic protocol, Schalley [128] reported the synthesis (Scheme 7b) of the amide-containing [2]rotaxane **46**. Initially, the diamine **44** is treated with a mild base, prompting it to thread onto the same starting macrocycle **40** to give a [2]pseudorotaxane [40 \supset 44] $^-$. The threading is followed by end-capping reactions with triphenylacetic acid chloride **45** at both ends, generating the resulting [2]rotaxane **46**. Use of esterification to add two stoppers in a one-pot reaction leads to a significantly lower yield 20–30%, compared with that for the mono-alkylation (95%) of a single stopper in the former example.

2.3.4

Dipyridiniummethane Templates

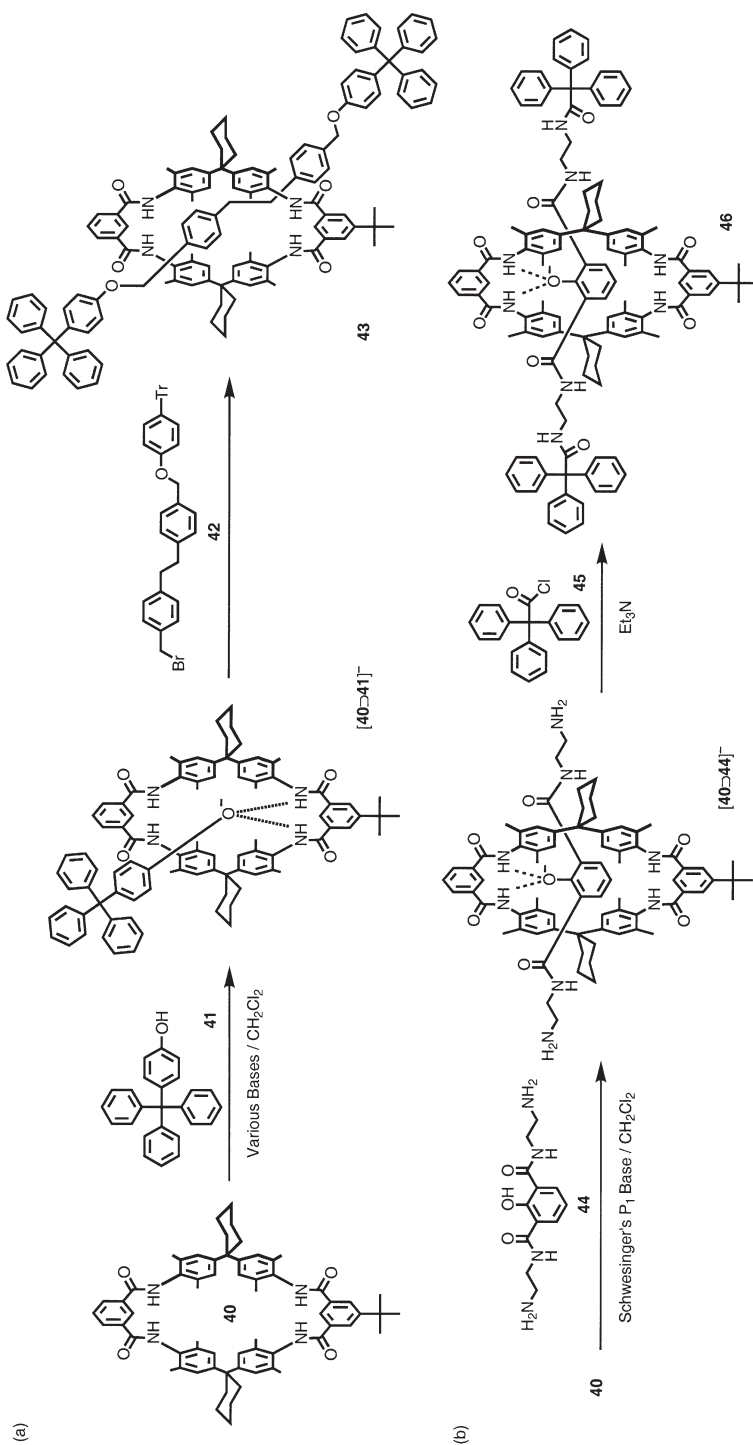
In 1998, Loeb and Wisner [19, 130] reported that 1,2-bis(pyridinium)ethane and DB24C8 self-assemble to form [2]pseudorotaxanes ($K_a=1,200\text{ M}^{-1}$ in MeCN at 298 K). The complex is held together by two modes of attractive interactions, namely [N $^+$ CH $_2\cdots$ O] hydrogen-bonding and [N $^+\cdots$ O] ion-dipole interactions. This finding led these researchers to prepare new rotaxane [131–132] and catenane [133] derivatives. For example, the [3]rotaxanes **50**·5BF $_4$ and **51**·6CF $_3$ SO $_3$ (Scheme 8a) were made by the monoalkylation of the pyridinium salt **47**·4BF $_4$ or dialkylation of the pyridinium salt **48**·4CF $_3$ SO $_3$ [131] with 4-*tert*-butylbenzyl bromide **49**, respectively, in the presence of an excess of DB24C8, to afford the [3]rotaxanes, both in about 18% yield. In each series, however, the [2]rotaxanes can also be prepared by using a limiting amount of the crown ether [132].

Alternatively, Loeb [133] has demonstrated (Scheme 8b) that, when various crown ethers, such as 24C8, B24C8, N24C8, BN24C8, DN24C8, and DB24C8, are treated separately with the pyridinium salt **52**·2Br and the dibromide **53**, then a large number of [3]catenanes **54**·8CF $_3$ SO $_3$ can be produced. According to the nature of the crown ether, the percentage yields vary from 17% to 66%, with DB24C8 giving the best result.

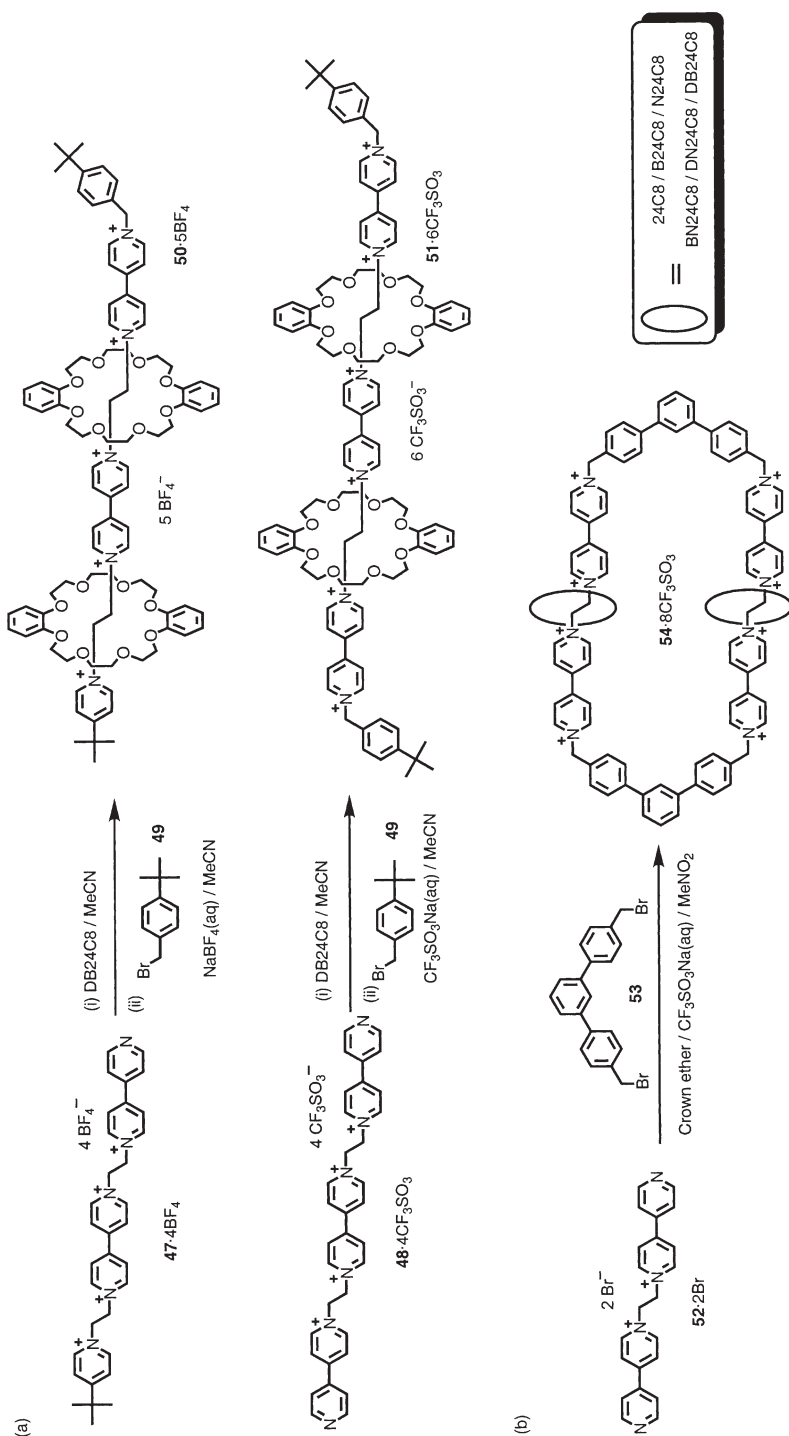
2.4

Summary

Mechanically interlocked molecules, such as catenanes and rotaxanes, can be synthesized in high efficiencies by utilizing organic or inorganic templates un-



Scheme 7 Anion-templated synthesis of the [2]rotaxanes 43 and 46 by the threading-followed-by-stoppering approach under kinetic control



Scheme 8 Template-directed syntheses of the dipyrindinium-based [3]rotaxanes 50-5BF₄, 51-6CF₃SO₃ and the [3]catenanes 54-8CF₃SO₃

der kinetic control. The efficiency of these template-directed syntheses relies upon a supramolecular approach that utilizes a combination of cooperative noncovalent bonding interactions such as, metal–ligand interactions, π – π stacking and hydrogen bonding to form intermediates, leading to the irreversible formation of mechanically interlocked molecules by the formation of a final covalent bond under kinetic control.

3

Thermodynamic Approaches to the Synthesis of Interlocked Molecules

3.1

Introduction

During the past 30 years, the synthesis of mechanically interlocked molecular compounds such as rotaxanes and catenanes has relied, for the most part, upon kinetically controlled reactions. However, as a result of the irreversible nature of this synthetic approach, non-interlocked by-products (free dumbbell components and free macrocycles) that are formed during the final post-assembly step, invariably reduce the yield of the mechanically interlocked compounds. So, in recent years, dynamic chemistry [134] has become the focus of some interest, leading to molecular assemblies that are formed in a thermodynamically controlled manner. In contrast with the kinetic process, the reversible thermodynamic regime allows the undesired or competitive by-products to be recycled to afford the most energetically favored mechanically interlocked compound.

3.2

Synthesis of Interlocked Molecules by Slippage

The so-called slippage approach has been employed successfully, in the past three decades to self-assemble a series of linear [135–139] and branched [n]rotaxanes [140–142] under thermodynamic control. In this strategy, the macrocycle and the dumbbell, which are synthesized independently prior to self-assembly, are usually heated together in an appropriate solvent until the macrocycle slips over the dumbbell's stopper by overcoming the associated free energy of activation. The resulting pseudorotaxane is stabilized by noncovalent bonding interactions. The rotaxane comes into being when the solution is cooled down to ambient temperature, at which point the free energy barrier to its dissociation back into its components becomes insurmountable.

In 1972, Harrison [143] reported the synthesis of a rotaxane using a thermodynamically controlled slippage process. This interlocked molecular compound was obtained by heating a solution containing macrocyclic hydrocarbons with ring sizes between C_{14} and C_{42} and a dumbbell-shaped compound, namely 1,10-bis(triphenylmethoxy)decane, up to 120 °C. After cooling the solution down to room temperature, Harrison was able to isolate chromatographically

a [2]rotaxane comprised of the thread and the C_{29} -macrocycle. It transpires that at high temperatures, the C_{29} macrocycle has sufficient energy to stretch out and pass over the triarylmethane stoppers to afford, after cooling, a [2]rotaxane.

Macrocycles with a ring size of C_{30} are instead free to pass freely over the end groups of the dumbbell and hence assemblies containing these rings are simply [2]pseudorotaxanes (1:1 complexes) at room temperature and dissociate into their components when chromatographic purification is attempted. When this type of slippage experiment was repeated in the presence of a small amount of trichloroacetic acid, a number of [2]rotaxanes containing cyclics ranging from C_{25} – C_{29} could be separated chromatographically. Thus, Harrison postulated that, as a result of the acid-catalyzed reversible cleavage of the triaryl group, the species that threads through the C_{25} – C_{29} rings, is now only the monotriphenylmethyl ether (i.e., the half dumbbell) prior to reformation of the ether linkage. In 1986, Schill [144] reported a similar synthesis of interlocked molecular compounds obtained by the reversible covalent bond approach but using thioethers instead of ethers.

Recently, the Stoddart group has demonstrated [135–136] the efficiency of the slippage approach by self-assembling a number of linear and branched [2]-, [3]-, and [4]rotaxanes, incorporating π -electron-rich hydroquinone-based macrocyclic polyethers and π -electron-deficient bipyridinium-based dumbbell-shaped compounds. A kinetic investigation of the slippage process revealed [138, 145] that the free energies of activation associated with the slipping-on and slipping-off processes are correlated with the size of the cavity of the macrocyclic component, as well as with the size of the stoppers attached to the dumbbell-shaped component. The free energy of activation was observed to increase upon reducing the size of the cavity of the macrocycle and/or enlarging the bulk of the stoppers. Rotaxanes have also been synthesized [146–148] by slippage using other well-known recognition motifs. For example [146], the interaction of secondary dialkylammonium ions with commercially available dibenzo[24]crown-8. In 1997, Vögtle [148] reported the synthesis of the first amide-type rotaxane using the slippage approach. The rotaxane-like structure was achieved by briefly melting the macrocycle and dumbbell components together in order to overcome the high energy of activation for the slippage process. The reported examples demonstrate the efficiency of the thermodynamically controlled slippage approach to achieve a range of rotaxanes using a wide variety of noncovalent interactions by tuning the size between the stoppers and the macrocycle.

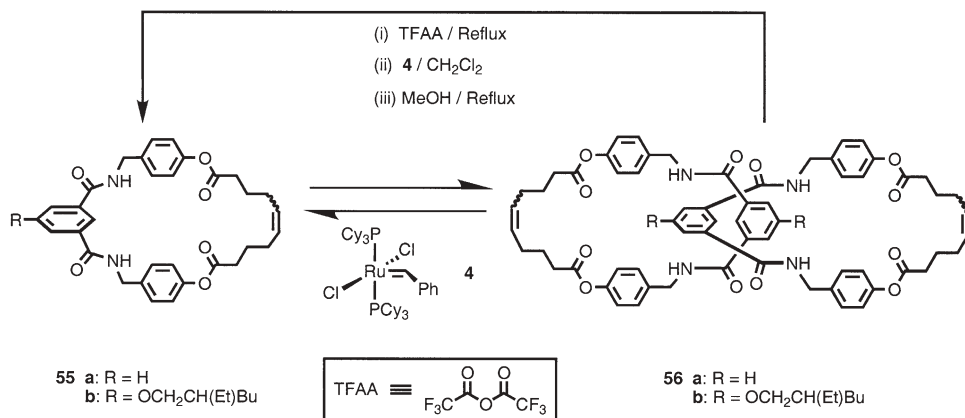
The slippage approach leads to rotaxanes that are only stable under certain conditions. In fact an increase in temperature, solvent polarity or acidity can drastically affect [146] the stability of rotaxanes obtained by slippage. Thus, in the last decade, more and more attention has become focussed on dynamic covalent chemistry. In this case, by utilizing reversible bond formation, in conjunction with supramolecular assistance, it is possible to make mechanically interlocked compounds by thermodynamically controlled stoppering or clipping reactions that can, in principle, produce rotaxanes that are stable under a broader range of conditions.

3.3

Ring-Closing Metathesis Mediated Syntheses

In 1998, the Sanders group [149] explored the use of dynamic covalent bond formation for synthesizing neutral π -associated [2]catenanes by ring-closing metathesis (RCM) [150–160]. The mechanically interlocked structure was achieved using the electronic complementarity of π -electron-deficient aromatic diimides substituted with olefin terminated alkyl chains and the π -electron-rich dinaphtho[38]crown-10 (DN38C10) in the presence of the catalyst **4**. The Cambridge group proved that, in the absence of the RCM catalyst, the main product formed is a white precipitate containing presumably only a mixture of oligomeric species. However, upon treatment of this product with the catalyst **4**, the mixture of linear and cyclic oligomers re-equilibrates to afford isomeric [2]catenanes. Some competition experiments were performed using an alternative diimide derivative to confirm the reversibility of these reactions. The slow reaction kinetics, however, prevents the system from reaching the ultimate equilibrium. Despite these difficulties, the Sanders group was able to demonstrate that a reversible thermodynamic process, such as olefin metathesis, can lead to the formation of an interlocked structure. Once again, the use of noncovalent bonding interactions to direct the synthesis of the [2]catenane led to greatly improved yields compared to the previous statistical methods.

A similar approach was employed by the Leigh group [161] in the synthesis of a [2]catenane wholly stabilized by hydrogen bonds. The combination of ring-closing olefin metathesis and hydrogen bond-mediated assembly of self-complementary macrocycles, under appropriate condition leads to the formation (Scheme 9) of [2]catenanes in >95% yield. A mixture of benzylic amide macrocycles (*E*- and *Z*-diastereoisomers) **55a** (or **55b**) was used in



Scheme 9 Reversible olefin metathesis is employed for the synthesis of [2]catenanes **56a** and **56b** under thermodynamic control. Their complete disassembly is achieved upon protection of the amide groups, followed by treatment with Grubbs I catalyst **4**, and subsequent deprotection

the metathesis experiments. Reversible ring-opening ring-closing metathesis (RORCM) reactions were carried out in a noncompeting solvent (typically CH_2Cl_2) to maximize the strength of the inter-ring hydrogen bonding interactions in the presence of the catalyst **4**.

Under these conditions, the formation of the [2]catenane is readily detected in high yields (>95%) reminiscent of the “magic” interlocking rings trick. In the RORCM experiment, the product distribution is, as expected, strongly dependent on the concentrations of the monomers. Thus, at low concentrations (0.2 mM), only the macrocycles can be detected. By increasing the reaction concentrations progressively, however, more and more of the [2]catenane is produced until, at 0.2 M, more than 95% of a mixture of the three diolefin isomers (*EE*, *EZ*, *ZZ*) is produced. The isolated mixture of these isomers can subsequently be converted into a single kinetically stable product by simply hydrogenating the double bonds catalytically.

As further proof that the metathesis reaction proceeds under thermodynamic control, the product mixture from one particular reaction was re-exposed at a different concentration to the catalyst **4**. The product distribution readjusted to that obtained if only the macrocycle (or catenane) was subjected to metathesis originally at that same concentration of the solution. Finally, to complete the magic ring-trick, the [2]catenane was disassembled into the macrocyclic components by trifluoroacetylation of the amide group in **56a** and **56b**. This protection procedure provides a mild and efficient method for switching “off” the inter-macrocyclic hydrogen bonding interactions. Although these chemically modified macrocycles are stable in the interlocked structure, when the Grubbs I catalyst **4** is added to the mixture, the dynamic nature of the [2]catenane shifts the equilibrium towards the formation of the free macrocycles **55**. Subsequently, cleavage of the trifluoroacetyl groups by refluxing in MeOH, prior to removal of the metathesis catalyst, affords the starting parent macrocyclic compound **55**.

Recently, in an extension of this work, the Leigh group [162] reported the synthesis of a rotaxane based on hydrogen bonding under thermodynamic control. In this research, a benzylic amide macrocycle, a rod containing two bulky stoppers, peptide-based template sites, and an olefinic bond are exposed to the Grubbs I catalyst **4**. In a manner similar to that observed for the magic rings, the rod is broken and the macrocycle binds to the template through four-point hydrogen bonding. Upon reformation of the carbon–carbon double bond and removal of the metathesis catalyst, the macrocycle is then trapped on the dumbbell component of the now kinetically stable [2]rotaxane. Since the dumbbell contains two templation sites, the interlocked structure obtained can be easily converted into a [3]rotaxane by another round of metathesis. The reversibility of the magic rod systems can be convincingly demonstrated either by concentration or disassembly experiments.

In summary, the Leigh group has demonstrated with the magic ring and dumbbell experiments that the combination of the olefin metathesis reaction with hydrogen bonding interactions represents a powerful method for inte-

grating thermodynamically controlled “error-checking” with a kinetically robust final product in the shape of mechanically interlocked compounds.

3.4

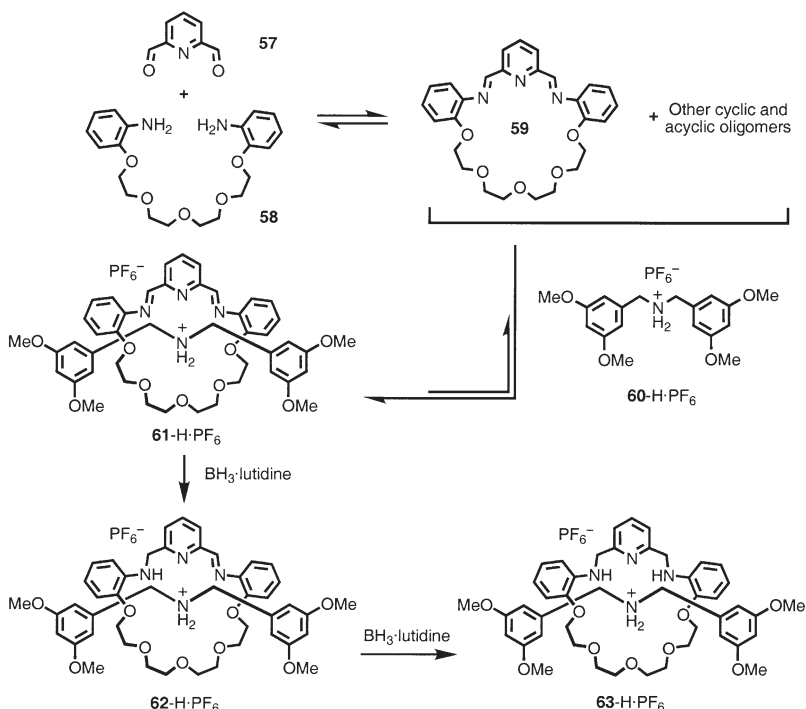
Ammonium Ion Templated Syntheses

Even although the introduction of supramolecular assistance to covalent synthesis leads to a tremendous improvement in reaction yields compared with the early statistical methods, the thermodynamic approach to the synthesis of wholly organic interlocked structures remained largely unexplored prior to the exploitation of the reversible imine bond [163]. Recently, the Stoddart group [164] reported a simple and effective dynamic procedure for the synthesis of a [2]rotaxane combining the reversible formation of the imine bond with the widely investigated secondary ammonium ion/crown recognition motif [119, 165–176]. Mixing a bis(4-formylbenzyl)ammonium salt with two equivalents of 3,5-di-*tert*-butylaniline, as a stoppering precursor, in the presence of one equivalent of DB24C8 afforded, after five days, the expected diimine [2]rotaxane as the major species (47%) present in solution. This reaction was demonstrated to proceed under thermodynamic control by the observation that the equilibrium composition was independent of the order of the addition of components. Finally, the dynamic system can be readily converted into the kinetically stable product by addition of benzeneselenol [177], leading to the isolation of the “fixed” diamine [2]rotaxane in 18% yield.

Further investigations into the reversibility of the imine bond were conducted by Rowan and Stoddart [178] in the dynamic synthesis of [2]rotaxanes based upon π -electron-rich/ π -electron-deficient recognition expressed by diaryl ethers and bipyridinium cations [66, 179–181]. This study not only explored the reversible behavior of imine bond formation but also illustrated its ability to undergo exchange reactions with competing amines to form new imines.

All the thermodynamically controlled syntheses of interlocked molecular compounds discussed so far in this Section have, as a common feature, the location of the reversible covalent linkage in the dumbbell component. This approach has led to the preparation of rotaxanes by either threading-followed-by-stoppering [152, 182–184] or slippage [135–148] protocols. However, in 2001, the Stoddart group [185] reported a simple and highly effective dynamic procedure (Scheme 10) for the formation of a [2]rotaxane by the clipping of a diamine with a dialdehyde, as the precursor components of a [24]crown-8-like macrocycle, around a dialkylammonium center that also acts as a template.

When an equimolar mixture of 2,6-diformylpyridine **57** and the diamine **58** are mixed together in acetonitrile- d_3 , the ^1H -NMR spectrum revealed broad peaks that clearly arise from a complex mixture of many different cyclic and acyclic oligomeric species. However, addition of bis(3,5-dimethoxybenzyl)ammonium hexafluorophosphate **60**·H·PF₆ to this equilibrating mixture has an immediate and dramatic effect. After only a few minutes, a new equilibrium state is established in which the main component is the [2]rotaxane **61**·H·PF₆.



Scheme 10 Reaction of the pyridine-containing macrocycle with **60-H·PF₆** leads to the equilibrium being shifted to form almost exclusively the [2]rotaxane **61-H·PF₆**. Subsequent reduction affords the kinetically stable [2]rotaxane **63-H·PF₆** in essentially quantitative yield

This result indicates that the dibenzylammonium ion templates the formation of the [24]crown-8-like macrocycle, thus generating the mechanically interlocked compound.

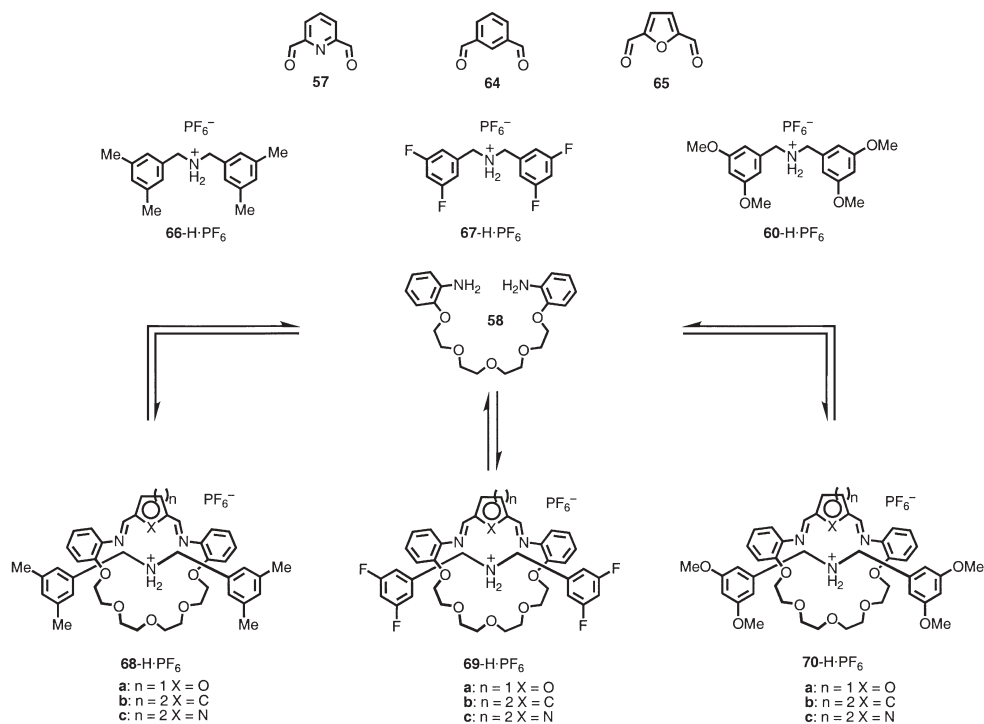
The [2]rotaxane obtained in this manner is thermodynamically stable, even although it interconverts slowly with its free components as a result of the presence of easily hydrolyzable imino groups. These groups can be subsequently reduced to the corresponding kinetically stable amino functions using the borane·2,6-lutidine complex [178].

The reaction between the equilibrium mixture set up by the dialdehyde **57**, the diamine **58**, and the dialkylammonium salt **60-H·PF₆**, in the presence of a slight excess of the $\text{BH}_3 \cdot \text{lutidine}$ complex in CD_3CN , was monitored by $^1\text{H-NMR}$ spectroscopy. The [2]rotaxane **61-H·PF₆** is consumed gradually with the initial appearance and subsequent disappearance of the monoreduced rotaxane **62-H·PF₆** being detected until, ultimately, the fully reduced rotaxane **63-H·PF₆** is produced.

Interestingly, the free dibenzylammonium ion signals also disappear while the reduction of the imine bonds takes place. This result indicates that the reduction of the imine bonds in the interlocked structures occurs at a rate faster

than those of the imine bonds in the free macrocycles or acyclic oligomers. Therefore, as more of the kinetically stable $63\text{-H}\cdot\text{PF}_6$ is formed, its removal from the equilibrium mixture is compensated by a shifting of the equilibrium between threaded and free macrocycles to form more of $61\text{-H}\cdot\text{PF}_6$. Although the imino groups of the interlocked structures are not as accessible sterically as those in free macrocycles or acyclic species, the presence of the NH_2^+ center in the rotaxanes provides a mildly acidic environment for the addition of the B-H bond to these particular imines, thereby catalyzing their reduction. The whole process, namely, thermodynamic formation of the diimine [2]rotaxane followed by kinetically controlled borane reduction, is somewhat reminiscent of enzyme catalysis [186] and also catalysis employing synthetic enzyme mimics (for an example of a synthetic receptor with enzyme-like activity, see [187]), wherein an initial recognition process results in a substrate pre-organization and hence access to a conformation that lowers the activation barrier for the final reaction.

The clipping approach based on the reversible imine bond [188] was investigated further by the preparation of a library of [2]rotaxanes (Scheme 11). This study describes the influence that the constitutions of two of the three precursor components have on the kinetic and thermodynamic stabilities of these



Scheme 11 Dynamic covalent syntheses of the imine [2]rotaxanes by clipping of the dialdehydes (57, 64 and 65) and the diamine 58 around the dialkylammonium ions ($60\text{-H}\cdot\text{PF}_6$, $66\text{-H}\cdot\text{PF}_6$, $67\text{-H}\cdot\text{PF}_6$)

dynamically interlocked compounds. In particular, the donor-acceptor nature of the terminal benzyl stoppering groups of the dumbbell-shaped dialkylammonium ions is varied from the π -electron-rich **60**-H·PF₆ [189] through the π -electron-neutral **66**-H·PF₆ to the π -electron-deficient **67**-H·PF₆. The dialdehyde is varied between 2,6-diformylpyridine **57** [190], isophthalaldehyde **64** and 2,5-diformylfuran **65** [191]. The tetraethylene glycol bis(2-aminophenyl)ether **58** is used as the diamine monomer in all the cases. On combining these dumbbell-shaped ions and the three dialdehydes with the diamine monomer, a library of nine dynamic [2]rotaxanes is obtained. The stabilities and stoichiometry of the dynamic [2]rotaxanes are established by mass spectrometry and ¹H-NMR spectroscopy. The non-existence of higher-order assemblies, such as double-stranded [3]pseudorotaxanes, in this dynamic equilibrating system confirms that the [2]rotaxanes are by far the most stable entities.

The rates of rotaxane formation vary drastically, however, depending on the components used in the assembly. In general, the 2,6-diformylpyridine **57** is associated with the fastest clipping reactions with all of the three dumbbells, and the 2,5-diformylfuran **65** results in the slowest. Clipping of isophthalaldehyde **64** occurs at an intermediate rate. This reactivity scale is consistent [183–195] with the electrophilicities of the different formyl groups. As expected, the dialdehyde **57** exhibits the most electrophilic behavior, while **65** exhibits the least. The donor-acceptor nature of the dumbbell-shaped dialkylammonium ion also affects the rates of clipping. In particular, the **67**-H·PF₆ dumbbell establishes the fastest reaction equilibria with all of the three dialdehydes. This result can be attributed to the higher acidity of the NH₂⁺ center relative to those of the other dumbbells and so increases the rate of imine bond formation. Additionally, during the clipping process, there are likely to be significant aromatic–aromatic interactions occurring between the stoppers on the dumbbell and the aryl units (π -electron-rich units in the diamine **58** and π -electron-deficient ones in **64** and **65**) of the forming macrocycle.

Some predictions on the rate of clipping can be made by considering the π -electron density alone, based on the simple model of charge distribution in π -systems proposed by Hunter and Sanders [81]. This model indicates that fast clipping reactions would occur for the most π -electron-rich dumbbell with the most π -electron-deficient dialdehyde (i.e., **60**-H·PF₆ with **57**) and the most π -electron-deficient dumbbell with the most π -electron-rich dialdehyde (i.e., **67**-H·PF₆ with **65**), as well as for pairs of π -electron-deficient dumbbells and dialdehydes (i.e., **67**-H·PF₆ with **57**). Based on the same idea, the slowest clipping reactions should occur for the interaction of the most π -electron-rich dumbbell with the most π -electron-rich dialdehyde (i.e., **60**-H·PF₆ with **65**). The Hunter–Sanders model turns out to be a good one for explaining the rates of the dynamic reactions obtained by ¹H-NMR spectroscopic studies. Another factor that influences the rate of reaction is the number of hydrogen bond acceptors in the nascent macrocycles. Thus, macrocycles containing either pyridine or furan units bind to all of the dialkylammonium-ions more strongly than the one derived from the isophthalaldehyde.

Estimations of the effective association constants (K_{eff})¹ between the macrocycles and dumbbells are available for all nine systems. The K_{eff} values support the fact that [2]rotaxanes **68a,c**-H·PF₆, **69a,c**-H·PF₆ and **70a,c**-H·PF₆ are more thermodynamically stable (i.e., they have high values of K_{eff}) on account of the incorporation of eight heteroatoms into their macrocycles. By contrast, low values of K_{eff} are estimated for the remaining three [2]rotaxanes **68b**-H·PF₆, **69b**-H·PF₆ and **70b**-H·PF₆ incorporating the isophthaloyl unit and are related to the absence of the extra heteroatom as well as to the presence of an aryl hydrogen atom, which may interact sterically in an unfavorable manner with the dumbbell.

The [2]rotaxanes **69a-c**-H·PF₆, which incorporate the most π -electron-deficient dumbbell, are the most stable thermodynamically; a feature that is probably a consequence of a combination of enhanced [N⁺-H...X] hydrogen bonding and significant aromatic π - π stacking interactions. Finally, K_{eff} values for [2]rotaxanes containing pyridine or furan units are similar for each dumbbell-shaped ion and are comparable to the strengths of binding in CD₃CN of disubstituted dibenzylammonium salts with the crown ethers DB24C8 [118, 196–198] and dipyridyl[24]crown-8 [199].

Several competition experiments were also conducted to evaluate the relative stabilities of pairs of [2]rotaxanes formed from a choice of either two dialdehydes or two dumbbell-shaped components. These experiments were carried out in CD₃CN with equimolar mixtures of four chosen components in which either (a) the four components were mixed together and then equilibrated or (b) the competing dumbbell or dialdehyde was added to a pre-equilibrated mixture of a single [2]rotaxane and the reaction was monitored until re-equilibration occurred. The times (6–30 days) required for these systems to reach equilibrium are generally longer than those found for the formation of a [2]rotaxane on combining the three single components – namely the diamine, the dialdehyde, and the dibenzylammonium salt. This observation suggests that the rates of macrocyclic ring opening of the [2]rotaxanes are relatively slow when compared to the rates of their clipping. Once again, the data showed that the [2]rotaxanes formed by using the fluorine-containing dialkylammonium ion **60**-H·PF₆ were the most stable. The differences in the stabilities of the [2]rotaxanes, incorporating either methoxy or methyl units in the dumbbell, were found to be negligible. Comparing the K_{eff} values with the data collected from the competitive experiments, it

¹ K_{eff} values between a macrocycle and a dumbbell in a rotaxanes were obtained using the equation: $K_{\text{eff}} = \frac{\text{Rotaxane}}{\text{Macrocycle}}$ Dumbbell. This equation is based on the assumption that,

in an equimolar mixture of dialdehyde, diamine, and dumbbell, all of the diamine and dialdehyde that is not incorporated into a [2]rotaxane is condensed into a free macrocycle whose concentration is equal to that of the uncomplexed dumbbell minus the concentration of the free dialdehyde. The real concentration of each free macrocycle is smaller than that, but, by making this assumption, we reduce the complexity of the system down to a bimolecular self-assembly involving one macrocycle and one dialkylammonium ion.

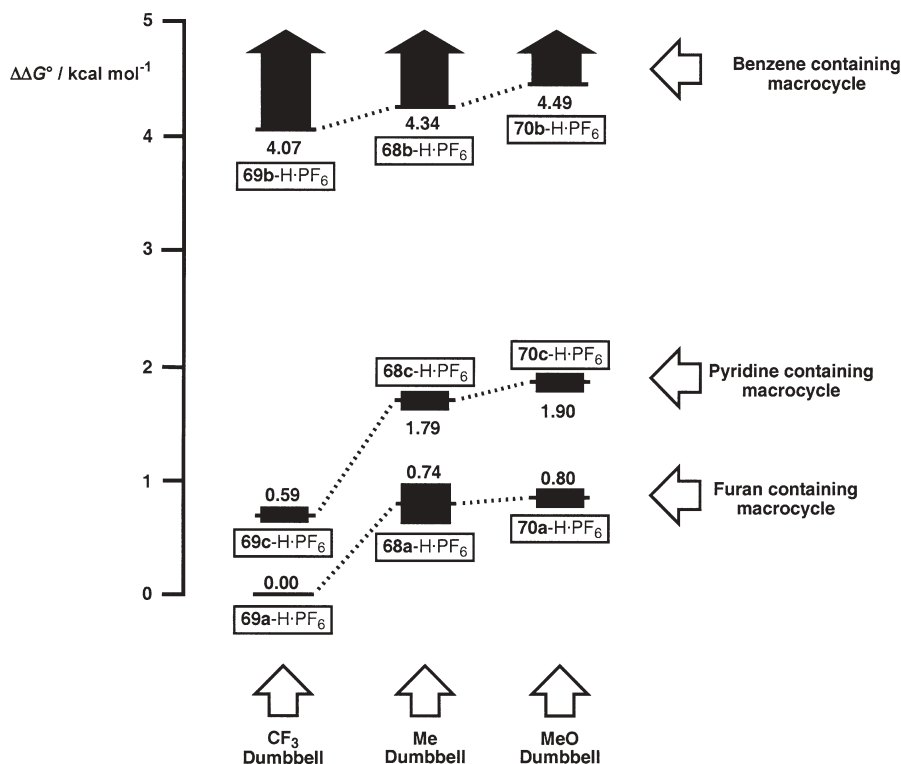


Fig. 4 Stabilities of the nine [2]rotaxanes in a competition experiment relative to the stability of [2]rotaxane **69a-H·PF₆**, which is designated as zero. The thickness of each black bar indicates the error associated with each measurement

is possible to obtain the complete sequence of relative stabilities for the nine [2]rotaxanes studied. These are portrayed graphically in Fig. 4.

The fluorine-containing [2]rotaxanes **69a-c-H·PF₆** are found to be the most stable compounds, whereas [2]rotaxanes derived from isophthalaldehyde **64** are the least stable. An unexpected result is the higher stability of furan-containing [2]rotaxanes **68a-H·PF₆**, **69a-H·PF₆** and **70a-H·PF₆** compared to the interlocked structures incorporating the pyridine ring. One might expect that a pyridine ring, being more basic than the furan one, would form the stronger hydrogen bonds. It is suggested, however, that the relative basicities of the pyridine and furan rings incorporated in the macrocycles is only one of the factors that play a part in determining the relative stabilities of the structure and that the basicities of their imino nitrogen atoms must be considered as well.²

² The solid-state structure of a reduced form of **61-H·PF₆** suggests that the aminophenyl nitrogen atoms are important for hydrogen bonding with the NH_2^+ center.

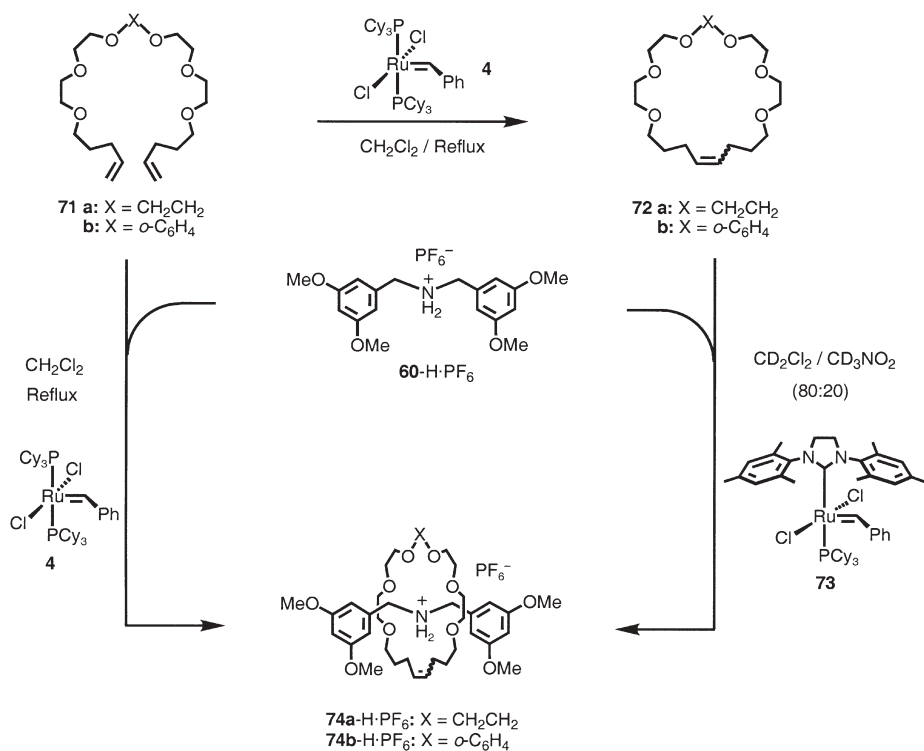
In fact, any partial positive charge that these groups receive upon hydrogen bonding to an NH_2^+ center is better stabilized by the furan ring than by a pyridine one, by virtue of the former's greater π -electron density. The pyridine ring may be expected to also withdraw a significant amount of electron density mesomerically from the phenolic ether oxygen atoms of the macrocycle. Thus, although the furan ring, when compared with the pyridine ring, is not as capable of accepting a hydrogen bond directly, the enhanced basicity of its neighboring imino and phenoxy units results in a more strongly coordinating macrocycle.³ To our knowledge, this study represents the most complete piece of work on [2]rotaxanes that are thermodynamically equilibrating with their starting products, based on a dynamic imine clipping. These systems are remarkably sensitive to small changes in the constitutions of the macrocyclic and dumbbell-shaped components, which in turn have dramatic effects on the kinetics and thermodynamics of the assemblies.

Another important investigation on some interlocked molecular compounds synthesized thermodynamically was recently reported by the Grubbs group [200]. In this work, the well established mutual recognition exhibited by secondary dialkylammonium (R_2NH_2^+) ions and suitably sized crown ethers is combined, in an elegant fashion, with the versatile reversible RCM reaction. In this manner, a terminal diolefin macrocyclic precursor **71** (Scheme 12) was designed in an effort to mimic the significant R_2NH_2^+ ion-binding capability of DB24C8.

Treatment of this linear oligomer **71** with the Grubbs I catalyst **4** [201] under dilute conditions, gave the 24-membered olefinic crown ether analog **72** as a mixture of *E* and *Z* isomers. The constitution of the macrocycle is strikingly similar in nature to the macrocyclic skeleton of 24C8. ¹H-NMR spectroscopic analyses showed that compound **72** interacts readily with a dibenzylammonium ion rod to form a 1:1 complex with a threaded geometry, i.e., a [2]pseudorotaxane. Therefore, repeating the same RCM reaction of the terminal diolefin **71** in the presence of a dumbbell-shaped template containing an ammonium ion **60**·H·PF₆ leads to the isolation of the corresponding [2]rotaxane as a mixture of *E* and *Z* isomers in 73% yield.

The significant templating effect of the NH_2^+ ion center can be appreciated by comparing this reaction with the untemplated macrocyclization of **71** to form the cyclic compound **72**. In fact, while the untemplated reaction is carried out at low concentration (5 mM) to avoid oligo/polymerization and yields only 48% of the desired macrocycle, the templated reaction can be performed at

³ Inspection of molecular models (Chem3D) suggests that the bite angle of a 2,5-diimino-furyl unit ($\text{N}\cdots\text{O}\cdots\text{N}$ angle of ca. 144°) is somewhat larger than that of a corresponding pyridyl unit ($\text{N}\cdots\text{N}\cdots\text{N}$ angle of ca. 125°). This larger bite angle suggests that any NH_2^+ unit that hydrogen bonds to the two imino nitrogen atoms of these subunits will be positioned about 0.4 Å closer to the furan oxygen atom than to the pyridine nitrogen atom. This small structural effect may result in more favourable electrostatic interactions and help to explain the stability of [2]rotaxanes incorporating the furan unit.



Scheme 12 Synthesis of the olefin macrocycles **72**, via their corresponding diolefin precursors **71**. Rotaxane synthesis can be achieved through either a ring-closing-metathesis approach, by utilizing **71** as starting material (lower left pathway), or by a magic ring synthesis in which the preformed macrocycles **72** are employed (lower right pathway)

much higher concentrations (ca. 100 mM in this case) to give 73% of the mechanically interlocked system.

The inherent reversibility of this system was investigated by performing a magic ring experiment. The second generation Grubbs II catalyst **73** was added to a mixture containing equimolar quantities of the dumbbell **60-H·PF₆** and the macrocycle **72**. ¹H-NMR spectroscopic analysis, prior to the addition of any catalyst, confirmed that the terminally bulky substituted secondary dialkylammonium ion **60-H·PF₆** cannot pass through the cavity of the 24-membered macrocyclic ring. However, upon the addition of the Grubbs II catalyst **73** [202] (10 mol%), the system re-equilibrates to a new thermodynamic minimum⁴ and results in the formation of the [2]rotaxane **74a/b**. The equilibrium was achieved after only 45 min and more than 95% of the species in solution was identified as the desired interlocked compound.

⁴ A thermodynamic minimum is a process driven by the creation of N⁺-H...O and C-H...O hydrogen bonds.

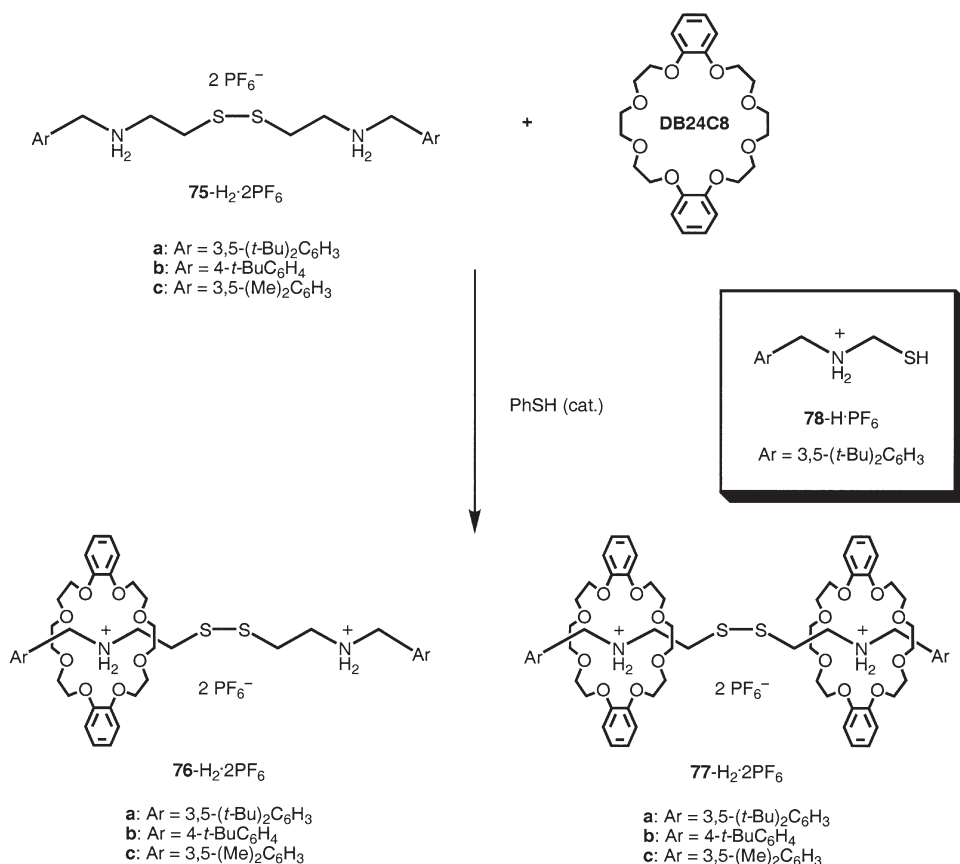
3.5

Disulfide-Based Systems

A common dynamic covalent bond, widespread in natural systems (i.e., stabilizing protein structures), is the thiol-disulfide redox system. Extensive mechanistic studies on thiols and disulfides by Whitesides [203] has shown that disulfide exchange takes place efficiently under mild conditions in the presence of a catalytic amount of a thiol and that disulfides are stable toward many different functional groups. Although disulfide linkages have been employed in the synthesis of both catenanes [204] and rotaxanes⁵ [205], this potentially reversible covalent bond was employed for the first time to construct an interlocked molecule under thermodynamic control in early 2000 by the Takata group [206–207]. A symmetrical dumbbell-shaped compound **75**-H₂·2PF₆ possessing two secondary dialkylammonium ion centers in addition to a centrally located disulfide linkage was synthesized. In the knowledge that DB24C8 can bind secondary dialkylammonium ions within its macrocyclic cavity, two equivalents of this crown ether were added (Scheme 13) to a solution of **75**-H₂·2PF₆ in CD₃CN. No crown ether was observed to thread onto the dumbbell containing two NH₂⁺ centers since the 3,5-di-*tert*-butylphenyl end groups are far too large to pass through the cavity of the DB24C8 macrocycle, even when the solution is heated to 100 °C. Upon addition of a catalytic amount of benzenethiol, however, the slow formation (equilibrium is reached after 30 days) of both a [2]- and a [3]rotaxane (8 and 58%, respectively) was observed. In the event, the small amount of catalytic thiol acts to “unlock” the disulfide bond in the dumbbell and create two threads containing NH₂⁺ centers, both of which are capable of threading through a DB24C8 macrocycle. Subsequent attack of the thiol-terminated [2]pseudorotaxane on any of the disulfides present in solution results in the formation of either a [2]- or a [3]rotaxane, **76**-H₂·2PF₆ and **77**-H₂·2PF₆, respectively.

Takata [207] also went on to show that increases in both temperature and catalyst loading resulted in the equilibrium being reached more quickly in this dynamic system. In a similar experiment, a small amount of benzenethiol was added to a solution of the dumbbell and DB24C8 (1:2 ratio, respectively) in CD₃CN. The mixture was heated at 50 °C and the progress of the reaction was monitored by ¹H-NMR spectroscopy. This time, the [2]rotaxane **76**-H₂·2PF₆ was formed faster, and its yield gradually increased to reach a maximum value (69%) after only 4 h. Eventually the signals in the ¹H-NMR spectrum relating to the [3]rotaxane start to appear and they increase rapidly with a concomitant decrease in the amount of the [2]rotaxane in the mixture. Finally, the system reached equilibrium after about 36 h (instead of 30 days) and the final yields

⁵ The kinetically controlled crystallization of a dynamic system appears to have been used to advantage in a high yielding preparation of a [3]rotaxane following a reversible oxidative coupling of the thiol groups of two [2]pseudorotaxane supermolecules by a so-called molecular riveting action.



Scheme 13 Synthesis of the [2]- and [3]rotaxane **76-H₂·2PF₆** and **77-H₂·2PF₆**, respectively, by thiol-disulfide bond interchange

of **76-H₂·2PF₆** and **77-H₂·2PF₆** were 29 and 65%, respectively. If the system is cooled down to room temperature for 80 h, the reaction mixture reaches another equilibrium state in which the yields of [2]- and [3]rotaxanes are 15 and 81%, respectively. Since the main driving force for rotaxane formation is the exothermic hydrogen-bonding interaction between the secondary dialkylammonium group and DB24C8, the equilibrium shifts to the [3]rotaxane side on lowering the reaction temperature. And, of course, raising the temperature again to 50 °C returns the equilibrium to its original state. These observations are wholly consistent with a reversible process where the yields of the rotaxanes can be changed under thermodynamic control.

Changing the solvent polarity also drastically affects the yields of the interlocked species. By using a mixture of CDCl₃/CD₃OD (1:1) instead of CD₃CN as solvent, the equilibrium shifts to give predominately the [2]rotaxane (37% at 50 °C). When nitromethane (CD₃NO₂) was used as the solvent, the highest yield

(83%) of [3]rotaxane **77**-H₂·2PF₆ was observed, while the use of dimethylformamide (DMF) as solvent resulted in a dramatic decrease in yield (total yield of interlocked compounds <10%). Both the experiments were carried out at 50 °C.

As expected, increasing the amount of the DB24C8 also shifts the equilibrium of the reaction mixture. When equimolar amounts of DB24C8 and **76**-H₂·2PF₆ were employed, the [2]rotaxane was obtained preferentially (at 50 °C). Increasing the DB24C8/dumbbell ratio dramatically shifts the equilibrium to the [3]rotaxane **77**-H₂·2PF₆ [208–209].

To evaluate the effect of the thiol catalyst, the monomer **78**-H·PF₆ and *tert*-BuSH were used as initiators. The use of **78**-H·PF₆ retarded the reaction rate and the yield of the [2]rotaxane reached a maximum 33 h after initiation, indicative of a much slower rate than that obtained with PhSH. The advantage of this slow rate, however, is that it makes it easier to isolate the [2]rotaxanes. When *tert*-BuSH was employed as an initiator, the reaction rate was much slower than that obtained with PhSH and **78**-H·PF₆. The system did not reach equilibrium, even after 300 h. This result can be attributed to the low nucleophilicity of *tert*-BuSH because of the steric hindrance of *tert*-Bu group.

In fact, the disulfide linkages can be cleaved by various nucleophiles other than thiols [210], such as 4-nitrophenol, diethylamine, and hexamethylphosphoric triamide (HMPT). Diethylamine was observed to catalyze the rotaxane synthesis, yielding 25% and 4%, of the [2]- and [3]rotaxane, respectively, at 50 °C after 67 h, but the reaction rate was as slow as that with *tert*-BuSH. HMPT also catalyzed the formation of [2]- and [3]rotaxane **76**-H₂·2PF₆ and **77**-H₂·2PF₆, (the yields were 60 and 25%, respectively, at 50 °C after 54 h). Finally, 4-nitrophenol did not react with **75**-H₂·2PF₆ at 50 °C, even after 60 h. Thus, amines and phosphines are potential catalysts for rotaxane synthesis utilizing the reversible nature of disulfide linkages.

3.6

Summary

To the best of our knowledge, four dynamic interlocked architectures have been examined to date (Fig. 5). A dynamic [2]catenane, in which each ring contains one or more reversibly formed covalent bonds (I), can be utilized for the self-assembly of homocircuit [2]catenanes, as demonstrated by Leigh [161].

However, as shown by the Sanders group [149], it is possible to assemble a dynamic [2]catenane (II) that is comprised of one static ring and one reversibly formed ring, thereby affording a heterocircuit [2]catenane. It has been shown that both structures **III** and **IV** can be utilized successfully in the self-assembly of dynamic [2]rotaxanes [164, 178, 185, 200, 208–209]. The reversibly formed component can be located in either the dumbbell (**III**) or the ring (**IV**) components, thus allowing for threading-followed-by-stoppering and clipping approaches, respectively. It should be noted that structure **V**, in which both components of the [2]rotaxane contain reversibly formed linkages, is largely

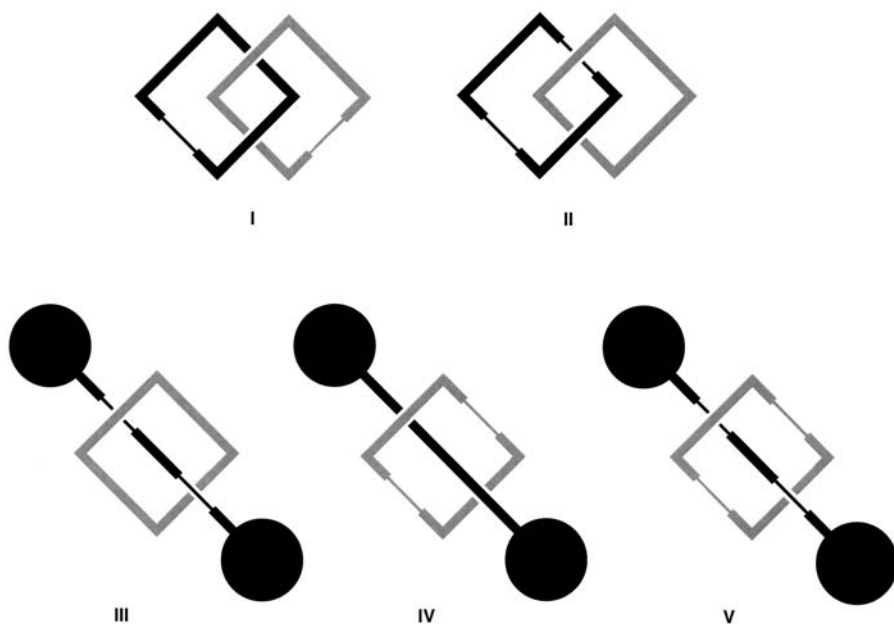


Fig. 5 Selected examples of dynamic [2]catenanes (I and II) and dynamic [2]rotaxanes (III–V). The *thin lines* represent dynamic covalent bonds

redundant as the only advantage of each component in an interlocked assembly having dynamic covalent bonds arises in cases where a homocircuit [2]catenane is desired. A [2]rotaxane comprised of a dynamic ring, as well as of a dynamic dumbbell, requires a certain orthogonality in the choice of the reversible reactions chosen for each component, i.e., the formation of the ring should not interfere with the formation of the dumbbell and vice versa.

In summary, the use of thermodynamically controlled approaches for the synthesis of wholly organic interlocked molecules is slowly growing in popularity. The use of olefin metathesis, imine formation/exchange and disulfide exchange as the reversible covalent step – in addition to the exploitation of different molecular recognition motifs – demonstrates the generality of thermodynamically controlled approaches for the synthesis of mechanically interlocked molecules.

4

Multivalency and Interlocked Molecules

The preparation of increasingly complex and functional mechanically interlocked molecules using template-directed methods will depend to a great extent on our understanding of the concept of multivalency [211–215]. The coordi-

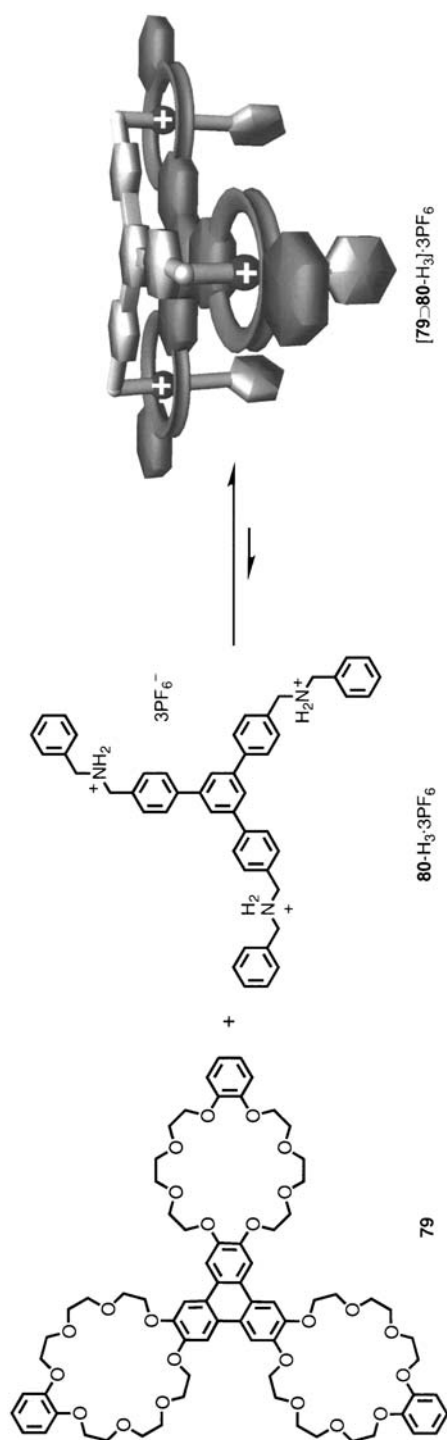
nated binding of multiple ligands on one chemical entity to multiple receptors on another is typically defined as a multivalent interaction and it can be much stronger than the sum of the corresponding monovalent interactions [216–225]. The relative ease of increasing binding affinities by multiplying the number of existing interactions [226–229], rather than addressing the more complicated task of evolving a new and stronger interaction could be an efficient way forward in the design of more effective receptors, drug delivery agents, inhibitors, and catalysts [230–235]. In an effort (i) to enhance noncovalent associations of molecules in unnatural settings, and (ii) to be able to build mechanically interlocked molecules beyond rotaxanes and catenanes, the complexation of multi-ligand with multi-receptor compounds and the construction of multivalent two-component mechanically interlocked bundles [236–240] have been investigated.

The formation of a triply threaded, two-component supramolecular bundle $[79\supset 80\text{-H}_3]\cdot 3\text{PF}_6$ (Scheme 14) has been demonstrated [241–242], wherein each arm of a trifurcated trication $80\text{-H}_3\cdot 3\text{PF}_6$ (in which three dibenzylammonium ions are linked 1,3,5 to a central benzenoid core) is threaded through each macroring of a tritopic receptor **79**, in which three benzo[24]crown-8 macrorings are fused onto a triphenylene core. Spectroscopic, photophysical and electrochemical experiments corroborated the formation of a very stable 1:1 adduct ($K_a > 10^7 \text{ mol L}^{-1}$ in CH_2Cl_2) with the averaged C_{3V} symmetry in solution. The supramolecular bundle $[79\supset 80\text{-H}_3]\cdot 3\text{PF}_6$ is both kinetically and thermodynamically stable, lending itself to studies in which template-directed methods could be probed in the syntheses of multivalent interlocked molecules.

[1,3]-Dipolar cycloaddition reactions have been used to pursue the post-assembly covalent modification of a multivalent supramolecular assembly, wherein one molecular structure interpenetrates another molecular structure⁶ [243] to yield a mechanically interlocked molecular compound. The triply threaded superbundle $83\text{-H}_3\cdot 3\text{PF}_6$ (Scheme 15) containing the tritopic crown ether **79** and the trifurcated trisammonium trication $81\text{-H}_3\cdot 3\text{PF}_6$, which carries azidomethyl functions on the *para* positions of its three benzyl groups, was initially assembled [244] in $\text{CH}_2\text{Cl}_2/\text{MeCN}$ (3:2) in 40% yield. Interestingly, neither the singly nor the doubly threaded mechanically interlocked compounds were detected or isolated⁷ [245]. The complete mechanical entanglement was

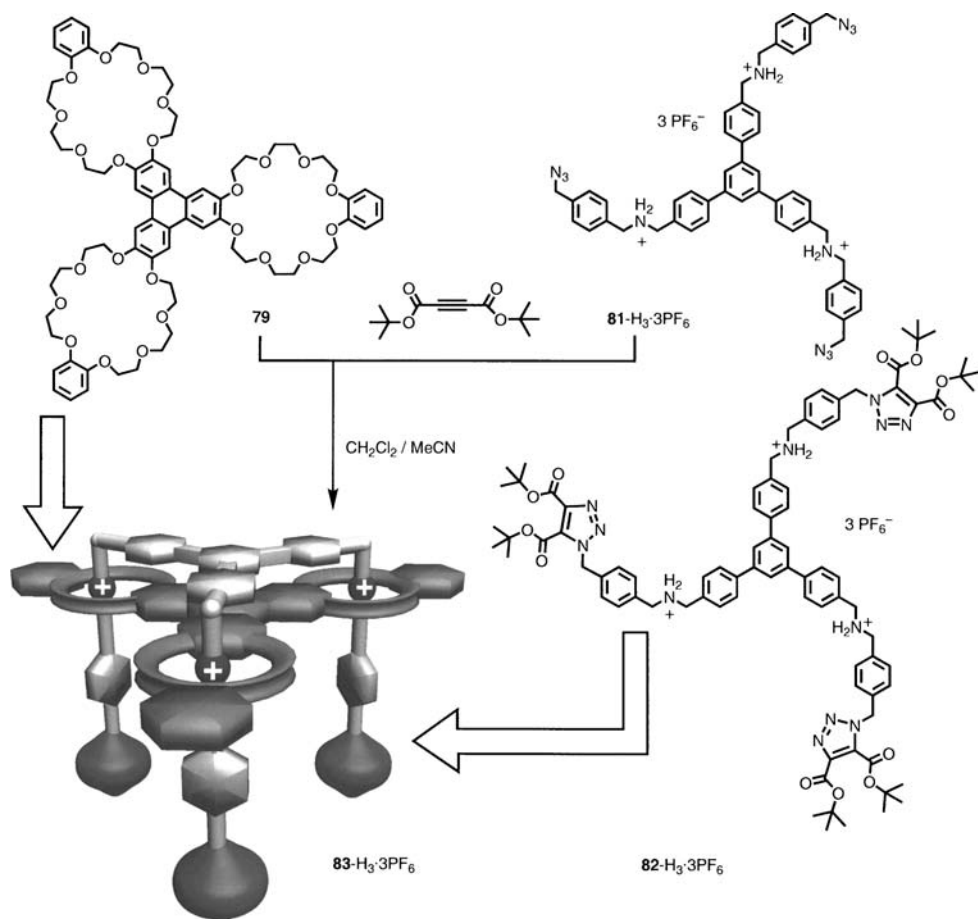
⁶ [1,3]-Dipolar cycloadditions have already been used successfully in the template-directed synthesis of [2]-rotaxanes, using a threading-followed-by-stoppering approach, see [17]. Furthermore, a range of virtually instantaneous reactions, i.e., click chemistry, may be utilized in the place of the cycloaddition.

⁷ In the strict self-assembly of a triply threaded two-component superbundle, starting from a tritopic receptor in which three benzo[24]crown-8 macrorings are fused onto a triphenylene core and a trifurcated trication wherein three bipyridinium units are linked 1,3,5 to a central benzenoid core, it transpires that the rapid formation of a doubly threaded two-component complex is followed by an extremely slow conversion over a week at 253 K in CD_3COCD_3 to reach equilibrium of this kinetically controlled product into a thermodynamically controlled one – namely, a triply threaded two-component superbundle.



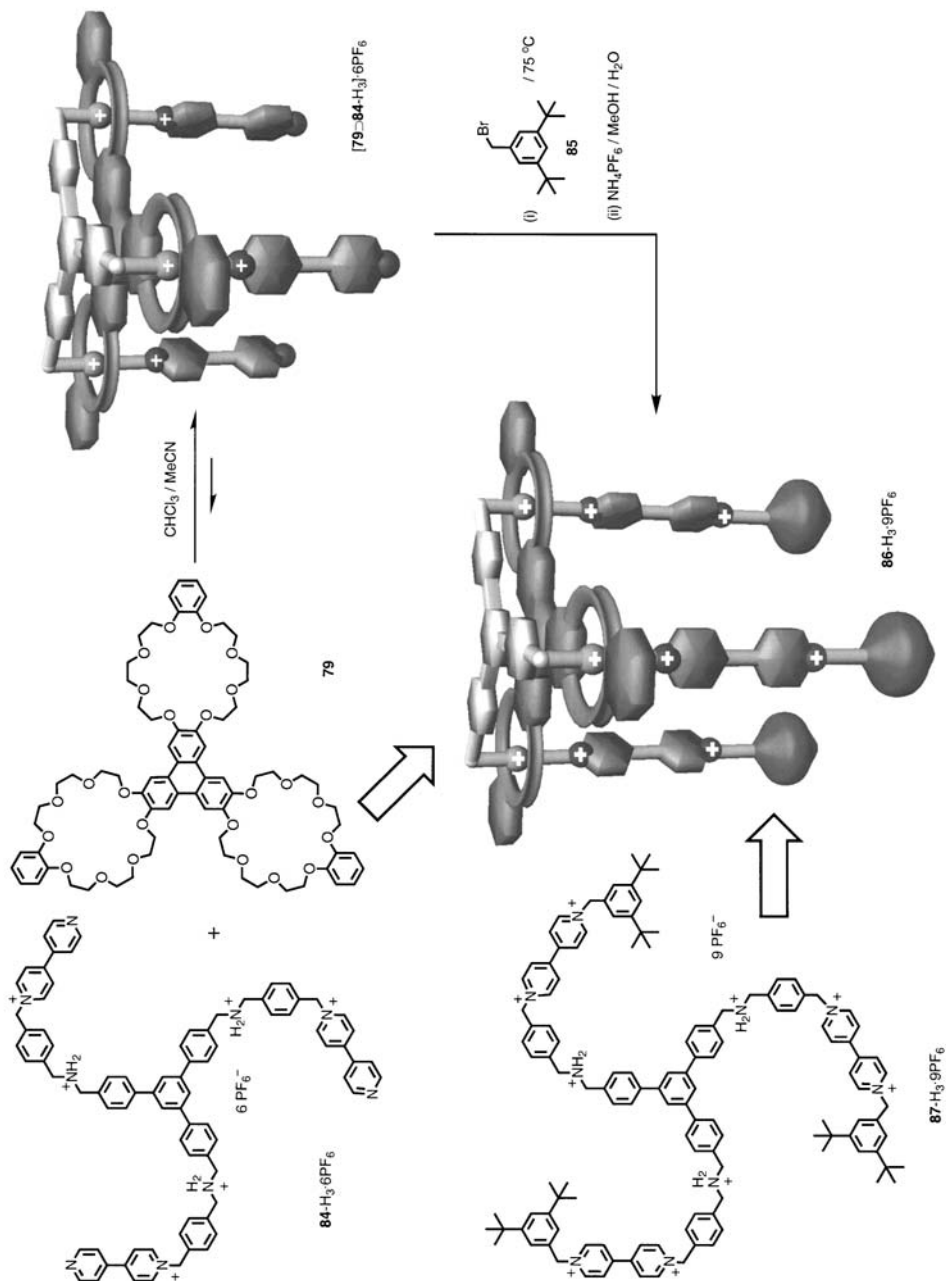
Scheme 14 Equilibrium between the tris-crown ether 79 and the tris-ammonium ion 80-H₃⁺·3PF₆⁻ lies very much over to the right in favor of the 1:1 adduct [79⊃80-H₃⁺]·3PF₆⁻ in solvents such as MeCN and CH₂Cl₂. In Me₂SO, the 1:1 adduct becomes completely dissociated into its components

vindicated in experiments where the bundle $83\text{-H}_3\cdot 3\text{PF}_6$ was fully deprotonated using a strong base *tert*-BuOK. Although the deprotonation did loosen the interlocked molecular structure, a result of replacing relatively strong $[\text{N}^+-\text{H}\cdots\text{O}]$ hydrogen bonds by much weaker $[\text{N}-\text{H}\cdots\text{O}]$ ones, the two matching components stayed mechanically interlocked, as confirmed by ^1H -NMR and fluorescence spectroscopies.



Scheme 15 Template-directed synthesis of the mechanically interlocked bundle $83\text{-H}_3\cdot 3\text{PF}_6$ using kinetically controlled, [1,3]-dipolar cycloadditions to trap the superbundle formed in $\text{CH}_2\text{Cl}_2/\text{MeCN}$ (3:2) at 40 °C between the tritopic triscrown ether **79** and the trifurcated trisammonium salt **81-H₃·3PF₆**

Incorporating the architectural features of the previously designed mechanically interlocked bundle, a two-component molecule $86\text{-H}_3\cdot 9\text{PF}_6$ that behaves like a nanometer-scale elevator was synthesized (Scheme 16) efficiently on account of the template-direction, coupled with the multivalency effect [246].



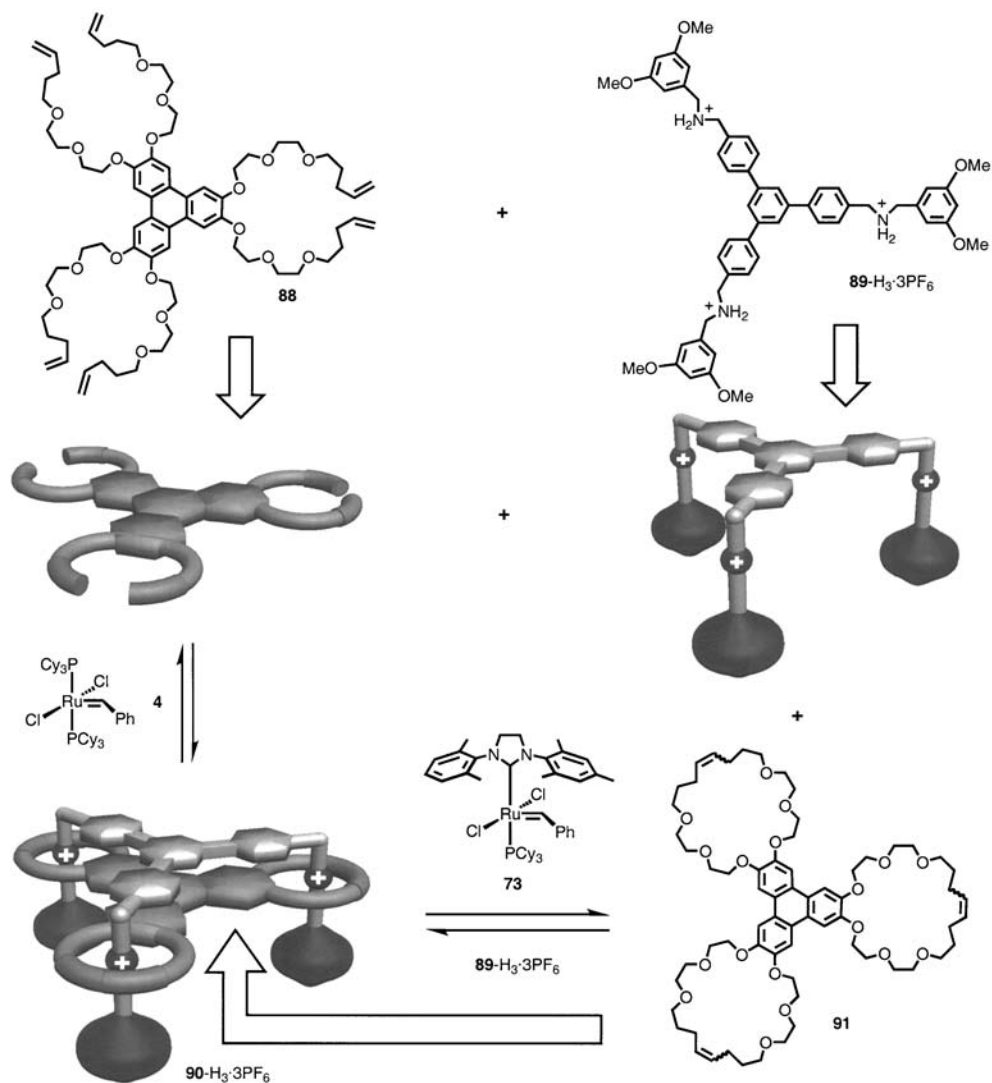
Scheme 16 Triturfacted guest salt $84\text{-H}_3\cdot 6\text{PF}_6$ and the tritopic host **79** (each 6.6 mM) in a $\text{CHCl}_3/\text{MeCN}$ solution (3.0 mL, 2:1) form a 1:1 adduct (superbundle) that is converted, at elevated temperature (75°C), to the mechanically interlocked elevator $86\text{-H}_3\cdot 9\text{PF}_6$ in a reaction with 3,5-di-*tert*-butylbenzylbromide **85** (200 mM), followed by the counterion-exchange ($\text{NH}_4\text{PF}_6/\text{MeOH}/\text{H}_2\text{O}$)

The trifurcated trisammonium hexacation **84**-H₃·6PF₆ and the tritopic crown ether **79** forms, in CH₃CN/CHCl₃ solution, an extremely stable 1:1 supramolecular bundle. The trifurcated trisammonium hexacation [79⊃84-H₃]·6PF₆ containing three terminal pyridyl groups, each threading through one of the three macrocyclic rings associated with the triscrown ether **79**, was reacted with bulky 3,5-di-*tert*-butylbenzyl bromide **85**, affording [247] the mechanically interlocked species **86**-H₃·9PF₆ in 33% yield. ¹H-NMR, absorption and fluorescence spectroscopies, in addition to electrochemistry measurements, indicated that **86**-H₃·9PF₆ has averaged C_{3v} symmetry with the platform's three crown ether loops encircling the three NH₂⁺ centers (Scheme 16). Acid/base treatment of the **86**-H₃·9PF₆ drives the crown ether platform between the NH₂⁺ and BIPY²⁺ recognition sites, a mechanical motion that resembles the operation of a nano-scale elevator.

The advent of dynamic covalent chemistry has opened up attractive alternative routes to mechanically interlocked molecules, *vide supra*. It has already been shown that reversible RCM and RORCM reactions, mediated by Grubbs catalysts, can be used in the thermodynamically controlled synthesis of catenanes and rotaxanes [149, 157, 161–162, 200, 248–249]. If multivalent sites between two or more components could be created spontaneously *in situ* by dynamic covalent chemistry [134], it seems reasonable that the multivalency effect, which is primarily a thermodynamic phenomenon, could assist in the formation of elaborate multiply threaded interlocked molecules [250].

When the triphenylene hexa-olefin **88** (Scheme 17) was subjected to the RCM reaction with and without the monovalent *bis*-3,5-dimethoxydibenzylammonium ion template and using Grubbs I catalyst **4**, neither the desired crown ether analog nor [4]rotaxane, respectively, was observed. When an equimolar mixture of the triphenylene hexa-olefin **88** and trifurcated trisammonium trication **89**-H₃·3PF₆ was subjected to an RCM reaction using Grubbs I catalyst **4**, the exclusive product was the mechanically interlocked molecular “bundle” **90**-H₃·3PF₆, containing C=C double bonds with both *E* and *Z* configurations and with averaged quasi-C_{3v} symmetry, as confirmed by ¹H-NMR spectroscopy.

The almost quantitative production of **90**-H₃·3PF₆ is presumably the result of the build-up of cooperative binding interactions, which result from the three productive RCM reactions assisted by the statistical and cluster effects associated with the multivalency that characterizes the thermodynamically stable product. The assembly of the mechanically interlocked **90**-H₃·3PF₆ was also attempted (Scheme 17) using already preformed components **89**-H₃·3PF₆ and **91**. The two components do *not* form a supramolecular bundle in solution. However, RORCM reactions do take place upon addition of Grubbs II catalyst **73**, leading to the opening and closing of **91**. The equilibration process led to the exclusive formation of the mechanically interlocked compound **90**-H₃·3PF₆, as evidenced by ¹H-NMR spectroscopy and mass spectrometry. The dynamic interplay between molecular recognition and the reversible formation of covalent and mechanical bonds, using suitable catalysts, in combination with template-directing effects can apparently be used in the efficient production of



Scheme 17 Efficient preparation of the mechanically interlocked “bundle” $90\text{-H}_3\cdot 3\text{PF}_6$ as a mixture of isomers containing C=C double bonds with both (*E*) and (*Z*) configurations can be achieved through either RCM reaction, starting from an equimolar mixture (CH_2Cl_2 at 40°C) of the trifurcated trisammonium salt $89\text{-H}_3\cdot 3\text{PF}_6$ and hexa-olefin **88** using the functional-group tolerant Grubbs I catalyst **4** or RORCM reaction starting from an equimolar mixture (CH_2Cl_2 at 25°C) of the trifurcated trisammonium salt $89\text{-H}_3\cdot 3\text{PF}_6$ and tris-crown **91** using the Grubbs II catalyst **73**

intriguing and functional molecular assemblies, and also hopefully of high molecular weight polymers with appealing materials properties. As the need for elaborate functional systems grows, the concept of multivalency is likely to play a significant role in the areas of supramolecular, medicinal, and materials chemistry.

5

Templating the Future of Technology

Template-directed synthesis allows for the precise control over the mutual location of the components in mechanically interlocked molecules. This high degree of organization lays the foundations for the production of molecular machinery [251–259]. In particular, with the addition of more than one templating unit, a property of higher order emerges – *motion* [78, 260]. Specifically, when two different templates are utilized [261–265], mechanically operating switchable molecules can be realized, wherein it is now their *movements* that can be controlled by an external chemical [266–268], electrochemical [269–271], or photochemical [272–275] stimulus. The stimulants are utilized to turn off and on the recognition motifs, namely the very templates that were employed in the compound's preparation. Additional criteria – organization and integration onto surfaces and ultimately into multi-scale devices [251–252, 276–278] – have been recognized and are presently being addressed in order to give molecular machines their rightful place in a technological world. As a first step, some of the molecular machines outlined in this review are being tethered to a variety of surfaces. In one significant instance, bistable [2]catenanes and [2]rotaxanes have been used to template the emergence of binary molecular memory.

5.1

Molecular Switching

Building on the early successes, a truly bistable [2]catenane **17b**⁴⁺ was prepared [91, 262] that displays (Fig. 6) an “all-or-nothing” preference for one of the translational isomers until stimulated, whereupon the preference switches from the ground state to an excited translational state or even to the other translational isomer, a metastable one. In this example, the TTF unit of the aromatic cyclic polyether component is preferentially bound within the CBPQT⁴⁺ cyclophane's cavity with the DNP ring system on the outside. Solution phase studies reveal that upon two-electron oxidation of the TTF unit, the now-charged aromatic cyclic polyether circumrotates as a result of charge repulsion, thus relocating the DNP ring system inside the cavity of the CBPQT⁴⁺ cyclophane. This design is exemplary for controlling molecular motion because (a) one of the recognition units can be easily switched – in this case the redox active TTF unit – and (b) both of the recognition units can be selected to have vastly different binding affinities for the mechanically mobile cyclophane.

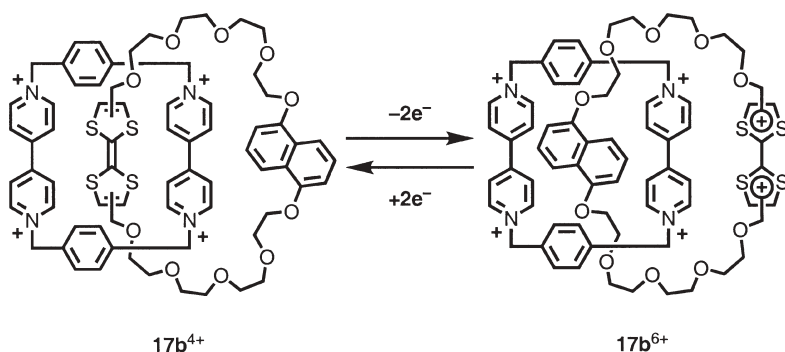


Fig. 6 Electrochemically stimulated circumrotational motion in the bistable [2]catenane $17b^{4+}$ allows two distinct redox states to be reversibly accessed

A bistable light-driven switch [110] in the form of a [2]rotaxane **32** has been designed so that the hydrogen-bond accepting ability of a photoactive naphthalimide (Fig. 7) is “turned on” by a photochemical reaction with a secondary electron donor. In the electronic ground state, the benzylic amide macrocycle is located preferentially at the succinamide site (MeCN, 329 K). Electrochemical reduction drives the translocation of the macrocycle to encircle the now-reduced naphthalimide unit. Consequently, the reduced form of the rotaxane can be considered a viable candidate for photo-induced electron transfer. In particular, the photo-excited (355 nm) naphthalimide unit of **32** accepts an electron from the

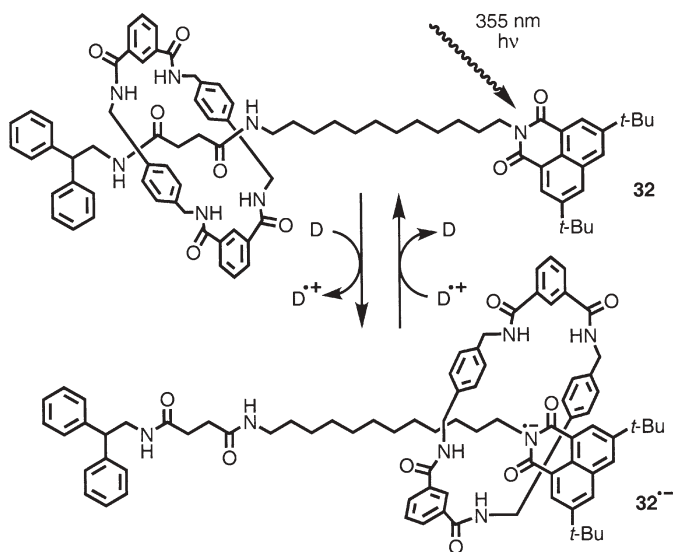


Fig. 7 Linear motions in the photoactive [2]rotaxane **32** can be driven by light in the presence of the secondary electron donor 1,4-diazabicyclo[2.2.2]octane (D)

triplet transfer agent 1,4-diazabicyclo[2.2.2]octane (D), generating the reduced state and thus turning on the unit's attraction for the macrocycle. In this manner, photo-induced translational motion is not only achieved but is also time-resolved to occur in $\sim 1 \mu\text{s}$, with subsequent relaxation over a much longer ($\sim 100 \mu\text{s}$) time-scale. The utilization of a secondary reagent has been employed in other instances [272], highlighting the fact that totally intramolecular photo-driven motion is an ongoing challenge.

The design of the component parts of a machine is becoming increasingly dictated by the desired functional outcome. Unidirectional motion [279–280] has been demonstrated [105] recently by utilizing (Fig. 8) a switchable hydrogen-bonded [3]catenane **92**, which is a by-product in the synthesis of the [2]catenane **30**. In this instance, the second macrocycle acts as a blocking group that directs the movement of the other macrocycle. This example underscores the level of complexity that has been achieved and will continue to be demanded in the design of molecular machinery based on interlocked molecules.

Analogous bistable catenates and metallated rotaxanes, which can be electrochemically activated, have been developed that are based on the translocation of transition metal ions. In particular, Sauvage [281] has made effective use of the differences in coordination requirements between Cu(I) and Cu(II) redox centers. The former prefers a four-coordinate arrangement, whereas the latter likes a five-coordinate environment. For example, an electrochemically active copper [2]catenate **93**⁺ involves [282] one macrocycle that incorporates both a bidentate and tridentate polypyridyl ligand into its ring. In the presence of

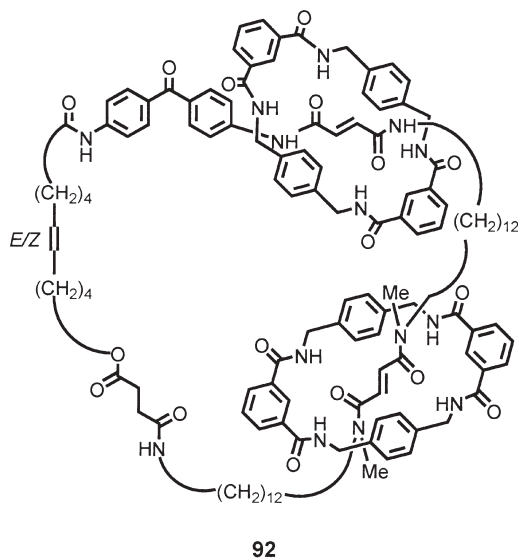


Fig. 8 Unidirectional circumrotational motion has been demonstrated from a [3]catenane **92** with four recognition units in which one of the two smaller rings acts as a blocking group

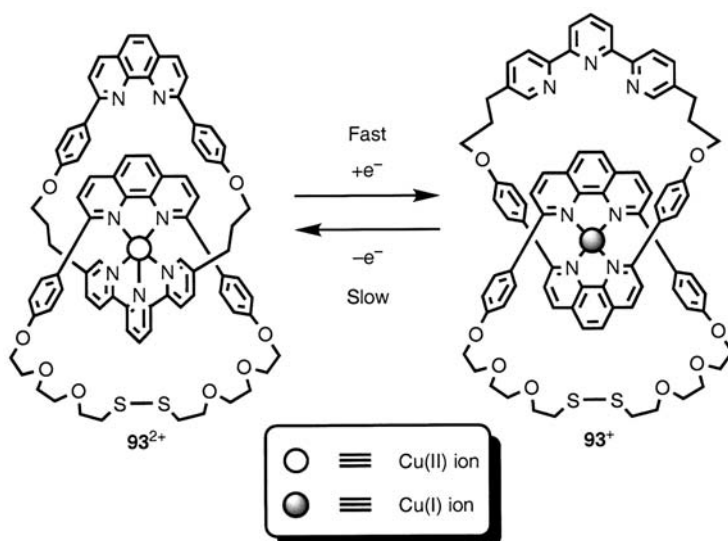


Fig. 9 Circumrotational motion in a metallated copper [2]catenane **93**^{2+/+} can be driven electrochemically in order to accommodate the 5- and 4-coordinate bonding preferences of Cu(II) and Cu(I), respectively

Cu(I), the two bidentate sites from the interlocked macrocycles are coordinated to the copper center. Oxidation to the Cu(II) state causes circumrotation and situates the tridentate ligand within the coordination sphere in order to accommodate the five-coordinate bonding requirement of the Cu center. This process (Fig. 9) can be stimulated electrochemically by beginning in the Cu(II) state. In addition to the circumrotational motions, the macrocycles can also be made to spin around the axes of rotaxanes [76, 265] and similarly, linear motion can be activated in rotaxanes [264].

5.2

Surface Switching

The linear motions of the moving components in a large number of controllable molecular machines distributed randomly in the solution state can be expressed coherently in a mechanical context by organizing them at interfaces [273, 282–283], either as Langmuir–Blodgett (LB) films [284–288] or as self-assembled monolayers (SAMs). Before any multi-scale and integrated devices based on molecular machines become viable for real technological applications, the conditions required to ensure that mechanical switching persists when the molecules are mounted onto solid supports are currently being investigated.

Molecular design motifs based on *intramolecular* disulfide bonding have been incorporated into a series of rotaxanes [289] and catenates [282] in order to facilitate their self-assembly onto gold surfaces. However, in both cases, the

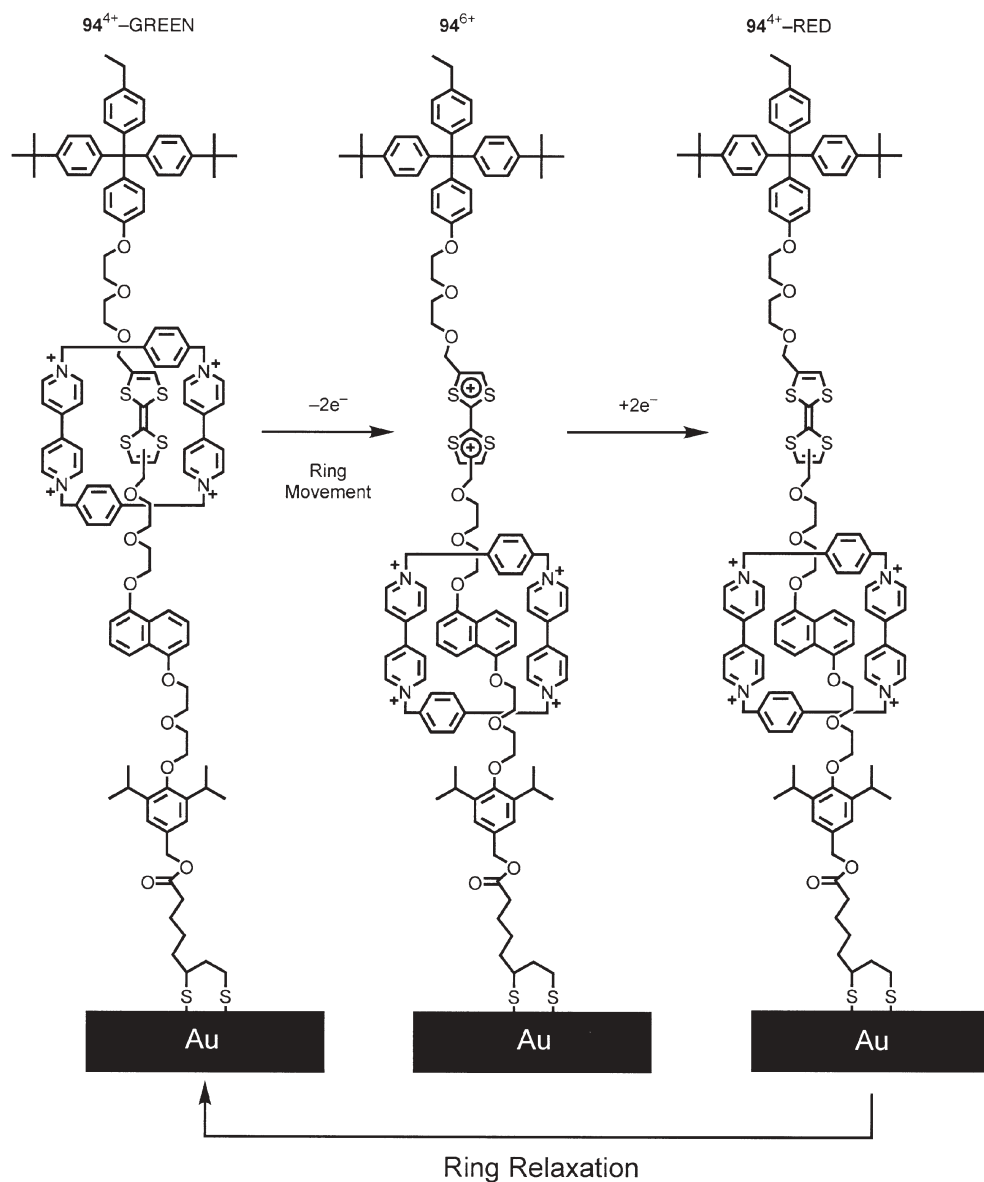


Fig. 10 The interlocked macrocycle of a surface-bound bistable [2]rotaxane **94** displays electrochemically driven linear motions between two recognition sites. The binding of the macrocycle to the weaker donor, 1,5-dioxynaphthalene, in the metastable state is sufficiently strong to forestall the reformation of the ground state, following electrochemical reset

molecular movements were found to be highly hindered or quenched in comparison to the solution-phase behavior. For example, the circumrotation of the [2]catenate **93**⁺ operates in solution following electrochemical stimulation according to the hysteresis observed in the CV. However, when either the Cu(II) or Cu(I) form of the [2]catenate SAM were examined electrochemically, negligible hysteresis in the CV was observed.

A switchable [2]rotaxane, based on viologen recognition units, has been attached [278] to 6 nm TiO₂ nanoparticles by a rigid tripodal stopper with phosphonate tethers. In this instance, switching within the hetero[2]rotaxane is achieved by chemical or electrochemical reduction. Analysis of the CV reveals a complex sequence of mechanical movements that differ from the solution dynamics. This result illustrates how the dynamics of surface-bound species may not always behave exactly as those observed in solution. Consequently, the study of molecular machines in the context of surface-bound species is important in order to understand just how to optimize their molecular structure in order to elicit controllable molecular functions.

Taking advantage of the modularity of template-directed synthesis of mechanically interlocked molecules, a [2]rotaxane **94**⁴⁺ was prepared with a disulfide tether attached to one of its two stoppers so that it can form a SAM on gold electrodes. These rotaxanes display redox-controlled motions (Fig. 10) of the CBPQT⁴⁺ cyclophane from the TTF unit to the DNP ring system. In an illuminating study using cyclic voltammetry (CV), fast redox switching at variable temperatures allowed the translational isomer with the CBPQT⁴⁺ cyclophane stationed at the DNP ring system to be identified and time-resolved. This translational isomer persists for a short period of time (~s) even although the TTF unit has returned to its neutral and therefore more attractive redox state. This metastable state was found [283] to relax to the ground state in about 1 s at room temperature over a barrier of 18 kcal mol⁻¹. Such DNP-based metastability had been observed in other systems [282] but had never been fully investigated. The presence of the metastable state, together with the barrier to motion, is consistent with the supramolecular history of these compounds from the perspective of the molecule's properties.

5.3

Molecular Electronics

Electrical crossbar devices (Fig. 11) built around the catenane **17b**⁴⁺, the amphiphilic bistable rotaxane **95**⁴⁺, and others have been investigated [92–94, 290–291] for their ability to display binary switching. The general method for constructing such devices relies upon depositing a LB monolayer of closely packed molecular switches onto a highly doped polysilicon (*p*-Si) electrode. A top electrode of Ti, followed by Al, is subsequently vapor-deposited on top of the monolayer.

The molecular devices display switching between high and low conductance states. Each device is interrogated and characterized by applying a “write” volt-

age, V and recording the “read” current, I . The ON state is accessed at +2 V, which is equivalent to net oxidizing conditions, whereas the OFF state is triggered at -2 V, or net reducing conditions. These data reveal that, in addition to the reversible voltage-gated switching of the device ON and OFF more than 30 times, the ON state is metastable, displaying a temperature-dependant re-setting of the device back to the OFF state.

A molecule-based nano-electromechanical switching mechanism has been proposed to account for the device’s observed experimental behavior. The OFF state corresponds to the translational isomer, with the cyclophane encircling the MPTTF unit. In the device, application of a +2 V bias generates an oxidized form of the MPTTF unit in the rotaxane. Just as observed in solution, the

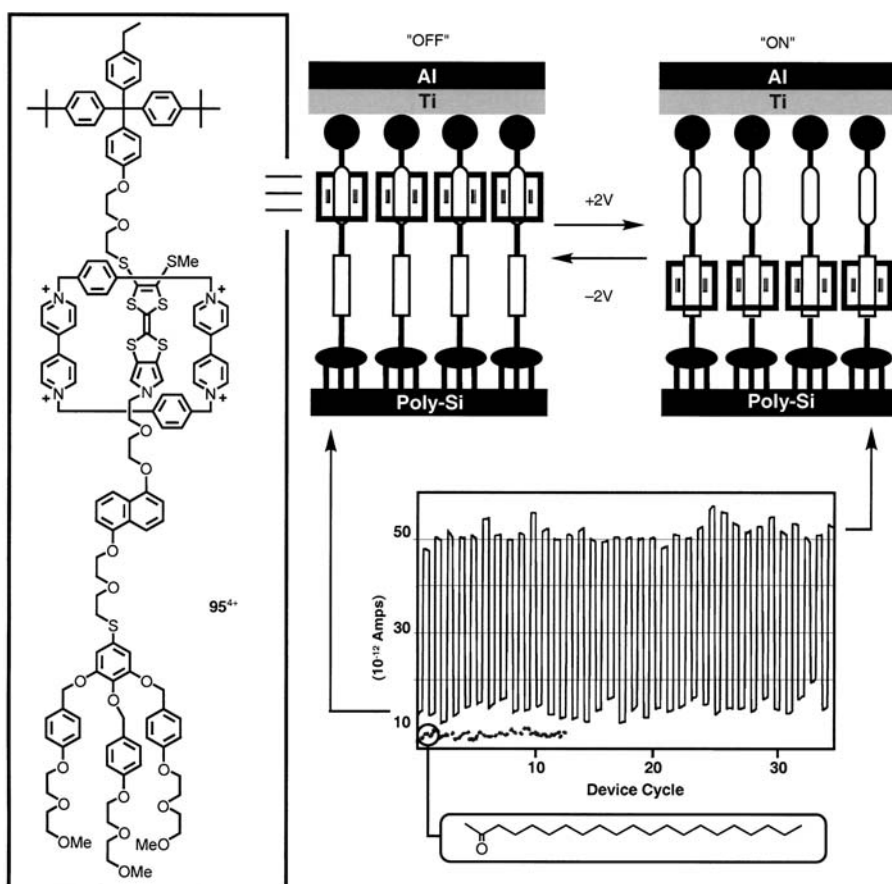


Fig. 11 The amphiphilic bistable [2]rotaxane 95^{4+} has been integrated into a crossbar device between two electrodes as a Langmuir-Blodgett monolayer. The ON and OFF states of the device are accessed at +2 V and -2 V, respectively, and are assigned to two different translational isomers, the metastable and the ground states, respectively

resulting charge–charge repulsive force drives a linear movement of the cyclophane along the dumbbell component to a position encircling the DNP ring system. When the bias is lowered to +0.1 V, for the purpose of reading the device, the charge on the MPTTF unit is neutralized and yet the cyclophane remains around the DNP ring system on account of the mutually attractive noncovalent interactions. This new metastable translational isomer is responsible for the high-conductance ON state. This metastable state of the device, and by inference the molecule, is observed to decay to the OFF state in a manner that is qualitatively similar [283] to the movements of the tetracationic cyclophane in rotaxanes that are self-assembled (*vide supra*) onto a gold electrode. Therefore, the decay rate is concomitant with the thermally activated linear movement of the cyclophane back along the dumbbell to the MPTTF unit. Alternatively, applying a reverse bias of –2 V causes the electrochemical reduction of the tetracationic cyclophane, allowing the facile reformation of the most stable translational isomer.

The proposed switching mechanism, while based on the molecule's known mechanical movements in solution, is supported experimentally by the comparison to control devices. In particular, devices utilizing the dumbbell-only compounds and non-redox active molecules, such as eicosanoic acid (Fig. 11), do not display any switching behavior.

5.4

Summary

The tenet for the molecular sciences that structure follows function is equally apparent for mechanically interlocked molecules where their potential to be harnessed as molecular machines is becoming increasingly attractive both academically and technologically. Beyond synthesis, the template and its recognition partner(s) serve many other purposes. Selection of strong binding templates allows for sub-nanometer control over the mutual location of the interlocked components. Switchable templates open the door to controllable motion. Topological design allows for different types of motions, including unidirectional rotations. Integration of mechanically interlocked molecules into larger self-organized assemblies can be easily attained, although the mechanical movements become more challenging to identify. Consequently, structure–function analyses are required in order to elicit understanding, as much as they are essential to optimize the molecules' function for a desired technological application. Where an example is apparent in molecular electronics, there are likely more, as yet unexplored, areas of research and development for these classes of molecules that utilize purely the mechanical machinery paradigm to herald a new technology at the boundary between soft and hard matter.

6

Conclusions and Perspectives

Mechanically interlocked molecules, such as catenanes and rotaxanes, can be synthesized at high efficiency by utilizing organic or inorganic templates under kinetic control. The efficiency of these templated syntheses relies upon a supramolecular approach that utilizes a combination of cooperative noncovalent bonding interactions (such as metal–ligand interactions, π – π stacking and hydrogen bonding) to form a weakly bonded intermediate complex, leading to the irreversible formation of interlocked molecules on the formation of a strong chemical (covalent) bond.

The use of thermodynamically controlled approaches for the synthesis of wholly organic interlocked molecules is slowly growing in popularity. The use of olefin metathesis, imine formation/exchange, or disulfide exchange as the reversible covalent step – in addition to the exploitation of different molecular recognition motifs – demonstrates the generality of thermodynamically controlled approaches for the synthesis of interlocked molecules.

The dynamic interplay between molecular recognition and the reversible formation of covalent and mechanical bonds, using catalysts where appropriate, in combination with template-directed effects, can be used in the efficient production of intriguing and functional molecular assemblies and high molecular weight polymers with appealing materials properties. As the need for elaborate functional systems grows, the concepts of multivalency and cooperativity are likely to play significant roles in the areas of supramolecular, medicinal, and materials chemistry.

Beyond synthesis, the template and its recognition partner(s) serve many other purposes, such as control over the mutual location of the interlocked components. Switchable templates lead to controllable motion, and topological design affords the opportunity for different types of motions, including unidirectional rotations. The integration of mechanically interlocked molecules into larger self-organized assemblies, as revealed by structure function analyses, is beginning to show some technological promise in areas such as molecular electronics.

References

1. Schill G (1971) *Catenanes, rotaxanes and knots*. Academic, New York
2. Amabilino DB, Stoddart JF (1995) *Chem Rev* 95:2725
3. Vögtle F, Dünwald T, Schmidt T (1996) *Acc Chem Res* 29:451
4. Sauvage J-P, Dietrich-Buchecker CO (1999) (eds) *Molecular catenanes, rotaxanes and knots*. Wiley-VCH, Weinheim
5. Hubin TJ, Busch DH (2000) *Coord Chem Rev* 200–202:5
6. Tauber SJ (1963) *J Res Nat Bur Stand Sect A* 67A:591
7. Wasserman E (1960) *J Am Chem Soc* 82:4433
8. Dietrich-Buchecker CO, Sauvage J-P, Kintzinger J-P (1983) *Tetrahedron Lett* 46:5095

9. Johnson AG, Leigh DA, Pritchard RJ, Deegan MD (1995) *Angew Chem Int Ed Engl* 34:1209
10. Andrievsky A, Ahuis F, Sessler JL, Vögtle F, Gudat D, Moini M (1998) *J Am Chem Soc* 120:9712
11. Fujita M (1999) *Acc Chem Res* 32:53
12. Roh SG, Park KM, Park GJ, Sakamoto S, Yamaguchi K, Kim K (1999) *Angew Chem Int Ed* 38:638
13. McArdle CP, Vittal JJ, Puddenphatt RJ (2000) *Angew Chem Int Ed* 112:3819
14. Wiseman MR, Marsh PA, Bishop PT, Brisdon BJ, Mahon MF (2000) *J Am Chem Soc* 122:12598
15. Harrison IT, Harrison S (1967) *J Am Chem Soc* 89:5723
16. Kolchinski AG, Busch DH, Alcock NW (1995) *J Chem Soc Chem Commun* 1289
17. Ashton PR, Glink PT, Stoddart JF, Tasker PA, White AJP, Williams DJ (1996) *Chem Eur J* 2:729
18. Anderson S, Claridge TDW, Anderson HL (1997) *Angew Chem Int Ed Engl* 36:1310
19. Loeb SJ, Wisner JA (1998) *Chem Commun* 2757
20. Solladie N, Chambron H-C, Sauvage J-P (1999) *J Am Chem Soc* 121:3684
21. Kawaguchi Y, Harada A (2000) *J Am Chem Soc* 122:3797
22. Seel C, Vögtle F (2000) *Chem Eur J* 6:21
23. Brouwer AM, Frochot C, Gatti FG, Leigh DA, Mottier L, Paolucci F, Roffia S, Wurpel GWH (2001) *Science* 291:2124
24. Jeppesen JO, Perkins J, Becher J, Stoddart JF (2001) *Angew Chem Int Ed* 40:1216
25. Ng Y-F, Meillon J-C, Ryan T, Dominey AP, Davis AP, Sanders JKM (2001) *Angew Chem Int Ed* 40:1757
26. Tseng H-R, Vignon SA, Stoddart JF (2003) *Angew Chem Int Ed* 42:1492
27. Chichak KS, Cantrill SJ, Pease AR, Chiu S-H, Cave GWV, Atwood JL, Stoddart JF (2004) *Science* 304:1308
28. Balzani V, Credi A, Raymo FM, Stoddart JF (2000) *Angew Chem Int Ed* 39:3348
29. Balzani V, Venturi M, Credi A (2003) *Molecular devices and machines – A journey into the nanoworld*. Wiley-VCH, Weinheim
30. Cram DJ (1986) *Angew Chem Int Ed Engl* 25:1039
31. Lehn J-M (1995) *Supramolecular chemistry: Concepts and perspectives*. Wiley-VCH, Weinheim
32. Busch DH, Stephenson NA (1990) *Coord Chem Rev* 100:119
33. Lindsey JS (1991) *New J Chem* 15:153
34. Whitesides GM, Mathias JP, Seto CT (1991) *Science* 254:1312
35. Anderson S, Anderson HL, Sanders JKM (1993) *Acc Chem Res* 26:465
36. Hoss R, Vögtle F (1994) *Angew Chem Int Ed Engl* 33:375
37. Schneider JP, Kelly JW (1995) *Chem Rev* 95:2169
38. Philp D, Stoddart JF (1996) *Angew Chem Int Ed Engl* 35:1155
39. Fyfe MCT, Stoddart JF (1997) *Acc Chem Res* 30:393
40. Hubin TJ, Kolchinski AG, Vance AL, Busch DL (1999) *Adv Supramol Chem* 5:237
41. Diederich F, Stang PJ (2000) (eds) *Templated organic synthesis*. Wiley-VCH, Weinheim
42. Hunter CA (1994) *Chem Soc Rev* 23:101
43. Johnston AG, Leighton DA, Pritchard RJ, Deegan MD (1995) *Angew Chem Int Ed Engl* 34:1209
44. Glink PT, Schiavo C, Stoddart JF, Williams DJ (1996) *Chem Commun* 1483
45. Leigh DA, Moody K, Smart JP, Watson KJ, Slawin AMZ (1996) *Angew Chem Int Ed Engl* 35:306
46. Otteus-Hildebrand S, Meier S, Schmidt W, Vögtle F (1994) *Angew Chem Int Ed Engl* 33:1767

47. Kolchinski AG, Alcock NW, Roesner RA, Busch DH (1998) *Chem Commun* 1437
48. Fyfe MCT, Stoddart JF (1999) *Coord Chem Rev* 183:139
49. Sauvage J-P (1990) *Acc Chem Res* 23:319
50. Bickelhaupt F (1994) *J Organomet Chem* 475:1
51. Chambron J-C, Dietrich-Buchecker CO, Sauvage J-P (1996) In: Atwood JL, Davies JED, MacNicol DD, Vögtle F (eds) *Comprehensive supramolecular chemistry*, vol 9. Pergamon, Oxford, p 43
52. Fujita M, Ogura K (1996) *Chem Rev* 148:249
53. Whang D, Park KM, Heo J, Ashton PR, Kim K (1998) *J Am Chem Soc* 120:4899
54. Amabilino DB, Stoddart JF (1993) *Pure Appl Chem* 65:2351
55. Pasini D, Raymo FM, Stoddart JF (1995) *Gazz Chim Ital* 125:431
56. Amabilino DB, Raymo FM, Stoddart JF (1996) In: Atwood JL, Davies JED, MacNicol DD, Vögtle F (eds) *Comprehensive supramolecular chemistry*, vol 9. Pergamon, Oxford, p 85
57. Hamilton DG, Davies JE, Prodi L, Sanders JKM (1998) *Chem Eur J* 4:608
58. Raymo FM, Stoddart JF (1998) *Chemtracts* 11:491
59. Try AC, Harding MM, Hamilton DG, Sanders JKM (1998) *Chem Commun* 723
60. Hamilton DG, Prodi L, Feeder N, Sanders JKM (1999) *J Chem Soc Perkin Trans 1*:1057
61. Stoddart JF (1992) *Angew Chem Int Ed Engl* 31:846
62. Isnin R, Kaifer AE (1993) *Pure Appl Chem* 65:495
63. Wenz G (1994) *Angew Chem Int Ed Engl* 33:802
64. Harada A (1996) *Coord Chem Rev* 148:115
65. Nepogodiev SA, Stoddart JF (1998) *Chem Rev* 98:1959
66. Gillard RE, Raymo FM, Stoddart JF (1997) *Chem Eur J* 3:1933
67. Thompson MC, Busch DH (1964) *J Am Chem Soc* 86:3651
68. Blinn EL, Busch DH (1968) *Inorg Chem* 7:820
69. Thompson MC, Busch DH (1962) *J Am Chem Soc* 84:1762
70. Curry JD, Busch DH (1964) *J Am Chem Soc* 86:592
71. Melson GA, Busch DH (1965) *J Am Chem Soc* 97:1706
72. Collin J-P, Dietrich-Buchecker CO, Gavina P, Jiménez-Molero MC, Sauvage J-P (2001) *Acc Chem Res* 34:477
73. Sauvage J-P (1998) *Acc Chem Res* 31:611
74. Mobian P, Kern J-M, Sauvage J-P (2003) *J Am Chem Soc* 125:2016
75. Mobian P, Kern J-M, Sauvage J-P (2003) *Inorg Chem* 42:8633
76. Poleschak I, Kern J-M, Sauvage J-P (2004) *Chem Commun* 474
77. Odell B, Reddington MV, Slawin AMZ, Spencer N, Stoddart JF, Williams DJ (1988) *Angew Chem Int Ed Engl* 27:1547
78. Ashton PR, Goodnow TT, Kaifer AE, Reddington MV, Slawin AMZ, Spencer N, Stoddart JF, Vicent C, Williams DJ (1989) *Angew Chem Int Ed Engl* 28:1396
79. Stoddart JF, Tseng H-R (2002) *Proc Natl Acad Sci USA* 99:4797
80. Hernandez R, Tseng H-R, Wong JW, Stoddart JF, Zink JI (2004) *J Am Chem Soc* 126:3370
81. Hunter CA, Sanders JKM (1990) *J Am Chem Soc* 112:5525
82. Hunter CA (1993) *Angew Chem Int Ed Engl* 32:1584
83. Houk KN, Menzer S, Newton SP, Raymo FM, Stoddart JF, Williams DJ (1999) *J Am Chem Soc* 121:1479
84. Raymo FM, Barberger MD, Houk KN, Stoddart JF (2001) *J Am Chem Soc* 123:9264
85. Philp D, Slawin AMZ, Spencer N, Stoddart JF, Williams DJ (1991) *J Chem Soc Chem Commun* 1584
86. Nielsen MO, Jeppesen JO, Lau J, Lomholt C, Damgaard D, Jacobsen JP, Becher J, Stoddart JF (2001) *J Org Chem* 66:3559

87. Amabilino DB, Ashon PR, Reder AS, Spencer N, Stoddart JF (1994) *Angew Chem Int Ed Engl* 33:1286
88. Asakawa M, Ashton PR, Balzani V, Boyd SE, Credi A, Mattersteig G, Menzer S, Montalti M, Raymo FM, Ruffilli C, Stoddart JF, Venturi M, Williams DJ (1999) *Eur J Org Chem* 985
89. Asakawa M, Ashton PR, Balzani V, Brown CL, Credi A, Matthews OA, Newton SP, Raymo FM, Shipway AN, Spencer N, Quick A, Stoddart JF, White AJP, Williams DJ (1999) *Chem Eur J* 3:860
90. Asakawa M, Ashton PR, Balzani V, Credi A, Hamers C, Mattersteig, Montalti M, Shipway AN, Spencer N, Stoddart JF, Tolley MS, Venturi M, White AJP, Williams DJ (1998) *Angew Chem Int Ed* 37:333
91. Balzani V, Credi A, Mattersteig G, Matthews OA, Raymo FM, Stoddart JF, Venturi M, White AJP, Williams DJ (2000) *J Org Chem* 65:1924
92. Collier CP, Mattersteig G, Wong EW, Luo Y, Beverly K, Sampaio J, Raymo FM, Stoddart JF, Heath JR (2000) *Science* 289:1172
93. Collier CP, Wong EW, Belohradsky M, Raymo FM, Stoddart JF, Kuekes PJ, Williams RS, Heath JR, (1999) *Science* 285:391
94. Collier CP, Jeppesen JO, Luo Y, Perkins J, Wong EW, Heath JR, Stoddart JF (2001) *J Am Chem Soc* 123:12632
95. Jeppesen JO, Nielsen KA, Perkins J, Vignon SA, Fabio AD, Ballardini R, Gandolfi MT, Venturi M, Balzani V, Becher J, Stoddart JF (2003) *Chem Eur J* 9:2982
96. Jeppesen JO, Vignon SA, Stoddart JF (2003) *Chem Eur J* 9:4611
97. Raehm L, Hamilton DG, Sanders JKM (2002) *Synlett* 11:1743
98. Hamilton DG, Lynch DE, Byriel KA, Kennard CHL (1997) *Aust J Chem* 50:439
99. Hamilton DG, Sanders JKM, Davies JE, Clegg W, Teat SJ (1997) *Chem Commun* 897
100. Hamilton DG, Montalti M, Prodi L, Fontani M, Zanello P, Sanders JKM (2000) *Chem Eur J* 6:608
101. Hansen JG, Feeder N, Hamilton DG, Gunter MJ, Becher J, Sanders JKM (2000) *Org Lett* 2:449
102. Hunter CA (1992) *J Am Chem Soc* 114:5303
103. Vögtle F, Meier S, Hoss R (1992) *Angew Chem Int Ed Engl* 31:1619
104. Adams H, Carver FJ, Hunter CA (1995) *J Chem Soc Chem Commun* 809
105. Leigh DA, Wong JKY, Dehez F, Zerbetto F (2003) *Nature* 424:174
106. Lane AS, Leigh DA, Murphy A (1997) *J Am Chem Soc* 119:11092
107. Gatti FG, Leigh DA, Nepogodiev SA, Slawin AMZ, Teat SJ, Wong JKY (2001) *J Am Chem Soc* 123:5983
108. Asakawa M, Brancato G, Fanti M, Leigh DA, Shimizu T, Slawin AMZ, Wong JKY, Zerbetto F, Zhang S (2002) *J Am Chem Soc* 124:2939
109. Da Ros T, Guldi DM, Morales AF, Leigh DA, Prato M, Turco R (2003) *Org Lett* 5:689
110. Altieri A, Gatti FG, Kay ER, Leigh DA, Martel D, Paolucci F, Slawin AMZ, Wong JKY (2003) *J Am Chem Soc* 125:8644
111. Altieri A, Bottari G, Dehez F, Leigh DA, Wong JKY, Zerbetto F (2003) *Angew Chem Int Ed* 42:2296
112. Keaveney CM, Leigh DA (2004) *Angew Chem Int Ed* 43:1222
113. Jäger R, Vögtle F (1997) *Angew Chem Int Ed Engl* 36:930
114. Safarowsky O, Nieger M, Fröhlich R, Vögtle F (2000) *Angew Chem Int Ed* 39:1616
115. Li QY, Vogel E, Parham AH, Nieger M, Bolte M, Fröhlich R, Saarenketo P, Rissanen K, Vögtle F (2001) *Eur J Org Chem* 4041
116. Li XY, Illigen J, Nieger M, Michel S, Schalley CA (2003) *Chem Eur J* 9:1332
117. Seel C, Parham AH, Safarowsky O, Hübner GM, Vögtle F (1999) *J Org Chem* 64:7236

118. Ashton PR, Chrystal EJT, Glink PT, Menzer S, Schiavo C, Spencer N, Stoddart JF, Tasker PA, White AJP, Williams DJ (1996) *Chem Eur J* 2:709 and references therein
119. Cantrill SJ, Pease AR, Stoddart JF (2000) *J Chem Soc Dalton Trans* 3715
120. Martínez-Díaz MV, Spencer N, Stoddart JF (1997) *Angew Chem Int Ed Engl* 36:1904
121. Rowan SJ, Cantrill SJ, Stoddart JF (1999) *Org Lett* 1:129
122. Rowan SJ, Stoddart JF (2000) *J Am Chem Soc* 122:164
123. Chiu S-H, Rowan SJ, Cantrill SJ, Stoddart JF, White AJP, Williams DJ (2002) *Chem Eur J* 8:5170
124. Hübner GM, Gläser J, Seel C, Vögtle F (1999) *Angew Chem Int Ed* 38:383
125. Reuter C, Wienand W, Hübner GM, Seel C, Vögtle F (1999) *Chem Eur J* 9:2692
126. Schmieder R, Hübner G, Seel C, Vögtle F (1999) *Angew Chem Int Ed* 38:3528
127. Mahoney JM, Shukla R, Marshall RA, Beatty AM, Zajicek J, Smith BD (2002) *J Org Chem* 67:1436
128. Ghosh P, Mermagen O, Schalley CA (2002) *Chem Commun* 2628
129. Linnartz P, Bitter S, Schalley CA (2003) *Eur J Org Chem* 4819
130. Loeb SJ, Wisner JA (1998) *Angew Chem Int Ed* 37:2838
131. Loeb SJ, Wisner JA (2000) *Chem Commun* 845
132. Loeb SJ, Wisner JA (2000) *Chem Commun* 1939
133. Hubbard AL, Davidson GJE, Patel RH, Wisner JA, Loeb SJ (2004) *Chem Commun* 138
134. Rowan SJ, Cantrill SJ, Cousins GRL, Sanders JKM, Stoddart JF (2002) *Angew Chem Int Ed* 41:898
135. Ashton PR, Belohradsky M, Philp D, Stoddart JF (1993) *J Chem Soc Chem Commun* 1269
136. Amabilino DB, Ashton PR, Belohradsky M, Raymo FM, Stoddart JF (1995) *J Chem Soc Chem Commun* 747
137. Ashton PR, Ballardini R, Balzani V, Belohradsky M, Gandolfi MT, Philp D, Prodi L, Raymo FM, Reddington MV, Spencer N, Stoddart JF, Venturi M, Williams DJ (1996) *J Am Chem Soc* 118:4931
138. Asakawa M, Ashton PR, Ballardini R, Balzani V, Belohradsky M, Gandolfi MT, Kocian O, Prodi L, Raymo FM, Stoddart JF, Venturi M (1997) *J Am Chem Soc* 119:302
139. Raymo FM, Stoddart JF (1997) *Pure Appl Chem* 69:1987
140. Amabilino DB, Ashton PR, Belohradsky M, Raymo FM, Stoddart JF (1995) *J Chem Soc Chem Commun* 751
141. Amabilino DB, Asakawa M, Ashton PR, Ballardini R, Balzani V, Belohradsky M, Credi A, Higuchi M, Raymo FM, Shimizu T, Stoddart JF (1998) *New J Chem* 959
142. Elizarov AM, Chang T, Chiu SH, Stoddart JF (2002) *Org Lett* 21:3565
143. Harrison IT (1972) *J Chem Soc Chem Commun* 231
144. Schill G, Beckmann W, Schweikert, Fritz H (1986) *Chem Ber* 119:2647
145. Raymo FM, Houk KN, Stoddart JF (1998) *J Am Chem Soc* 120:9318
146. Ashton PR, Baxter I, Fyfe, Raymo FM, Spencer N, Stoddart JF, White AJP, Williams DJ, Venturi M (1998) *J Am Chem Soc* 120:2297
147. Macartney DH (1996) *J Chem Soc Perkin Trans 2* 2775
148. Händel M, Plevovets M, Gestermann S, Vögtle F (1997) *Angew Chem Int Ed Engl* 36: 1199
149. Hamilton DG, Feeder N, Teat SJ, Sanders JKM, (1998) *New J Chem* 1019
150. Fujita M, Ibukuro F, Hagihara H, Ogura K (1994) *Nature* 367:720
151. Dietrich-Buchecker CO, Geum N, Hori A, Fujita M, Sakamoto S, Yamaguchi K, Sauvage J-P (2001) *Chem Commun* 1182
152. Chichak K, Walsh MC, Branda NR (2000) *Chem Commun* 847
153. Gunter MJ, Bampas N, Johnstone KD, Sanders JKM (2001) *New J Chem* 25:166

154. Hogg L, Leigh DA, Lusby PJ, Morelli A, Parsons S, Wong JKY (2004) *Angew Chem Int Ed* 43:1218
155. Mohr B, Weck M, Sauvage J-P, Grubbs RH (1997) *Angew Chem Int Ed Engl* 36:1308
156. Weck M, Mohr B, Sauvage J-P, Grubbs RH (1999) *J Org Chem* 64:5463
157. Arico F, Mobian P, Kern J-M, Sauvage J-P (2003) *Org Lett* 11:1887
158. Mobian P, Kern J-M, Sauvage J-P (2004) *Angew Chem Int Ed* 43:2392
159. Belfrekh N, Dietrich-Buchecker CO, Sauvage J-P (2000) *Inorg Chem* 38:5169
160. Dietrich-Buchecker CO, Rapenne GN, Sauvage J-P, (1997) *Chem Commun* 2053
161. Kidd TJ, Leigh DA, Wilson AJ (1999) *J Am Chem Soc* 121:1599
162. Hannam JS, Kidd JT, Leigh DA, Wilson AJ (2003) *Org Lett* 5:1907
163. Dayagi S, Degani Y (1970) In: Patai S (ed) *The chemistry of the carbon–nitrogen double bond*. Interscience, NewYork, p 64
164. Cantrill SJ, Rowan SJ, Stoddart JF (1999) *Org Lett* 1:1363
165. Amirsakis DG, Garcia-Garibay MA, Rowan SJ, Stoddart JF, White AJP, Williams DJ (2001) *Angew Chem Int Ed* 40:4256
166. Ashton PR, Becher J, Fyfe MCT, Nielsen MB, Stoddart JF, White AJP, Williams DJ (2001) *Tetrahedron* 57:947
167. Cantrill SJ, Youn GJ, Stoddart JF, Williams DJ (2001) *J Org Chem* 66:6857
168. Duggan SA, Fallon G, Langford SJ, Lau VL, Satchell JF, Paddon-Row MN (2001) *J Org Chem* 66:4419
169. Zehnder II DW, Smithrud DB (2001) *Org Lett* 3:2485
170. Clifford T, Abushamleh A, Busch DH (2002) *Proc Natl Acad Sci USA* 99:4830
171. Gibson HW, Yamaguchi N, Hamilton L, Jones JW (2002) *J Am Chem Soc* 124:4653
172. Tokunaga Y, Seo T (2002) *Chem Commun* 970
173. Tokunaga Y, Kakuchi S, Akasaka K, Nishikawa N, Shimomura Y, Isa K, Seo T (2002) *Chem Lett* 8:810
174. Furusho Y, Rajkumar GA, Oku T, Takata T (2002) *Tetrahedron* 58:6609
175. Chiu SH, Rowan SJ, Cantrill SJ, Ridvan L, Ashton PR, Garrell RL, Stoddart JF (2002) *Tetrahedron* 58:807
176. Elizarov AM, Chiu S-H, Glink PT, Stoddart JF (2002) *Org Lett* 4:679; (2000) *Chem Eur J* 6:2274
177. Fujimori K, Yoshimoto H, Oae S (1980) *Tetrahedron Lett* 21:3385
178. Rowan SJ, Stoddart JF (1999) *Org Lett* 1:1913
179. Anelli PL, Ashton PR, Ballardini R, Balzani V, Delgado M, Gandolfi MT, Goodnow TT, Kaifer AE, Philp D, Pietraszkiewicz M, Prodi L, Reddington MV, Slawin AMZ, Spencer N, Stoddart JF, Vicent C, Williams DJ (1992) *J Am Chem Soc* 114:193
180. Ballardini R, Balzani V, Gandolfi MT, Gillard RE, Stoddart JF, Tabellini E (1998) *Chem Eur J* 4:449
181. Amabilino DB, Ashton PR, Stoddart JF, White AJP, Williams DJ (1998) *Chem Eur J* 4:460
182. Lyon AP, Macartney DH (1997) *Inorg Chem* 36:729
183. Fisher C, Nieger M, Mogck O, Bohmer V, Umgaro R, Vögtle F (1998) *Eur J Org Chem* 155
184. Benniston AC, Herrimen A, Lynch VM (1995) *J Am Chem Soc* 117:5275
185. Glink PT, Oliva AI, Stoddart JF, White AJP, Williams DJ (2001) *Angew Chem Int Ed* 10:1870
186. Kirby AJ (1996) *Angew Chem Int Ed Engl* 35:707
187. Nakash M, Clyde-Watson Z, Feeder N, Davies JE, Teat SJ, Sanders JKM (2000) *J Am Chem Soc* 122:5286
188. Horn M, Ihringer J, Glink PT, Stoddart JF (2003) *Chem Eur J* 9:4046
189. Cantrill SJ, Fyfe MCT, Heiss AM, Stoddart JF, White AJP, Williams DJ (2000) *Org Lett* 2:61
190. Luening U, Baumstark R, Peters K, von Schnering HG (1990) *Liebigs Ann.* 1990:129

191. van Reijndam JW, Heeres GJ, Janssen MJ (1970) *Tetrahedron* 26:1291
192. Lewis KG, Mulquiney CE (1979) *Aust J Chem* 32:1079
193. Dominguez C, Escobar G, Plumet J, Gaset A, Rigal L (1986) *An Quim Ser C* 82:241
194. Kavallieratos K, Crabtree RH (1999) *Chem Commun* 2109
195. Youngman MA, Dax SL (2001) *J Comb Chem* 3:469
196. Yamaguchi N, Gibson HW (1998) *Chem Commun* 789
197. Ashton PR, Fyfe MCT, Hickingbottom SK, Stoddart JF, White AJP, Williams DJ (1998) *J Chem Soc Perkin Trans 2*:2117
198. Cantrill SJ, Fulton DA, Heiss AM, Pease AR, Stoddart JF, White AJP, Williams DJ (2000) *Chem Eur J* 6:2274
199. Chang T, Heiss AM, Cantrill SJ, Fyfe MCT, Pease AR, Rowan SJ, Stoddart JF, White AJP, Williams DJ (2000) *Org Lett* 2:2947
200. Kilbinger AFM, Cantrill SJ, Waltman AW, Day MW, Grubbs RH (2003) *Angew Chem Int Ed* 42:3281
201. Schwab P, Grubbs RH, Ziller JW (1996) *J Am Chem Soc* 118:100
202. Scholl M, Ding S, Lee CW, Grubbs RH (1999) *Org Lett* 1:953
203. Lee WJ, Whitesides GM (1993) *J Org Chem* 58:642
204. Raehm L, Hamann C, Kern J-M, Sauvage J-P (2000) *Org Lett* 2:1991
205. Kolchinski AG, Alcock NW, Roesner RA, Busch DH (1998) *Chem Commun* 1437
206. Furusho Y, Hasegawa T, Tsuboi A, Kihara N, Takata T (2000) *Chem Lett* 18
207. Furusho Y, Oku T, Hasegawa T, Tsuboi A, Kihara N, Takata T (2003) *Chem Eur J* 9:2895
208. Takata T, Kawasaki H, Kihara N, Furusho Y (2001) *Macromolecules* 34:5449
209. Furusho Y, Rajkumar GA, Oku T, Takata T (2002) *Tetrahedron* 58:6609
210. Field L, Oae S (eds) (1997) *Organic chemistry of sulfur*. Plenum, New York
211. Lee RT, Lee YC (1995) *Acc Chem Res* 28:321
212. Lundquist JL, Toone EJ (2002) *Chem Rev* 102:555
213. Kitov PI, Bundle DR (2003) *J Am Chem Soc* 125:16271
214. Ercolani G (2003) *J Am Chem Soc* 125:16097
215. Christensen T, Gooden DM, Kung JE, Toone EJ (2003) *J Am Chem Soc* 125:7357
216. Breslow R, Greenspoon N, Guo T, Zarzycki R (1989) *J Am Chem Soc* 111:8296
217. Zhang B, Breslow R (1993) *J Am Chem Soc* 113:9353
218. Drickamer K (1995) *Struct Biol* 2:437
219. Jayaraman N, Nepogodiev SA, Stoddart JF (1997) *Chem Eur J* 3:1193
220. Venema F, Nelissen HFM, Berthault P, Birlirakis N, Rowan AE, Feiters NC, Nolte RJM (1998) *Chem Eur J* 4:2237
221. Rockendorf N, Lindhorst TH (2001) *Top Curr Chem* 217:201
222. Turnbull WB, Stoddart JF (2002) *Rev Mol Biotech* 90:231
223. Gibson HW, Yamaguchi N, Hamilton L, Jones JW (2002) *J Am Chem Soc* 124:4653
224. Dubber M, Fréchet JMJ (2003) *Bioconjugate Chem* 14:239
225. Huang F, Fronczek FR, Gibson HW (2003) *J Am Chem Soc* 125:9272
226. Mammen M, Choi S-K, Whitesides GM (1998) *Angew Chem Int Ed* 37:2754
227. Lee RT, Lee YC (2000) *Glyconjugate J* 17:543
228. Kiessling LL, Gestwicki JE, Strong LE (2000) *Curr Opin Chem Biol* 4:696
229. Arranz-Plaza E, Tracy AS, Siriwardena A, Pierce JM, Boons GJ (2002) *J Am Chem Soc* 124:13035
230. Rao J, Lahiri J, Isaacs L, Weiss RM, Whitesides GM (1998) *Science* 280:708
231. Kitov PI, Sadawska JM, Mulvey G, Armstrong GD, Ling H, Pannu NS, Read RJ, Bundle DR (2000) *Nature* 403:669
232. Rao J, Lahiri J, Weiss RM, Whitesides GM (2000) *J Am Chem Soc* 122:2698
233. Calama MC, Timmerman P, Reinhoudt DN (2000) *Angew Chem Int Ed* 39:755

234. Gestwicki JE, Cairo CW, Strong LE, Oetjen KA, Kiessling LL (2002) *J Am Chem Soc* 124:14922
235. Woller EK, Walter ED, Morgan JR, Singel DJ, Cloninger MJ (2003) *J Am Chem Soc* 125:8820
236. Tobey SL, Anslyn EV (2003) *J Am Chem Soc* 125:10963
237. Ashton PR, Fyfe MCT, Glink PT, Stephan MJ, Stoddart JF, White AJP, Williams DJ (1997) *J Am Chem Soc* 119:12514
238. Chang T, Heiss AM, Cantrill SJ, Fyfe MCT, Pease AR, Rowan SJ, Stoddart JF, Williams DJ (2000) *Org Lett* 2:2943
239. Fulton DA, Cantrill SJ, Stoddart JF (2002) *J Org Chem* 67:7968
240. Lowe JN, Fulton DA, Chiu S-H, Elizarov AM, Cantrill SJ, Rowan SJ, Stoddart JF (2004) *J Org Chem* 69:4390
241. Fyfe MCT, Lowe JN, Stoddart JF, Williams DJ (2000) *Org Lett* 2:1221
242. Balzani V, Clemente-Leon M, Credi A, Lowe JN, Badjic JD, Stoddart JF, Williams DJ (2003) *Chem Eur J* 9:5348
243. Kolb HC, Finn MG, Sharpless KB (2001) *Angew Chem Int Ed* 40:2004
244. Badjic JD, Balzani V, Credi A, Lowe JN, Silvi S, Stoddart JF (2004) *Chem Eur J* 10:1926
245. Badjic JD, Cantrill SJ, Stoddart JF (2004) *J Am Chem Soc* 126:2288
246. Badjic JD, Balzani V, Credi A, Silvi S, Stoddart JF (2004) *Science* 303:1845
247. Ashton PR, Ballardini R, Balzani V, Baxter I, Credi A, Fyfe MCT, Gandolfi MT, Gómez-López M, Martínez-Díaz MV, Piersanti A, Spencer N, Stoddart JF, Venturi M, White AJP, Williams DJ (1998) *J Am Chem Soc* 120:11932
248. Wisner JA, Beer PD, Drew MGB, Sambrook MR (2002) *J Am Chem Soc* 124:12469
249. Coumans RGE, Elemans JAAW, Thordarson P, Nolte RJM, Rowan AE (2003) *Angew Chem Int Ed* 42:650
250. Badjic JD, Cantrill SJ, Grubbs RH, Guidry EN, Orenes R, Stoddart JF (2004) *Angew Chem Int Ed* 43:3273
251. Stoddart JF (1992) *Chem Aust* 59:576,581
252. Gómez-López M, Preece JA, Stoddart JF (1996) *Nanotechnology* 7:183
253. Balzani V, Gómez-López M, Stoddart JF (1998) *Acc Chem Res* 31:405
254. Tseng H-R, Stoddart JF (2002) In: Astruc D (ed) *Modern arene chemistry*. Wiley-VCH 574
255. Harada A (2001) *Acc Chem Res* 34:456
256. Schalley CA, Beizai K, Vögtle F (2001) *Acc Chem Res* 34:465
257. Ballardini R, Balzani V, Credi A, Gandolfi MT, Venturi M (2001) *Struct Bonding* 99:55
258. Stanier CA, Alderman SJ, Claridge TDW, Anderson HL (2002) *Angew Chem Int Ed* 41:1769
259. Balzani V, Credi A, Venturi M (2002) *Chem Eur J* 8:5524
260. Anelli PL, Spencer N, Stoddart JF (1991) *J Am Chem Soc* 113:5131
261. Bissell RA, Córdova E, Kaifer AE, Stoddart JF (1994) *Nature* 369:133
262. Flood AH, Ramirez RJA, Deng W-Q, Muller RP, Goddard III WA, Stoddart JF (2004) *Aust J Chem* 57:301
263. Livoreil A, Dietrich-Buchecker CO, Sauvage J-P (1994) *J Am Chem Soc* 116:9399
264. Collin J-P, Gaviña P, Sauvage J-P (1997) *New J Chem* 21:525
265. Raehm L, Kern J-M, Sauvage J-P (1999) *Chem Eur J* 5:3310
266. Martínez-Díaz M-V, Spencer N, Stoddart JF (1997) *Angew Chem Int Ed Engl* 36:1904
267. Kelly TR, De Silva H, Silva RA (1999) *Nature* 401:150
268. Elizarov AM, Chiu S-H, Stoddart JF (2002) *J Org Chem* 67:9175
269. Raehm L, Kern J-M, Sauvage J-P (1999) *Chem Eur J* 5:3310
270. Gaviña P, Sauvage J-P (1997) *Tetrahedron Lett* 38:3521

271. Armaroli N, Balzani V, Collin J-P, Gaviña P, Sauvage J-P (1999) *J Am Chem Soc* 121:4397
272. Ashton PR, Ballardini R, Balzani V, Credi A, Dress KR, Ishow E, Kleverlaan CJ, Kocian O, Preece JA, Spencer N, Stoddart JF, Venturi M, Wenger S (2000) *Chem Eur J* 6:3558
273. Feringa BL, Koumara N, van Delden RA, Ter Wiel MKJ (2002) *Appl Phys A* 75:301
274. Blanco MJ, Jimenez MC, Chambron JC, Heitz V, Linke M, Sauvage J-P (1999) *Chem Soc Rev* 28:293
275. Mulder A, Jukovic A, Lucas LN, van Esch J, Feringa BL, Huskens J, Reinhoudt DN (2002) *Chem Commun* 2734
276. Preece JA, Stoddart JF (1994) *Nanobiology* 3:149
277. Colasson BX, Dietrich-Buchecker CO, Jimenez-Molero MC, Sauvage J-P (2002) *J Phys Org Chem* 15:476
278. Pease AR, Jeppesen JO, Stoddart JF, Luo Y, Collier CP, Heath JR (2001) *Acc Chem Res* 34:433
279. Hess H, Clemmens J, Qin D, Howard J, Vogel V (2001) *Nano Lett* 1:235
280. Yurke B, Turberfield AJ, Mills AP Jr, Simmel FC, Neumann JL (2000) *Nature* 406:605
281. Collin JP, Dietrich-Buchecker CO, Gaviña P, Jimenez-Molero MC, Sauvage J-P (2001) *Acc Chem Res* 34:477
282. Raehm L, Kern J-M, Sauvage J-P, Hamann C, Palacin S, Bourgoin J-P (2002) *Chem Eur J* 8:2153
283. Tseng H-R, Wu DM, Fang NXL, Zhang X, Stoddart JF (2004) *Chem Phys Chem* 5:111
284. Asakawa M, Higuchi M, Mattersteig G, Nakamura T, Pease AR, Raymo FM, Shimizu T, Stoddart JF (2000) *Adv Mater* 12:1099
285. Ahuja RC, Caruso PL, Mobius D, Wildburg G, Ringsdorf H, Philp D, Preece JA, Stoddart JF (1993) *Langmuir* 9:1534
286. Ahuja RC, Caruso PL, Mobius D, Philp D, Preece JA, Ringsdorf H, Stoddart JF, Wildburg G (1996) *Thin Solid Films* 285:671
287. Brown CL, Jonas U, Preece JA, Ringsdorf H, Seitz M, Stoddart JF (2000) *Langmuir* 16:1924
288. Long B, Nikitin K, Fitzmaurice D (2003) *J Am Chem Soc* 125:15490
289. Weber N, Hamann C, Kern J-M, Sauvage J-P (2003) *Inorg Chem* 42:6780
290. Luo Y, Collier CP, Jeppesen JO, Nielsen KA, Delonno E, Ho G, Perkins J, Tseng H-R, Yamamoto T, Stoddart JF, Heath JR (2002) *Chem Phys Chem* 3:519
291. Diehl MR, Steuerman DW, Tseng H-R, Vignon SA, Star A, Celestre PC, Stoddart JF, Heath JR (2003) *Chem Phys Chem* 4:1335

Molecular Knots

Christiane Dietrich-Buchecker · Benoît X. Colasson ·
Jean-Pierre Sauvage (✉)

Laboratoire de Chimie Organo-Minérale, CNRS UMR 7513, Faculté de Chimie,
Université Louis Pasteur, 67070 Strasbourg, France
sauvage@chimie.u-strasb.fr

1	Introduction	262
1.1	Topology: from the Arts to Mathematics	262
1.2	Biological Topology: DNA and Proteins	263
2	The Early Days of Chemical Topology	264
3	Towards Molecular Knots: Early Attempts	265
4	Molecular Knots Constructed on Dicopper(I) Helical Complexes	268
4.1	Strategy	268
4.2	A Synthetic Molecular Trefoil Knot: First Results [57]	270
4.3	Generalization and Improvements	271
4.4	Resolution of a Molecular Knot into its Enantiomers	275
5	Templated Synthesis of Molecular Knots Based on Hydrogen Bond-Sets	277
6	Conclusion	280
	References	281

Abstract Knots are fascinating non-trivial topological entities. They are not only present in art and history but in many scientific fields as well, from mathematics to biology. By targeting this tantalizing structure, chemists have contributed to the promotion of their beauty. So far, two very different template syntheses of molecular knots have been developed. The first one is based on the template effect induced by a transition metal, which gathers and disposes fragments in a predictable geometry. The second relies on the use of a suitable hydrogen bond-set. Together with the presentation of these two reliable strategies, this chapter stresses one of the intrinsic properties of a knot: its chirality. The resolution of the two kinds of molecular knots into their enantiomers is discussed.

Keywords Knot · Topology · Chirality · Coordination chemistry · Hydrogen bonding

1

Introduction

The present review article will mostly be focused on artificial molecular knots, but other types of molecular knots belonging to the biological world are very important. These synthetic knots used to represent very challenging chemical problems but, nowadays, they are reasonably accessible. If the synthesis of amazingly complex natural products is still an extremely active area of research (for recent work on antitumor drugs, see [1]), with formidable challenges¹, unnatural compounds also represent exciting objectives for many reasons. Beyond aims related to applications (molecular materials, pharmaceutical use, sensors, etc...), the making of a novel molecular system can represent an exciting challenge in itself, not only for possibly discovering the new properties of a so-far-unknown compound, but also for its attractive shape, topology, etc. In other words, the synthesis itself of the compound and the hypothetical properties of the target molecules are two distinct incitements. The synthesis of interlocking ring molecular systems and knots combines both sets of motivation but it also adds an aesthetic dimension to the chemical problem. Indeed the search for aesthetically attractive molecules has been a goal since the very origin of chemistry.

1.1

Topology: from the Arts to Mathematics

The aesthetic aspect of any object is usually connected to its shape in Euclidian geometry: the object is conveniently represented by points and lines, the metric properties (length of a segment, angles, etc.) being of utmost importance. In this case, the object cannot be put out of shape. However, another interesting facet of beauty rests in the topological properties of the object. Among the most fascinating objects displaying non-trivial topological properties, interlaced designs and knots occupy a special position.

Interlocking and knotted rings occupied a privileged position in the art of the most ancient civilizations. This virtually universal art reached its zenith in the Celtic culture. The magnificent illuminations consisting of the extremely complex interlaced designs and knots of the *Book of Kells* [3], an Irish incunabulum of the 8th century, give evidence of the fascination that braids, wreaths and knots exert on man. Some views of interlaced designs and knots are presented in Fig. 1. Modern art has also devoted special attention to knotted threads. The Dutch artist Cornelius Escher [4] is certainly one of the most popular artists among the community of chemists since many of his works contain volumes

¹ An impressively complex natural molecule is maitotoxin, a remarkable biologically active compound produced by the dinoflagellate *Gambierdiscus toxicus*. Presently, the total synthesis of this natural substance seems to be beyond the possibilities offered by modern synthesis [2].

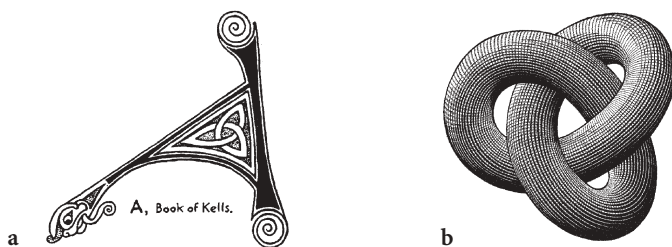


Fig. 1 a Remarkable lettering example taken from the *Book of Kells* (8th century) [3]. b Escher: the trefoil knot [4]

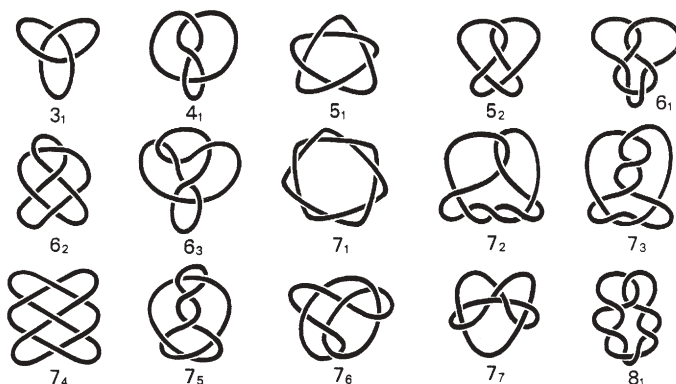


Fig. 2 First fifteen prime knots

and interlaces closely related to modern molecular sciences. The simplicity of his view of the trefoil knot makes it particularly attractive (Fig. 1b).

In mathematics, knots and links occupy a special position. They have been the object of active thinking for more than a century [5–7]. Any interested reader should have a look at a relatively recent and accessible small book entitled *The Knot Book* [8]. In Fig. 2 are represented the first twenty prime knots. These knots are single-knotted loops, in contrast to “links” (or catenanes, in chemistry), which are sets of knotted or unknotted loops, all interlocked together.

In 1994, Liang and Mislow presented fascinating discussions on knots and links in relation to chirality [9–10]. This breakthrough work should help bridge the gap between the communities of mathematical topologists and molecular chemists.

1.2

Biological Topology: DNA and Proteins

The discovery that DNA forms catenanes and knots, some of them being of extreme complexity, initiated a new field of research that has been called “bio-chemical topology” [11]. In 1967, Vinograd and coworkers detected in mito-

chondria “isolable DNA molecules that consist of independent, double-stranded, closed circles that are topologically interlocked or catenated like the links in a chain” [12, 13]. A few years later, catenanes had been observed everywhere that circular DNA molecules were known [14] and the first knot was found by Liu and coworkers in single-stranded circular phage fd DNA treated with *Escherichia coli* ω -protein [15]. In 1980, knots were also generated in double-stranded circular DNA [16]. A whole class of enzymes effect these topological transformations perfectly: they are called topoisomerases [17, 18]. Their possible role in a large variety of biological functions was, and still is, intensively studied. It is today commonly assumed that topoisomerases are able to solve the topological problems arising during replication, site-specific recombination and transcription of circular DNA [16, 19].

Besides naturally occurring DNA catenanes and knots, a fascinating family of related molecules has been synthesized and described by Seeman and coworkers [20]. The elegant approach of this group utilizes synthetic single-stranded DNA fragments, which are combined and knotted by topoisomerases.

Interestingly, DNA is not the only biological molecular system to have the privilege of forming catenanes and knots. Liang and Mislow examined X-ray structures of many proteins and, to the surprise of many molecular chemists and biochemists, they found catenanes and even trefoil knots [9, 10]. This remarkable finding addresses the general question of whether the topological properties of proteins have any biological significance. Recent work by Zhou seems to demonstrate that catenation of proteins increases very significantly the stability of their folded structures [21]. Similar conclusion were drawn from an interesting study on knotted properties [22]. It is particularly interesting to observe that Nature has utilized topology as a functional tool in order to control the properties of given proteins.

2

The Early Days of Chemical Topology

Turning now to pure chemistry and synthetic molecular objects, it is clear that the concept of catenanes has fascinated chemists for several decades. The application of graph theory to chemistry has created a new field called “chemical topology”. However, it must be stressed that rigorous mathematical treatments applied to molecules has existed only since the 1980s thanks to Walba’s use of graph theory for describing molecular systems [23].

Before being put into rigorous theory, chemical topology received much interest from many scientists and several contributions of utmost importance are worth mentioning. The famous book written by Schill and published in 1971 [24] is an absolute “must”. But the first theoretical written discussion to appear on chemical topology was a publication by Frisch and Wasserman [25]. This general article seems to be the cornerstone of the field since it contains, expressed in a very chemical and accessible language, most of the notions that

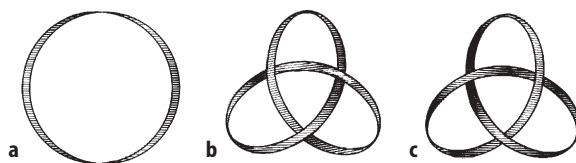


Fig. 3 Trefoil knot: a closed ring with a minimum of three crossing points. The rings **a**, **b** and **c** are topological stereoisomers; the two knots **b** and **c** are topological enantiomers

constitute the background of chemical topology. The idea of topological isomers was introduced in this pioneering paper. It is best exemplified using a single closed curve: normal (topologically trivial) or knotted cycle (the most simple non-trivial knot being the trefoil knot). The three objects **a**, **b**, and **c** of Fig. 3 are topological stereoisomers: although they may consist of exactly the same atoms and chemical bonds connecting these atoms, they cannot be interconverted by any type of continuous deformation in three-dimensional space. In addition, the compounds of Fig. 3b and Fig. 3c are topological enantiomers since the mirror image of any presentation of Fig. 3b is identical to a given presentation of Fig. 3c.

Two other historically important discussions are worth mentioning: (i) A very imaginative paper was written by Van Gülick (Eugene, University of Oregon, USA) at the beginning of the 1960s but, unfortunately, the manuscript was not accepted for publication at that time. It was published [26] in a special issue of the *New Journal of Chemistry* devoted to chemical topology, along with many other contributions spanning from mathematical topology to polymers and DNA [27]. (ii) A review by Sokolov [28] which appeared in Russian literature and which is particularly relevant to the present discussion since it mentions the possible use of a transition metal center as template to prepare a trefoil knot.

3 Towards Molecular Knots: Early Attempts

The “Möbius strip” approach, depicted in Fig. 4 and first suggested by Frisch and Wasserman in 1961 [25], is attractive although extremely difficult to realize.

In this approach, it is envisaged that the target molecule **3** can be obtained after cleavage of the vertical rungs of compound **2**, which in turn is prepared from the ladder-shaped molecule **1**, the ends of which are able to twist prior to

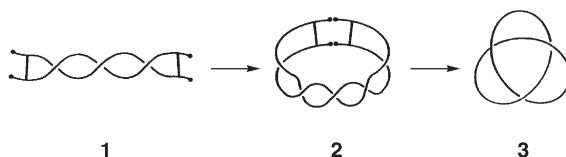


Fig. 4 Möbius strip approach (three half-twists) to a trefoil knot

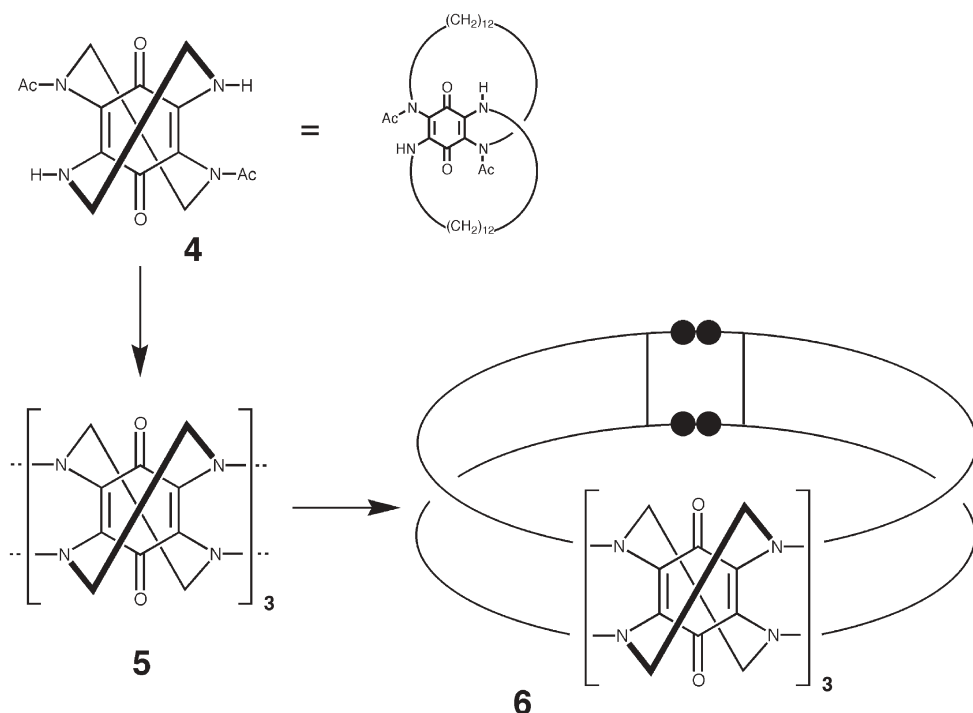


Fig. 5 Particularly attractive way of introducing three half twists in a molecular ladder, as envisaged by Schill and group [30]

bimacrocyclization. Walba and coworkers [29] have done very elegant work along a strategy close to that of Fig. 4. Unfortunately, formation of twisted species similar to **3** could not be demonstrated.

A directed knot synthesis relying upon the Möbius strip principle was conceived by Schill and coworkers [30–39] who synthesized the doubly bridged tetraamino-*p*-benzoquinone **4**. Connection of three such molecules by long chains should give the molecular ladder **5**, precursor of the three half-twist containing Möbius strip **6** (Fig. 5).

Nevertheless, despite the elegance of its principle, this synthesis did not yield a trefoil knot, because of the large number of steps required. The same authors also attempted the directed synthesis of a trefoil knot, which relied on the use of a benzo-acetal central core [32, 33]. These syntheses are closely related to the ones that this group had already used successfully to prepare various [2]- and [3]catenanes [34–38].

A very interesting approach towards a trefoil knot can be found in Sokolov's review [28]. The principle of the synthesis imagined by this author as early as 1973 is given in Fig. 6.

Three bidentate chelates disposed in a suitable fashion around an octahedral transition metal used as a matrix may, after connection of their ends, lead to a

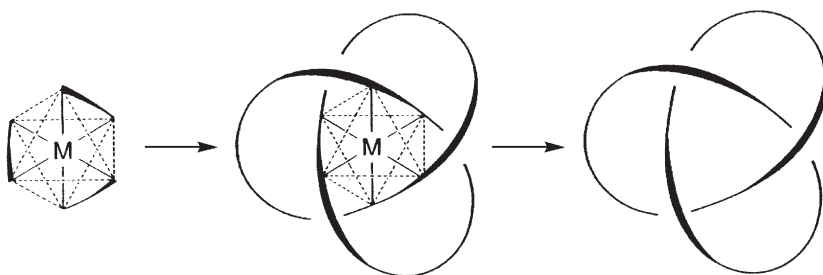


Fig. 6 Sokolov's strategy for constructing a trefoil knot on an octahedral tris-chelate complex [28]

molecular knot. Obviously, the probability that the six ends will connect (two by two) in the required fashion is quite low. Nevertheless, strict geometrical control of the involved coordinated fragments or slight changes in the above proposed scheme may one day give access to a knot using this strategy. Recently, an “open” knot was prepared using a different but related strategy by Hunter and coworkers [40]. The three chelates have been incorporated in a single linear fragment 7. The synthesis of the knotted molecule 8^{2+} is represented in Fig. 7.

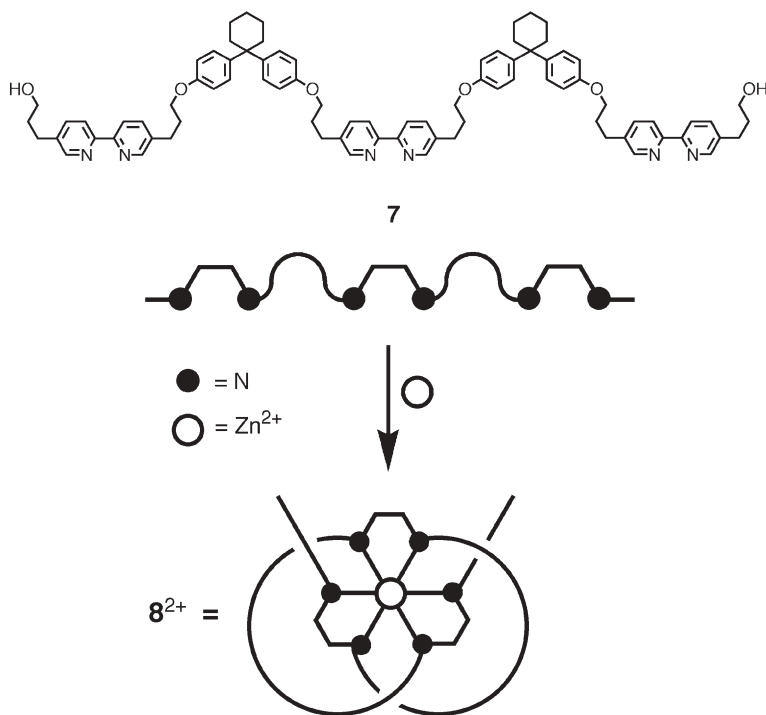


Fig. 7 Synthesis of an “open” knot using a linear fragment 7, which can wrap itself around an octahedral metal center such as Zn^{2+} to afford an “open” knot 8^{2+} [40]

4

Molecular Knots Constructed on Dicopper(I) Helical Complexes

4.1

Strategy

The templated synthesis towards a trefoil knot derives directly from the synthetic concept that had already afforded an easy access to catenanes. The strategy of the catenane synthesis relied on the well-known specific property of transition metals, namely their ability to gather and dispose ligands in a given predictable geometry, thus inducing what is generally called a template effect.

In the presence of copper(I), 2,9-dianisyl-1,10-phenanthroline or related compounds such as **9** form a very stable pseudo-tetrahedral complex (**10⁺**) in which the two ligands are intertwined around the metallic center. Due to its very special topography [41], this complex appeared to be a perfect precursor for a templated catenane synthesis as shown in Fig. 8.

The functionalized ligand 2,9-di(p-hydroxyphenyl)-1,10-phenanthroline **9** was prepared by the addition of lithioanisole to 1,10-phenanthroline, leading to 2,9-dianisyl-1,10-phenanthroline, which was subsequently deprotected by the pyridine hydrochloride procedure [42–44]. In the presence of $\text{Cu}(\text{CH}_3\text{CN})_4\text{BF}_4$, two ligands **9** fit together by forming the very stable copper(I) complex **10⁺**. The

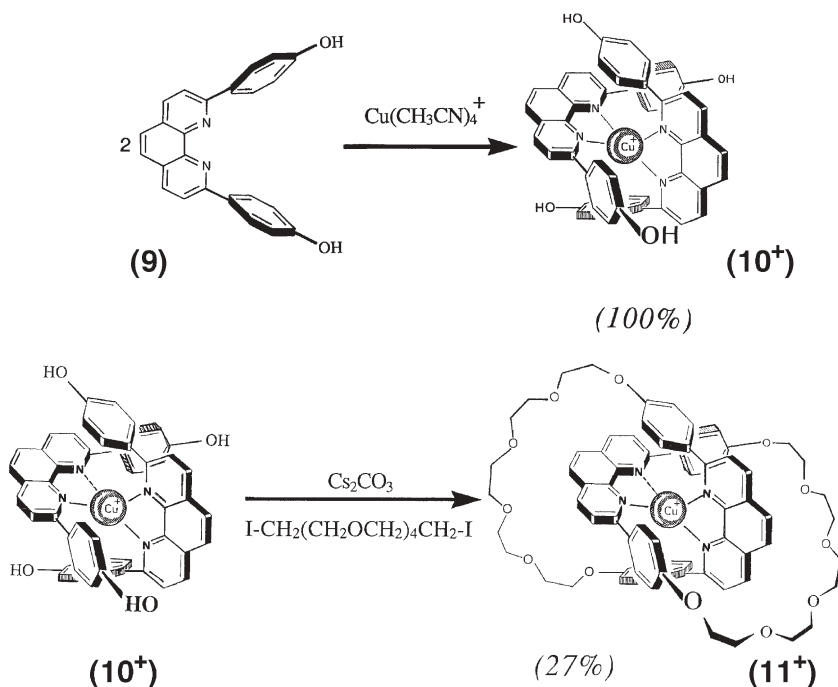


Fig. 8 One-pot preparation of the first metallo-catenane (=catenane) **11⁺** [43]

latter reacts with two equivalents of di-iodo derivative of pentaethylene glycol under high-dilution conditions in the presence of cesium carbonate in dimethylformamide. By this very convenient one-pot synthesis, the expected copper(I) [2]catenane **11**⁺ could be obtained in 27% yield. It should be noted that, more recently, two different, also highly efficient template catenane syntheses have been developed; one of them, first introduced by Stoddart and his coworkers [45] is based on the π -donor/ π -acceptor gathering effect between aromatic nuclei, whereas in the second one, mainly developed by Hunter and Vögtle and their coworkers, gathering and orientation of the various subunits of the future catenane are induced by hydrogen bondings [46–48].

The success encountered in the synthesis of various catenanes following the strategy depicted in Fig. 8 led to a molecular trefoil knot synthesis by extending the former synthetic concept from one to two copper(I) ions. As shown in Fig. 9, two bis-chelating molecular threads (A) can be interlaced on two transition metal centers, leading to a double helix (B). After cyclization to (C) and demetalation, a knotted system (D) should be obtained. An important prerequisite for the success of this approach is the formation of a helical dinuclear complex (B).

Although the preparation of double helices from various transition metals and bis-chelate ligands is very likely to have occurred long ago, it is only relatively recently that the first such system was recognized and characterized [49]. Moreover, the scientific interest of these arrangements was not at all obvious. One of the earliest dinuclear helical complex was identified by Fuhrhop and coworkers in 1976 [49]. During the 1980s, several laboratories prepared and investigated double-stranded helical complexes, the systems containing either pyrrolic ligands [50] and derivatives [51] (with Zn^{2+} , Ag^+ , Cu^+) or oligomers of

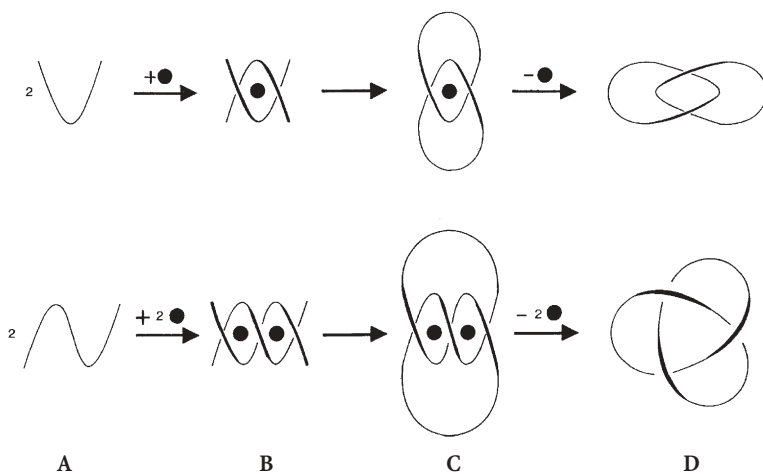


Fig. 9 Strategy leading to a trefoil knot is represented on the *bottom line*. It involves two metal centers and two coordinating organic threads. On the *upper line*, the synthesis principle of a [2]catenane is also given, to show the analogy between both strategies

2,2'-bipyridine [52, 53]. "Helicates" [52–56] may consist of up to five copper(I) centers and these systems are reminiscent of the DNA double helix.

4.2

A Synthetic Molecular Trefoil Knot: First Results [57]

After many attempts with various linkers, it was found that 1,10-phenanthroline nuclei connected via their 2-positions by a $-(\text{CH}_2)_4$ -linking unit will indeed form a double helix when complexed to two copper(I) centers. In addition, by introducing appropriate functions at the 9-positions, the strategy of Fig. 9 could be followed to achieve the synthesis of a molecular knot of the (D) type. The precursors used and the reactions carried out are represented in Fig. 10.

The diphenolic bis-chelating molecular thread **12** (prepared in a few steps starting from 1,10-phenanthroline and $\text{Li}-(\text{CH}_2)_4\text{-Li}$ [58]) was reacted with a stoichiometric amount of $\text{Cu}(\text{CH}_3\text{CN})_4\text{BF}_4$ to afford the dinuclear precursor double helix **13**²⁺ together with an important proportion of other copper(I) complexes. The complex mixture containing the double helix was reacted under high dilution conditions with two equivalents of the di-iodo derivative of hexaethyleneglycol in the presence of cesium carbonate. After a long and difficult purification process, the bis-copper(I) complex **14**²⁺ could be isolated in 3% yield. Its knotted topology, first evidenced by mass and NMR spectroscopy, was later fully confirmed by an X-ray structure determination [59] (Fig. 11).

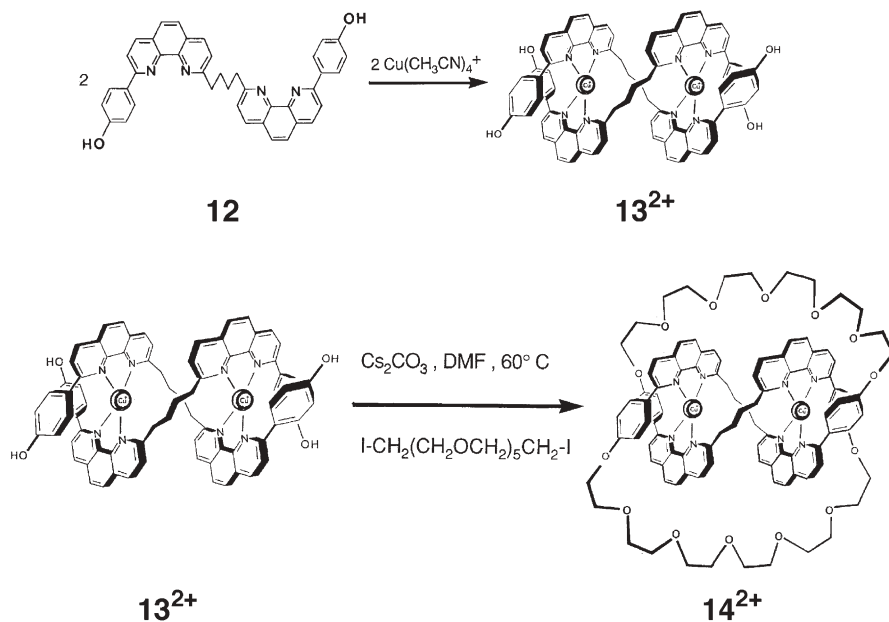


Fig. 10 Organic precursor and the reaction scheme leading to the dicopper(I) trefoil knot **14**²⁺. The main limitation is due to the poor yield of the double-stranded helical precursor **13**²⁺

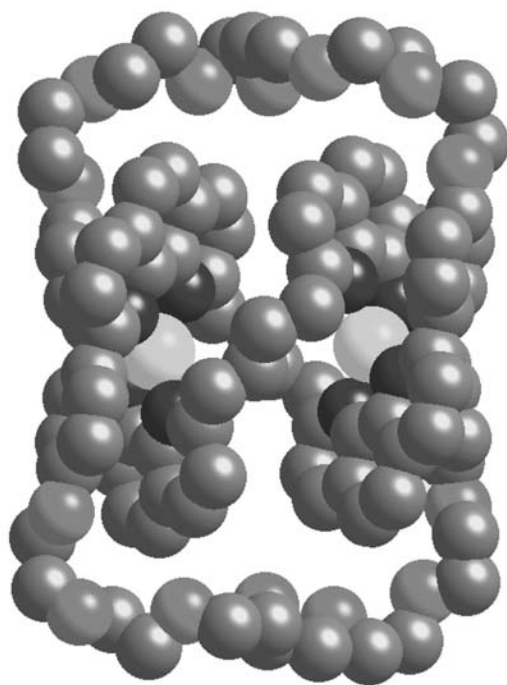


Fig. 11 X-ray structure of the knot 14^{2+} [59]

Treatment of 14^{2+} by a large excess of potassium cyanide led quantitatively to the free knot **15** whose topological chirality could be demonstrated by NMR and mass spectroscopy (Fig. 12).

4.3

Generalization and Improvements

The modest yield (only 3%) obtained for the original dicopper knotted 86-membered ring could be significantly improved by modifying the length of the linker connecting the two chelates and the long functionalized chain used in the cyclization step [60]. The best yields obtained were in the range of 8% but, using polymethylene linkers between the phenanthroline nuclei, it turned out to be the upper limit.

A spectacular improvement could be obtained by using a 1,3-phenylene spacer between the coordinating units [61]. The bis-chelate organic precursor **16** as well as the reactions leading to the dicopper(I) trefoil knot 17^{2+} are represented in Fig. 13.

The diphenolic bis-chelate **16** was obtained in good yield by reacting 2-(*p*-anisyl)-1,10-phenanthroline with 1,3-dilithio-benzene in tetrahydrofuran, followed by hydrolysis, MnO_2 oxidation and subsequent demethylation in usual conditions.

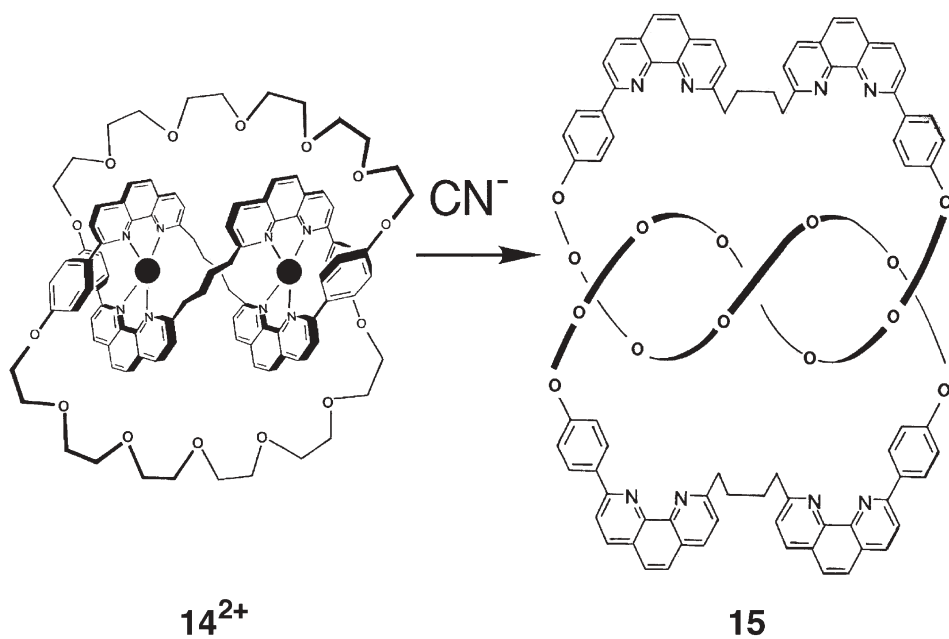


Fig. 12 Demetalation of the dicopper(I) knot **14²⁺** by CN^- leading to the free trefoil knot **15**

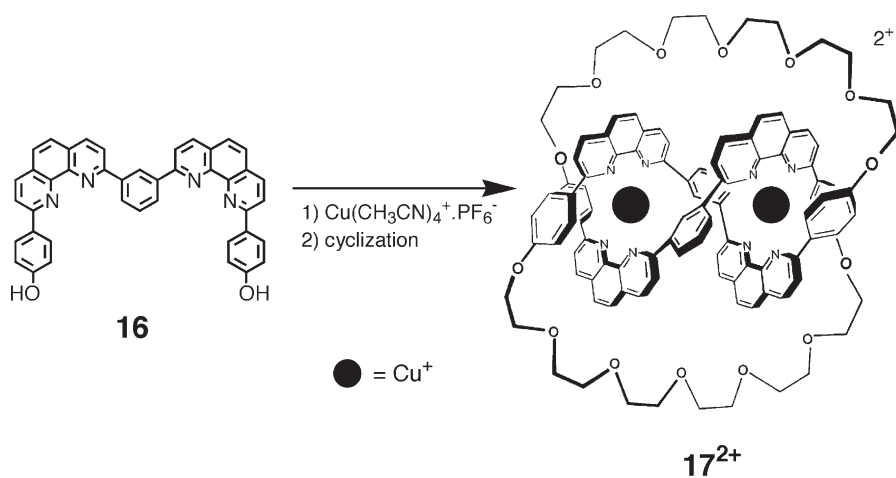


Fig. 13 Reaction scheme leading to the dicopper(I) trefoil knot **17²⁺**. In this case, the formation of the helical precursor from copper(I) and the bis-chelate **16** is quantitative

Preparation of the double-stranded helical precursor turned out to be quantitative. Reaction of this tetraphenolic double helix with two equivalents of the di-iodo derivative of hexaethyleneglycol, in the presence of cesium carbonate, afforded a single isolable copper(I) complex (Fig. 13). The dicopper(I) knot 17^{2+} was isolated in 29% yield after chromatography. It forms sea urchin-shaped aggregates of crystals (as BF_4^- salt).

^1H -NMR spectroscopy data [61] indicate that 17^{2+} contains a compact helical core. This was fully confirmed by its subsequent X-ray structure determination [62].

In 1992, Grubbs and coworkers published the synthesis of a new family of metallo-carbenes and developed their use as catalysts for ring-closing metathesis (RCM) reactions [63–65]. Gradually, these compounds were used by a large number of research groups and, nowadays, this new methodology can be considered as one of the major developments of transition metal-assisted organic synthesis of the last decade. In a collaborative research project between the Grubbs group and our team, we could show that the RCM strategy is particularly well adapted to the synthesis of copper(I)-complexed catenanes [66]. A natural extension of this work was the preparation of a trefoil knot following the strategy depicted in Fig. 14.

The helical precursor 19^{2+} was obtained in quantitative yield from **18** and Cu(I). The double ring closing metathesis reaction of the terminal olefins catalyzed by $\text{RuCl}_2(\text{PCy}_3)_2(=\text{CHPh})$ (Ph=phenyl, Cy=cyclohexyl) afforded the trefoil knot 20^{2+} in 74% yield [67] (Fig. 15). The only other products were oligomers due to intermolecular metathesis reactions.

The dicopper(I) trefoil knot 20^{2+} was first obtained as a mixture of isomers (*cis-cis*, *cis-trans* and *trans-trans* products), due to the *cis* or *trans* nature of the two cyclic olefins formed. These olefins can be easily and quantitatively reduced at room temperature by catalytic hydrogenation.

Combining the quantitative formation and high stability of the helical precursor composed of Cu(I) bisphenanthroline units with 1,3-phenylene linkers (between the phen moieties) and the highly efficient RCM methodology developed by Grubbs and coworkers, the dicopper(I) trefoil knot 20^{2+} could be obtained in seven steps from commercially available 1,10-phenanthroline, with an overall yield of 35% [67].

Due to the significant yield improvements, it became possible to study the specific properties of the knots related to their topology, to resolve both enan-

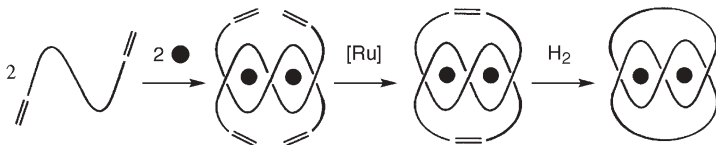


Fig. 14 Synthetic strategy: Two coordinating fragments bearing terminal olefins are gathered and interlaced around two copper(I) centers. Ring-closing metathesis with Grubbs ruthenium catalyst affords the knot

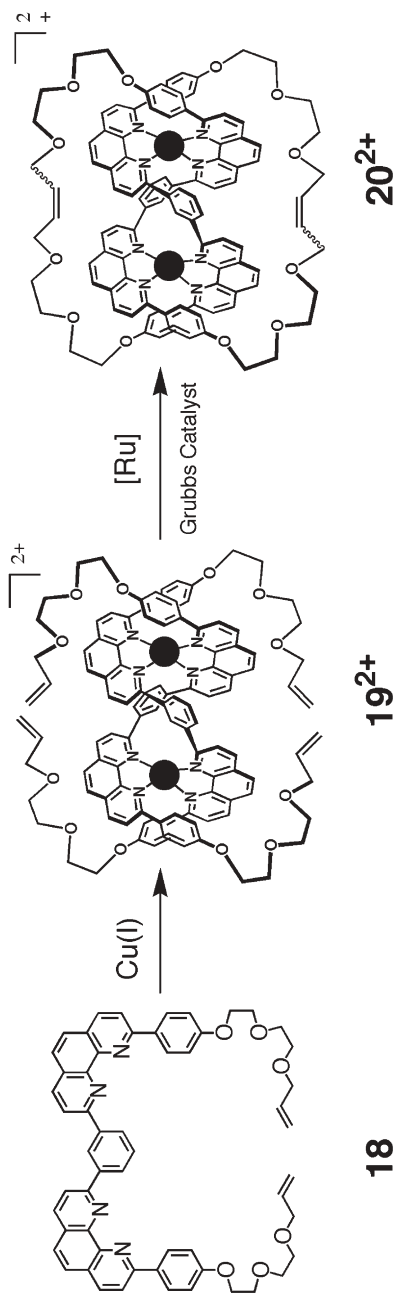


Fig. 15 The dicopper(II) knot prepared by ring-closing metathesis and its precursors

tiomers, and also to study their coordination chemistry. It also became possible to prepare the first chemical knot composite [68] and to prove its complex and unusual topology. For space reasons, we will not discuss in detail the coordination properties of the knotted ligands. However, it should be noted that the various complexes of such ligands display extraordinary kinetic inertness towards de-metalation [69]. In addition, due the close proximity between the two copper centers in the helical core of the knot, novel electronic properties could be evidenced [70]. In particular, the Cu(II)-Cu(II) oxidation state is strongly destabilized, as shown by the extremely high redox potential of the system (~ 0.9 V vs. SCE in acetonitrile) which makes it almost unique in copper chemistry.

4.4

Resolution of a Molecular Knot into its Enantiomers

The chirality of a molecular system can generally be analyzed in terms of Euclidian geometry, using metric elements (distances and angles) [71–72]. Topological chirality is an upper level of description of a molecular object, which implies that its molecular graph be non-planar [73–75]. Made of a single-knotted closed ring, the trefoil knot, which requires a minimum of three crossing points for its representation in a two-dimensional space, can be considered as the prototypical example of an unconditionally topologically chiral object (no need to orient nor color edges for the species to be chiral) [76, 77].

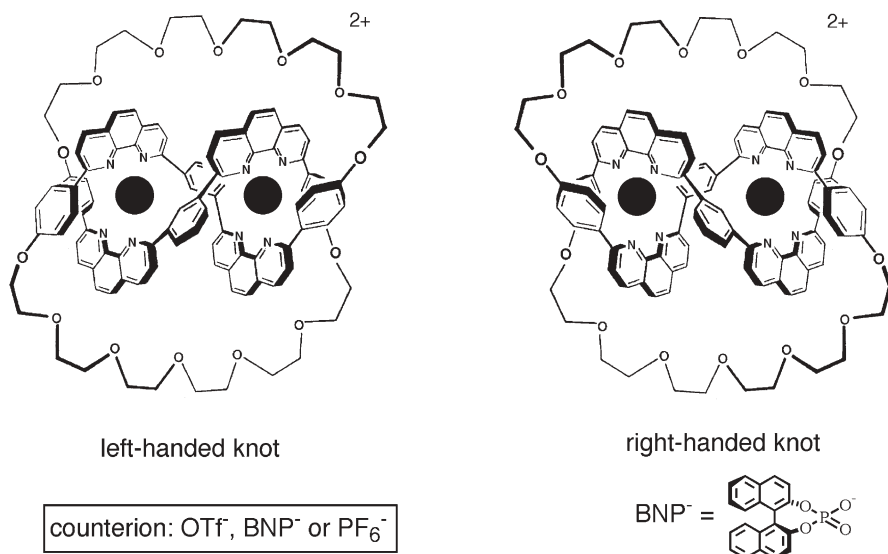


Fig. 16 Resolution of the dicopper(I) molecular trefoil knot 17^{2+} . The chiral auxiliary used is (S)-(+)-1,1'-binaphthyl-2,2'-diyl phosphate (BNP⁻). The cationic species are true topological enantiomers

Resolution using chiral supports in HPLC turned out to be successful for the separation of chiral catenates [78, 79]. Unfortunately, this technique seemed to be inappropriate to the resolution of the knot.

The copper(I)-templated syntheses of knots implies that the target molecules are obtained as cationic dicopper(I) complexes. Therefore, the possibility of interconverting both enantiomers into a pair of diastereomeric salts [80, 81] by combining them with an optically active anion was considered. The chirality of binaphthyl phosphate (BNP^-) [82] arises from the binaphthyl core, which is twisted. This helical structure is of the same type as that of the copper(I) double helix, precursor of the knot. Besides, both compounds are aromatic and thus we could expect some potentially helpful stacking interactions. These structural similarities should enable strong interactions between the two moieties, possibly leading to a marked differentiation of the properties of both diastereomers (e.g., their solubility), making their resolution possible by selective crystallization.

The molecular structure of the chiral auxiliary used is represented in Fig. 16. Both enantiomers of the dicopper(I) knots are also depicted.

To introduce the chiral auxiliary, a labile anion, unlike the classical BF_4^- or PF_6^- , which cannot be exchanged, is required. Preliminary studies showed the triflate to be appropriate. It was introduced during the formation step of the double helix. One equivalent of copper(I) triflate was added to the bischelating diphenolic strand **16** (Fig. 13) in a reductive medium. ^1H -NMR showed that the dinuclear copper(I) double helix **17**²⁺ (Fig. 13) was formed quantitatively, the counterion being now $\text{CF}_3\text{-SO}_3^-$. The bicyclization reaction afforded the racemic copper(I) knot triflate **17**²⁺.**2TfO**⁻ in 23% yield.

The racemic mixture of the knot was converted into diastereomers using a liquid-liquid extractor taking advantage of the solubility of potassium triflate in water compared to the insolubility of binaphthylphosphate salts.

The ^1H -NMR spectrum of the diastereomeric mixture appeared to be very striking: each signal was split into two, which clearly indicated a strong difference of association between the chiral auxiliary and each enantiomer of the knot. This difference was large enough to give the two diastereomers different solubilities. Indeed (+)-**17**²⁺.**2(+)-BNP**⁻ could be crystallized in a mixture of nitromethane and benzene [83], whereas the laevorotatory knot remained in the mother liquor.

To our knowledge, this was the first preparative resolution of topological enantiomers.

In order to obtain the pure topological enantiomers, and not diastereomeric salts, the chiral auxiliary was easily replaced by the hexafluorophosphate anion. The optical rotatory power was found to be very high. Considering the D-ray of sodium (589 nm), the optical rotatory power was + or $-7,000^\circ\text{mol}^{-1}\text{L dm}^{-1}$. The circular dichroism (CD) spectra of both enantiomers are shown in Fig. 17. As one would expect for such molecules, the two spectra are mirror images of one another.

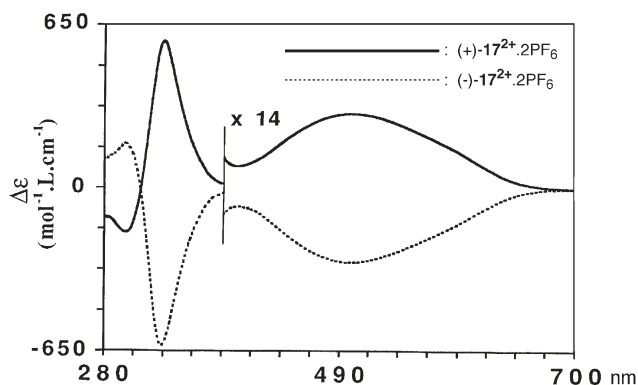


Fig. 17 Circular dichroism spectra of both enantiomers (in CH_2Cl_2); these are perfect mirror images

Of course, it also seemed to be of great interest to obtain the enantiomerically pure free ligands, in order to investigate the properties of a molecule for which chirality was exclusively originating from its topology (i.e., had nothing to do with that of transition metal complexes). It should be mentioned here that pure classical Euclidian chirality is present in the double helix of the metalated species. Each enantiomer was thus demetalated using cyanide as copper(I) quencher. The optical rotatory power of the free knot [(+) or (-)-(K-84)_p] was then + or $-2.000^\circ \text{mol}^{-1} \text{L dm}^{-1}$. Interestingly, the demetalated knot can be considered as two intertwined helices and the values obtained can be compared to those measured for heterohelices of similar structures [84–86].

By definition, topologically chiral molecules are those whose enantiomers cannot be interconverted by continuous deformation and therefore racemization is totally excluded as long as no bond in their organic backbone is broken. In addition, the combination of this latter topological property with the high thermodynamic stability of copper(I) 2,9-diphenylphenanthroline complexes provides such complexes with promising catalytic properties for enantioselective processes.

5

Templated Synthesis of Molecular Knots Based on Hydrogen Bond-Sets

Until the recent contribution by Vögtle and coworkers, only one example of a molecular trefoil knot synthesis based on organic templates had been reported in the literature [87]. Due to its sophisticated topology, this synthesis must be based on a reliable template intermediate. The work of Vögtle and coworkers on the templated synthesis of [2]catenanes based on hydrogen bonds serendipitously led to a very efficient preparation of a molecular knot [88]. In the course of the synthesis of [n]catenanes, the macrocycle **21**, presenting two concave

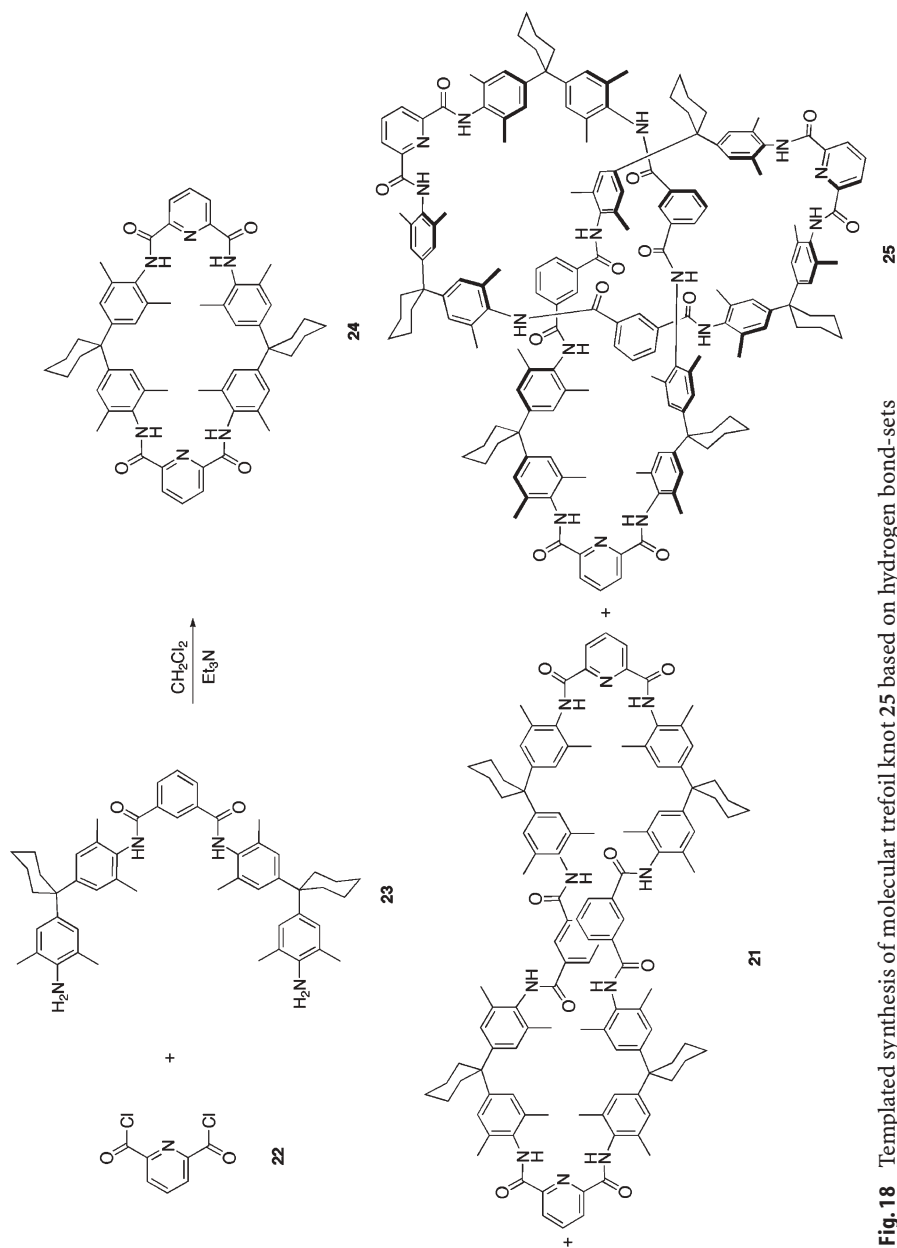


Fig. 18 Templated synthesis of molecular trefoil knot 25 based on hydrogen bond-sets

sites for hydrogen bonding interactions, was identified as a good intermediate. The synthesis of **21**, consisting of the reaction between 2,6-pyridinedicarboxylic acid dichloride **22** and diamine **23**, in the presence of triethylamine under high dilution conditions (10^{-3} mM in dichloromethane), gave **25** as a colorless product in 20% yield along with the smaller macrocycle **24** (15% yield) and **21** (23% yield) (Fig. 18).

The first analysis (^1H NMR and mass spectrometry) did not provide enough information to determine the structure of **25** (knotted or not knotted? Catenated or not catenated?). The molecular weight of **25** corresponded to a 3:3 macrocyclization. The [3]catenane-type structure (consisting of 2 macrocycles of **24** and one macrocycle of **21**) was excluded because of the fragmentation pattern of the mass spectrum. No more structural evidence could be obtained before the successful crystallization of **25** which, unexpectedly, was found to be a molecular trefoil knot.

The knotted structure could be rationalized from the crystal structure of **25**, which showed a pattern of hydrogen bonds between amide groups (Fig. 19). A similar pattern is also found in the templated synthesis of [2]catenanes and rotaxanes [46].

Further studies of the two precursors **22** and **23** proved the reliability of this templated synthesis and leading to a large number of molecular knot analogs of **25** [89–90] and more exotic structures [91].

The intrinsic chirality of a molecular knot was introduced earlier. Chromatographic methods were not suitable for the separation of the two enantiomers of the metal-templated trefoil knot, however, these techniques were successful in the amide-containing knot. In collaboration with the group of Prof. Okamoto, the

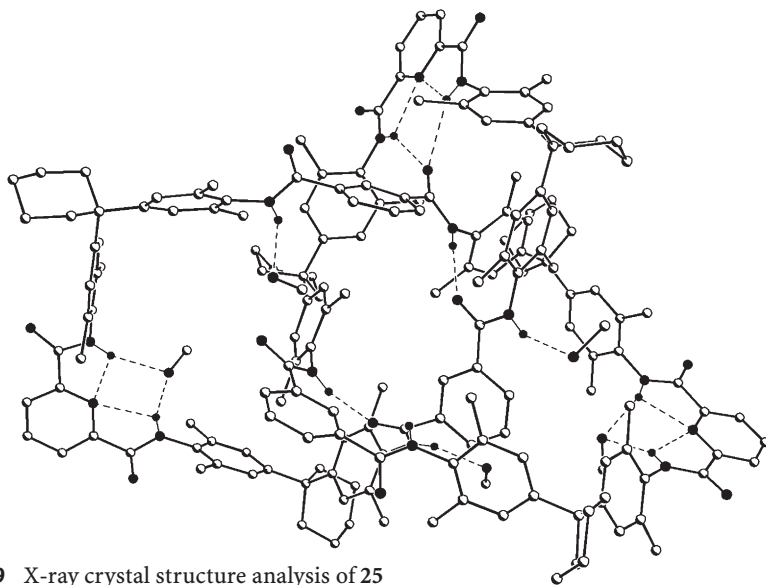


Fig. 19 X-ray crystal structure analysis of **25**

separation of the two enantiomers of six different knots was achieved [89]. A non-commercially available column (Chiral-AD type) was required since trichloromethane was needed to obtain an optimal separation. The silica gel and the chiral stationary phase were covalently bound so that the material did not bleed out when the lipophilic eluent was used.

Moreover, comparison of the experimental CD of the pure enantiomers of **25** with a theoretically calculated CD (based on X-ray structure and a fully optimized AM1 geometry) permitted assignment of the absolute configuration of this knot

6

Conclusion

Looking back at the first discussion on non-trivial knots in the chemical literature (1960), it is clear that very significant progress has been made as far as their synthesis is concerned. Transition metals have proved extremely useful in their ability to gather and intertwine string-like molecular fragments, before the appropriate ring-forming reactions are carried out. The second efficient approach is based on hydrogen bonding. This impressive synthetic achievement was probably not totally predicted by the authors themselves but the result is that another novel and really preparative method is now available. Because the first series of molecular knots stem from coordination chemistry, most of their interesting properties are related to transition metal chemistry. On the other hand, the Bonn series made by Vögtle and coworkers is purely organic and structurally much closer to biological molecules, new properties could be expected in relation to modeling biological processes such as the knotting or the catenation of proteins. Both series of molecular knots are thus complementary and it is expected that, in the future, other families of knotted molecules with distinct properties will also be made and studied. In this context, the properties of a pure polymethylene knotted ring should be fascinating, although the synthesis of such a compound seems to be presently out of reach.

Where will the chemistry of knots lead us? Today, it is of course difficult to know whether practical applications will be found, although one could easily imagine that polymers containing knotted fragments could be interesting organic materials or that knotted compounds able to interact in a specific way with DNA could display new biological properties. It remains that the field is still fascinating from a purely fundamental viewpoint. The challenge of making non-trivial prime knots beyond the trefoil knot is certainly worth considering, although when looking at the beautiful but very complex knots of Fig. 2, one can foresee great chemical difficulties.

Obviously, chirality is an essential property in molecular chemistry, and knots are exciting systems in this context. With a touch of fantasy, it could be conceived that some of the chemical processes for which chirality is essential

(enantioselection of substrates, asymmetric induction and catalysis, cholesteric phases and ferroelectric liquid crystals molecular materials for non linear optics etc.) could one day use enantiomerically pure knots. The future of molecular knots will, to a large extent, be determined by their accessibility and, even if the transition metal-templated strategy and the hydrogen bond-approach represent interesting synthetic achievements, there is still a long way to go before molecular knots can be made at a preparative scale compatible with industrial applications.

References

1. Nicolaou KC, Van Delft F, Ohshima T, Vourloumis D, Xu J, Hosokawa S, Pfefferkorn J, Kim S, Li T (1997) *Angew Chem Int Ed* 36:2520–2524
2. Sasaki M, Matsumori N, Maruyama T, Nonomura T, Murata M, Tachibana K, Yasumoto T (1996) *Angew Chem Int Ed* 35:1672–1674
3. Bain G (1973) In: *The methods of construction of Celtic art*. Dover, New-York
4. Locher JC (1971) In: *The world of M.C. Escher*. Abram, New York
5. Michel F, Weber C (1988) In: *Noeuds et Entrelacs*. Institut de Mathématiques, University of Geneva, Switzerland
6. Conway JH (1970) In: *Computational problems in abstract algebra*. Pergamon, New-York
7. Flapan E (1998) *Chaos Solit Frac* 9:547–560
8. Adams CC (1994) *The knot book*. Freeman, New York
9. Liang C, Mislow K (1994) *J Am Chem Soc* 116:11189–11190
10. Liang C, Mislow K (1995) *J Am Chem Soc* 117:4201–4213
11. Wasserman SA, Cozzarelli NR (1986) *Science* 232:951–960
12. Hudson B, Vinograd J (1967) *Nature* 216:647–652
13. Clayton DA, Vinograd J (1967) *Nature* 216:652–657
14. Kreuzer KN, Cozzarelli NR (1980) *Cell* 20:245–254
15. Liu LF, Depew RE, Wang JC (1976) *J Mol Biol* 106:439–452
16. Liu LF, Liu CC, Alberts BM (1980) *Cell* 19:697–707
17. Wang JC (1971) *J Mol Biol* 55:523–533
18. Gellert M, Mizuuchi K, O'Dea MH, Nash HA (1976) *Proc Natl Acad Sci USA* 73:3872–3876
19. Yang L, Wold MS, Li JJ, Kelly TJ, Liu LF (1987) *Proc Natl Acad Sci USA* 84:950–954
20. Seeman NC (1997) *Acc Chem Res* 30:357–363
21. Zhou HX (2003) *J Am Chem Soc* 125:9280–9281
22. Taylor WR, Lin K (2003) *Nature* 421:25
23. Walba DW (1985) *Tetrahedron* 41:3161–3212
24. Schill G (1971) In: *Catenanes, rotaxanes and knots*. Academic, New-York
25. Frisch HL, Wasserman E (1961) *J Am Chem Soc* 83:3789–3795
26. Van Gülick N (1993) *New J Chem* 17:619–625
27. Sauvage JP (ed) (1993) *Special issue*. *New J Chem* 17
28. Sokolov VI (1973) *Russian Chem Rev* 42:452–463
29. (a) Walba DW, Armstrong JD, Perry AE, Richards RM, Homan TC, Haltiwanger RC (1986) *Tetrahedron* 42:1883–1894; (b) Walba DW, Zheng QY, Schilling K (1992) *J Am Chem Soc* 114:6259–6260
30. Schill G, Tafelmair L (1971) *Synthesis* 10:546–548
31. Schill G, Keller U, Fritz H (1983) *Chem Ber* 116:3675–3684

32. Schill G, Doerjers G, Logemann E, Fritz H (1979) *Chem Ber* 112:3603–3615
33. Boeckmann J, Schill G (1974) *Tetrahedron* 30:1945–1957
34. Schill G, Lüttringhaus A (1964) *Angew Chem* 76:567–568
35. Schill G (1967) *Chem Ber* 100:2021–2037
36. Schill G, Zollenkopf H (1969) *Liebigs Ann. Chem* 721:53–74
37. Schill G, Zürcher C (1971) *Naturwissenschaften* 58:40–45
38. Schill G, Zürcher C (1969) *Angew Chem* 81:996–997
39. Schill G, Zürcher C (1977) *Chem Ber* 110:2046–2066
40. Adams H, Ashworth E, Breault GA, Guo J, Hunter CA, Mayers PC (2001) *Nature* 411:763
41. Dietrich-Buchecker CO, Marnot PA, Sauvage JP, Kintzinger JP, Maltès P (1984) *Nouv J Chim* 8:573–582
42. Dietrich-Buchecker CO, Sauvage JP (1983) *Tetrahedron Lett* 24:5091–5094
43. Dietrich-Buchecker CO, Sauvage JP, Kern JM (1984) *J Am Chem Soc* 106:3043–3045
44. Dietrich-Buchecker CO, Sauvage JP (1990) *Tetrahedron* 46:503–512
45. Ashton PR, Goodnow TT, Kaifer KE, Reddington MV, Slawin AMZ, Spencer N, Stoddart JF, Vincent C, Williams DJ (1989) *Angew Chem Int Ed* 28:1396–1399
46. Vögtle F, Meier S., Hoss R (1992) *Angew Chem Int Ed* 31:1619–1622
47. Jäger R, Vögtle F (1997) *Angew Chem Int Ed* 36:930–944
48. Hunter CA (1992) *J Am Chem Soc* 114:5303–5311
49. Fuhrhop JH, Struckmeier G, Thewalt U (1976) *J Am Chem Soc* 98:278–279
50. Sheldrick WS, Engel J (1980) *J Chem Soc Chem Commun* pp 5–6
51. Van Stein GC, Van der Poel H, Van Koten G (1980) *J Chem Soc Chem Commun* pp 1016–1018
52. Lehn JM, Rigault A, Siegel J, Harrowfield J, Chevrier B, Moras D (1987) *Proc Natl Acad Sci USA* 84:2565–2569
53. Lehn JM, Rigault A (1988) *Angew Chem Int Ed* 27:1095–1097
54. Constable EC, Drew MGB, Ward MD (1987) *J Chem Soc Chem Commun* 1600–1601
55. M. Barley, Constable EC, Corr SA, Mc Queen RCS, Nutkins JC, Ward MD, Drew MGB (1988) *J Chem Soc Dalton Trans* 2655–2662
56. Constable EC, Ward MD (1990) *J Am Chem Soc* 112:1256–1258
57. Dietrich-Buchecker CO, Sauvage JP (1989) *Angew Chem Int Ed* 28:189–192
58. West R, Rochow EG (1953) *J Org Chem* 18:1739–1742
59. Dietrich-Buchecker CO, Guilhem J, Pascard C, Sauvage JP (1990) *Angew Chem Int Ed* 29:1154–1156
60. (a) Dietrich-Buchecker CO, Nierengarten JF, Sauvage JP (1992) *Tetrahedron Lett* 33:3625–3628. Dietrich-Buchecker CO, Nierengarten JF, Sauvage JP, Armaroli N, Balzani V, De Cola L (1993) *J Am Chem Soc* 115:11237–11244;
(b) Albrecht-Gary AM, Dietrich-Buchecker CO, Guilhem J, Meyer M, Pascard C, Sauvage JP (1993) *Recl Trav Chim Pays-Bas* 112:427–428
61. Dietrich-Buchecker CO, Sauvage JP, De Cian A, Fischer J (1994) *J Chem Soc Chem Commun* 2231–2232
62. Dietrich-Buchecker CO, Rapenne G, Sauvage JP (1999) *Coord Chem Rev* 185–186:167–176
63. Fu GC, Grubbs RH (1994) *J Am Chem Soc* 114:5426–5427
64. Dias EL, Nguyen ST, Grubbs RH (1997) *J Am Chem Soc* 119:3887–3897
65. Schwab P, Grubbs RH, Ziller JW (1996) *J Am Chem Soc* 118:100–110
66. Mohr B, Weck M, Sauvage JP, Grubbs RH (1997) *Angew Chem Int Ed* 36:1308–1310
67. (a) Dietrich-Buchecker CO, Rapenne G, Sauvage JP (1997) *J Chem Soc Chem Commun* 21:2053–2054;
(b) Rapenne G, Dietrich-Buchecker CO, Sauvage JP (1999) *J Am Chem Soc* 121, 994–1001

68. Carina RF, Dietrich-Buchecker C, Sauvage JP (1996) *J Am Chem Soc* 118:9110–9116
69. Meyer M, Albrecht-Gary AM, Dietrich-Buchecker CO, Sauvage JP (1997) *J Am Chem Soc* 119:4599–4607
70. Dietrich-Buchecker CO, Sauvage JP, Armaroli N, Ceroni P, Balzani V (1996) *Angew Chem Int Ed* 35:1119–1121
71. Cahn RS, Ingold C, Prelog V (1966) *Angew Chem Int Ed* 5:385–415
72. Mislow K (1977) *Bull Soc Chim Belg* 86:595–601
73. Mislow K, Siegel J (1984) *J Am Chem Soc* 106:3319–3328
74. Eliel EL (1982) *Top Curr Chem* 105:1–76
75. Chambron JC, Dietrich-Buchecker CO, Sauvage JP (1993) *Top Curr Chem* 165:131–162
76. Liang C, Mislow K (1994) *J Math Chem* 15:35–62
77. Liang C, Mislow K (1994) *J Math Chem* 15:245–260
78. Mitchell DK, Sauvage JP (1988) *Angew Chem Int Ed* 27:930–931
79. Kaida Y, Okamoto Y, Chambron JC, Mitchell DK, Sauvage JP (1993) *Tetrahedron Lett* 34:1019–1022
80. Jacques J, Collet A, Wilen SH (1981) *Enantiomers, racemates and resolutions*, 1st edn. Wiley, New York
81. Pasteur L (1853) *CR Acad Sci* 37:162–166
82. Jacques J, Fouquey C (1989) *Org Synth* 67:1–12
83. (a) Rapenne G, Dietrich-Buchecker CO, Sauvage JP (1996) *J Am Chem Soc* 118:10932–10933; (b) Dietrich-Buchecker CO, Rapenne G, Sauvage JP, De Cian A, Fischer J (1999) *Chem Eur J* 5:1432–1439
84. Laarhoven WH, W.J.C. Prinsen (1984) *Top Curr Chem* 125:63–130
85. Meurer KP, Vögtle F (1985) *Top Curr Chem* 127, 1–76
86. Pereira DE, Leonard NJ (1990) *Tetrahedron* 46:5895–5908
87. Ashton PR, Matthews OA, Menzer S, Raymo FM, Spencer N, Stoddart JF Williams DJ *Liebigs Ann* (1997) 2485
88. Safarowsky O, Nieger M, Fröhlich R, Vögtle F (2000) *Angew Chem Int Ed* 39:1616
89. Vögtle F, Hüntten A, Vogel E, Buschbeck S, Safarowsky O, Recker J, Parham AH, Knott M, Müller WM, Müller U, Okamoto Y, Kubota T, Lindner W, Francotte E, Grimme S (2001) *Angew Chem Int Ed* 40:2468
90. Lukin O, Müller WM, Müller U, Kaufmann A, Schmidt C. Leszczynski J, Vögtle F (2003) *Chem Eur J* 9:3507
91. (a) Lukin O, Recker J, Böhmer A, Müller WM, Kubota T, Okamoto Y, Nieger M, Fröhlich R, Vögtle F (2003) *Angew Chem Int Ed* 42:442; (b) Recker J, Müller WM, Müller U, Kubota T, Okamoto Y, Nieger M, Vögtle F (2002) *Chem Eur J* 8:4434; (c) Lukin O, Kubota T, Okamoto Y, Schelhase F, Yoneva A, Müller WM, Müller, Vögtle F (2003) *Angew Chem Int Ed* 42:4542

Templation in Noncovalent Synthesis of Hydrogen-Bonded Rosettes

Mercedes Crego-Calama (✉) · David N. Reinhoudt ·
Mattijs G. J. ten Cate

Laboratory of Supramolecular Chemistry and Technology, MESA⁺ Institute
for Nanotechnology, University of Twente, PO Box 217, 7500 AE Enschede,
The Netherlands
m.cregocalama@utwente.nl

1	Introduction	286
2	Formation and Characterization of Rosette Assemblies	288
3	Guest Templated Selection and Amplification of the Strongest Binding Receptor in Dynamic Libraries	292
4	Templation for the Control of the Chirality in Supramolecular Systems . . .	294
4.1	Amplification of Chirality: “Sergeant and Soldiers Principle”	294
4.2	Enantioselective Noncovalent Synthesis: Memory of Supramolecular Chirality	296
4.3	Diastereomeric and Enantiomeric Noncovalent Synthesis of Double Rosettes by Guest Templation	298
4.4	Diastereomeric Noncovalent Synthesis of Tetra-rosettes by Guest Templation	301
5	Templated Synthesis by Noncovalent Assemblies	303
5.1	Templated Synthesis of Covalent Cyclic Calix[4]Arene Dimelamine Trimers	303
5.2	Templated Synthesis of Noncovalent Cyclic Hydrogen-Bonded Trimers	306
6	Surface Templation	307
6.1	Gold Surfaces	309
6.2	Graphite Surfaces	310
6.2.1	First-Order Template Effect	310
6.2.2	First- and Second-Order Template Effect	311
	References	315

Abstract In this chapter, hydrogen-bonded assemblies based on the rosette motif are used to describe some examples of templation in noncovalent synthesis.

After a brief description of the synthesis and characterization of these assemblies, the guest-templated selection and amplification of the strongest binding receptor in dynamic libraries is explained. The equilibrating mixtures of the rosette structures (dynamic combinatorial libraries) allow for the target-driven generation of the active constituents of the

library. A template effect for the formation and amplification of the strongest hydrogen-bonded receptor is obtained when a guest molecule is added to a library of potential hydrogen-bonded receptors that are under thermodynamic control.

Additionally, templation for the control of the chirality in these supramolecular systems is described at three different levels:

1. Amplification of chirality (“Sergeant and Soldiers” principle), where the achiral building blocks of the assemblies “follow” the templated helicity induced by the chiral components even when chiral molecules are present in very small fractions.
2. Enantioselective noncovalent synthesis (memory of supramolecular chirality), where use of a chiral template interacts stereoselectively to give preferentially one of the two possible enantiomeric forms (P or M-helix). After the template is replaced by an achiral analog the induced chirality is preserved allowing the synthesis of enantiomerically enriched self-assembled double rosette assemblies.
3. Diastereomeric and enantiomeric noncovalent synthesis of double and tetra-rosettes by guest templation, where chiral guest molecules can be used as templates to induce the formation of one specific helicity of the double and tetra-rosette assemblies.

Furthermore, the concept of templated synthesis by hydrogen-bonded rosette assemblies is also illustrated with the templated synthesis of covalent cyclic calix[4]arene dimelamine trimers. The synthesis of this trimer is impossible without the template role provided by one of the building blocks of the assembly. The templated synthesis by a double rosette of noncovalent cyclic hydrogen-bonded trimers is also described.

The role of gold and graphite surfaces as template for the formation of hydrogen-bonded nanostructures is also revised. The topology of the structure that is formed by noncovalent interactions on the surfaces is determined by the noncovalent interactions between the surface template and the substrates. Specifically, the growth of individual nanometer-sized hydrogen-bonded assemblies on gold monolayers is templated through an exchange reaction between a double rosette in solution and a single calix[4]arene dimelamine embedded into hexanethiol self-assembled monolayers (SAMs).

On the other hand, first- and second-order template effects using graphite surfaces as templates are shown. The formation of linear rod-like structures on a graphite surface was observed by TM-AFM after deposition of double rosette on the graphite template (*first-order template effect*). Also, double rosettes having gold atoms coordinated to phosphane groups form nanorod domains after deposition on HOPG template. These metal-containing nanorod arrays might constitute a viable route for the templated (*second-order template effect*) bottom-up fabrication of, for example, conducting nanowires.

Keywords Hydrogen-bonded assemblies · Noncovalent templation · Supramolecular chirality · Combinatorial dynamic libraries · Nanowires

1 Introduction

In this chapter, hydrogen-bonded assemblies based on the rosette motif are used to describe some examples of templation in noncovalent synthesis. In self-organizing systems the building blocks contain all the information to form an assembly with specific geometry, while templated systems involve the use of

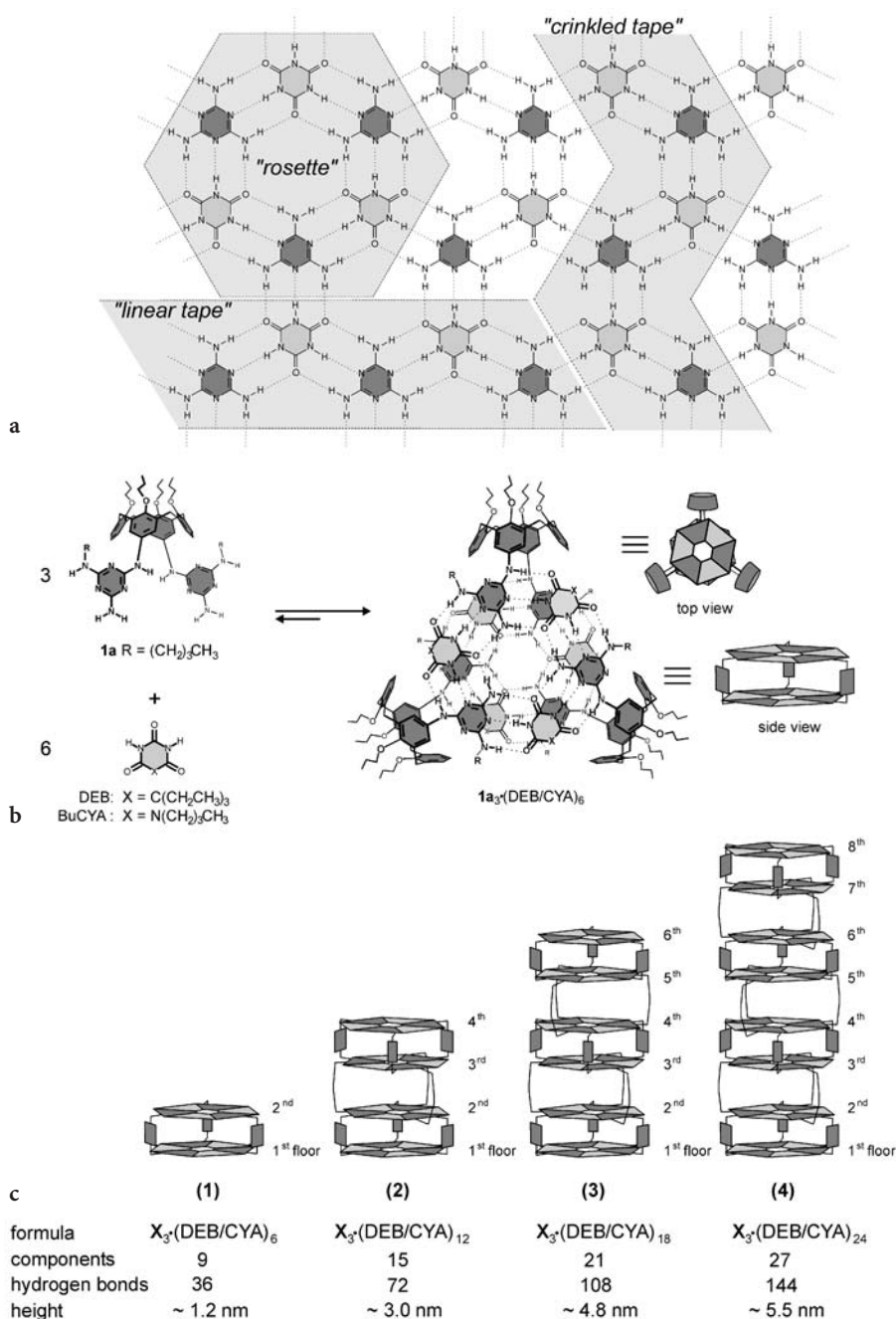


Fig. 1 **a** 2-D lattice of alternating isocyanuric acid (light grey) and melamine (dark grey) molecules. The three possible motifs, i.e., linear tape, crinkled tape, and rosette are highlighted. **b** Formation of double rosette assembly 1a₃-(DEB/BuCYA)₆ from three calix[4]arene dimelamines 1a and six 5,5-diethylbarbiturate (DEB) or *n*-butyl cyanurate (BuCYA) molecules. **c** Schematic representation of 1 double rosette, 2 tetrarosette, 3 hexarosette, and 4 octarosette. Each floor represents one rosette motif

temporary or permanent species that assist the assembly of supramolecular structures into a specific geometry.

The rosette motif is a self-assembled circular network of complementary hydrogen bonds formed between three melamines and three barbituric (BAR) or cyanuric acids (CYA) (Fig. 1a) [1]. This rosette motif is used to form large and well-defined hydrogen-bonded assemblies. Calix[4]arenes, diametrically substituted with two melamine units at the upper rim, form double rosette assemblies (Fig. 1b) in the presence of two equivalents of BAR or CYA [2]. Extended tetra-, hexa- and octarosettes are obtained when calix[4]arene dimelamine units are covalently linked [3–5]. In these nanostructures, each rosette motif is formed through 18 hydrogen bonds. The rapid increase of the number of hydrogen bonds (double rosette=36, tetra-rosette=72, hexarosette=108 and octarosette=142) in these extended assemblies renders a high thermodynamic stability (Fig. 1c). The molecular weight of the rosette assemblies reaches that of small proteins. For example, the octarosette has a size of 3.0 nm×3.3 nm×5.5 nm and a molecular weight of ~20 kD, which is larger than small proteins like cytochrome *c* (~12 kD) and myoglobin (~16 kD).

Functionalization of the melamine moieties of the rosette assemblies allows for the concave 3-D positioning of functionalities around this template, providing the basis for the formation of several receptor assemblies that are able to complex small substrates. Moreover, ordered nanostructures are obtained by the self-organization of the rosette assemblies on graphite templates.

2

Formation and Characterization of Rosette Assemblies

Using the rosette motif introduced by Whitesides [6], we have reported the noncovalent synthesis of the thermodynamically stable double rosette assemblies $1_3 \cdot (\text{DEB/CYA})_6$ that are held together by a total of 36 hydrogen bonds. The assemblies are formed spontaneously by mixing of calix[4]arenes diametrically substituted at the upper rim with two melamine units (1) and 2 equivalents of either BAR or CYA derivatives (Fig. 1b). The assemblies consist of two flat rosette motifs connected via three calix[4]arene molecules. The assemblies are stable in apolar solvents like chloroform, benzene, and toluene even at 10^{-4} M [2, 7].

Three conformational isomers of double rosette assemblies can be formed, i.e., one staggered (D_3) isomer and two eclipsed (symmetrical C_{3h} and unsymmetrical C_s) isomers (Fig. 2). In the staggered isomer the two melamines on each calix[4]arene are in an anti-parallel orientation with respect to each other, while in the eclipsed isomers the melamines on each calix[4]arene unit are parallel.

Rosette assemblies are easily characterized by ^1H -NMR spectroscopy in solution [8]. In the region between 13 and 16 ppm, diagnostic signals for the BAR/CYA hydrogen-bonded imide NH protons are present (Fig. 3b). The number of signals that are observed depends on the type of rosette and their

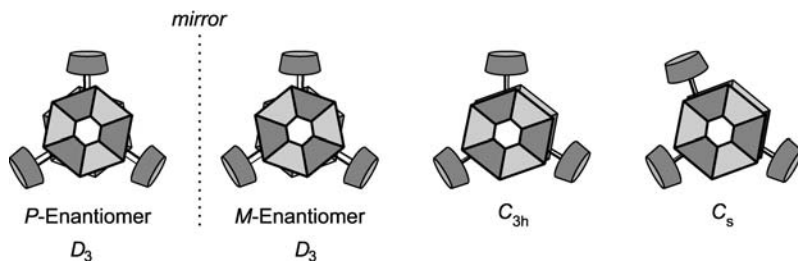


Fig. 2 Schematic representations of the three isomeric forms for double rosette assemblies: staggered (D_3), symmetrical eclipsed (C_{3h}), and unsymmetrical eclipsed (C_s)

symmetry. For example, the D_3 and the C_{3h} isomers of the double rosette have only two different hydrogen-bonded imide NH protons and therefore two different signals are observed in the $^1\text{H-NMR}$ spectrum. For the C_s isomer, six hydrogen-bonded imide NH protons are magnetically different and thus six signals are observed. If the assemblies are formed with certain bulky CYA derivatives, all possible isomers are formed [9], while with BAR derivatives the D_3 isomers are obtained preferentially. For the D_3 isomer of the tetra- and octa- rosettes $\text{X}_3\cdot(\text{DEB/CYA})_{12}$, four different hydrogen-bonded imide NH protons can be distinguished and therefore four different signals are observed in the $^1\text{H-NMR}$ spectra (Fig. 3c). Similarly, for the D_3 isomer of the hexa- and the octa- rosettes, six and eight signals are observed in the $^1\text{H-NMR}$ spectra, respectively.

Rosette assemblies $\text{X}_3\cdot(\text{BAR/CYA})_{3n}$ ($n=2$ double, $n=4$ tetra-, $n=6$ hexa-, and $n=8$ octa- rosette) are formed as an equal mixture of (*M*)- and (*P*)-enantiomers when the components do not contain chiral centers. [2, 7, 10]. Nevertheless, in double rosette assemblies $\text{I}_3\cdot(\text{BAR/CYA})_6$ for example, when one of the building blocks (1 or BAR/CYA) is chiral, complete induction of supramolecular chirality is observed; i.e., when *R,R* dimelamines assemble with BAR or CYA only the (*M*)-diastereomer is formed, while the assembly of *S,S* dimelamines with BAR or CYA gives only the (*P*)-diastereomer. This property makes it possible to study double (and tetra-, hexa-, and octa-) rosette formation using circular dichroism (CD) spectroscopy [11]. For example, double rosette assemblies exhibit a very strong induced CD signal ($|\Delta\epsilon_{\text{max}}| \sim 100 \text{ L mol}^{-1} \text{ cm}^{-1}$ for double rosettes), while the individual chiral components are hardly CD active ($|\Delta\epsilon_{\text{max}}| < 8.1 \text{ L mol}^{-1} \text{ cm}^{-1}$) (Fig. 4). The observed CD is a direct result of the assembly formation. The CD curves of the (*M*)- and (*P*)-assemblies are perfect mirror images, reflecting their enantiomeric relationship. Therefore, the sign of the CD curve is a good probe for the supramolecular chirality of double (and larger) rosette assemblies.

MALDI-TOF mass spectrometry using the Ag^+ -labeling technique [12] also gives evidence for rosette formation. This technique is extremely mild and provides a nondestructive method to generate positively charged assemblies by coordination of Ag^+ to a cyano group or by complexation of Ag^+ between two phenyl rings.

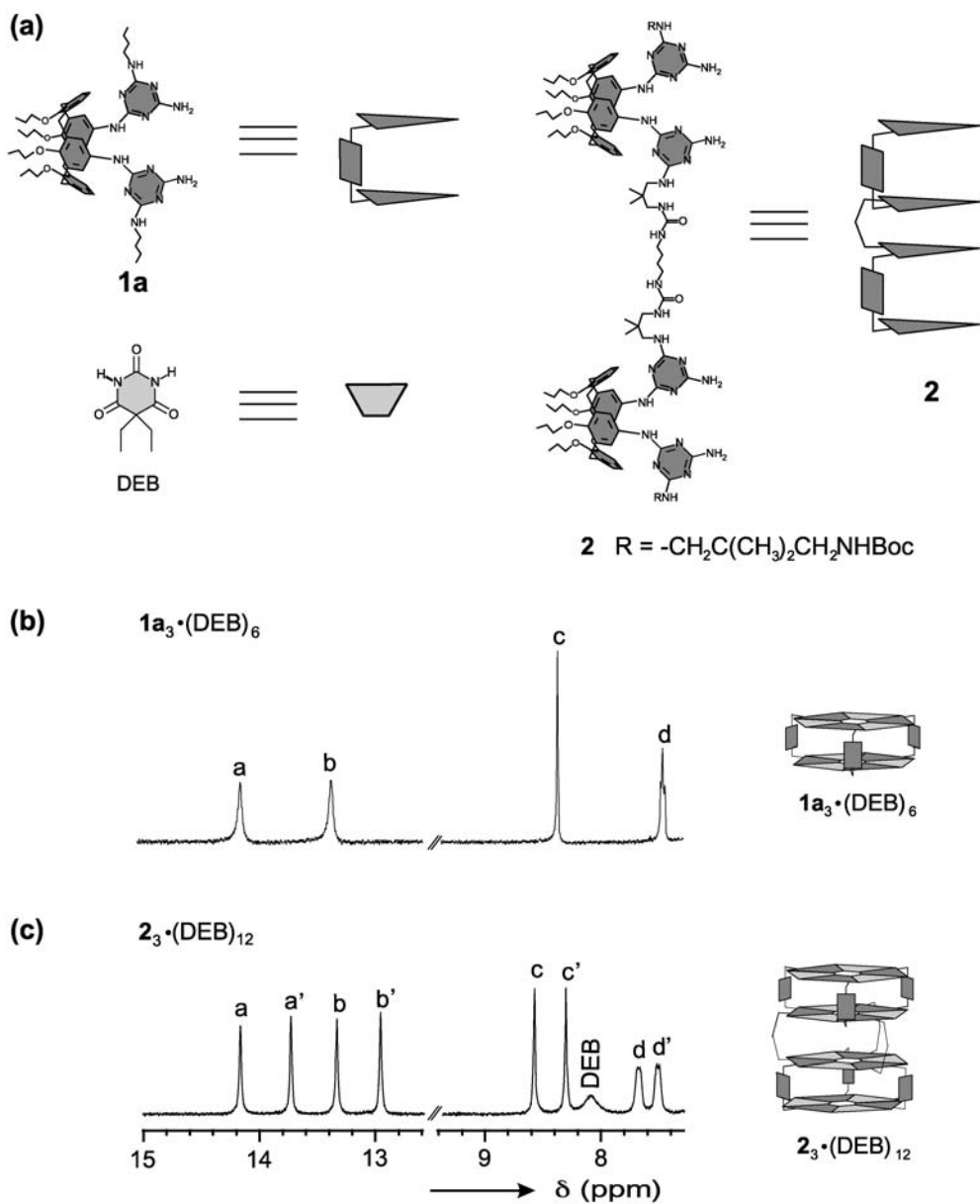


Fig. 3 a Chemical structure and schematic representation of dimelamine **1a**, tetramelamine **2** and DEB and part of the ^1H -NMR spectrum (CDCl_3 , 298 K) of **b** $1\text{a}_3 \cdot (\text{DEB})_6$ and **c** $2_3 \cdot (\text{DEB})_{12}$

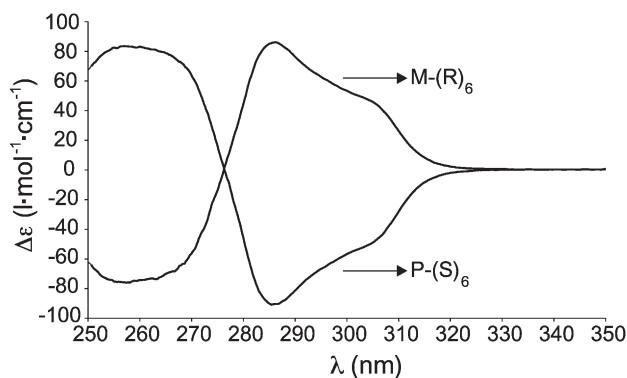


Fig. 4 Example of the CD spectra obtained for (*M*)- and (*P*)-double rosettes (*M*-(*R*)₆ and *P*-(*S*)₆) after chiral induction by *R,R*-dimelamines and *S,S*-dimelamines, respectively

The X-ray crystal structure of assembly **1a**₃·(DEB)₆ provides unequivocal evidence that the assembly exists as the *D*₃-isomer (Fig. 5). Furthermore, it shows that the calix[4]arene units are fixed in a pinched cone conformation, which is the only conformation that allows simultaneous participation of the calix[4]arene units in both the upper and the lower rosette motif. The two rosette motifs are stacked on top of each other with an interatomic separation of 3.5 Å at the edges to 3.2 Å in the centre of the rosette [7]. The assemblies have a height of 1.2 nm and a width of ~3 nm.

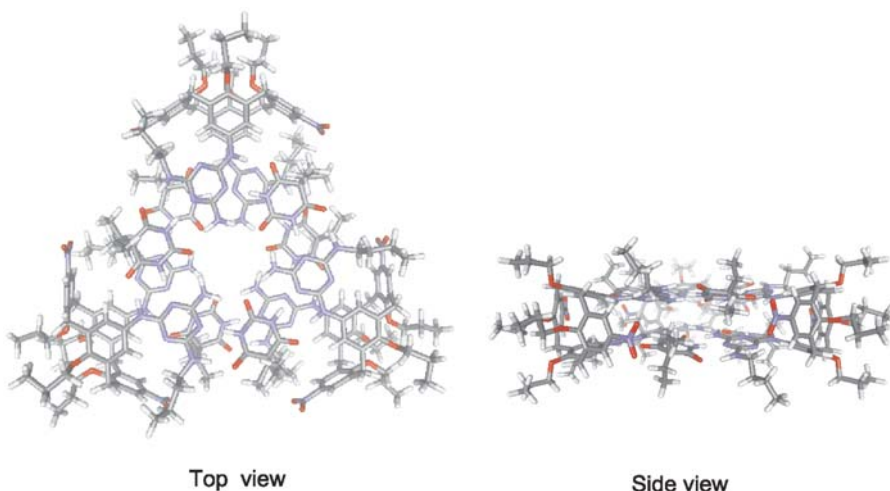


Fig. 5 Top and side view of the X-ray crystal structure of assembly **1a**₃·(DEB)₆

3

Guest Templated Selection and Amplification of the Strongest Binding Receptor in Dynamic Libraries

Combinatorial chemistry (CC) allows for the generation of molecular diversity and is widely used in the search for biologically active compounds, new materials, and catalysts [13]. Its combination with supramolecular chemistry has led to the new research field of dynamic combinatorial chemistry (DCC) [13]. The concept of DCC relies on the reversible interchange of components between supramolecular structures. The equilibrating mixtures of supramolecular structures (dynamic combinatorial libraries) allow for the target-driven generation of the active constituents of the library [14]. For example, a template effect for the formation and amplification of the strongest binding receptor can be expected when a guest molecule is added to a library of potential receptors that are under thermodynamic control.

Dynamic libraries of double rosette assemblies are formed under thermodynamically controlled conditions in solution when different substituted calix[4]arene dimelamines and 5,5'-diethylbarbituric acid (DEB) are mixed [15]. These libraries exist as a statistical mixture of homomeric and heteromeric double rosettes. For example, mixing of equimolar solutions of the individual assemblies $1a_3 \cdot (DEB)_6$ and $1b_3 \cdot (DEB)_6$, bearing butyl and zinc porphyrin moieties, respectively, distributes the calix[4]arene dimelamines **1a** and **1b** (Fig. 6a) over four different double rosettes. The assemblies $1a_3 \cdot (DEB)_6$, $1a_2 \cdot 1b \cdot (DEB)_6$, $1a \cdot 1b_2 \cdot (DEB)_6$, $1b_3 \cdot (DEB)_6$ are formed in a statistical ratio of 1:3:3:1, respectively (Fig. 6b).

The H_c - H_e ($\delta=8.0$ – 9.0) and the H_p , H_g proton signals ($\delta=2.5$ – 2.7) clearly illustrate the mixing process (Fig. 7a–c). For the H_c proton signal of the mixture $1a_{(3-n)} \cdot 1b_n \cdot (DEB)_6$ ($n=0$ – 3) at least five signals ($\delta=8.3$ – 8.5) are present, while this signal appears as a single resonance at $\delta=8.32$ for the pure homomeric assembly $1b_3 \cdot (DEB)_6$ (Fig. 7a). Similarly, the H_d , H_e and H_p , H_g protons of the mixture give rise to multiple resonances. Integration of the various proton signals clearly proves the almost statistical composition of the mixture (30% versus 25% homomeric, 70% versus 75% heteromeric).

Addition of template **3** to this dynamic library shifts the equilibrium towards the maximum formation of the strongest 3-binding receptor $1b_3 \cdot (DEB)_6$, resulting in a mixture of $1a_3 \cdot (DEB)_6$ and $1b_3 \cdot (DEB)_6 \cdot 3_2$ (1:1) (Fig. 6b) [16]. In this way, guest **3** serves as a template that drives the chemical evolution of the dynamic mixture $1a_{(3-n)} \cdot 1b_n \cdot (DEB)_6$ ($n=0$ – 3) toward the amplification of the best receptor. The amplification of receptor $1b_3 \cdot (DEB)_6$ is a factor 3.3 (from ~15% before addition to ~50% after addition of **3**). Evidence for this comes from the disappearance of the proton signals for the heteromeric assemblies $1a_2 \cdot 1b \cdot (DEB)_6$ and $1a \cdot 1b_2 \cdot (DEB)_6$ in the 1H -NMR spectrum (Fig. 7d). From the five H_c protons resonancing at $\delta=8.3$ – 8.4 , only two signals corresponding to the homomeric assemblies $1a_3 \cdot (DEB)_6$ and $1b_3 \cdot (DEB)_6 \cdot 3_2$ are present after addition of the guest template **3**.

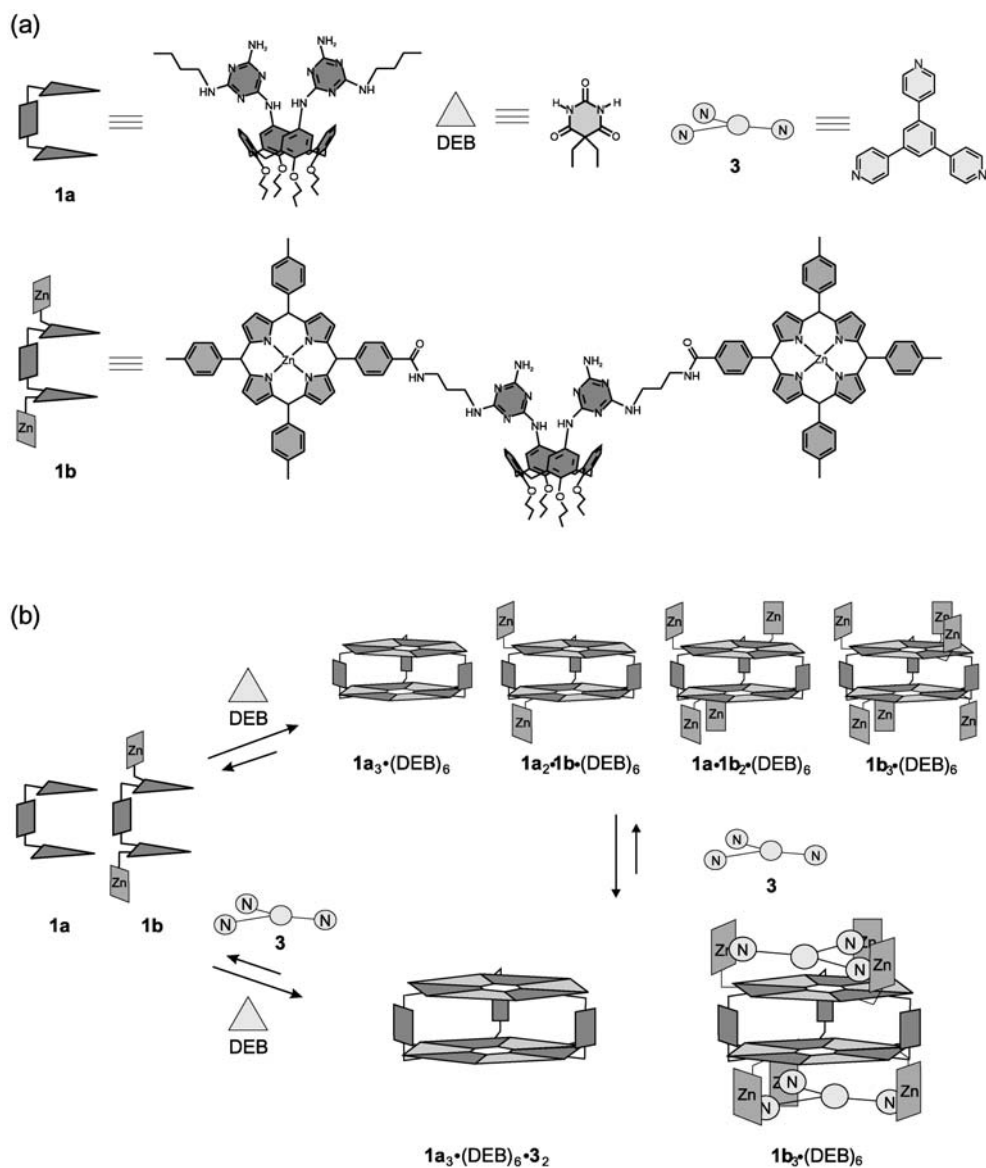


Fig. 6 a Molecular and schematic representations calix[4]arene dimelamines **1a** and **1b** and tripyridine **3**. b Schematic representation of the formation of four component library $1a_{(3-n)} \cdot 1b_n \cdot (DEB)_6$ ($n=0-3$) and templated selection of the best receptor upon addition of the guest **3**

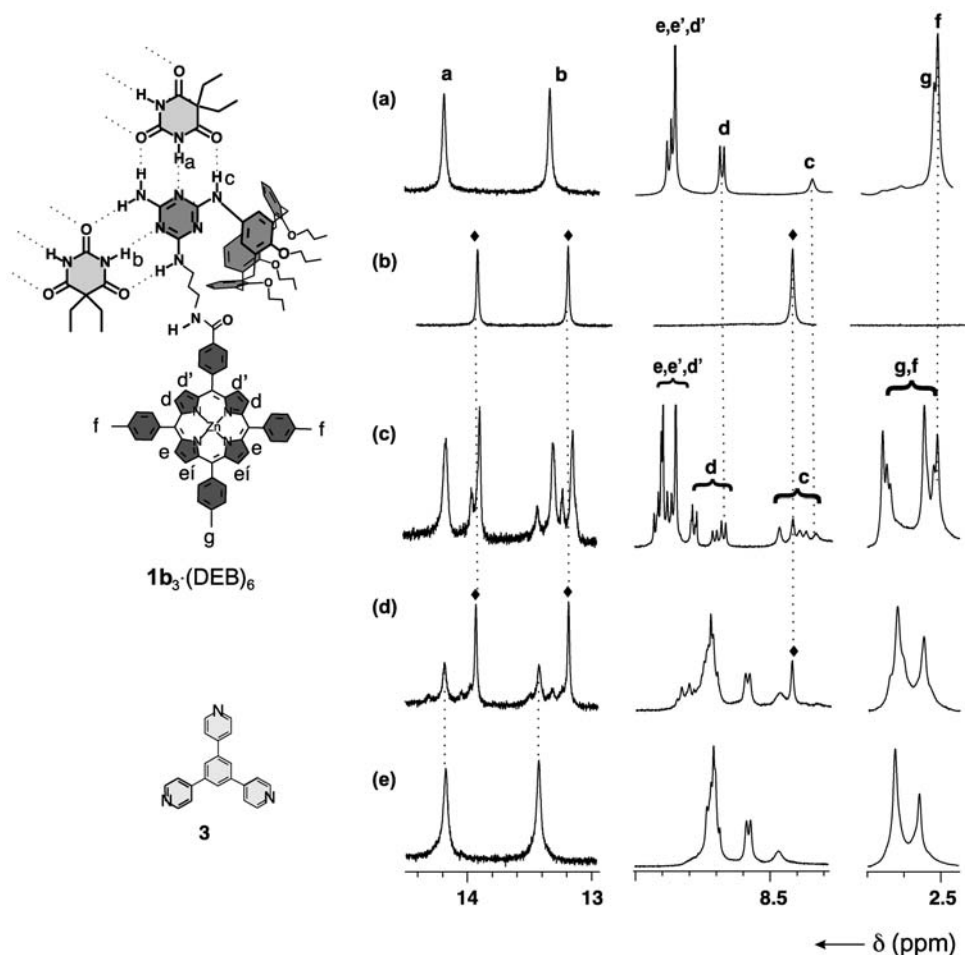


Fig. 7 Parts of the ^1H -NMR spectra of **a** assembly $1\text{a}_3 \cdot (\text{DEB})_6$, **b** assembly $1\text{b}_3 \cdot (\text{DEB})_6$, **c** mixture of $1\text{a}_3 \cdot (\text{DEB})_6$ and $1\text{b}_3 \cdot (\text{DEB})_6$ (1:1), **d** mixture of $1\text{a}_3 \cdot (\text{DEB})_6$ and $1\text{b}_3 \cdot (\text{DEB})_6$ (1:1) after addition of 4 equiv of **3**, and **e** assembly $1\text{b}_3 \cdot (\text{DEB})_6$ after addition of 2 equiv of **3**. Spectra were recorded at 300 MHz in CDCl_3 at room temperature. The signals marked with ? are from $1\text{a}_3 \cdot (\text{DEB})_6$ protons

4

Templation for the Control of the Chirality in Supramolecular Systems

4.1

Amplification of Chirality: "Sergeant and Soldiers Principle"

In the absence of elements of chirality, double rosettes are formed as a racemic mixture of *M*- and *P*-enantiomers but, when one of the components (melamine or BAR/CYA) is chiral, total chiral induction is achieved and they assemble in

two diastereomeric forms with either the *M*- or *P*-enantiomers (see Sect. 2). More interestingly, double rosettes also exhibit amplification of chirality. In this case, the achiral components of the assemblies “follow” the templated helicity induced by the chiral components even when chiral molecules are present in very small fractions. This is known as the “Sergeants and Soldiers” principle.

Meijer and coworkers have also studied the “Sergeants and Soldiers” principle in dynamic macromolecular aggregates that are held together via noncovalent interactions, such as π - π stacking or hydrogen bonding [17]. Large optical activities were observed for chiral columnar assemblies containing only a small fraction (~5%) of chiral components [17a, 18].

In this section, the principle applied to double rosette assemblies is described. The “Sergeants and Soldiers” experiments with the rosette assemblies (templation of chirality) have been carried out under thermodynamically controlled conditions.

Mixing of solutions of diastereomerically pure assembly (*M*)-**1c**·(DEB)₆ [15] and racemic assembly **1d**·(DEB)₆ (mixtures were prepared at ratio **1c**·(DEB)₆:**1d**·(DEB)₆ ranging from 1:9 to 9:1; see Fig. 8a for molecular structures) results

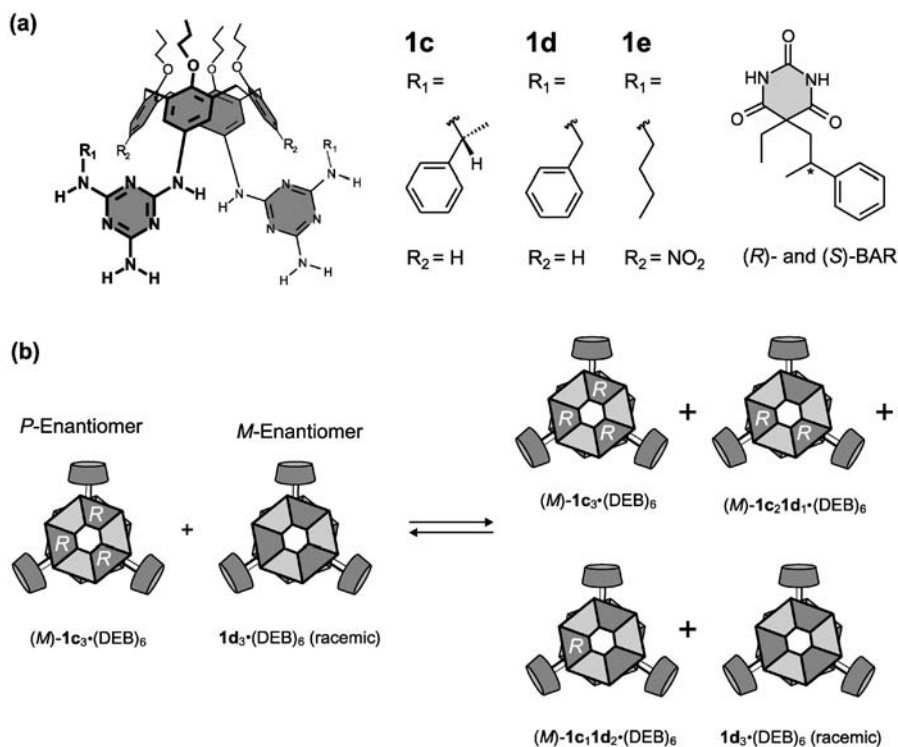


Fig. 8 a Molecular structures of calix[4]arene dimelamines **1c**-**e** and (*R*)- and (*S*)-BAR. b Mixing of the diastereomeric double rosettes (*M*)-**1c**₃·(DEB)₆ and racemic assembly **1d**₃·(DEB)₆

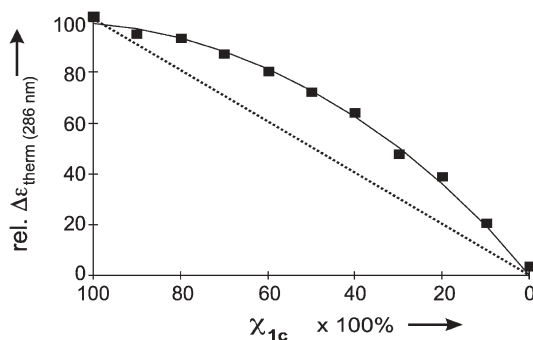


Fig. 9 Relative CD intensity (■, measured at 286 nm) versus the mole fraction of chiral component **1c** (χ_{1c}), measured in chloroform at room temperature. The dotted line represents the expected CD intensity in the absence of chiral amplification

in the formation of a mixture of assemblies $\mathbf{1c}_n\mathbf{1d}_{3-n}\cdot(\text{DEB})_6$ ($n=0-3$), due to the continuous exchange of **1c** and **1d** in solution (Fig. 8b). In chloroform, the thermodynamic equilibrium is reached within seconds after mixing because of the high exchange rate of dimelamines **1c** and **1d** when barbiturate form part of the assemblies. Two-dimensional NMR analysis has shown that for this type of assembly the distribution of the dimelamine components over the four assemblies $\mathbf{1c}_n\mathbf{1d}_{3-n}\cdot(\text{DEB})_6$ ($n=0-3$) is nearly statistical (1:3:3:1) [10b].

The CD intensities of the different mixtures of $(M)\text{-}\mathbf{1c}_3\cdot(\text{DEB})_6$ and $\mathbf{1d}_3\cdot(\text{DEB})_6$ are significantly higher than the sum of the CD intensities of the individual assemblies (corrected for the relative ratio **1c**/**1d**, see Fig. 9). This phenomenon is an example of chiral amplification and is caused by the presence of the heteromeric assemblies $\mathbf{1c}_2\mathbf{1d}_1\cdot(\text{DEB})_6$ and $\mathbf{1c}_1\mathbf{1d}_2\cdot(\text{DEB})_6$. These assemblies contain four or two (*R*)-substituents, respectively, which act as a chiral template leading to the preferential formation of the corresponding (*M*)-diastereomers for the heteromeric assemblies. Apparently, the d.e. for these assemblies is significantly higher than 66% ($\mathbf{1c}_2\mathbf{1d}_1\cdot(\text{DEB})_6$) or 33% ($\mathbf{1c}_1\mathbf{1d}_2\cdot(\text{DEB})_6$), values expected when the d.e. is related in a linear fashion to the number of chiral centers present. This is a clear example of the phenomenon first described by Green and coworkers as the “Sergeants and Soldiers” principle [19], which indicates here that within the heteromeric assemblies the achiral dimelamines follow the helicity induced by the chiral dimelamines that act as a chiral template.

4.2

Enantioselective Noncovalent Synthesis: Memory of Supramolecular Chirality

The synthesis of enantiopure self-assembled aggregates from achiral components has been achieved using the “chiral memory” concept previously reported by the groups of Yashima for the enantioselective synthesis of covalent *P*- or

M-helical polymers [20]. The chiral memory concept implies the use of a chiral template that interacts stereoselectively in a noncovalent manner to give preferentially one of the two possible enantiomeric forms. Subsequently, the template is replaced by an achiral analog while the induced chirality is preserved. This replacement of the chiral template is the crucial step in this strategy. The resulting structure is still optically active, although none of its components are chiral. This strategy has been used to synthesize enantiomerically enriched self-assembled double rosette assemblies [10b].

As explained earlier (Sect. 2), the use of a chiral barbiturate compound leads to the formation of a diastereomeric double rosette with a d.e. of 96% (total induction of supramolecular chirality). For example, when BuCYA is added to a solution containing the diastereomerically pure *P*-**1e**₃·((*S*)-BAR)₆ or *M*-**1e**₃·((*R*)-BAR)₆ (for molecular structures see Fig. 8a), the exchange of the chiral barbiturate (*S*)-BAR for the achiral cyanurate BuCYA gives an enantiopure assembly with an e.e. of 96% (Fig. 10a). This exchange of the barbiturate for a cyanurate is possible because of the formation of stronger hydrogen bonds between the melamine–cyanurate pair than between the melamine–barbiturate pair due to the higher acidity of the cyanurate [21]. Thus, enantiopure rosettes *P*-**1e**₃·(BuCYA)₆ (or *M*-**1e**₃·(BuCYA)₆) are obtained without any chiral center due

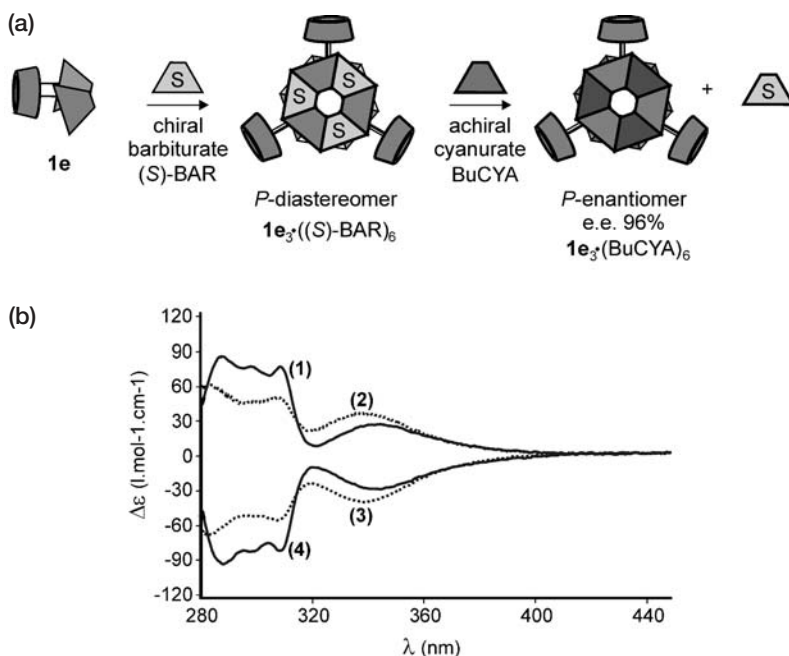


Fig. 10 **a** Schematic representation of the chiral memory effect by exchange of a chiral barbiturate for an achiral cyanurate. **b** CD spectra of assemblies **1** (*M*)-**1e**₃·(BuCYA)₆, **2** (*M*)-**1e**₃·((*R*)-BAR)₆, **3** (*P*)-**1e**₃·((*S*)-BAR)₆, and **4** (*P*)-**1e**₃·(BuCYA)₆. Assemblies were recorded in benzene-*d*₆ (1.0 mM) at 298 K

to the templation exerted by the chiral barbiturate. This memory of supramolecular chirality is clearly demonstrated by CD spectroscopy (Fig. 10b).

4.3

Diastereomeric and Enantiomeric Noncovalent Synthesis of Double Rosettes by Guest Templation

Chiral guest molecules can be used as templates to induce the formation of one specific helicity of the double rosette assemblies. Assemblies $1f_3 \cdot (BuCYA)_6$ and $1g_3 \cdot (BuCYA)_6$ are formed predominantly as the D_3 -isomer and exist as a racemic mixture of the *P*- and *M*-enantiomers (Fig. 11) [9]. We have shown that

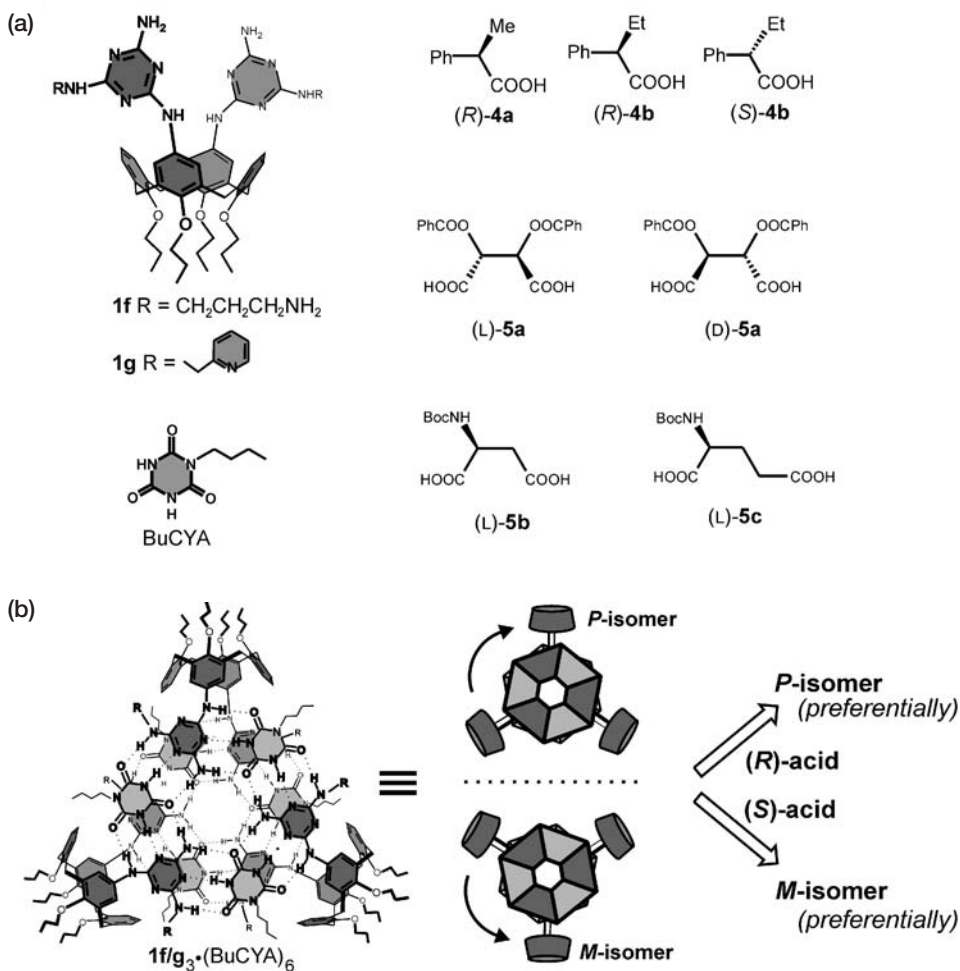


Fig. 11 a Structures of dimelamines 1f and 1g, *n*-butylcyanurate, chiral acids 4 and 5. b Illustration of templation of supramolecular chirality by chiral acids 4 and 5

the six amino or pyridyl functionalities positioned on the assemblies $1\mathbf{f}_3 \cdot (\text{BuCYA})_6$ and $1\mathbf{g}_3 \cdot (\text{BuCYA})_6$, respectively, are able to interact with chiral carboxylic acids to form diastereoselectively a *P*- or *M*-assembly depending on the chirality of the guest (Fig. 11) [22]. Thus, the chiral acids template the diastereoselective formation of preferably one of the two possible diastereomeric assemblies.

Typically, six equivalents of $4\mathbf{a-b}$ were added to a racemic solution of $1\mathbf{f}_3 \cdot (\text{BuCYA})_6$ (1.0 mM, 298 K), which has six amino functionalities that serve as binding sites for complexation of the chiral carboxylic acids in toluene- d_8 . The interaction between host and guest becomes apparent from shifts in the ^1H -NMR spectrum. For example, in the case of acid (*S*)- $4\mathbf{b}$ (6 equiv), the H_k and H_l shift is 0.09–0.18 ppm upfield and 0.32 ppm downfield, respectively, upon addition of guest (Fig. 12). In addition, the H_b , H_c , H_k , and H_l protons are split because of the formation of the diastereomeric assemblies (*M*)- $1\mathbf{f}_3 \cdot (\text{BuCYA})_6 / (\text{S})\text{-}4\mathbf{b}$ and (*P*)- $1\mathbf{f}_3 \cdot (\text{BuCYA})_6 / (\text{S})\text{-}4\mathbf{b}$, which are no longer mirror images. The chiral acids (*R*)- $4\mathbf{a}$, (*R*)- $4\mathbf{b}$, (*S*)- $4\mathbf{b}$ also express a clear selectivity towards one of the two enantiomers (*M* or *P*) of assembly $1\mathbf{f}_3 \cdot (\text{BuCYA})_6$ that are present in solution. As a result, the enantiomer that is bound most strongly is amplified in the mixture as both enantiomers are in dynamic equilibrium. This increase causes the CD spectrum of assembly $1\mathbf{f}_3 \cdot (\text{BuCYA})_6$ to show reliable and reproducible Cotton effects in the presence of chiral acids $4\mathbf{a-b}$ (Fig. 12a). With six equivalents of acids $4\mathbf{a}$ and $4\mathbf{b}$, enantioselectivities of 19% and 21% d.e., respectively, were observed.

On the other hand, double rosette assembly $1\mathbf{g}_3 \cdot (\text{BuCYA})_6$ with six 2-pyridyl functionalities is able to complex chiral dicarboxylic acids $5\mathbf{a-c}$. The interaction between the assembly and the chiral diacid can be seen from the shifts and the splitting of the signals in the ^1H -NMR spectra. For example, when L- $5\mathbf{a}$ (3 equiv) was added to a solution of $1\mathbf{g}_3 \cdot (\text{BuCYA})_6$ (1.0 mM, 298 K) in toluene- d_8 , the signals of protons H_a , H_b , H_c , H_h , and H_i are split and shifted (Fig. 13) because of the formation of the diastereomeric assemblies (*M*)- $1\mathbf{g}_3 \cdot (\text{BuCYA})_6 / (\text{L-}5\mathbf{a})$ and (*P*)- $1\mathbf{g}_3 \cdot (\text{BuCYA})_6 / (\text{L-}5\mathbf{a})$, which are no longer mirror images and exhibit different signals in the ^1H -NMR spectrum. The ratio of these signals shows that the diacids $5\mathbf{a-c}$ bind preferentially to either the *M*- or *P*-enantiomer of the assembly $1\mathbf{g}_3 \cdot (\text{BuCYA})_6$, leading to amplification of that particular enantiomer in the mixture. The addition of dicarboxylic acids $5\mathbf{a-c}$ (3 equiv) gives a very high enantioselectivity (Fig. 13) that is ascribed to a two-point hydrogen-bonding interaction between one molecule of $5\mathbf{a-c}$ and two 2-pyridyl moieties of $1\mathbf{g}_3 \cdot (\text{BuCYA})_6$. The highest selectivity was achieved with $5\mathbf{a}$ (90% d.e.). In absence of the chiral auxiliary, the racemic mixture of *P*- and *M*-enantiomers is not CD active. When the chiral diacids are added, the CD spectra of $1\mathbf{g}_3 \cdot (\text{BuCYA})_6$ show reproducible Cotton effects, indicating that the chiral acids interact with the assembly and, thus, amplify either the *P*- or the *M*-enantiomer in the mixture. Generally, it was found that chiral L-acids induce the *M*-helicity and D-acids the *P*-helicity, as indicated from a positive and negative CD sign, respectively.

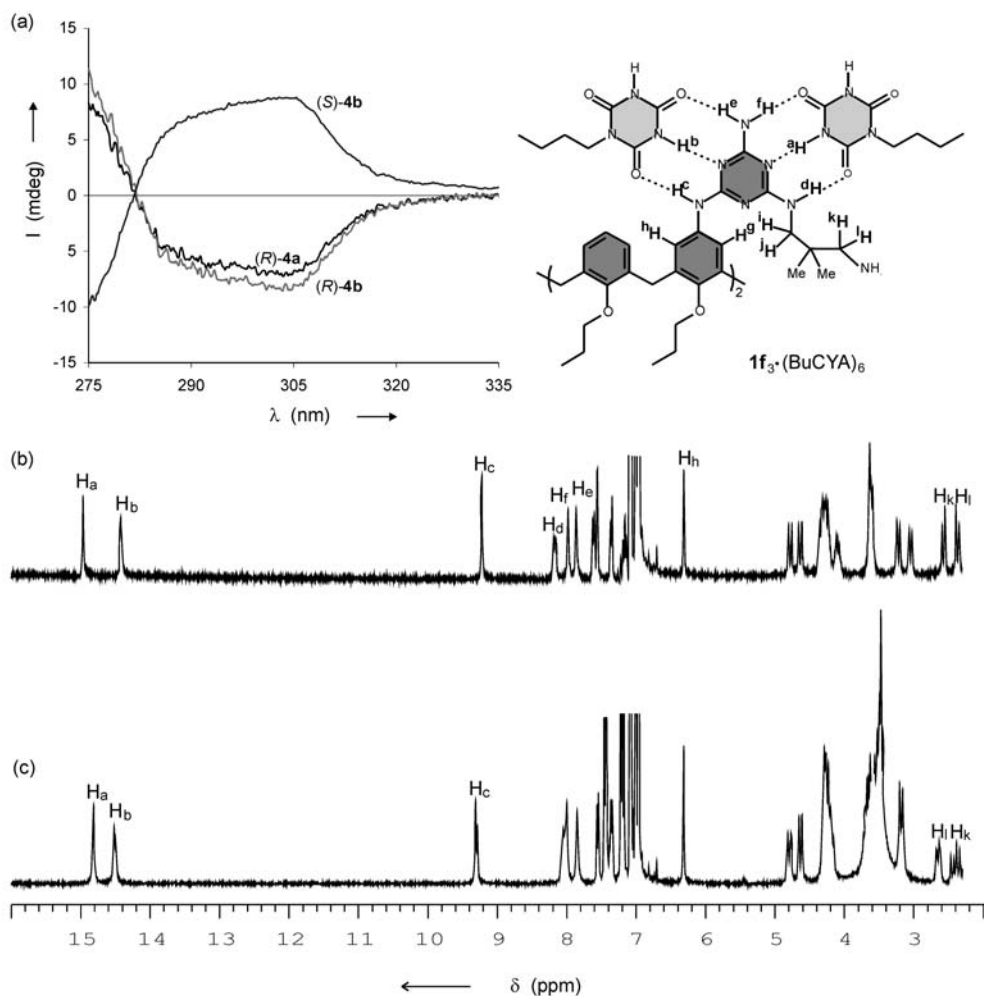


Fig. 12 a CD spectra of $1f_3 \cdot (\text{BuCYA})_6$ after addition of 6 equiv of acids (R) -4a, (R) -4b, and (S) -4b and parts of the ^1H -NMR spectra ($\text{toluene-}d_8$) of $1f_3 \cdot (\text{BuCYA})_6$ b before and c after addition of 6 equiv (S) -4b

Moreover, removal of the template **5a** leaves one of the original enantiomers in 90% *ee*, which racemizes only slowly ($t_{1/2} \approx 1$ week). ^1H -NMR spectroscopy indicated that within a few minutes after addition of ethylenediamine (3 equiv) the L-**5a** moieties are removed by complexation with the ethylenediamine. As monitored by CD spectroscopy, removal of L-**5a** from complex $1g_3 \cdot (\text{BuCYA})_6 / (\text{L-5a})$ leads to the formation of mainly the *M*-enantiomer of $1g_3 \cdot (\text{BuCYA})_6$. Thus, the assembly memorizes the chirality templated by the guest even after removal of the template.

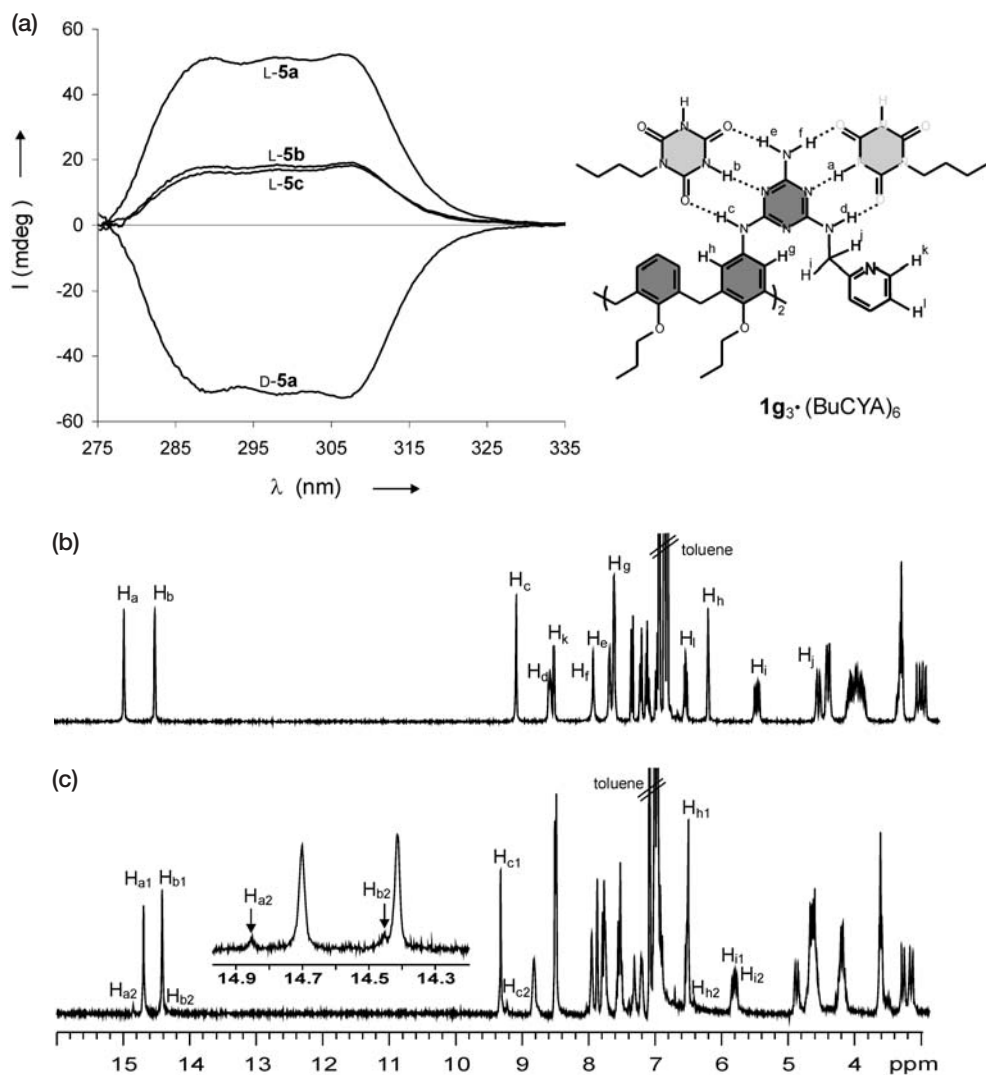


Fig. 13 a CD spectra of $1g_3 \cdot (BuCYA)_6$ after addition of 3 equiv of acids (L)-5a, (D)-5a, (L)-5b and (L)-5c and part of the 1H -NMR spectra ($toluene-d_8$) of $4_3 \cdot (BuCYA)_6$ b before and c after addition of 3 equiv (L)-5a

4.4

Diastereomeric Noncovalent Synthesis of Tetra-rosettes by Guest Templating

Another interesting case of templating of supramolecular chirality can be seen with tetra-rosettes upon saccharide complexation. Recognition of n -octyl β -D-glucopyranoside (β -D-6) by the tetra-rosette $2_3 \cdot (DEB)_{12}$ is, among other things, reflected by the shifts and splitting of the hydrogen-bonded proton

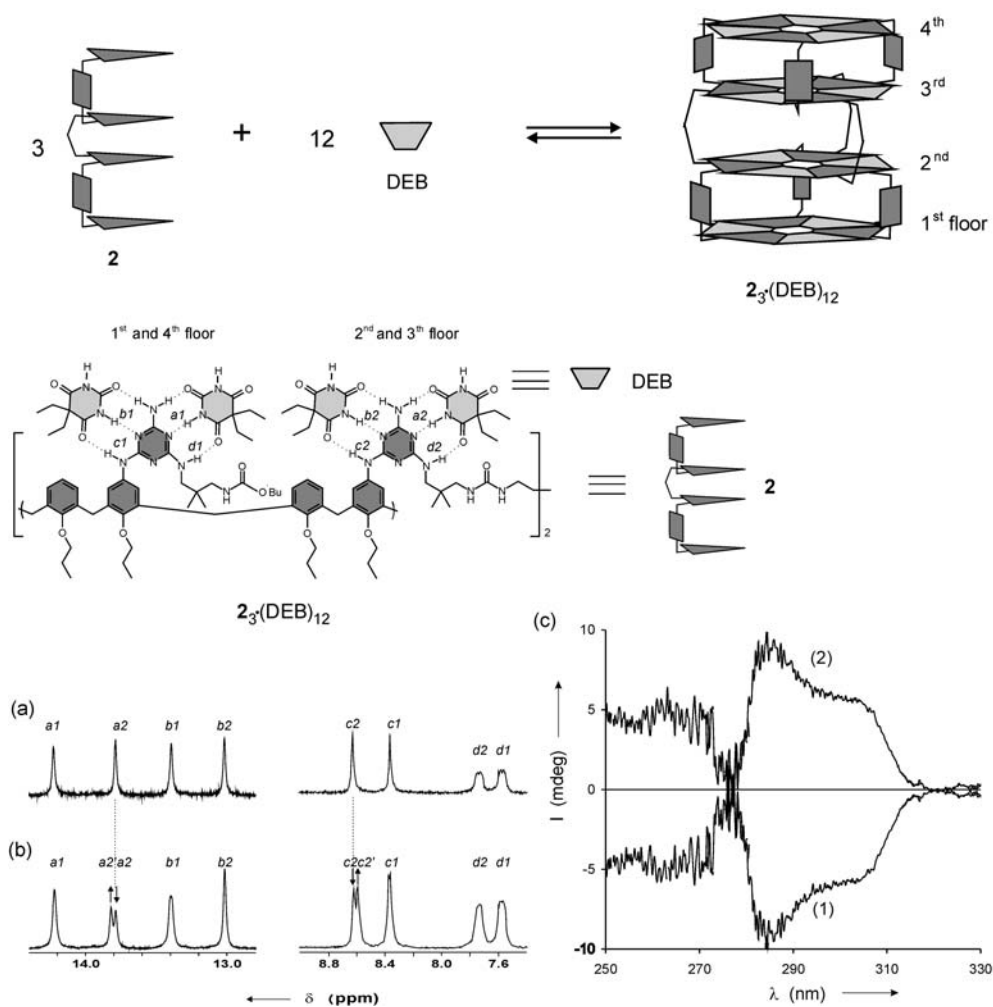


Fig. 14 Top: Formation of tetrarosette assembly $2_3 \cdot (\text{DEB})_{12}$ from three tetramelamines **2** and twelve 5,5-diethylbarbiturate (DEB) molecules; Bottom: Parts of the ¹H-NMR spectra (CDCl₃) of $2_3 \cdot (\text{DEB})_{12}$ (1 mM) in CDCl₃ at 293 K **a** before and **b** after addition of 10 equiv of β-D-6. **c** CD spectra of $2_3 \cdot (\text{DEB})_{12}$ (1 mM) in CDCl₃ at 293 K after addition of 1 β-D-6 and 2 β-L-6

signals H_{a2} and H_{c2} on the second and third rosette floors in the ¹H-NMR spectrum (293 K, CDCl₃), whereas the corresponding signals of the first and fourth floor show no splitting (Fig. 14).

The intensities of the new signals ($\text{H}_{a2'}$ and $\text{H}_{c2'}$) increase when β-D-6 is added, while the original signals decrease. This means that only one of the two enantiomers from the racemic mixture of the *P* and *M* isomers of $2_3 \cdot (\text{DEB})_{12}$ recognizes the chiral guest stereoselectively and results in the formation of one diastereomeric complex. This conclusion is supported by the induced CD spec-

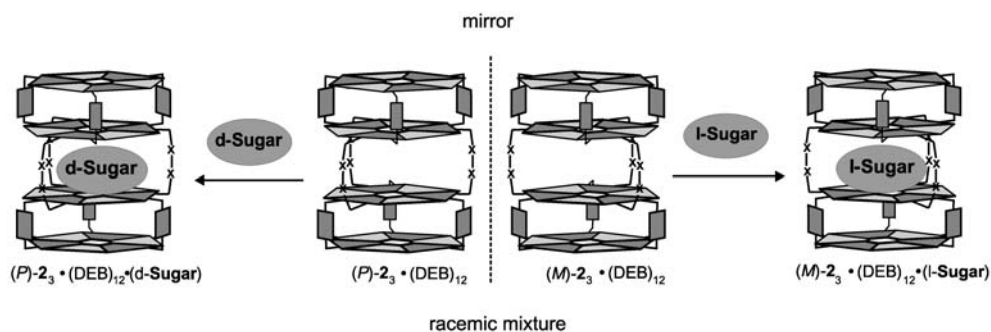


Fig. 15 Schematic representation of the templation of the supramolecular chirality of tetra-rosette $2_3 \cdot (\text{DEB})_{12}$ by chiral saccharides $\beta\text{-D-6}$ and $\beta\text{-L-6}$

trum. The racemic mixture of $(M)\text{-}2_3 \cdot (\text{DEB})_{12}$ and $(P)\text{-}2_3 \cdot (\text{DEB})_{12}$ is CD silent, while addition of $\beta\text{-D-6}$ induces a negative Cotton effect, evidencing the preferential formation of a *P* rosette assembly (Fig. 14c). As a result of the chiral templation, the *P* enantiomer, which binds $\beta\text{-D-6}$ more strongly, is amplified in the mixture as both enantiomers are in dynamic equilibrium. The templation of the *M* rosette assembly is observed when *n*-octyl $\beta\text{-L-glucopyranoside}$ ($\beta\text{-L-6}$) is added to the racemic mixture of $(M)\text{-}2_3 \cdot (\text{DEB})_{12}$ and $(P)\text{-}2_3 \cdot (\text{DEB})_{12}$. Thus, the chirality of the guest template ($\beta\text{-D-6}$ or $\beta\text{-L-6}$) determines the supramolecular chirality of the resulting tetra-rosette assembly (Fig. 15).

5

Templated Synthesis by Noncovalent Assemblies

The principle of templated synthesis is based on a template that provides the instructions for the formation of a specific product from substrates that otherwise have the potential to assemble and react in a variety of ways or do not assemble at all [23]. After the template has directed the formation of the product the template can often be removed to yield the template-free product, but it is also possible that the template is required for the stabilization of the non-stable products [23].

5.1

Templated Synthesis of Covalent Cyclic Calix[4]Arene Dimelamine Trimers

The covalent capture or post-modification of a supramolecular assembly is the fixation of the different components comprising the noncovalent assembly through the formation of covalent bonds. Such modification on hydrogen-bonded double rosettes was performed with the intent to increase their overall stability. In addition, with the covalent fixation the structural information present in the assemblies is stored on a covalent level, which allows for the

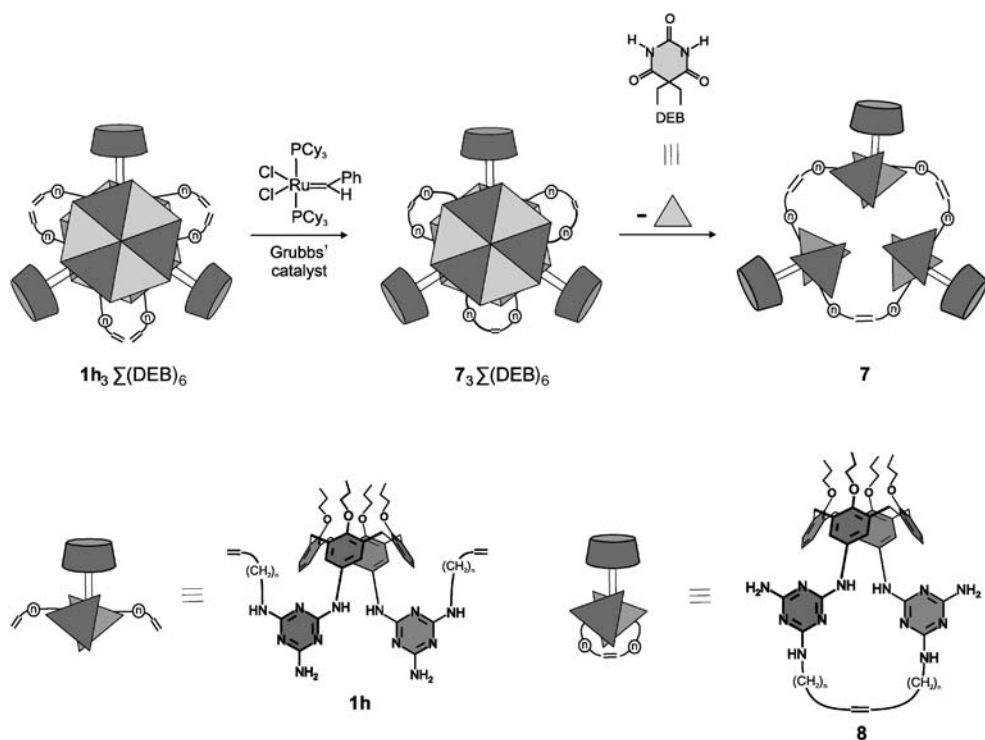


Fig. 16 Top: Schematic representation of the formation of cyclic calix[4]arene dimelamine trimer **7**. Bottom: Molecular structures and schematic representations of calix[4]arene dimelamine **1h** and cyclic monomer **8**

characterization of the assembly. Furthermore, covalent post-modification allows for the formation of a cyclic calix[4]arene dimelamine trimer in >95% yield. The synthesis of this trimer is virtually impossible without the template role provided by the DEB (Fig. 16). For covalent capture the ring closing metathesis reaction (RCM) [24] was chosen since it occurs under conditions that are compatible with the hydrogen-bonded network in assembly $1h_3 \cdot (DEB)_6$ (Fig. 16) (for application of the metathesis on hydrogen-bonded systems see [25] and for application of the metathesis in other supramolecular systems see [26]).

Reaction of assembly $1h_3 \cdot (DEB)_6$ ($n=6$) [7], having oct-7-enyl side chains, with Grubbs catalyst in CH_2Cl_2 resulted in the covalent linkage of the three calix[4]arene dimelamine units **1h** (Fig. 16) via a threefold metathesis reaction giving macrocycle **7** as the corresponding assembly $7 \cdot (DEB)_6$ in 96% yield [27]. Upon formation of assembly $1h_3 \cdot (DEB)_6$, the oct-7-enyl side chain of one calix[4]arene dimelamine is in close contact with an oct-7-enyl side chains of an adjacent calix[4]arene dimelamine. This pre-organization of the 7-octenyl side chains obtained upon addition of DEB and formation of the double rosette

causes the templated formation of macrocycle **7**, rather than the formation of cyclic monomer **8**.

The reaction monitored by ^1H -NMR spectroscopy clearly showed that the reaction occurs without destroying the assembly. The signals for the terminal vinylic protons of $1\text{h}_3\cdot(\text{DEB})_6$ at δ 5.8 and 4.9 (Fig. 17a) gradually disappear during the reaction and a new signal at δ 5.5 for the vinylic protons in $7\cdot(\text{DEB})_6$ is observed (Fig. 17b). The clean formation of **7** was also confirmed by MALDI-TOF ($m/z=3,100$ for $[\text{7}+\text{H}]^+$ containing the most abundant natural isotopes as

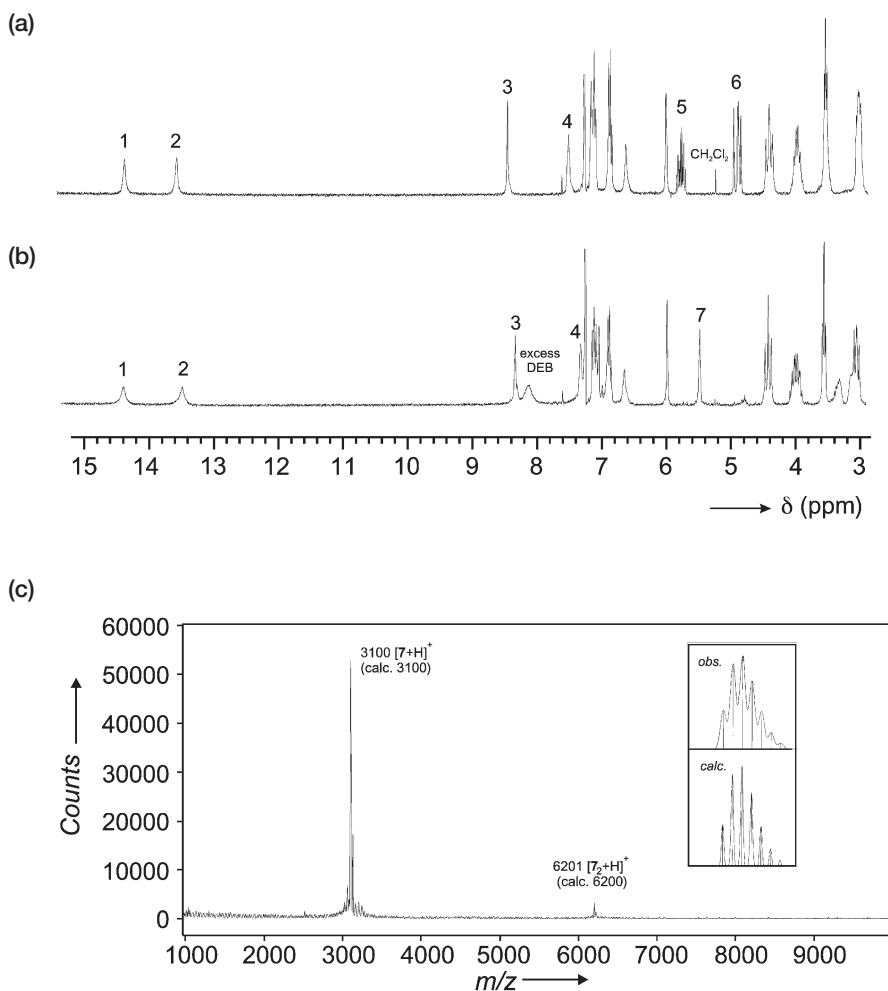


Fig. 17 Parts of the ^1H -NMR spectra (CDCl_3 , 298 K) of **a** assembly $1\text{h}_3\cdot(\text{DEB})_6$ and **b** assembly $7_3\cdot(\text{DEB})_6$ after reaction of assembly $1\text{h}_3\cdot(\text{DEB})_6$ with Grubbs catalyst. Peak assignment: NH_{DEB} protons (1 and 2), NH_{Ar} protons (3), NH_{CH_2} protons (4), terminal (5, 6) and internal (7) vinylic protons. **c** MALDI-TOF mass spectra of the crude reaction mixture of the covalent capture of assembly $1\text{h}_3\cdot(\text{DEB})_6$

calculated for $C_{180}H_{240}N_{36}O_{12}=3,100$). Both, HPLC and MALDI-TOF MS clearly showed that the cyclic monomer **8** is not formed, which emphasizes the degree of pre-organization of the reactive double bonds within the assembly. The clean formation of $7 \cdot (DEB)_6$ is only formed under conditions where assembly $1h_3 \cdot (DEB)_6$ is present. RCM reactions carried out at concentrations where extensive dissociation of the assembly is observed give the cyclic monomer **8** as the major product.

5.2

Templated Synthesis of Noncovalent Cyclic Hydrogen-Bonded Trimers

The double rosette $1a_3 \cdot (DEB)_6$ (see Fig. 1 for molecular structure) also acts as a template for the formation of the noncovalent hydrogen-bonded trimer **9**, which is not formed in the absence of this double rosette (Fig. 18). $1a_3 \cdot (DEB)_6$ is a self-assembled nanometer-sized molecular box that can encapsulate three molecules of alizarin **9** (Fig. 18). Both the top and the bottom of this highly thermodynamically stable molecular container comprise the cyclic hydrogen-bonded rosette motif, with the calix[4]arene units acting as side walls, while the space between the two rosette floors limits the encapsulation area. The dynamic character of the self-assembled box allows the rearrangement of the building blocks to obtain the “perfect” fit for three alizarin molecules forming a trimeric species [28]. The driving force for the encapsulation of alizarin is π - π stacking between host and guest, while the trimer formation arises from the formation of a hydrogen-bonded network between the entrapped molecules.

The crystal structure of the complex $1a_3 \cdot (DEB)_6 \cdot 9_3$ (Fig. 19) revealed that the two melamines of one calix[4]arene are in an *eclipsed* orientation, while before the encapsulation of **9**, these melamines were in a *staggered* orientation. The electron-deficient aromatic ring of **9** (ring B; see Fig. 18) is stacked in between the two relatively electron-poor rings of the melamine units, with a slight

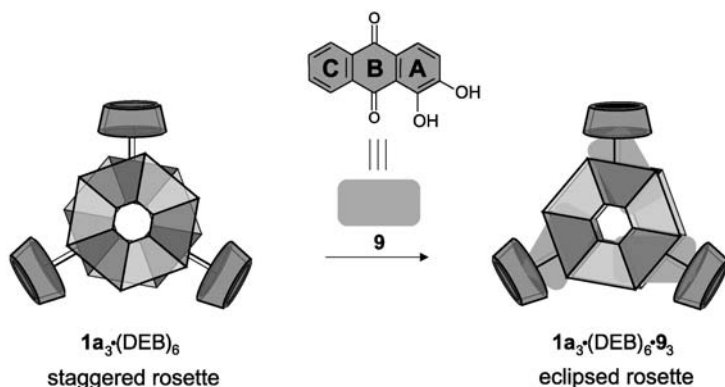


Fig. 18 Schematic illustration of the encapsulation of three molecules alizarine **9** by double rosette $1a_3 \cdot (DEB)_6$ and the conformational changes of double rosette $1a_3 \cdot (DEB)_6$ to fit **9**

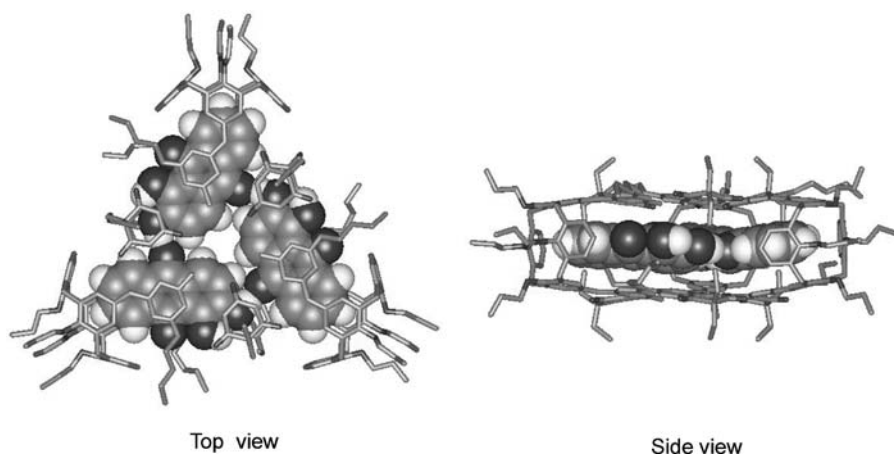


Fig. 19 Top and side view of the crystal structure of the complex $1a_3 \cdot (DEB)_6 \cdot 9_3$. A stick model is used for the representation of the molecular cage $1a_3 \cdot (DEB)_6$, while a space-filling representation is chosen for the trimer 9_3 . Hydrogens of the assembly are not shown and only the main parts for the disordered butyl and propyl groups are depicted

offset of the face-to-face arrangement [28]. Furthermore, the crystal structure showed that the three **9** molecules of the trimer are interlocked by an array of hydrogen bonds between the carbonyl groups and the 2-hydroxyl groups of **9**.

The symmetry of the complex, reflected by the relatively simple ^1H -NMR spectrum, indicated that three molecules of **9** are also complexed in solution between the two rosette layers (Fig. 20). The large shifts observed for the alizarin protons (>3 ppm) clearly indicate the encapsulation of the guest molecules. The aromatic protons H_r , H_s , and H_t of **9** (ring C, see Fig. 20) shifted 3.28–3.88 ppm upfield upon complexation, indicating that ring C is partially included in the calix[4]arene cone. The 2-hydroxyl group (OH_n) shifted 3.63 ppm downfield, suggesting that the hydroxyl group is involved in the formation of an hydrogen bond. Furthermore, the NH_{DEB} -protons H_a and H_b in the complex $1a_3 \cdot (DEB)_6 \cdot 9_3$ were shifted upfield in comparison with the free host $1a_3 \cdot (DEB)_6$. In summary, all the shifts confirmed the formation of the hydrogen-bonded alizarine trimer **9**₃ between the two rosette planes of the template $1a_3 \cdot (DEB)_6$ in solution.

6 Surface Templation

The topology of a structure that is formed by noncovalent interactions on a surface is determined by the noncovalent interactions between the surface template and the substrates [23]. The surface holds the organic groups in the correct orientation for a specific structure.

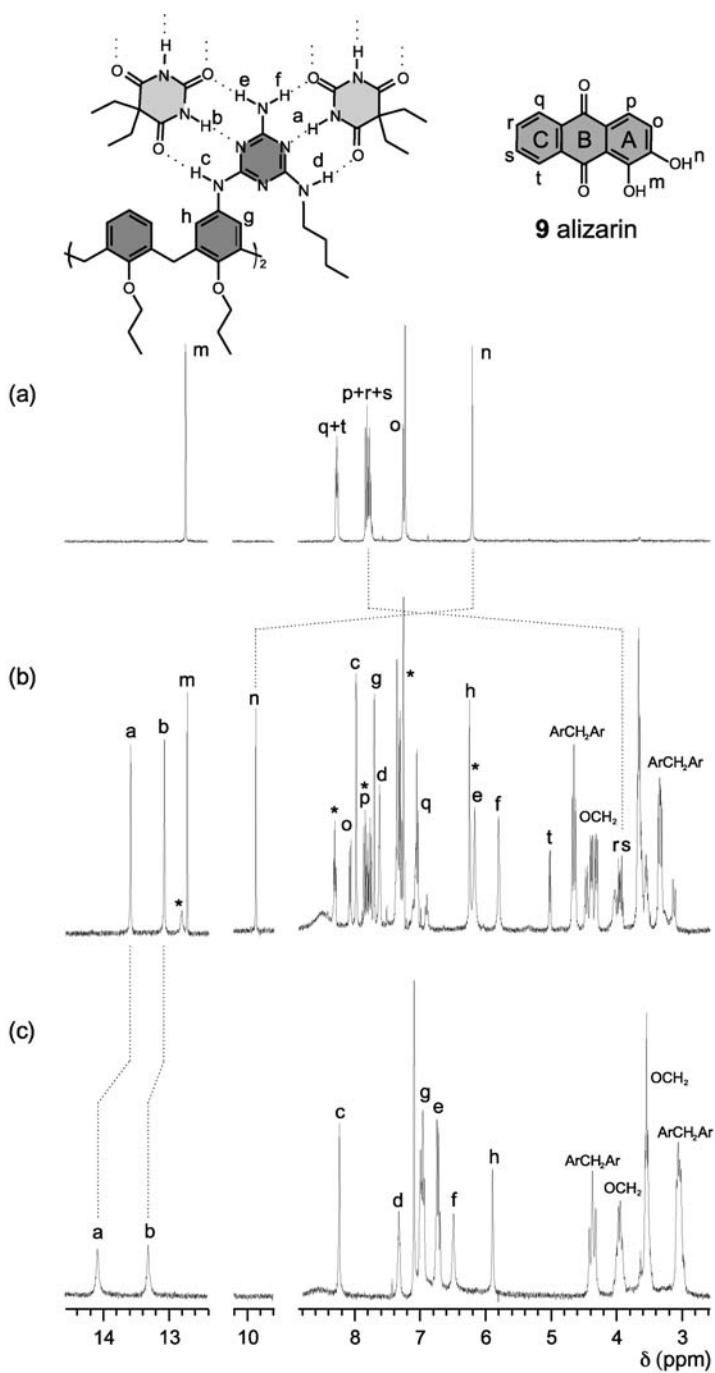


Fig. 20 Part of the ^1H -NMR spectra (CDCl₃) of **a** guest molecule **9**, **b** complex **1a₃·(DEB)₆·9**, and **c** receptor **1a₃·(DEB)₆**. The signals corresponding to free **9** are marked with *

7.1

Gold Surfaces

The growth of individual nanometer-sized hydrogen bonded assemblies on gold monolayers is templated through an exchange reaction between double rosette $1a_3 \cdot (DEB)_6$ (for molecular structures see Fig. 1) in solution and single calix[4]arene dimelamine **1i** embedded into hexanethiol self-assembled monolayers (SAMs) (Fig. 21) [29]. When gold Au (111) substrates covered with hexanethiol monolayer are exposed to a solution of absorbate **1i**, single isolated features with an average height of 1.1 ± 0.2 nm are visible in TM-AFM images in air. The calix[4]arene dimelamines **1i** are positioned at the surface of the monolayers. Subsequently, TM-AFM images recorded after immersing of the monolayers in a solution of absorbate $1a_3 \cdot (DEB)_6$ results in two different size features. The height of the largest feature is 3.51 nm, which agrees well with the expected size for the heteromeric assembly $1a_2 \cdot 1i \cdot (DEB)_6$ considering the crystal structure of a similar double rosette assembly [7]. The height of the smallest features (0.95 nm) corresponds to single isolated molecules of **1i** that are not involved in exchange reactions with $1a_3 \cdot (DEB)_6$.

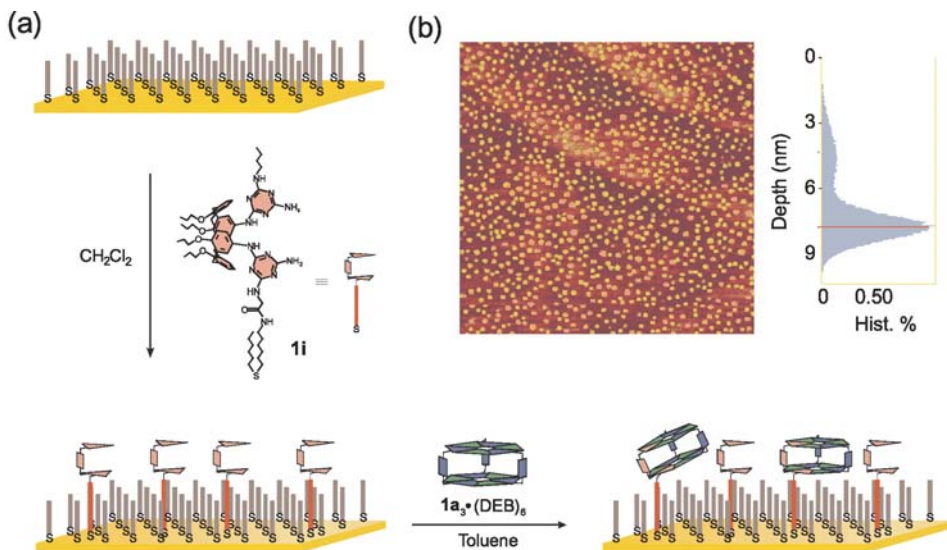


Fig. 21 a Schematic representation of the growth of assemblies $1a_2 \cdot 1i \cdot (DEB)_6$ on gold monolayers. b TM-AFM image in air ($1 \times 1 \mu m$) and histogram analysis of hexanethiol monolayers on Au (111) after sequential treatment with a solution of calix[4]arene dimelamine **1i** and a solution of assembly $1a_3 \cdot (DEB)_6$. Color scale from dark to yellow: $Z=10$ nm

6.2

Graphite Surfaces

6.2.1

First-Order Template Effect

The formation of linear rod-like structures on a graphite surface was observed by TM-AFM after deposition of double rosette $1a_3 \cdot (DEB)_6$ (0.01 mg/mL) on the graphite template (Fig. 22a) [30]. These rod-like structures are most likely formed by the face-to-face arrangement of multiple disc-like assemblies $1a_3 \cdot (DEB)_6$, a process that is driven by solvophobic interactions. The TM-SFM data were analyzed according to the model presented in Fig. 22b. The heart-to-heart distance is experimentally determined from the SFM images by averaging the distance spanned by 10–15 adjacent strands. This parameter is related to the others via $h=d+n$. The diameter (d) is calculated from the crystal structure of $1a_3 \cdot (DEB)_6$ via the relation $d=2L/(3)^{0.5}$ [7]. These calculations assume that stacking occurs with the alkyl chains organized in a circular fashion around the structure. For the rod-like nanostructures with $1a_3 \cdot (DEB)_6$ a diameter of 3.4 nm was calculated from the TM-SFM data. It was found that the heart-to-heart distance (3.8 nm) is always larger than the diameter, indicating that the short C_3 side chains of the calix[4]arene units are not interdigitating ($n=0.4$ nm).

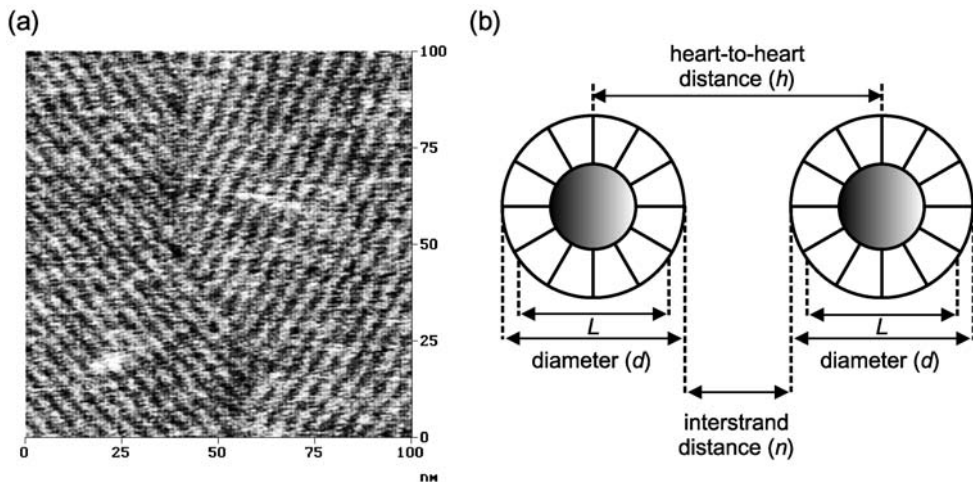


Fig. 22 a TM-SFM images of rod-like nanostructure $[1a_3 \cdot (DEB)_6]_n$ (chloroform). b Schematic front view of the nanostructures indicating the “heart-to-heart” distance (h), the diameter (d), and the inter-strand distance (n)

6.2.2

First- and Second-Order Template Effect

Double rosette $1\mathbf{l}_3\cdot(\text{DEB})_6$ having gold atoms coordinated to phosphane groups also form nanorod domains after deposition on HOPG template (first-order template effect), as unveiled by intermittent contact mode AFM (Fig. 23) [31]. The observed structure is characterized by a heart-to-heart distance of 5.1 nm and is thereby forming structurally similar 2-D arrays as observed for double rosette $1\mathbf{a}_3\cdot(\text{DEB})_6$. The observed inter-row distances (heart-to-heart) are a function of the substituents as well as the rosette size and, together with evidence from molecular modeling, led to the conclusion that the rosettes are stacked approximately face-to-face in these rows. The direct real-space observation of the individual rosettes comprising the nanorod domains was attempted in high-resolution AFM measurements. As shown in Fig. 23, the 2-D fast Fourier transform (2-D FFT) shows several reflections in addition to the reflections that correspond to the inter-row distance. From analysis of the 2-D FFT, an oblique lattice structure was obtained, which is characterized by $a=4.0\pm0.1$ nm, $b=5.2\pm0.1$ nm, and $\gamma=105\pm3^\circ$. This unit cell probably contains four double rosette structures, which correspond to a formal area requirement of 5.0 nm²/rosette. The gas-phase-minimized structure possesses an area requirement of 3.64 nm²/rosette. These values are in good agreement with each other considering earlier reports of related double rosettes [30].

On the other hand, the feasibility of $1\mathbf{l}_3\cdot(\text{DEB})_6$ to serve as a scaffold for the formation of metal-containing nanorod arrays might constitute a viable route for the templated (second-order template effect) bottom-up fabrication of, for example, conducting nanowires.

The formation of rod-like nanostructures with the larger tetra-rosette assembly $2_3\cdot(\text{DEB})_{12}$ (for molecular structure see Fig. 14 top) has also been studied by atomic force microscopy (AFM) [32]. The self-assembly of tetra-rosettes $2_3\cdot(\text{DEB})_{12}$ from a dilute solution on highly oriented pyrolytic graphite (HOPG) by slow evaporation and subsequent vacuum treatment resulted in the formation of multiphase films (Fig. 24a). The most prominent features of these films are the ordered domains, which consist of parallel stripes as revealed by tapping mode AFM images. The tetra-rosettes $2_3\cdot(\text{DEB})_{12}$ form nanorod assemblies on HOPG that are similar to the structures observed for double rosette $1\mathbf{a}_3\cdot(\text{DEB})_6$. The mutual directions of the rods in different domains possess relative angles of 0°, 60°, and 120°, respectively (Fig. 24). Hence, the alignment is determined by the template substrate HOPG.

The nanorods observed by AFM are characterized by a highly reproducible inter-row distance (heart-to-heart) of 4.6 nm, and appears to be an intrinsic property of the tetra-rosette $2_3\cdot(\text{DEB})_{12}$ nanorod assembly on the template HOPG.

In higher resolution AFM images, a superstructure with smaller periodicity is also present, suggesting the presence of inclined elongated features along the rows. The quantitative analysis of the 2-D fast Fourier transforms (Fig. 25b

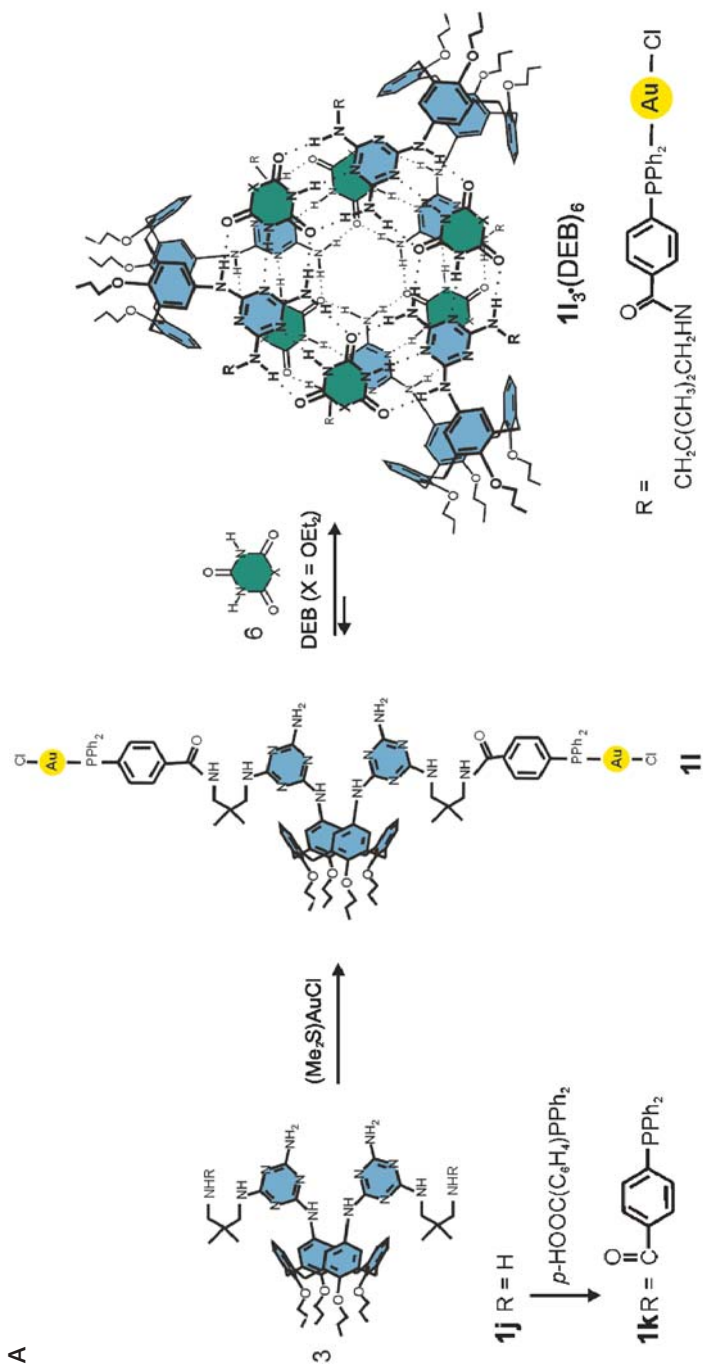


Fig. 23 a Synthesis of gold-functionalized calix[4]arene dimelamine **11** and formation of double-rosette **11₃(DEB)₆** containing six Au(I) atoms. b Schematic representation of the formation of **11₃(DEB)₆** from **11**. c Tapping mode AFM phase images of rosettes **11₃(DEB)₆** on HOPG acquired in air (*I*). High resolution TM-AFM image of nanorod domain of rosettes **11₃(DEB)₆** (*insets*; 2-D FFT *left*; FFT filtered section *right*) (*2*) and unit cell derived from an analysis of the 2-D FFT of high resolution TM-AFM image. This cell contains probably four double rosettes. TM-AFM image of different domain orientations of nanorod domains of rosettes **11₃(DEB)₆** on HOPG (*3*) (domains labeled *a* and *b* differ in orientation by 6°; the bulk crystalline phase is denoted *c*). *Inset*: 2-D FFT of section of *3*

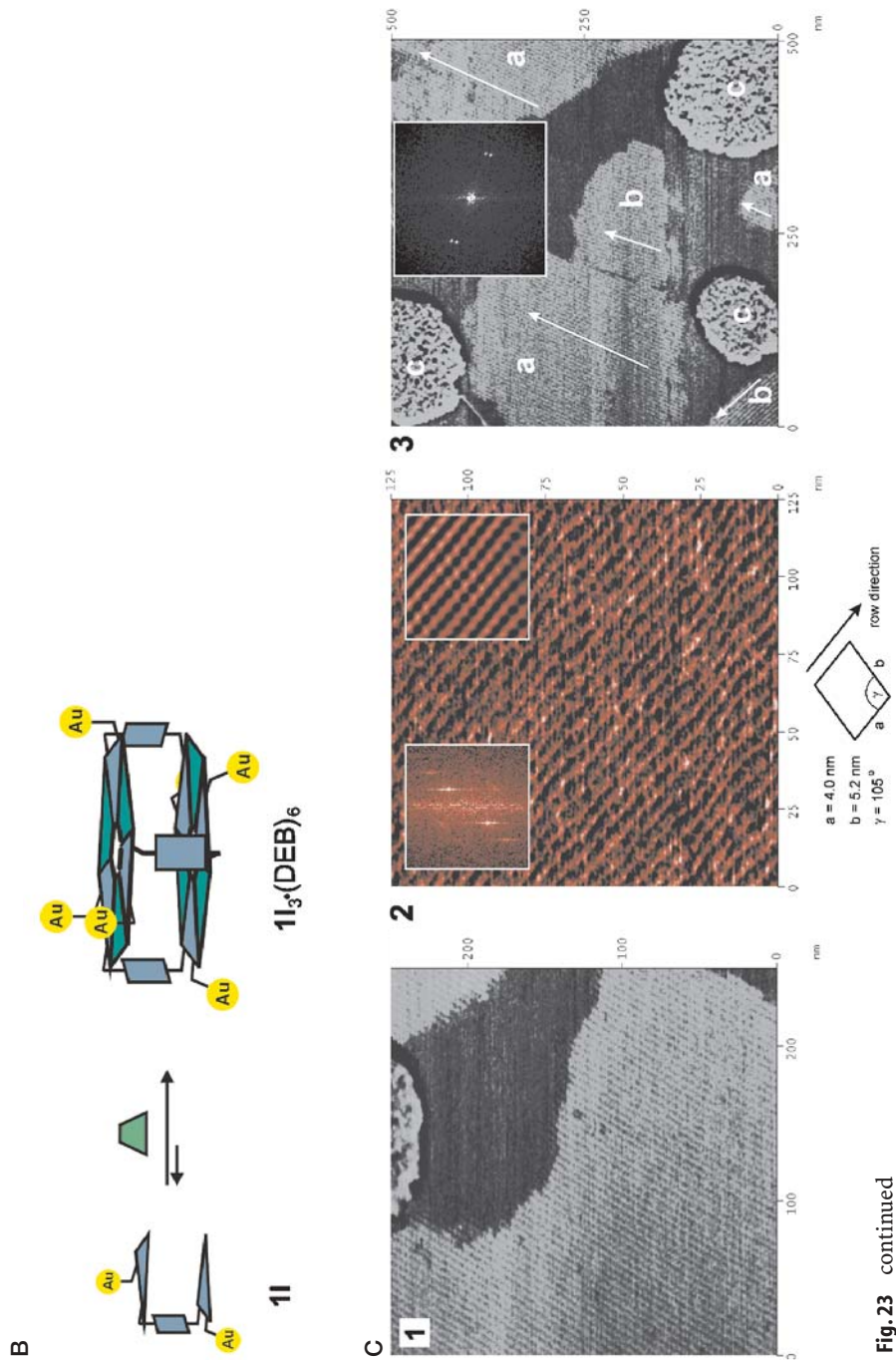


Fig. 23 continued

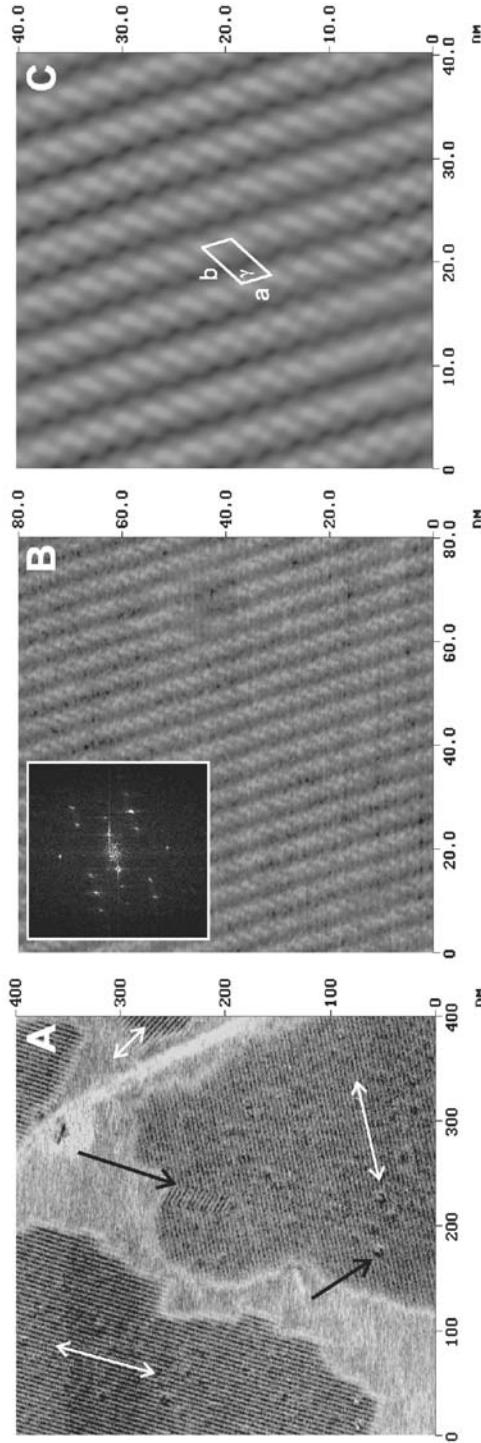


Fig. 24 a Tapping mode AFM phase image of nanorod domains of tetraosettes $2_3'(\text{DEB})_{12}$ on HOPG. b Unfiltered high resolution tapping mode AFM phase image of tetraosette $2_3'(\text{DEB})_{12}$ nanorod domain structure (inset: 2-D fast Fourier transform). c Fourier filtered section of raw data shown in a and unit cell of the lattice structure

inset) reveals an oblique lattice structure with $a=2.5\pm0.3$ nm, $b=5.0\pm0.1$ nm, and $\gamma=122\pm3^\circ$. This unit cell, which has an area of 10.6 nm^2 and contains probably one rosette nanostructure, is indicated in the Fourier filtered section shown in Fig. 25c. Considering the known crystal structure of the double rosette **1a**₃-(DEB)₆ and the gas-phase minimized structure of the tetra-rosettes [33], the observed nanorods can be concluded to consist of rows of tetra-rosettes.

References

1. Seto CT, Whitesides GM (1993) *J Am Chem Soc* 115:905
2. Vreekamp RH, van Duynhoven JPM, Reinhoudt DN (1996) *Angew Chem Int Ed* 35:1215
3. Jolliffe KA, Timmerman P, Reinhoudt DN (1999) *Angew Chem Int Ed* 38:933
4. Paraschiv V, Crego-Calama M, Timmerman P, Reinhoudt DN (2001) *J Org Chem* 66:8297
5. Prins LJ, Neuteboom EE, Paraschiv V, Crego-Calama M, Timmerman P, Reinhoudt DN (2002) *J Org Chem* 67:4808
6. a) Seto CT, Whitesides GM (1990) *J Am Chem Soc* 112:6409; b) Zerkowski JA, Seto CT, Wierdo DA, Whitesides GM (1990) *J Am Chem Soc* 112:9025
7. Timmerman P, Vreekamp RH, Hulst R, Verboom W, Reinhoudt DN, Risannen K, Udachin KA, Ripmeester J (1997) *Chem Eur J* 3:1823
8. a) Timmerman P, Prins LJ (2001) *Eur J Org Chem* 17:3191; b) Reinhoudt DN, Timmerman P, Cardullo F, Crego-Calama M (1999) In: *Supramolecular science: where it is and where it is going*. Ungaro R, Dalcanele E (eds) Kluwer, Dordrecht, pp 181–195
9. Prins LJ, Jolliffe KA, Hulst R, Timmerman P, Reinhoudt DN (2000) *J Am Chem Soc* 122:3617
10. a) Prins LJ, Huskens J, De Jong F, Timmerman P, Reinhoudt DN (1999) *Nature* 398:498; b) Prins LJ, De Jong F, Timmerman P, Reinhoudt DN (2000) *Nature* 408:181
11. Eliel EL, Wilen SH (1994) *Stereochemistry of organic compounds*. Wiley, New York
12. a) Timmerman P, Jolliffe KA, Crego-Calama M, Weidmann JL, Prins LJ, Cardullo F, Snellink-Ruel BHM, Fokkens RH, Nibbering NMM, Shinkai S, Reinhoudt DN (2000) *Chem Eur J* 6:4104; b) Jolliffe KA, Crego-Calama M, Fokkens R, Nibbering NMM, Timmerman P, Reinhoudt DN (1998) *Angew Chem Int Ed* 37:1247
13. a) Otto S, Furlan RLE, Sanders JKM (2001) *Curr Opin Chem Biol* 6:321; b) Lehn J-M, Eliseev AV (2001) *Science* 291:2331; c) Otto S, Furlan RLE, Sanders JKM (2002) *Drug Discov Today* 7:117; d) Ramstrom O, Lehn J-M (2002) *Nat Rev Drug Disc* 1:26; e) Rowan SJ, Cantrill SJ, Cousins GRL, Sanders JKM, Stodart J F (2002) *Angew Chem Int Ed* 41:898
14. a) Farlan RLE, Ng Y-F, Otto S, Sanders JMK (2001) *J Am Chem Soc* 123:8876; b) Hiraoka S, Kubota Y, Fujita M (2000) *Chem Commun*:1509
15. Crego-Calama M, Hulst R, Fokkens R, Nibbering NMM, Timmerman P, Reinhoudt DN (1998) *Chem Commun* 1021
16. Crego-Calama M, Timmerman P, Reinhoudt DN (2000) *Angew Chem Int Ed* 39:755
17. a) Palmans ARA, Vekemans JAJM, Havinga EE, Meijer EW (1997) *Angew Chem Int Ed* 36:2648; b) Brunsveld L, Schenning APHJ, Broeren MAC, Janssen HM, Vekemans JAJM, Meijer EW (2000) *Chem Lett* 292; c) Brunsveld L, Lohmeijer BGG, Vekemans JAJM, Meijer EW (2000) *Chem Commun* 2305
18. Van der Schoot MMAJ, Brunsveld L, Sijbesma RP, Ramzi A (2000) *Langmuir* 16:10076
19. Green MM, Reddy MP, Johnson RJ, Darling G, O'Leary DJ, Willson G (1989) *J Am Chem Soc* 111:6452
20. Yashima E, Maeda K, Okamoto Y (1999) *Nature* 399:449
21. Bielejewska AG, Marjo CE, Prins LJ, Timmerman P, De Jong F, Reinhoudt DN (2001) *J Am Chem Soc* 123:7518

22. a) Ishi-i T, Crego-Calama M, Timmerman P, Reinhoudt DN, Shinkai S (2002) *Angew Chem Int Ed* 41:1924; b) Ishi-i T, Crego-Calama M, Timmerman P, Reinhoudt DN, Shinkai S (2002) *J Am Chem Soc* 124:14631
23. Anderson S, Anderson HL, Sanders JKM (1993) *Acc Chem Res* 26:469
24. a) Grubbs RH, Chang S (1998) *Tetrahedron* 54:4413; b) Armstrong SK (1998) *J Chem Soc, Perkin Trans* 1:371; c) Schuster M, Blechert S (1997) *Angew Chem Int Ed* 36:2036
25. a) Clark TD, Ghadiri MR (1995) *J Am Chem Soc* 117:12364; b) Miller SJ, Grubbs RH (1995) *J Am Chem Soc* 117:5855
26. a) Marsella MJ, Maynard HD, Grubbs RH (1997) *Angew Chem Int Ed* 36:1101; b) Mohr B, Weck M, Sauvage J-P, Grubbs RH (1997) *Angew Chem Int Ed* 36:1308; c) Hamilton DG, Sanders JM (1998) *Chem Commun*: 1749
27. Cardullo F, Crego-Calama M, Snellink-Ruël, Weidmann J-L, Bielejewska A, Fokkens R, Nibbering NMM, Timmerman P, Reinhoudt DN (2000) *Chem Commun* 367
28. Kerckhoffs JMCA, Van Leeuwen FWB, Spek AL, Kooijman H, Crego-Calama M, Reinhoudt DN (2003) *Angew Chem Int Ed* 42:5717
29. Garcia-Lopez JJ, Zapotoczny S, Timmerman P, Van Veggel FCJM, Vancso GJ, Crego-Calama M, Reinhoudt DN (2003) *Chem Commun* 352
30. Klok H-A, Jolliffe KA, Schauer CL, Prins LJ, Spatz JP, Möller M, Timmerman P, Reinhoudt DN (1999) *J Am Chem Soc* 121:7154
31. Manen H-J, Paraschiv V, García-López JJ, Schönherr H, Zapotoczny S, Vancso GJ, Crego-Calama M, Reinhoudt DN (2004) *Nano Lett* 4:441
32. Schönherr H, Paraschiv V, Zapotoczny S, Crego-Calama M, Timmerman P, Frank CW, Vancso GJ, Reinhoudt DN (2002) *Proc Natl Acad Sci* 99:5024
33. Timmerman P, Weidmann J-L, Jolliffe KA, Prins LJ, Reinhoudt DN, Shinkai S, Frish L, Cohen Y (2000) *J Chem Soc Perkin Trans* 2:2077

Imprinted Polymers

Andrew J. Hall · Marco Emgenbroich · Börje Sellergren (✉)

INFU, University of Dortmund, Otto Hahn Strasse 6, 44221 Dortmund, Germany
b.sellergren@infu.uni-dortmund.de

1	Introduction	317
2	General Approaches	319
3	Binding Site Design in Non-Covalent Imprinting	323
3.1	New Host Monomers for Non-Covalent Imprinting	323
3.2	Introducing Secondary Functions to Non-Covalent Binding Monomers	328
3.3	Binding Site Monomers in Metal-Mediated Imprinting	330
3.4	Molecularly Imprinted Dendrimers	333
4	Catalysis with Imprinted Polymers	333
4.1	Bio-inspired MIPs Catalysing Hydrolysis Reactions	335
4.2	Chemoinspired catalytically active MIPs – Imprints of metal catalysts or their analogues	343
5	Perspectives	346
	References	347

1 Introduction

Recent progress in the area of host-guest chemistry has resulted in low molecular weight hosts capable of selective and strong complexation of a variety of guests in various matrix environments [1–3]. One drawback of such receptors is the difficulty in engineering them in useful formats for the recognition of guests of higher complexity or of larger size. Thus, general recognition strategies directed towards more complex targets based on artificial receptors remain an important challenge [4]. In this context the concept of molecular imprinting appears very appealing [5–7]. Here, monomers are chosen in order to complement functional groups of a template molecule. After incorporation of the monomer–template complexes in a cross-linked polymer matrix and removal of the template, binding sites remain that are capable of rebinding the template with high affinity and selectivity (Fig. 1).

The advantage of this “top-down” approach in receptor design lies in its use of the self-assembly principle to guide the binding groups to their positions in the receptor site; thus, the structure of the final binding site is, a priori, unknown. Recent advances in molecular imprinting have opened up new ways

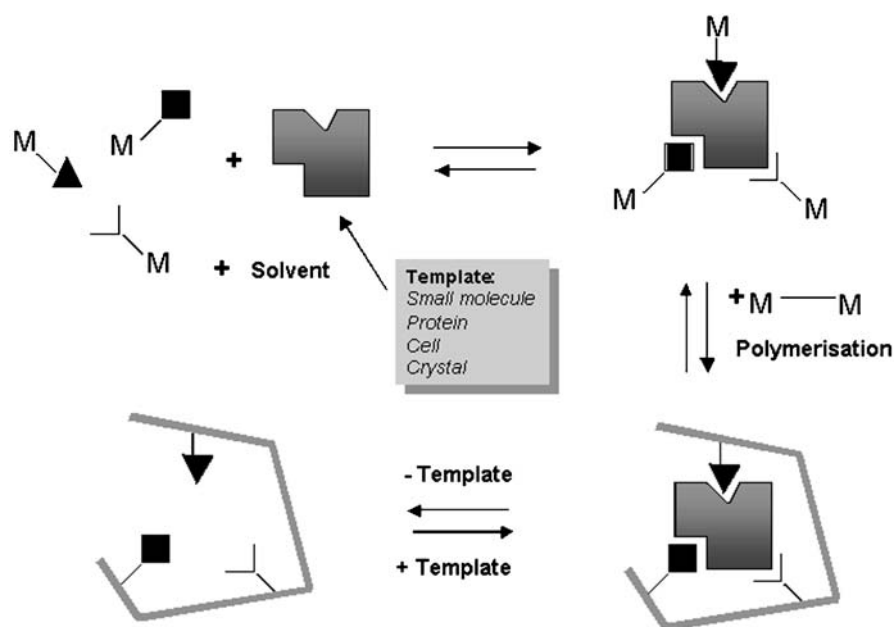


Fig. 1 General principle for imprinting of polymers starting from templates and monomers

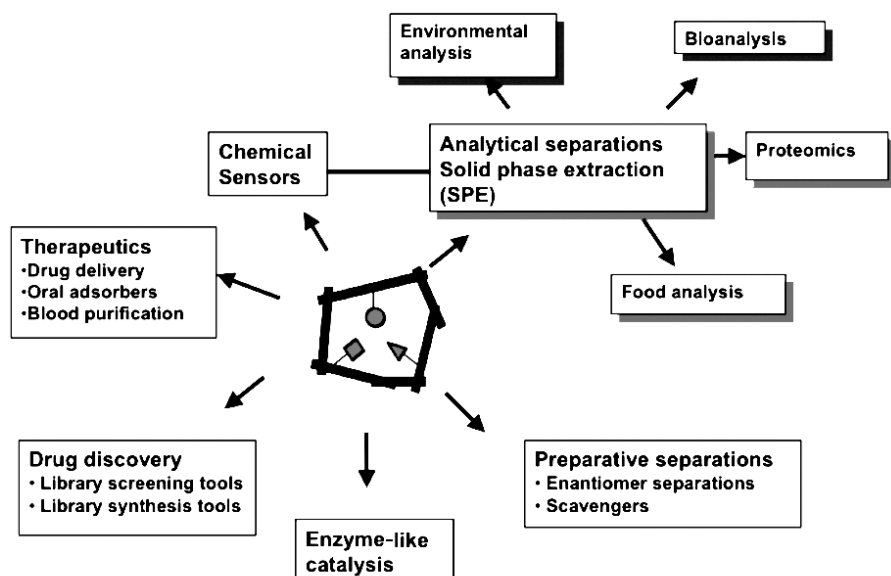


Fig. 2 Scheme outlining the main applications envisaged for MIPs

to custom-make robust molecular recognition elements with relatively little effort. A range of applications using these so-called molecularly imprinted polymers (MIPs) are under investigation (Fig. 2).

For instance, stable recognition elements capable of strong and selective binding of molecules could be used in areas with urgent needs for methods enabling selective separation [8], extraction [9] and sensing [10] of low molecular weight or macromolecular targets in biological fluids. Alternatively, such recognition elements could be used as scavengers to remove undesirable compounds from foods or biological fluids [11], for targeted delivery of drugs [12], or as tools in drug discovery [13]. If these recognition elements can be designed to bind specific proteins, a number of important applications in areas such as biotechnology (including downstream processing, sensors and diagnostics) can be foreseen.

Although MIPs are good at binding specific targets they have been less successful in catalysing chemical reactions [14]. However, using stable transition state analogues as templates, recent advances indicate that they may someday compete with their biological counterparts.

We will review here the recent advances in this field from the above-mentioned aspects. In the context of templates we will discuss the different roles templates have in molecular imprinting, from achieving molecular recognition to achieving catalysis, and the chemistry involved in achieving this using mainly the non-covalent imprinting approach. For a comprehensive coverage of the field, the reader is referred to a number of excellent books and reviews [5, 7, 10, 14–16].

2

General Approaches

MIPs are highly reticulated network polymers consisting of a common matrix structure and binding sites formed by a template present during polymer synthesis (Fig. 1).

The 3-D arrangement of the binding functional groups in MIPs is obtained by linking the functional monomers covalently or noncovalently to the template during polymerisation (Fig. 3). Removal of the template from the formed polymer then generates a structure complementary to the template structure. These sites can be reoccupied by the template or an analogous structure through reformation of the binding interactions present during synthesis or, alternatively, through weaker, kinetically more favourable interactions.

Essentially, three main approaches exist to date to generate high fidelity imprinted sites, which are distinguished by the nature of the linkage during synthesis and during rebinding.

The first example of molecular imprinting of organic network polymers introduced by Wulff was based on a covalent attachment strategy, i.e. covalent monomer–template, covalent polymer–template (Fig. 3A) [17, 18]. This approach has the advantage of a known stoichiometry between the functional

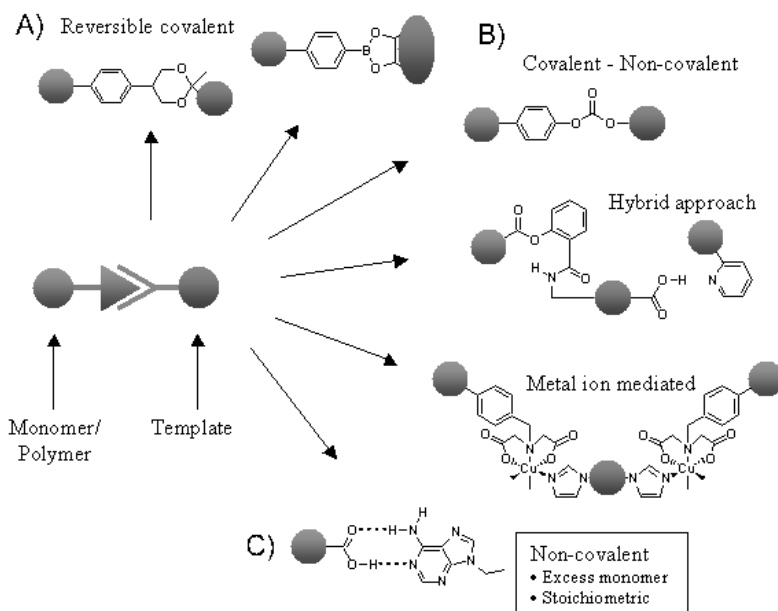


Fig. 3 Strategies used to place binding or catalytic functional groups at defined positions in imprinted sites of network polymers

monomer and the template. Provided that the template can be recovered in high yields, a high density of well-defined sites can be expected. One problem with this approach is the limited number of covalent linkages that satisfy these criteria. Furthermore, considerable synthetic effort may be required to prepare the template, and slow kinetics are often observed for rebinding by reformation of the covalent bond. This approach is therefore difficult to combine with applications where fast on-off kinetics are required. In this respect, the use of sacrificial spacers has found more widespread use [11]. Here the functional monomer is bound to the template through a disposable spacer that is removed after polymerisation is completed. This results in a disposition of the functional groups allowing rebinding to occur through hydrogen bonding interactions (Fig. 3B). Therefore, this approach can be more amenable to chromatographic applications and furthermore allows more freedom in the choice of polymerisation conditions (*vide infra*). However, the most widely used approach in imprinting involves functional monomers that are chosen to associate non-covalently with the template (Fig. 3C) [19]. Here the template is directly mixed with one or several functional monomers followed by polymerisation. It can thereafter be easily extracted from the polymer and recycled. Generally, the resulting materials can be directly used to perform separations with high affinity and selectivity, for instance as chromatographic stationary phases.

For example, a simple commodity monomer such as methacrylic acid (MAA) can be used to create good binding sites for a large variety of template structures

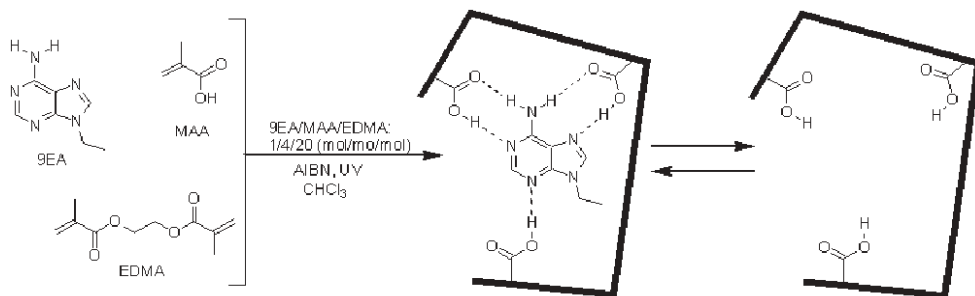


Fig. 4 Non-covalent imprinting of 9-ethyladenine (9EA) leading to highly cross-linked monoliths from which particles are obtained by repetitive crushing and sieving cycles

containing hydrogen bond- or proton-accepting functional groups (see Fig. 4 for the imprinting of 9-ethyladenine 9EA) [20]. MAA forms complementary hydrogen bonds or hydrogen-bonded ion pairs with the template, with individual binding constants ranging from units for weak hydrogen bonds to several hundreds for cyclic hydrogen bonds or hydrogen-bonded ion pairs formed in weakly polar aprotic solvents such as chloroform.

Otherwise, templates containing acids are often well targeted using basic functional monomers such as vinylpyridine, or amide monomers such as methacrylamide. For templates with multiple functionalities, obtaining the best result may require the use of a multitude of the above functional monomers. Often, the optimum combination is only found after time-consuming trial and error, which has spurred the development of parallel synthesis and assessment techniques and computational approaches to identify suitable functional monomers [21].

Although the preparation of a MIP by this method is technically simple it relies on the success of the stabilisation of the relatively weak interactions between the template and the functional monomers. This typically requires the use of solvents of low polarity and the addition of an excess of functional monomer (typically four equivalents, but sometimes higher) in order to ensure that the template molecule is complexed to a maximal degree. This, in turn, means that a large proportion of the functional monomer is not involved in complexation of the template and is instead distributed randomly throughout the polymer matrix during the polymerisation. This is a major cause of the high levels of non-specific binding and binding site heterogeneity observed in these materials.

The result is often a material that exhibits a small class of high affinity binding sites capable of discriminating the template from close structural analogues (see Fig. 5a) superimposed on a larger class of non-discriminating sites [20].

As shown for a polymer imprinted with 9-ethyladenine, these materials exhibit binding isotherms (Fig. 5b), that can only be fitted with multiple site models. This typically results in a poor performance when the materials are used as chromatographic stationary phases. Furthermore, it results in a low saturation capacity, which restricts the use of such materials mainly to low load

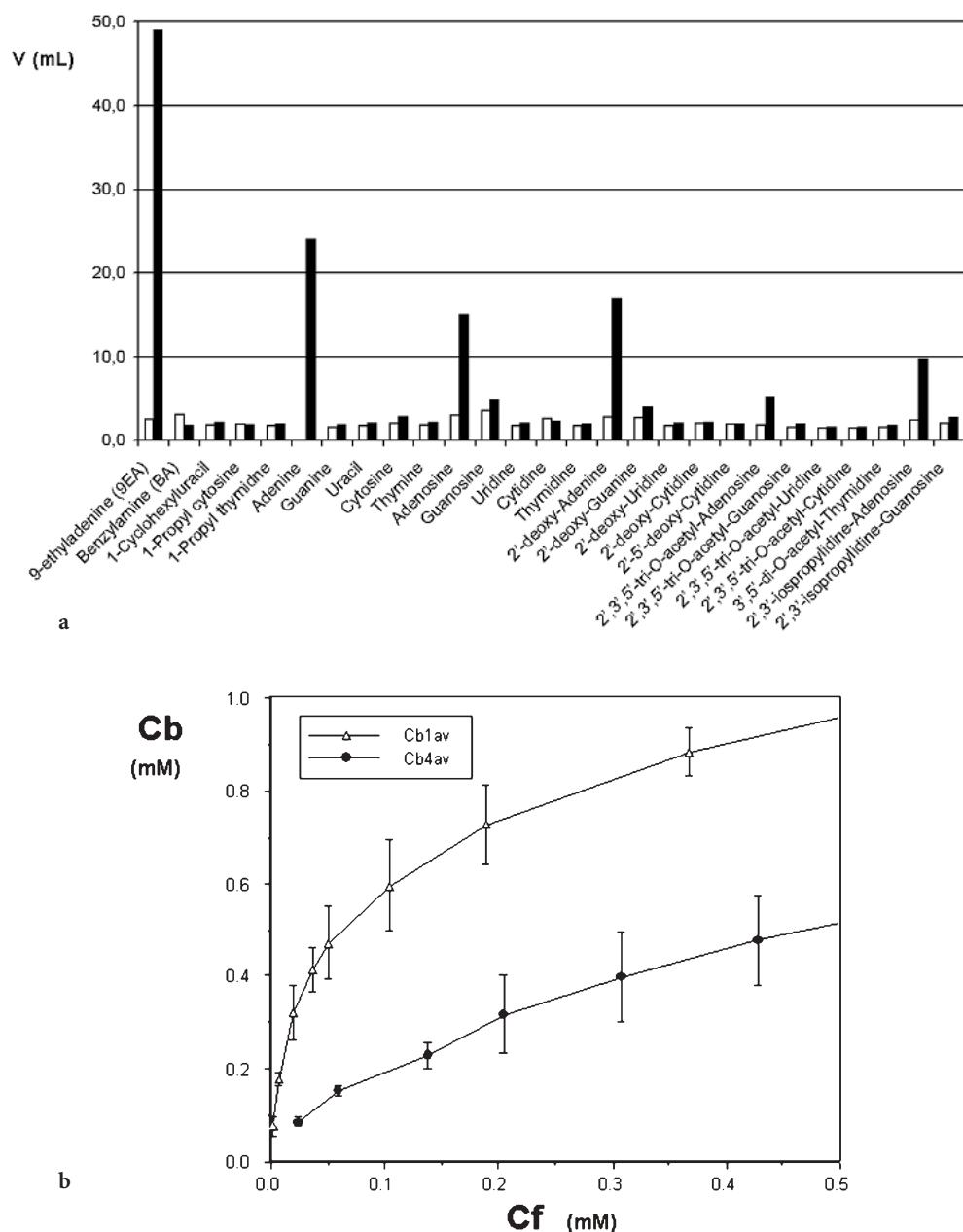


Fig. 5 **a** Elution volumes of the DNA bases, nucleosides and their derivatives from chromatographic runs using columns packed with a polymer imprinted with 9EA (black bars) or a control polymer imprinted with benzylamine (white bars). The mobile phase was acetonitrile/acetic acid/water: 92.5/5/2.5 (v/v/v). **b** Binding isotherms obtained from equilibrium binding experiments in chloroform showing the binding to a 9EA-imprinted polymer (*upper curve*) and a control polymer imprinted with benzylamine (*lower curve*). From [20]

analytical applications. One solution to this problem is to extend the monomer tool box drawing inspiration from the area of host-guest chemistry. Thus, designed functional monomers and recent examples of their use to achieve molecular recognition or catalysis are the subjects of the following sections.

3

Binding Site Design in Non-Covalent Imprinting

In the previous section, the various methods of molecular imprinting have been described. In this section we will focus on some of the more successful approaches that have been investigated towards the design of improved binding sites within MIPs. These concern firstly developments in “non-covalent” imprinting, especially with regards to the design of new “breeds” of functional monomers capable of stronger interactions than those traditionally used in imprinting and, secondly, on developments in “metal-mediated” imprinting.

The use of designed functional monomers also allows the opportunity to build in secondary functions, such as units capable of signalling a binding event or cross-linking functional monomers which can increase binding site fidelity. Developments of this nature will also be discussed.

3.1

New Host Monomers for Non-Covalent Imprinting

There have been a number of advances in recent years in the design of new functional monomers for non-covalent imprinting. Here, the aim is the preparation of monomers capable of strong binding to the template molecule, such that no excess of functional monomer is required during the imprinting process. The achievement of this ultimate goal has thus far been demonstrated in only a limited number of examples. To describe such examples Wulff has coined the phrase “stoichiometric non-covalent imprinting” [6].

One of the first reports of a designed functional monomer in molecular imprinting came from Takeuchi et al., [22] who used the bis-amidopyridine monomer **1** in the imprinting of barbitol. The monomer presents a donor-acceptor-donor (DAD) array of hydrogen bond sites, which is complementary to the ADA sites within the template. The polymeric binding site obtained was postulated to resemble the structure of small molecule receptors prepared by Hamilton et al. [23] for the same purpose (Fig. 6). MIPs prepared with this monomer showed relatively high imprinting factors and a degree of selectivity for barbitol over differently substituted barbiturates when tested in the chromatographic mode. Further, analytes where some of the hydrogen bonding sites had been removed were much less retained on these polymers. Takeuchi et al. extended their use of **1** to the imprinting of uracils (thymines) [24, 25].

Concurrently with this latter work, we used **1** in the imprinting of similar imide-containing templates, e.g. 1-substituted uracils [26, 27] and flavins (es-

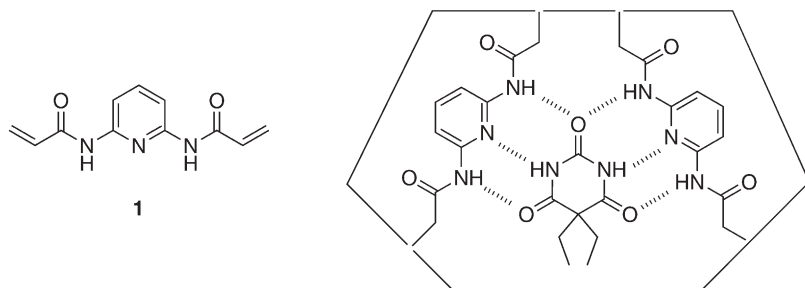


Fig. 6 2,6-Bis-acrylamidopyridine (**1**) and the proposed polymeric binding site with barbital

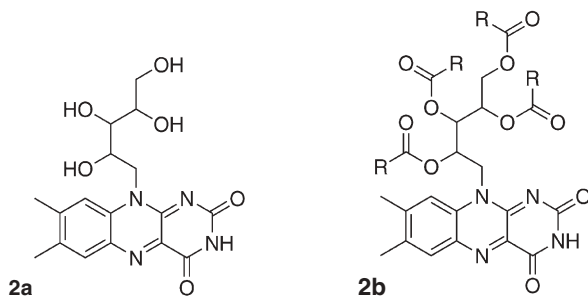


Fig. 7 Structures of **2a** riboflavin and **2b** template analogues used for imprinting (R=CH₃, C₂H₅, C₃H₇)

pecially riboflavin, vitamin B₂(**2a**)) (Fig. 7) [28]. We first quantified the solution binding of the monomer to the templates. By performing ¹H-NMR titrations (in CDCl₃), we obtained association constants of ca. 780 M⁻¹ for the binding to (1-benzyl) uracil (**1BU**) and ca. 600 M⁻¹ for a chloroform-soluble flavin derivative. This implies that, at “normal” imprinting concentrations (ca. 0.1 M in template), stoichiometric use of the monomer would lead to ca. 80% complexation of the template molecule. However, due to difficulties in solubilising **1** and **1BU** in the chosen polymerisation medium (containing EDMA as cross-linking monomer), we used much lower concentrations (ca. 0.05 M), while keeping the ratios of **1** and **1BU** stoichiometric with the template functionality. Even under these imprinting conditions, the obtained MIPs exhibited large imprinting factors.

We then extended our studies to the preparation of riboflavin-selective MIPs, again using **1** as the functional monomer. Due to the insolubility of riboflavin in organic media, we used a series of tetraesters (acetate, propionate and butyrate) as “template analogues” during the imprinting protocols and used **1** in a stoichiometric manner. The resulting MIPs showed extremely high imprinting factors (>100) for their respective templates when organic media were used as chromatographic mobile phases. Furthermore, recognition of riboflavin in predominantly aqueous phases (85% water) was also achieved.

Aiming to increase the performance of our MIPs, we then prepared bis-amidopyrimidines **3** and **4** [27] (Fig. 8), expecting that the electron-donating substituents at the 6-position of the ring would lead to an enhancement of the hydrogen-bond accepting properties of the ring N3. However, the strengths of the binding to **1BU** of both **3** (K_a ca. 600 M⁻¹) and **4** (K_a ca. 560 M⁻¹) were found to be lower than that with **1**. This is in keeping with the reports of Sijbesma et al. [29], who reported that such molecules show a strong tendency to dimerise (K_d ca. 170 M⁻¹ in CDCl₃), thus masking their binding affinity towards uracils. We estimate $K_d(\mathbf{3})$ to be ca. 700 M⁻¹. Given that the K_a value for the **3:2** complexation is not so different from that obtained for **1:2** complexation, we believe that the intrinsic binding ability of **3** is higher than that of **1**.

Despite this “masking” effect, anti-2 MIPs prepared with **3** as the functional monomer, under the same conditions used previously with **1**, exhibited increased imprinting factors. A possible explanation is as follows: In the pre-polymerisation solution, **1** is either free or complexed (to **1BU**). This leads to the formation of a mixture of non-specific and imprinted sites in the MIP. With **3**, there will be a mixture of free **3**, **1BU:3** complexes and (**3**)₂ dimers, which are duly incorporated into the polymer matrix. After extraction of **2**, only monomer residues that were previously free or complexed to **2** are available for template rebinding as the dimers are now locked irreversibly into the 3-D network. Given the values for the association and dimerisation constants, it is reasonable to suggest that only limited amounts of **3** exist in the free state prior to polymerisation, thus reducing non-specific binding to the MIP.

In an interesting approach to imprinting in aqueous media, Komiyama et al. [30] have introduced the use of functionalised β -cyclodextrins as functional monomers in the imprinting of steroids and dipeptides, taking advantage of hydrophobic effects. In the latter example, it was demonstrated that the latent enantioselectivity exhibited by the host molecule was enhanced by the imprinting process.

Turning to the recognition of oxyacids, a number of reports concerning the use of novel monomers have appeared. In the majority of cases, these monomers offer only slightly improved binding compared to the commercially available functional monomers, with the exception of the amidine-based monomer of Wulff, which will be discussed later.

Steinke et al. [31] proposed the use of 2-amidopyridines for the imprinting of carboxylic acids, although no results on MIPs were presented. Whitcombe et al. prepared MIPs against glutamate-containing secondary metabolites of a fermentation process, using 6-methyl-2-(methacrylamido) pyridine (**5**) (Fig. 8) as functional monomer, with the aim of applying the materials to downstream processing applications. An association constant for the interaction of the monomer with acid (K_a ca. 100 M⁻¹) was measured prior to MIP preparation. The MIP prepared using **5** performed less well than another prepared using 4-aminostyrene as functional monomer and no further studies were performed with this MIP. We have also prepared a series of such monomers and found that subtle increases in solution association with model acids may be achieved via

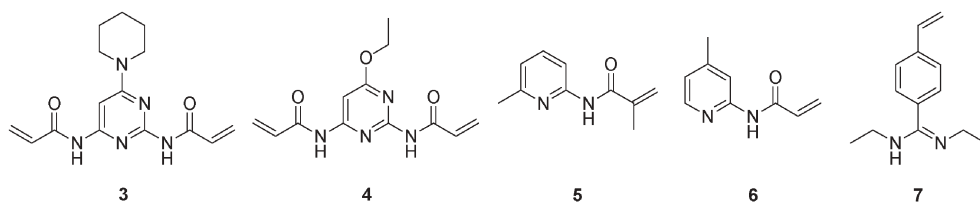


Fig. 8 Some monomers used for stoichiometric imprinting of imides (3, 4) carboxylic and phosphonic acids (5–7)

simple variation of substitution patterns (at the pyridine 4- and 6-positions). There appears to be a delicate balance between enhanced basicity and steric factors affecting the extent of association, with monomer **6** showing the optimum binding properties ($K_a=780\text{ M}^{-1}$ in CDCl_3) [33].

Spivak and Shea prepared a range of functional monomers for the imprinting of acids [34]. Included were 2-amidopyridines, adenine-based monomers and monomers containing guanidinium functions. However, MIPs prepared from these monomers showed negligible imprinting effects. This is presumably due to the fact that the poor solubility of the monomers necessitated the use of an extremely polar solvent (DMF) as polymerisation solvent.

To date, the most successful functional monomer for the imprinting of neutral acids is the amidine-based monomer **7** reported by the group of Wulff [35]. This monomer is capable of engaging in electrostatic and cyclic hydrogen bonding interactions with carbon and phosphorous acids. In CDCl_3 , the interactions ($K_a>10^6\text{ M}^{-1}$) are strong enough to allow beaded MIP preparation via traditional, aqueous-based suspension polymerisation techniques [36]. The association is also strong in CD_3CN ($K_a\approx 10^4\text{ M}^{-1}$). The stoichiometric use of **7** in such solvents leads to $>95\%$ complexation prior to the polymerisation, which has been shown to translate to a near-quantitative yield of imprinted sites in the final polymer. A limitation of **7** is that the association strength falls dramatically on moving to solvents of yet higher polarity, e.g. $\text{DMSO}-d_6$ ($K_a<10\text{ M}^{-1}$), due to the adoption of an unfavourable conformation for binding. The highly impressive use of **7** in the preparation of catalytically active MIPs will be discussed in more detail in the following section.

Whitcombe et al. described two novel functional monomers for the preparation of MIPs against ampicillin, an antibiotic (Fig. 9) [37]. To target the carboxylic acid (in its anionic form) they prepared a polymerisable version of a previously reported receptor (**8**). Unfortunately, the binding of this monomer to carboxylates (ca. 280 M^{-1} in $\text{DMSO}-d_6$) was an order of magnitude lower than the receptor upon which the monomer was based. It was suggested that the decrease in binding strength arose from the electron-releasing group by which the polymerisable function was introduced. To target the amino group the chloranil-based monomer **9** was prepared. According to Job plot analysis, one amino group should be complexed by two molecules of **9**. The interaction between the template and **9** (in $\text{DMSO}-d_6$) was too strong to

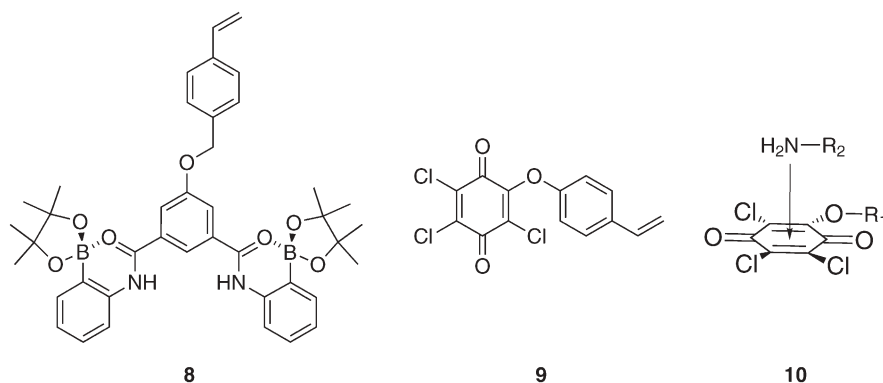


Fig. 9 Novel monomers used in the “orthogonal” imprinting of ampicillin. 10 is the proposed complex formed between 9 and a 1° amine

be determined quantitatively (via ¹H-NMR titration), but was estimated to be $>10^4 \text{ M}^{-1}$. Stoichiometric use of 9 (postulated to give a complex such as 10), together with monomer 8, led to a MIP capable of selective ampicillin uptake in buffered aqueous media. It is also interesting to note that the monomers may be used in an orthogonal manner, as there are no competing monomer–monomer interactions.

We have recently introduced a new type of monomers, containing 1,3-di-substituted urea moieties, for targeting oxyanions (Fig. 10) [38]. This moiety has been extensively used in small-molecule receptors [39] and it has been shown that, by manipulation of the urea substituents, extremely strong binding to oxyanions may be achieved [40], even in polar environments, e.g. DMSO.

In our first study we prepared the bis-urea monomer 11 and used it in an attempt to prepare MIPs able to recognise the anti-cancer drug methotrexate (12), which contains a glutamic acid residue. Thus, a MIP was prepared against the tetrabutylammonium (TBA) salt of N-Z-L-glutamic acid using 11 stoichiometrically. Prior to this we determined K_a between 11 and bis-TBA-glutarate to be ca. $1,500 \text{ M}^{-1}$ (DMSO-*d*₆). Initial chromatographic mode testing, using pure acetonitrile as the mobile phase, led to minimal differences being observed between the MIP and non-imprinted (NIP) control polymer with respect to the

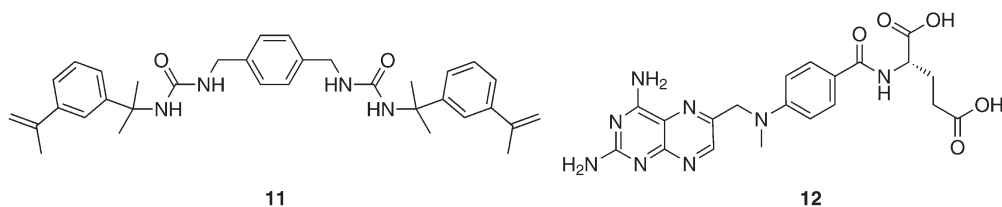


Fig. 10 A bis-urea monomer, targeted towards glutamate recognition, and the anti-cancer drug methotrexate

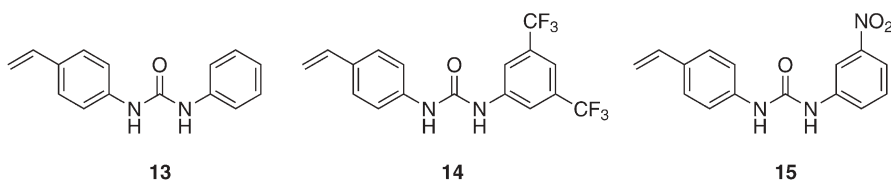


Fig. 11 Bis-aryl mono-urea monomers providing for strong binding to oxyanions

retention of *N*-Z-L-Glu. However, addition of small amounts (1–2%) of a base, triethylamine, to the mobile phase caused large differences in the behaviours of the polymers. Thus, the “template” now exhibited far greater retention on the MIP. Further, the MIP was able to separate an equimolar mixture of *N*-Z-L-Glu, *N*-Z-L-aspartic acid and *N*-Z-glycine, while the NIP was not. Finally, the aim of the study was achieved by showing that the MIP was also capable of retaining 12.

We have since turned our attention to the preparation and use of polymerisable 1,3-diaryl mono-ureas (Fig. 11) [41, 42]. These monomers provide for strong interactions in polar media, which may be further tuned by the appropriate choice of substituents on the phenyl groups. A “base” value for this interaction strength is provided by 1-(4-vinylphenyl)-3-phenyl urea (13); complexation of 13 with benzoate (in $\text{DMSO}-d_6$) gives K_a ca. $1,300 \text{ M}^{-1}$.

Placement of electron-withdrawing groups (NO_2 , CF_3 , etc.) on the 3-phenyl ring lead to significant increases in binding, e.g. binding of 14 to benzoate gives K_a ca. $9,000 \text{ M}^{-1}$. We have used monomer 15 (K_a with benzoate ca. $8,000 \text{ M}^{-1}$) to create another MIP against *N*-Z-L-glutamic acid. Once again, base-modified mobile phases are necessary for the recognition properties of the MIP to become “activated”. However, in comparison to the 11-based polymers, far greater binding strength is observed. Thus, addition of water (6%) to the mobile phase leads to elution of the template from the NIP, though not the MIP. At a water content of 7%, the template also elutes from the MIP, but is much more retained than on the NIP. In equilibrium binding experiments, a significant difference between the uptake of the imprinted enantiomer and its antipode was observed (the difference in uptake amounting to an impressive amount of ca. $13 \mu\text{mol g}^{-1}$ polymer).

3.2

Introducing Secondary Functions to Non-Covalent Binding Monomers

As well as enhancing binding strength by the design and synthesis of novel binding elements, there is also the possibility to introduce interesting secondary functions to the monomer, e.g. signalling subunits, cross-linking ability.

In this context, the preparation of monomers that can give a readable signal of the binding event within the polymer would surely advance the use of MIPs in sensory applications and some examples of non-covalent functional monomers possessing such properties have begun to appear.

The first example of this kind was reported by Turkewitch et al. [43]. Imprinted polymers were prepared against cAMP incorporating a fluorescent dye, trans-4-[*p*-(*N,N*-dimethylamino)styryl]-*N*-vinylbenzylpyridinium chloride, as an integral part of the recognition cavity. This served as both the recognition element and the measuring element for the fluorescence detection of cAMP in aqueous media.

Another recent example of a monomer exhibiting both binding and signalling properties came from Takeuchi's group [44]. Imprinted polymers exhibiting selectivity for 9-ethyladenine were prepared by combining MAA and vinyl-substituted zinc(II) porphyrin as functional monomers (see also the following section). Compared to MIPs using only methacrylic acid or zinc porphyrin as a functional monomer, the terpolymer showed higher affinity and selectivity for the template. Interestingly, these polymers showed fluorescence quenching correlating with the binding of 9-ethyladenine, and the quenching was significant in the low-concentration range, suggesting that the high-affinity binding sites contain the porphyrin residue.

Monomer **1** has been shown, by ourselves [27] and Takeuchi [45], to be fluorescence active. In our work, addition of the template **1BU** to a chloroform solution of **1** leads to quenching of this fluorescence [33]. This is also carried through to the polymeric systems, i.e. the MIP and the control NIP, as seen from equilibrium binding experiments (although the emission maximum is shifted in the polymers, a phenomenon which is discussed below). The quenching of fluorescence agrees well with the quantity of **1BU** rebound to the polymers. Further, the quenching of fluorescence for the MIP is far greater than that seen for the NIP, again in agreement with the earlier chromatographic and rebinding experiments. Addition of non-template species leads to far less fluorescence quenching on the MIP, but only minimal alteration of the response of the NIP, thus showing the existence of selective sites within the MIP. Monomer **3** shows similar effects, but there is a more pronounced selectivity in the fluorescence quenching response of the MIP, again consistent with the earlier results obtained from chromatographic testing.

Conversely, Takeuchi et al. have recently reported that MIPs prepared against barbitol using **1** as the functional monomer exhibit enhancements in their fluorescence emission when template binding occurs [45]. While interesting, the inherent fluorescence of the barbiturate molecule appears to have been overlooked.

The urea monomer **15** exhibits a chromogenic response to carboxylate binding in solution, with a bathochromic shift in the absorbance maximum being observed (from 349 nm to 364 nm) [41]. Although this shift is small, it is sufficient for the binding event to be seen with the naked eye. These effects are also carried through to the anti-*N-Z-L*-Glu MIP, which exhibits a stronger chromogenic response than the NIP. We are currently investigating the use of the urea moiety as a platform for the generation of binding monomers, which show larger responses (chromogenic or fluorogenic) on binding.

Other examples of non-covalent functional monomers combining both binding and reporting ability are rare. Shea et al. [46] have reported some

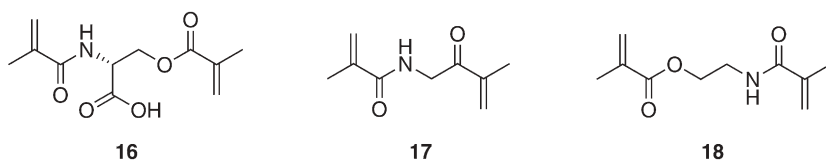


Fig. 12 Novel cross-linking functional monomers by Spivak et al.

interesting examples recently, but their use in MIPs has yet to be demonstrated.

Monomers **1** and **3** are also, potentially, cross-linking monomers. That they are incorporated into the polymeric matrix via polymerisation of both their C=C bonds is indicated by the change in the fluorescence emission maximum of the monomer units once polymerised; the polymers showing emission maxima very similar to those of saturated models [27]. These measurements show, at least qualitatively, that “double” incorporation of **1** and **3** into the polymer matrix occurs. This is probably an added factor in their success as binding monomers in molecular imprinting.

Most of a MIP is made up from cross-linking monomer. More recently, in recognition of this fact, Spivak et al. have introduced a series of small-molecule cross-linkers containing carboxylic acid or amide residues for use in imprinting protocols (Fig. 12) [47–49].

The results of imprinting using such cross-linking monomers, compared to more “traditional” protocols, have been reasonably impressive. The use of **16** leads to enhancements (cf. using methacrylic acid as functional monomer) in enantioselectivity when imprinting nicotine and chiral amines [47]. Further, MIPs prepared using **17** showed much better enantioseparation of N-protected amino acids than those formulated with the more traditional cross-linker, EDMA [48]. Most recently, this group has coined the term “OMNiMIP” (One MoNomer MIPs) after the discovery that monomer **18** could be used alone (i.e. in the absence of other functional or cross-linking monomers) to create MIPs showing good enantioselectivity, albeit for a limited range of target species [49]. Also, as these monomers function via weak interactions, the problems relating to binding site heterogeneity and the need for low polar media during imprinting are not overcome using this approach.

3.3

Binding Site Monomers in Metal-Mediated Imprinting

The use of functional monomer–metal ion–template complexes in imprinting protocols is rare, which is surprising given that metal ion–ligand complexes are generally extremely strong, even in water. One problem perhaps lies in the preparation of well-defined ternary (or higher) metal ion complexes. Indeed, there are few examples where the structures proposed to be present in the imprinting mixture have been definitively confirmed, e.g. by crystal structure determination.

Notable early examples of this technique came from the group of Arnold, particularly the use of polymerisable Cu(II)-iminodiacetic acid complexes for the imprinting of benzimidazole-containing molecules [50]. More recently, Striegler has used the Cu(II) complex of a polymerisable ethylene triamine ligand as a functional monomer for the imprinting of carbohydrates (mono- and disaccharides) with some success [51–53]. However, the use of Cu(II) complexes can lead to problems in free radical polymerisation protocols, especially with regards to incomplete polymerisation of monomers.

To avoid such problems, the group of Shea used polymerisable Ni(II)-nitrilotriacetic acid (NTA) complexes for the preparation of MIPs capable of recognition of histidine residues in small oligopeptides [54, 55]. Histidine is known to form an octahedral ternary complex of considerable strength with Ni(II) and NTA in water ($K_d=0.0093$ mM). The 1:1:1 ternary template complex (19) between His-Ala, Ni(II) and the polymerisable NTA ligand (20) is depicted in Fig. 13.

This ternary complex was characterised by absorption spectroscopy and mass spectroscopy. It is notable that both the imprinting step and the subsequent rebinding experiments were performed in purely aqueous media. In the rebinding step, uptake of His-Ala was found to exceed that of His-Phe, while minimal binding of Ala-Phe was observed. This implies firstly that there is restricted access to the binding cavity in the case of the larger dipeptide and, secondly, that the terminal His-residue is required for binding. On imprinting His-Phe, no selectivity for the two dipeptides was observed, indicating accessibility to the binding site for the smaller dipeptide. Further, when a pentapeptide, His-Ala-Ala-Ala-Ala, was imprinted, the uptake of both His-Ala and His-Phe by the MIP was found to be greater than that of the template (and His-Ala-Phe and His-Phe-Ala-Ala-Ala). Finally, kinetic binding studies, using His-Trp as a fluorescent probe, indicated that the rebinding was reasonably fast, leading to equilibration in ca. 1 h.

As mentioned in the previous section, Takeuchi's group used a polymerisable Zn(II)-porphyrin complex, in combination with methacrylic acid, for the preparation of MIPs against 9-ethyl adenine [44] and (–)cinchonidine [56]. The

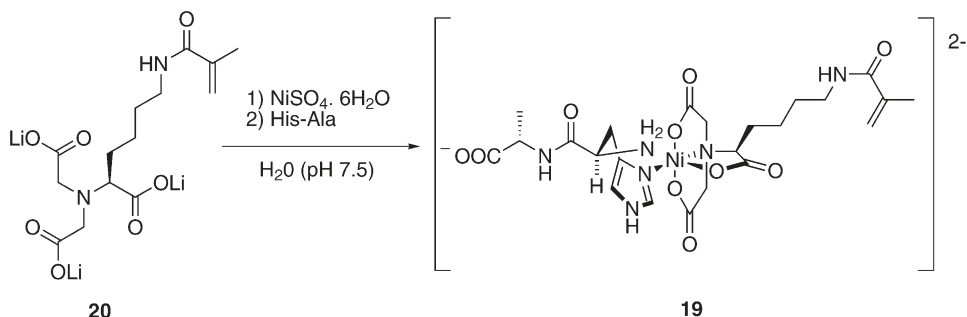


Fig. 13 Formation of template complex in the imprinting of His-containing peptides

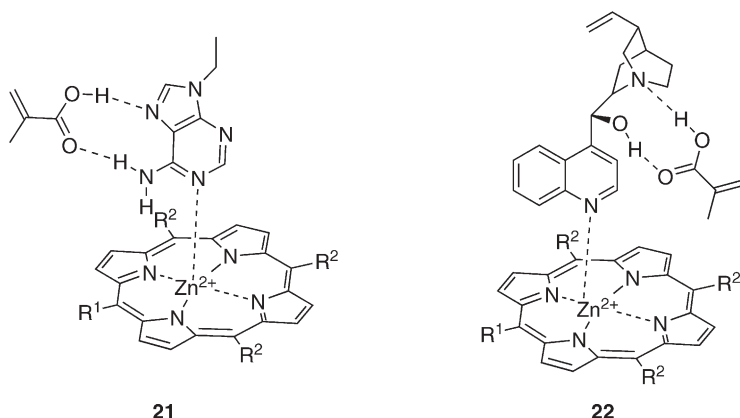
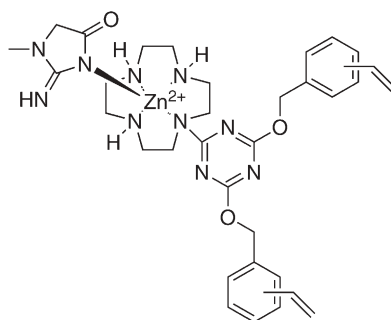


Fig. 14 Proposed complexes in the imprinting of 9-ethyladenine and (–)-cinchonidine using a polymerisable Zn(II)-porphyrin functional monomer possessing secondary signalling properties in combination with methacrylic acid. $R^1 = \text{CH}_2=\text{C}(\text{CH}_3)\text{COOC}_6\text{H}_4$; $R^2 = (\text{CH}_3)_2\text{CHC}_6\text{H}_4$.

proposed complexes, **21** and **22**, are shown in Fig. 14. There appears to be a high degree of co-operativity in each of these systems, as MIPs made with each monomer individually were shown to be less effective in uptake of the template. In the case of (–)-conchinidine MIP, the uptake of (+)-cinchonine was lower than that of the template, indicating a certain degree of diastereoselectivity. In both systems, it was demonstrated that rebinding of the template was accompanied by a change in UV-Vis and/or fluorescence behaviour, while the response was much lower for the non-template species tested. Thus, a secondary signalling property is introduced by incorporation of the metal ion complex into the binding cavities of the polymers. However, it should be mentioned that very little characterisation data for the proposed complexes was provided. Further, the polymerisation was performed in chloroform and rebinding studies were carried out predominantly in dichloromethane. It would be interesting to see if the proposed ternary complexes could be of use for imprinting in more polar media.

König et al. have recently published on the use of a polymerisable Zn(II)-cyclen complex in the imprinting of creatinine; the template complex **23** is depicted in Fig. 15 [57].

This report is one of the few in which the structure of the imprinted complex has been definitively confirmed (by X-ray crystallography). Also notable is that imprinting was carried out using water as the polymerisation solvent and that the rebinding experiments were conducted in water at physiological pH. In solution, the Zn(II)-cyclen complex is known to bind to thymine in preference to creatinine, with the association constant being ca. 34 times higher. Imprinting of the complex led to a MIP capable of reversing this preference, with creatinine absorbed ca. 3.5 times more than thymine. Further, the MIP



23

Fig. 15 Ternary template complex used in the imprinting of creatinine

could be used in repeated absorption-desorption cycles with little loss in activity. Control polymers lacking the metal ion displayed no significant affinity for either creatinine or thymine, while a flavin absorbed non-specifically to all polymers.

A further recent example has come from the group of Wulff [58, 59]. This may be viewed as a combination of non-covalent and metal-mediated imprinting approaches. Thus, a functional monomer possessing both an amidine group (for acid binding) and a Zn(II)-aza-macrocycle complex, separated by a suitable spacer, has been used in the preparation of catalytically active MIPs, as will be discussed later.

3.4

Molecularly Imprinted Dendrimers

Very recently, in a new approach to binding site design, Zimmerman et al. have introduced the idea of imprinting in dendrimers, whereby one macromolecule is furnished with a single binding site (similar to the case of enzymes) [60]. While the synthetic effort is certainly greater than in traditional imprinting protocols, there is the benefit that homogeneous binding sites may be formed using this technique. Developments in this work have been reviewed recently [61].

4

Catalysis with Imprinted Polymers

Given the receptor-like molecular recognition properties displayed by several imprinted polymers, the idea of combining the recognition event with a chemical transformation in an enzyme-like fashion seems obvious. This approach to heterogeneous catalysts was first proposed by Wulff in the early 1970s, but only the last couple of years has seen promising advances towards this end [14].

Enzymes catalyse a large variety of chemical and biochemical reactions with high reaction rates and specificity under relatively mild conditions. Thus, chemists have sought to create mimics that could match the catalytic properties of enzymes. Early approaches to enzyme mimics were based on macromolecular receptors, e.g. cyclodextrins or crown ethers containing suitably placed functional groups to mimic the amino acid residues known to be involved in the catalytic mechanism [62]. Such models were able to mimic the main features of enzymes (i.e. substrate selectivity, Michaelis-Menten kinetics and turnover) although commonly showing modest rate enhancements using activated non-natural substrates and non-aqueous environments. However, no such simple model system shows catalytic activity on a par with the biological counterparts.

Catalytic antibodies have come closer in this regard and have been regarded as the most successful enzyme mimics [63, 64]. Here, antibodies are elicited using antigens containing stable transition state analogues (TSAs), for the reaction to be catalysed, as haptens. These mimic the shape and charge of the transition state of the reaction to be catalysed and define the active site of the antibody. This builds on the idea of Pauling [65] and Jencks [66] that enzymes owe their enormous power to catalyse a reaction mainly to their ability to lower the energy required for passing the transition state of the reaction.

Based on similar concepts, MIPs showing catalytic activity have been developed. Here, first of all, a proper cavity equipped with catalytically active functional groups is required. This should furthermore exhibit binding and shape complementarity towards the substrate or the transition state of the reaction.

There are two main strategies to achieve this (Fig. 16). The most common method is to place suitable functional groups in the cavity by choosing the substrate or the product of the reaction, or alternatively analogues of these, as the template. In line with catalytic antibodies, however, the most successful approach is the use of stable transition state analogues (TSA) as templates.

The second strategy is to incorporate a low molecular weight metallorganic catalyst as a complex with a template molecule (e.g. the substrate, its analogue or a transition state analogue) to form the active sites in the polymer. In this

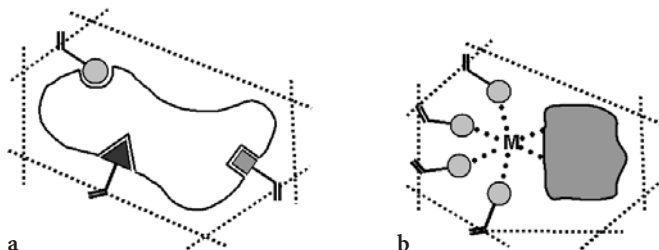


Fig. 16 Two approaches to achieve molecularly imprinted catalysts (MIC). **a** Bio-inspired MICs by constructing catalytically active sites using stable transition state analogues. **b** Chemo-inspired MICs by imprinting of a metallorganic catalyst in a complex with, e.g. a transition state or substrate analogue

case the polymer plays the role of improving an already established solution catalyst. Thus, apart from achieving simple immobilisation of the catalyst, the imprinted site may allow the introduction of further catalytically active or binding functional groups and to provide shape selectivity in the reaction. In this manner the selectivity and activity may be improved in the resulting heterogeneous catalyst.

These two main strategies for creating MICs will be described in more detail below. Under the first group we will focus on models inspired by hydrolytic enzymes. These constitute by far the most widely studied and developed group and also the group that has come closest in mimicking the key features of enzymes. As stated in the introduction we have limited the review to include systems based on organic network polymers. Comprehensive reviews of earlier work can be found elsewhere [14, 67].

4.1

Bio-inspired MIPs Catalysing Hydrolysis Reactions

In the chemistry of enzyme mimics one general strategy is to generate a host that is capable of binding to a transition state analogue (TSA) of a reaction. Upon removal of the template the host should behave as an artificial enzyme for the chosen reaction [68]. This strategy has met with considerable success in the field of catalytic antibodies [64], which further inspired research to produce imprinted catalysts based on the same principle. The first examples of catalytically active MIPs were published in the 1980s. Thus templates similar or identical to previously used antibody haptens were used to create an imprinted polymer [14]. The functional monomers in these systems have to fulfil several requirements that are somewhat oppositional. On the one hand, the functional monomers have to form a stable complex with the template molecule during the polymerisation step, leading to their incorporation into the polymer matrix in the correct orientation and position. On the other hand, the interactions must be readily reversible in order to allow release of the template to form the empty cavity. Further, during the catalytic process these groups must bind the substrate and/or the transition state and provide catalysis allowing for fast kinetics and product release.

The earliest and most extensive efforts towards MIP-based catalysts concerned the mimicking of serine protease enzymes. This is mainly due to the extensive knowledge available concerning their mechanism of action and the structure of the active site and intermediates [69]. A further factor is the fact that serine proteases, lipases, cholesterases and other hydrolytic enzymes share similar catalytic machineries and mechanisms. Chymotrypsin, an enzyme with a well documented catalytic mechanism, has been the model of choice in these efforts [68].

Most reports up to now have concerned imprinted polymers that mimic their hydrolytic activity by incorporating some or all of the key features of the active site, e.g. the Ser-His-Asp catalytic triad, transition state stabilisation and a stereoselective binding pocket, into the synthetic polymer.

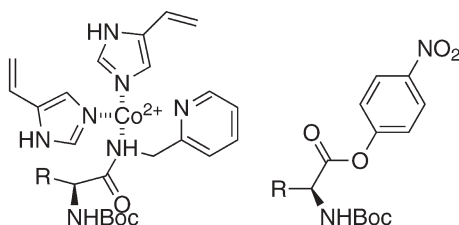


Fig. 17 Template complex and substrate in esterase mimic by Leonhardt and Mosbach

In the first report by Leonhardt and Mosbach, imidazole residues were employed as the catalytically active groups to hydrolyse activated amino acid nitrophenyl esters (Fig. 17) [70]. A complex comprising 2-vinyl imidazole and a substrate analogue coordinated to Co(II) was copolymerised with DVB. The MIPs showed a four- to eightfold rate enhancement of the hydrolysis of BOC-Leu(or Met)-*p*-nitrophenylester over the control polymer containing statistically distributed imidazole groups.

With the hope of creating more active catalysts, the use of stable TSAs as templates came soon after the first reports on catalytic antibodies. By using a phosphonic acid as a TSA template for the hydrolysis of 4-nitrophenyl esters, polymer catalysts developed by the groups of Mosbach [71] and Ohkubo [72] showed modest rate enhancement (ca. sevenfold for Ohkubo's catalyst) with reference to the uncatalysed solution reaction. The lack of proper controls in some of these reports makes it difficult to ascribe these effects to the presence of templated sites alone.

More recently Ohkubo and co-workers synthesised polymers imprinted with a racemic TSA corresponding to the hydrolysis of *Z*-Leu-4-nitrophenyl ester using *N*-acryloyl-L-histidine methylester as the functional monomer (Fig. 18) [73, 74]. MIPs were synthesised using different cross-linkers and by using styrene as a hydrophobic co-monomer. Thus polymers were obtained giving faster hydrolysis for the *L*-isomer over the *D*-isomer by factors of 1.15–2.54 and showed catalytic rate enhancements of 3.4–29, depending on the cross-linkers and co-monomers used (see Table 1).

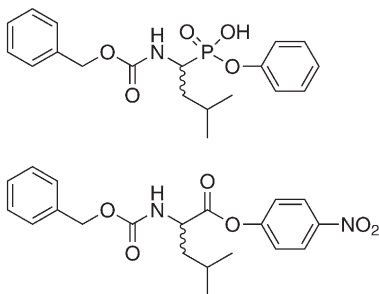


Fig. 18 *rac*-TSA and substrate used by Ohkubo et al.

Table 1 Comparison of kinetic data in reports on MIPs exhibiting esterase-like activity

Ref.	Template type	Template binding	Polymer format	Substrate type	$k_{\text{cat}}/k_{\text{sol}}$	Enantio-selectivity	$k_{\text{cat}}/k_{\text{ctrl}}$	K_M (mM)	k_{cat} (min^{-1})	v_{max} (mM/min)	K_i (mM)
[70]	SubA	I	CM	PNP	–		4–8				
[71]	TSA	I	CM	PNP	6.7		–				
[74]	TSA	II	CM	PNP	29 ^a 3.4 ^b	1.15 ^a 2.54 ^b	–				
[75]	TSA	II+III	CM	PNP (ethyl ester)	10	1.85	2.5	5.4	0.0014	–	–
[35]	TSA	IV	CM	Phenyl ester	102–235		5.0	0.6	0.00008	–	0.025
[36]	TSA	IV	CM	Carbonate	588		7.8	5.01	0.012	0.023	0.094
[36]	TSA	IV	CM	Carbamate	1435		4.2	3.33	0.022	–	0.285
[78]	TSA	IV	Beads	Carbonate	168 ^c 293 ^d		24 ^c 9.7 ^d	13.4 ^c	0.004 ^c	0.008 ^c	0.22 ^c
[78]	TSA	IV	Beads	Carbamate	140 ^e		11 ^e				
[80]	TSA	IV	CM	Cholesterol carbonate	27		2.4	3.7	0.000222	–	0.9
[79]	TSA	IV	CM	Phenyl ester	325	1.39 ^f 1.65 ^g	79	0.51	0.000474	–	0.016

Table 1 (continued)

Ref.	Template type	Template binding	Polymer format	Substrate type	$k_{\text{cat}}/k_{\text{sol}}$	Enantio-selectivity	$k_{\text{cat}}/k_{\text{ctrl}}$	K_{M} (mM)	k_{cat} (min^{-1})	v_{max} (mM/min)	K_{i} (mM)
[81]	SubA	I	Without emulsion	PNP	1.8		–	1.63	–	0.0625	–
[58]	TSA	I+IV	CM	Carbonate	3264 ^h		61.5 ^h	2.01 ^h	0.035 ^h	–	–
					76570 ⁱ		80.1 ⁱ	0.58 ⁱ	28.0 ⁱ		
[82]	TSA	IV	Microgels	Carbonate	530		–	2.38	–	0.0804	–

$k_{\text{cat}}/k_{\text{sol}}$ is the enhancement determined from pseudo-first-order kinetics as the ratio between the first-order rate constants of the imprinted polymer(k_{cat}) and the solution (k_{sol}). $k_{\text{cat}}/k_{\text{ctrl}}$ is the imprinting efficiency determined from the first-order rate constants of the imprinted polymer (k_{cat}) and the control polymer t (k_{ctrl})

SubA substrate analogue, TSA transition state analogue, PNP *p*-nitrophenyl ester, I metal coordination, II non-covalent, III covalent, IV stoichiometric non-covalent, CM crushed monolith.

^a Cross-linker: ethylene bisacrylamide.

^b Cross-linker: butylene bisacrylamide+styrene.

^c Porogen: cyclohexanol/dodecanol (91/9), 20 wt% NaCl and 8 wt% starch in water.

^d Porogen: toluene. Suspension stabiliser: 1 wt% poly(*N*-vinylpyrrolidone) and 2 wt% poly(vinylalcohol) solution in water.

^e Porogen: cyclohexanol/dodecanol (91/9), 0.1 wt% poly(*N*-vinylpyrrolidone) and 0.2 wt % poly(vinylalcohol) solution in water.

^f Calculated from pseudo-first-order kinetics.

^g Calculated from Michaelis-Menten kinetics.

^h Metal: Zn²⁺.

ⁱ Metal: Cu²⁺.

Using a hybrid covalent/non-covalent imprinting approach, Sellergren and Shea developed polymers incorporating most of the catalytically important features found in chymotrypsin (Fig. 19) [75, 76]. The MIP catalysts were constructed by copolymerisation of MAA, EGDMA and a template monomer consisting of a phenol-imidazole monomer linked via a labile phosphonate ester linkage to a phosphonic acid analogue of BOC-D-phenylalanine. After template removal this would leave behind a site equipped with a mimic of the Ser-His-Asp catalytic triad, a TSA complementary site and a stereoselective binding pocket complementary towards BOC-D-phenylalanine.

The maximum rate enhancement for the hydrolysis of D-*p*-nitrophenyl ester was tenfold greater than the reaction in solution. As expected, the control polymers showed less activity, approximately 5.7-fold or less over the reaction in solution and a complete absence of enantioselectivity. The polymer catalyst showed a 1.85-fold rate enhancement for the D-isomer over the L-isomer; the control polymers (one using an achiral template and without the tetrahedral phosphonate and the other without the phenol-imidazole functionality) showed no preference for one isomer over the other. Notably, modest stereoselective rate enhancements for the hydrolysis of the non-activated ethyl ester were also observed for BOC-D-PheOEt: $K_m=1.92$ mM, $k_{cat}=2.32\times10^{-5}$ min⁻¹ and for BOC-L-PheOEt: $K_m=1.96$ mM, $k_{cat}=1.91\times10^{-5}$ min⁻¹. As seen in Table 1, these K_m -values are lower than those observed for the corresponding *p*-nitro-

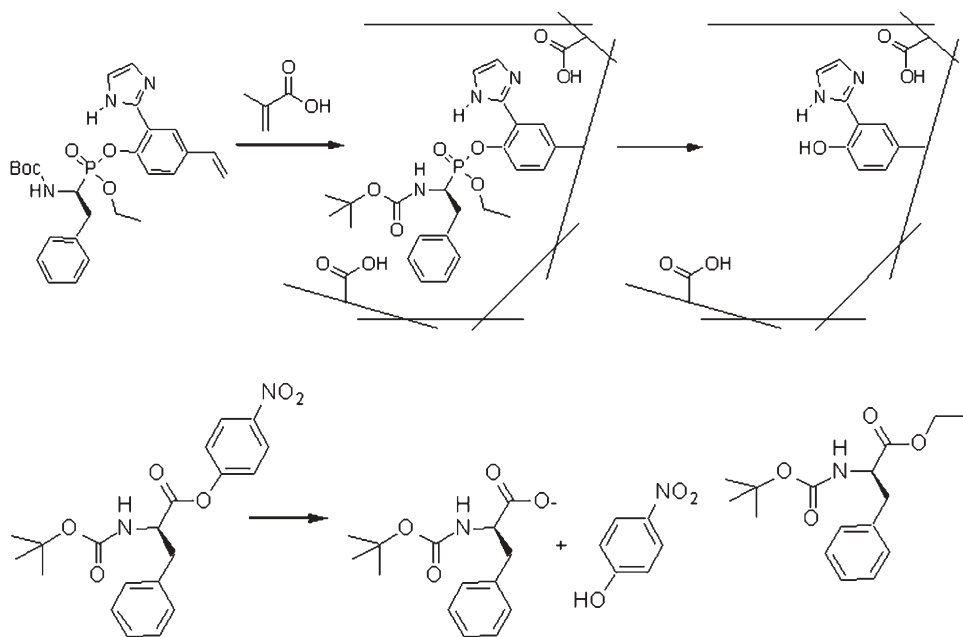


Fig. 19 MIP chymotrypsin mimic prepared by Sellergren and Shea. As substrates either *p*-nitro phenyl ester (lower left) or ethyl ester (lower right) were used

phenylester substrate ($K_m=5.4$ mM). This indicates that the ethyl substituent of the TSA template has given rise to a shape complementary site where the ethyl ester fits better than the *p*-nitrophenylester.

Much stronger esterase activity was reported by Wulff and co-workers using a polymerisable amidine, in particular *N,N'*-diethyl(4-vinylphenyl)amidine (7) (see also Sect. 3.1), as functional monomer in combination with a phosphonate TSA template (Fig. 20) [35]. This follows in part the findings that the charged guanidine group of arginine plays an essential role in the mechanism of esterolytic antibodies [77]. The authors reasoned that a complementary shape to the transition state analogue itself may not be sufficient for catalysis and that an appropriately positioned amidine functionality, with similar properties to that of arginine, could be envisaged to provide additional electrostatic stabilisation of the transition state oxyanion. Thus the 7-phosphonate TSA complex provided an "oxyanion hole" for transition state stabilisation similar to that found in serine proteases. This monomer was henceforth used in several systems to create active polymers as described in the following section.

In the first application, the basic hydrolysis of a phenyl ester (Fig. 20) was shown to be accelerated >100-fold in the presence of the MIP catalyst [35]. This was accompanied by Michaelis-Menten kinetics ($K_m=0.60$ mM; $k_{cat}=0.8\times10^{-4}$ min⁻¹). The low k_{cat} value reflects a poor turnover; in fact, in addition to the template, the product was also found to competitively inhibit the reaction. The postulated mechanism is shown in Fig. 21. The bound substrate (b) is converted into the tetrahedral intermediate (c), which in turn breaks down into the acid and alcohol (d). Product inhibition was attributed to the carboxylate group ($X=CH_2$), which binds strongly to the amidine residue (see Sect. 3.1).

To avoid the product inhibition in further studies Wulff et al. investigated the hydrolysis of carbonates and carbamates, which liberate CO₂ and alcohols, with no significant affinity for the amidine site [37]. Thus, the hydrolysis of diphenyl carbonate and diphenyl carbamate were catalysed by the MIP (imprinted with diphenyl phosphate and DEVPA) with rate enhancements of 588 and 1435,

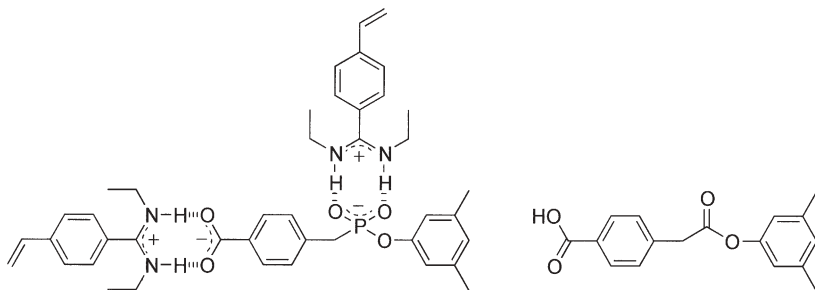


Fig. 20 Left: Two equivalents of 7 forming hydrogen-bonded ion pairs with one equivalent of TSA. Right: Phenylester substrate

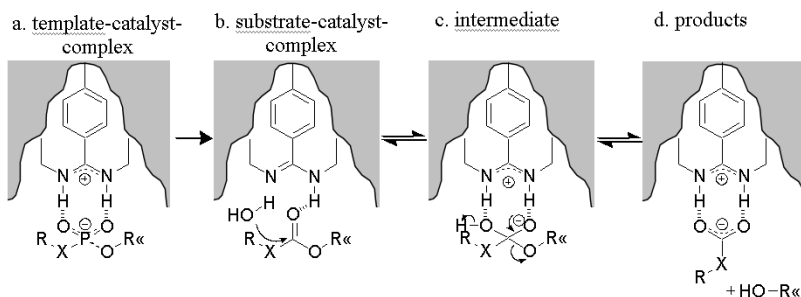


Fig. 21 Proposed mechanism of the basic hydrolysis of esters, carbonates and carbamates ($X=CH_2$, O, NH) in the cavity

respectively, compared to the rates of the uncatalysed reactions. Relative to that of the control polymer, the MIP catalyst showed rate enhancements of 10 and 24, respectively.

As an alternative to the classical technique to produce MIPs as crushed monoliths, an aqueous suspension polymerisation technique for creating MIPs in bead form was introduced (see also Sect. 3.1) [78]. The pseudo-first order rate constants showed enhancements by factors of 293 for carbonate and 160 for carbamate, compared to the uncatalysed reactions. These results were somewhat poorer than those given by the MIPs produced as crushed monoliths. On the other hand, the rate enhancements with respect to the control polymer were 24-fold for carbonate and 11-fold for the carbamate, which showed an improvement compared to the enhancements obtained with the crushed monoliths (tenfold for carbonate; 5.8-fold for carbamate).

Again based on 7, Emgenbroich and Wulff recently reported on an enzyme model exhibiting enantioselective esterase activity (Fig. 22) [79]. Two enantiomerically pure stable α -amino phosphonic monoesters (L-LeuP and L-ValP) were connected by stoichiometric non-covalent interactions to two equivalents of 7. The complex was thereafter copolymerised with EDMA and the resulting polymer freed from template generating enantioselective catalytic sites. The

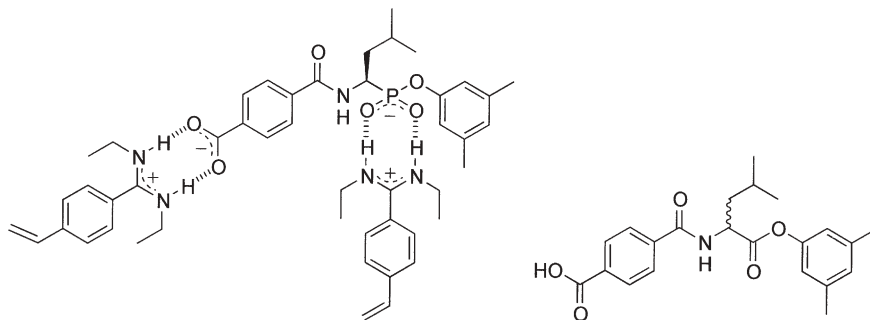


Fig. 22 Complex of chiral TSA L-LeuP with 7 and chiral substrate

catalyst prepared by imprinting of L-LeuP enhanced the hydrolysis of the corresponding substrate L-Leu by a factor of 325 relative to that of a buffered solution. Relative to a control polymer, the enhancement was still about 80-fold, showing one of highest imprinting effects in MIP-based catalysis. The polymers exhibited Michaelis-Menten kinetics, allowing the Michaelis constant K_M and the catalytic constant k_{cat} to be estimated. The ratio of the catalytic efficiency k_{cat}/K_M between the hydrolysis of the two enantiomers, representing the enantioselectivity, was 1.65. This derives from both selective binding of the substrate ($K_{ML}/K_{MD}=0.82$), and selective formation of the transition state ($k_{catL}/k_{catD}=1.36$). Thus, these catalysts show good catalysis together with high imprinting and substrate selectivity. They also showed strong competitive inhibition caused by the template, which further reflects the enzyme-analogue behaviour of the model.

Based on a similar principle, Resmini et al. developed guanidine functionalised soluble polymer microgels imprinted with a TSA for the hydrolysis of activated carbonates [82]. In contrast to the heterogeneous systems the resulting gel was soluble in DMSO/buffer 9:1 allowing direct monitoring of the kinetics by UV-Vis spectroscopy. The Michaelis-Menten kinetics, for the hydrolysis of the *p*-nitro phenyl carbonate, gave a rate enhancement of $k_{cat}/k_{uncat}=530$.

The inapplicability of water-soluble substrates and the mass transfer problems with conventional MIPs prompted Goto et al. to investigate a “surface molecular imprinting technique” [83]. Briefly, the MIP was prepared by polymerising water-in-oil (W/O) emulsions containing the functional host molecule (oleyl imidazole), the template (*N*-*t*-Boc-L-histidine) and the cross-linking monomer (DVB). Co^{2+} ions were used to coordinate the imidazole residues of the host molecule. The host-guest complex was formed at the interior surface of the water droplets, and the surrounding organic layer was polymerised. Subsequently the ability of the monoliths to catalyse the hydrolysis of *N*-*t*-Boc-L-alanine *p*-nitrophenyl ester was investigated. Using a substrate analogue a 1.8-fold rate enhancement was found for the imprinted polymer over the control.

The latest generation of catalytic MIPs from Wulff's group mimic carboxypeptidase A, an exopeptidase catalysing the hydrolysis of C-terminal peptides [58, 59]. The enzyme contains a stereoselective binding site complementary to peptides containing C-terminal large hydrophobic amino acids and nearby a catalytically important zinc ion coordinating the water or hydroxide for the hydrolysis reaction. The bio-inspired catalytically-active monomer is again based on the amidine monomer 7 but with one of the *N*-ethyl groups substituted with a chelating ligand site for Zn^{2+} or Cu^{2+} (Fig. 23). By using a pyridyl-containing TSA that can form a coordinative bond to the metal a catalytically-active polymer was prepared by polymerising the complex with EDMA as cross-linking monomer.

The resulting activities are very high and show rate enhancements of up to 3,264 compared to the background reaction in solution. However, the imprinting efficiency, compared to the control polymer, is only 62. According to the mechanism, the authors assumed that the Zn^{2+} ion coordinates to a water mole-

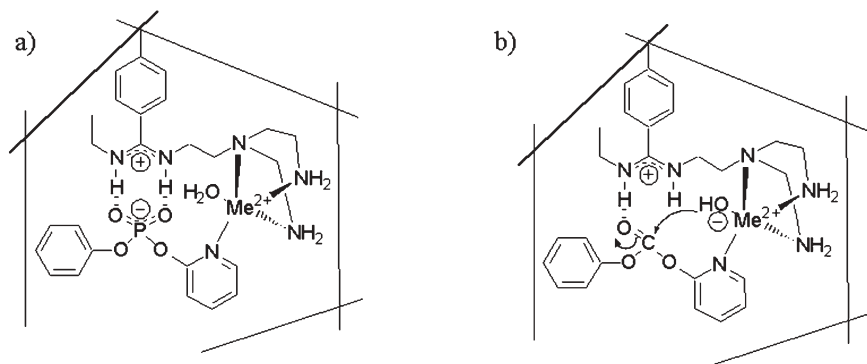


Fig. 23 Preparation and function of imprinted carboxypeptidase A mimic by Wulff et al. **a** Cavity imprinted with the template and functional monomer in presence of Me^{2+} ($\text{Me}=\text{Zn}$, Cu). **b** Substrate carbonate in the cavity attacked by the metal-coordinated hydroxide

cule, causing an increase of the acidity of the water. The resultant α -coordinated hydroxy groups can then attack the substrate. In a following paper they changed the metal ion to Cu^{2+} [59]. This change led to further dramatic effects in the catalytic enhancement of the resulting polymer, up to a $k_{\text{MIP}}/k_{\text{solution}} \approx 77,000$. By comparing with a control polymer they detected an imprinting effect of 80, whereby only a small part of the catalysis is caused by the imprinting effect. Also, the enzyme-like catalysis showed extraordinary turnover numbers with $k_{\text{cat}} = 28 \text{ min}^{-1}$, thus outperforming all previous MIP-based catalysts. By comparing the Michaelis-Menten kinetics for the polymer with the background reaction a catalytic activity $k_{\text{cat}}/k_{\text{uncat}}$ of up to 110,000 was calculated. For carbonate hydrolysis this is the fastest enzyme mimic presented and is even one order of magnitude better than catalytic antibodies, although, admittedly, the antibodies exhibit higher rate enhancements compared to controls.

4.2

Chemoinspired catalytically active MIPs – Imprints of metal catalysts or their analogues

An alternative approach to imprinted catalysts is via the incorporation of a low molecular weight catalyst that already exhibits activity in solution. To achieve this the catalyst needs polymerisable groups that are located remote from the active centre. Next, a complex is formed with a suitable template molecule. The template may be the substrate (or analogue), a TSA or the product (or analogue) of the reaction. This depends on the reaction, the accessibility of the required molecules and their ability to coordinate to the catalyst. By imprinting such a complex, a cavity is formed that is complementary to the catalyst and the bound template. After template removal, the formed cavity supports the binding and recognition of the substrate molecules. Thus, in addition to simple catalyst immobilisation, the formed cavity introduces shape selectivity,

which may also result in enhanced activities. Clearly, given the wide field of metallo-enzymes, this approach may also be classified as “bio-inspired” (see previous section). However, the literature reports so far are based on metallo-organic complexes, which exhibit high solution activity per se.

The first examples of the combination of inorganic catalysts with the imprinting technique were published in the mid 1990s. The group of Lemaire presented a polyurethane-supported Rh-catalyst, imprinted to promote hydride transfer to form alcohols by using the product as template (1-(*S*)-phenylethanolate) [84, 85]. The enantioselectivity of the homogeneous catalyst of maximum 67% (e.e.) was hereby slightly improved (e.e. 70%) by the cross-linked polymer support. Without cross-linking the catalyst was less effective.

Severin et al. reported on a defined polymerisable ruthenium-complex with a TSA template as one of the ligands (Fig. 24) [86, 87]. The crystal structure indicated the phosphinic acid complex to be analogous to the six-membered transition state of the transfer hydrogenation catalysed by Ru. After incorporation of the complex into a polymer matrix, then template removal, the resulting imprinted catalyst was active in catalysing the hydrogenation of aromatic ketones. The selectivity of the MIP was demonstrated with a competition experiment with seven similar substrates where the substrate, being the analogue of the TSA, showed the highest activity.

In a further development of these catalysts the authors used a rhodium(III)-complex with a chiral chelating ligand [88]. The resulting MIPs (Fig. 25) showed a high enantioselectivity (up to 95% e.e.) for the transfer hydrogenation of acetophenone derivatives, whereas the control polymer imprinted without the TSA showed similar e.e. but only half the yield compared to the MIP.

In an effort to enhance the stereoselectivity of the platinum catalysed reaction shown in Fig. 26, Gagné and co-workers synthesised platinum(II) complexes between a polymerisable chiral diphosphine ligand and chiral binaphthol (BINOL) ligands [89]. Removal of BINOL would leave behind a chiral BINOL shaped cavity. This resulted in an immobilised precatalyst that could be

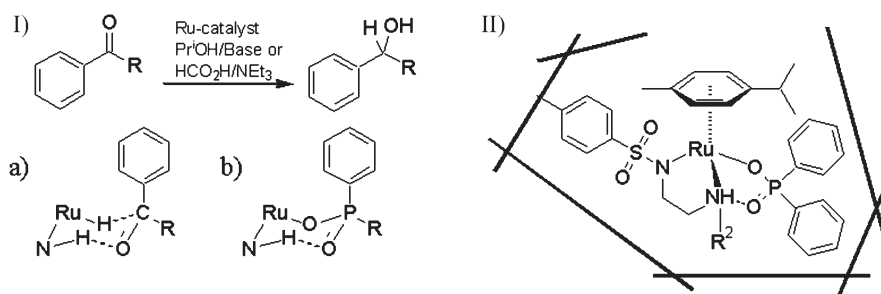


Fig. 24 I) Hydrogen transfer to aromatic ketones catalysed by ruthenium half-sandwich complexes. a) Proposed transition structure. b) TSA mimicked by the phosphinato complex. II) Imprinted Ru-catalyst in complex with TSA-template ($\text{R}^2=\text{H}$, $\text{CH}_2\text{C}_6\text{H}_4\text{CH}=\text{CH}_2$)

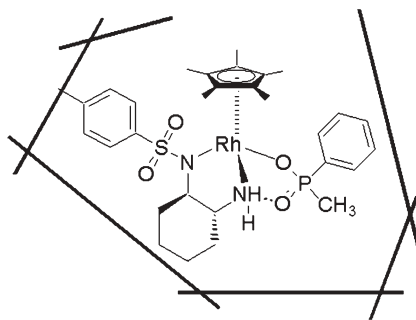


Fig. 25 TSA mimicked by the phosphinato complex imprinted Rh-catalyst in complex with TSA template

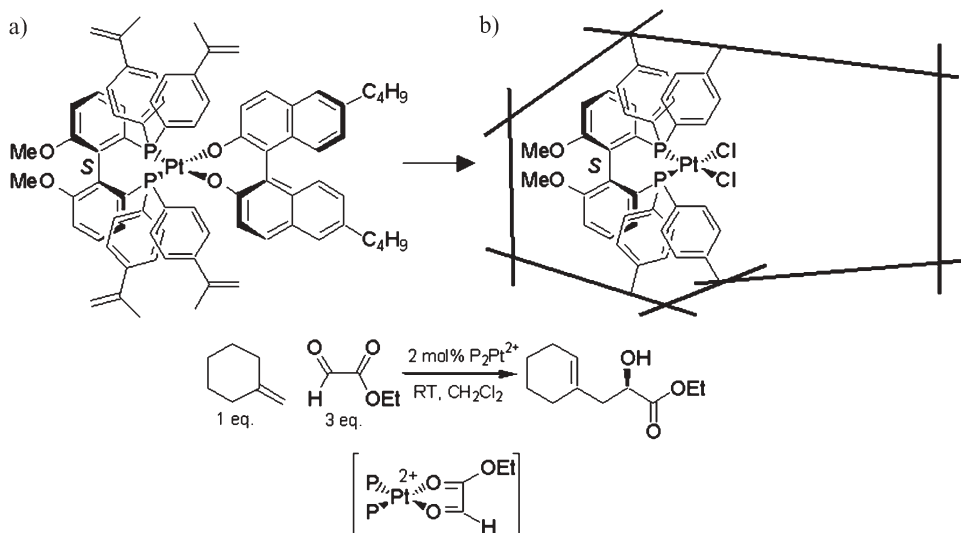


Fig. 26 a) Polymerisable catalyst complex with *S*-BINOL as template ligand. b) Empty cavity remaining after template removal. After activation the polymer can catalyse the shown ene reaction

activated for asymmetric catalysis. Poisoning experiments using the chiral poison (*R*)- or (*S*)-1,1'-binaphthyl-2,2'-diamine showed that the generated active sites exhibited similar reactivity and selectivity for the ene reaction. However, the enantioselectivity was unfortunately poor, reflecting the relatively large influence of the chiral diphosphine ligand in controlling the enantioselectivity of the reaction rather than the cavity shape.

Cambridge and Gagne have recently reported molecularly imprinted catalysts for the Suzuki coupling shown in Fig. 27. In both approaches palladium catalysts containing phosphine ligands were imprinted. Cambridge et al. used

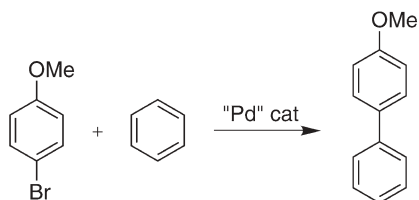


Fig. 27 Suzuki reaction catalysed by Pd-MIPs

a Pd-complex with two polymerisable phosphine ligands and a benzene-1,2-diol as template ligand [90]. The imprinted catalyst gave a higher yield (81%) compared to the homogeneous catalyst (56%). Importantly, the catalyst was reusable with no reduction in the yield, whereas the homogeneous catalyst lost activity on repeated usage (45% at second use).

Gagne et al. used a bipodal phosphine ligand and 4,6-dinitrobenzene-1,2,3-triol as a template ligand [91]. In addition to this complex a primary amine, stabilised by a polymerisable crown ether, was added to form a polymerisable ternary complex via non-covalent interactions, thus creating a hybrid crown-ether functionalised active site during the imprinting step (Fig. 28). Using this original approach they improved the activity of the resulting MIP catalyst by factors of up to 2.5.

5 Perspectives

The number of reports of the use of “non-traditional” functional monomers in molecular imprinting has grown steadily in recent years. While we hope to

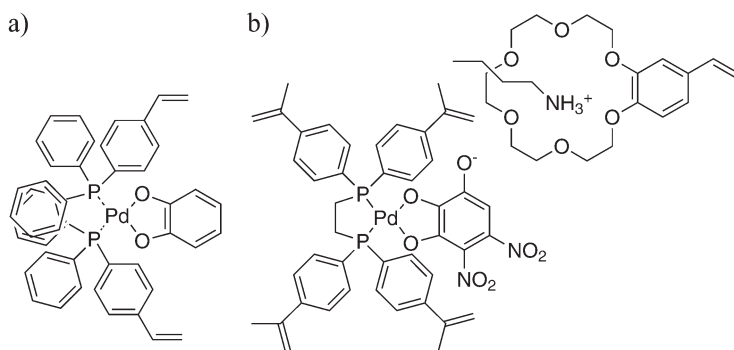


Fig. 28 Pd-catalysts complexed with template for the catalysis of Suzuki couplings by a) two phosphine ligands with benzene-1,2-diol as template and b) a chelating bisphosphine ligand with 4,6-dinitro-benzene-1,2,3-triol as template in a ternary complex with a primary amine stabilised by a crown ether

have demonstrated that there are obvious benefits to be gained from the preparation of new binding monomers for both recognition and catalysis, such developments are still at an early stage within the field. Undoubtedly this will change in the near future as more researchers in the field discover the advantages in binding site homogeneity and affinity that these monomers can bring to their macromolecular receptors. The recent examples of MIPs exhibiting enzyme-like catalysis convincingly demonstrate these benefits. By combining the type of chemistry described in this review for construction of the binding or catalytic sites with techniques to generate the polymer as beads, nanoparticles, microgels or thin films we envisage a new generation of imprinted receptors or catalysts exhibiting strong improvements compared to state-of-the-art materials.

References

1. Best MD, Tobey SL, Anslyn EV (2003) *Coord Chem Rev* 240:3–15
2. Gale PA (2003) *Coord Chem Rev* 240:191–221
3. Suksai C, Tuntulani T (2003) *Chem Soc Rev* 32:192–202
4. Peczu, MW, Hamilton AD (2000) *Chem Rev* 100:2479–2494
5. Sellergren B (ed) (2001) *Molecularly imprinted polymers. Man-made mimics of antibodies and their applications in analytical chemistry*, vol 23. Elsevier, Amsterdam
6. Wulff G, Knorr K (2002) *Bioseparation* 10:257
7. Shea KJ (2002) *Molecularly imprinted materials – sensors and other devices*, vol 723. MRS, San Francisco
8. Sellergren B (2001) In: Subramanian G (ed) *Chiral separation techniques*, 2nd edn. Wiley-VCH, Weinheim
9. Andersson LI, Schweitz L (2003) *Handbook of analytical separations*, vol 4. Elsevier, Amsterdam, pp 45–71
10. Haupt K, Mosbach K (2000) *Chem Rev* 100:2495–2504
11. Whitcombe MJ, Rodriguez ME, Villar P, Vulfson EN (1995) *J Am Chem Soc* 117:7105–7111
12. Oral E, Peppas NA (2004) *J Biomed Mat Res Part A* 68A:439–447
13. Mosbach K (2001) *Anal Chim Acta* 435:3–8
14. Wulff G (2002) *Chem Rev* 102:1
15. Komiyama M, Takeuchi T, Mukawa T, Asanuma H (eds) (2002) *Molecular imprinting – from fundamentals to applications*. Wiley-VCH, Weinheim
16. Wulff G (1995) *Angew Chem Int Ed Engl* 34:1812–32
17. Wulff G, Sarhan A (1972) *Angew Chem Int Ed Engl* 11:341
18. Shea KJ, Dougherty TK (1986) *J Am Chem Soc* 108:1091–1093
19. Sellergren B, Lepistoe M, Mosbach K (1988) *J Am Chem Soc* 110:5853–60
20. Shea KJ, Spivak DA, Sellergren B (1993) *J Am Chem Soc* 115:3368–3369
21. Lanza F, Sellergren B (2004) *Macromol Rapid Commun* 25:59–68
22. Tanabe K, Takeuchi T, Matsui J, Ikebukuro K, Yano K, Karube I (1995) *J Chem Soc Chem Commun* 22:2303–4
23. Chang SK, Van Engen D, Fan E, Hamilton AD (1991) *J Am Chem Soc* 113:7640
24. Kugimiya A, Mukawa T, Takeuchi T (2001) *Analyst* 126:772–774
25. Yano K, Tanabe K, Takeuchi T, Matsui J, Ikebukuro K, Karube I (1998) *Anal Chim Acta* 363:111–117

26. Hall AJ, Manesiotis P, Mossing JT, Sellergren B (2002) *Mat Res Soc Symp Proc* 723: M1.3.1–5
27. Manesiotis P, Hall AJ, Sellergren B (2005) *J Org Chem* 70: 2729–2738
28. Manesiotis P, Hall AJ, Courtois J, Irgum K, Sellergren B (2005) *Angew. Chem.* in press
29. Beijer FH, Kooijman H, Speck AL, Sijbesma RP, Meijer EW (1998) *Angew Chem Int Ed* 37:75–78
30. Hishiya T, Shibata M, Kakazu M, Asanuma H, Komiyama M (1999) *Macromolecules* 32:2265–2269
31. Steinke J, Sherrington D, Dunkin I (1995) *Adv Polym Sci* 123:80
32. Ju JY, Shin CS, Whitcombe MJ, Vulfson EN (1999) *Biotechnol Bioeng* 64:232–239
33. Hall AJ, Manesiotis P, Sellergren B (unpublished work)
34. Spivak D, Shea KJ (1999) *J Org Chem* 64:4627–4634
35. Wulff G, Gross T, Schönfeld, R (1997) *Angew Chem Int Ed Engl* 36:1962–1964
36. Strikovskiy AG, Kasper D, Gruen M, Green HJ, Wulff G (2000) *J Am Chem Soc* 122:6295–6296
37. Lübke C, Lübke M, Whitcombe MJ, Vulfson EN (2000) *Macromolecules* 33:5098–5105
38. Hall AJ, Achilli L, Manesiotis P, Quaglia M, De Lorenzi E, Sellergren B (2003) *J Org Chem* 68, 9132–9135
39. Fan E, Van Arman SA, Kincaid S, Hamilton AD (1993) *J Am Chem Soc* 115:369–370
40. Wilcox CS, Kim E, Romano D, Kuo LH, Burt LB, Curran DP (1995) *Tetrahedron* 51:621
41. Manesiotis P, Hall AJ, Emgenbroich M, Quaglia M, De Lorenzi E, Sellergren B (2004) *Chem Commun* 2278–2279
42. Hall AJ, Manesiotis P, Emgenbroich M, Quaglia M, De Lorenzi E, Sellergren B (2005) *J. Org. Chem.* 70:1732–1736
43. Turkewitsch P, Wandelt B, Darling GD, Powell WS (1998) *Anal. Chem* 70:2025–2030
44. Matsui J, Higashi M, Takeuchi T (2000) *J Am Chem Soc* 122:5218–5219
45. Kubo H, Nariai H, Takeuchi T (2003) *Chem Commun* 2792–2793
46. Batra D, Shea K (2003) *J Org Lett.* 5:3895–3898
47. Sibrian-Vazquez M, Spivak DA (2003) *Macromolecules* 36:5105–5113
48. Sibrian-Vazquez M, Spivak DA (2003) *J Organic Chem* 68:9604–9611
49. Sibrian-Vazquez M, Spivak DA (2004) *J Am Chem Soc* 126:7827–2833
50. Dahl PK, Arnold FH (1991) *J Am Chem Soc* 113:7417–7418
51. Striegler S (2001) *Tetrahedron* 57:2349–2354
52. Striegler S (2002) *Bioseparation* 10:307–314
53. Striegler S (2003) *Macromolecules* 36, 1310–1317
54. Hart BR, Shea KJ (2001) *J Am Chem Soc* 123:2072–2073
55. Hart BR, Shea K (2002) *J Macromolecules* 35:6192–6201
56. Takeuchi T, Mukawa T, Matsui J, Higashi M, Shimizu KD (2001) *Anal Chem* 73:3869–3874
57. Subat M, Borovik AS, König B (2004) *J Am Chem Soc* 126:3185–3190
58. Lui J-Q, Wulff G (2004) *Angew Chem Int Ed Eng* 43
59. Lui J-Q, Wulff G (2004) *J Am Chem Soc* 126:7452–7453
60. Zimmerman SC, Zharov I, Wendland, M. S, Rakow NA, Suslick KS (2003) *J Am Chem Soc* 125:13504–13518
61. Zimmerman SC, Lemcoff NG (2004) *Chemical Commun* 5–14
62. Kirby A (1996) *Angew Chem Int Ed Engl* 35:707–724
63. Lerner RA, Benkovic SJ, Schultz PG (1991) *Science* 252:659–667
64. Tanaka F (2002) *Chem Rev* 102:4885–4906
65. Pauling L (1946) *Chem Eng News* 1375–1377
66. Jencks WP (1969) *Catalysis in chemistry and enzymology*. McGraw-Hill, New York
67. Alexander C, Davidson L, Hayes W (2003) *Tetrahedron* 59:2025–2057

68. Motherwell WB, Bingham MJ, Six Y (2001) *Tetrahedron* 57:4663–4686
69. Fersht A (1985) *Enzyme structure and mechanism*, 2nd edn. Freeman, New York
70. Leonhardt A, Mosbach K (1987) *React Polym* 6:285–290
71. Robinson DK, Mosbach K (1989) *J Chem Soc Chem Commun* 969–70
72. Ohkubo K, Urata Y, Hirota S, Honda Y, Fujishita Y-I, Sagawa T (1994) *J Mol Catal* 93:189–93
73. Ohkubo K, Sawakuma K, Sagawa T (2001) *J Mol Catal A: Chem* 165:1–7
74. Ohkubo K, Sawakuma K, Sagawa T (2000) *Polymer* 42:2263–2266
75. Sellergren B, Shea KJ (1994) *Tetrahedron Assym* 5:1403
76. Sellergren B, Karmalkar R, Shea KJ (2000) *J Org Chem* 65:4009–4027
77. Stewart JD, Liotta LJ, Benkovic S (1993) *Acc Chem Res* 26:396–404
78. Strikovskiy A, Hradil J, Wulff G (2003) *React Funct Polym* 54:49–61
79. Emgenbroich M, Wulff G (2003) *Chem-A Eur J* 9:4106–4117
80. Kim J-M, Ahn K-D, Wulff G (2001) *Macromol Chem Phys* 202:1105–1108
81. Toorisaka E, Uezu K, Goto M, Furusaki S (2003) *Biochem Eng J* 14:85–91
82. Maddock SC, Pasetto P, Resmini M (2004) *Chem Commun* 536–537
83. Toorisaka E, Yoshida M, Uezu K, Goto M (1999) *Chem Lett* 387–388
84. Gamez P, Dunjic B, Pinel C, Lemaire M (1995) *Tetrahedron Lett* 36:8779–82
85. Locatelli F, Gamez P, Lemaire M (1998) *J Mol Catal A: Chem* 135:89–98
86. Polborn K, Severin K (2000) *Chem Eur J* 6:4604–4611
87. Severin K (2000) *Curr Opin Chem Biol* 4:710–714
88. Polborn K, Severin K (2000) *Eur J Inorg Chem* 8:1687–1692
89. Koh JH, Larsen A O, White PS, Gagne MR (2002) *Organometallics* 21:7–9
90. Cammidge AN, Baines NJ, Bellingham RK (2001) *Chem Commun* 2588–2589
91. Becker JJ, Gagne MR (2003) *Organometallics* 22:4984–4998

Author Index Volumes 201–249

Author Index Vols. 26–50 see Vol. 50

Author Index Vols. 51–100 see Vol. 100

Author Index Vols. 101–150 see Vol. 150

Author Index Vols. 151–200 see Vol. 200

The volume numbers are printed in italics

- Achilefu S, Dorshow RB (2002) Dynamic and Continuous Monitoring of Renal and Hepatic Functions with Exogenous Markers. 222: 31–72
- Alajarín M, López-Leonardo C, Llamas-Lorente P (2005) The Chemistry of Phosphinous Amides (Aminophosphanes): Old Reagents with New Applications. 250: 77–106
- Albert M, see Dax K (2001) 215: 193–275
- Albrecht M (2004) Supramolecular Templating in the Formation of Helicates. 248: 105–139
- Ando T, Inomata S-I, Yamamoto M (2004) Lepidopteran Sex Pheromones. 239: 51–96
- Angyal SJ (2001) The Lobry de Bruyn-Alberda van Ekenstein Transformation and Related Reactions. 215: 1–14
- Antzutkin ON, see Ivanov AV (2005) 246: 271–337
- Anupöld T, see Samoson A (2005) 246: 15–31
- Aricó F, Badjic JD, Cantrill SJ, Flood AH, Leung KC-F, Liu Y, Stoddart JF (2005) Templated Synthesis of Interlocked Molecules. 249: 203–259
- Armentrout PB (2003) Threshold Collision-Induced Dissociations for the Determination of Accurate Gas-Phase Binding Energies and Reaction Barriers. 225: 227–256
- Astruc D, Blais J-C, Cloutet E, Djakovitch L, Rigaut S, Ruiz J, Sartor V, Valério C (2000) The First Organometallic Dendrimers: Design and Redox Functions. 210: 229–259
- Augé J, see Lubineau A (1999) 206: 1–39
- Baars MWPL, Meijer EW (2000) Host-Guest Chemistry of Dendritic Molecules. 210: 131–182
- Bach T, see Basler B (2005) 243: 1–42
- Bächinger H-P, see Engel J (2005) 247: 7–33
- Badjic JD, see Aricó F (2005) 249: 203–259
- Balazs G, Johnson BP, Scheer M (2003) Complexes with a Metal-Phosphorus Triple Bond. 232: 1–23
- Balbo Block MA, Kaiser C, Khan A, Hecht S (2005) Discrete Organic Nanotubes Based on a Combination of Covalent and Non-Covalent Approaches. 245: 89–150
- Balczewski P, see Mikoloajczyk M (2003) 223: 161–214
- Ballauff M (2001) Structure of Dendrimers in Dilute Solution. 212: 177–194
- Ballauff M, see Likos CN (2005) 245: 239–252
- Baltzer L (1999) Functionalization and Properties of Designed Folded Polypeptides. 202: 39–76
- Balzani V, Ceroni P, Maestri M, Saudan C, Vicinelli V (2003) Luminescent Dendrimers. Recent Advances. 228: 159–191
- Bandichhor R, Nosse B, Reiser O (2005): Paraconic Acids – The Natural Products from Lichen Symbiont. 243: 43–72
- Bannwarth W, see Horn J (2004) 242: 43–75
- Barré L, see Lasne M-C (2002) 222: 201–258

- Bartlett RJ, see Sun J-Q (1999) 203: 121–145
- Basler B, Brandes S, Spiegel A, Bach T (2005) Total Syntheses of Kelsoene and Preussin. 243: 1–42
- Bäuerle P, see Kaiser A (2005) 249: 127–201
- Bauer RE, Grimsdale AC, Müllen K (2005) Functionalised Polyphenylene Dendrimers and Their Applications. 245: 253–286
- Beaulac R, see Bussière G (2004) 241: 97–118
- Beifuss U, Tietze M (2005) Methanophenazine and Other Natural Biologically Active Phenazines. 244: 77–113
- Bélisle H, see Bussière G (2004) 241: 97–118
- Bergbreiter DE, Li J (2004) Applications of Catalysts on Soluble Supports. 242: 113–176
- Bertrand G, Bourissou D (2002) Diphosphorus-Containing Unsaturated Three-Membered Rings: Comparison of Carbon, Nitrogen, and Phosphorus Chemistry. 220: 1–25
- Betzemeier B, Knochel P (1999) Perfluorinated Solvents – a Novel Reaction Medium in Organic Chemistry. 206: 61–78
- Bibette J, see Schmitt V (2003) 227: 195–215
- Birk DE, Bruckner P (2005) Collagen Suprastructures. 247: 185–205
- Blais J-C, see Astruc D (2000) 210: 229–259
- Bogár F, see Pipek J (1999) 203: 43–61
- Bohme DK, see Petrie S (2003) 225: 35–73
- Boillot M-L, Zarembowitch J, Sour A (2004) Ligand-Driven Light-Induced Spin Change (LD-LISC): A Promising Photomagnetic Effect. 234: 261–276
- Boukheddaden K, see Bousseksou A (2004) 235: 65–84
- Boukheddaden K, see Varret F (2004) 234: 199–229
- Bourissou D, see Bertrand G (2002) 220: 1–25
- Bousseksou A, Varret F, Goiran M, Boukheddaden K, Tuchagues J-P (2004) The Spin Crossover Phenomenon Under High Magnetic Field. 235: 65–84
- Bousseksou A, see Tuchagues J-P (2004) 235: 85–103
- Bowers MT, see Wyttenbach T (2003) 225: 201–226
- Brady C, McGarvey JJ, McCusker JK, Toftlund H, Hendrickson DN (2004) Time-Resolved Relaxation Studies of Spin Crossover Systems in Solution. 235: 1–22
- Braekman J-C, see Laurent P (2005) 240: 167–229
- Brand SC, see Haley MM (1999) 201: 81–129
- Brandes S, see Basler B (2005) 243: 1–42
- Bravic G, see Guionneau P (2004) 234: 97–128
- Bray KL (2001) High Pressure Probes of Electronic Structure and Luminescence Properties of Transition Metal and Lanthanide Systems. 213: 1–94
- Brinckmann J (2005) Collagens at a Glance. 247: 1–6
- Bronstein LM (2003) Nanoparticles Made in Mesoporous Solids. 226: 55–89
- Brönstrup M (2003) High Throughput Mass Spectrometry for Compound Characterization in Drug Discovery. 225: 275–294
- Brücher E (2002) Kinetic Stabilities of Gadolinium(III) Chelates Used as MRI Contrast Agents. 221: 103–122
- Bruckner P, see Birk DE (2005) 247: 185–205
- Brüggemann J, see Schalley CA (2004) 248: 141–200
- Brunel JM, Buono G (2002) New Chiral Organophosphorus catalysts in Asymmetric Synthesis. 220: 79–106
- Buchwald SL, see Muci AR (2002) 219: 131–209
- Bunz UHF (1999) Carbon-Rich Molecular Objects from Multiply Ethynylated *p*-Complexes. 201: 131–161
- Buono G, see Brunel JM (2002) 220: 79–106

- Burger BV (2005) Mammalian Semiochemicals. 240: 231–278
- Busch DH (2005) First Considerations: Principles, Classification, and History. 249: 1–65
- Bussière G, Beaulac R, Bélisle H, Lescop C, Luneau D, Rey P, Reber C (2004) Excited States and Optical Spectroscopy of Nitronyl Nitroxides and Their Lanthanide and Transition Metal Complexes. 241: 97–118
- Cadierno V, see Majoral J-P (2002) 220: 53–77
- Cámara M, see Chhabra SR (2005) 240: 279–315
- Caminade A-M, see Majoral J-P (2003) 223: 111–159
- Cantrill SJ, see Aricó F (2005) 249: 203–259
- Carmichael D, Mathey F (2002) New Trends in Phosphametallocene Chemistry. 220: 27–51
- Caruso F (2003) Hollow Inorganic Capsules via Colloid-Templated Layer-by-Layer Electrostatic Assembly. 227: 145–168
- Caruso RA (2003) Nanocasting and Nanocoating. 226: 91–118
- Ceroni P, see Balzani V (2003) 228: 159–191
- Chamberlin AR, see Gilmore MA (1999) 202: 77–99
- Chasseau D, see Guionneau P (2004) 234: 97–128
- Che C-M, see Lai S-W (2004) 241: 27–63
- Chhabra SR, Philipp B, Eberl L, Givskov M, Williams P, Cámara M (2005) Extracellular Communication in Bacteria. 240: 279–315
- Chivers T (2003) Imido Analogues of Phosphorus Oxo and Chalcogenido Anions. 229: 143–159
- Chow H-F, Leung C-F, Wang G-X, Zhang J (2001) Dendritic Oligoethers. 217: 1–50
- Chumakov AI, see Winkler H (2004) 235: 105–136
- Clarkson RB (2002) Blood-Pool MRI Contrast Agents: Properties and Characterization. 221: 201–235
- Cloutet E, see Astruc D (2000) 210: 229–259
- Co CC, see Hentze H-P (2003) 226: 197–223
- Codjovi E, see Varret F (2004) 234: 199–229
- Colasson BX, see Dietrich-Buchecker C (2005) 249: 261–283
- Constant S, Lacour J (2005) New Trends in Hexacoordinated Phosphorus Chemistry. 250: 1–41
- Cooper DL, see Raimondi M (1999) 203: 105–120
- Cornils B (1999) Modern Solvent Systems in Industrial Homogeneous Catalysis. 206: 133–152
- Corot C, see Idee J-M (2002) 222: 151–171
- Crego-Calama M, Reinhoudt DN, ten Cate MGJ (2005) Templatation in Noncovalent Synthesis of Hydrogen-Bonded Rosettes 249: 285–316
- Crépy KVL, Imamoto T (2003) New P-Chirogenic Phosphine Ligands and Their Use in Catalytic Asymmetric Reactions. 229: 1–40
- Cristau H-J, see Taillefer M (2003) 229: 41–73
- Crooks RM, Lemon III BI, Yeung LK, Zhao M (2001) Dendrimer-Encapsulated Metals and Semiconductors: Synthesis, Characterization, and Applications. 212: 81–135
- Croteau R, see Davis EM (2000) 209: 53–95
- Crouzel C, see Lasne M-C (2002) 222: 201–258
- Curran DP, see Maul JJ (1999) 206: 79–105
- Currie F, see Häger M (2003) 227: 53–74
- Dabkowski W, see Michalski J (2003) 232: 93–144
- Dalozé D, see Laurent P (2005) 240: 167–229
- Daniel C (2004) Electronic Spectroscopy and Photoreactivity of Transition Metal Complexes: Quantum Chemistry and Wave Packet Dynamics. 241: 119–165

- Davidson P, see Gabriel J-C P (2003) 226: 119–172
- Davis EM, Croteau R (2000) Cyclization Enzymes in the Biosynthesis of Monoterpenes, Sesquiterpenes and Diterpenes. 209: 53–95
- Davies JA, see Schwert DD (2002) 221: 165–200
- Dax K, Albert M (2001) Rearrangements in the Course of Nucleophilic Substitution Reactions. 215: 193–275
- De Jaeger R, see Gleria M (2005) 250: 165–251
- de Keizer A, see Kleinjan WE (2003) 230: 167–188
- de la Plata BC, see Ruano JLG (1999) 204: 1–126
- de Meijere A, Kozhushkov SI (1999) Macrocyclic Structurally Homoconjugated Oligo-acetylenes: Acetylene- and Diacetylene-Expanded Cycloalkanes and Rotanes. 201: 1–42
- de Meijere A, Kozhushkov SI, Khlebnikov AF (2000) Bicyclopropyldiene – A Unique Tetra-substituted Alkene and a Versatile C₆-Building Block. 207: 89–147
- de Meijere A, Kozhushkov SI, Hadjiaraoglou LP (2000) Alkyl 2-Chloro-2-cyclopropylideneacetates – Remarkably Versatile Building Blocks for Organic Synthesis. 207: 149–227
- Dennig J (2003) Gene Transfer in Eukaryotic Cells Using Activated Dendrimers. 228: 227–236
- de Raadt A, Fechter MH (2001) Miscellaneous. 215: 327–345
- Desai B, Kappe CO (2004) Microwave-Assisted Synthesis Involving Immobilized Catalysts. 242: 177–208
- Desreux JF, see Jacques V (2002) 221: 123–164
- Dettner K, see Francke W (2005) 240: 85–166
- Diederich F, Gobbi L (1999) Cyclic and Linear Acetylenic Molecular Scaffolding. 201: 43–79
- Diederich F, see Smith DK (2000) 210: 183–227
- Diederich F, see Thilgen C (2004) 248: 1–61
- Dietrich-Buchecker C, Colasson BX, Sauvage J-P (2005) Molecular Knots 249: 261–283
- Djakovitch L, see Astruc D (2000) 210: 229–259
- Dolle F, see Lasne M-C (2002) 222: 201–258
- Donges D, see Yersin H (2001) 214: 81–186
- Dormán G (2000) Photoaffinity Labeling in Biological Signal Transduction. 211: 169–225
- Dorn H, see McWilliams AR (2002) 220: 141–167
- Dorshow RB, see Achilefu S (2002) 222: 31–72
- Dötz KH, Wenzel B, Jahr HC (2004) Chromium-Templated Benzannulation and Haptotropic Metal Migration. 248: 63–103
- Drabowicz J, Mikołajczyk M (2000) Selenium at Higher Oxidation States. 208: 143–176
- Drain CM, Goldberg I, Sylvain I, Falber A (2005) Synthesis and Applications of Supramolecular Porphyrinic Materials. 245: 55–88
- Dutasta J-P (2003) New Phosphorylated Hosts for the Design of New Supramolecular Assemblies. 232: 55–91
- Dyer PW, see Hissler M (2005) 250: 127–163
- Eberl L, see Chhabra SR (2005) 240: 279–315
- Eckert B, Steudel R (2003) Molecular Spectra of Sulfur Molecules and Solid Sulfur Allotropes. 231: 31–97
- Eckert B, see Steudel R (2003) 230: 1–79
- Eckert H, Elbers S, Epping JD, Janssen M, Kalwei M, Strojek W, Voigt U (2005) Dipolar Solid State NMR Approaches Towards Medium-Range Structure in Oxide Glasses. 246: 195–233
- Ehes M, Romerosa A, Peruzzini M (2002) Metal-Mediated Degradation and Reaggregation of White Phosphorus. 220: 107–140

- Eder B, see Wrodnigg TM (2001) The Amadori and Heyns Rearrangements: Landmarks in the History of Carbohydrate Chemistry or Unrecognized Synthetic Opportunities? 215: 115–175
- Edwards DS, see Liu S (2002) 222: 259–278
- Elaissari A, Ganachaud F, Pichot C (2003) Biorelevant Latexes and Microgels for the Interaction with Nucleic Acids. 227: 169–193
- Elbers S, see Eckert H (2005) 246: 195–233
- Emgenbroich M, see Hall AJ (2005) 249: 317–349
- Enachescu C, see Varret F (2004) 234: 199–229
- End N, Schöning K-U (2004) Immobilized Catalysts in Industrial Research and Application. 242: 241–271
- End N, Schöning K-U (2004) Immobilized Biocatalysts in Industrial Research and Production. 242: 273–317
- Engel J, Bächinger H-P (2005) Structure, Stability and Folding of the Collagen Triple Helix. 247: 7–33
- Epping JD, see Eckert H (2005) 246: 195–233
- Esumi K (2003) Dendrimers for Nanoparticle Synthesis and Dispersion Stabilization. 227: 31–52
- Eyre DR, Wu J-J (2005) Collagen Cross-Links. 247: 207–229
- Falber A, see Drain CM (2005) 245: 55–88
- Famulok M, Jenne A (1999) Catalysis Based on Nucleic Acid Structures. 202: 101–131
- Fechter MH, see de Raadt A (2001) 215: 327–345
- Fernandez C, see Rocha J (2005) 246: 141–194
- Ferrier RJ (2001) Substitution-with-Allylic-Rearrangement Reactions of Glycal Derivatives. 215: 153–175
- Ferrier RJ (2001) Direct Conversion of 5,6-Unsaturated Hexopyranosyl Compounds to Functionalized Glycohexanones. 215: 277–291
- Flood AH, see Aricó F (2005) 249: 203–259
- Förster S (2003) Amphiphilic Block Copolymers for Templating Applications. 226: 1–28
- Francke W, Dettner K (2005) Chemical Signalling in Beetles. 240: 85–166
- Frey H, Schlenk C (2000) Silicon-Based Dendrimers. 210: 69–129
- Friščić T, see MacGillivray LR (2004) 248: 201–221
- Frullano L, Rohovec J, Peters JA, Geraldès CFGC (2002) Structures of MRI Contrast Agents in Solution. 221: 25–60
- Fugami K, Kosugi M (2002) Organotin Compounds. 219: 87–130
- Fuhrhop J-H, see Li G (2002) 218: 133–158
- Furukawa N, Sato S (1999) New Aspects of Hypervalent Organosulfur Compounds. 205: 89–129
- Gabriel J-C P, Davidson P (2003) Mineral Liquid Crystals from Self-Assembly of Anisotropic Nanosystems. 226: 119–172
- Gamelin DR, Güdel HU (2001) Upconversion Processes in Transition Metal and Rare Earth Metal Systems. 214: 1–56
- Ganachaud F, see Elaissari A (2003) 227: 169–193
- García R, see Tromas C (2002) 218: 115–132
- García Y, Gütlich P (2004) Thermal Spin Crossover in Mn(II), Mn(III), Cr(II) and Co(III) Coordination Compounds. 234: 49–62
- García Y, Niel V, Muñoz MC, Real JA (2004) Spin Crossover in 1D, 2D and 3D Polymeric Fe(II) Networks. 233: 229–257
- Gaspar AB, see Ksenofontov V (2004) 235: 23–64
- Gaspar AB, see Real JA (2004) 233: 167–193

- Gates DP (2005) Expanding the Analogy Between P=C and C=C Bonds to Polymer Science. 250: 107–126
- Geraldes CFGC, see Frullano L (2002) 221: 25–60
- Gibb BC, see Laughrey ZR (2005) 249: 67–125
- Gilmore MA, Steward LE, Chamberlin AR (1999) Incorporation of Noncoded Amino Acids by In Vitro Protein Biosynthesis. 202: 77–99
- Givskov M, see Chhabra SR (2005) 240: 279–315
- Glasbeek M (2001) Excited State Spectroscopy and Excited State Dynamics of Rh(III) and Pd(II) Chelates as Studied by Optically Detected Magnetic Resonance Techniques. 213: 95–142
- Glass RS (1999) Sulfur Radical Cations. 205: 1–87
- Gleria M, De Jaeger R (2005) Polyphosphazenes: A Review. 250: 165–251
- Gobbi L, see Diederich F (1999) 201: 43–129
- Goiran M, see Bousseksou A (2004) 235: 65–84
- Goldberg I, see Drain CM (2005) 245: 55–88
- Göltner-Spickermann C (2003) Nanocasting of Lyotropic Liquid Crystal Phases for Metals and Ceramics. 226: 29–54
- Goodwin HA (2004) Spin Crossover in Iron(II) Tris(diimine) and Bis(terimine) Systems. 233: 59–90
- Goodwin HA, see Gütllich P (2004) 233: 1–47
- Goodwin HA (2004) Spin Crossover in Cobalt(II) Systems. 234: 23–47
- Goux-Capes L, see Létard J-F (2004) 235: 221–249
- Gouzy M-F, see Li G (2002) 218: 133–158
- Grandjean F, see Long GJ (2004) 233: 91–122
- Greenspan DS (2005) Biosynthetic Processing of Collagen Molecules. 247: 149–183
- Gries H (2002) Extracellular MRI Contrast Agents Based on Gadolinium. 221: 1–24
- Grimsdale AC, see Bauer RE (2005) 245: 253–286
- Gruber C, see Tovar GEM (2003) 227: 125–144
- Grunert MC, see Linert W (2004) 235: 105–136
- Gudat D (2003): Zwitterionic Phospholide Derivatives – New Ambiphilic Ligands. 232: 175–212
- Guionneau P, Marchivie M, Bravic G, Létard J-F, Chasseau D (2004) Structural Aspects of Spin Crossover. Example of the $[\text{Fe}^{\text{II}}\text{L}_n(\text{NCS})_2]$ Complexes. 234: 97–128
- Güdel HU, see Gamelin DR (2001) 214: 1–56
- Guga P, Okruszek A, Stec WJ (2002) Recent Advances in Stereocontrolled Synthesis of P-Chiral Analogues of Biophosphates. 220: 169–200
- Guionneau P, see Létard J-F (2004) 235: 221–249
- Gulea M, Masson S (2003) Recent Advances in the Chemistry of Difunctionalized Organo-Phosphorus and -Sulfur Compounds. 229: 161–198
- Gütllich P, Goodwin HA (2004) Spin Crossover – An Overall Perspective. 233: 1–47
- Gütllich P (2004) Nuclear Decay Induced Excited Spin State Trapping (NIESST). 234: 231–260
- Gütllich P, see Garcia Y (2004) 234: 49–62
- Gütllich P, see Ksenofontov V (2004) 235: 23–64
- Gütllich P, see Kusz J (2004) 234: 129–153
- Gütllich P, see Real JA (2004) 233: 167–193
- Haag R, Roller S (2004) Polymeric Supports for the Immobilisation of Catalysts. 242: 1–42
- Hackmann-Schlichter N, see Krause W (2000) 210: 261–308
- Hadjiraoglou LP, see de Meijere A (2000) 207: 149–227
- Häger M, Currie F, Holmberg K (2003) Organic Reactions in Microemulsions. 227: 53–74
- Haley MM, Pak JJ, Brand SC (1999) Macrocyclic Oligo(phenylacetylenes) and Oligo(phenyldiacetylenes). 201: 81–129

- Hall AJ, Emgenbroich M, Sellergren B (2005) Imprinted Polymers 249: 317–349
- Hamilton TD, see MacGillivray LR (2004) 248: 201–221
- Harada A, see Yamaguchi H (2003) 228: 237–258
- Hartmann T, Ober D (2000) Biosynthesis and Metabolism of Pyrrolizidine Alkaloids in Plants and Specialized Insect Herbivores. 209: 207–243
- Haseley SR, Kamerling JP, Vliegenthart JFG (2002) Unravelling Carbohydrate Interactions with Biosensors Using Surface Plasmon Resonance (SPR) Detection. 218: 93–114
- Hassner A, see Namboothiri INN (2001) 216: 1–49
- Hauser A (2004) Ligand Field Theoretical Considerations. 233: 49–58
- Hauser A (2004) Light-Induced Spin Crossover and the High-Spin/Low-Spin Relaxation. 234: 155–198
- Hauser A, von Arx ME, Langford VS, Oetliker U, Kairouani S, Pillonnet A (2004) Photo-physical Properties of Three-Dimensional Transition Metal Tris-Oxalate Network Structures. 241: 65–96
- Häusler H, Stütz AE (2001) d-Xylose (d-Glucose) Isomerase and Related Enzymes in Carbohydrate Synthesis. 215: 77–114
- Hawker CJ, see Wooley KL (2005) 245: 287–305
- Hecht S, see Balbo Block MA (2005) 245: 89–150
- Heckrodt TJ, Mulzer J (2005) Marine Natural Products from Pseudopterogorgia Elisabethae: Structures, Biosynthesis, Pharmacology and Total Synthesis. 244: 1–41
- Heinmaa I, see Samoson A (2005) 246: 15–31
- Helm L, see Tóth E (2002) 221: 61–101
- Helmboldt H, see Hiersemann M (2005) 243: 73–136
- Hemscheidt T (2000) Tropane and Related Alkaloids. 209: 175–206
- Hendrickson DN, Pierpont CG (2004) Valence Tautomeric Transition Metal Complexes. 234: 63–95
- Hendrickson DN, see Brady C (2004) 235: 1–22
- Hennel JW, Klinowski J (2005) Magic-Angle Spinning: a Historical Perspective. 246: 1–14
- Hentze H-P, Co CC, McKelvey CA, Kaler EW (2003) Templating Vesicles, Microemulsions and Lyotropic Mesophases by Organic Polymerization Processes. 226: 197–223
- Hergenrother PJ, Martin SF (2000) Phosphatidylcholine-Preferring Phospholipase C from *B. cereus*. Function, Structure, and Mechanism. 211: 131–167
- Hermann C, see Kuhlmann J (2000) 211: 61–116
- Heydt H (2003) The Fascinating Chemistry of Triphosphabenzene and Valence Isomers. 223: 215–249
- Hiersemann M, Helmboldt H (2005): Recent Progress in the Total Synthesis of Dolabellane and Dolastane Diterpenes. 243: 73–136
- Hirsch A, Vostrowsky O (2001) Dendrimers with Carbon Rich-Cores. 217: 51–93
- Hirsch A, Vostrowsky O (2005) Functionalization of Carbon Nanotubes. 245: 193–237
- Hissler M, Dyer PW, Reau R (2005) The Rise of Organophosphorus Derivatives in *p*-Conjugated Materials Chemistry. 250: 127–163
- Hiyama T, Shirakawa E (2002) Organosilicon Compounds. 219: 61–85
- Holmberg K, see Häger M (2003) 227: 53–74
- Horn J, Michalek F, Tzschucke CC, Bannwarth W (2004) Non-Covalently Solid-Phase Bound Catalysts for Organic Synthesis. 242: 43–75
- Houseman BT, Mrksich M (2002) Model Systems for Studying Polyvalent Carbohydrate Binding Interactions. 218: 1–44
- Hricovinová Z, see Petruš L (2001) 215: 15–41
- Idee J-M, Tichowsky I, Port M, Petta M, Le Lem G, Le Greneur S, Meyer D, Corot C (2002) Iodinated Contrast Media: from Non-Specific to Blood-Pool Agents. 222: 151–171
- Igau A, see Majoral J-P (2002) 220: 53–77

- Ikeda Y, see Takagi Y (2003) 232: 213–251
- Imamoto T, see Crépy KVL (2003) 229: 1–40
- Inomata S-I, see Ando T (2004) 239: 51–96
- Ivanov AV, Antzutkin ON (2005) Natural Abundance ^{15}N and ^{13}C CP/MAS NMR of Dialkylidithio-carbamate Compounds with Ni(II) and Zn(II). 246: 271–337
- Iwaoka M, Tomoda S (2000) Nucleophilic Selenium. 208: 55–80
- Iwasawa N, Narasaka K (2000) Transition Metal Promoted Ring Expansion of Alkynyl and Propadienylcyclopropanes. 207: 69–88
- Imperiali B, McDonnell KA, Shogren-Knaak M (1999) Design and Construction of Novel Peptides and Proteins by Tailored Incorporation of Coenzyme Functionality. 202: 1–38
- Ito S, see Yoshifuji M (2003) 223: 67–89
- Jacques V, Desreux JF (2002) New Classes of MRI Contrast Agents. 221: 123–164
- Jahr HC, see Dötz KH (2004) 248: 63–103
- James TD, Shinkai S (2002) Artificial Receptors as Chemosensors for Carbohydrates. 218: 159–200
- Janssen AJH, see Kleinjan WE (2003) 230: 167–188
- Janssen M, see Eckert H (2005) 246: 195–233
- Jas G, see Kirschning A (2004) 242: 208–239
- Jenne A, see Famulok M (1999) 202: 101–131
- Johnson BP, see Balazs G (2003) 232: 1–23
- Jung JH, Shinkai S (2004) Gels as Templates for Nanotubes. 248: 223–260
- Junker T, see Trauger SA (2003) 225: 257–274
- Jurenka R (2004) Insect Pheromone Biosynthesis. 239: 97–132
- Kairouani S, see Hauser A (2004) 241: 65–96
- Kaiser C, see Balbo Block MA (2005) 245: 89–150
- Kaiser A, Bäuerle P (2005) Macrocycles and Complex Three-Dimensional Structures Comprising Pt(II) Building Blocks 249: 127–201
- Kaler EW, see Hentze H-P (2003) 226: 197–223
- Kalesse M (2005) Recent Advances in Vinylogous Aldol Reactions and their Applications in the Syntheses of Natural Products. 244: 43–76
- Kalwei M, see Eckert H (2005) 246: 195–233
- Kalsani V, see Schmittel M (2005) 245: 1–53
- Kamerling JP, see Haseley SR (2002) 218: 93–114
- Kappe CO, see Desai B (2004) 242: 177–208
- Kashemirov BA, see Mc Kenna CE (2002) 220: 201–238
- Kato S, see Murai T (2000) 208: 177–199
- Katti KV, Pillarsetty N, Raghuraman K (2003) New Vistas in Chemistry and Applications of Primary Phosphines. 229: 121–141
- Kawa M (2003) Antenna Effects of Aromatic Dendrons and Their Luminescence Applications. 228: 193–204
- Kazmierski S, see Potrzebowski M J (2005) 246: 91–140
- Kee TP, Nixon TD (2003) The Asymmetric Phospho-Aldol Reaction. Past, Present, and Future. 223: 45–65
- Keeling CI, Plettner E, Slessor KN (2004) Hymenopteran Semiochemicals. 239: 133–177
- Kepert CJ, see Murray KS (2004) 233: 195–228
- Khan A, see Balbo Block MA (2005) 245: 89–150
- Khlebnikov AF, see de Meijere A (2000) 207: 89–147
- Kim K, see Lee JW (2003) 228: 111–140
- Kirschning A, Jas G (2004) Applications of Immobilized Catalysts in Continuous Flow Processes. 242: 208–239

- Kirtman B (1999) Local Space Approximation Methods for Correlated Electronic Structure Calculations in Large Delocalized Systems that are Locally Perturbed. *203*: 147–166
- Kita Y, see Tohma H (2003) *224*: 209–248
- Kleij AW, see Kreiter R (2001) *217*: 163–199
- Klein Gebbink RJM, see Kreiter R (2001) *217*: 163–199
- Kleinjan WE, de Keizer A, Janssen AJH (2003) Biologically Produced Sulfur. *230*: 167–188
- Klibanov AL (2002) Ultrasound Contrast Agents: Development of the Field and Current Status. *222*: 73–106
- Klinowski J, see Hennel JW (2005) *246*: 1–14
- Klopper W, Kutzelnigg W, Müller H, Noga J, Vogtner S (1999) Extremal Electron Pairs – Application to Electron Correlation, Especially the R12 Method. *203*: 21–42
- Knochel P, see Betzemeier B (1999) *206*: 61–78
- Knoelker H-J (2005) Occurrence, Biological Activity, and Convergent Organometallic Synthesis of Carbazole Alkaloids. *244*: 115–148
- Koide T, Nagata K (2005) Collagen Biosynthesis. *247*: 85–114
- Kolodziejski W (2005) Solid-State NMR Studies of Bone. *246*: 235–270
- Koser GF (2003) C-Heteroatom-Bond Forming Reactions. *224*: 137–172
- Koser GF (2003) Heteroatom-Heteroatom-Bond Forming Reactions. *224*: 173–183
- Kosugi M, see Fugami K (2002) *219*: 87–130
- Koudriavtsev AB, see Linert W (2004) *235*: 105–136
- Kozhushkov SI, see de Meijere A (1999) *201*: 1–42
- Kozhushkov SI, see de Meijere A (2000) *207*: 89–147
- Kozhushkov SI, see de Meijere A (2000) *207*: 149–227
- Krause W (2002) Liver-Specific X-Ray Contrast Agents. *222*: 173–200
- Krause W, Hackmann-Schlichter N, Maier FK, Mller R (2000) Dendrimers in Diagnostics. *210*: 261–308
- Krause W, Schneider PW (2002) Chemistry of X-Ray Contrast Agents. *222*: 107–150
- Kräuter I, see Tovar GEM (2003) *227*: 125–144
- Kreiter R, Kleij AW, Klein Gebbink RJM, van Koten G (2001) Dendritic Catalysts. *217*: 163–199
- Krossing I (2003) Homoatomic Sulfur Cations. *230*: 135–152
- Ksenofontov V, Gaspar AB, Gütllich P (2004) Pressure Effect Studies on Spin Crossover and Valence Tautomeric Systems. *235*: 23–64
- Ksenofontov V, see Real JA (2004) *233*: 167–193
- Kuhlmann J, Herrmann C (2000) Biophysical Characterization of the Ras Protein. *211*: 61–116
- Kunkely H, see Vogler A (2001) *213*: 143–182
- Kusz J, Gütllich P, Spiering H (2004) Structural Investigations of Tetrazole Complexes of Iron(II). *234*: 129–153
- Kutzelnigg W, see Klopper W (1999) *203*: 21–42
- Lacour J, see Constant S (2005) *250*: 1–41
- Lai S-W, Che C-M (2004) Luminescent Cyclometalated Diimine Platinum(II) Complexes. Photophysical Studies and Applications. *241*: 27–63
- Lammertsma K (2003) Phosphinidenes. *229*: 95–119
- Landfester K (2003) Miniemulsions for Nanoparticle Synthesis. *227*: 75–123
- Langford VS, see Hauser A (2004) *241*: 65–96
- Lasne M-C, Perrio C, Rouden J, Barré L, Roeda D, Dolle F, Crouzel C (2002) Chemistry of *b*⁺-Emitting Compounds Based on Fluorine-18. *222*: 201–258
- Laughrey ZR, Gibb BC (2005) Macrocyclic Synthesis Through Templatation. *249*: 67–125
- Laurent P, Braekman J-C, Daloze D (2005) Insect Chemical Defense. *240*: 167–229
- Lawless LJ, see Zimmermann SC (2001) *217*: 95–120

- Leal WS (2005) Pheromone Reception. *240*: 1–36
- Leal-Calderon F, see Schmitt V (2003) *227*: 195–215
- Lee JW, Kim K (2003) Rotaxane Dendrimers. *228*: 111–140
- Le Bideau, see Vioux A (2003) *232*: 145–174
- Le Greneur S, see Idee J-M (2002) *222*: 151–171
- Le Lem G, see Idee J-M (2002) *222*: 151–171
- Leclercq D, see Vioux A (2003) *232*: 145–174
- Leitner W (1999) Reactions in Supercritical Carbon Dioxide (scCO₂). *206*: 107–132
- Lemon III BI, see Crooks RM (2001) *212*: 81–135
- Lescop C, see Bussière G (2004) *241*: 97–118
- Leung C-F, see Chow H-F (2001) *217*: 1–50
- Leung KC-F, see Aricó F (2005) *249*: 203–259
- Létard J-F, Guionneau P, Goux-Capes L (2004) Towards Spin Crossover Applications. *235*: 221–249
- Létard J-F, see Guionneau P (2004) *234*: 97–128
- Levitzi A (2000) Protein Tyrosine Kinase Inhibitors as Therapeutic Agents. *211*: 1–15
- Li G, Gouzy M-F, Fuhrhop J-H (2002) Recognition Processes with Amphiphilic Carbohydrates in Water. *218*: 133–158
- Li J, see Bergbreiter DE (2004) *242*: 113–176
- Li X, see Paldus J (1999) *203*: 1–20
- Licha K (2002) Contrast Agents for Optical Imaging. *222*: 1–29
- Likos CN, Ballauff M (2005) Equilibrium Structure of Dendrimers – Results and Open Questions. *245*: 239–252
- Linarès J, see Varret F (2004) *234*: 199–229
- Linclau B, see Maul JJ (1999) *206*: 79–105
- Lindhorst TK (2002) Artificial Multivalent Sugar Ligands to Understand and Manipulate Carbohydrate-Protein Interactions. *218*: 201–235
- Lindhorst TK, see Röckendorf N (2001) *217*: 201–238
- Linert W, Grunert MC, Koudriavtsev AB (2004) Isokenetic and Isoequilibrium Relationships in Spin Crossover Systems. *235*: 105–136
- Liu S, Edwards DS (2002) Fundamentals of Receptor-Based Diagnostic Metalloradiopharmaceuticals. *222*: 259–278
- Liu Y, see Aricó F (2005) *249*: 203–259
- Liz-Marzán L, see Mulvaney P (2003) *226*: 225–246
- Llamas-Lorente P, see Alajarín M (2005) *250*: 77–106
- Long GJ, Grandjean F, Reger DL (2004) Spin Crossover in Pyrazolylborate and Pyrazolylmethane. *233*: 91–122
- López-Leonardo C, see Alajarín M (2005) *250*: 77–106
- Loudet JC, Poulin P (2003) Monodisperse Aligned Emulsions from Demixing in Bulk Liquid Crystals. *226*: 173–196
- Lubineau A, Augé J (1999) Water as Solvent in Organic Synthesis. *206*: 1–39
- Lundt I, Madsen R (2001) Synthetically Useful Base Induced Rearrangements of Aldonolactones. *215*: 177–191
- Luneau D, see Bussière G (2004) *241*: 97–118
- Loupy A (1999) Solvent-Free Reactions. *206*: 153–207
- MacGillivray LR, Papaefstathiou GS, Friščić T, Varshney DB, Hamilton TD (2004) Template-Controlled Synthesis in the Solid State. *248*: 201–221
- Madhu PK, see Vinogradov E (2005) *246*: 33–90
- Madsen R, see Lundt I (2001) *215*: 177–191
- Maestri M, see Balzani V (2003) *228*: 159–191
- Maier FK, see Krause W (2000) *210*: 261–308

- Majoral J-P, Caminade A-M (2003) What to do with Phosphorus in Dendrimer Chemistry. 223: 111–159
- Majoral J-P, Igau A, Cadierno V, Zablocka M (2002) Benzyne-Zirconocene Reagents as Tools in Phosphorus Chemistry. 220: 53–77
- Manners I (2002), see McWilliams AR (2002) 220: 141–167
- March NH (1999) Localization via Density Functionals. 203: 201–230
- Marchivie M, see Guionneau P (2004) 234: 97–128
- Marque S, Tordo P (2005) Reactivity of Phosphorus Centred Radicals. 250: 43–76
- Martin SF, see Hergenrother PJ (2000) 211: 131–167
- Mashiko S, see Yokoyama S (2003) 228: 205–226
- Masson S, see Gulea M (2003) 229: 161–198
- Mathey F, see Carmichael D (2002) 220: 27–51
- Maul JJ, Ostrowski PJ, Ublacker GA, Linclau B, Curran DP (1999) Benzotrifluoride and Derivates: Useful Solvents for Organic Synthesis and Fluorous Synthesis. 206: 79–105
- McCusker JK, see Brady C (2004) 235: 1–22
- McDonnell KA, see Imperiali B (1999) 202: 1–38
- McGarvey JJ, see Brady C (2004) 235: 1–22
- McGarvey JJ, see Toftlund H (2004) 233: 151–166
- McGarvey JJ, see Tuchagues J-P (2004) 235: 85–103
- McKelvey CA, see Hentze H-P (2003) 226: 197–223
- McKenna CE, Kashemirov BA (2002) Recent Progress in Carbonylphosphonate Chemistry. 220: 201–238
- McWilliams AR, Dorn H, Manners I (2002) New Inorganic Polymers Containing Phosphorus. 220: 141–167
- Meijer EW, see Baars MWPL (2000) 210: 131–182
- Merbach AE, see Tóth E (2002) 221: 61–101
- Metz P (2005) Synthetic Studies on the Pamamycin Macrodiolides. 244: 215–249
- Metzner P (1999) Thiocarbonyl Compounds as Specific Tools for Organic Synthesis. 204: 127–181
- Meyer D, see Idee J-M (2002) 222: 151–171
- Mezey PG (1999) Local Electron Densities and Functional Groups in Quantum Chemistry. 203: 167–186
- Michalek F, see Horn J (2004) 242: 43–75
- Michalski J, Dabkowski W (2003) State of the Art. Chemical Synthesis of Biophosphates and Their Analogues via PIII Derivatives. 232: 93–144
- Mikołajczyk M, Balczewski P (2003) Phosphonate Chemistry and Reagents in the Synthesis of Biologically Active and Natural Products. 223: 161–214
- Mikołajczyk M, see Drabowicz J (2000) 208: 143–176
- Millar JG (2005) Pheromones of True Bugs. 240: 37–84
- Miura M, Nomura M (2002) Direct Arylation via Cleavage of Activated and Unactivated C-H Bonds. 219: 211–241
- Miyaura N (2002) Organoboron Compounds. 219: 11–59
- Miyaura N, see Tamao K (2002) 219: 1–9
- Möller M, see Sheiko SS (2001) 212: 137–175
- Molnár G, see Tuchagues J-P (2004) 235: 85–103
- Morais CM, see Rocha J (2005) 246: 141–194
- Morales JC, see Rojo J (2002) 218: 45–92
- Mori H, Miller A (2003) Hyperbranched (Meth)acrylates in Solution, in the Melt, and Grafted From Surfaces. 228: 1–37
- Mori K (2004) Pheromone Synthesis. 239: 1–50
- Mrksich M, see Houseman BT (2002) 218: 1–44

- Muci AR, Buchwald SL (2002) Practical Palladium Catalysts for C-N and C-O Bond Formation. 219: 131–209
- Müllen K, see Wiesler U-M (2001) 212: 1–40
- Müllen K, see Bauer RE (2005) 245: 253–286
- Müller A, see Mori H (2003) 228: 1–37
- Müller G (2000) Peptidomimetic SH2 Domain Antagonists for Targeting Signal Transduction. 211: 17–59
- Müller H, see Kloppe W (1999) 203: 21–42
- Müller R, see Krause W (2000) 210: 261–308
- Mulvaney P, Liz-Marzán L (2003) Rational Material Design Using Au Core-Shell Nanocrystals. 226: 225–246
- Mulzer J, see Heckrodt TJ (2005) 244: 1–41
- Muñoz MC, see Real JA (2004) 233: 167–193
- Muñoz MC, see Garcia Y (2004) 233: 229–257
- Murai T, Kato S (2000) Selenocarbonyls. 208: 177–199
- Murray KS, Kepert CJ (2004) Cooperativity in Spin Crossover Systems: Memory, Magnetism and Microporosity. 233: 195–228
- Muscat D, van Benthem RATM (2001) Hyperbranched Polyesteramides – New Dendritic Polymers. 212: 41–80
- Mutin PH, see Vioux A (2003) 232: 145–174
- Myllyharju J (2005) Intracellular Post-Translational Modifications of Collagens. 247: 115–148
- Nagata K, see Koide T (2005) 247: 85–114
- Naka K (2003) Effect of Dendrimers on the Crystallization of Calcium Carbonate in Aqueous Solution. 228: 141–158
- Nakahama T, see Yokoyama S (2003) 228: 205–226
- Nakayama J, Sugihara Y (1999) Chemistry of Thiophene 1,1-Dioxides. 205: 131–195
- Namboothiri INN, Hassner A (2001) Stereoselective Intramolecular 1,3-Dipolar Cycloadditions. 216: 1–49
- Narasaka K, see Iwasawa N (2000) 207: 69–88
- Narayana C, see Rao CNR (2004) 234: 1–21
- Niel V, see Garcia Y (2004) 233: 229–257
- Nierengarten J-F (2003) Fullerodendrimers: Fullerene-Containing Macromolecules with Intriguing Properties. 228: 87–110
- Nishibayashi Y, Uemura S (2000) Selenoxide Elimination and [2,3] Sigmatropic Rearrangements. 208: 201–233
- Nishibayashi Y, Uemura S (2000) Selenium Compounds as Ligands and Catalysts. 208: 235–255
- Nixon TD, see Kee TP (2003) 223: 45–65
- Noga J, see Kloppe W (1999) 203: 21–42
- Nomura M, see Miura M (2002) 219: 211–241
- Nosse B, see Bandichhor R (2005) 243: 43–72
- Nubbemeyer U (2001) Synthesis of Medium-Sized Ring Lactams. 216: 125–196
- Nubbemeyer U (2005) Recent Advances in Charge-Accelerated Aza-Claisen Rearrangements. 244: 149–213
- Nummelin S, Skrifvars M, Rissanen K (2000) Polyester and Ester Functionalized Dendrimers. 210: 1–67
- Ober D, see Hemscheidt T (2000) 209: 175–206
- Ochiai M (2003) Reactivities, Properties and Structures. 224: 5–68
- Oetliker U, see Hauser A (2004) 241: 65–96
- Okazaki R, see Takeda N (2003) 231: 153–202
- Okruszek A, see Guga P (2002) 220: 169–200

- Okuno Y, see Yokoyama S (2003) 228: 205–226
- Onitsuka K, Takahashi S (2003) Metallo dendrimers Composed of Organometallic Building Blocks. 228: 39–63
- Osanaï S (2001) Nickel (II) Catalyzed Rearrangements of Free Sugars. 215: 43–76
- Ostrowski PJ, see Maul JJ (1999) 206: 79–105
- Otomo A, see Yokoyama S (2003) 228: 205–226
- Pak JJ, see Haley MM (1999) 201: 81–129
- Paldus J, Li X (1999) Electron Correlation in Small Molecules: Grafting CI onto CC. 203: 1–20
- Paleos CM, Tsiourvas D (2003) Molecular Recognition and Hydrogen-Bonded Amphiphilics. 227: 1–29
- Papaefstathiou GS, see MacGillivray LR (2004) 248: 201–221
- Past J, see Samoson A (2005) 246: 15–31
- Paulmier C, see Ponthieux S (2000) 208: 113–142
- Paulsen H, Trautwein AX (2004) Density Functional Theory Calculations for Spin Crossover Complexes. 235: 197–219
- Penadés S, see Rojo J (2002) 218: 45–92
- Perrio C, see Lasne M-C (2002) 222: 201–258
- Peruzzini M, see Ehses M (2002) 220: 107–140
- Peters JA, see Frullano L (2002) 221: 25–60
- Petrie S, Bohme DK (2003) Mass Spectrometric Approaches to Interstellar Chemistry. 225: 35–73
- Petruš L, Petrušov M, Hricovíniová (2001) The Blik Reaction. 215: 15–41
- Petrušová M, see Petruš L (2001) 215: 15–41
- Petta M, see Idee J-M (2002) 222: 151–171
- Philipp B, see Chhabra SR (2005) 240: 279–315
- Pichot C, see Elaissari A (2003) 227: 169–193
- Pierpont CG, see Hendrickson DN (2004) 234: 63–95
- Pillarsetty N, see Katti KV (2003) 229: 121–141
- Pillonnet A, see Hauser A (2004) 241: 65–96
- Pipek J, Bogár F (1999) Many-Body Perturbation Theory with Localized Orbitals – Kapuy's Approach. 203: 43–61
- Platner DA (2003) Metalorganic Chemistry in the Gas Phase: Insight into Catalysis. 225: 149–199
- Plettner E, see Keeling CI (2004) 239: 133–177
- Pohnert G (2004) Chemical Defense Strategies of Marine. 239: 179–219
- Ponthieux S, Paulmier C (2000) Selenium-Stabilized Carbanions. 208: 113–142
- Port M, see Idee J-M (2002) 222: 151–171
- Potrzebowski MJ, Kazmierski S (2005) High-Resolution Solid-State NMR Studies of Inclusion Complexes. 246: 91–140
- Poulin P, see Loudet JC (2003) 226: 173–196
- Raghuraman K, see Katti KV (2003) 229: 121–141
- Raimondi M, Cooper DL (1999) Ab Initio Modern Valence Bond Theory. 203: 105–120
- Rao CNR, Seikh MM, Narayana C (2004) Spin-State Transition in LaCoO_3 and Related Materials. 234: 1–21
- Real JA, Gaspar AB, Muñoz MC, Gütllich P, Ksenofontov V, Spiering H (2004) Bipyrimidine-Bridged Dinuclear Iron(II) Spin Crossover Compounds. 233: 167–193
- Real JA, see García Y (2004) 233: 229–257
- Reau R, see Hissler M (2005) 250: 127–163
- Reber C, see Bussière G (2004) 241: 97–118
- Reger DL, see Long GJ (2004) 233: 91–122

- Reinhold A, see Samoson A (2005) 246: 15–31
- Reinhoudt DN, see van Manen H-J (2001) 217: 121–162
- Reinhoudt DN, see Crego-Calama M (2005) 249: 285–316
- Reiser O, see Bandichhor R (2005) 243: 43–72
- Renaud P (2000) Radical Reactions Using Selenium Precursors. 208: 81–112
- Rey P, see Bussière G (2004) 241: 97–118
- Ricard-Blum S, Ruggiero F, van der Rest M (2005) The Collagen Superfamily. 247: 35–84
- Richardson N, see Schwert DD (2002) 221: 165–200
- Rigaut S, see Astruc D (2000) 210: 229–259
- Riley MJ (2001) Geometric and Electronic Information From the Spectroscopy of Six-Coordinate Copper(II) Compounds. 214: 57–80
- Rissanen K, see Nummelin S (2000) 210: 1–67
- Rocha J, Morais CM, Fernandez C (2005) Progress in Multiple-Quantum Magic-Angle Spinning NMR Spectroscopy 246: 141–194
- Röckendorf N, Lindhorst TK (2001) Glycodendrimers. 217: 201–238
- Roeda D, see Lasne M-C (2002) 222: 201–258
- Røeggen I (1999) Extended Geminal Models. 203: 89–103
- Rohovec J, see Frullano L (2002) 221: 25–60
- Rojo J, Morales JC, Penads S (2002) Carbohydrate-Carbohydrate Interactions in Biological and Model Systems. 218: 45–92
- Roller S, see Haag R (2004) 242: 1–42
- Romerosa A, see Ehses M (2002) 220: 107–140
- Rouden J, see Lasne M-C (2002) 222: 201–258
- Ruano JLG, de la Plata BC (1999) Asymmetric [4+2] Cycloadditions Mediated by Sulf-oxides. 204: 1–126
- Ruggiero F, see Ricard-Blum S (2005) 247: 35–84
- Ruijter E, see Wessjohann LA (2005) 243: 137–184
- Ruiz J, see Astruc D (2000) 210: 229–259
- Rychnovsky SD, see Sinz CJ (2001) 216: 51–92
- Salaün J (2000) Cyclopropane Derivates and their Diverse Biological Activities. 207: 1–67
- Samoson A, Tuherm T, Past J, Reinhold A, Anupöld T, Heinmaa I (2005) New Horizons for Magic-Angle Spinning NMR. 246: 15–31
- Sanz-Cervera JF, see Williams RM (2000) 209: 97–173
- Sartor V, see Astruc D (2000) 210: 229–259
- Sato S, see Furukawa N (1999) 205: 89–129
- Saudan C, see Balzani V (2003) 228: 159–191
- Sauvage J-P, see Dietrich-Buchecker C (2005) 249: 261–283
- Schalley CA, Weilandt T, Brüggemann J, Vögtle F (2004) Hydrogen-Bond-Mediated Template Synthesis of Rotaxanes, Catenanes, and Knotanes. 248: 141–200
- Scheer M, see Balazs G (2003) 232: 1–23
- Scherf U (1999) Oligo- and Polyarylenes, Oligo- and Polyarylenevinyls. 201: 163–222
- Schlenk C, see Frey H (2000) 210: 69–129
- Schlüter AD (2005) A Covalent Chemistry Approach to Giant Macromolecules with Cylindrical Shape and an Engineerable Interior and Surface. 245: 151–191
- Schmitt V, Leal-Calderon F, Bibette J (2003) Preparation of Monodisperse Particles and Emulsions by Controlled Shear. 227: 195–215
- Schmitt M, Kalsani V (2005) Functional, Discrete, Nanoscale Supramolecular Assemblies. 245: 1–53
- Schoeller WW (2003) Donor-Acceptor Complexes of Low-Coordinated Cationic p-Bonded Phosphorus Systems. 229: 75–94
- Schöning K-U, see End N (2004) 242: 241–271

- Schöning K-U, see End N (2004) 242: 273–317
- Schröder D, Schwarz H (2003) Diastereoselective Effects in Gas-Phase Ion Chemistry. 225: 129–148
- Schwarz H, see Schröder D (2003) 225: 129–148
- Schwert DD, Davies JA, Richardson N (2002) Non-Gadolinium-Based MRI Contrast Agents. 221: 165–200
- Sefkow M (2005) Enantioselective Synthesis of C(8)-Hydroxylated Lignans – Early Approaches and Recent Advances. 243: 185–224
- Seikh MM, see Rao CNR (2004) 234: 1–21
- Sellergren B, see Hall AJ (2005) 249: 317–349
- Sergeyev S, see Thilgen C (2004) 248: 1–61
- Sheiko SS, Möller M (2001) Hyperbranched Macromolecules: Soft Particles with Adjustable Shape and Capability to Persistent Motion. 212: 137–175
- Shen B (2000) The Biosynthesis of Aromatic Polyketides. 209: 1–51
- Shinkai S, see James TD (2002) 218: 159–200
- Shinkai S, see Jung JH (2004) 248: 223–260
- Shirakawa E, see Hiyama T (2002) 219: 61–85
- Shogren-Knaak M, see Imperiali B (1999) 202: 1–38
- Sinou D (1999) Metal Catalysis in Water. 206: 41–59
- Sinz CJ, Rychnovsky SD (2001) 4-Acetoxy- and 4-Cyano-1,3-dioxanes in Synthesis. 216: 51–92
- Siuzdak G, see Trauger SA (2003) 225: 257–274
- Skrifvars M, see Nummelin S (2000) 210: 1–67
- Slessor KN, see Keeling CI (2004) 239: 133–177
- Smith DK, Diederich F (2000) Supramolecular Dendrimer Chemistry – A Journey Through the Branched Architecture. 210: 183–227
- Sorai M (2004) Heat Capacity Studies of Spin Crossover Systems. 235: 153–170
- Sour A, see Boillot M-L (2004) 234: 261–276
- Spiegel A, see Basler B (2005) 243: 1–42
- Spiering H (2004) Elastic Interaction in Spin-Crossover Compounds. 235: 171–195
- Spiering H, see Real JA (2004) 233: 167–193
- Spiering H, see Kusz J (2004) 234: 129–153
- Stec WJ, see Guga P (2002) 220: 169–200
- Steudel R (2003) Aqueous Sulfur Sols. 230: 153–166
- Steudel R (2003) Liquid Sulfur. 230: 80–116
- Steudel R (2003) Inorganic Polysulfanes H_2S_n with $n > 1$. 231: 99–125
- Steudel R (2003) Inorganic Polysulfides S_n^{2-} and Radical Anions $S_n^{\cdot -}$. 231: 127–152
- Steudel R (2003) Sulfur-Rich Oxides S_nO and S_nO_2 . 231: 203–230
- Steudel R, Eckert B (2003) Solid Sulfur Allotropes. 230: 1–79
- Steudel R, see Eckert B (2003) 231: 31–97
- Steudel R, Steudel Y, Wong MW (2003) Speciation and Thermodynamics of Sulfur Vapor. 230: 117–134
- Steudel Y, see Steudel R (2003) 230: 117–134
- Steward LE, see Gilmore MA (1999) 202: 77–99
- Stocking EM, see Williams RM (2000) 209: 97–173
- Stoddart JF, see Aricó F (2005) 249: 203–259
- Streubel R (2003) Transient Nitrilium Phosphanylid Complexes: New Versatile Building Blocks in Phosphorus Chemistry. 223: 91–109
- Strojek W, see Eckert H (2005) 246: 195–233
- Stütz AE, see Häusler H (2001) 215: 77–114
- Sugihara Y, see Nakayama J (1999) 205: 131–195

- Sugiura K (2003) An Adventure in Macromolecular Chemistry Based on the Achievements of Dendrimer Science: Molecular Design, Synthesis, and Some Basic Properties of Cyclic Porphyrin Oligomers to Create a Functional Nano-Sized Space. 228: 65–85
- Sun J-Q, Bartlett RJ (1999) Modern Correlation Theories for Extended, Periodic Systems. 203: 121–145
- Sun L, see Crooks RM (2001) 212: 81–135
- Surján PR (1999) An Introduction to the Theory of Geminals. 203: 63–88
- Sylvain I, see Drain CM (2005) 245: 55–88
- Taillefer M, Cristau H-J (2003) New Trends in Ylide Chemistry. 229: 41–73
- Taira K, see Takagi Y (2003) 232: 213–251
- Takagi Y, Ikeda Y, Taira K (2003) Ribozyme Mechanisms. 232: 213–251
- Takahashi S, see Onitsuka K (2003) 228: 39–63
- Takeda N, Tokitoh N, Okazaki R (2003) Polysulfido Complexes of Main Group and Transition Metals. 231: 153–202
- Tamao K, Miyaura N (2002) Introduction to Cross-Coupling Reactions. 219: 1–9
- Tanaka M (2003) Homogeneous Catalysis for H-P Bond Addition Reactions. 232: 25–54
- Tanner PA (2004) Spectra, Energy Levels and Energy Transfer in High Symmetry Lanthanide Compounds. 241: 167–278
- ten Cate MGJ, see Crego-Calama M (2005) 249: 285–316
- ten Holte P, see Zwanenburg B (2001) 216: 93–124
- Thiem J, see Werschkun B (2001) 215: 293–325
- Thilgen C, Sergeyev S, Diederich F (2004) Spacer-Controlled Multiple Functionalization of Fullerenes. 248: 1–61
- Thutewohl M, see Waldmann H (2000) 211: 117–130
- Tichowsky I, see Idee J-M (2002) 222: 151–171
- Tiecco M (2000) Electrophilic Selenium, Selenocyclizations. 208: 7–54
- Tietze M, see Beifuss U (2005) 244: 77–113
- Toftlund H, McGarvey JJ (2004) Iron(II) Spin Crossover Systems with Multidentate Ligands. 233: 151–166
- Toftlund H, see Brady C (2004) 235: 1–22
- Tohma H, Kita Y (2003) Synthetic Applications (Total Synthesis and Natural Product Synthesis). 224: 209–248
- Tokitoh N, see Takeda N (2003) 231: 153–202
- Tomoda S, see Iwaoka M (2000) 208: 55–80
- Tordo P, see Marque S (2005) 250: 43–76
- Tóth E, Helm L, Merbach AE (2002) Relaxivity of MRI Contrast Agents. 221: 61–101
- Tovar GEM, Kruter I, Gruber C (2003) Molecularly Imprinted Polymer Nanospheres as Fully Affinity Receptors. 227: 125–144
- Trauger SA, Junker T, Siuzdak G (2003) Investigating Viral Proteins and Intact Viruses with Mass Spectrometry. 225: 257–274
- Trautwein AX, see Paulsen H (2004) 235: 197–219
- Trautwein AX, see Winkler H (2004) 235: 105–136
- Tromas C, García R (2002) Interaction Forces with Carbohydrates Measured by Atomic Force Microscopy. 218: 115–132
- Tsiourvas D, see Paleos CM (2003) 227: 1–29
- Tuchagues J-P, Bousseksou A, Molnár G, McGarvey JJ, Varret F (2004) The Role of Molecular Vibrations in the Spin Crossover Phenomenon. 235: 85–103
- Tuchagues J-P, see Bousseksou A (2004) 235: 65–84
- Tuherm T, see Samoson A (2005) 246: 15–31
- Turecek F (2003) Transient Intermediates of Chemical Reactions by Neutralization-Reionization Mass Spectrometry. 225: 75–127

- Tzschucke CC, see Horn J (2004) 242: 43–75
Ublacker GA, see Maul JJ (1999) 206: 79–105
Uemura S, see Nishibayashi Y (2000) 208: 201–233
Uemura S, see Nishibayashi Y (2000) 208: 235–255
Uggerud E (2003) Physical Organic Chemistry of the Gas Phase. Reactivity Trends for Organic Cations. 225: 1–34
Uozumi Y (2004) Recent Progress in Polymeric Palladium Catalysts for Organic Synthesis. 242: 77–112
Valdemoro C (1999) Electron Correlation and Reduced Density Matrices. 203: 187–200
Valrio C, see Astruc D (2000) 210: 229–259
van Benthem RATM, see Muscat D (2001) 212: 41–80
van der Rest M, see Ricard-Blum S (2005) 247: 35–84
van Koningsbruggen PJ (2004) Special Classes of Iron(II) Azole Spin Crossover Compounds. 233: 123–149
van Koningsbruggen PJ, Maeda Y, Oshio H (2004) Iron(III) Spin Crossover Compounds. 233: 259–324
van Koten G, see Kreiter R (2001) 217: 163–199
van Manen H-J, van Veggel FCJM, Reinhoudt DN (2001) Non-Covalent Synthesis of Metallo dendrimers. 217: 121–162
van Veggel FCJM, see van Manen H-J (2001) 217: 121–162
Varret F, Boukheddaden K, Codjovi E, Enachescu C, Linares J (2004) On the Competition Between Relaxation and Photoexcitations in Spin Crossover Solids under Continuous Irradiation. 234: 199–229
Varret F, see Bousseksou A (2004) 235: 65–84
Varret F, see Tuchagues J-P (2004) 235: 85–103
Varshney DB, see MacGillivray LR (2004) 248: 201–221
Varvoglis A (2003) Preparation of Hypervalent Iodine Compounds. 224: 69–98
Vega S, see Vinogradov E (2005) 246: 33–90
Verkade JG (2003) $P(RNCH_2CH_2)_3N$: Very Strong Non-ionic Bases Useful in Organic Synthesis. 223: 1–44
Vicinelli V, see Balzani V (2003) 228: 159–191
Vinogradov E, Madhu PK, Vega S (2005) Strategies for High-Resolution Proton Spectroscopy in Solid-State NMR. 246: 33–90
Vioux A, Le Bideau J, Mutin PH, Leclercq D (2003): Hybrid Organic-Inorganic Materials Based on Organophosphorus Derivatives. 232: 145–174
Vliegthart JFG, see Haseley SR (2002) 218: 93–114
Vogler A, Kunkely H (2001) Luminescent Metal Complexes: Diversity of Excited States. 213: 143–182
Vogtner S, see Kloppe W (1999) 203: 21–42
Vögtle F, see Schalley CA (2004) 248: 141–200
Voigt U, see Eckert H (2005) 246: 195–233
von Arx ME, see Hauser A (2004) 241: 65–96
Vostrowsky O, see Hirsch A (2001) 217: 51–93
Vostrowsky O, see Hirsch A (2005) 245: 193–237
Waldmann H, Thutewohl M (2000) Ras-Farnesyltransferase-Inhibitors as Promising Anti-Tumor Drugs. 211: 117–130
Wang G-X, see Chow H-F (2001) 217: 1–50
Weil T, see Wiesler U-M (2001) 212: 1–40
Weilandt T, see Schalley CA (2004) 248: 141–200
Wenzel B, see Dötz KH (2004) 248: 63–103

- Werschkun B, Thiem J (2001) Claisen Rearrangements in Carbohydrate Chemistry. 215: 293–325
- Wessjohann LA, Ruijter E (2005) Strategies for Total and Diversity-Oriented Synthesis of Natural Product(-Like) Macrocycles. 243: 137–184
- Wiesler U-M, Weil T, Müllen K (2001) Nanosized Polyphenylene Dendrimers. 212: 1–40
- Williams P, see Chhabra SR (2005) 240: 279–315
- Williams RM, Stocking EM, Sanz-Cervera JF (2000) Biosynthesis of Prenylated Alkaloids Derived from Tryptophan. 209: 97–173
- Winkler H, Chumakov AI, Trautwein AX (2004) Nuclear Resonant Forward and Nuclear Inelastic Scattering Using Synchrotron Radiation for Spin Crossover Systems. 235: 105–136
- Wirth T (2000) Introduction and General Aspects. 208: 1–5
- Wirth T (2003) Introduction and General Aspects. 224: 1–4
- Wirth T (2003) Oxidations and Rearrangements. 224: 185–208
- Wong MW, see Steudel R (2003) 230: 117–134
- Wong MW (2003) Quantum-Chemical Calculations of Sulfur-Rich Compounds. 231: 1–29
- Wooley KL, Hawker CJ (2005) Nanoscale Objects: Perspectives Regarding Methodologies for their Assembly, Covalent Stabilization and Utilization. 245: 287–305
- Wrodnigg TM, Eder B (2001) The Amadori and Heyns Rearrangements: Landmarks in the History of Carbohydrate Chemistry or Unrecognized Synthetic Opportunities? 215: 115–175
- Wu J-J, see Eyre DR (2005) 247: 207–229
- Wytenbach T, Bowers MT (2003) Gas-Phase Confirmations: The Ion Mobility/Ion Chromatography Method. 225: 201–226
- Yamaguchi H, Harada A (2003) Antibody Dendrimers. 228: 237–258
- Yamamoto M, see Ando T (2004) 239: 51–96
- Yersin H, Donges D (2001) Low-Lying Electronic States and Photophysical Properties of Organometallic Pd(II) and Pt(II) Compounds. Modern Research Trends Presented in Detailed Case Studies. 214: 81–186
- Yersin H (2004) Triplet Emitters for OLED Applications. Mechanisms of Exciton Trapping and Control of Emission Properties. 241: 1–6
- Yeung LK, see Crooks RM (2001) 212: 81–135
- Yokoyama S, Otomo A, Nakahama T, Okuno Y, Mashiko S (2003) Dendrimers for Optoelectronic Applications. 228: 205–226
- Yoshifuji M, Ito S (2003) Chemistry of Phosphanlydene Carbenoids. 223: 67–89
- Zablocka M, see Majoral J-P (2002) 220: 53–77
- Zarembowitch J, see Boillot M-L (2004) 234: 261–276
- Zhang J, see Chow H-F (2001) 217: 1–50
- Zhdankin VV (2003) C-C Bond Forming Reactions. 224: 99–136
- Zhao M, see Crooks RM (2001) 212: 81–135
- Zimmermann SC, Lawless LJ (2001) Supramolecular Chemistry of Dendrimers. 217: 95–120
- Zwanenburg B, ten Holte P (2001) The Synthetic Potential of Three-Membered Ring Aza-Heterocycles. 216: 93–124

Subject Index

- AFM 311
Alizarin, encapsulation 306
Amide templates 214
Amidopyridines 325
Amines 330
4-Aminostyrene 325
Anchors 10, 11, 30
–, hydrophobic 15
–, metal ion 20, 35
–, π - π 11, 12
Archimedean structures 188
Aspartic acid 328
- Binding sites, endotopic 178
BINOL 345
Bis-amidopyrimidines 325
Bis-*p*-phenylene₃₄crown₁₀ 30
1,2-Bispyridinium ethane 38, 42
Bite angle 131, 174
Borromean link 4, 10, 58
- Cages 128
–, ligands 22, 24
Calix[4]arene dimelamine 303
Calixarene, containing macrocycle 94
Carbamates 340
–, hydrolysis 341
Carbohydrates 331
Carbonates, hydrolysis 341
Carboxypeptidase A 342
Catenanes 11, 26, 32, 69, 85–89, 103–109, 114, 119, 121, 191, 204, 205, 263–280
–, diimide-based 32
–, directed synthesis 35
–, iso-phthaloylamide-based 33
–, phthaloylamide-based 32
–, polymeric 69, 109
Cavity 334
Chirality 167, 179, 190, 295
- Cinchonidine 332
Clathro-chelate 22
Clipping 204, 205
Comuter chip, molecular 50
Copper 269–277
Cotton effect 299
Counterions 156
Coupling, Glaser-Hay 214
Creatinine 332
Crocheting 56
Crossbar devices 248
Crown ethers 81, 83, 216
Cucurbituril 15, 16, 44
Cycloaddition, 1,3-dipolar 237, 239
Cyclobis(paraquat-*p*-phenylene) 211, 212, 243, 247, 248–250
Cyclodextrin 15
Cyclophane 211
- Daisy-chain polymer 44
DEB 292
Dendrimers 42, 333
Diastereomers 289
Dicopper(I) 268–275
Diimides 213
Dioxynaphthalene 212
Dipyridinium axle 48
Dipyridiniummethane 218
Directional bond 131, 177, 180
DNA 2, 50, 136, 263
Donor-acceptor interactions 194
Donor-acceptor-donor 323
Dumbbell molecule 57
Dynamic combinatorial library (DCL) 68, 76, 78, 111, 118, 285, 292
- EDMA 324
Eicosanoic acid 250
Electron configuration 129

- Elimination, reductive 162, 172, 174, 195, 197
Equilibrium 134, 142, 149, 153, 155, 177, 196
Esterase 341
Esters, hydrolysis 341
9-Ethyladenine 320

Flavins 323

Glutamic acid 328
Glycine 328
Glycylglycine 15
Gold surfaces 309
Granny 53
Grubbs catalysts 231, 232, 304
Guest 292, 317

H-bonding anchor 13
Haptens 334
Helical macrocycle, sugar binding 84, 85
Helix 269–277
Hoop-snake vision 17
HOPG 311
Host monomers 323
Host-guest chemistry 141, 147, 150
– –, cage structures 183
– –, induced fit 157
– –, tweezer complexes 147, 162, 164
Hydrogen bonds 153, 261, 288
Hydrolysis reaction 335

Imprinted polymers 317
Imprinting, non-covalent 323
Interlocked molecules 203
Isomerization, by light 148
–, *cis*-to-*trans* 131, 166
–, *trans*-to-*cis* 166

Job plot 326

Ketones, hydrogenation 344
Knitting 56
Knotanes 54–58
Knots 53, 54, 58, 261–281
–, composite 2, 10, 53
–, square 53

Langmuir-Blodgett film 246, 249
Ligand reaction 20, 21
MAA 320
Macramé 56
Macrochelate 136, 179
Macrocycle 17
– templation 68
Macrocycles, annulated 183
–, conjugated 174, 195
–, porphyrin-containing 88, 109, 116
–, preformed 133
–, strategies 133
MALDI-TOF 289
Mass spectrometry 134
Medicine delivery 58
Metal template approach 133, 183, 187, 191
Metallo-enzymes 343
Metal-to-ligand charge transfer 158
Metathesis 176, 181, 304
Methacrylamide 321
MIPs 335
Mitsunobu reaction 214
MO scheme 129
Möbius strip 58, 266
Molecular device 43, 58
Molecular knot 91, 111
Molecular machines 50, 204
Molecular reactor 58
Molecular riveting 233
Molecular shuttle 42
Molecular switch/switching 43, 243
Multivalency 204

Nanorods 311
Nanowires 286
Network structures 182
Nicotine 330
Noncovalent synthesis 298, 303
Nucleobases 136

Olefin metathesis 209, 223, 224, 231, 232, 241, 242, 251
Oligo-catenate 50
Olympiadane 32, 211
OMNiMIP 330

Pd(II) 127, 345
Phosphamacrocycle 81, 82
Platonic structures 188
Polycatenane 31
Polyethylene glycol axle 50
Porphyrin 329

- Pseudorotaxanes 205
Pt(II) complexes 127, 345
Pyrolysis 183
- Rearrangement 179
Reduction, asymmetric 170
Resorcinarene templates 71
Riboflavin 324
Ring closing metathesis (RCM) 29, 41, 51, 68, 86–91, 102, 109, 223
– – –, catenane synthesis 86–89, 109
– – –, knot synthesis 91
– – –, macrocycle synthesis 76, 94
– – –, rotaxane synthesis 102
RORCM 224
Rosettes, hydrogen-bonded 285
Rotaxanes 37, 42, 89, 97, 100–102, 142, 157, 195, 204, 205
–, pseudo- 4, 8, 35
–, semi- 41
- SAMs 286
Scavengers 319
Self-assembly 128, 133, 191
–, monolayers 246
Sergeant and soldier principle 294
Slipping 204
Smart materials 43
Smectite clay template 75
Spacers, sacrificial 320
Steroids 325
Stopping 205
Surface switching 246
Surface templation 307
Surfaces, gold 309
–, graphite 310
- Suzuki reaction, Pd-MIPs 346
Switch 58
- Tecton 56
Template 265, 268, 269, 276–281
–, anchor 4, 8
–, element 6, 8, 28
–, small molecule 59
Template synthesis 133, 183, 187, 191
– –, metal template approach 172 195
Templation, macrocycle synthesis 67
–, surface 307
–, π -donor/ π -acceptor 211
Tetraamide macrocycle 38
Tetrasilicates 301
Tetrathiafulvalene 211–213, 243, 247–250
Thermodynamic control 134, 193, 196
Threading 55
–, molecular 3
Threading-followed-by-stoppering 204
Thymine 323, 332
TM-SFM 310
Topology 3, 4, 35, 264
Trefoil knot 51, 52, 270
Trimers 303
–, hydrogen-bonded 306
Tweezer complexes 147, 162, 164
- Uracils 323
- Vinylpyridine 321
- Wittig reaction 216
- Zinc porphyrin 329